Developing and Understanding Iridium-Catalysed Arene Borylation

HARRISSON, PETER

Developing and Understanding Ir-Catalysed Arene Borylation

Peter Harrisson
Ph.D. Thesis

University of Durham
Department of Chemistry
2011

Statement of Copyright

Declaration

The work described in this thesis was carried out in the Department of Chemistry at Durham University and Syngenta, Jealott's Hill International Research Centre, Bracknell between October 2007 and December 2010, under the supervision of Dr Patrick G. Steel, Prof. Todd B. Marder and Dr James Morris. All the work is my own work, unless otherwise stated, and has not been submitted previously for a degree at this or any other university.

Peter Harrisson

Acknowledgements

I would like to thank my supervisors Dr Patrick G. Steel, Prof. Todd B. Marder and Dr James Morris for their guidance and help throughout my studies. My time in both Durham and Bracknell has been enjoyable and challenging and I thank them for giving me the opportunity. Special thanks go to my lab colleagues for the help and advice which helped to make my studies productive.

I would also like to thank the departmental service staff, especially those from the NMR service, Dr Alan Kenwright, Ian McKeag and Catherine Heffernan; Dr Andrei Batsanov of the X-ray crystallography service for getting results from the smallest of crystals; Dr Mike Jones, Dr Jackie Mosely for help with Mass Spectrometry.

Many thanks to all past and current members of CG 1 and 52: Dr Jonathan Sellars, Dr Tom Woods, Dr Kathryn Knight, Nick Hughes, Dr Marvis Erhunmwunse, Dr Michel Czyewski, John Dunwell, Dr John Mina, Hazmi Tajuddin, Dr Matt Burton, Hannah Straker, Dr Chris Coxon, Dr Bianca Bitterlich, Dr Jon Collings, Dr Marie-Hélène Thibault, Dr Christian Kleeberg, Dr Andreas Steffen, Nim Chaiyaveij, Dr Kittiya Wongkhan, Chao Liu, Dr Andrew Crawford.

I am also grateful to others from around the department for keeping me amused, especially, Dr Matt Cargill, Jessica Breen, Dr Chris McPake, Dr Ian Wilson, Ffion Abraham, Rich Delley, Katharine Linton, Dr Neil Brown, Dr Phil Schauer and Professor Graham Sandford.

I thank my parents for their help, support and guidance throughout the past 26 years. Finally, I would like to thank Catherine for supporting me throughout my PhD and helping me continually along the way.

Conferences Attended

41st Sheffield Stereochemistry Meeting, (Day Meeting)

University of Sheffield, 15th January 2008

RSC Organic Division North East Regional Meeting, (Day Meeting)

Newcastle University, 2nd April 2008

Investigating Chemical Processes Through Designed Experiments (Residential Workshop)

University of Southampton, 3rd - 5th September 2008

42nd Sheffield Stereochemistry Meeting (Day Meeting)

University of Sheffield, 13th January 2009

RSC Pre-Grasmere Meeting and Symposium (Day Meeting)

University of York, 6th May 2009

2nd NEPIC Organic Chemistry and Catalysis Symposium (Oral Presentation)

University of Durham - 30th June 2009

EPSRC Summer School on Catalysis (Poster)

University of Liverpool, 13th - 17th July 2009

SCI Challenges in Catalysis for Pharmaceuticals and Fine Chemicals II (Poster)

SCI, London, 20th October, 2009

SCI Key Elements in Organic Synthesis (Poster)

SCI, London, 4th December 2009

SCI Graduate Symposium (Oral Presentation)

University of Manchester, 31st March 2010

RSC Organic Division Regional Meeting (Poster)

University of Durham, 15th April 2010

RSC Dalton Division USIC 2010 (Organising Committee)

University of Durham, 8th - 9th July 2010

ACS National Meeting, Boston (Oral Presentation)

Boston, MA, USA, 22nd - 26th August 2010

Syngenta CASE Conference (Oral Presentation) - Awarded 1st prize

Jealott's Hill, Bracknell, 9th - 10th September 2010

RSC Dalton Discussions 12 (Poster)

University of Durham, 13th - 15th September 2010

NORSC Symposium (Oral Presentation)

University of York, 28th October 2010

J-NOST-6 (Oral Presentation)

University of Hyderabad, India, 28th - 31st January 2011

Publications

1) **A One-Pot, Single Solvent Process for Tandem, Catalyzed C-H Borylation/Suzuki-Miyaura Cross-Coupling Sequences.**

   Harrisson, P.; Morris, J.; Steel, P. G.; Marder T. B *Synlett*, 2009, *1*, 149

2) **Microwave Accelerated Iridium Catalyzed Borylation of Aromatic C-H Bonds.**

   Harrisson, P.; Morris, J.; Marder, T. B.; Steel, P. G. *Org. Lett*., 2009, *11*, 3589

3) **Iridium Catalyzed C-H Borylation of Quinolines and Unsymmetrical 1,2-disubstituted Benzenes: Insights into Selectivity.**

   Peter Harrisson, Bianca Bitterlich, Hazmi Tajuddin, Andrei Batsanov, Aoife Maxwell, Lena Shukla, James Morris, Todd. B. Marder and Patrick G. Steel

   J. Am. Chem. Soc., **2011** (In Preparation)

Abstract

Developing and Understanding Ir-Catalysed Arene Borylation

Iridium catalysed C-H borylation has moved from an interesting observation to an efficient catalytic reaction. This work has developed and improved upon some of the key issues associated with the methodology.

The one-pot conversion of aryl boronates, generated by C-H borylation, to other functionality has been one area of interest. However, reactions typically require a change in reaction solvent to make this possible. This thesis describes a one-pot, single solvent C-H borylation/Suzuki-Miyaura cross-coupling sequence. The key to this transformation is the use of methyl tert-butyl ether (MTBE). This procedure allows efficient synthesis of biaryls by initial C-H borylation of aromatic substrates followed by addition of water, subsequent reagents and aryl halide to complete the Suzuki-Miyaura cross-coupling without the need for change in reaction solvent.

Another issue associated with the C-H borylation reaction is the extended reaction times required for some substrates. This issue was tackled by development of a microwave accelerated C-H borylation reaction. Microwave reactions are conducted at the same temperature as standard heated reactions with accelerations of 2 - 24 times affording comparable product yields. Typically reaction times were reduced from hours to minutes. A microwave accelerated one-pot, single solvent C-H borylation/Suzuki-Miyaura cross-coupling sequence allowed synthesis of biaryls from arene plus aryl halides in reaction times of minutes.

Subsequent work focussed on the borylation of novel substrates classes, in particular quinolines. The borylation of substituted quinolines highlighted interesting electronic selectivity of the reaction. The site of borylation can be directed by changing the nature of the substituent on the ring. DFT calculations have been conducted to gain understanding into the causes of selectivity. A link between C-H acidity, calculated by DFT methods, and the borylation site was observed. Preliminary studies into the borylation of azaindoles are discussed. Studies towards a procedure to convert aryl boronates to trifluoromethyl groups are also been introduced.

Abbreviations

Å	angstrom	di-CO_2H-bpy	2,2'-bipyridine-4,4'-dicarboxylic acid
acac	acetoacetyl	dippe	1,2-bis(diisopropyl-phosphino)ethane
Ar	aryl	D*o*M	Directed *ortho*-metalation
ASAP	Atmospheric pressure Solid Analysis Probe	DMAP	4-dimethylaminopyridine
B3LYP	Becke-3 + LYP hybrid functional	DME	dimethoxyethane
Bn	benzyl	DMF	N,N-dimethylformamide
B_2neop_2	dis(neopentyl glycolato)diboron	dmpe	1,2-bis(dimethyl-phosphino) ethane
Boc	*tert*-butoxycarbonyl	DMSO	dimethylsulfoxide
B_2pin_2	bis(pinacolato)diboron	dppb	1,4-bis(diphenyl-phosphino) butane
bpy	2,2'-bipyridine	dppe	1,2-bis(diphenyl-phosphino) ethane
cat	catacholato (1,2-$O_2C_6H_4$)	dppf	1,1'-bis(diphenyl-phosphino) ferrocene
cat.	catalyst	dtbpy	4,4 di-*tert*-butyl-2,2-bipyridine
cod	1,5-cyclooctadiene	eg	ethylenegyloclato (OCH_2CH_2O)
coe	cyclooctene	EI	Electron Ionisation
Conv.	conversion	eq.	equivalents
Cp	cyclopentadienyl	Et	ethyl
Cp*	pentamethylcyclopentadienyl	Et_2O	diethyl ether
Cy	cyclohexyl	EtOAc	ethyl acetate
dba	dibenzylideneacetone	eV	electron volt
DCE	1,2-dichloroethane		
DCM	dichloromethane		
DFT	Density Functional Theory		
DIBAL	di-isobutyl-aluminium hydride		

GC-MS	Gas Chromatography-Mass Spectrometry	*n*Bu	n-butyl
		NCS	N-chloro-succinimide
GHz	gigahertz	neop	neopentylglycolato ($OCH_2CMe_2CH_2O$)
h	hour		
HRMS	High Resolution Mass Spectrometry	NHC	N-hetrocyclic carbene
		NIS	N-iodo-succinimide
Ind	indenyl	NXS	N-halo-succinimide
^{i}Pr	iso-propyl	OAc	acetate
K	Kelvin	OTf	triflate
L	litre	Oxone®	potassium peroxymonosulfate
LA	Lewis acid	$P^{i}Pr_3$	triisopropylphosphine
m	metre	Ph	phenyl
M	molar	phen	1,10-phenanthroline
m.p.	melting point	pin	pinacolato ($OCMe_2CMe_2$)
m/z	*mass/charge* ratio	PMe_3	trimethylphosphine
MAOS	Microwave Assisted Organic Synthesis	PPh_3	triphenylphosphine
		R	group
Me	methyl	rt	room temperature
MeCN	acetonitrile	Selectfluor®	1-chloromethyl-4-fluoro-1,4-diazoniabicyclo-[2.2.2]octane bis (tetrafluoroborate)
2-Me-THF	2-methyl-tetrahydrofuran		
Mes	mesitylene		
mg	milligram	Si-SMAP	Silica Supported Mono Alkyl Phosphine
min	minute		
mL	millilitre	S-Phos	2-dicyclohexylphosphino-2',6'-dimethoxybiphenyl
mmol	millimole		
MTBE	methyl *tert*-butyl ether	t	time
μW	microwave	tan δ	loss tangent
NBS	N-bromo-succinimide	^{t}Bu	*tert*-butyl

Temp.	temperature	Tp	hydrotris(pyrazolyl)borate
tert	tertiary	TSE	2-(trimethylsilyl)ethyl
THF	tetrahydrofuran	X	halide
TIPS	triisopropylsilyl	Δ	standard heating
TMS	trimethylsilyl	ε′	dielectric constant
TON	turnover number	ε″	dielectric loss

NMR Abbreviations

d	doublet	m	multiplet
Hz	hertz	MHz	megahertz
J	coupling constant	q	quartet
s	singlet	t	triplet
ppm	parts per million	NMR	Nuclear Magnetic Resonance

Table of Contents

Statement of Copyright i

Declaration i

Acknowledgements ii

Conferences Attended iii

Publications iv

Abstract v

Abbreviations vi

NMR Abbreviations viii

Table of Contents ix

Table of Graphs xxiv

Table of Tables xxiv

CHAPTER I - METAL CATALYSED C-H BORYLATION REACTIONS 1

1.1 Introduction 2

1.2 Introduction to C-H Activation 2

1.3 C-H Functionalisation Strategies 2

1.4 Aryl C-H to C-B Bond Formation 3

1.5 Synthesis of Aryl Boronates 4

1.6 Metal Catalysed Aromatic C-H Borylation 6

1.6.1 Stoichiometric C-H Borylation 6

1.6.2 Catalytic C-H Borylation 8

1.6.3 Iridium Catalysts with Phosphine Ligands 11

1.6.4 $[Ir(X)cod]_2$ Catalysed Borylation of Arenes 12

1.6.5 Proposed Mechanism for the Borylation of Arenes with $[Ir(OMe)cod]_2$ 17

1.6.6 Selectivity of C-H Borylation in Simple Aromatic Systems 19

1.6.7 Variation of Ligand System 22

1.6.8 Directed *ortho*-Borylation 26

1.6.8.1 Silica Supported *ortho*-Borylation 28

1.7 Borylation of Arenes With the $[Ir(X)cod]_2$/dtbpy Catalyst Systems (X = Cl, OMe) 29
1.7.1 Polyaromatic Substrates 30
1.7.2 Heteroaromatic Substrates 30
1.7.2.1 5-Membered Heteroarenes 31
1.7.2.2 Fused 5-Membered Heteroarenes 33
1.7.2.3 Pyridines 35
1.7.3 Novel Applications of C-H Borylation 38
1.7.4 Application of C-H Borylation to the Synthesis of Complex Molecules 41
1.8 Conclusions 42
1.9 Chapter I -References 43

2 CHAPTER II - ONE-POT, SINGLE SOLVENT C-H BORYLATION/SUZUKI-MIYAURA CROSS-COUPLING SEQUENCE 49
2.1 Introduction 50
2.2 Transformations from Arylboronates 50
2.2.1 *Ipso*-Substitution of the Aryl Boronate Group 51
2.2.1.1 Phenol Synthesis 51
2.2.1.2 *Ipso*-Nitration 53
2.2.1.3 Azide Synthesis 54
2.2.1.4 Aniline Synthesis 54
2.2.1.5 *Ipso*-Halogenation 55
2.2.1.5.1 *Ipso*-Chlorination, Bromination and Iodination 55
2.2.1.5.2 *Ipso*-Fluorination 57
2.2.1.6 *Ipso*-Cyanation 57
2.2.1.7 *Ipso*-Trifluoromethylation 58
2.2.2 C-N and C-O Bond Forming Reactions 59
2.2.3 C-C bond Forming Reactions 61
2.2.3.1 Petasis Borono-Mannich Reaction - Addition of Aryl Boronates to Imines 61

2.2.3.2 Rhodium Catalysed Conjugate Addition to α,β-Unsaturated Carbonyl Compounds 63
2.2.3.3 Oxidative Heck-Type Couplings to Alkenes 63
2.2.3.4 Suzuki-Miyaura Cross-Coupling 64
2.3 One-pot Borylation/Functionalisation Strategies 66
2.3.1 One-pot C-H Borylation/Suzuki-Miyaura Cross-coupling strategies 67
2.3.2 Conclusions 69
2.4 Results and Discussion 69
2.4.1 Initial Studies 69
2.4.2 Catalyst and Base Screen 72
2.4.3 One-Pot, Single-Solvent C-H Borylation/Suzuki-Miyaura Cross-Coupling Sequence 74
2.4.4 Variation of the Aryl Halide Coupling Partner 78
2.5 Conclusions 80
2.6 Chapter II - References 80

3 CHAPTER III - MICROWAVE ACCELERATED C-H BORYLATION 84
3.1 Introduction 85
3.2 Microwave Chemistry 85
3.2.1 Microwave Heating Theory 86
3.2.2 Microwave Effects 89
3.2.2.1 Specific Microwave Effects 90
3.2.2.2 Non-thermal Microwave Effects 91
3.2.3 Microwave Assisted Organic Synthesis 91
3.3 Microwave Heating in C-H Borylation Reactions 92
3.4 Summary 93
3.5 Results and Discussion 94
3.5.1 Initial Reaction Screen 94
3.5.2 Cause of Microwave Acceleration Effect 97

3.5.2.1 Investigation of Substrate Scope for the Microwave Accelerated C-H Borylation Reaction 97
3.5.2.1.1 Carbocyclic Substrates 98
3.5.2.1.2 Pyridine and Quinoline Substrates 99
3.5.2.1.3 Pyrazine Substrates 102
3.5.2.1.4 5-Membered Heterocycles 104
3.5.2.1.5 Indole Based Substrates 108
3.5.2.1.6 Conclusions 112
3.5.2.2 Microwave Absorbing Solvents 113
3.5.2.3 Nano-Particle Formation 114
3.5.2.4 Origins of the Microwave Acceleration Effect 114
3.5.3 Microwave Accelerated One-Pot C-H Borylation/Suzuki-Miyaura Cross-Coupling Sequence 114
3.6 Conclusions 115
3.7 Chapter III - References 116

4 CHAPTER IV- C-H BORYLATION OF SUBSTITUTED QUINOLINES 119
4.1 Introduction 120
4.2 Uses of Quinoline Derivatives 120
4.3 Quinoline Synthesis 121
4.3.1 Functionalisation of Quinolines 123
4.3.2 Selectivity of C-H Borylation in Analogous Systems to Quinoline 126
4.3.2.1 C-H Borylation of Quinoline 126
4.3.2.2 Analogy to Naphthalene Borylation 127
4.3.2.3 Analogy to Pyridine Borylation 127
4.4 Results and Discussion 130
4.4.1 Borylation of 2,6-Disubstituted Quinolines 130
4.4.2 Borylation of 4,7-Disubstituted Quinolines 134
4.4.3 2,7-Disubstituted Quinolines 138

4.4.3.1 Synthesis of 2-Methyl-7-Substituted Quinolines 139
4.4.3.1.1 The Döbner-Miller Reaction 139
4.4.3.1.1.1 Mechanism of the Döbner-Miller Reaction 139
4.4.3.1.2 Döbner-Miller Synthesis of 2-Methyl-7-Substituted Quinolines 142
4.4.3.1.2.1 Synthesis of 2-Methyl-7-Bromoquinoline 142
4.4.3.1.2.2 Synthesis of 2-Methyl-7-(Trifluoromethyl)quinoline 143
4.4.3.1.2.3 Synthesis of 7-Methoxy-2-Methylquinoline 144
4.4.3.1.2.4 Synthesis of 7-Cyano-2-Methylquinoline 145
4.4.3.1.2.5 Synthesis of 2-Methyl-7-(Trimethylsilyl)quinoline 146
4.4.3.2 Borylation of 2-Methyl-7-Substituted Quinolines 147
4.4.4 Conclusions 155
4.4.5 Investigation of Electronic Effects in the Borylation Reaction 155
4.4.5.1 Borylation of Heteroaromatic Substrates 155
4.4.5.2 DFT method for the Calculation of pK_a Values in Aromatic Systems 158
4.4.5.2.1 pK_a of Substituted Quinolines 160
4.4.5.3 Calculated pK_a Values for substituted quinolines 160
4.5 Conclusions 162
4.6 Chapter IV - References 162

5 CHAPTER V - AZAINDOLE PROTECTION AND BORYLATION 167
5.1 Introduction 168
5.2 C-H Borylation of 7-Azaindoles 169
5.2.1 Synthesis of *N*-Protected 7-Azaindoles 170
5.2.2 C-H Borylation of *N*-protected 7-Azaindoles 173
5.2.3 *N*-Boc-7-Azaindole Borylation Study 175
5.2.3.1 Variation of B_2pin_2 Stoichiometry for the Borylation of *N*-Boc-7-Azaindole 175
5.2.3.2 Variation of Reaction Solvent for the Borylation of *N*-Boc-7-Azaindole 177
5.2.3.3 Application of Microwave Heating to the Borylation of *N*-Boc-7-Azaindole 179

5.3 Conclusions 180

5.4 Chapter V - References 180

6 CHAPTER VI - *IPSO*-TRIFLUOROMETHYLATION OF ARYL BORONATES 181

6.1 Introduction 182

6.2 Classical Methods 183

6.3 Metal Mediated Conversion of ArX to $ArCF_3$ 183

6.3.1 Copper Mediated Trifluoromethylation 183

6.4 Palladium Catalysed Trifluoromethylation 185

6.5 Reactions of Cu^I and Ag^I Salts with Aryl Boronates 187

6.5.1 Electrophilic Trifluoromethylating Reagents 189

6.6 Results and Discussion 190

6.6.1 Trifluoromethylation of Aryl boronates 191

6.6.2 Copper (I) Source Screen 192

6.7 Future Outlook and Conclusion 194

6.8 Chapter VI - References 196

7 CHAPTER VII - CONCLUSIONS AND FUTURE WORK 198

7.1 Conclusions 199

7.2 Future Work 200

8 CHAPTER VIII - EXPERIMENTAL DETAILS 201

8.1 General Experimental Considerations 202

8.2 General Procedures 204

8.3 Experimental Details - References 257

APPENDIX I - NMR SPECTRA 259

APPENDIX II - X-RAY CRYSTAL STRUCTURES & DATA TABLES 325

APPENDIX III - DFT CALCULATION DATA TABLES (ON ENCLOSED CD)

Table of Figures

Figure 1 **-** Selected examples of C-H functionalisation reactions by Yu, Sanford, Fagnou & Gaunt. 3

Figure 2 **- S**elected examples of classical methods for the formation of aryl boron reagents. 4

Figure 3 **-** The first (sub-stoichiometric) aromatic C-H borylation. 7

Figure 4 **-** The photolytic borylation of benzene with $M(CO)_5(Bcat)$ (M = Mn, Re) or $[CpFe(CO)_2(Bcat)]$. 7

Figure 5 **-** The catalytic borylation of benzene with $[Cp^*Ir(PMe_3)(H)(Bpin)]$. 8

Figure 6 - The photocatalysed borylation of benzene with $[Cp^*Mn(CO)_3]$. 8

Figure 7 - Catalytic borylation of terminal alkanes and benzene with $[Cp^*Rh(\eta^4\text{-}C_6Me_6)]$. 9

Figure 8 **-** The borylation of substituted arenes with **41** and **44**. 9

Figure 9 **-** The borylation of disubstituted arenes with $[Cp^*Rh(\eta^4\text{-}C_6Me_6)]$ in an inert cyclic alkane solvent**.** 10

Figure 10 **-** The borylation of benzene with **52**. 11

Figure 11 **-** The borylation of benzene using **52** and **33.** 11

Figure 12 **-** The borylation of arenes and heteroarenes with **33** dmpe/dppe catalyst system. 12

Figure 13 **-** Aromatic C-H borylation of benzene using **62.** 13

Figure 14 **-** C-H borylation competition experiment. 14

Figure 15 **-** Borylation of benzene with a range of Ir^I precursors and bpy ligands. 15

Figure 16 **-** A proposed catalytic cycle for aromatic borylation by $[Ir(X)cod]_2$/dtbpy and B_2pin_2. 18

Figure 17 **-** A proposed mechanism showing the dissociation of the coe ligand. 19

Figure 18 **-** Borylation of mono substituted arenes by the $[Ir(Cl)cod]_2$/bpy catalyst system. 20

Figure 19 **-** Borylation of 1,2-disubstituted benzenes with the $[Ir(X)cod]_2$/bpy catalyst system. 20

Figure 20 **-** The *ortho*-borylation of benzodioxole and 1,2-bismethoxybenzene. 21

Figure 21 **-** Borylation of 1,3-disubstituted benzenes with the $[Ir(X)cod]_2$/bpy catalyst system. 21

Figure 22 **-** Borylation of 4-benzonitriles with the $[Ir(OMe)cod]_2$/dtbpy catalyst system. 22

Figure 23 **-** Selected examples of borylation using recyclable carboxylic acid catalyst system. 23

Figure 24 **-** The catalytic borylation of arenes with the "TpIr" catalyst system. 24

Figure 25 **-** Catalytic borylation of aromatic C-H bonds using $[Ir(cod)(NHC)_2]^+$ as catalyst precursor. 25

Figure 26 **-** Borylation of arenes using Ir CCC-NHC pincer complex **105**. 25

Figure 27 **-** The dialkylsilyl directed *ortho*-borylation. 26

Figure 28 - Mechanism of the dialkylsilyl directed *ortho*-borylation. 27

Figure 29 **-** *Ortho*-borylation of methyl benzoates. 27

Figure 30 **-** Silica supported *ortho*-borylation of arenes and heteroarenes. 28

Figure 31 **-** The *ortho*-borylation of phenol derivatives using the Silica-SMAP-Ir catalyst. 29

Figure 32 **-** Borylation of polycyclic aromatics using the $[Ir(OMe)cod]_2$/dtbpy catalyst system. 30

Figure 33 **-** Mono-borylation of 5-membered heteroarenes using the $[Ir(OMe)cod]_2$/dtbpy catalyst system. 31

Figure 34 **-** Synthesis of 2,5-bis(boryl)heteroarenes using the $[Ir(OMe)cod]_2$/dtbpy catalyst system. 31

Figure 35 **-** Borylation of substituted thiophenes using the $[Ir(OMe)cod]_2$/dtbpy catalyst system. 32

Figure 36 - Borylation of *N*-Boc-protected azaheterocycles using the $[Ir(OMe)cod]_2$/dtbpy catalyst system. 32

Figure 37 **-** Thermally initiated decarboxylation of *N*-Boc azoles. 33

Figure 38 **-** Borylation of benzofused heteroarenes using the $[Ir(Cl)cod]_2$/dtbpy catalyst system. 33

Figure 39 **-** Borylation of 2-substituted indoles using the $[Ir(OMe)cod]_2$/dtbpy catalyst system. 34

Figure 40 **-** Silicon directed C-H borylation of indoles using the $[Ir(Cl)cod]_2$/dtbpy catalyst system. 35

Figure 41 **-** Borylation and cross-coupling of 9-benzyl-6-phenylpyrolo[2,3,d]pyrimidine. 35

Figure 42 **-** Borylation of **193** and **195** using the $[Ir(Cl)cod]_2$/dtbpy catalyst system. 36

Figure 43 **-** Proposed coordination of the pyridine nitrogen to a Lewis acid (LA) blocking borylation at the *ortho*- position. 36

Figure 44 - Borylation of **57** using the [Ir(Ind)cod]/dppe catalyst system. 37

Figure 45 **-** Borylation of **1** using the $[Ir(OMe)cod]_2$/dtbpy catalyst system. 37

Figure 46 **-** Borylation of **79** using the $[Ir(OMe)cod]_2$/dtbpy catalyst system. 38

Figure 47 **-** Borylation of **199** using the $[Ir(OMe)cod]_2$/dtbpy catalyst system. 39

Figure 48 **-** Borylation of porphyrin **201** using the $[Ir(OMe)cod]_2$/dtbpy catalyst system. 39

Figure 49 **-** Borylation of dipyrroles and BODIPYs using the $[Ir(OMe)cod]_2$/dtbpy catalyst system. 40

Figure 50 **-** Borylation of amino acid derivatives using the $[Ir(OMe)cod]_2$/dtbpy catalyst system. 40

Figure 51 **-** Synthesis of Rhazinicine via a C-H borylation strategy. 41

Figure 52 **-** Synthesis of (+)-Complanadine. 41

Figure 53 **-** Synthesis of SM-130686. 42

Figure 54 - Selected transformations from arylboronate moiety. 51

Figure 55 - Hydrogen peroxide oxidation of 4-chloro- and 4-methyl- phenylboronic acid to the corresponding phenol. 52

Figure 56 - Mechanism of aqueous oxidation of phenyl boronic acid with hydrogen peroxide. 52

Figure 57 -Mechanism of *ipso*-nitration of *meta*-chloroboronic acid with TMSCl-silver nitrate. 53

Figure 58 - Copper catalysed conversion of aryl boronic acid to aryl azide. 54

Figure 59 - Copper catalysed conversion of aryl boronic acids to anilines. 55

Figure 60 - *Ipso*-halogenation of aryl boronic acids, esters and trifluoroborates. 56

Figure 61 - C-H borylation followed by oxidative cleavage to boronic acid and subsequent silver mediated fluorination. 57

Figure 62 - Cyanation of aryl pinacolboronate ester and subsequent transformations. 58

Figure 63 - Oxidative trifluoromethylation of aryl boronic acids. 59

Figure 64 - Proposed mechanism of oxidative trifluoromethylation of aryl boronic acids. 59

Figure 65 - Initial reports of phenol and amine couplings with boronic acids. 60

Figure 66 - Mechanism of Chan-Lam coupling. 61

Figure 67 - Petasis Borono-Mannich reaction in the synthesis of α-arylglycines. 62

Figure 68 - Proposed mechanism for the Petasis Borono-Mannich reaction. 62

Figure 69 - Rhodium catalysed conjugate addition of phenylboronic acid to α,β-unsaturated ketones. 63

Figure 70 - Palladium (II) catalysed oxidative heck reaction of *para*-methoxyphenylboronic acid with *tert*-butyl-acrylate. 64

Figure 71 - Catalytic cycle of Suzuki-Miyaura reaction. 65

Figure 72 - Suzuki-Miyaura cross-coupling of chloro-4-methoxybenzene with phenyl boronic acid. 66

Figure 73 - C-H borylation of 1,3-dichlorobenzene and Suzuki-Miyaura cross-coupling with 3-bromotoluene. 67

Figure 74 - Borylation of 2-phenyl pyridine and cross-coupling of the boronates formed with 1-iodonapthalene. 68

Figure 75 - Borylation with $[Ir(OMe)cod]_2$/dtbpy catalyst system followed by Suzuki-Miyaura reaction in DMF. 68

Figure 76 - C-H Borylation solvent screen. 70

Figure 77 - Preliminary Suzuki-Miyaura reaction. 71

Figure 78 - Crude GS-MS chromatogram of **94** (top) and **302** (bottom). 75

Figure 79 - ^{1}H NMR spectrum of **302** (400 MHz, $CDCl_3$). 76

Figure 80 - Substrate scope of the one-pot procedure. 77

Figure 81 - ^{1}H NMR spectrum of **301** (400 MHz, $CDCl_3$). 78

Figure 82 - One-pot C-H Borylation/Suzuki-Miyaura coupling strategy. 79

Figure 83 - Microwave accelerated Claisen-rearrangement. 86

Figure 84 - Calculation of tan δ from dielectric constant, ε′ and dielectric loss ε″. 87

Figure 85 - Temperature profile after 1 minute of heating for microwave reaction (left) and oil bath heated reaction (right). 89

Figure 86 - Temperature profile for sample of methanol heated under microwave conditions (*p*=pressure, T = temperature, P = power). 90

Figure 87 - Specific Microwave effects. 91

Figure 88 - Synthesis of 4-aryl-2-quinolinone via microwave assisted synthesis. 92

Figure 89 - Nanoparticle catalysed C-H borylation of benzene. 93

Figure 90 - Borylation and cross-coupling of *N*-Boc pyrrole. 93

Figure 91 - C-H borylation of *m*-xylene under thermal conditions. 96

Figure 92 - C-H borylation of *p*-xylene under thermal and microwave conditions. 99

Figure 93 - C-H borylation of 2,6-substituted pyridines. 100

Figure 94 - C-H borylation of quinoline with the $[Ir(Cl)cod]_2$/dtbpy catalyst system. 101

Figure 95 - C-H borylation of quinoline under thermal and microwave conditions. 101

Figure 96 - C-H borylation of dtbpy and borylation/Suzuki-Miyaura cross-coupling of 2,3-dimethylpyrazine. 103

Figure 97 - Borylation products of 2,3- and 2,5-dimethyl pyrazine. 103

Figure 98 - Borylation of 2,5-dimethylthiophene by Smith and co-workers. 106

Figure 99 - Room temperature borylation of 2,5-dibromothiophene. 106

Figure 100 - Borylation of 1,2,3-tetrahydrocyclopenta[b]indole with $[Ir(OMe)cod]_2$/dtbpy and HBpin. 108

Figure 101 - Molecular structure of **172** (Thermal ellipsoids drawn at 50% probability). 111

Figure 102 - C-H borylation of *N*-Boc-7-azaindole at room temperature by Smith. 111

Figure 103 - Borylation and cross-coupling of *N*-Boc pyrrole. 112

Figure 104 - Borylation of *N*-Boc pyrrole by Smith and co-workers. 112

Figure 105 - Borylation of *N*-Boc pyrrole under microwave conditions. 112

Figure 106 - Microwave accelerated one-pot, single solvent C-H borylation/Suzuki-Miyaura cross coupling sequence. 115

Figure 107 - Applications of quinolines. 121

Figure 108 - Classical methods for the synthesis of quinolines. 122

Figure 109 - Novel synthetic methodologies of quinoline scaffolds. 123

Figure 110 - Nucleophilic halide displacement with 2-chloroquinoline. 123

Figure 111 - Electrophilic bromination and nitration of quinoline. 124

Figure 112 - Nucleophilic addition to quinoline. 124

Figure 113 - Nickel catalysed direct arylations of quinoline and palladium catalysed oxidative Heck-coupling to quinoline *N*-Oxide. 125

Figure 114 - *N*-directed magnesiation of 3-bromoquinoline. 125

Figure 115 - C-H borylation of quinoline with $[Ir(Cl)cod]_2$/dtbpy catalyst system. 126

Figure 116 - C-H borylation of quinoline under thermal and microwave conditions. 126

Figure 117 - C-H borylation of naphthalene using the $[Ir(OMe)cod]_2$/dtbpy catalyst system. 127

Figure 118 - C-H borylation of pyridine $[Ir(Cl)cod]_2$/dtbpy catalyst system. 128

Figure 119 - Borylation of 2,6-dimethylpryride and *m*-xylene. 128

Figure 120 - Borylation of 2-phenylpyridine using the $[Ir(OMe)cod]_2$/dtbpy catalyst system. 129

Figure 121 - Borylation of dtbpy using the $[Ir(OMe)cod]_2$/dtbpy catalyst system. 129

Figure 122- Borylation of 2,6-disubstituted quinolines. 131

Figure 123 - ^{1}H NMR spectrum of 2,6-dimethyl-4-Bpin-quinoline (400 MHz, $CDCl_3$). 132

Figure 124 - Molecular structure of 2-methyl-6-chloro-4-Bpin-quinoline and 2-methyl-6-bromo-4-Bpin-quinoline (Thermal ellipsoids drawn at 50% probability). 133

Figure 125 - Temperature dependent borylation of thiophene and furan. 134

Figure 126- Borylation of 4,7-disubstituted quinolines. 135

Figure 127 - Borylation of 4,4′-$(OMe)_2$-2,2′-bipyridine. 136

Figure 128 - *Ortho*-borylation of chlorobenzene and anisole with Si-SMAP-Ir catalyst system. 136

Figure 129 - Suzuki-Miyaura cross coupling of methyl boronic acid. 137

Figure 130 - Synthesis of **432** by palladium catalysed methylation of **426**. 137

Figure 131 - Attempted C-H borylation of **432**. 138

Figure 132 - Proposed mechanism for the formation of 2-methyl-7-chloroquinoline via the Döbner-Miller reaction. 140

Figure 133 - Purification of 2-methyl-7-chloroquinoline with $ZnCl_2$. 141

Figure 134 - Two-phase solvent system used in the Döbner-Miller reaction. 141

Figure 135 - Döbner-Miller reaction utilising *p*-chloranil as a chemical oxidant. 142

Figure 136 - Synthesis of 2-methyl-7-bromoquinoline. 143

Figure 137 - Synthesis of 2-methyl-7-(trifluoromethyl)quinoline. 144

Figure 138 - Copper catalysed anisole synthesis. 145

Figure 139 - Synthesis of 2-methyl-7-methoxyquinoline. 145

Figure 140 - Microwave assisted synthesis of aryl nitriles. 146

Figure 141 - Palladium catalysed synthesis of **454** from **450**. 146

Figure 142 - Synthesis of **459** by lithium-halogen exchange and trapping with a TMS electrophile. 147

Figure 143 - C-H borylation of 2,7-disubstituted quinolines. 147

Figure 144 - ^{1}H NMR chemical shifts of 2,7-dimethylquinoline (400 MHz, $CDCl_3$). 149

Figure 145 - Aromatic region of ^{1}H NMR spectrum of **460.** 150

Figure 146 - Aromatic region of ^{1}H NMR spectra of **464.** 151

Figure 147 - Molecular structures of 2,7-dimethyl-4-Bpin-quinoline and 2-methyl-7-chloro-5-Bpin quinoline (Thermal ellipsoids drawn at 50% probability). 152

Figure 148 - Room temperature borylation of **450**. 152

Figure 149 - Room temperature borylation of **452**. 153

Figure 150 - Borylation reaction with 2-methyl-6-chloro- and 2-methyl-7-chloro-quinoline. 154

Figure 151 - Borylation of thiophene and quinoline. 156

Figure 152 - Calculated pK_a values for thiophene and quinoline. 156

Figure 153 - The *ortho*-borylation of benzodioxole. 156

Figure 154 - Proton transfer in the transition state for C-H borylation reaction. 157

Figure 155 - Direct arylations via the ligand assisted deprotonation pathway. 157

Figure 156 - Proton exchange reaction used as the basis for pK_a calculations. 158

Figure 157 - Calculation of $\Delta G_{(gas)}$. 159

Figure 158 - Equation for the calculation of $\Delta_{(solv)}G$ and Total $\Delta_{(solv)}G$. 159

Figure 159 - Calculation of $\Delta G_{(exchange)}$. 159

Figure 160 - Theoretical proton exchange reaction with furan and calculation of target arene pK_a. 160

Figure 161 - pK_a values and observed selectivities for 2,7-disubstituted quinolines. 161

Figure 162 - Calculated pK_a values for **424.** 161

Figure 163 - Calculated pK_a values for **425**, **426**, **434.** 161

Figure 164 - Structures of 4- , 5- , 6- and 7- azaindole. 168

Figure 165 - Selected Biologically active 4-, 5-, 6- and 7-azaindoles. 168

Figure 166 - Attempted C-H borylation of 7-azaindole. 169

Figure 167 - C-H borylation of pyridine, indole and pyrole. 169

Figure 168 - Synthesis of *N*-methyl-7-azaindole. 170

Figure 169 - Synthesis and molecular structure of **482** and **483** (Thermal ellipsoids drawn at 50% probability). 171

Figure 170 - Synthesis and molecular structure of **365** (Thermal ellipsoids drawn at 50% probability). 171

Figure 171 - Synthesis and molecular structure of **484** (Thermal ellipsoids drawn at 50% probability). 172

Figure 172 - Synthesis and molecular structure of **485** (Thermal ellipsoids drawn at 50% probability). 173

Figure 173 - C-H borylation of protected azaindole. 173

Figure 174 - ^{1}H NMR spectrum of 1-*N*-Boc-7-azaindole borylation products. 175

Figure 175 - Open borylation of **365.** 176

Figure 176 - Solvent screen for C-H borylation of *N*-Boc-7-azaindole. 178

Figure 177 - CF_3 containing active pharmaceutical and agrochemical compounds.[2] 182

Figure 178 - Copper (I) mediated trifluoromethylation. 183

Figure 179 - Copper NHC mediated trifluoromethylation. 184

Figure 180 - Copper catalysed trifluoromethylation of aryl iodides. 184

Figure 181 - Reductive elimination of $PhCF_3$ from Pd^{II}. 185

Figure 182 - Palladium catalysed trifluoromethylation of aryl chlorides. 186

Figure 183 - Copper catalysed *ipso*-carboxylation of aryl boronates. 187

Figure 184 - Copper mediated Suzuki-Miyaura cross coupling. 188

Figure 185 - Silver mediated fluorination of aryl boronates. 188

Figure 186 - Electrophilic trifluoromethylating reagents. 189

Figure 187 - Application of hypervalent iodine trifluoromethylating reagents. 189

Figure 188 - Synthesis of **521.** 190

Figure 189 - Copper mediated trifluoromethylation test reaction. 191

Figure 190 - Copper (I) salt screen. 193

Figure 191 - Oxidative trifluoromethylation of aryl boronic acids. 194

Figure 192 - Electrophilic trifluoromethylation of aryl boronic acids. 195

Figure 193 - Potential substrates to probe electronic selectivity of C-H borylation reaction. 200

Table of Graphs

Graph 1 **-** Time/conversion plot for the thermal borylation of *m*-xylene. 96

Graph 2 - Time/conversion plot for the microwave borylation of *m*-xylene. 96

Table of Tables

Table 1 **-** Competition experiments of electron rich vs. electron poor arenes (mixture of all borylated isomers). 14

Table 2 **-** Variation of anionic ligand of $[Ir(X)cod]_2$ catalyst precursor. 15

Table 3 **-** Variation of substituents on bpy ligand. 16

Table 4 **-** C-H borylation of mono-substituted arenes with $[Ir(Cl)cod]_2$/bpy catalyst system. 20

Table 5 **-** Borylation of 1,2-disubstituted benzenes with the $[Ir(X)cod]_2$/bpy catalyst system. 20

Table 6 - C-H Borylation Solvent Screen. 71

Table 7 - Catalyst & Base screen for Suzuki-Miyaura cross-coupling reaction. 73

Table 8 - Aryl halide coupling partners for one-pot sequence. 79

Table 9 - Dielectric constant (ε) and Loss factor (tan δ) for common organic solvents. 88

Table 10 - Temperature time relationship for simple first order reaction. 89

Table 11 - C-H borylation of 2,6-disubstituted pyridines under thermal and microwave conditions. 100

Table 12 - Thermal and microwave borylation of 2,3- and 2,5-dimethyl pyrazine. 103

Table 13 - Borylation of substituted 5 membered heterocycles. 105

Table 14 - Borylation of indole based substrates. 109

Table 15 - Microwave assisted C-H borylation of 2,6-disubstituted quinolines. 131

Table 16 - C-H borylation of 4,7-disubstituted quinolines. 135

Table 17 - C-H borylation of 2,7-disubstituted quinolines. 148

Table 18 **-** C-H borylation of protected azaindoles. 173

Table 19 **-** Open borylation reaction of **365**. 176

Table 20 - Solvent screen for C-H borylation of *N*-Boc-7-azaindole. 178

Table 21 **-** Microwave heating for C-H borylation of *N*-Boc-7-azaindole. 179

Table 22 - Copper (I) salt screen. 193

CHAPTER I - METAL CATALYSED C-H BORYLATION REACTIONS

1.1 Introduction

This thesis describes work carried out in the area of iridium catalysed C-H borylation. Improvements have been made to the methodology associated with subsequent functionalisation of aryl boronates formed from the reaction; along with addressing issues associated with the borylation methodology itself. The borylation of novel substrate classes for the reaction have been explored. The remainder of this chapter will highlight the development and important aspects of the C-H borylation reaction, with particular reference to reactivity and selectivity of the catalysts used.

1.2 Introduction to C-H Activation

The prevalence of the C-H bond in organic molecules means that, typically, it is not considered as a functional group. This is demonstrated in the standard drawing of organic molecules, where the presence of hydrogens are implied by their omission.[1] This assumption of the presence of C-H bonds highlights their abundance and low reactivity. Due to their prevalence, methods to selectively functionalise C-H bonds could lead to broadly applicable routes to interesting organic molecules. The advent of green chemistry has also invigorated interest in C-H activation due to the reduction in waste through not requiring a classical 'leaving group'.[2] This chapter will examine C-H functionalisation as a general topic before exploring the field of C-H borylation.

1.3 C-H Functionalisation Strategies

C-H functionalisation strategies convert the ubiquitous C-H bond to synthetically useful functionality. Methods have been developed to allow functionalisation of sp, sp^2 and sp^3 C-H bonds but, given the focus of this thesis, this chapter will only discuss developments in aromatic C-H functionalisation.

Aromatic C-H functionalisation can be considered to include electrophilic and nucleophilic aromatic substitution reactions such as nitration and halogenation. However, these reactions

typically require harsh conditions and, as such, low functional group tolerance and low selectivity for the desired product are often observed.[3,4]

More recently, metal catalysed C-H activation reactions have received significant attention due to their ability to provide milder conditions and higher selectivities. Transformations from C-H to C-C, C-O, C-N and C-X bonds have been reported by such methods (***Figure 1***).[5-8]

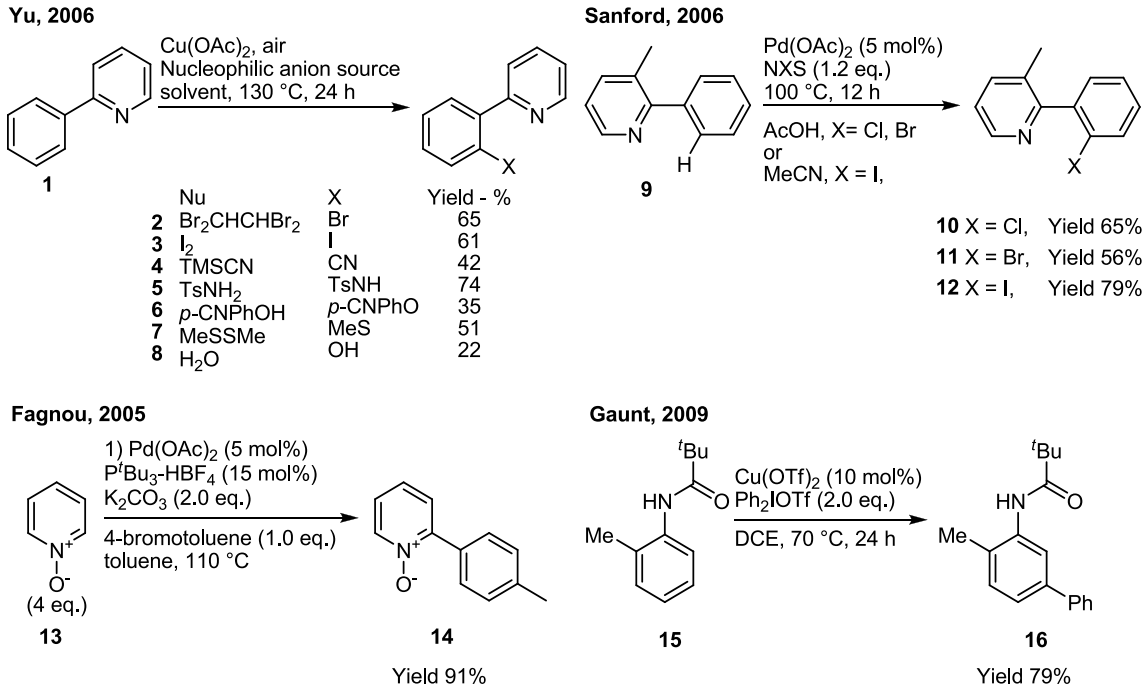

Figure 1 - Selected examples of C-H functionalisation reactions by Yu,[5] Sanford,[6] Fagnou[7] & Gaunt.[8]

This thesis will focus on the conversion of aryl C-H to C-B bonds. This transformation is the subject of a recent comprehensive review[9] and, as such, this introduction highlights only the key points of the current literature.[10-13]

1.4 Aryl C-H to C-B Bond Formation

Interest in the formation of aryl C-B bonds has stemmed from their importance in a number of areas of chemistry, with particular focus on their use as intermediates in organic synthesis.[10,11] This use has been realised in a wide range of reactions[12] which include the Suzuki-Miyaura cross-coupling reaction[14,15] and copper catalysed C-O and C-N couplings by

Chan, Lam and Evans.[16-18] Developments in the use of aryl boronates in the synthesis of organic molecules will be discussed in more detail in chapter II.

1.5 Synthesis of Aryl Boronates

In order to assess the impact of aromatic C-H borylation, classical methods for the synthesis of C-B bonds must first be considered. A number of methods have been employed in the synthesis of aryl boron reagents (***Figure 2***).

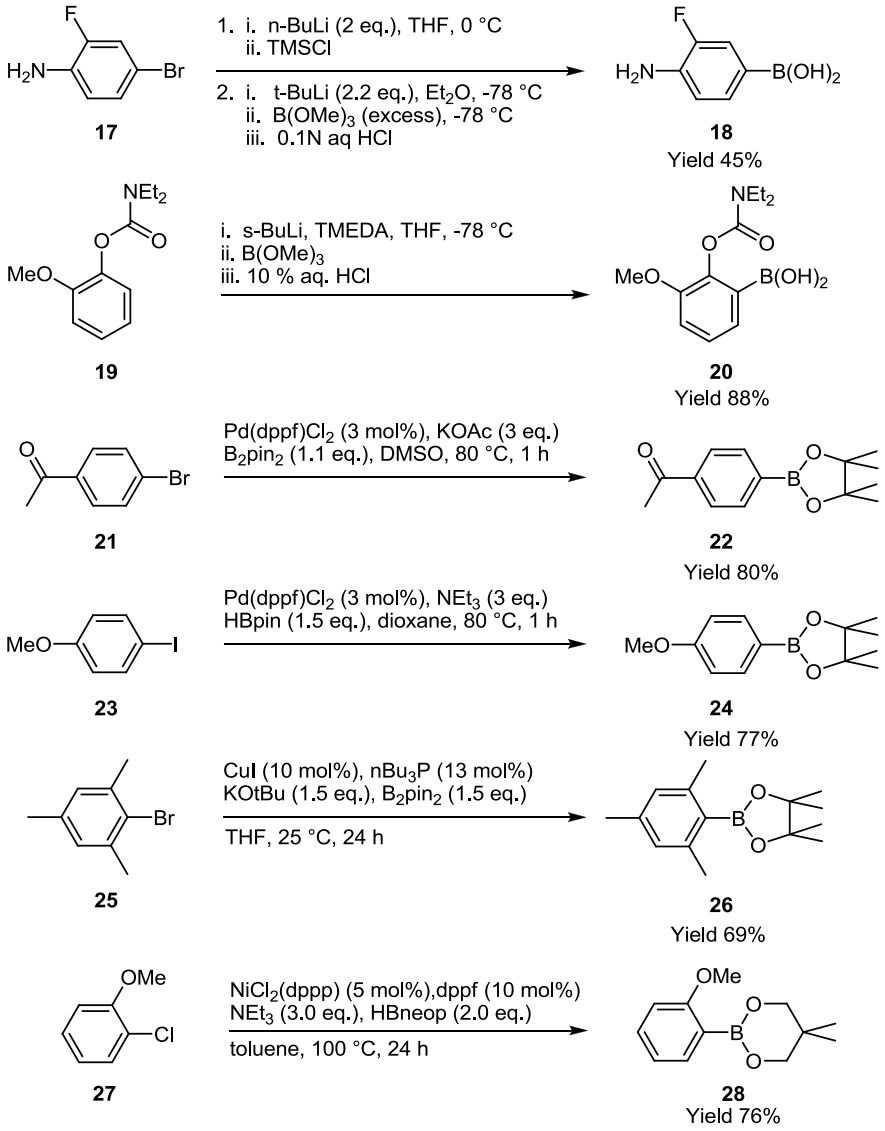

Figure 2 **- S**elected examples of classical methods for the formation of aryl boron reagents.[10-12,19-29]

The most widely used route to access aryl boronates involves the reaction of hard organometallic intermediates (e.g. Li) with trialkoxyborates at low temperature which, upon acidic work-up, afford aryl boronic acids (**17** → **18**).[19]

This route can be applied through either lithium halogen exchange of the corresponding aryl halide or by Directed *ortho*-Metalation (DoM) using suitable directing groups such as amines, esters, anilides, carbamates or amides (**19** → **20**).[20] These methods have become widely used as they are cheap, highly efficient and can be carried out on a large scale.[12] However, low functional group tolerance and substrate instability in the presence of strongly basic and nucleophilic organolithium reagents can be problematic.[12] The requirement for rigorously anhydrous conditions and cryogenic cooling (-78 °C) of the reactions are also a drawback of the methodologies.

Transition metal catalysed methods have been developed using palladium,[21,23-25] copper[22] or nickel[26-29] catalysts to convert aryl halides to aryl boronate esters. These reactions utilise milder reaction conditions, than the metalation reactions, allowing for greater functional group tolerance.

Systems developed by Miyaura[21] and Masuda[23-25] utilise Pd(dppf)Cl_2 with B_2pin_2 or HBpin respectively, to convert aryl halides to aryl boronates (**21** → **22, 23** → **24)**. The initial reports were limited to reactions of aryl bromides and iodides;[21,23-25] however, application of biarylmonophosphines as ligands to palladium (II) precursors has enabled aryl chlorides to be used in the reaction.[30,31] The palladium catalyst systems are most effective with unhindered, electron deficient, aryl halides with electron rich examples typically requiring longer reaction times.

The copper catalyst system, developed by Marder and co-workers,[22] has, to date, been limited to aryl bromides and iodides. However, this system is effective with both electron deficient and electron rich aryl halides along with sterically hindered substrates (**25** → **26**).[22]

The nickel catalyst system, developed by Percec and co-workers,[26-29] utilises nickel salts with bidentate phosphine ligands and HBneop (neop = $OCH_2CMe_2CH_2O$) to convert aryl chlorides, bromides, iodides, triflates or mesylates to aryl boronates (**27** → **28**). The reaction is effective with both electron deficient and electron rich arene systems.

The nickel and copper catalyst systems have provided a cheap alternative to the use of more expensive palladium catalysts. However, the requirement to remove metals to ppm levels for use in pharmaceutical applications is an issue for all metal catalysed reaction.

Methods utilising borane reagents (HBpin, HBneop) were developed due to the high cost of diboron reagents (B_2pin_2, B_2neop_2). However, the large scale production (e.g. 100 kg) of diboron reagents has caused their price to drop making them a more attractive choice for use in synthetic strategies.[22]

The key limitation of the methodologies discussed is that they require pre-activation of the substrate with either halide or D*o*M group. Methods for the synthesis of aryl boronates from C-H bonds have become an area of significant interest.[9] This allows the boronate functionality to be introduced into synthetically important compounds without the prerequisite of the corresponding aryl halide starting material being available.

This chapter will detail the early stoichiometric systems, development of the catalytic borylation of aromatic substrates, mechanistic insights into the reaction and application of the reaction to a wide range of different aromatic scaffolds.

1.6 Metal Catalysed Aromatic C-H Borylation

The area of aromatic C-H borylation has received much interest due to the promise of direct functionalisation of typically unreactive aromatic C-H bonds. A number of metal systems have been found to mediate this transformation. The following section will examine each system in turn, looking at the selectivity and catalytic activity offered by each of them.

1.6.1 Stoichiometric C-H Borylation

The first system was reported in 1993, by Marder and co-workers.[32] During the preparation of the iridium complex $[Ir(\eta^6\text{-}MeC_6H_5)(Bcat)_3]$ **29** (cat = 1,2-$O_2C_6H_4$), substoichiometric amounts of the toluene solvent were borylated to form small amounts of two isomers of tolylBcat **30** in a 2:1 ratio. Similar results were also observed when benzene or C_6D_6 were used as solvents with the production of PhBcat **31** and C_6D_5Bcat **32,** respectively (***Figure 3***).[32] This

system was inefficient at producing borylated arene but represented a starting point for the stoichiometric and catalytic systems that followed.

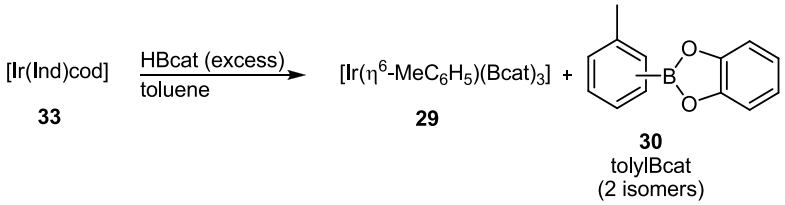

Figure 3 **-** The first (sub-stoichiometric) aromatic C-H borylation.

Subsequently, in 1995, Hartwig and co-workers[33] reported the stoichiometric borylation of benzene and toluene under photolytic conditions using $[Mn(CO)_5(Bcat)]$ **34**, $[Re(CO)_5(Bcat)]$ **35** and $[CpFe(CO)_2(Bcat)]$ **36** (***Figure 4***).

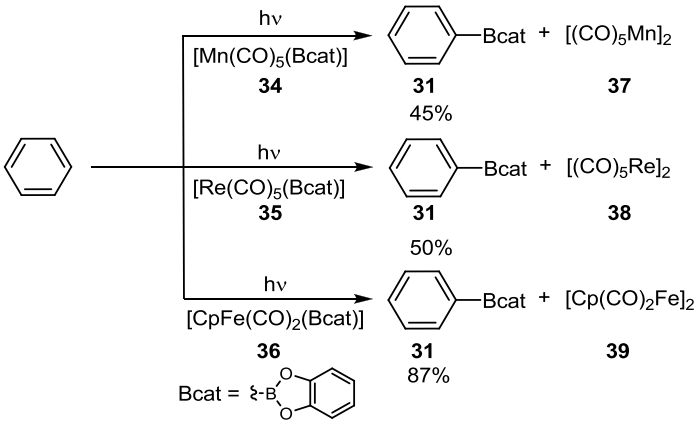

Figure 4 **-** The photolytic borylation of benzene with $M(CO)_5(Bcat)$ (M = Mn, Re) or $[CpFe(CO)_2(Bcat)]$.

Reactions with toluene showed no *ortho*- product formation and *meta:para* ratios of 1.6:1 and 1.1:1 for $[CpFe(CO)_2(Bcat)]$ **36** and $[Cp^*Fe(CO)_2(Bcat)]$ **40** respectively. Subsequent work showed that the photolysis of **36** and **40** in benzene afforded PhBcat **31** in 99% and 100% yield, respectively.[34] Complexes **34**, **35** and **36** were also shown to be reactive towards the borylation of alkenes.[34] This system was the first example in which isolable quantities of borylated arenes were formed by transition metal mediated reactions. The selectivity for positions not adjacent to

substituents, observed for toluene, highlights the steric selectivity of the C-H borylation reaction which will be discussed in further detail throughout this chapter.

The stoichiometric borylation reactions discussed so far offer insight into the types of metal systems which are able to promote the C-H borylation reaction. However, these methods are not suitable for preparative synthesis of the desired products due to the use of stoichiometric metal complexes to mediate the reactions

1.6.2 Catalytic C-H Borylation

Four years later, in 1999, Smith and co-workers demonstrated the first catalytic aromatic C-H borylation using [Cp*Ir(PMe_3)(H)(Bpin)] **41** with HBpin to borylate neat benzene at 150 °C (***Figure 5***).[35] The reaction was only able to facilitate 3 catalytic turnovers affording PhBpin **42** in 53% yield.

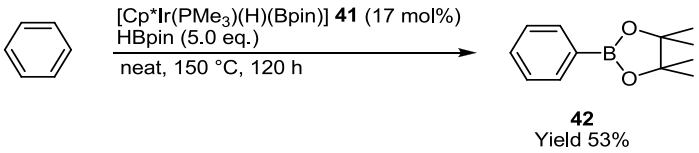

Figure 5 - The catalytic borylation of benzene with [Cp*Ir(PMe_3)(H)(Bpin)].

In the same year, Hartwig and co-workers[36] reported the photocatalytic borylation of benzene with [Cp*Mn$(CO)_3$] **43** and B_2pin_2 (***Figure 6***). Complex **43** was also reactive towards alkenes, in analogy to previously reported manganese complexes.[33]

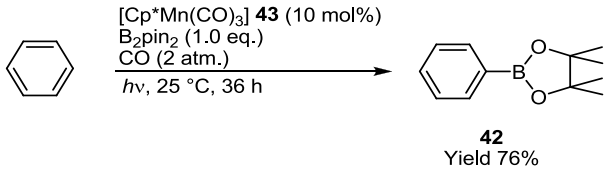

Figure 6 - The photocatalysed borylation of benzene with [Cp*Mn$(CO)_3$].

Hartwig and co-workers[37] reported [Cp*Rh(η^4-C_6Me_6)] **44** as a catalyst for the selective borylation of linear alkanes. The reaction of *n*-octane afforded terminal borylated product **45** in

84% yield. The catalyst was also applied to the borylation of benzene affording **42** in 92% yield, after a 2.5 hour reaction time (***Figure 7***). Although benzene was the only aromatic substrate used, the catalyst system was, to date, the most active reported. However, the requirements of running reactions in neat substrate at high reaction temperatures (150 °C) are key limitations of this reaction.

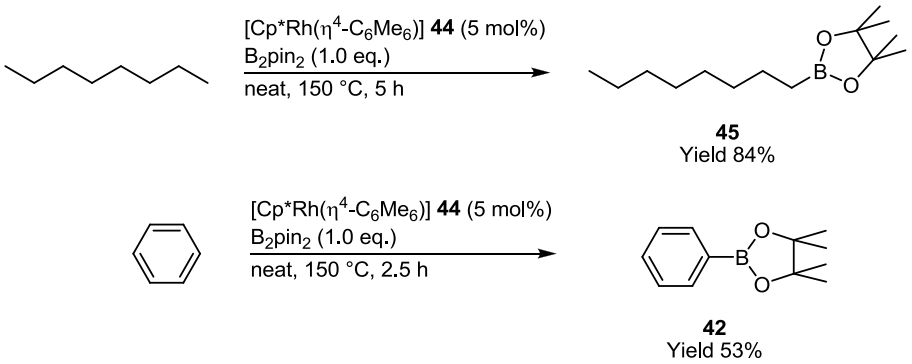

Figure 7 - Catalytic borylation of terminal alkanes and benzene with [Cp*Rh(η^4-C_6Me_6)].

Smith and co-workers[38] utilised both Hartwig's [Cp*Rh(η^4-C_6Me_6)] **44** along with their own [Cp*Ir(PMe_3)(H)(Bpin)] **41,** in a comparative study, to borylate a range of arenes. Mono substituted arenes provided an approximately statistical mixture (2:1) of *meta:para* products alluding to the steric influence on the regioselectivity of the reaction (***Figure 8***).

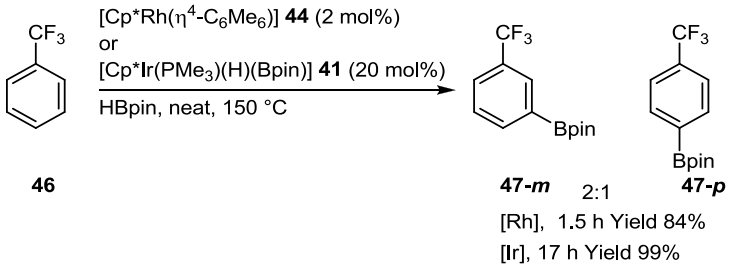

Figure 8 - The borylation of substituted arenes with **41** and **44**.

Rhodium catalyst **44** demonstrated higher reactivity than the iridium system **41**, allowing a 10 fold lower catalyst loading to be used for the rhodium system. However, the high reaction

temperature and requirement for reactions to be conducted in neat arene solvent limit the general applicability of these systems to aromatic borylation.

The issue of using neat arene to conduct reactions was addressed by Smith and co-workers.[39] Cyclohexane was used as an inert solvent for the borylation of disubstituted arenes in the presence of, Hartwig's catalyst, **44**. This allowed the arene to be used as the yield limiting reagent for the transformation, making the reaction a preparative option for the installation of the boronate ester group to aromatic substrates.

Borylation of 1,3-disubstituted arenes afforded 5-borylated products where as 1,2-disubstituted arenes resulted in 4-borylated products (***Figure 9*****).** The catalyst was more reactive towards electron deficient substrates than electron rich ones. However, high reaction temperatures (150 °C) were still required to facilitate the reaction. The solvent choice exploited the high terminal selectivity of **44** for the borylation of alkanes. The absence of primary C-H bonds in the cyclic alkane meant the solvent remained unborylated.

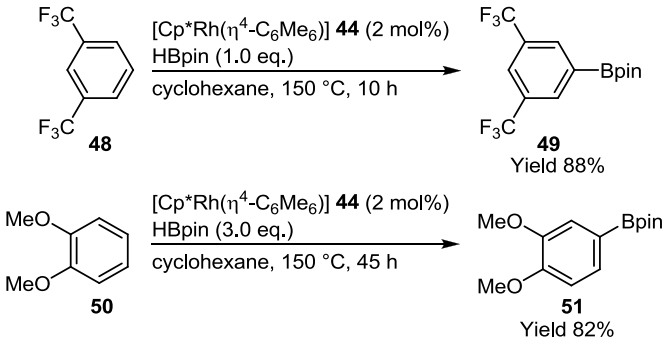

Figure 9 **-** The borylation of disubstituted arenes with [Cp*Rh(η^4-C_6Me_6)] in an inert cyclic alkane solvent**.**

Using a phosphine containing rhodium catalyst system, in 2001, Marder and co-workers[40] demonstrated the catalytic borylation of methylarenes and benzene. The reaction was highly selective for benzylic borylation over aromatic borylation. The reaction with toluene afforded 76% yield with 81% selectivity for benzylic borylation. The borylation of benzene afforded **42** in 62% yield over a 14 hour reaction time, increasing to 86% after 58 hours when using 1 mol% catalyst. When using 0.3 mol% of **52**, PhBpin **42** was afforded in 67% yield after 104 h (***Figure***

10). The high selectivity of the catalyst towards benzylic borylation is due to the formation of a η^3-benzyl intermediate.

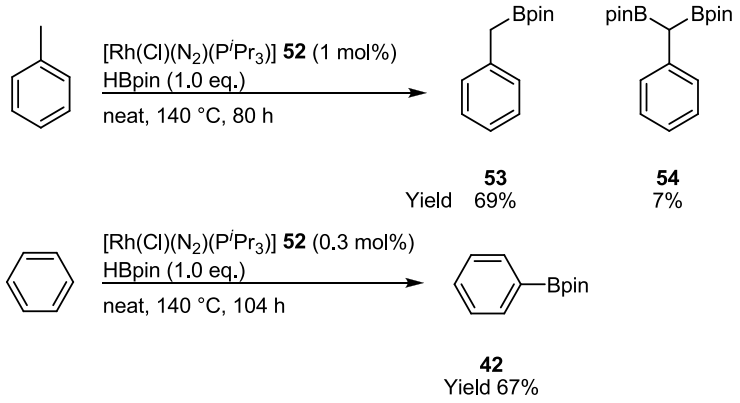

Figure 10 **-** The borylation of benzene with **52**.

The catalytic borylation systems discussed so far represented a significant step forward from the stoichiometric systems; however, they still required high reaction temperatures and extended reaction times.

1.6.3 Iridium Catalysts with Phosphine Ligands

In 2002, Smith and co-workers[41] borylated neat arene solvents with [Ir(η^6-Mes)(Bpin)$_3$] **55** and [Ir(Ind)cod] **33** as catalysts in the presence of phosphine ligands. Borylation of benzene showed that the use of bidentate phosphine ligands afforded higher efficiency, compared to other catalyst systems, with catalyst loadings as low as 0.02 mol% being achieved with the [Ir(Ind)cod]/dmpe catalyst system (***Figure 11***).

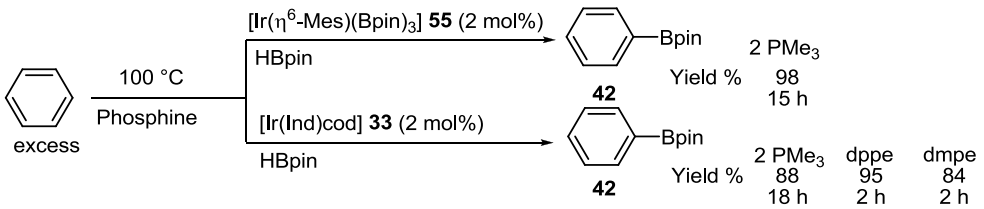

Figure 11 **-** The borylation of benzene using **52** and **33.**

The [Ir(Ind)cod] dmpe/dppe catalyst system was then applied to a range of substituted arenes. In all cases, the regiochemical outcome of the reactions was in agreement with the previous observations, with mono substituted arenes affording approximately statistical mixtures (2:1) of *meta*:*para* borylation products. Borylation of 1,3-disubstituted arenes occurred at the mutually *meta*- 5-position (***Figure 12***).

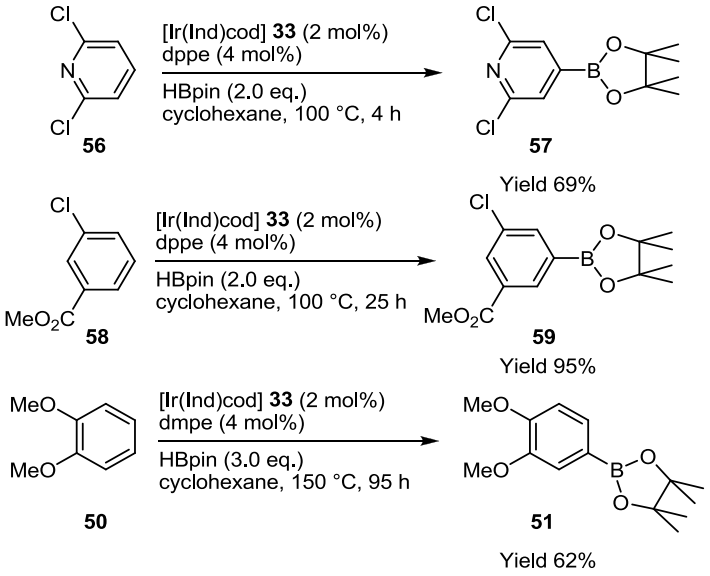

Figure 12 **-** The borylation of arenes and heteroarenes with **33** dmpe/dppe catalyst system.

This system offered significant advantages over the earlier examples due to the lower catalyst loadings and shorter reaction times which could be achieved. However, high reaction temperatures (100 - 150 °C) were still required for the reaction to proceed. Even then, short reaction times were not achievable with all substrates as 95 hours was required to borylate more electron rich substrates, e.g., 1,2-dimethoxybenzene **50**.

1.6.4 [Ir(X)cod]$_2$ Catalysed Borylation of Arenes

In an effort to address the high temperatures and long reaction times associated with the phosphine ligated systems, Hartwig, Miyaura and co-workers[42] developed a catalyst system containing [Ir(Cl)cod]$_2$ **60**, 2,2-bipyridine **61** (bpy) and B_2pin_2. This enabled reactions to be carried out at 80 °C for 16 hours in neat arene (***Figure 13***).

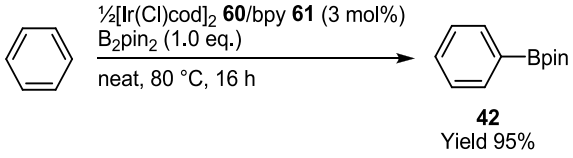

Figure 13 **-** Aromatic C-H borylation of benzene using **62.**

The regioselectivity of this catalyst system was again consistent with previously reported borylation catalysts. In general, C-H activation did not occur at positions adjacent to substituents. Mono-substituted arenes reacted to give statistical mixtures (ca. 2:1) of *meta*:*para* products; 1,3-disubstituted arenes and symmetrical 1,2-disubstituted arenes borylated in the 5- and 4- positions, respectively. The borylation of *p*-xylene was more challenging due to all position being sterically hindered and as such reduced yields were achieved compared to less hindered arenes. However, the catalyst was shown to have greater reactivity towards electron rich arenes than the previously reported rhodium[37,38,40] and iridium catalyst systems.[35,39,41]

Subsequently, Hartwig, Miyaura and co-workers,[42] investigated the relative reactivity of electron-poor and electron-rich arenes through a series of competition experiments involving reaction of equimolar mixtures of trifluoromethylbenzene **46** and toluene **62**, trifluoromethylbenzene **46** and anisole **63**, and toluene **62** and anisole **63**, (***Figure 14***, ***Table 1***). The results demonstrate the greater reactivity of electron-deficient compared to electron-rich arenes towards C-H borylation. This study also provides some of the first evidence that steric effects are not the only important factor influencing the borylation. Inductive effects also influence the reaction, exemplified by the faster rate of borylation for anisole compared to toluene.

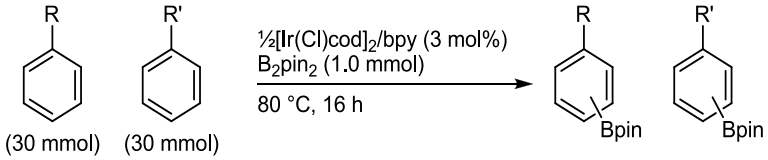

Figure 14 - C-H borylation competition experiment.

Table 1 - Competition experiments of electron rich vs. electron poor arenes (mixture of all borylated isomers).

Arenes		GC Product Ratio (%)	
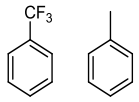		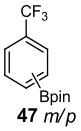	
46	**62**	**47** *m/p*	**64** *m/p*
1:1		90	10
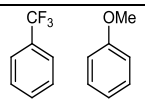		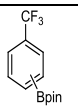	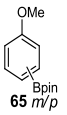
46	**63**	**47** *m/p*	**65** *m/p*
1:1		85	15
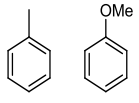		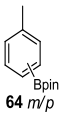	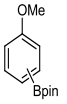
62	**63**	**64** *m/p*	**65** *m/p*
1:1		40	60

Further development of the catalyst system by Hartwig, Miyaura and co-workers[43] allowed direct C-H borylation of arenes and heteroarenes at room temperature in an inert solvent, hexane. A study was conducted by varying both the anionic ligand of the iridium precursor (***Table 2***) and then the bpy ligand (***Table 3***) to find a more active catalyst system in the presence of excess benzene substrate (***Figure 15***).

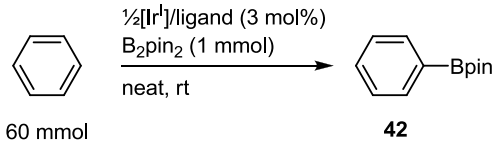

Figure 15 **-** Borylation of benzene with a range of Ir^{I} precursors and bpy ligands.

Table 2 **-** Variation of anionic ligand of $[Ir(X)cod]_2$ catalyst precursor.

Entry	Ir (I) precursor	Ligand	Time (h)	Conversion of B_2pin_2 (%)	GC Yield of **42** (%)
1	$[Ir(Cl)cod]_2$ **60**	bpy **61**	24	0	0
2	$[Ir(cod)_2]BF_4$ **66**	**61**	24	3	0
3	$[Ir(OH)cod]_2$ **67**	**61**	4	100	88
4	$[Ir(OPh)cod]_2$ **68**	**61**	4	100	84
5	$[Ir(OAc)cod]_2$ **69**	**61**	24	19	1
6	$[Ir(OMe)cod]_2$ **70**	**61**	4	100	90
7	$[Ir(Cl)cod]_2$ **60** /4NaOMe **71**	**61**	4	100	73

Halide and cationic complexes were ineffective at catalysing the room temperature reaction (***Table 2***, entries 1 & 2). Complexes **67**, **68** and **70** containing hydroxide or alkoxide anions (***Table 2***, entries 3, 4 & 6) were comparably successful in forming active room temperature catalysts with **70** providing a slightly higher yield of **42** (***Table 2***, entry 6). The reaction with **69,** (***Table 2***, entry 5) was unable to create a viable catalyst system due to the lower basicity of the acetate anion. The relatively higher reactivity of the hydroxide and alkoxide containing precursors can be explained by the greater ease with which these species form (boryl)iridium complexes, the key active intermediates in the catalyst cycle, which will be further discussed in section 1.6.5.[43] The effect of varying the size and electronics of the substituents on the 2,2′-bipyridine ligand were also investigated (***Table 3***).

Table 3 - Variation of substituents on bpy ligand.

Entry	Ir (I) precursor	Ligand	Time (h)	Conversion of **22** (%)	GC Yield of **44** (%)
1	**70**	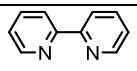 **61**	4	100	90
2	**70**	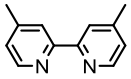 **72**	4	100	89
3	**70**	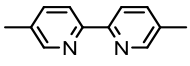 **73**	2	100	82
4	**70**	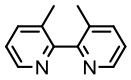 **74**	8	100	60
5	**70**	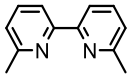 **75**	24	27	0
6	**70**	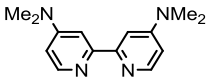 **76**	2	100	89
7	**70**	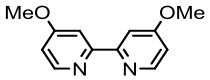 **77**	4	100	90
8	**70**	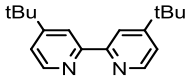 **78**	4	100	83
9	**70**	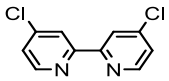 **79**	24	16	0
10	**70**	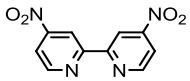 **80**	24	46	0

Introduction of the electron donating methyl substituent into the 4,4′- **72** and 5,5′ **73** positions showed little improvement in catalyst activity with the **73** being slightly more reactive (***Table 3***, entries 2 & 3). However, introduction of methyl groups into the 3,3′- **74** and 6,6′- **75** positions adversely affected the reactivity of the system. This reduction in activity is due to restriction in the conformational freedom of the ligand for **74** and inhibition of iridium binding for **75** (***Table 3***, entries 4 & 5).

Investigations into the electronic influence of ligand substituents on reactivity were carried out by variation of functionality at the 4,4′-position. The results demonstrated that ligands containing electron donating substituents (NMe_2, OMe, ^{t}Bu) (***Table 3***, entries 6 - 8) exhibited

superior reactivity to those containing electron withdrawing substituents (Cl, NO_2) (***Table 3***, entries 9 & 10). Although complexes of ligands **61**, **76**, **77**, and **78** showed comparable reactivity, **78** was selected for further study due to its higher solubility in the reaction solvent, hexane.

Since this report, the $[Ir(X)cod]_2$/4,4′-di-*tert*-butyl-2,2′bipyridine (dtbpy) (X = Cl, OMe) catalyst system has dominated the field of aromatic C-H borylation. Using this system, the substrate scope of the reaction has been extensively explored and will be discussed later in this chapter. However, further investigation into the effect of the ligand on the reaction has been limited to a few isolated examples. which will be discussed later in the chapter. In order to gain an understanding of the effect that ligands have on the reactivity and selectivity of the reaction, the mechanism of this catalyst system will now be discussed.

1.6.5 Proposed Mechanism for the Borylation of Arenes with $[Ir(OMe)cod]_2$

Hartwig, Miyaura and co-workers[42] suggested $[Ir(dtbpy)(Bpin)_3]$ **81**, related to other tris(boryl)Ir(III) complexes,[32,41] is a likely intermediate in the catalyst cycle for aromatic borylation. The synthesis of $[Ir(dtbpy)(coe)(Bpin)_3]$ **82** was performed and its structure was confirmed by X-ray crystallography. The instantaneous formation of C_6D_5Bpin **83** when **82** was dissolved in C_6D_6 is indicative that **82** is a competent reactive intermediate in the catalytic cycle.[42,44]

The proposed mechanism for borylation involves the reaction of B_2pin_2 with the $Ir^{(I)}$ complex [Ir(X)(dtbpy)] to generate the tris(boryl)$Ir^{(III)}$ intermediate **81**. The next step is thought to be the oxidative addition of an arene to afford an $Ir^{(V)}$ species **84**, followed by reductive elimination of a borylated arene to giving the $[(Bpin)_2Ir^{(III)}(H)]$ complex **85**, this step could either proceed via a formal two stage process as described or via a concerted σ-bond metathesis mechanism which gives rise to the same products. A definitive answer as to which route occurs has not been elucidated and is the topic of ongoing research within the field.[45-49] Oxidative addition of B_2pin_2 to **85** affords **86** which undergoes reductive elimination of HBpin to regenerate **81 (*Figure 16*)**. The proposed cycle has been supported by experimental and theoretical studies. [49-52]

A two-stage cycle has been suggested with fast consumption of B_2pin_2 followed by slow consumption of HBpin.[51] This cycle requires oxidative addition of HBpin to **85** to afford **87**, which then undergoes reductive elimination of H_2 to regenerate **81**.

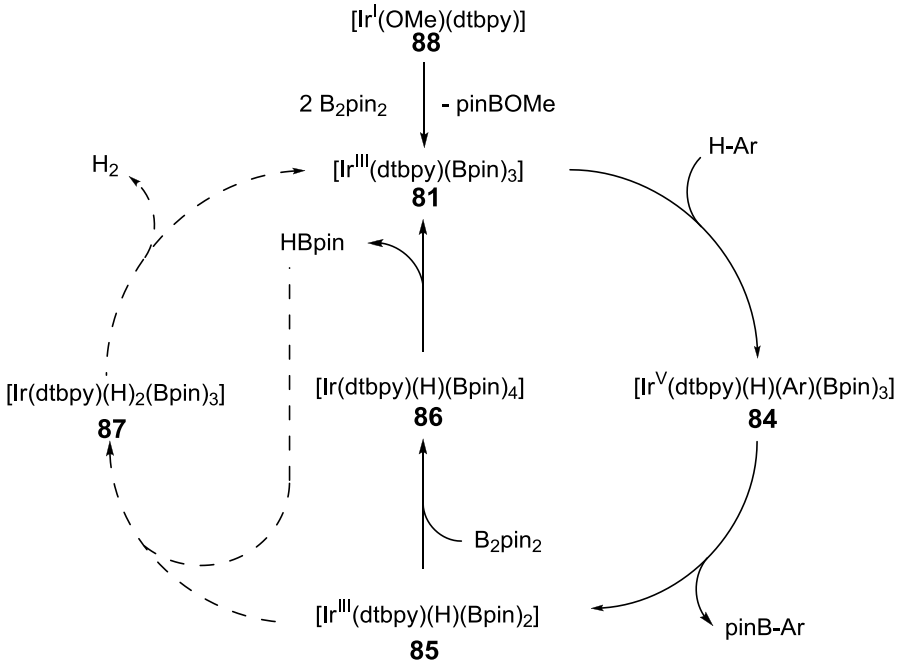

Figure 16 **-** A proposed catalytic cycle for aromatic borylation by $[Ir(X)cod]_2$/dtbpy and B_2pin_2.

Theoretical backing for the proposed mechanism was provided by Sakaki and co-workers.[51] The tris(boryl)iridium$^{(III)}$ complex [Ir(bpy)(Bpin)$_3$] **89** was again implicated as the active species. The theoretical calculations favoured the oxidative addition pathway via a hindered Ir$^{(V)}$ **85**. However, the calculations were conducted using the smaller Beg (eg = OCH_2CH_2O) instead of Bpin. Beg is less σ-donating than Bpin and as a result less nucleophilic and less basic, due to lack of donating methyl groups in Beg.[48] These factors may influence the calculated oxidative addition route being favoured over the alternative σ-bond metathesis pathway. The oxidative addition route is supported by the strong σ-donating properties of the boryl and bpy ligands combining to stabilise the high formal oxidation state, seven coordinate route iridium$^{(V)}$ intermediate **85**.

Hartwig and co-workers[50] reported experimental data for the proposed mechanism by isolation of **82** from the reaction of $[Ir(OMe)cod]_2$ **70** with dtbpy **78**, cyclooctene (coe) and

HBpin. A kinetic study was carried out showing that complex **82** reacts with arenes following reversible dissociation of coe. Subsequent oxidative addition of arene C-H bond and reductive elimination of the borylated arene regenerates the active species (***Figure 17***).

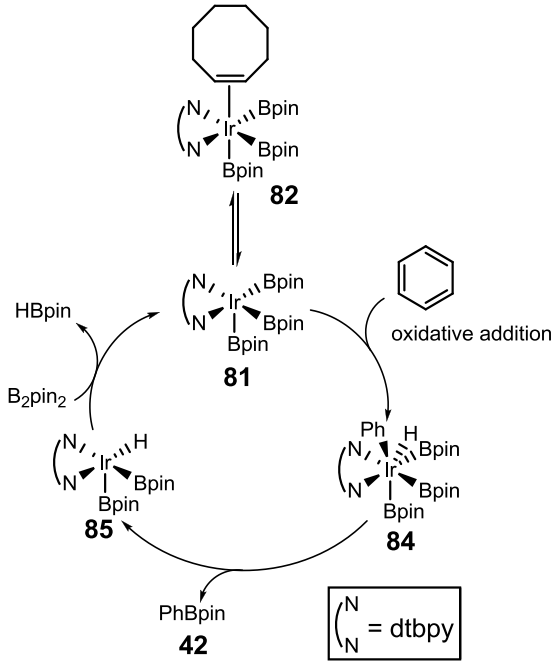

Figure 17 **-** A proposed mechanism showing the dissociation of the coe ligand.

The identification of the sterically hindered $Ir^{(III)}$ tris(boryl) active species explains the origins of the regioselectivity observed in the experimental reactions. The highly hindered nature of this species results in the most unhindered C-H bond being activated.

1.6.6 Selectivity of C-H Borylation in Simple Aromatic Systems

In general, for substrates examined in the early studies, borylation was controlled, at least to a large extent, by steric factors. This led to preferential activation at positions which are not *ortho*- to substituents or ring junctions. This results in mono-substituted arenes giving an approximately statistical ratio (*ca.* 2:1) of *meta:para* products with no, or very little, *ortho*-product being formed (***Figure 18***, ***Table 4***)[42]

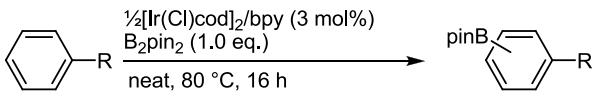

Figure 18 **-** Borylation of mono substituted arenes by the $[Ir(Cl)cod]_2$/bpy catalyst system.

Table 4 **-** C-H borylation of mono-substituted arenes with $[Ir(Cl)cod]_2$/bpy catalyst system.

R	GC Yield based on B_2pin_2 (%) *(o:m:p)*
Me	82 (0:69:31)
OMe	95 (1:74:25)
CF_3	80 (0:70:30)

However, significant variance from the 2:1 ratio is observed for the borylation of anisole which gives a 3:1 ratio of *meta:para* products, suggesting that an electronic influence may play a role; this topic will be discussed in more detail in chapter IV.

The borylation of symmetrical 1,2-disubstituted benzenes has been shown to give the 4-borylated product regiospecifically, due to the inherent preference for reaction at positions which are not adjacent to substituents (***Figure 19***, ***Table 5***).[42,43]

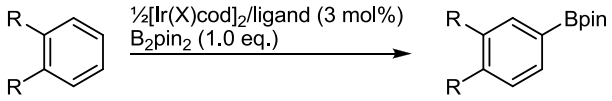

Figure 19 **-** Borylation of 1,2-disubstituted benzenes with the $[Ir(X)cod]_2$/bpy catalyst system.

Table 5 **-** Borylation of 1,2-disubstituted benzenes with the $[Ir(X)cod]_2$/bpy catalyst system.

R	Ir^I precursor	Ligand	solvent	time (h)	GC Yield based on B_2pin_2 (%)
Me	$[Ir(Cl)cod]_2$	bpy	neat	16	83
OMe	$[Ir(Cl)cod]_2$	bpy	neat	16	86
Cl	$[Ir(OMe)cod]_2$	dtbpy	hexane	16	82

Recently, Smith and co-workers[46] reported the borylation of benzodioxole **90** with isolable iridium complexes [(dippe)Ir(Bpin)$_3$] **91** and [(dtbpy)Ir(Bpin)$_3$(coe)] **82** affording *ortho*-

borylated benzodioxole **92**. Although *ortho*-borylation systems have been developed, this represents the first example of electronically selective *ortho*-borylation utilising a standard ligand system, without the requirement for coordinating directing groups (e.g. CO_2Me). The CH_2 linker between the oxygen atoms of **90** causes the *ortho*- C-H bonds to be less hindered than in the related 1,2-dimethoxybenzene. This allows the most electronically activated position to be preferential borylated (***Figure 20***).

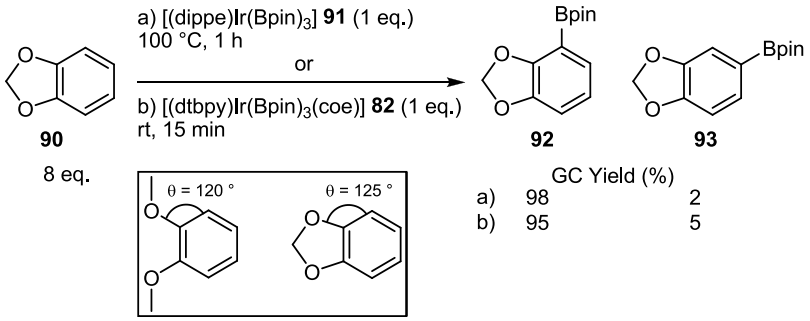

Figure 20 - The *ortho*-borylation of benzodioxole and 1,2-bismethoxybenzene.

As with symmetrical 1,2-disubstituted benzenes, 1,3-disubstituted benzenes borylate in the most sterically accessible position, namely the 5-position, which is mutually *meta*- to the substituents (***Figure 21***).[42] On account of the large number of commercially available 1,3-disubstituted arenes, the formation of a single borylated product and the difficulty in installing functionality to the 5-position by other means, this class of substrate has received more attention than any other.[42] This is especially true with regard to conversion of aryl boronates to other useful functionality after installation; this topic will be further discussed in chapter II.

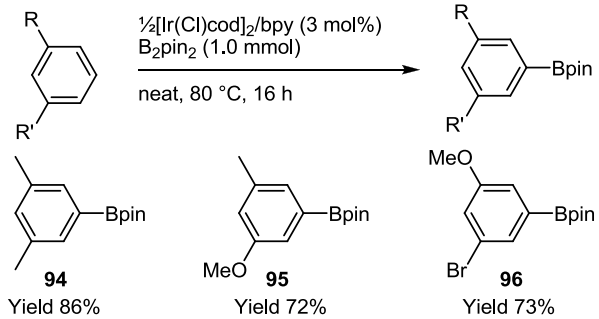

Figure 21 - Borylation of 1,3-disubstituted benzenes with the $[Ir(X)cod]_2$/bpy catalyst system.

In contrast to the high reactivity exhibited by 1,2- and 1,3-disubstituted benzenes, the symmetrical 1,4-disubstituted benzene, c.f., *p*-xylene, afforded reduced yields due to all positions being sterically hindered.[42,43] Smith and co-workers[53] examined the borylation of unsymmetrical 1,4-disubstituted benzenes, in particular, 4-substituted benzonitriles, which showed borylation *ortho*- to the cyano group when the 4-substituent was large and borylation *ortho*- to the 4-substituent when it was smaller than the cyano group (***Figure 22***).

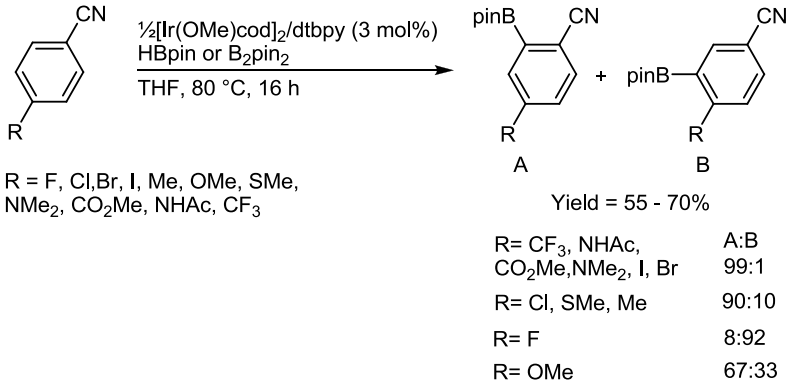

Figure 22 - Borylation of 4-benzonitriles with the $[Ir(OMe)cod]_2$/dtbpy catalyst system.

A few attempts have been made to alter the ligand environment in order to improve reactivity and/or affect the selectivity of the reaction. The following section will focus on the success of these reports relative to the $[Ir(X)cod]_2$/dtbpy catalyst system (X = Cl , OMe) in terms of both reactivity and selectivity.

1.6.7 Variation of Ligand System

Attempts to vary the ligand used for the C-H borylation reaction have been successful in providing catalyst systems able to perform the reaction. However, the majority of systems investigated have retained classical steric selectivity and exhibited only similar or lower reactivity compared to the standard $[Ir(X)cod]_2$/dtbpy (X = Cl, OMe) catalyst system. Recently, there have been monodentate phosphine systems which have enabled *ortho*-borylation of substrates; this will be discussed in section 1.6.8.

Nishida and co-workers[54] utilised a bpy analogue **97** containing carboxylic acid functionality at the 4,4′ positions, which results in the catalyst being soluble in hexane at elevated temperatures, but insoluble at room temperature. As such, the catalyst can be recovered by filtration and has been recycled 10 times in the borylation of benzene, with no loss of activity or iridium leaching (***Figure 23***).

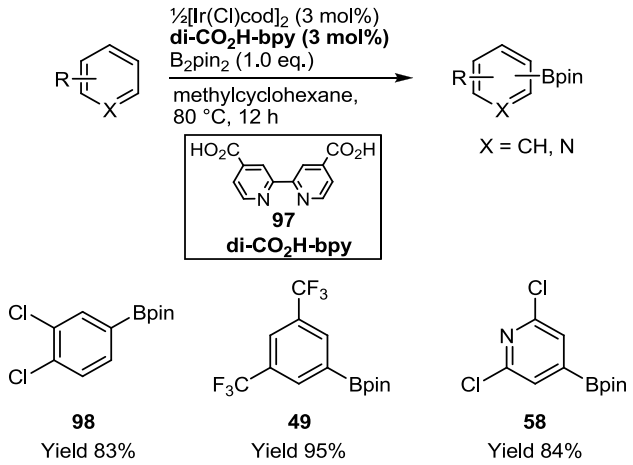

Figure 23 **-** Selected examples of borylation using recyclable carboxylic acid catalyst system.

A flow reactor has been developed with this catalyst system. A preformed solid catalyst was packed into a fritted column through which heated solvent containing substrate and B_2pin_2 were passed. Borylation has been achieved at a rate of up to 0.3 mmol/h.[55] The catalyst derived from **97** offers comparable reactivity to the system derived from dtbpy **78,** but has the added advantage of being recyclable. Nonetheless, elevated temperatures are still required to achieve the transformation.

The high reactivity of this system contrasts with the results of ligand studies by Hartwig, Miyaura and co-workers,[43] who found that the most active systems contained electron donating groups. Ligands containing electron withdrawing groups Cl **79** and NO_2 **80** led to significantly reduced yields. The high activity of the catalyst system containing **97** suggests that the electronic nature of the substituents is not the only factor governing activity.

Moving away from bipyridine containing ligands, Murata and co-workers[56] have showed that iridium (I) complexes coordinated with hydrotris(pyrazolyl)borate (Tp) derivatives are able to catalyse the C-H borylation of arenes with HBpin (***Figure 24***).

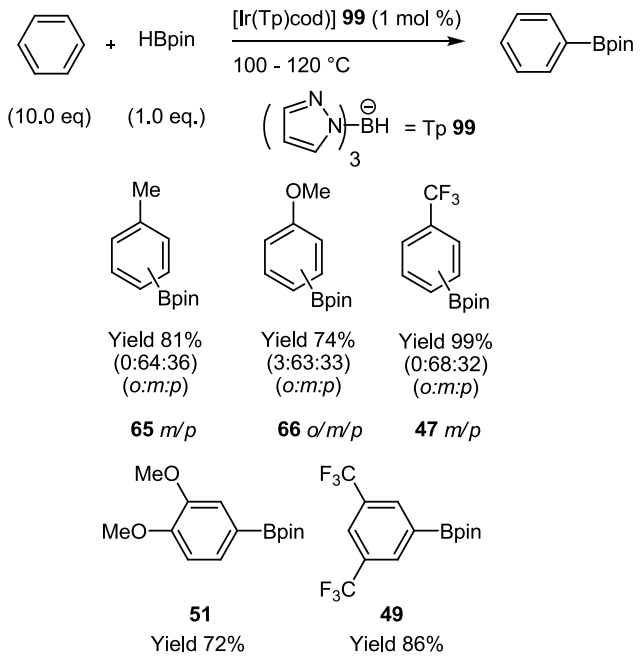

Figure 24 **-** The catalytic borylation of arenes with the "TpIr" catalyst system.

A number of mono-substituted, 1,2-disubstituted, 1,3-disubstituted and 1,4-disubstituted arenes have been borylated with selectivity mirroring that of the $[Ir(X)cod]_2$/dtbpy (X = Cl, OMe) catalyst system. Elevated temperatures (100 - 120 °C) are again required in order to achieve good activity. The nature of the active species in this system has not been determined.

The use of N-heterocyclic carbene ligands (NHC's) in catalytic chemistry has become increasingly widespread,[57] and has been reported within the field of aromatic C-H borylation.[58-60] Herrmann and co-workers[58] have shown that a range of alkyl-substituted NHC ligand systems are effective for C-H borylation (***Figure 25***). Selectivity for the reaction mirrors that expected from the standard system, with borylation avoiding positions *ortho* to substituents and ring junctions. The strong σ-donating properties and 2:1 NHC:Ir ratio suggests that a similar catalytically active species to the dtbpy system will be generated upon addition of B_2pin_2.

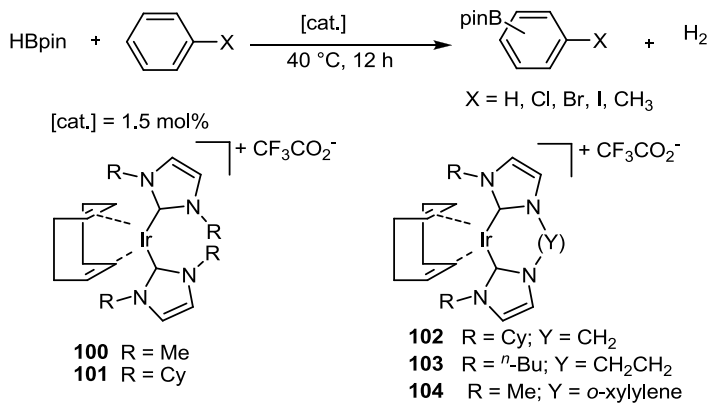

Figure 25 **-** Catalytic borylation of aromatic C-H bonds using $[Ir(cod)(NHC)_2]^+$ as catalyst precursor.

In an adaptation of simple NHC ligands, Bremer and co-workers[60] have reported a CCC-NHC pincer complex which is able to borylate arenes in moderate yields and classical selectivities. The system employs NaO^{t}Bu (4 mol%) as an additive to enhance the reactivity of the catalyst (***Figure 26***). The strong σ-donor property of the ligand in **105** is again similar to that of dtbpy. However, the tridentate nature of the ligand would prevent an iridium tris boryl complex from being the active species, as all coordination sites would be filled.

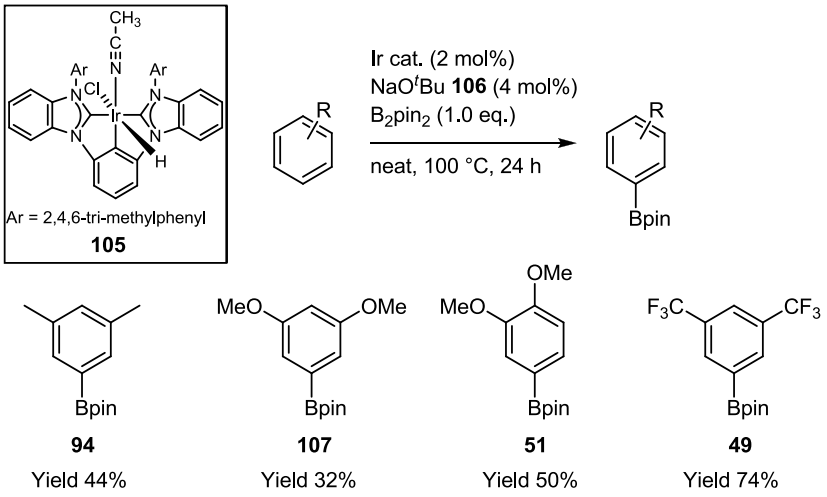

Figure 26 **-** Borylation of arenes using Ir CCC-NHC pincer complex **105**.

Of the ligand systems detailed, none have been able to provide improved reactivity compared to the $[Ir(OMe)cod]_2$/dtbpy catalyst system (described in section 1.6.4). For this reason, the $[Ir(OMe)cod]_2$/dtbpy catalyst system has been most widely applied throughout the published literature.

In contrast to the sterically directed systems which have been discussed in the previous sections, a number of groups have explored o*rtho*-borylation utilising a range of substrates with *ortho*-coordinating groups.

1.6.8 Directed *ortho*-Borylation

Hartwig and co-workers[61] demonstrated a directed *ortho*-borylation of benzyl and phenolic dialkylhydrosilanes using the $[Ir(Cl)cod]_2$/dtbpy, B_2pin_2 catalyst system. The dialkyl hydrosilyl directing group[62] acts as a tether, directing the catalyst close to the *ortho*-position and thus facilitating activation in this position (***Figure 27***, ***Figure 28***). The methodology has also been used in the functionalisation of indole, which will be discussed in section 1.7.2.2.

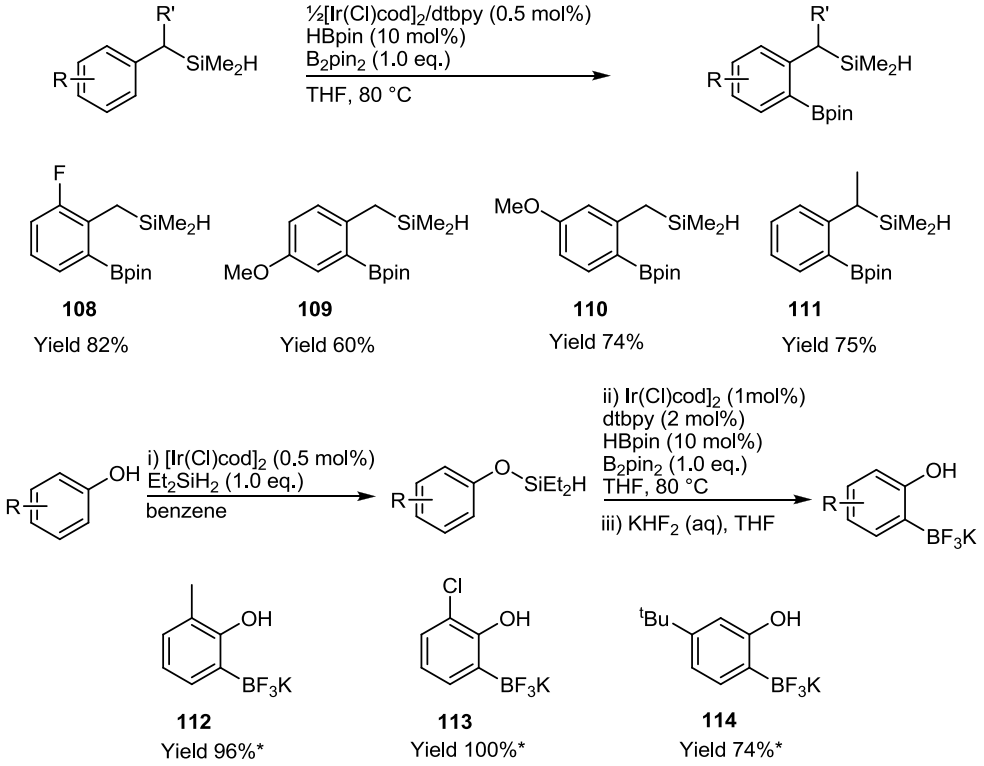

Figure 27 **-** The dialkylsilyl directed *ortho*-borylation.

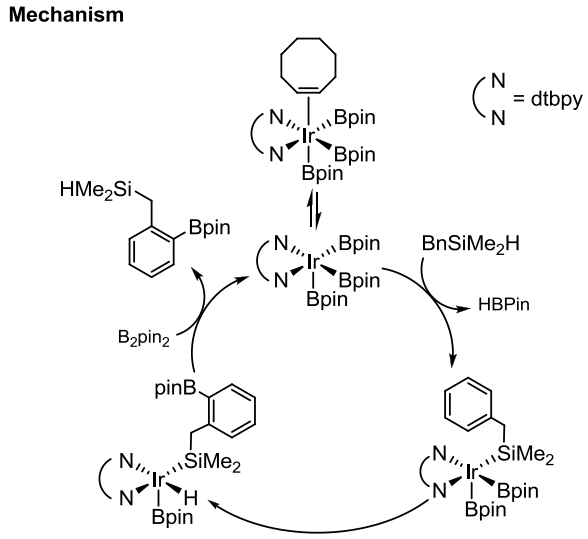

Figure 28 - Mechanism of the dialkylsilyl directed *ortho*-borylation.

The field of *ortho*-borylation has been further extended by Ishiyama, Miyaura, and co-workers.[13,63] The reaction utilises $[Ir(OMe)cod]_2$ and a bulky electron deficient mono-dentate phosphine $(3,5\text{-}(CF_3)_2C_6H_3)_3P$) **115** (2.0 eq.) to *ortho*-borylate a range of methyl benzoates with high selectivity for the *ortho*-product (***Figure 29***). This methodology is again thought to rely on coordination of the directing group to guide the catalyst to the desired position of activation.

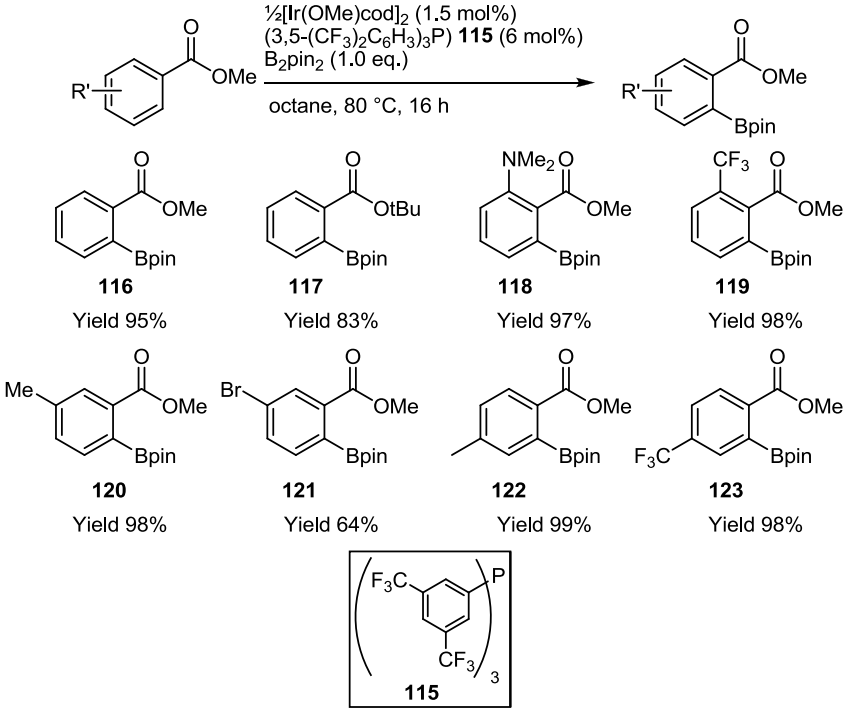

Figure 29 - *Ortho*-borylation of methyl benzoates.

1.6.8.1 Silica Supported *ortho*-Borylation

In related work, Sawamura and co-workers[64,65] presented the first example of a solid supported iridium catalyst for C-H borylation. This system offers analogous selectivity for *ortho*-borylation to the monodentate phosphine system developed by Miyaura and co-workers.[63] A silica supported monodentate phosphine is key to the reaction, enabling excellent regioselectivities, along with high activity and turnover numbers of up to 20000 being achieved (***Figure 30***). The catalyst system allows activation of substrates in an orthogonal manner to classical homogeneous borylations. Interestingly, similar reactivity and selectivity are achieved for both monodentate phosphine systems, despite the ligands being electronically and sterically very different. The Miyaura system utilises a bulky electron deficient triarylphosphine whilst the Sawamura system utilises a small trialkylphosphine.

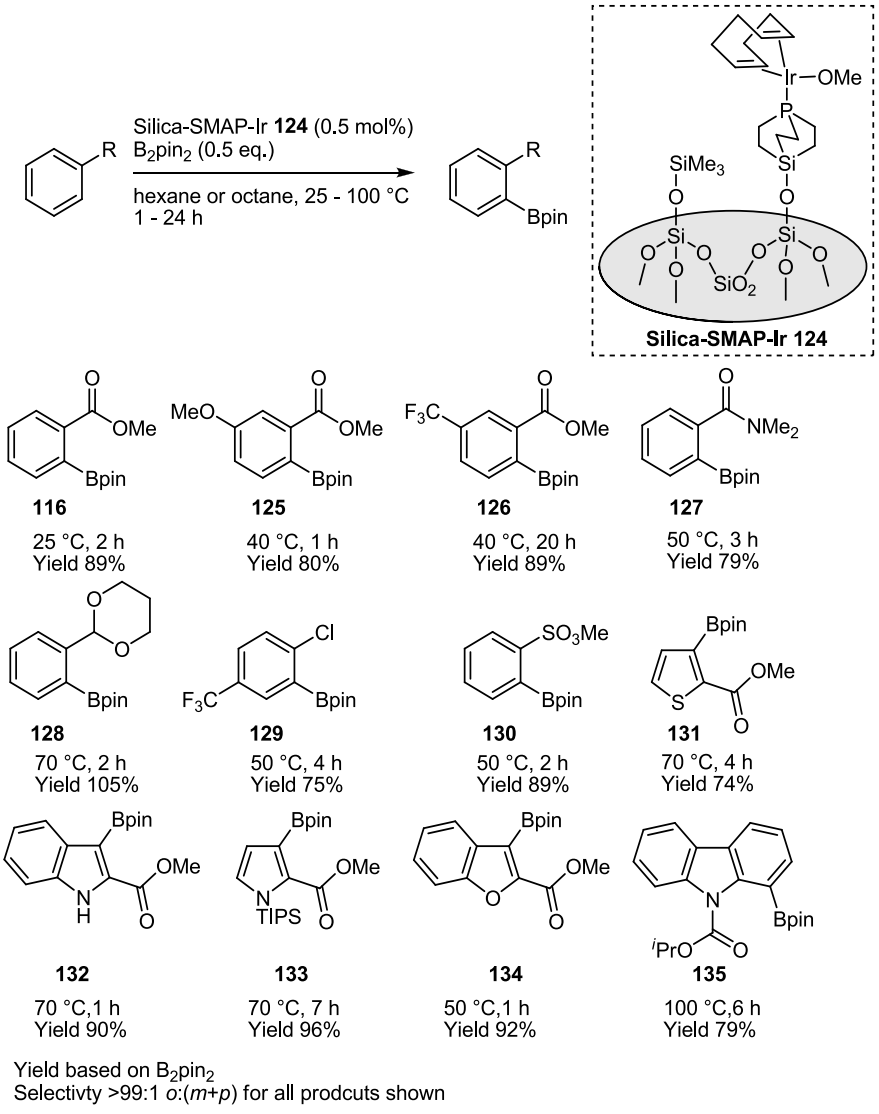

Figure 30 - Silica supported *ortho*-borylation of arenes and heteroarenes.

The Silica-SMAP-Ir system has most recently been applied to the *ortho*-borylation of phenol derivatives further extending the range of functionality able to undertake *ortho*-directed borylation (***Figure 31***).[66]

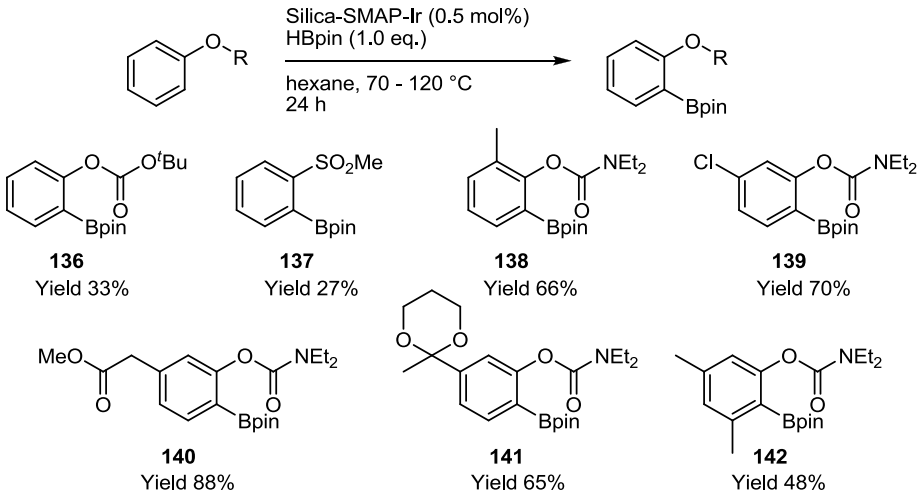

Figure 31 - The *ortho*-borylation of phenol derivatives using the Silica-SMAP-Ir catalyst.

The area of *ortho*-borylation has been the most recent development within the field and is of significant interest due to the non-classical products which are produced. This, in conjunction with the standard catalyst systems, has made C-H borylation an applicable technology to a wide range of different substrate classes. As such, the methodology has developed from an interesting observation to a main stream synthetic method for accessing borylated materials. The following section will highlight the selectivity and reactivity of the most commonly used $[Ir(X)cod]_2$/dtbpy catalyst system (X = Cl , OMe) towards a range of arenes and heteroarenes.

1.7 Borylation of Arenes With the $[Ir(X)cod]_2$/dtbpy Catalyst Systems (X = Cl, OMe)

The $[Ir(X)cod]_2$/dtbpy catalyst system has dominated the area of aromatic C-H borylation since its discovery. Borylation occurs under mild conditions, exhibiting increased reactivity relative to other catalyst systems. The catalyst system has been applied to a number of more unusual substrates which will also be highlighted in this section.

1.7.1 Polyaromatic Substrates

The borylation of polyaromatic systems has demonstrated another facet of the selectivity of the C-H borylation reaction.[67-71] This was highlighted by Marder and co-workers[67] who reported the borylation of a series of polycyclic arenes. In analogy to simple substituted benzene substrates, positions *ortho*- to ring junctions are not borylated. Naphthalene, pyrene and perylene were all borylated selectively at the least hindered positions (***Figure 32***). Interestingly, for pyrene **147** and perylene **150**, the site of borylation is not the normal site of electrophilic aromatic substitution.[67] This allows access to unusually substituted products and also suggests that an electrophilic substitution type mechanism is not taking place.

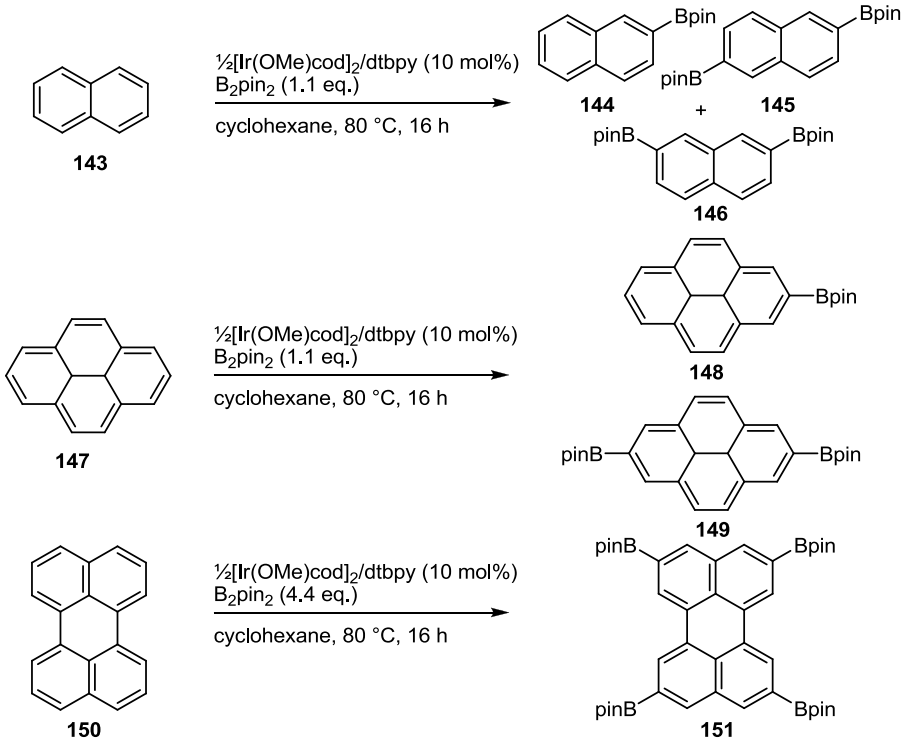

Figure 32 **-** Borylation of polycyclic aromatics using the $[Ir(OMe)cod]_2$/dtbpy catalyst system.

1.7.2 Heteroaromatic Substrates

The prevalence of heteroarenes in pharmaceuticals, agrochemicals and materials has resulted in the borylation of such substrates becoming an area of interest.[72] Particular focus has been placed on the reactivity and selectivity towards such substrates.

1.7.2.1 5-Membered Heteroarenes

Ishiyama, Miyaura and co-workers[73] reported the borylation of a series 5-membered heteroarenes. Their results demonstrated that borylation occurred adjacent to the heteroatom in high yields and with short reaction times (***Figure 33***). This preference for reaction at the 2-position is not fully understood. However, the C-H bond at the 2-position has higher acidity relative to the 3-position which might relate to the observed selectivity, as discussed further in chapter IV.[74] The regioselectivity of the borylation of **154** can be directed away from the most active 2-position by introduction of a steric blocking group (e.g. *N*-TIPS **158)** causing borylation to occur at the 3-position (***Figure 33***).[44,73,75]

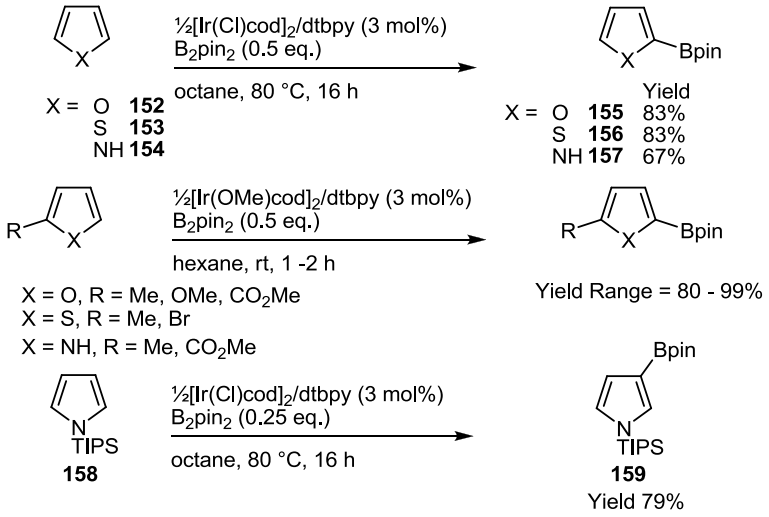

Figure 33 - Mono-borylation of 5-membered heteroarenes using the $[Ir(OMe)cod]_2$/dtbpy catalyst system.

Thiophene, furan and pyrrole all gave the corresponding 2,5-diborylated products with high regioselectivity in the presence of 1.1 equiv. of B_2pin_2 (***Figure 34***).

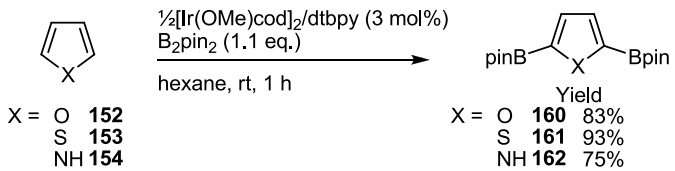

Figure 34 - Synthesis of 2,5-bis(boryl)heteroarenes using the $[Ir(OMe)cod]_2$/dtbpy catalyst system.

Borylation of a greater range of substituted thiophenes was carried out by Smith and co-workers.[76] Again, preferential borylation took place at the most sterically accessible position on thiophene (***Figure 35***).

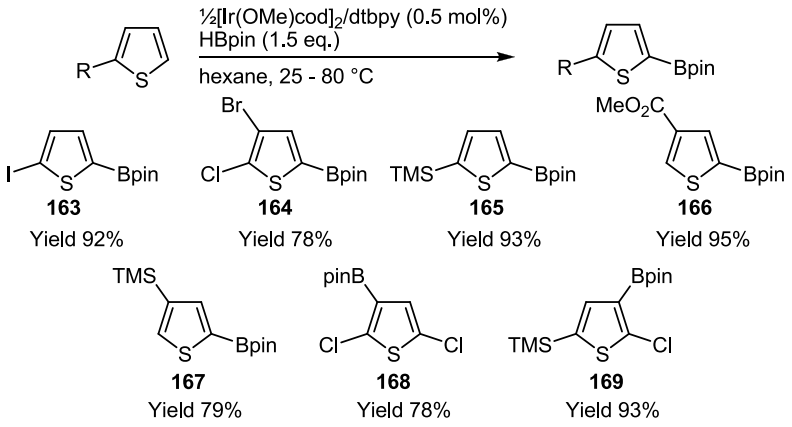

Figure 35 **-** Borylation of substituted thiophenes using the [Ir(OMe)cod]$_2$/dtbpy catalyst system.

In analogy to *N*-TIPS protected pyrrole, Smith and co-workers[77] utilised the *N*-Boc protecting group to control the regiochemistry of the borylation of a range of azaheterocycles. In all examples reported, the borylated products were obtained in moderate to good yields (***Figure 36***).

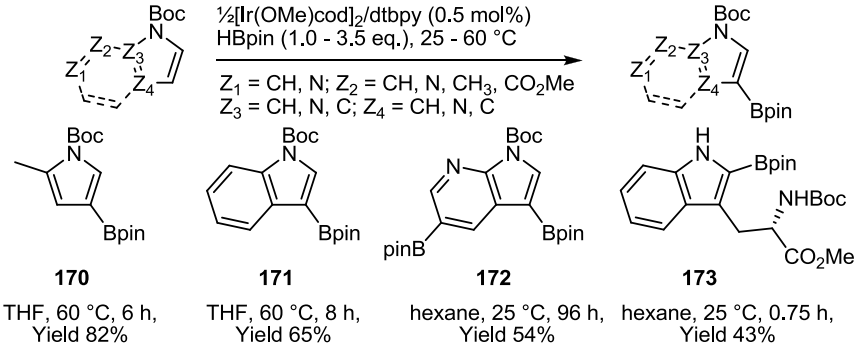

Figure 36 - Borylation of *N*-Boc-protected azaheterocycles using the [Ir(OMe)cod]$_2$/dtbpy catalyst system.

A thermally initiated deprotection strategy provides a method for removal of the *N*-Boc group, enabling production of the parent borylated heterocycle, without the need for strong acids which would otherwise affect the Bpin group (***Figure 37***).

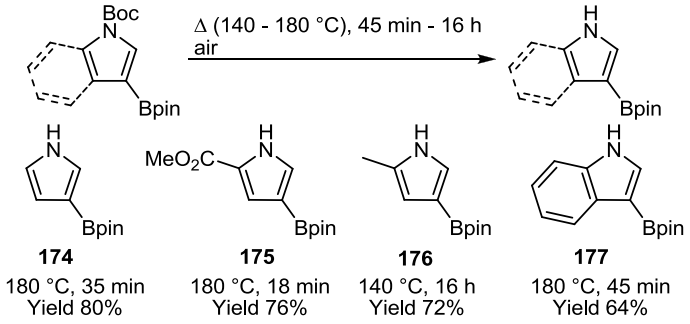

Figure 37 **-** Thermally initiated decarboxylation of *N*-Boc azoles.

This offers a useful method for the removal of protecting groups in the presence of aryl boronate esters, but may not be widely applicable to more complex molecules containing sensitive functionality due to the high temperatures involved in the deprotection step.

1.7.2.2 Fused 5-Membered Heteroarenes

Along with work on 5-membered heteroarenes, studies have been carried out on benzofused heterocycles. The borylation of simple benzofused analogues of furan, thiophene and pyrrole show similar selectivity to the parent 5-membered heterocycle, with an inherent selectivity for the heteroaromatic over the carbocyclic ring. Protection of the indole nitrogen with *N*-TIPS causes borylation at the 3-position, in a similar fashion to **158** (***Figure 38***)[44,73,75]

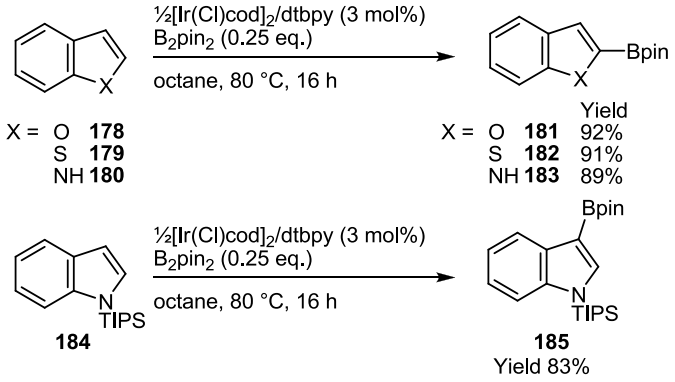

Figure 38 **-** Borylation of benzofused heteroarenes using the [Ir(Cl)cod]$_2$/dtbpy catalyst system.

The selectivity for mono-borylated products highlights the significantly higher reactivity of the heterocycle over the carbocycle. The cause of this reactivity difference is not fully understood as both electron rich and electron deficient heterocycles are more reactive than

carbocyclic arenes.[73] C-H acidity has been suggested as a possible cause of selectivity in certain aromatic and heteroaromatic systems.[46,58] This topic will be discussed in more detail in chapter IV.

Substitution at the 2-position of indole allows the less reactive benzofused ring to be activated.[78,79] Smith and co-workers,[78] demonstrated this through the regiospecific borylation at the 7-position of 2-substituted indoles. This preference for borylation at the 7-position was attributed to *N*-coordination to the Ir catalyst (***Figure 39***). The intermediate described by Smith would result in all coordination sites of the catalyst active species being filled. Alternatively, Marder, Hartwig and co-workers[9] have suggested that an interaction between the indole-nitrogen and a vacant p-orbital on a boryl ligand could direct the site of borylation.[9] The longer reaction times required for borylation of the benzofused ring again highlight the inherently lower reactivity of carbocyclic substrates.[44,73,75]

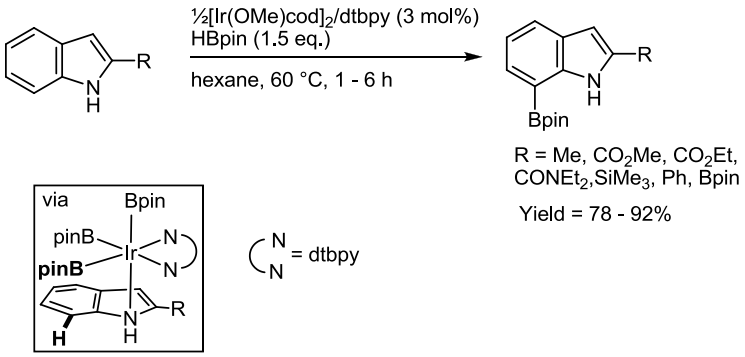

Figure 39 - Borylation of 2-substituted indoles using the $[Ir(OMe)cod]_2$/dtbpy catalyst system.

More recently, Hartwig and co-workers[80] have demonstrated a route to 7-borylated indoles without the requirement of a 2-substituent by introduction of a dialkylsilyl directing group. This group can subsequently be removed to yield 7-borylated indoles (***Figure 40***). This strategy relies on a similar mechanism to Hartwig's *ortho*-borylation of benzyl and phenolic dialkylhydrosilanes (***Figure 27***).[61]

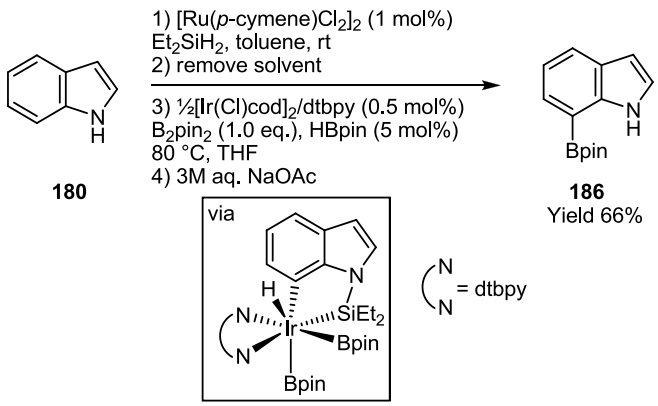

Figure 40 - Silicon directed C-H borylation of indoles using the $[Ir(Cl)cod]_2$/dtbpy catalyst system.

Finally, Hocek and co-workers,[81] have demonstrated the borylation of 9-benzyl-6-phenylpyrolo[2,3,d]pyrimidine **187** and the subsequent Suzuki-Miyaura cross-coupling with various aryl halides in good yields over the two reaction steps (***Figure 41***). Interestingly, borylation avoids both the seemingly more sterically accessible 6-phenyl and 9-benzyl groups of **187** and takes place at the 8-position on the heteroarene.

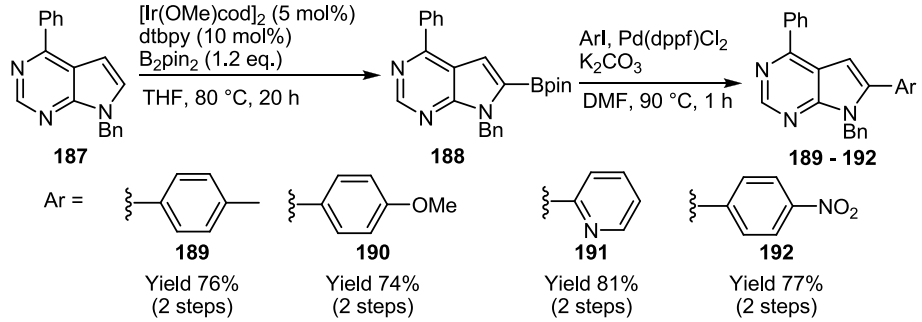

Figure 41 - Borylation and cross-coupling of 9-benzyl-6-phenylpyrolo[2,3,d]pyrimidine.

1.7.2.3 Pyridines

Pyridine **193** gave a statistical mixture (2:1) of *meta:para* borylation products **194** ***m/p*** whilst quinoline **195** selectively borylated at the 3-position on the nitrogen containing ring (***Figure 42***).[44,73] In both cases, borylation *ortho*- to nitrogen is not observed.

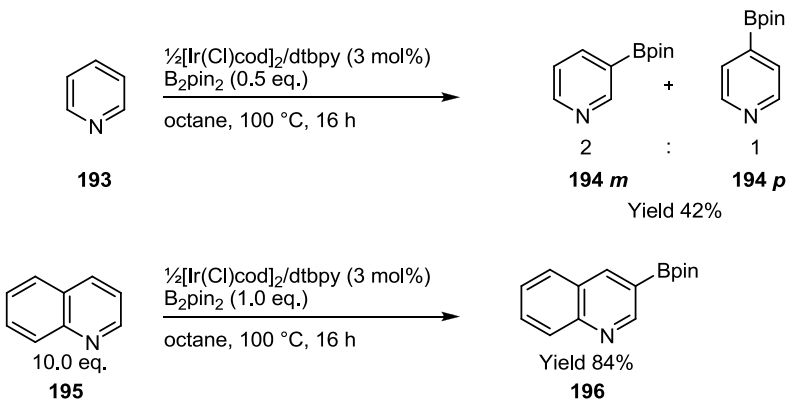

Figure 42 **-** Borylation of **193** and **195** using the $[Ir(Cl)cod]_2$/dtbpy catalyst system.

The reactivity of unsubstituted pyridine has been shown to be low. Pyridine's strong affinity for Lewis acids may provide an explanation for this. It was suggested that coordination of the basic nitrogen to iridium or boron may both activate the pyridine ring towards oxidative addition and in turn block borylation α to the heteroatom (***Figure 43***)[44] The poor reactivity of pyridine may be due to its coordination to iridium sequestering a significant quantity of the active catalyst thus reducing the efficiency with which the substrate is able to borylate.

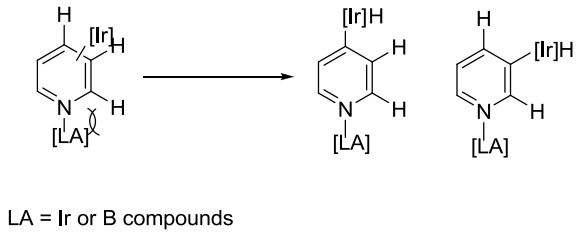

Figure 43 **-** Proposed coordination of the pyridine nitrogen to a Lewis acid (LA) blocking borylation at the *ortho*- position.

The higher reactivity of quinoline compared to pyridine, can be attributed the benzofused ring inhibiting coordination to the active catalyst and preventing it from being sequestered from the reaction. As observed for benzofused-5-membered heterocycles, the heterocyclic ring of quinoline is more reactive than the carbocyclic ring.

The effect of blocking coordination of the pyridine nitrogen to Ir was demonstrated by Smith and co-workers[41] in the reaction of 2,6-dichloropyridine **57**. Borylation *ortho*- to the chlorine substituent is hindered resulting in borylation exclusively at the 4-position, comparable with analogous 1,3-disubstituted benzenes (***Figure 44***).

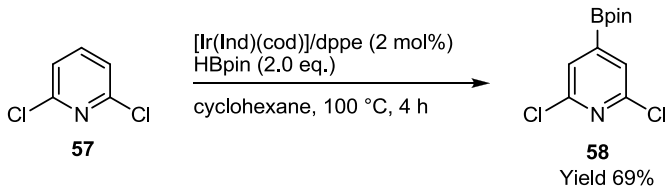

Figure 44 - Borylation of **57** using the [Ir(Ind)cod]/dppe catalyst system.

Marder and co-workers[82] demonstrated that borylation of 2-phenylpyridine **1** occurs exclusively at the 4- and 5- positions on the pyridine ring. This highlights the improved reactivity caused by the presence substituents at the 2-position or 2,6-positions in pyridines, along with the enhanced reactivity of the heterocycle and the fact that steric inhibition of *N*-coordination to Ir does not lead to borylation adjacent to nitrogen (***Figure 45***).

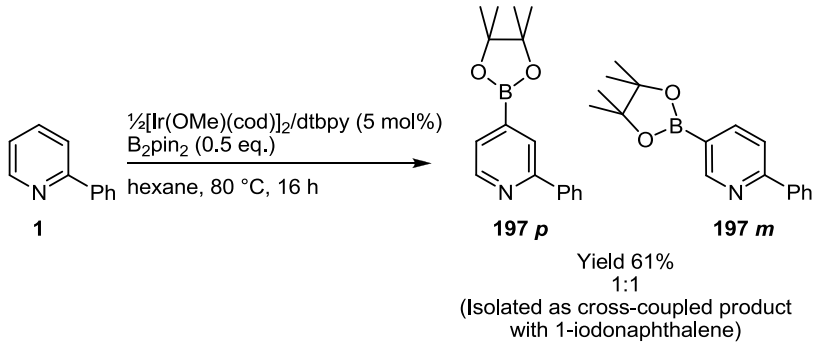

Figure 45 - Borylation of **1** using the $[Ir(OMe)cod]_2$/dtbpy catalyst system.

The reason that borylation adjacent to nitrogen is inhibited is not yet fully understood. Facile proteodeboronation of 2-pyridyl boronates, which can occur under conditions such as those employed in Suzuki-Miyaura reactions,[83] could explain why they are not observed. However, this argument is not supported by the observation that borylation of dtbpy takes place at the 6 and 6′ positions (***Figure 46***).

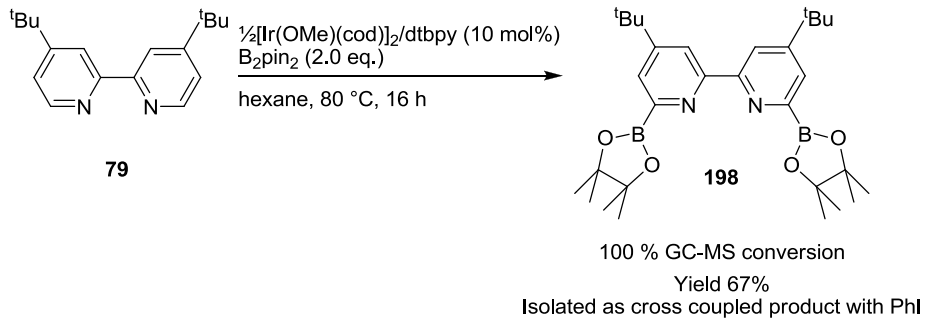

Figure 46 - Borylation of **79** using the $[Ir(OMe)cod]_2$/dtbpy catalyst system.

The reaction was conducted by premixing the catalyst components in hexane to form the active species followed by addition of **79** as substrate. The highly hindered nature of all other positions forces reaction to occur adjacent to the pyridine nitrogen. Whilst **198** was characterised by GC-MS and ^{1}H NMR spectroscopy, it should be noted that attempted purification by silica gel chromatography did result in proteodeboronation.

The acidity of the C-H bonds could explain the lower reactivity of the 2- relative to the 3- and 4- positions; this hypothesis will be discussed further in Chapter IV.

1.7.3 Novel Applications of C-H Borylation

The continued development of C-H borylation as a method for the synthesis of aryl boronates from simple aromatic substrates has been extremely successful, and application of the methodology to more complex aromatic systems have been described.

The borylation of arenes coordinated to metals and metalloid elements has been described. Plenio and co-workers[84] have thus demonstrated the borylation of ferrocenes and other half-sandwich compounds (***Figure 47***). Interestingly, it was not possible to obtain bis-borylated products, suggesting that the mono-borylated metallocene is significantly less reactive than the unsubstituted one.

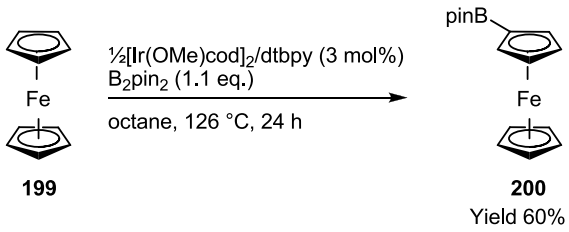

Figure 47 **-** Borylation of **199** using the $[Ir(OMe)cod]_2$/dtbpy catalyst system.

Osuka and co-workers have also demonstrated the borylation of a number of porphyrin cores as the free and zinc complexed porphyrins[85,86] (***Figure 48***). Formation of poly-borylated products was avoided through the use of steric blocking groups on the aryl substituents. The Suzuki-Miyaura cross-coupling of brominated and borylated porphyrins has also been demonstrated forming a zinc-porphyrin tetramer.[87]

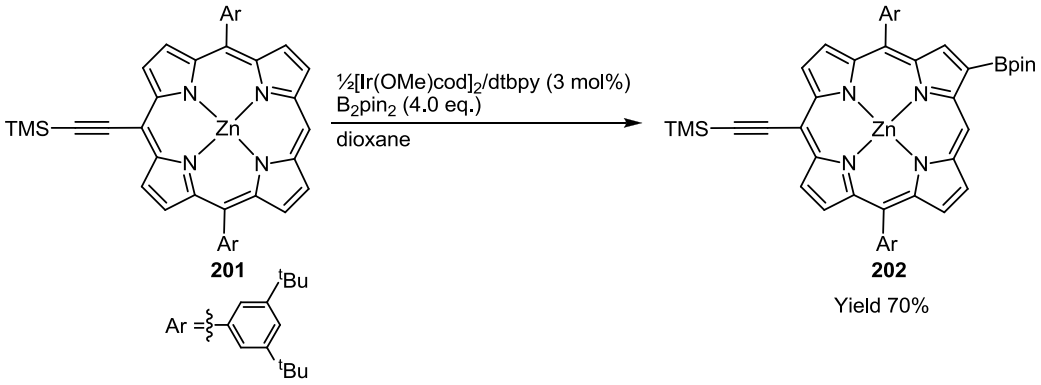

Figure 48 **-** Borylation of porphyrin **201** using the $[Ir(OMe)cod]_2$/dtbpy catalyst system.

Regioselective borylation of both dipyrroles and BODIPY's has also been demonstrated by Osuka and co-workers[88] (***Figure 49***). The free dipyrrole was borylated at the 2-positions of the pyrrole rings, in analogy to other 5-membered heteroarenes (***Figure 33***). In contrast, the analogous BODIPY **206** gives the 3-borylated product. This switch in selectivity may be due to steric blocking of the 2-position in analogy to other *N*-protected pyrroles (***Figure 33***, ***Figure 36***)

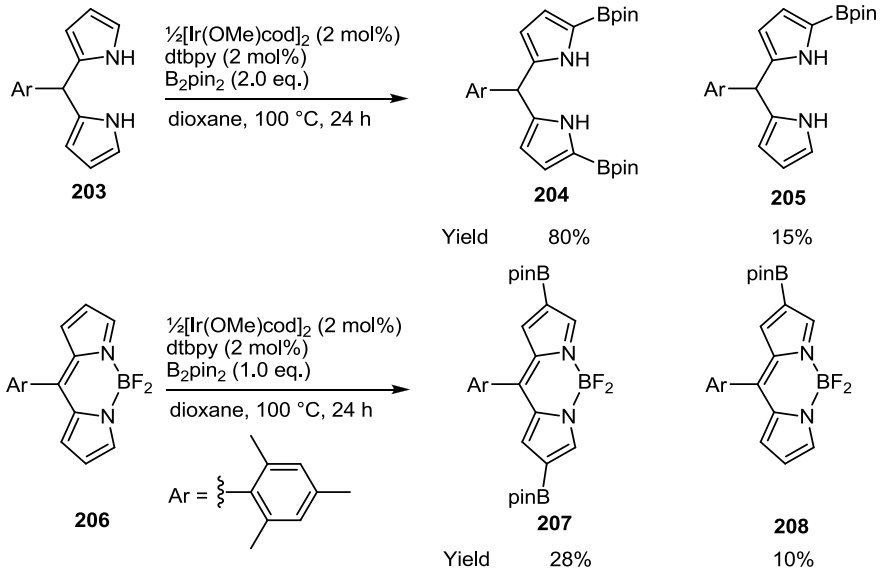

Figure 49 **-** Borylation of dipyrroles and BODIPYs using the $[Ir(OMe)cod]_2$/dtbpy catalyst system.

In a biologically relevant system, James and co-workers[89] borylated a range of protected amino acids. The borylation of amino acids was first demonstrated by Smith and co-workers;[77] however, the substrate scope has been significantly expanded in this report (***Figure 50***).

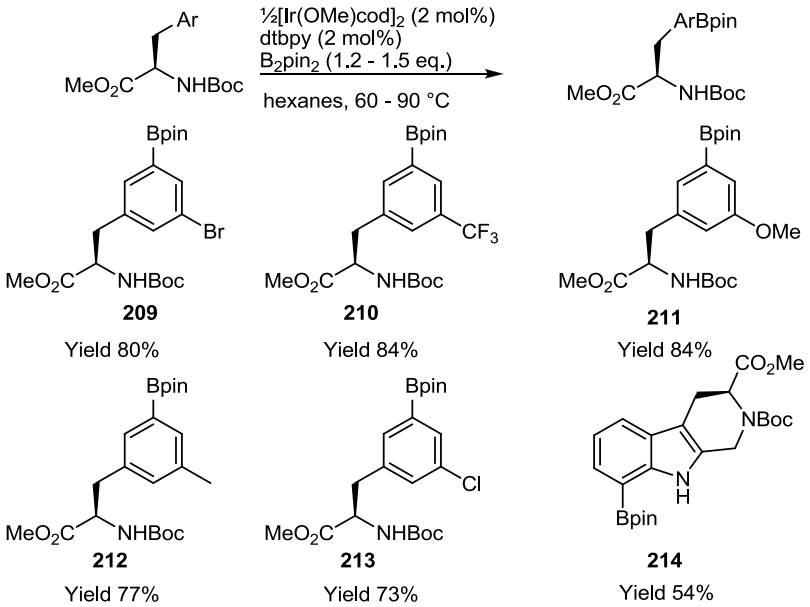

Figure 50 **-** Borylation of amino acid derivatives using the $[Ir(OMe)cod]_2$/dtbpy catalyst system.

1.7.4 Application of C-H Borylation to the Synthesis of Complex Molecules

The ability for mild and selective late stage introduction of boronate esters into advanced intermediates has resulted in the incorporation of C-H borylation/Suzuki-Miyaura cross-coupling sequences into the syntheses of complex molecules.[90-92]

Gaunt and co-workers[90] utilised this sequence to install an aryl group at the 3-position of an *N*-Boc protected pyrole in the total synthesis of Rhazinicine. This strategy gave access to the key arylboronate intermediate which was then cross-coupled to iodo-2-nitrobenzene allowing access to the desired regiochemistry for the remainder of the synthesis (***Figure 51***).

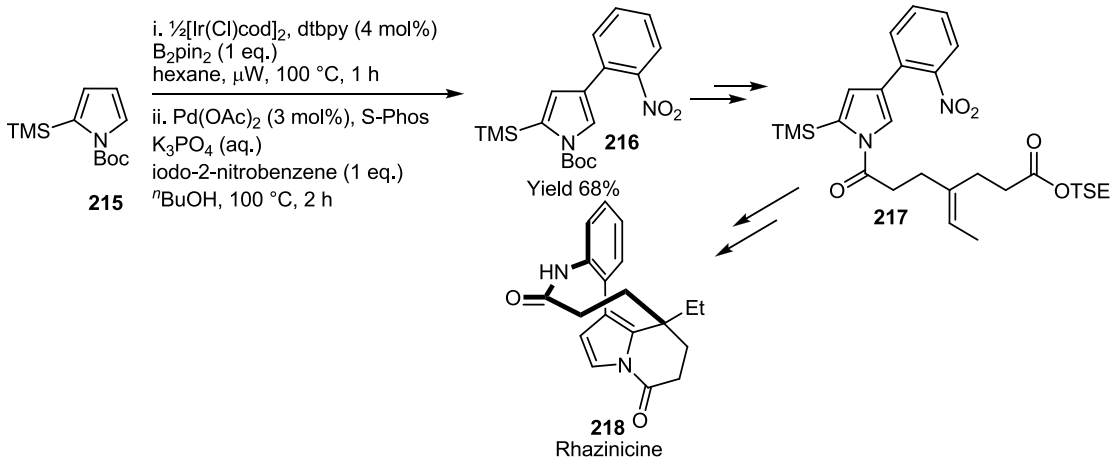

Figure 51 - Synthesis of Rhazinicine via a C-H borylation strategy.

Sarpong and co-workers[91] utilised the sequence in a synthesis of (+)-Complanadine, a member of the Lycopodium alkaloids. The strategy involved the selective C-H borylation of a late-stage 2,3-disubstituted pyridine intermediate giving the 5-borylated compound, which underwent Suzuki-Miyaura cross-coupling to yield the natural product **221** (***Figure 52***).

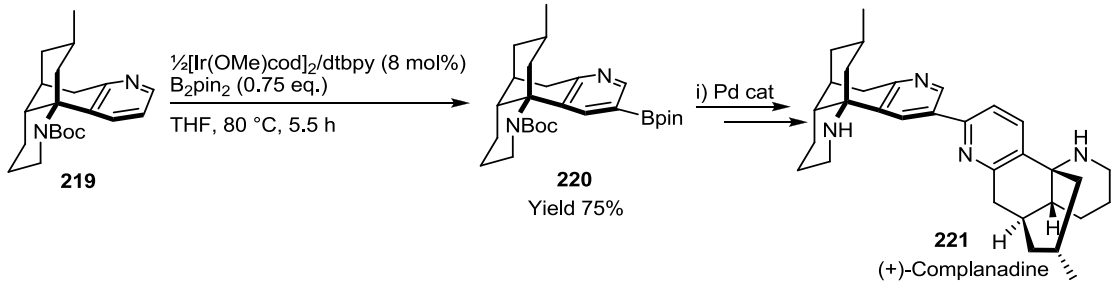

Figure 52 - Synthesis of (+)-Complanadine.

Shibasaki and co-workers[92] have reported the synthesis of SM-130686, a growth hormone secretagogue, with a key reaction step being the iridium-catalysed C-H borylation of a 1,2,3-trisubstituted benzene to yield the 5-borylated product (***Figure 53***).

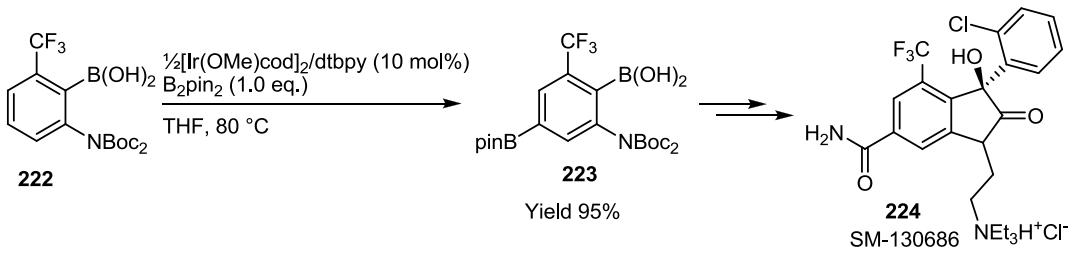

Figure 53 - Synthesis of SM-130686.

Although borylation has been applied to the synthesis of a few natural products, its use has only been incorporated early in these syntheses for the borylation of relatively simple molecules. Application of the methodology to functionalise advanced intermediates has yet to be exploited. This may be due to the potential for the catalyst to yield poly-borylated products where more than one sterically available position exists.

However, as observed for the borylation of purine analogue **187**, careful choice of substrate can lead to selectivity in the presence of multiple possible activation sites.

1.8 Conclusions

Since the first observation of aromatic C-H borylation in 1993,[32] there have been wide ranging advances in the field. Initial success was found with improvements in the stoichiometric reaction, followed by the first catalytic processes. Ligand screening led to development of catalysts showing high activity even at room temperature.

The substrate scope has also increased dramatically from benzene and other mono-substituted arenes to a wide range of substitution patterns, heteroarenes and polyaromatics.

The broad functional group tolerance of the reaction has seen it become more widely used and included in natural product syntheses, amino acid functionalisation and the borylation of substrates such as porphyrins, 7-deazapurines and BOPIDY's.

There have been many studies of the C-H borylation reaction, but there are still unresolved issues. Key areas of current interest include elucidation of the electronic influences on regioselectivity and expansion of substrate scope. Future challenges for the field will be associated with ligand development in order to direct borylation without the need for tether groups. This thesis highlights some areas for improvement and demonstrates attempts to bring about efficient and general solutions to these problems.

One area of recent research has been the development of transformations of the aryl boronate moiety once formed. The work in this area has enabled the C-H borylation reaction to grow in importance as there are now a diverse range of transformations possible, many of which can be carried out in a one-pot process, without purification of the intermediate aryl boronate. This area will be reviewed in greater detail in Chapter II, which reports an efficient one-pot, single-solvent, C-H borylation/Suzuki-Miyaura cross-coupling sequence.

1.9 Chapter I -References

1 Goldman, A. S.; Goldberg, K. I., *Activation and Functionalization of C-H Bonds*. American Chemical Society: Washington, DC, 2004.

2 Crabtree, R. H., *Chem. Rev.* **2010**, *110*, 575.

3 Tochilkin, A. I.; Kovel'man, I. R.; Prokof'ev, E. P.; Gracheva, I. N.; Levinskii, M. V., *Chem. Heterocycl. Compd.* **1988**, *24*, 892.

4 Königs, W., *Chem. Ber.* **1879**, *12*, 448.

5 Chen, X.; Hao, X-S.; Goodhue, C. E.; Yu, J-Q., *J. Am. Chem. Soc.* **2006**, *128*, 6790.

6 Kalyani, D.; Dick, A. R.; Anani, W. Q.; Sanford, M. S., *Org. Lett.* **2006**, *8*, 2523.

7 Campeau, L-C.; Rousseaux, S.; Fagnou, K., *J. Am. Chem. Soc.* **2005**, *127*, 18020.

8 Phipps, R. J.; Gaunt, M. J., *Science* **2009**, *323*, 1593.

9 Mkhalid, I. A. I.; Barnard, J. H.; Marder, T. B.; Murphy, J. M.; Hartwig, J. F., *Chem. Rev.* **2010**, *110*, 890.

10 Brown, H. C., *Boranes in Organic Chemistry*. Cornell University Press: Ithaca, 1972.

11 Muetterties, E. L., *The Chemistry of Boron and its Compounds*. John Wiley & Sons, Inc.: New York, 1976.

12 Hall, D. G., *Boronic Acids: Preparation and Applications in Organic Synthesis and Medicine*. Wiley-VCH: Weinheim, 2005; p 568.

13 Miyaura, N., *Bull. Chem. Soc. Jpn.* **2008**, *81*, 1535.

14 Miyaura, N.; Suzuki, A., *Chem. Rev.* **1995**, *95*, 2457.

15 Suzuki, A., *J. Organomet. Chem.* **1999**, *576*, 147.

16 Lam, P. Y. S.; Clark, C. G.; Saubern, S.; Adams, J.; Winters, M. P.; Chan, D. M. T.; Combs, A., *Tetrahedron Lett.* **1998**, *39*, 2941.

17 Chan, D. M. T.; Monaco, K. L.; Wang, R-P.; Winters, M. P., *Tetrahedron Lett.* **1998**, *39*, 2933.

18 Evans, D. A.; Katz, J. L.; West, T. R., *Tetrahedron Lett.* **1998**, *39*, 2937.

19 Dasa, S.; Alexeeva, V. L.; Sharmaa, A. C.; Geiba, S. J.; Asher, S. A., *Tetrahedron Lett.* **2003**, *44*, 7719.

20 James, C. A.; Coelho, A. L.; Gevaert, M.; Forgione, P.; Snieckus, V., *J. Org. Chem.* **2009**, *74*, 4094.

21 Ishiyama, T.; Murata, M.; Miyaura, N., *J. Org. Chem.* **1995**, *60*, 7508.

22 Kleeberg, C.; Dang, L.; Lin, Z.; Marder, T. B., *Angew. Chem. Int. Ed.* **2009**, *48*, 5350.

23 Murata, M.; Oyama, T.; Watanabe, S.; Masuda, Y., *J. Org. Chem.* **2000**, *65*, 164.

24 Murata, M.; Oyama, T.; Watanabe, S.; Masuda, Y., *Synthesis* **2000**, 778.

25 Murata, M.; Watanabe, S.; Masuda, Y., *Tetrahedron Lett.* **2000**, *41*, 5877.

26 Moldoveanu, C.; Wilson, D. A.; Wilson, C. J.; Corcoran, P.; Rosen, B. M.; Percec, V., *Org. Lett.* **2009**, *11*, 4974.

27 Moldoveanu, C.; Wilson, D. A.; Wilson, C. J.; Leowanawat, P.; Resmerita, A-M.; Liu, C.; Rosen, B. M.; Percec, V., *J. Org. Chem.* **2010**, *75*, 5438.

28 Wilson, D. A.; Wilson, C. J.; Moldoveanu, C.; Resmerita, A. M.; Corcoran, P.; Hoang, L. M.; Rosen, B. M.; Percec, V., *J. Am. Chem. Soc.* **2010**, *132*, 1800.

29 Wilson, D. A.; Wilson, C. J.; Rosen, B. M.; Percec, V., *Org. Lett.* **2008**, *10*, 4879.

30 Billingsley, K. L.; Buchwald, S. L., *J. Org. Chem.* **2008**, *73*, 5589.

31 Billingsley, K. L.; Barder, T. E.; Buchwald, S. L., *Angew. Chem. Int. Ed.* **2007**, *46*, 5359.

32 Nguyen, P.; Blom, H. P.; Westcott, S. A.; Taylor, N. J.; Marder, T. B., *J. Am. Chem. Soc.* **1993**, *115*, 9329.

33 Waltz, K. M.; He, X.; Muhoro, C.; Hartwig, J. F., *J. Am. Chem. Soc.* **1995**, *117*, 11357.

34 Waltz, K. M.; Muhoro, C. N.; Hartwig, J. F., *Organometallics* **1999**, *18*, 3383.

35 Iverson, C. N.; Smith, M. R., III., *J. Am. Chem. Soc.* **1999**, *121*, 7696.

36 Chen, H.; Hartwig, J. F., *Angew. Chem. Int. Ed.* **1999**, *38*, 3391.

37 Chen, H.; Schlecht, S; Semple, T. C.; Hartwig, J. F., *Science* **2000** *287*, 1995.

38 Cho, J. Y.; Iverson, C. N.; Smith, M. R., III., *J. Am. Chem. Soc.* **2000**, *122*, 12868.

39 Tse, M. K.; Cho, J. Y.; Smith, M. R., III., *Org. Lett.* **2001**, *3*, 2831.

40 Shimida, S.; Batsanov, A.; Howard, J. A. K.; Marder, T. B., *Angew. Chem. Int. Ed.* **2001**, *40*, 2168.

41 Cho, J.; Tse, M. K.; Holmes, D.; Maleczka, R. E., Jr.; Smith, M. R., III., *Science* **2002**, *295*, 305

42 Ishiyama, T.; Takagi, J.; Ishida, K.; Miyaura, N.; Anastasi, N. R.; Hartwig, J. F., *J. Am. Chem. Soc.* **2002**, *124*, 390.

43 Ishiyama, T.; Takagi, J.; Hartwig, J. F.; Miyaura, N., *Angew. Chem. Int. Ed.* **2002**, *41*, 3056.

44 Ishiyama, T.; Miyaura, N., *J. Organomet. Chem.* **2003**, *680*, 3.

45 Webster, C. E.; Fan, Y.; Hall, M. B.; Kunz, D.; Hartwig, J. F., *J. Am. Chem. Soc.* **2003**, *125*, 858.

46 Vanchura, I. I. B. A.; Preshlock, S. M.; Roosen, P.C.; Kallepalli, V. A.; Staples, R.J.; Maleczka, R. E., Jr.; Singleton, D. A.; Smith, M. R., III., *Chem. Commun.* **2010**, *46*, 7724.

47 Ess, D. H.; Nielsen, R. J.; Goddard, W. A., III.; Periana, R. A., *J. Am. Chem. Soc.* **2009**, *131*, 11686.

48 Dang, L.; Lin, Z.; Marder, T. B., *Chem. Commun.* **2009**, 3987.

49 Liskey, C. W.; Wei, C. S.; Pahls, D. R.; Hartwig, J. F., *Chem. Commun.* **2009**, *37*, 5603.

50 Boller, T. M.; Murphy, J. M.; Hapke, M.; Ishiyama, T.; Miyaura, N.; Hartwig, J. F., *J. Am. Chem. Soc.* **2005**, *127*, 14263.

51 Tamura, H.; Yamazaki, H.; Sato, H.; Sakaki, S., *J. Am. Chem. Soc.* **2003**, *125*, 16114.

52 Chotana, G. A.; Vanchura, B. A., II ; Tse, M. K.; Staples, R. J.; Maleczka, R. E., Jr.; Smith, M. R., III., *Chem. Commun.* **2009**, *38*, 5731.

53 Chotana, G. A.; Rak, M. A.; Smith, Milton R. III., *J. Am. Chem. Soc.* **2005**, *127*, 10539.

54 Tagata, T.; Nishida, M.; Nishida, A., *Tetrahedron Lett.* **2009**, *50*, 6176.

55 Tagata, T.; Nishida, M.; Nishida, A., *Adv. Synth. Catal.* **2010**, *352*, 1662.

56 Murata, M.; Odajima, H.; Watanabe, S.; Masuda, Y., *Bull. Chem. Soc. Jpn.* **2006**, *79*, 1980.

57 Diez-Gonzalez, S.; Marion, N.; Nolan, S. P., *Chem. Rev.* **2009**, *109*, 3612.

58 Frey, G. D.; Rentzsch, C. F.; Preysing, D. von; Scherg, T.; Mühlhofer, M.; Herdtweck, E.; Herrmann, W. A., *J. Organomet. Chem.* **2006**, *691*, 5725.

59 Rentzsch, C. F.; Tosh, E.; Herrmann, W. A.; Kühn, F. E., *Green Chem.* **2009**, *11*, 1610.

60 Chianese, A. R.; Mo, A.; Lampland, N.L.; Swartz, R. L.; Bremer, P. T., *Organometallics* **2010**, *29*, 3019.

61 Boebel, T. A.; Hartwig, J. F., *J. Am. Chem. Soc.* **2008**, *130*, 7534.

62 Whisler, M. C.; MacNeil, S.; Snieckus, V.; Beak, P., *Angew. Chem. Int. Ed.* **2004**, *43*, 2206.

63 Ishiyama, T.; Isou, H.; Kikuchi, T.; Miyaura, N., *Chem. Commun.* **2010**, *46*, 159.

64 Kawamorita, S.; Ohmiya, H.; Hara, K.; Fukuoka, A.; Sawamura, M., *J. Am. Chem. Soc.* **2009**, *131*, 5058.

65 Kawamorita, S.; Ohmiya, H.; Sawamura, M., *J. Org. Chem.* **2010**, *75*, 3855.

66 Yamazaki, K.; Kawamorita, S.; Ohmiya, H.; Sawamura, M., *Org. Lett.* **2010**, *12*, 3978.

67 Coventry, D. N.; Batsanov, A. S.; Goeta, A. E.; Howard, J. A. K.; Marder, T. B.; Perutz, R. N., *Chem. Commun.* **2005**, 2172.

68 Kimoto, T.; Tanaka, K.; Sakai, Y.; Ohno, A.; Yoza, K.; Kobayashi, K., *Org. Lett.* **2009**, *11*, 3658.

69 Fujinaga, M.; Murafuji, T.; Kurotobi, K.; Sugihara, Y., *Tetrahedron* **2009**, *65*, 7115.

70 Fujinaga, M.; Suetake, K.; Gyoji, K.; Murafuji, T.; Kurotobi, K.; Sugihara, Y., *Synthesis* **2008**, *2008*, 3745.

71 Kurotobi, K.; Miyauchi, M.; Takakura, K.; Murafuji, T.; Sugihara, Y, *Eur. J. Org. Chem.* **2003**, *2003*, 3663.

72 Keller, P. A.; Katritzky, A. R.; Ramsden, C. A.; Scriven, E. F. V.; Taylor, R. J. K., *Comprehensive Heterocyclic Chemistry III*. Elsevier: Oxford, 2008; Vol. 7, p 1066.

73 Takagi, J.; Sato, K.; Hartwig, J. F.; Ishiyama, T.; Miyaura, N., *Tetrahedron Lett.* **2002**, *43*, 5649.

74 Shen, K.; Fu, Y.; Li, J-N.; Liu, L.; Guo, Q-X., *Tetrahedron* **2007**, *63*, 1568.

75 Ishiyama, T.; Takagi, J.; Yonekawa, Y.; Hartwig, J. F.; Miyaura, N., *Adv. Synth. Catal.* **2003**, *345*, 1103.

76 Chotana, G. A.; Kallepalli, V. A.; Maleczka, Robert E. Jr.; Smith, Milton R. III., *Tetrahedron* **2008**, *64*, 6103.

77 Kallepalli, V. A.; Shi, F.; Paul, S.; Onyeozili, E. N.; Maleczka, R. E., Jr.; Smith, M. R., III., *J. Org. Chem.* **2009**, *74*, 9199.

78 Paul, S.; Chotana, G. A.; Holmes, D.; Reichle, R. C.; Maleczka, R. E., Jr.; Smith, M. R., III., *J. Am. Chem. Soc.* **2006**, *128*, 15552.

79 Lo, W. F.; Kaiser, H. M.; Spannenberg, A.; Beller, M.; Tse, M. K., *Tetrahedron Lett.* **2007**, *48*, 371.

80 Robbins, D. W.; Boebel, T. A.; Hartwig, J. F., *J. Am. Chem. Soc.* **2010**, *132*, 4068.

81 Klecka, M.; Pohl, R.; Klepetarova, B.; Hocek, M., *Org. Biomol. Chem.* **2009**, *7*, 866.

82 Mkhalid, I. A. I.; Coventry, D. N.; Albesa-Jove, D.; Batsanov, A. S.; Howard, J. A. K.; Perutz, R. N.; Marder, T. B., *Angew. Chem. Int. Ed.* **2006**, *45*, 489.

83 Deng, J. Z.; Paone, D. V.; Ginnetti, A. T.; Kurihara, H.; Dreher, S. D.; Weissman, S. A.; Stauffer, S. R.; Burgey, C. S., *Org. Lett.* **2009**, *11*, 345.

84 Datta, A.; Köllhofer, A.; Plenio, H., *Chem. Commun.* **2004**, 1508.

85 Hata, H.; Yamaguchi, S.; Mori, G.; Nakazono, S.; Katoh, T.; Takatsu, K.; Hiroto, S.; Shinokubo, H.; Osuka, A., *Chem. Asian J.* **2007**, *2*, 849.

86 Mori, G.; Shinokubo, H.; Osuka, A., *Tetrahedron Lett.* **2008**, *49*, 2170.

87 Chen, J.; Aratani, N.; Shinokubo, H.; Osuka, A., *Chem. Asian J.* **2009**, *4*, 1126.

88 Chen, J.; Mizumura, M.; Shinokubo, H.; Osuka, A., *Chem. Eur. J.* **2009**, *15*, 5942.

89 Meyer, F-M.; Liras, S.; Guzman-Perez, A.; Perreault, C.; Bian, J.; James, K., *Org. Lett.* **2010**, *12*, 3870.

90 Beck, E. M.; Hatley, R. ; Gaunt, M. J., *Angew. Chem. Int. Ed.* **2008**, *47*, 3004.

91 Fischer, D. F.; Sarpong, R., *J. Am. Chem. Soc.* **2010**, *132*, 5926.

92 Tomita, D.; Yamatsugu, K.; Kanai, M.; Shibasaki, M., *J. Am. Chem. Soc.* **2009**, *131*, 6946.

CHAPTER II - ONE-POT, SINGLE SOLVENT C-H BORYLATION/SUZUKI-MIYAURA CROSS-COUPLING SEQUENCE

2.1 Introduction

As discussed in chapter 1, efficient and facile methods towards the synthesis of aryl boronates have been developed. A key driving force for the development of these new methods has been the synthetic utility of the aryl boronate group in further elaboration to other functionality.[1]

A strategy which has been employed, for a wide range of examples, is C-H functionalisation followed by subsequent elaboration to other functionality in a one-pot manner. However, many of these reactions require a change in reaction solvent after the C-H borylation step. Development of a method which would allow for the reaction to be carried out in a single reaction solvent would be desirable. This chapter will discuss work undertaken to develop a one-pot, single solvent method for the conversion of arenes to biaryls.

The chapter will initially introduce the wide range of transformations developed to elaborate aryl boronates to other functionalities. Simple functional group interconversions will be systematically explored. Subsequently, examples of the use of aryl boronates for the formation of key C-C, C-N and C-O bonds in the synthesis of larger molecules will be discussed. Finally, one-pot C-H borylation/functionalisation strategies will be discussed to highlight the key issues concerning the methodologies which have been developed.

2.2 Transformations from Arylboronates

The arylboronate core is an extremely versatile group for elaboration to other functionality in a number of C-C, C-O, C-N and C-X (X = F, Cl, Br, I) bond forming reactions (***Figure 54***).[1,2] Many routes have been developed which constitute simple functional group interconversions from aryl boronates.

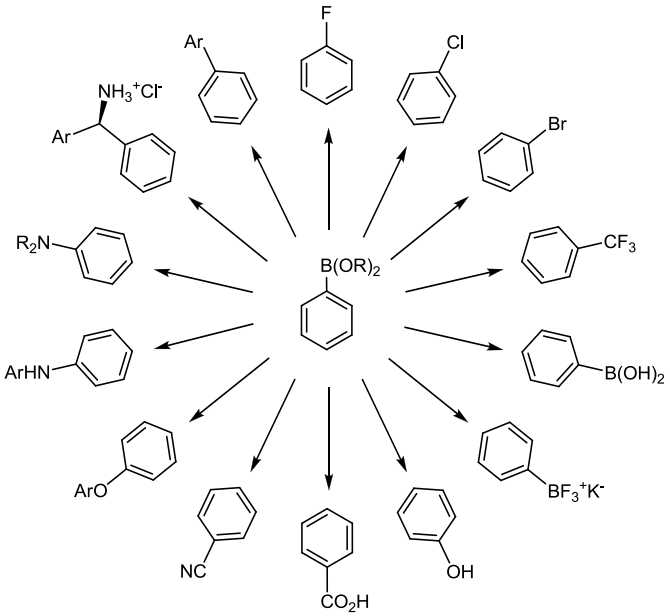

Figure 54 - Selected transformations from arylboronate moiety.

The discussion of reactions will start by introduction of the initial reaction discovery followed by highlighting areas of important development in the methodology. The reaction mechanism will be discussed along with the influence this has on the functional group tolerance and reactivity towards different substrates.

2.2.1 *Ipso*-Substitution of the Aryl Boronate Group

This section will examine a selection of the wide range of simple functional group interconversions developed by *ipso*-substitution of boron. This section highlights the key transformations in the field. However, due to the size of the body of published work, a full discussion of each method is not possible.

2.2.1.1 Phenol Synthesis

The *ipso*-oxidation of boronic acids to phenols was first described by Challenger and co-workers in 1930,[3] involving the use of alkaline hydrogen peroxide. Petasis and co-workers[4] later removed the requirement for base in the reaction by using aqueous hydrogen peroxide (30%) (***Figure 55***).

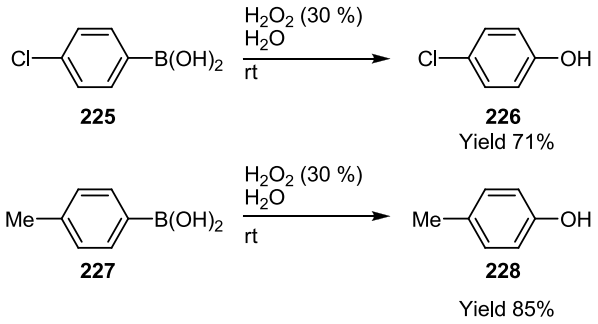

Figure 55 - Hydrogen peroxide oxidation of 4-chloro- and 4-methyl- phenylboronic acid to the corresponding phenol.

The issue with both of these procedures is the functional group tolerance to the strongly oxidising conditions. As such, other, milder methods have been developed with the use of Oxone®,[5] sodium perborate,[6] hydroxylamine[7] and, most recently, a copper catalysed hydroxylation in water.[8] These oxidation methodologies have been shown to operate on boronic acids, esters and trifluoroborate salts. For all of the hydroxylation strategies described above electron rich aryl boronates are more reactive than electron poor ones.

Consistent with this observation, Kuivila and co-workers,[9,10] investigated the mechanism of the oxidation of phenyl boronic acid and suggested that the reaction proceeded via a carbon migration from boron to oxygen followed by hydrolysis to the phenol product (***Figure 56***). Similar mechanisms have also been suggested for the other milder oxidants described.

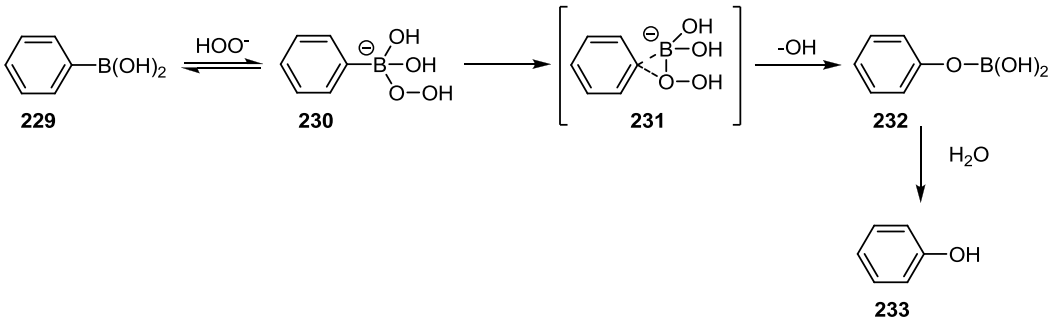

Figure 56 - Mechanism of aqueous oxidation of phenyl boronic acid with hydrogen peroxide.

2.2.1.2 *Ipso*-Nitration

Ipso-nitration of aryl boronates is a mild method for the introduction of nitro functionality to an arene, when compared to classically harsh nitration techniques.

Ipso-nitration was first described by Petasis and co-workers,[11] using Crivello's reagent[12] (ammonium nitrate/trifluoroacetic anhydride). However, this method is prone to formation of poly-nitrated compounds due to Crivello's reagent being an effective C-H nitrating reagent. In order to limit reactivity, and therefore side product formation, low temperature reactions (-35 °C) were employed.

Prakash and co-workers[13] developed a milder nitration method using silver or ammonium nitrate salts with TMSCl. This reagent combination forms TMS-O-NO_2 **238** *in situ* which attacks the boron atom of **229**. Subsequent migration of the arene from boron to nitrogen affords the nitro arene in an analogous mechanism to the phenol synthesis described above (***Figure 57***). Consistent with this mechanism, electron rich arenes are most reactive with electron deficient arenes requiring more forcing reaction conditions.

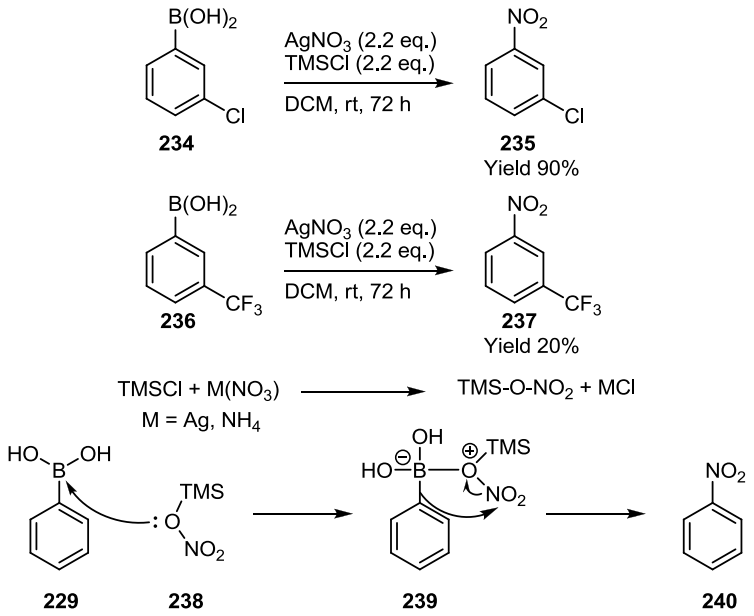

Figure 57 -Mechanism of *ipso*-nitration of *meta*-chloroboronic acid with TMSCl-silver nitrate.

2.2.1.3 Azide Synthesis

Azides have found use as coupling partners in 1,3-dipolar cycloaddition with alkynes to form 1,2,3-triazoles which have utilised in medicinal chemistry.[14] Routes to install the group selectively in a mild manner are therefore desirable. The formation of aryl azides from aryl boronic acids was first described by Pinhey and co-workers.[15,16] The process involved generation of a lead species through transmetalation of an aryl boronic acid to $Pb(OAc)_4$. Reaction of the aryl lead reagent with sodium azide affords the aromatic azide. Although efficient, this methodology has drawbacks due to the high toxicity the lead reagent used and as such has not been widely applied.

Recently, Aldrich and co-workers[17] have reported an adaptation of the Pinhey methodology using copper (II) acetate with sodium azide to yield the aryl azide products (***Figure 58***). The mechanism is reported to be similar to that of the Chan-Lam coupling which will be discussed in section 2.2.2. The reaction was shown to be effective with aryl boronic acids and boronate esters, but less so with potassium trifluoroborate salts. Both electron donating and withdrawing substituents are tolerated on the arene. Arenes containing strongly electron donating groups required shorter reaction times relative to those containing electron withdrawing substituents.

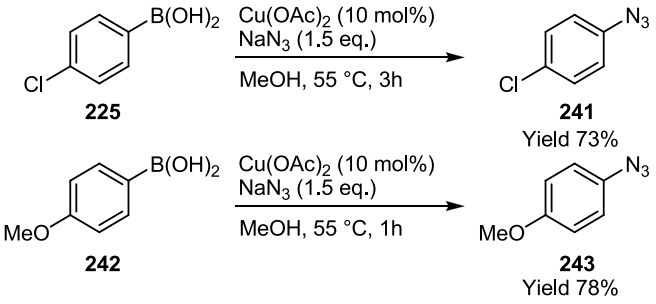

Figure 58 - Copper catalysed conversion of aryl boronic acid to aryl azide.

2.2.1.4 Aniline Synthesis

In a mechanistic analogy to the aryl azide synthesis described in the previous section, Fu and co-workers[18] demonstrated the conversion of aryl boronic acids and esters to anilines. The method utilises copper (I) oxide catalyst with aqueous ammonia as the nitrogen source (***Figure***

59). As with the azide synthesis, electron rich substrates require shorter reaction times and provide slightly higher yields than the more electron deficient substrates.

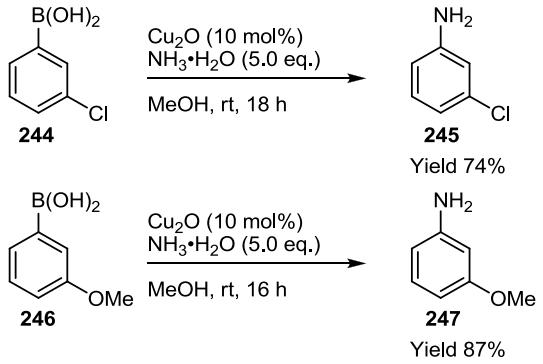

Figure 59 - Copper catalysed conversion of aryl boronic acids to anilines.

2.2.1.5 *Ipso*-Halogenation

The *ipso*-halogenation of arylboronates has received significant attention with methodology for chlorination and bromination being most widely reported. Reports of methods for iodination and fluorination are much less prevalent.

2.2.1.5.1 *Ipso*-Chlorination, Bromination and Iodination

Ipso-chlorination and bromination of arylboronic acids was first observed by Challenger and co-workers in the reaction of phenylboronic acid with chlorine or bromine water to afford the respective chloro or bromobenzene.[3] Subsequent to this initial observation there have been numerous reports of the transformation by several groups (***Figure 60***).

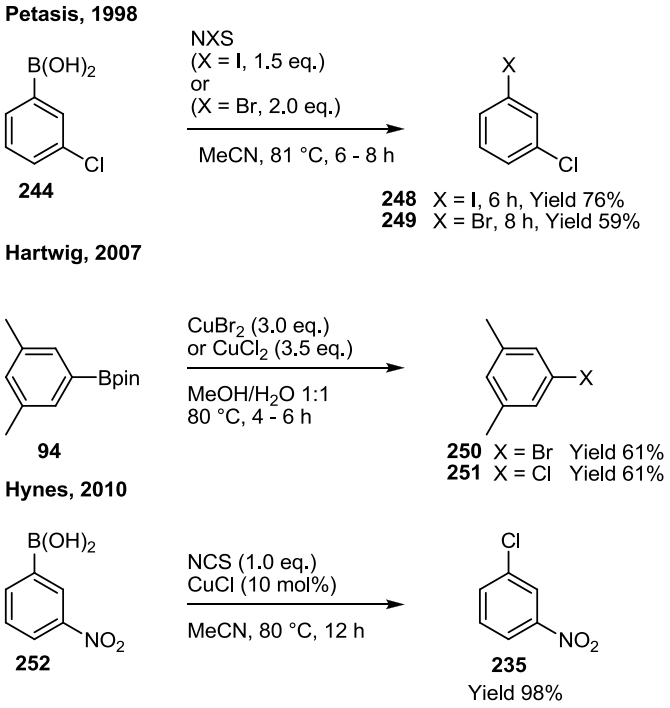

Figure 60 - *Ipso*-halogenation of aryl boronic acids, esters and trifluoroborates.

Petasis and co-workers[19] reported the *ipso*- bromination and iodination of simple boronic acids with the corresponding N-halosuccinimides; the analogous chlorination reaction with N-chlorosuccinimide was not successful. Electron deficient arylboronic acids afforded low yields and required long reaction times in agreement with an electrophilic nature of the reaction mechanism. Although arylboronate esters were viable substrates, they required longer reaction times and gave low yields.

Huffman and co-workers[20] demonstrated the use of copper (II) bromide to facilitate bromo-deboronation. This was subsequently extended to aryl chlorides by Hartwig and co-workers[21] through analogous use of copper (II) chloride. Moreover, both aryl boronate esters and acids were shown to be viable substrates. The major drawback of this method is the requirement for superstoichiometric quantities of Cu^{II} salts in the reaction.

The low reactivity towards electron deficient substrates and requirement for superstoichiometric reagent quantities was addressed by Hynes and co-workers.[22] In this method, based on the work of Petasis,[19] NCS is used to facilitate chlorodeboronation in a copper (I) chloride catalysed process. The reaction proceeds via oxidative addition of the copper (I)

chloride to NCS forming a Cu^{III} intermediate which then undergoes transmetalation with the aryl boronate followed by reductive elimination of the aryl chloride. This approach has been shown to be effective with CuBr/NBS and CuI/NIS systems, but has not been fully explored.

2.2.1.5.2 *Ipso*-Fluorination

The fluorination of aryl boronates has been a significant challenge with initial attempts using $CsSO_4F$ requiring low reaction temperatures (-40 °C - rt), affording only moderate yields and poor selectivity for fluoro-deboronation over competing C-H fluorination.[23]

Recently, Ritter and co-workers[24] have demonstrated the conversion of aryl boronic acids and esters to arylfluorides using silver(I)triflate and Selectfluor® (***Figure 61***). The reaction proceeds via an aryl silver species formed by transmetalation with the silver triflate. As with many transmetalations of aryl boronates, hydroxide base is used to facilitate the process.[2,25] Both electron-rich and electron-poor substrates give similarly good yields. Arenes containing protic, electrophilic, or nucleophilic functional groups are viable substrates. A one-pot C-H borylation/fluorination sequence giving access to selectively fluorinated arenes in high yields was also reported.

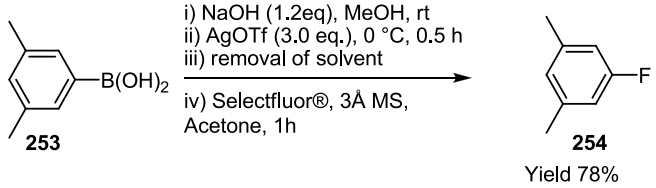

Figure 61 - C-H borylation followed by oxidative cleavage to boronic acid and subsequent silver mediated fluorination.

2.2.1.6 *Ipso*-Cyanation

In another copper mediated transformation, Hartwig and co-workers[26] have shown the conversion of arylboronic acids and esters to aryl nitriles with zinc (II) cyanide. Aryl boronic acids were more reactive than the aryl boronate esters, which required higher reaction

temperatures and longer reaction times. The methodology was developed as a one-pot, iridium catalysed C-H borylation/cyanation sequence.

The reaction is likely to proceed via a Cham-Lam type mechanism which will be further discussed in section 2.2.2. Both electron rich and poor arenes exhibited similar reactivity and gave good yields of the aryl nitrile product.

The aryl nitrile product could be further elaborated to form primary benzamides, benzoic acids, benzaldehydes, benzylamines, ketones and tetrazoles, further demonstrating the diverse range of functionality which can be installed via the aryl boronate moiety (***Figure 62***).

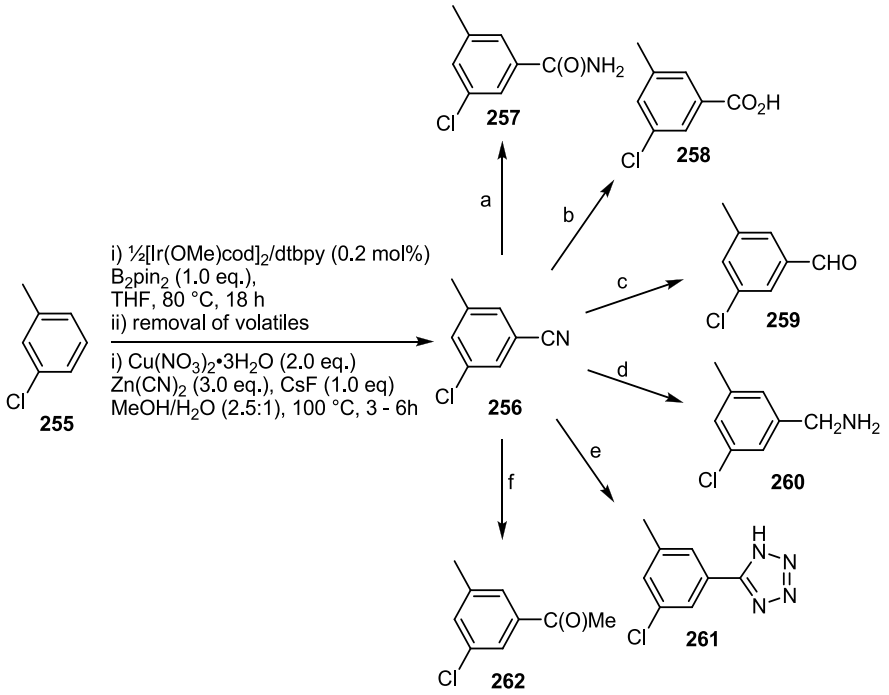

Figure 62 - Cyanation of aryl pinacolboronate ester and subsequent transformations.

2.2.1.7 *Ipso*-Trifluoromethylation

The selective installation of trifluoromethyl groups into molecules is an important goal in the synthesis of biologically active molecules as the group can be installed to enhance chemical and biological stability of active compounds.[27]

The *ipso*-trifluoromethylation of aryl boronic acids has recently been demonstrated by Qing and co-workers through a copper mediated oxidative coupling with $TMSCF_3$ (***Figure 63***).

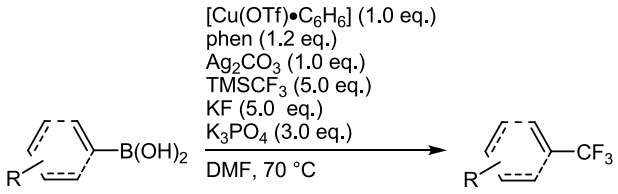

Figure 63 - Oxidative trifluoromethylation of aryl boronic acids.

The mechanism suggested for the transformation (***Figure 64***) requires initial formation of a copper (I) CF_3 species **B**, transmetalation with aryl boronic acid and oxidation by the silver salt then occurs to give either copper (II) or (III) **C.** Reductive elimination of trifluoromethyl arene **D** then follows. Both electron poor and electron rich aryl boronates are viable for the reaction with electron rich examples giving slightly higher yields.

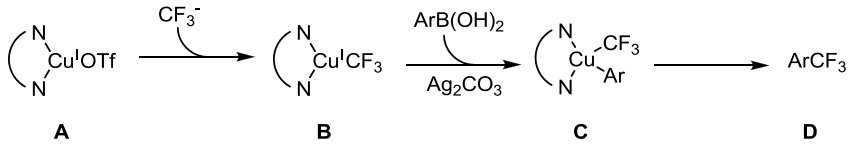

Figure 64 - Proposed mechanism of oxidative trifluoromethylation of aryl boronic acids.

The reactions described so far have been concerned with simple functional group interconversions from aryl boronates. One area where aryl boronate chemistry has been advanced is in the construction of key bonds in more complex molecular architectures. This concept will be now be explored further.

2.2.2 C-N and C-O Bond Forming Reactions

The coupling of aryl and heteroaryl boronic acids with molecules containing acidic heteroatoms such as phenols, thiols, amines and amides were first reported in independent reports by Chan,[28] Chan and Lam[29] and Evans.[30] All three reports utilised $Cu(OAc)_2$ in the coupling of aryl boronic acids with phenols, primary or secondary amines (***Figure 65***).

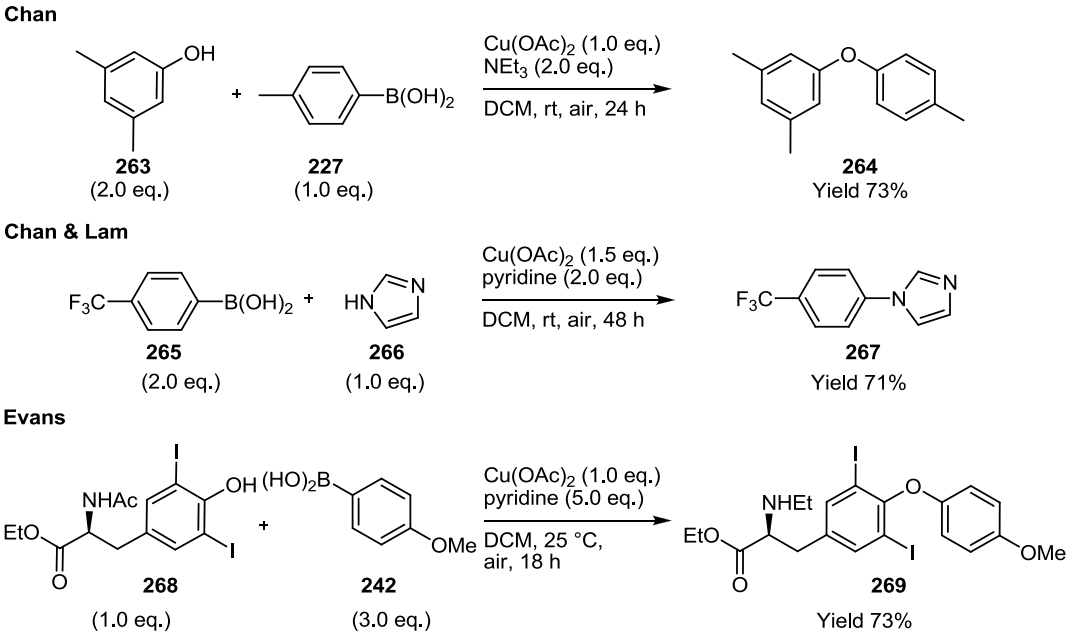

Figure 65 - Initial reports of phenol and amine couplings with boronic acids.

The mechanism of the reaction (***Figure 66***) has been suggested to involve initial coordination of the nucleophile followed by deprotonation to give a Cu^{II} species **271.** Transmetalation with the aryl boronic acid gives **272**. The following step either involves reductive elimination from the Cu^{II} species **272,** then oxidation to **270,** or oxidation to Cu^{III} species **274,** then reductive elimination to Cu^{II} species **270**. It has been suggested that the latter of these routes is more likely as reductive elimination is more facile from Cu^{III} than Cu^{II}.[31]

There has been significant work towards improvements in the catalysts employed and broadening of substrate scope. [2,31,32] The reaction has been shown to be more effective with aryl boronic acids but also viable with aryl boronate esters.[31] Catalytic variants have been developed which rely on efficient reoxidation of the copper source by molecular oxygen or added oxidants.[31] An excess of the aryl boronate coupling partner is routinely used which, along with the long reaction times, are the major limitations of the methodology.

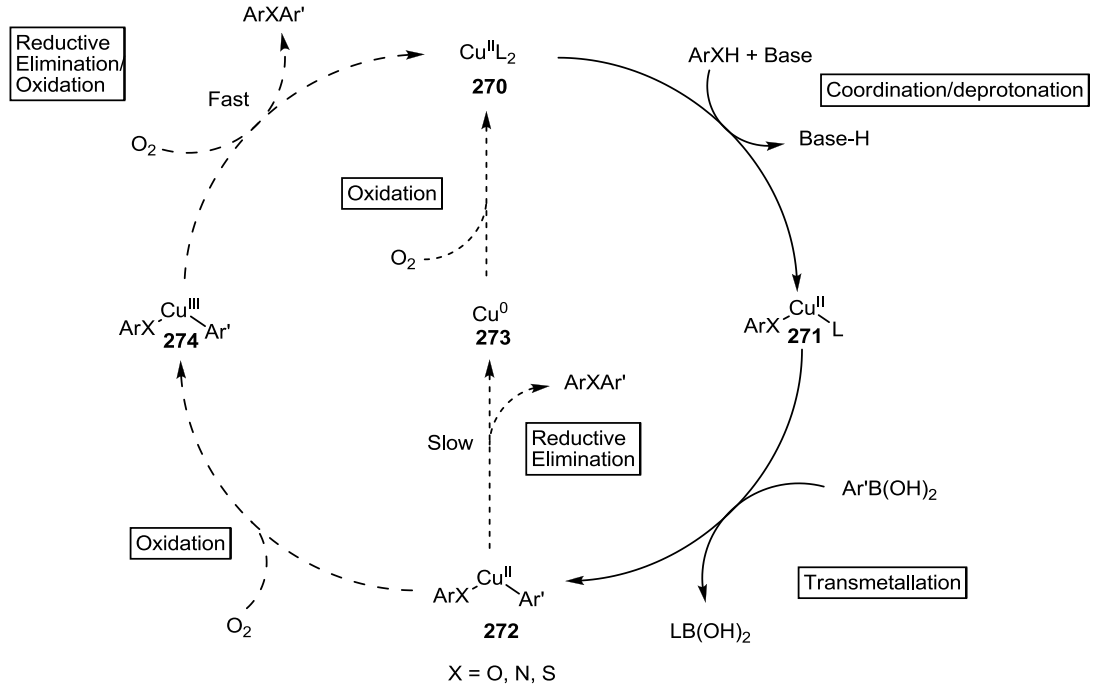

Figure 66 - Mechanism of Chan-Lam coupling.

2.2.3 C-C bond Forming Reactions

The use of aryl boronates in the formation of carbon-carbon bonds has been an area of research in which many transformations have been developed. The formation of Csp^2-Csp^2 bonds is of significant importance due to their prevalence in an extensive array of important molecules with applications in all areas of chemistry. This section will give a brief overview of the types of reactions which have been demonstrated in order to show the breadth of chemistry possible when forming simple C-C bonds.

2.2.3.1 Petasis Borono-Mannich Reaction - Addition of Aryl Boronates to Imines

Petasis and co-workers,[33] developed a three component reaction in which α-ketoacids, amines and boronic acids react to form α-amino acids. Initial work used aryl boronic acids in the synthesis of α-arylglycines[34] (***Figure 67***).

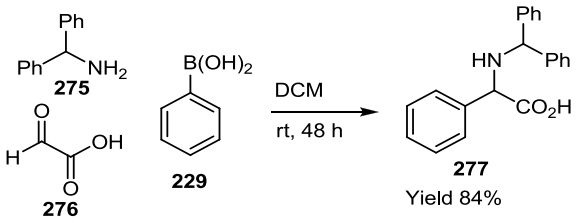

Figure 67 - Petasis Borono-Mannich reaction in the synthesis of α-arylglycines.

Detailed mechanistic studies have not been undertaken into the reaction, although initial reports suggest that both reactive imminium ion **283** and the quaternised boronic acid 'ate' complex **284** are required for addition to occur. However, the exact mode of addition of **283** to **284** is unknown. Reaction through complex **279** has also been suggested as a possibility (***Figure 68***).[2]

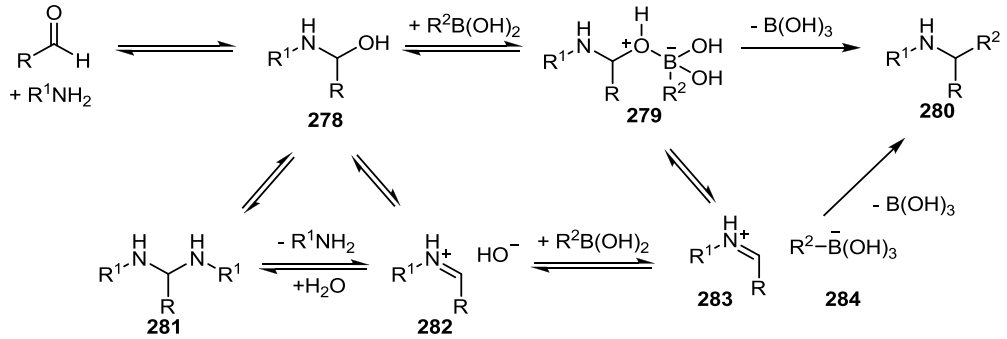

Figure 68 - Proposed mechanism for the Petasis Borono-Mannich reaction.

The reaction has mainly been limited to boronic acids with few boronate esters being shown to undergo the transformation.[35] Arylboronates containing electron donating groups exhibit higher reactivity than those bearing electron withdrawing substituents.[34] This improved reactivity of electron rich arenes reflects the nucleophilic roles of the arene in the mechanism of the reaction.

2.2.3.2 Rhodium Catalysed Conjugate Addition to α,β-Unsaturated Carbonyl Compounds

Miyaura and co-workers[36] reported the rhodium catalysed conjugate addition of aryl boronic acids to α,β-unsaturated ketones (***Figure 69***).

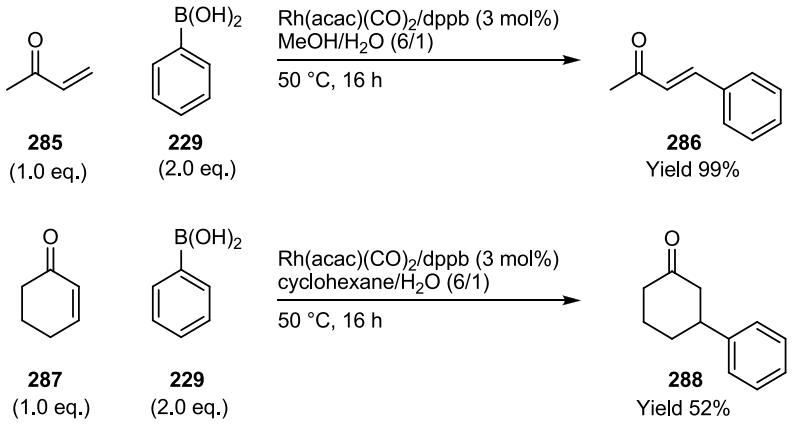

Figure 69 - Rhodium catalysed conjugate addition of phenylboronic acid to α,β-unsaturated ketones.

Hayashi and co-workers[37] have suggested a catalytic cycle for the reaction which proceeds via transmetalation of the boronic acid to rhodium followed by insertion of the enone into the Rh-Ph bond to give an oxa-π-allylrhodium species. Subsequent hydrolysis affords the product and regenerates the rhodium hydroxide active species.

The reaction has since been shown to be effective with enamides, enals and enoates as acceptors.[38] Asymmetric variants of the reaction have also been developed.[39] Aryl trifluoroborates exhibit the highest reactivity followed by aryl boronic acids and then aryl boronate esters.[2,38,39]

2.2.3.3 Oxidative Heck-Type Couplings to Alkenes

The palladium (0) catalysed oxidative Heck coupling of aryl boronic acids with olefins was first described by Uemura and co-workers.[40] Subsequent discoveries by Mori and co-workers[41] and Jung and co-workers[42] have shown that the reaction can be effectively carried out using $Pd^{(II)}$ chemistry with either copper (II) salts[41] or molecular oxygen[42] as the re-oxidant for the

palladium catalyst (***Figure 70***). The use of molecular oxygen or added chemical oxidants forms the major focus of reported examples.[43]

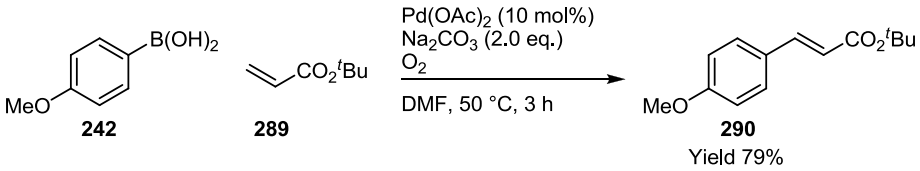

Figure 70 - Palladium (II) catalysed oxidative heck reaction of *para*-methoxyphenylboronic acid with *tert*-butyl-acrylate.

Reactions carried out under ruthenium[44] and rhodium[45] catalysis have also been developed along with asymmetric variants of the reaction.[43] For a more extensive insight into the chemistry, a recent review article has been published on the topic.[43]

2.2.3.4 Suzuki-Miyaura Cross-Coupling

The Suzuki-Miyaura reaction,[46] which forms a σ C-C bond *via* cross-coupling of an organoboron reagent and an organohalide or pseudohalide (OTf), is possibly one of the most important transformations of an aryl boronates.

Initial reports by Suzuki, Miyaura and co-workers[47] described the reaction of phenyl boronic acid with aryl halides under palladium (0) catalysis to yield biaryls. Since this publication, there have been significant adaptations made to the reaction conditions through variations in catalyst, ligands, bases, solvents and additives.

In analogy to other Pd cross-coupling reactions, the accepted mechanism proceeds via oxidative addition of the aryl halide to the $Pd^{(0)}$ catalyst giving a $Pd^{(II)}$ species. Subsequent transmetalation with the aryl boronate 'ate' complex and reductive elimination regenerates the catalyst releasing the biaryl product, (***Figure 71***).

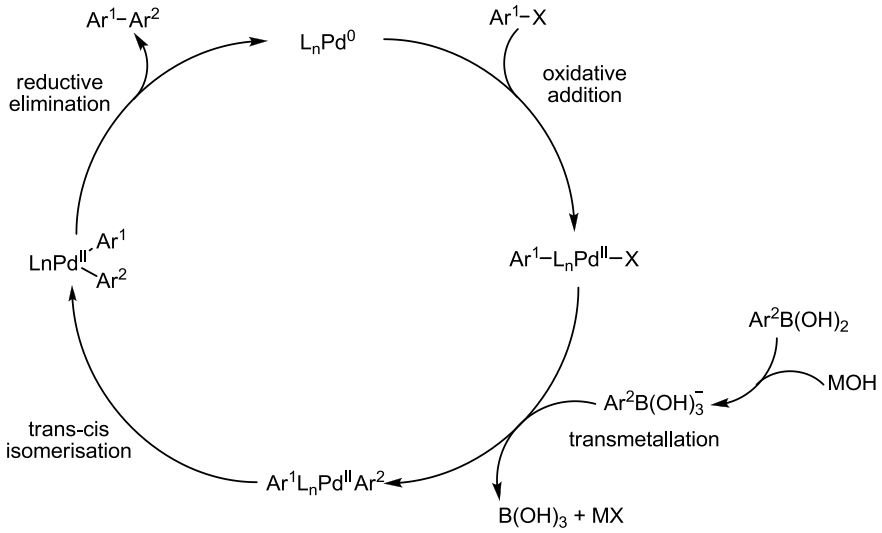

Figure 71 - Catalytic cycle of Suzuki-Miyaura reaction.[2]

A variety of Pd^0 sources, such as $Pd(PPh_3)_4$, have been used as catalysts as have combinations of Pd_2dba_3 with ligands which form ligated Pd^0 species *in situ*. The use of air stable Pd^{II} pre-catalysts such as $PdCl_2(PPh_3)_2$, $Pd(dppf)Cl_2$, $Pd(OAc)_2$/phosphine have also been effective in the reaction. Active Pd^0 species are generated from either phosphine mediated reduction[48] or from double transmetalation of aryl boronate to Pd^{II} followed by reductive elimination to give Pd^0 and the homocoupled biaryl.[49]

The transmetalation of aryl boronates to Pd^{II} halides has been shown to be ineffective due to the low nucleophilicity of the carbon attached to boron. In order to facilitate transmetalation, base is added. This causes quaternisation of boron to form a boron 'ate' complex ($Ar\text{-}B(OR)_3^-$) which increases nucleophilicity of the carbon attached to boron thus promoting transmetalation.[50] The reaction has been demonstrated with boronic acids, boronate esters and trifluoroborate salts.

The oxidative addition step has frequently been shown to be the rate determining step with the relative reactivity of aryl halides and pseudohalides being I>OTf>Br>>Cl.[46] As such, aryl iodides and bromides have classically been used for the transformation; however, through development of more electron donating ligand systems, aryl chlorides are now highly effective substrates (***Figure 72***).[51-53]

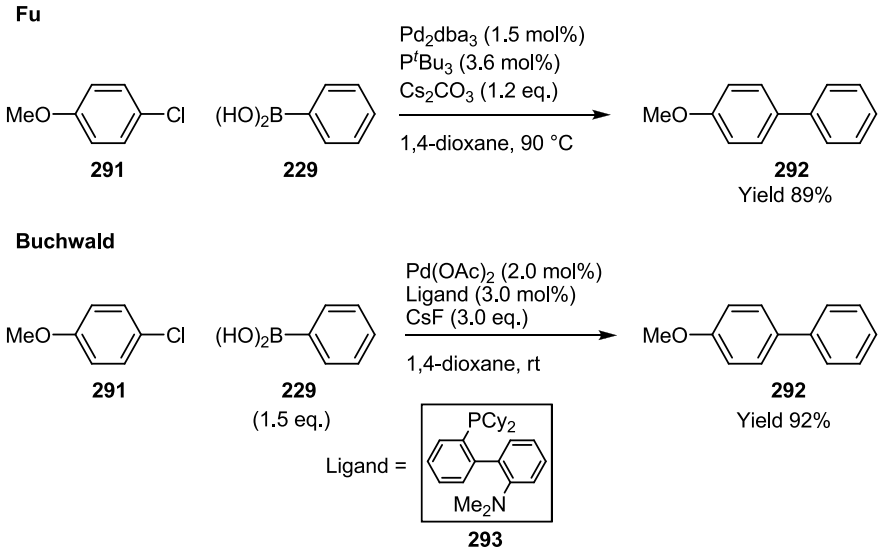

Figure 72 - Suzuki-Miyaura cross-coupling of chloro-4-methoxybenzene with phenyl boronic acid.[51,52]

2.3 One-pot Borylation/Functionalisation Strategies

One-pot reaction strategies carry out sequential reactions in a single reaction vessel without purification of the intermediate product. This approach has many benefits including increased procedural simplicity, reduction in waste, and removal of the need for extra purification.

This section will highlight how this concept has been applied to the functionalisation of arenes via iridium catalysed C-H borylation and subsequent one-pot functionalisation, without purification of the intermediate aryl boronate.

As discussed in sections 2.2.1 - 2.2.3, many transformations have been developed to convert the aryl boronates into useful functionality. Of these functionalisation methodologies, many have been developed into processes which can be carried out in the same reaction vessel as the C-H borylation reaction. Through this approach, aryl boronates generated by iridium catalysed C-H borylation have been transformed to aryl- boronic acids and trifluoroborate salts;[54] phenols;[55-57] aryl fluorides,[24] chlorides, [21] and bromides;[21] N-alkyl and aryl amines, diaryl ethers through Chan-Lam couplings,[58] enantioenriched chiral α,α-diaryl methylammonium chlorides through rhodium catalysed 1,2-addition to chiral sulfinimines;[59] and most widely studied, the synthesis of biaryls via the Suzuki-Miyaura reaction.[60-62]

Although success has been achieved in conversion of this wide range of transformations to one-pot processes there are still problems with the methodologies employed. These difficulties

and challenges are adequately highlighted in the attempts made towards the one-pot C-H borylation/Suzuki-Miyaura cross-coupling sequence. As this sequence will form the focus of the remainder of this chapter, the issues encountered in previous studies will be highlighted in this context.

2.3.1 One-pot C-H Borylation/Suzuki-Miyaura Cross-coupling strategies

The C-H borylation reaction, although highly efficient, has limitations concerning the solvents which can be used to carry out the transformation. Classically, C-H borylation has been carried out neat, in alkane solvents (hexane, octane, cyclohexane) or in THF.[63,64] However, the subsequent transformations often have very different solvent requirements. The incompatibility of solvents between reaction steps has been tackled by employing a number of methods. These will now be discussed in the context of the one-pot C-H borylation/Suzuki-Miyaura cross-coupling sequence.

One method to solve the problem of solvent incompatibility is to remove the first reaction solvent under reduced pressure, followed by addition of a reaction solvent compatible with the second reaction step. This strategy was described by Smith and co-workers.[60] Thus, following the borylation of 1,3-dichlorobenzene, the solvent was removed *in vacuo*. Subsequent addition of DME, 3-bromotoluene, $Pd(PPh_3)_4$ and K_3PO_4 afforded, after heating for 17 hours at 80 °C, the cross-coupled product in 80% yield (***Figure 73***).

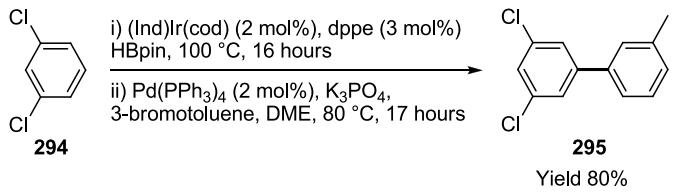

Figure 73 - C-H borylation of 1,3-dichlorobenzene and Suzuki-Miyaura cross-coupling with 3-bromotoluene.

In a similar fashion, Marder and co-workers[62] described a 'one-pot' borylation/Suzuki-Miyaura cross-coupling sequence of 2-substituted pyridines. After borylation in hexane, the

solvent was removed *in vacuo* and replaced by 1,4-dioxane. The subsequent cross-coupling with 1-iodonapthalene over 1 hour at 150 °C using focussed microwave heating afforded the desired biaryl products in 61% yield, (***Figure 74***).

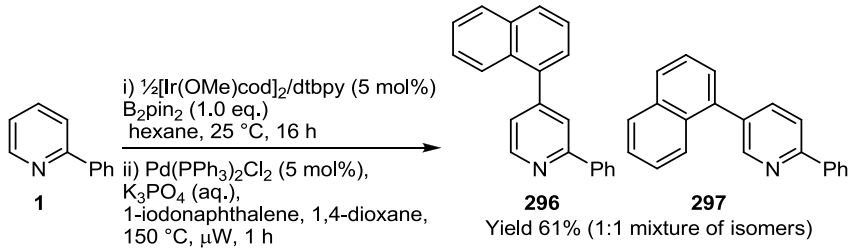

Figure 74 - Borylation of 2-phenyl pyridine and cross-coupling of the boronates formed with 1-iodonapthalene.

An alternative approach was employed by Ishiyama, Hartwig and Miyaura.[61] The borylation of 1,3-dichlorobenzene was carried out in hexane (2 mL). After borylation, DMF (4 mL) was added to the reaction vessel along with methyl-4-bromo-benzoate, $Pd(dppf)Cl_2$, K_3PO_4 to afford the desired biaryl in 91% yield (***Figure 75***).

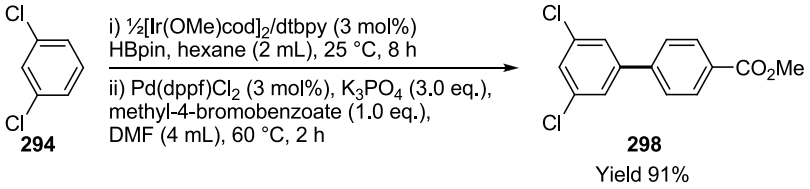

Figure 75 - Borylation with $[Ir(OMe)cod]_2$/dtbpy catalyst system followed by Suzuki-Miyaura reaction in DMF.

The methods described to date have either required removal of borylation solvent or addition of excess polar solvent. These methods both add to the procedural complexity of the reaction and increase waste. This is an area which the remainder of this chapter will address.

2.3.2 Conclusions

To date, the developments in the field have allowed the elaboration of a variety of arylboronates to a diverse range of functionalities with many of the reactions carried out in a one-pot manner with no purification of the intermediate aryl boronate. A common step in the majority of the transformations is to remove the volatiles from the borylation reaction. This step increases the procedural complexity, cost and waste from the reaction.

An alternative approach was sought through development of a one-pot, single solvent process whereby two reaction steps would be carried out in a single solvent. As a result, the need for an intermediate removal of volatiles step would be eliminated affording the cost, waste, time and procedural simplicity benefits discussed.

2.4 Results and Discussion

2.4.1 Initial Studies

As discussed in section 2.3, several groups have reported one-pot sequences combining C-H borylation with subsequent Suzuki-Miyaura cross-coupling. These methods allow access to biaryls via a one-pot procedure without purification of the intermediate aryl boronate. However, they require either the removal of volatiles, both borylation solvent and HBpin by-product as an intermediate step, or the addition of a large quantity of polar solvent (DMF, DME) in order enable the Suzuki-Miyaura reaction to proceed.[61,65]

In order to develop the methodology further, a single solvent system which would allow both steps to be carried out without the need for additional manipulations or secondary polar solvents, was sought.

The C-H borylation reaction has been reported to be most effective in non-polar solvents, with solvents such as octane, mesitylene, hexane and cyclohexane being routinely used for the reaction.[63,64] More recently, THF has been found to also be a viable solvent for the reaction.[21] However, there have been only a few studies examining the relative effectiveness of the solvents.[63,64] The relative rate of the borylation reaction was found to vary with solvent in the order hexane > mesitylene > DME > DMF. Coordinating solvents inhibit catalysis by binding to

the free site on the active species which is required for C-H activation. Consequently, it was decided to commence this study by carrying out a solvent screen comparing both previously reported and unreported solvents for the reaction.

In order to assess the different solvents, *m*-xylene was chosen as the model substrate as 1,3-arenes are known to borylate selectively at the mutually *meta*- position giving a single product.[1] Moreover, both the product and starting material are visible by GC-MS allowing for convenient monitoring of the reaction progress. This was assessed by preparation of an authentic sample of *m*-xylene-Bpin. Preparation was achieved by a literature procedure,[66] running the C-H borylation reaction in neat arene with $[Ir(OMe)cod]_2$ (1.5 mol%), dtbpy (3 mol%) and B_2pin_2 (1.0 eq.) affording the desired product in 94% isolated yield over a 6 hour reaction time.

The solvent screen was conducted by preparation of samples in a nitrogen filled glove box. The reagents, $[Ir(OMe)cod]_2$ (1.5 mol%), dtbpy (3 mol%) and B_2pin_2 (1.0 mmol), were combined in a Young's tap Schlenk tube followed by addition of the relevant solvent and the mixture was allowed to stir for 2 minutes to form the active catalyst species. The *m*-xylene substrate was then added and the sealed tube was removed from the glove box and heated in an aluminium heating block for 6 hours at 80 °C. Conversion was calculated by comparison of the integration areas of product and starting arene peaks in the GC-MS total ion chromatogram (***Figure 76***).

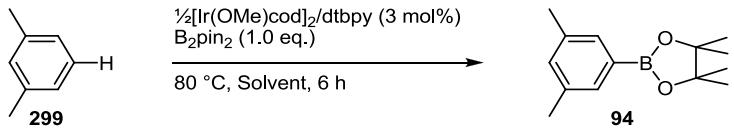

Figure 76 - C-H Borylation solvent screen.

Initial studies were carried out using solvents which were known to be good for Suzuki-Miyaura cross-coupling reactions. Ether based solvents containing steric groups to block coordination of the oxygen were chosen as another group of solvents to explore. THF has been shown to be a viable solvent for the C-H borylation reaction, but with reduced reactivity.[21] It

was postulated that a group to block oxygen coordination may allow for this class of more polar solvents to be viable for both reactions.

In agreement with previous reports in the literature,[63,64] polar coordinating solvents were ineffective in the C-H borylation reaction (***Table 6***, entries 1 - 3). However, both 2-methyl-THF and methyl tert-butyl ether (MTBE) were found to be efficient C-H borylation solvents. Of these, MTBE offered higher conversions over the same reaction time, so it was used for further studies.

Table 6 - C-H Borylation Solvent Screen.

Entry	Solvent	Conversion (%)
1	DMF	0
2	1,4-dioxane	25
3	MeCN	37
4	2-MeTHF	85
5	MTBE	100

MTBE has been widely used in process chemistry as a replacement for Et_2O and THF. The lower tendency to form peroxides, relative to other ether solvents, has made the use of MTBE popular. However there are no reports describing its use as a solvent for either the C-H borylation reaction or the Suzuki-Miyaura reaction. As a result, a simple preliminary evaluation of the viability of MTBE in the latter reaction was undertaken (***Figure 77***).

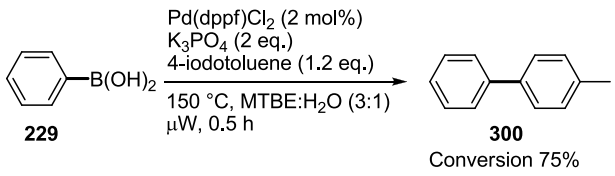

Figure 77 - Preliminary Suzuki-Miyaura reaction.

Following precedents for the Suzuki-Miyaura reaction developed in the group, phenyl boronic acid was heated in a microwave reactor at 150 °C for 30 minutes in the presence of

$Pd(dppf)Cl_2$ as catalyst, two equivalents of tri-potassium phosphate as base and 4-iodotoluene as the other coupling partner in a mixture of MTBE:H_2O (3:1).[62] The formation of product was confirmed by a molecular ion of 168 *m/z* in the GC-MS, giving 75% conversion based on recovered starting material. The remaining boronic acid was easily removed by silica gel flash column chromatography, but the biaryl product and homo-coupled biphenyl were inseparable, reflecting the highly similar structural nature of the two compounds. Having established that both the C-H borylation and Suzuki-Miyaura reaction could be undertaken in MTBE, optimised conditions for the Suzuki-Miyaura reaction were explored.

2.4.2 Catalyst and Base Screen

A catalyst and base screen was undertaken in order to find optimal conditions for the Suzuki-Miyaura reaction in MTBE (***Table 7***). Reactions were carried out using purified *m*-xylene-Bpin **94**. The initial reaction combined **94** with degassed water (0.8 mL), methyl 4-iodobenzoate (1.2 eq.), $Pd(dppf)Cl_2$ (3 mol%) and K_2CO_3 (2.0 eq.) in MTBE (2.4 mL) followed by heating at 80 °C for 3 hours. After this reaction time, minimal amounts of cross-coupled product could be detected by GC-MS. Further heating over 12 hours afforded 30% of the desired cross-coupled product, with the major product being the initial arene arising from proteodeboronation (***Table 7***, Entry 1 & 2). GC-MS analysis of the reaction mixture enabled conversion to product to be estimated by monitoring the relative integration of the peak at t = 5.74 min with a molecular ion of 232 *m/z* for the *m*-xylene boronate and the product peak at t = 8.32 min with a molecular ion of 240 *m/z* for the cross coupled product.

Common bases and catalysts for the Suzuki-Miyaura reaction were explored under the reaction conditions described above. All initial attempts using potassium carbonate and various different catalyst precursors did not give satisfactory conversions (***Table 7***, entries 3 & 4). Other potassium bases were explored, with potassium fluoride and K_3PO_4 giving 0 and 29% conversion, respectively (***Table 7***, entries 5 & 6). Barium hydroxide has been widely used within the group as a base for Suzuki-Miyaura reactions. The use of two equivalents of this base afforded 92% conversion and two and a half equivalents gave full conversion over the three hour reaction time (***Table 7***, entries 7 & 8). Whilst this combination of reagents was successful,

the use of barium hydroxide led to a thick slurry being generated during the reaction causing problems with work up and purification.

Consequently, alternative bases were then examined. Barium carbonate (***Table 7***, entry 9) gave no conversion to product suggesting that the nature of the cation was not a major factor. However, other hydroxide bases were effective, with both potassium and sodium hydroxide yielding near full conversion, along with easier work up (***Table 7***, entries 10 - 13). The optimised base and catalyst combination were chosen as $Pd(dppf)Cl_2$ and potassium hydroxide (5.0 eq.) (***Table 7***, entry 13). The reaction was shown to be effective with 2.5 equivalents of KOH but, in order to ensure full conversion, it was decided to use 5.0 equivalents for the reaction.

Table 7 - Catalyst & Base screen for Suzuki-Miyaura cross-coupling reaction.

Entry	Catalyst[a]	Base (eq.)	MTBE (mL)	H_2O (mL)	Time (h)	Conv. (%)[b]
1	$Pd(dppf)Cl_2$	K_2CO_3 (2.0)	2.4	1.0	3	0
2	$Pd(dppf)Cl_2$	K_2CO_3 (2.0)	2.4	1.0	12	30
3	$Pd(PPh_3)_2Cl_2$	K_2CO_3 (3.5)	2.4	1.0	3	0
4	$Pd(dppf)Cl_2$	K_2CO_3 (4.5)	2.4	1.0	3	0
5	$Pd(PPh_3)_2Cl_2$	KF (3.5)	2.4	1.0	3	0
6	$Pd(dppf)Cl_2$	K_3PO_4 (2.5)	2.4	1.0	3	29
7	$Pd(PPh_3)_2Cl_2$	$Ba(OH)_2$ (2.0)[c]	2.4	1.0	3	92
8	$Pd(dppf)Cl_2$	$Ba(OH)_2$ (2.5)[c]	2.4	1.0	3	100
9	$Pd(dppf)Cl_2$	$BaCO_3$ (2.5)	2.4	1.0	3	0
10	$Pd(dppf)Cl_2$	NaOH (2.5)	2.4	1.0	3	90
11	$Pd(dppf)Cl_2$	NaOH (5.0)	2.4	1.0	3	100
12	$Pd(dppf)Cl_2$	KOH (2.5)	2.4	1.0	3	100
13	$Pd(dppf)Cl_2$	KOH (5.0)	2.4	1.0	3	100
14	$Pd(dppf)Cl_2$	NaOH (5.0)	2.4	0.0	3	0

[a] 3 mol% catalyst loading, [b] GC-MS conversion, [c] $Ba(OH)_2 \cdot 8H_2O$ used

Significantly, the reaction was also shown to be ineffective in the absence of water (***Table 7***, entry 14). Moreover, the order of addition of the reagents for the cross-coupling reaction had a significant influence upon the outcome of the tandem reaction. It was found that if the catalyst and base were added before the water, reproducibility of the chemistry was problematic. However, when the water was added first, followed by the remaining reagents, the reaction proceeded effectively. As long as this order of addition was followed the reaction showed high reproducibility. Effervescence occurs upon addition of water, which is thought to be due to reaction with the HBpin by-product of the C-H borylation reaction to form a pinB-O-Bpin compound, visible by GC-MS.

2.4.3 One-Pot, Single-Solvent C-H Borylation/Suzuki-Miyaura Cross-Coupling Sequence

A key goal for the development of a single solvent sequence was to increase procedural simplicity. As such, the standard experimental procedure, as described for the solvent screen, was modified to allow the reagents to be added as a stock solution. The catalyst components, $[Ir(OMe)cod]_2$ (131 mg, 0.2 mmol), dtbpy (105 mg, 0.4 mmol), and B_2pin_2 (713 mg, 2.75 mmol) were added to a sealable vial and MTBE (26.4 mL) was added. The stock solution contained 20% of the B_2pin_2 required for the reaction and as such the remaining 80% (200 mg) was added to the Young's tap tube along with the substrate (1.0 mmol). The catalyst solution (2.0 mL) was then added along with a further MTBE (0.4 mL). The stock solution gave a catalyst loading of 3 mol% with 1.0 mmol of B_2pin_2.

With optimised conditions developed for each reaction step in isolation, the one-pot sequence was explored. Following borylation of *m*-xylene over a 6 hour reaction time, water, catalyst and base were added followed by methyl 4-iodobenzoate. Resealing of the reaction vessel and heating for a further 3 hours afforded the desired unsymmetrical biaryl in a 90% yield. The reaction was monitored by GC-MS with samples taken after the C-H borylation reaction and again upon completion of the Suzuki-Miyaura reaction (***Figure 78***). Both the C-H borylation and Suzuki-Miyaura cross-coupling were efficient and selective for formation of the

desired product with no reagent degradation. The only side product was 6 mol% of the biaryl 3,3',5,5'-tetramethylbiphenyl **301** formed by reduction of Pd^{II} to Pd^{0} in the catalyst activation step..

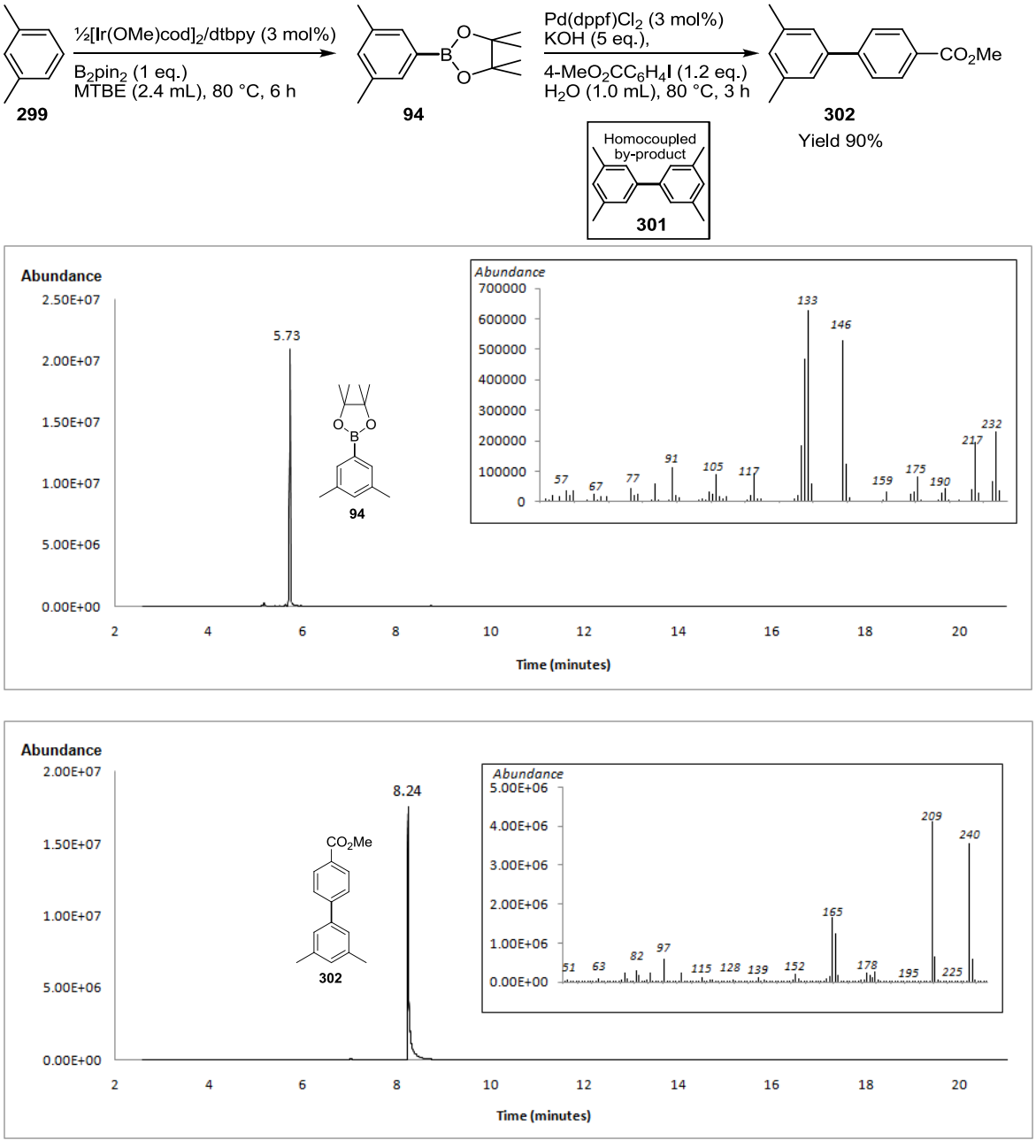

Figure 78 - Crude GS-MS chromatogram of **94** (top) and **302** (bottom).

The regio-chemical identity of the product was determined by ^{1}H NMR spectroscopy which showed a pair of doublets at 8.08 ppm and 7.64 ppm integrating to two protons each, with a coupling constant of J = 8.5 Hz consistent with the aromatic protons of a 1,4-disubstituted benzene. The presence of the 1,3,5-trisubstituted arene is confirmed by broad singlets for the

aromatic protons at 7.23 ppm and 7.03 ppm in a 2:1 ratio. The signal at 3.93 ppm corresponds to methyl ester group with the methyl groups on the 1,3,5-trisubstituted benzene giving rise to a singlet at 2.38 ppm, integrating for six protons (***Figure 79***).

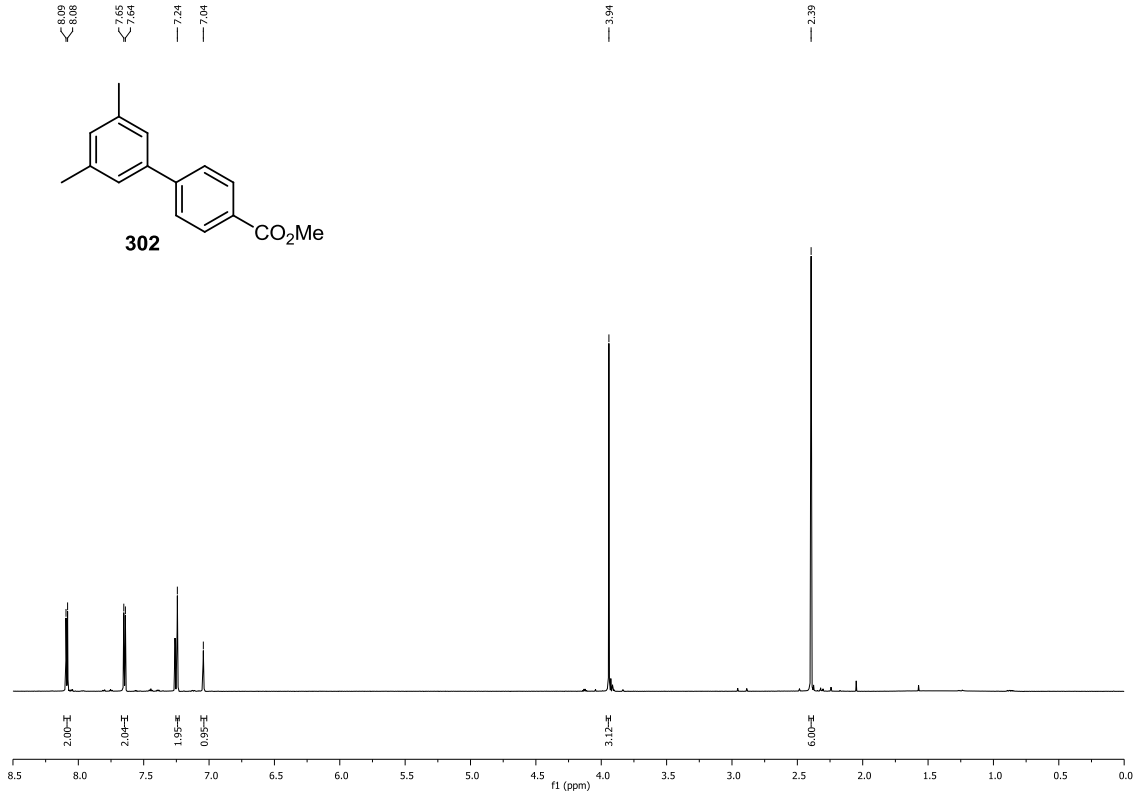

Figure 79 - ^{1}H NMR spectrum of **302** (400 MHz, $CDCl_3$).

With a highly efficient reaction procedure developed, a range of 1,3-arenes were chosen bearing groups with differing electronic effects of the substituents on the ring (***Figure 80***). The selectivity of the C-H borylation reaction is consistent with previous examples in the literature.[1] The results demonstrate the applicability of the tandem sequence to substrates containing a wide variety of functionality.

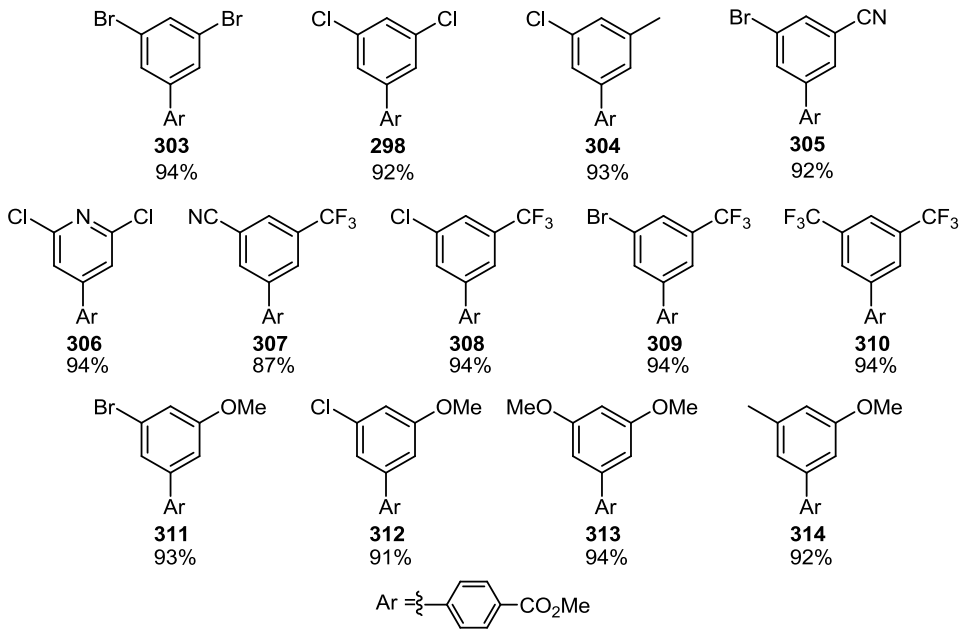

Figure 80 - Substrate scope of the one-pot procedure.

In each case, the reactions preceded in high yield over the two reaction steps. A maximum yield of 94% was achieved for the reaction sequence, due to the formation of 6 mol% homocoupled biaryl from the reduction of Pd^{II} to Pd^{0} as discussed in section 2.2.3.4,[49] confirmed by ^{1}H NMR spectroscopy with characteristic singlets at 7.20 ppm, 6.98 ppm and 2.38 ppm in a 2:1:6 ratio, respectively (***Figure 81***). Analysis by GC-MS showed a molecular ion of 210 *m/z* consistent with **301**.

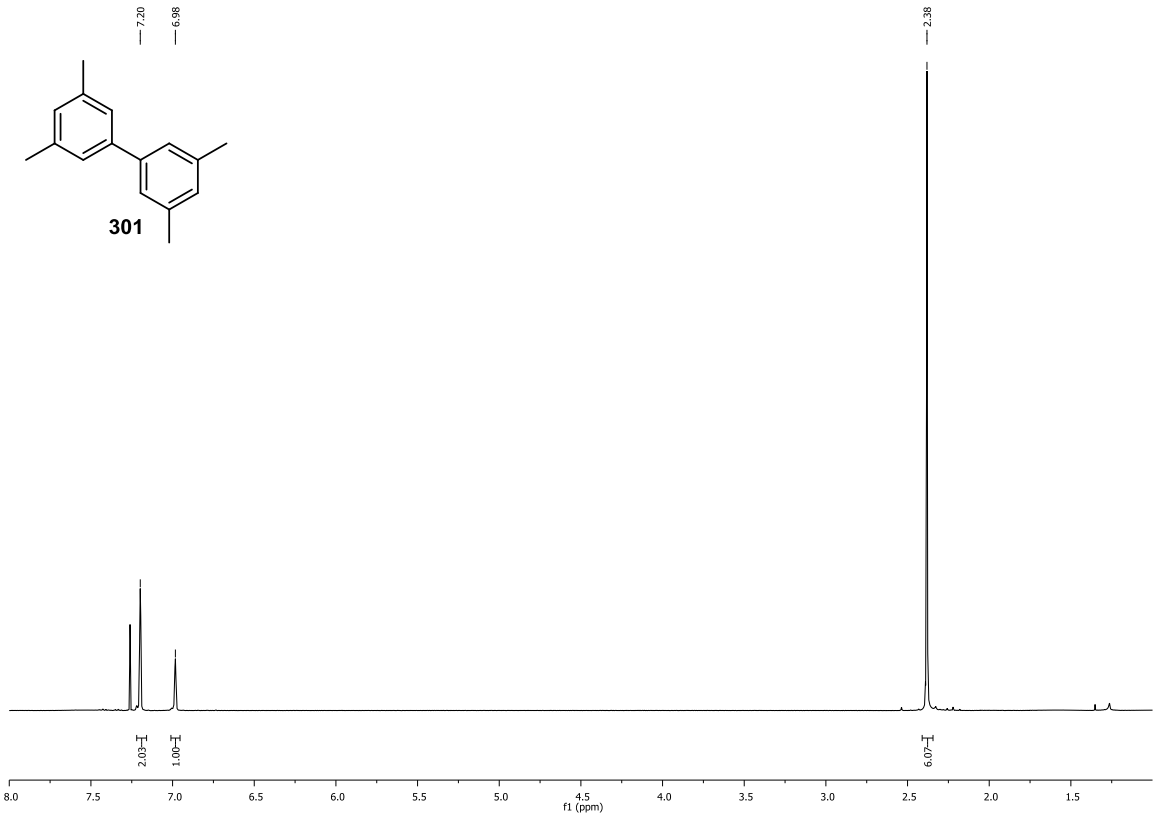

Figure 81 - ^{1}H NMR spectrum of **301** (400 MHz, $CDCl_3$).

The effectiveness of the sequence has been demonstrated by both the C-H borylation and Suzuki-Miyaura reactions reaching quantitative conversion and isolated yields. It should also be noted that base sensitive groups such as methyl esters were not affected by the reaction conditions and remained intact in the isolated products confirmed by characteristic ^{1}H NMR signal between 3.93 - 3.96 ppm.

2.4.4 Variation of the Aryl Halide Coupling Partner

As a wide range of different substituents were tolerated on the arene being borylated, a range of aryl halides containing electron withdrawing and donating substituents were investigated for use in the second step the one-pot reaction (***Figure 82, Table 8***).

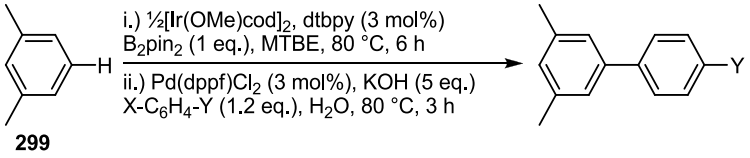

Figure 82 - One-pot C-H Borylation/Suzuki-Miyaura coupling strategy.

Table 8 - Aryl halide coupling partners for one-pot sequence.

Entry	X	Y	Product	Yield (%)[a,b]
1	I	CO_2Me	**301**	90[c]
2	I	Me	**315**	>95[d]
3	I	CF_3	**316**	91[c]
4	I	OMe	**317**	90[c]
5	I	NO_2	**318**	93[c]
6	Br	CO_2Me	**301**	92[c]
7	Br	CN	**319**	92[c]
8	Br	NMe_2	**320**	84
9	Br	Me	**315**	94[d]
10	Cl	CN	**319**	50[c,e]

a. Isolated, purified yields.

b. Small amounts of biaryl arising from homo-coupling of arylboronate ester detected in all cases by GC-MS.

c. Homocoupled product (6%) arising from arylboronate isolated.

d. No attempt was made to separate homocoupled by-product from cross-coupled product.

e. Unreacted boronate ester (44%) was recovered.

The one-pot methodology was tolerant to aryl iodides with electron donating (***Table 8***, entries 2 & 4)) and electron withdrawing substituents (***Table 8***, entries 1, 3 and 5). The reaction with aryl bromides containing similar functionalities (***Table 8***, entries 6 - 9) also proceeded well. When the reaction was carried out with 4-chlorobenzonitrile (***Table 8***, entry 10) a moderate yield of 50% was achieved with 45% of the intermediate aryl boronate recovered from

the reaction. This observation demonstrates that although the reaction is being carried out in the presence of 5.0 equivalents of KOH, the arylboronate does not undergo proteodeboronation.

Upon isolation of the reaction product, it was possible in a number of cases (***Table 8***, entries 1, 3 - 7 & 10) to isolate 6% of the homo-coupled arene arising from the reduction of 3 mol% of the Pd^{II} to Pd^{0} via double transmetalation of the aryl boronate followed by reductive elimination of the homo-coupled product, as previously discussed in section 2.2.3.4.

2.5 Conclusions

A fast and efficient method for the synthesis of unsymmetrical biaryls in a single reaction solvent has been demonstrated. The methodology has been shown to borylate arenes containing a wide range of functionalities efficiently and with high regiocontrol and quantitative conversion. The intermediate arylboronates were then efficiently converted to biaryls using simple and readily available reagents to offer a process with procedural simplicity and reduced cost and waste compared to previous reports in the literature.[60-62,65]

After the publication of this work, Sniekus and co-workers[67] employed this one-pot single solvent sequence noting that the procedure afforded cleaner reactions and improved yields of biaryl products compared to alternative processes. This report further highlights the benefits of the methodology.

2.6 Chapter II - References

1 Mkhalid, I. A. I.; Barnard, J. H.; Marder, T. B.; Murphy, J. M.; Hartwig, J. F., *Chem. Rev.* **2010**, *110*, 890.

2 Hall, D. G., *Boronic Acids: Preparation and Applications in Organic Synthesis and Medicine*. Wiley-VCH: Weinheim, 2005; p 568.

3 Ainley, A. D.; Challenger, F., *J. Chem. Soc.* **1930**, 2171.

4 Simon, J.; Salzbrunn, S.; Prakash, G. K. S.; Petasis, N. A.; Olah, G. A., *J. Org. Chem.* **2000**, *66*, 633.

5 Webb, Kevin S.; Levy, Daniel, *Tetrahedron Lett.* **1995**, *36*, 5117.

6 Nanni, E. J.; Sawyer, D. T., *J. Am. Chem. Soc.* **1980**, *102*, 7591.

7 Kianmehr, E.; Yahyaee, M.; Tabatabai, K., *Tetrahedron Lett.* **2007**, *48*, 2713.

8 Xu, J.; Wang, X.; Shao, C.; Su, D.; Cheng, G.; Hu, Y., *Org. Lett.* **2010**, *12*, 1964.

9 Kuivila, H. G., *J. Am. Chem. Soc.* **1954**, *76*, 870.

10 Kuivila, H. G.; Armour, A. G., *J. Am. Chem. Soc.* **1957**, *79*, 5659.

11 Salzbrunn, S.; Simon, J.; Prakash, G. K. S.; Petasis, N. A.; Olah, G. A., *Synlett* **2000**, 1485.

12 Crivello, J. V., *J. Org. Chem.* **1981**, *46*, 3056.

13 Prakash, G. K. S.; Panja, C.; Mathew, T.; Surampudi, V.; Petasis, N. A.; Olah, G. A., *Org. Lett.* **2004**, *6*, 2205.

14 Tron, G. C.; Pirali, T.; Billington, R. A.; Canonico, P. L.; Sorba, G.; Genazzani, A. A., *Med. Res. Rev.* **2008**, *28*, 278.

15 Morgan, J.; Pinhey, J. T., *J. Chem. Soc., Perkin. Trans. 1* **1990**, 715.

16 Huber, M-L.; Pinhey, J. T., *J. Chem. Soc., Perkin. Trans. 1* **1990**, 721.

17 Grimes, K. D. ; Gupte, A.; Aldrich, C. C. , *Synthesis* **2010**, *2010*, 1141.

18 Rao, H.; Fu, H.; Jiang, Y.; Zhao, Y., *Angew. Chem. Int. Ed.* **2009**, *48*, 1114.

19 Thiebes, C.; Prakash, G. K. S.; Petasis, N. A.; Olah, G. A., *Synlett* **1998**, 141.

20 Thompson, A. L. S.; Kabalka, G. W.; Akula, M. R.; Huffman, J. W., *Synthesis* **2005**, *4*, 547.

21 Murphy, J. M.; Liao, X.; Hartwig, J. F., *J. Am. Chem. Soc.* **2007**, *129*, 15434.

22 Wu, H.; Hynes, J., *Org. Lett.* **2010**, *12*, 1192.

23 Diorazio, L. J.; Widdowson, D. A.; Clough, J. M., *Tetrahedron* **1992**, *48*, 8073.

24 Furuya, T.; Ritter, T., *Org. Lett.* **2009**, *11*, 2860.

25 Martin, A. R.; Y. Yang, *Acta Chem. Scand.* **1993**, *47*, 221.

26 Liskey, C. W.; Liao, X.; Hartwig, J. F., *J. Am. Chem. Soc.* **2010**, *132*, 11389.

27 Chu, L.; Qing, F-L., *Org. Lett.* **2010**, *12*, 5060.

28 Chan, D. M. T.; Monaco, K. L.; Wang, R-P.; Winters, M. P., *Tetrahedron Lett.* **1998**, *39*, 2933.

29 Lam, P. Y. S.; Clark, C. G.; Saubern, S.; Adams, J.; Winters, M. P.; Chan, D. M. T.; Combs, A., *Tetrahedron Lett.* **1998**, *39*, 2941.

30 Evans, D. A.; Katz, J. L.; West, T. R., *Tetrahedron Lett.* **1998**, *39*, 2937.

31 Ley, S. V.; Thomas, A. W., *Angew. Chem. Int. Ed.* **2003**, *42*, 5400.

32 Chan, D. M. T.; Monaco, K. L.; Li, R.; Bonne, D.; Clark, C. G.; Lam, P. Y. S., *Tetrahedron Lett.* **2003**, *44*, 3863.

33 Petasis, N. A.; Zavialov, I. A., *J. Am. Chem. Soc.* **1997**, *119*, 445.

34 Petasis, N. A.; Goodman, A.; Zavialov, I. A., *Tetrahedron* **1997**, *53*, 16463.

35 Candeias, N. R.; Montalbano, F.; Cal, P. M. S. D.; Gois, P. M. P., *Chem. Rev.* **2010**, *110*, 6169.

36 Sakai, M.; Hayashi, H.; Miyaura, N., *Organometallics* **1997**, *16*, 4229.

37 Hayashi, T.; Takahashi, M.; Takaya, Y.; Ogasawara, M., *J. Am. Chem. Soc.* **2002**, *124*, 5052.

38 Fagnou, K.; Lautens, M., *Chem. Rev.* **2002**, *103*, 169.

39 Hayashi, T.; Yamasaki, K., *Chem. Rev.* **2003**, *103*, 2829.

40 Cho, C. S.; Uemura, S., *J. Organomet. Chem.* **1994**, *465*, 85.

41 Du, X.; Suguro, M.; Hirabayashi, K.; Mori, A.; Nishikata, T.; Hagiwara, N.; Kawata, K.; Okeda, T.; Wang, H. F.; Fugami, K.; Kosugi, M., *Org. Lett.* **2001**, *3*, 3313.

42 Jung, Y. C.; Mishra, R. K.; Yoon, C. H.; Jung, K. W., *Org. Lett.* **2003**, *5*, 2231.

43 Karimi, B.; Behzadnia, H.; Elhamifar, D.; Akhaven, P. F.; Esfahani, F. K., *Synthesis* **2010**, *9*, 1399.

44 Farrington, E. J.; Brown, J. M.; Barnard, C. F. J.; Rowsell, E., *Angew. Chem. Int. Ed.* **2002**, *41*, 169.

45 Zou, G.; Wang, Z.; Zhu, J.; Tang, J., *Chem. Commun.* **2003**, 2438.

46 Miyaura, N.; Suzuki, A., *Chem. Rev.* **1995**, *95*, 2457.

47 Miyaura, N.; Yanagi, T.; Suzuki, A., *Synth. Commun.* **1981**, *11*, 513.

48 Amatore, C.; Jutand, A.; M'Barki, M. A., *Organometallics* **1992**, *11*, 3009.

49 Parrish, J. P.; Jung, Y. C.; Floyd, R. J.; Jung, K. W., *Tetrahedron Lett.* **2002**, *43*, 7899.

50 Miyaura, Norio, *J. Organomet. Chem.* **2002**, *653*, 54.

51 Old, D. W.; Wolfe, J. P.; Buchwald, S. L., *J. Am. Chem. Soc.* **1998**, *120*, 9722.

52 Littke, A. F.; Fu, G. C., *Angew. Chem. Int. Ed.* **1998**, *37*, 3387.

53 Barder, T. E.; Walker, S. D.; Martinelli, J. R.; Buchwald, S. L., *J. Am. Chem. Soc.* **2005**, *127*, 4685.

54 Murphy, J. M.; Tzschucke, C. C.; Hartwig, J. F., *Org. Lett.* **2007**, *9*, 757.

55 Maleczka, R. E., Jr.; Shi, F.; Holmes, D.; Smith, M. R., III., *J. Am. Chem. Soc.* **2003**, *125*, 7792.

56 Shi, F.; Smith, M. R., III.; Maleczka, R. E., Jr., *Org. Lett.* **2006**, *8*, 1411.

57 Marshall, L. J.; Cable, K. M.; Botting, N. P., *Tetrahedron Lett.* **2010**, *51*, 2690.

58 Tzschucke, C.; Murphy, J. M.; Hartwig, J. F., *Org. Lett.* **2007**, *9*, 761.

59 Boebel, T. A.; Hartwig, J. F., *Tetrahedron* **2008**, *64*, 6824.

60 Cho, J.; Tse, M. K.; Holmes, D.; Maleczka, R. E., Jr.; Smith, M. R., III., *Science* **2002**, *295*, 305

61 Ishiyama, T.; Nobuta, Y.; Hartwig, J. F.; Miyaura, N., *Chem. Commun.* **2003**, 2924.

62 Mkhalid, I. A. I.; Coventry, D. N.; Albesa-Jove, D.; Batsanov, A. S.; Howard, J. A. K.; Perutz, R. N.; Marder, T. B., *Angew. Chem. Int. Ed.* **2006**, *45*, 489.

63 Ishiyama, T.; Isou, H.; Kikuchi, T.; Miyaura, N., *Chem. Commun.* **2010**, *46*, 159.

64 Ishiyama, T.; Takagi, J.; Hartwig, J. F.; Miyaura, N., *Angew. Chem. Int. Ed.* **2002**, *41*, 3056.

65 Kikuchi, T.; Nobuta, Y.; Umeda, J.; Yamamoto, Y.; Ishiyama, T.; Miyaura, N., *Tetrahedron* **2008**, *64*, 4967.

66 Ishiyama, T.; Takagi, J.; Ishida, K.; Miyaura, N.; Anastasi, N. R.; Hartwig, J. F., *J. Am. Chem. Soc.* **2002**, *124*, 390.

67 Hurst, T.; Macklin, T.; Becker, M.; Hartmann, E.; Kügel, W.; Parisienne-La Salle, J. C.; Batsanov, A.; Marder, T. B.; Snieckus, V., *Chem. Eur. J.* **2010**, *16*, 8155.

CHAPTER III - MICROWAVE ACCELERATED C-H BORYLATION

3.1 Introduction

As discussed in Chapter II, significant progress has been made in the development of processes to elaborate the aryl boronate group to synthetically useful functionalities. The majority of work in the field has focussed on developing one-pot methodologies with little attention devoted to the improvement of the C-H borylation reaction procedure. Many reactions reported in the literature require extend reaction times (16 h) at elevated temperatures (80 - 150 °C).[1] The goal of this chapter was to provide a method for the rapid synthesis of aryl boronates using iridium catalysed C-H borylation.

This chapter will describe work which resulted in the development of a general procedure for the microwave accelerated C-H borylation reaction. This gives access to borylated products from a diverse range of substrate classes in vastly reduced reaction times relative to the standard reaction when carried out at the same reaction temperature.

This chapter will discuss the background of using microwave irradiation to facilitate chemical reactions. The theory of how microwaves heat reactions will be discussed along with the effects which have been observed as a result. Previous reports of using microwave irradiation to facilitate the C-H borylation reactions will be examined and contrasted to the experimental approach which will be described subsequently. Along with the observation of an acceleration effect, the cause of the acceleration will also be discussed in context of the experimental work carried out.

3.2 Microwave Chemistry

The ideal chemical transformation that achieves full conversion in minutes and is carried out at room temperature and atmospheric pressure is often not an achievable goal.[2,3] Many synthetically important reactions require heating to elevated temperatures for prolonged periods of time to achieve high conversions to the desired products.[2,3]

Classical methods for facilitating these extended reactions have involved the use of round bottom flasks, equipped with condensers, heated by oil baths or heating blocks. In these situations, the reaction temperature is controlled by the boiling point of the solvent of choice. Due to heat being transferred from the outside in, heating of the reaction medium relies upon the

thermal conductivity of the equipment and solvent being used and as such is an inefficient method of heat transfer.

In recent years, a contrasting method for heating has been developed which utilises microwave radiation to transfer energy to the reaction. This field has been more recently termed Microwave-Assisted Organic Synthesis (MAOS). The field of MAOS has been widely studied since the first example was described in 1986 by Gedye[4] and Giguere/Majetich[5] (***Figure 83***).

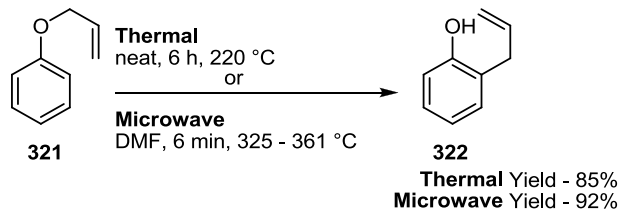

Figure 83 - Microwave accelerated Claisen-rearrangement.[5]

Following this initial discovery, more than 4000 papers have published on the topic.[6] Microwave heating has been applied to a vast array of reaction types and there have been a number of reviews describing the range of transformations that can be carried out.[2,3,7] Consequently, this introduction will not aim to re-review this wealth of literature. However, it will highlight the theory behind the mechanism of heating under microwave conditions and further explore some key reactions carried out using this technique.

3.2.1 Microwave Heating Theory

Microwave radiation forms part of the electromagnetic spectrum in the frequency range of 0.3 - 300 GHz. The frequency of microwaves used in all domestic microwave ovens and chemical synthesis reactors is 2.45 GHz which corresponds to a wavelength of 1.22 m. This frequency is used to avoid interference with frequencies used for telecommunication applications.[2,3]

At a frequency of 2.45 GHz, a microwave photon has an energy of 0.0016 eV which is too low to cause cleavage of a chemical bond and is also lower than the energy of Brownian motion.

With such low energy photons, microwave radiation cannot promote chemical reactions by inducing the breaking of bonds.[8-11]

An alternative theory for the way that microwave irradiation is able to facilitate chemical reactions is by the provision of efficient heating of reaction media. This is caused by microwave dielectric heating. The effectiveness of this process is strongly dependent on the ability of reaction components (solvent or reagents) to absorb the microwave energy and convert it to heat.

This heating of reaction components is caused by two effects; ionic conduction and dipole polarisation. When the reaction is subjected to microwave irradiation the dipoles and/or ions attempt to align with the applied electric field. The oscillation of the field leads to the polar species attempting to realign with the alternating electric field and causing heating through 'friction' with neighbouring molecules. The heat generated is related to the ability of the reaction media to carry out this process. If polar species do not have sufficient time to align with the field or realign too quickly then heating does not occur. The microwave frequency of 2.45 GHz allows polar molecules to align with the field, but insufficient time to allow them to follow the field oscillations exactly.[8,9]

This ability to convert the applied electromagnetic energy to heat for a given frequency is called the loss factor or tan δ. The tan δ is determined by the ability of a solvent to store electrical potential energy under the influence of an electric field (dielectric constant, ε′) along with a solvent's efficiency of converting absorbed energy into heat (dielectric loss, ε″) (***Figure 84***).[10,11]

$$\tan\delta = \frac{\varepsilon''}{\varepsilon'}$$

Figure 84 - Calculation of tan δ from dielectric constant, ε′ and dielectric loss ε″.

Solvents can be generally classified into good (tan δ > 0.5), medium (tan δ 0.1 - 0.5) and poor (tan δ < 0.1) microwave absorbers. A range of common organic solvents with their associated dielectric constant (ε) and loss tangent (tan δ) are listed in ***Table 9***.[2,3]

Table 9 - Dielectric constant (ε) and Loss factor (tan δ) for common organic solvents.

Entry	Solvent	ε	tan δ	Entry	Solvent	ε	tan δ
1	ethylene glycol	37.0	1.350	10	water	80.4	0.123
2	ethanol	24.6	0.941	11	chloroform	4.8	0.091
3	DMSO	47	0.825	12	acetonitrile	36.0	0.062
4	methanol	32.7	0.659	13	ethyl acetate	6.0	0.059
5	nitrobenzene	34.8	0.589	14	acetone	20.6	0.054
6	NMP	32.2	0.275	15	THF	7.6	0.047
7	acetic acid	6.2	0.174	16	DCM	9.1	0.042
8	DMF	36.7	0.161	17	toluene	2.2	0.040
9	DCE	10.4	0.127	18	hexane	1.9	0.020

Data obtained from ref 10 & 11

The most efficient heating is achieved with solvents of high tan δ, but it is still possible to use low tan δ, 'microwave transparent', solvents to carry out microwave reactions. This is due to the ability of other reaction components containing a dipole to respond to the electromagnetic radiation.[2,3,9]

Organic synthesis has classically been carried out using an external heat source, such as an oil bath or heating block. These methods of heat transfer to the reaction medium rely on good thermal conductivity of the reaction vessel and efficient mixing as heat transfer only takes place at the walls of the reaction vessel. In contrast to classical heating, microwave irradiation allows efficient and fast bulk heating of the reaction medium. The vessels typically used for microwave reactions are near transparent to microwave irradiation and as such an inverse temperature gradient to classical thermal heating is observed (***Figure 85***).[12]

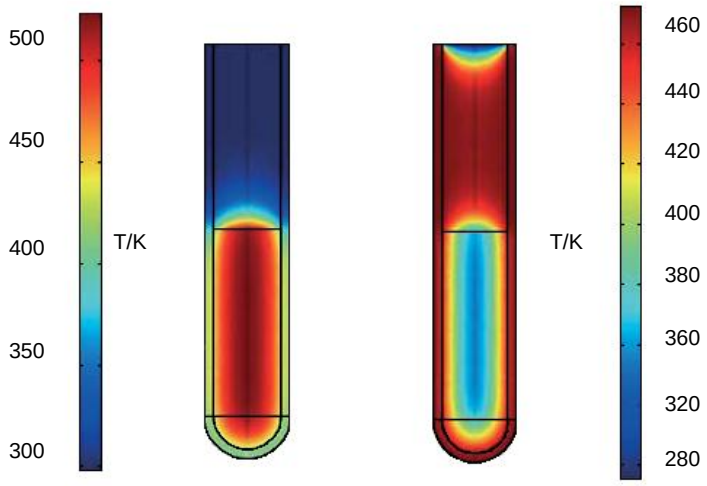

Figure 85 - Temperature profile after 1 minute of heating for microwave reaction (left) and oil bath heated reaction (right).[12]

3.2.2 Microwave Effects

One key benefit of microwave heated reactions is the ability to access higher reaction temperatures than would not be easily accessible under reflux conditions.

Rate enhancements between classically heated and microwave reactions are often observed when microwave reactions are carried out at a higher reaction temperature compared to the classically heated reaction. This was demonstrated by Mingos and co-workers[8] who applied the Arrhenius law [$k = A \exp(-E_a/RT)$] to a transformation which at 27 °C reaches 90% conversion in 68 days but would only require 1.61 seconds to reach the same conversion if carried out at 227 °C (***Table 10***).[8]

Table 10 - Temperature time relationship for simple first order reaction.[3]

Entry	Temperature / °C	k / s^{-1}	time[a]
1	27	1.55×10^{-7}	68 days
2	77	4.76×10^{-5}	13.4 hours
3	127	3.49×10^{-3}	11.4 minutes
4	177	9.86×10^{-2}	23.4 seconds
5	227	1.43	1.61 seconds

[a] required to reach 90% conversion

This degree of temperature increase is possible when using microwave irradiation as strongly absorbing solvents such as methanol can be heated to 160 °C in a sealed microwave vessel in a matter of seconds (***Figure 86***).[3]

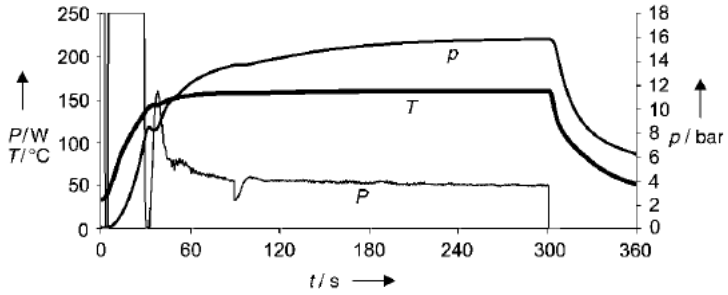

Figure 86 - Temperature profile for sample of methanol heated under microwave conditions (*p*=pressure, T = temperature, P = power).

3.2.2.1 Specific Microwave Effects

The rate enhancement observed by this increase in reaction temperature is common in many of the reports in the literature. However, there are also examples where it has been suggested that the acceleration effect is not due simply to rate enhancement from the higher reaction temperature. These have been termed 'specific microwave effects' and are cases in which the acceleration enhancements cannot be achieved by conventional heating.[13-16] The nature of these effects include the superheating of solvent (***Figure 86***).[17,18] Use of passive heating elements (e.g. silicon carbide or graphite-doped Teflon stirrer bar) allow poor microwave absorbing solvent to reach elevated temperatures (***Figure 87***).[2,19] Formation of molecular radiators from strongly absorbing reagents in a homogeneous reaction or metal nanoparticles can form microscopic hotspots in the reaction (***Figure 87***).[10,20-22] Removal of wall effects by rapid centre out heating has also been implicated as a specific microwave effect (***Figure 87***).[12,23,24] These enhancements are still controlled thermally, and as a consequence it is not be possible to determine the exact reaction temperature due to areas of higher temperature within the reaction.[2,3]

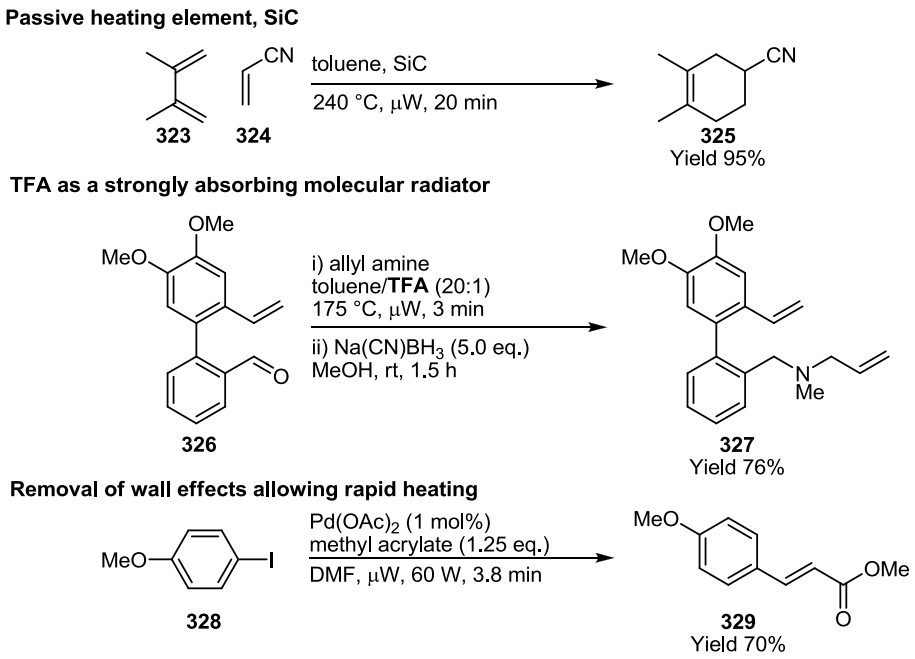

Figure 87 - Specific Microwave effects.

3.2.2.2 Non-thermal Microwave Effects

Not limited to thermal enhancements, there are also examples in the literature where 'non-thermal' microwave effects have been suggested. These are rate accelerations which cannot be explained simply by thermal/kinetic or specific microwave effects.[14,15] These effects have been rationalised as originating from direct interaction of reaction components with the applied electric field.

Suggestions have been put forward that the electric field can lead to orientation effects of molecules containing a dipole and, as such, effect the entropy term of the Arrhenius equation. Such an effect should be particularly significant in cases in which the reaction proceeds via an increase in polarity from ground state to transition state which should lead to an improved reactivity due to lowering of the activation energy.[14,15]

3.2.3 Microwave Assisted Organic Synthesis

Microwave Assisted Organic Synthesis has been applied to a wide range of reactions, with the synthesis of 4-aryl-2-quinolinone exhibiting the type of reactions which have been facilitated using microwave heating (***Figure 88***).[25]

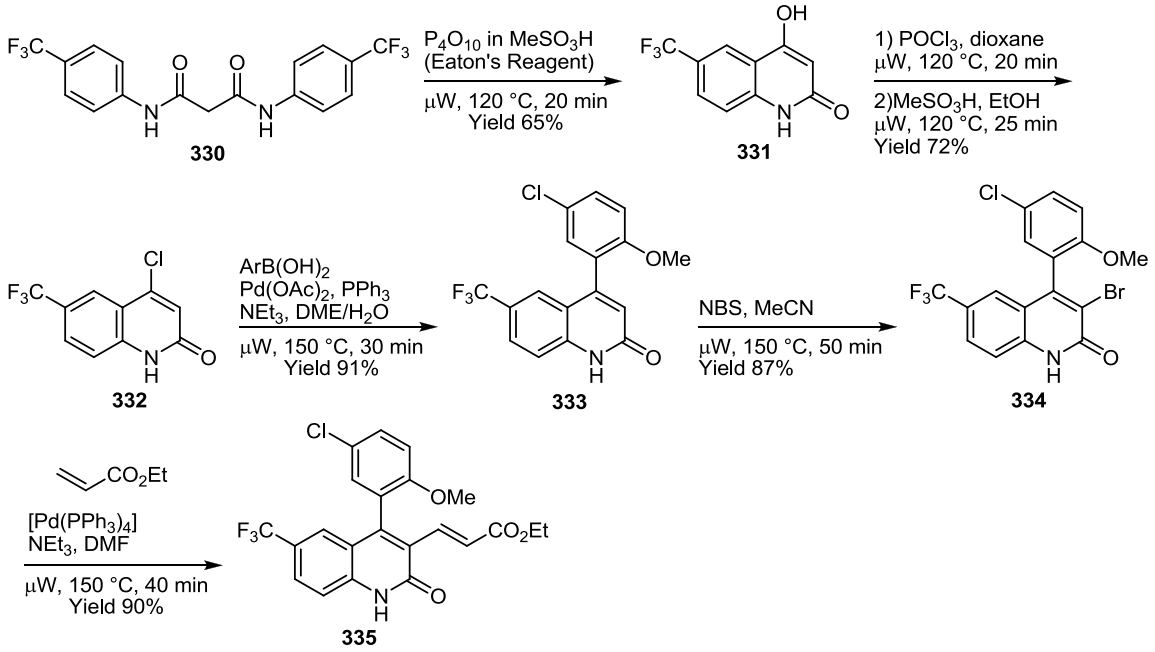

Figure 88 - Synthesis of 4-aryl-2-quinolinone via microwave assisted synthesis.

3.3 Microwave Heating in C-H Borylation Reactions

Although microwave heating has been applied to a wide range of different chemical reactions, prior to our work, the following were the only two reports of the use of microwave heating in C-H borylations.

Microwave assisted C-H borylation was first reported in 2008 by Maguire and co-workers.[26] The reaction was facilitated by an iridacarborane complex 3,3-$(Ph_3P)_2$-3-H-3,1,2-$IrC_2B_9H_{11}$ **336** in ethylene glycol under a hydrogen pressure of 10 bar. The arene borylation system contained HBpin, tetra-2-pyridylpyrazine (TPy) **337** as a stabilising ligand and an ionic liquid solvent of trihexyltetradecylphosphonium methylsulfonate [THTdP][MS] **338**. The reaction was heated with microwave irradiation for 1 hour at 130 °C with benzene as substrate. The reaction afforded the boronate ester which was subsequently treated with HCl to give the boronic acid in 91% yield (***Figure 89***). The active metal species was proposed to be iridium (0) nanoparticles stabilised by the TPy. The nanoparticles formed in the reaction could act as points of superheating within the reaction medium and promote the reaction.

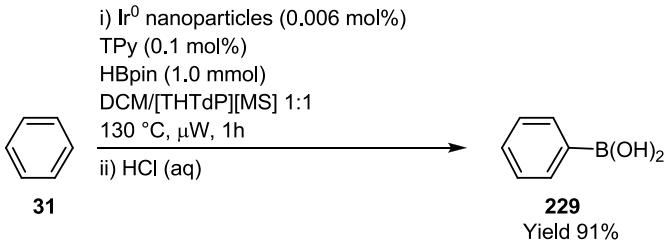

Figure 89 - Nanoparticle catalysed C-H borylation of benzene.

Whilst the work detailed in this chapter was in progress, Gaunt and co-workers[27] described the borylation of *N*-Boc protected pyrrole using microwave irradiation. This reaction, a step in the total synthesis of Rhazinicine **218,** was carried out in hexane at 100 °C for 1 hour (***Figure 90***). This report, although important, did not fully exploit the potential of the application of microwave heating to the C-H borylation reaction; this will form the basis of the remainder of this chapter.

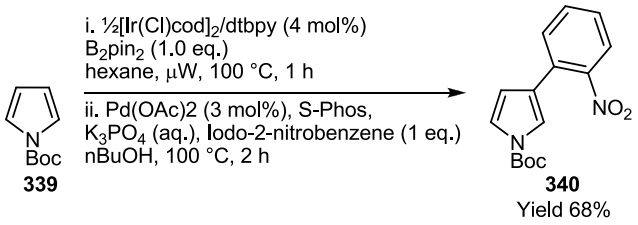

Figure 90 - Borylation and cross-coupling of *N*-Boc pyrrole.[27]

3.4 Summary

The application of microwave heating in the field of organic synthesis has become widespread with many reactions requiring heating being carried out via this methodology. The ability to access high reaction temperatures and dramatically accelerate reactions has made the technology of great use.

Of the substrates reported to undergo the C-H borylation reaction, many typically require reaction times of several hours, with 18 hour reaction times being routine.[1] It was postulated that the application of microwave heating may be able to reduce this reaction time to allow a more rapid and efficient route to borylated arenes.

Applications of microwave heating in the field of C-H borylation have been very limited, with the two reported examples not fully exploiting the potential of the technology. Neither reports offer a significant advantage over the classical methods of carrying out the reaction. As such it was sought to apply microwave synthesis to the C-H borylation to investigate whether a real synthetic advantage could be gained by using this technology.

3.5 Results and Discussion

3.5.1 Initial Reaction Screen

In order to assess the extent of any benefits provided by carrying out the C-H borylation reaction under microwave conditions, the reaction time of the standard thermal reaction was investigated. For this, the reaction of *m*-xylene was chosen based on previous studies described in chapter II.

Smith and co-workers[28] reported the borylation of *m*-xylene using both [Cp*Ir(PMe_3)(H)(Bpin)] and [Cp*Rh(η^4-C_6Me_6)] catalyst systems with long reaction times required to achieve moderate conversions. Ishiyama and co-workers[29] then reported the borylation of *m*-xylene carried out with the [Ir(Cl)cod]$_2$/bpy catalyst system at 3 mol% in neat arene using B_2pin_2 over a 16 hour reaction time at 80 °C to give 86% yield of the aryl boronate.

At the same time, practical enhancements to the reaction were also sought. In earlier work, although stock solutions of the catalyst components had been used, it had been necessary to weigh out B_2pin_2 for each individual reaction. In order to simplify this, the Ir-precursor, ligand and diboron reagents ([Ir(OMe)cod]$_2$ (104 mg, 0.156 mmol), dtbpy (83 mg, 0.312 mmol), B_2pin_2 (2.642 g, 10.4 mmol) were weighed into a sealable 25 mL volumetric flask. The flask was then sealed with a crimp top septum cap. Solvent was then added to the flask and the stock solution was shaken to mix the constituent parts of the catalyst efficiently until a dark red solution formed. A 2.4 mL aliquot of this catalyst stock solution contained [Ir(OMe)cod]$_2$ (0.015 mmol), dtbpy (0.03 mmol) and B_2pin_2 (1.0 mmol) which is equivalent to a 3 mol% catalyst loading for a 1.0 mmol scale reaction with a B_2pin_2 loading a 1.0 equivalent relative to the substrate. Using such aliquots, the stock solution contained sufficient reagents to facilitate 10 reactions on a 1 mmol scale through the use of 2.4 mL of the solution per reaction.

From previous studies, the C-H borylation of *m*-xylene had been carried out over a standardised 6 hour reaction time.[30] In order to assess the time required to reach full conversion, a series of reactions spanning a range of reaction times (0 - 6 hours) were carried out.

In order to ensure constant conditions, apart from the heating mode, all reactions were carried out using identical crimp top thick walled microwave reaction tubes; the same catalyst stock solution was used for both the microwave and thermal reactions with the same reaction volume. Moreover, the thermal reactions were carried out in a preheated aluminium heating block. The extent of the background reaction at room temperature was evaluated over a 12 hour time period, with no conversion observed after this time.

Separate reactions were carried out for each time point, with the relative conversion of starting material to product monitored by GC-MS. In order to ensure that the results were accurate, and the reaction times were as stated, each tube was cooled in an ice bath after the relevant heating time to ensure that no further conversion was achieved.

As described in chapter II, studies of the borylation of *m*-xylene[30] using conventional heating had shown that after 6 hours complete conversion had been achieved. However, it was not known whether this time could be reduced. Consequently, the borylation of *m*-xylene was carried out at time points between 5 minutes and 6 hours, with full conversion achieved at the 6 hour reaction time giving an isolated yield 98% (***Figure 91***, ***Graph 1***). Analysis of the product by GC-MS showed a molecular ion of 232 *m/z*, consistent with **94**. Analysis by ^{1}H NMR spectroscopy revealed singlet signals at 7.45 ppm and 7.11 ppm in a 2:1 ratio, consistent with the remaining aromatic hydrogens of **94**. The signal for hydrogens adjacent to the Bpin group of **94** (7.45 ppm) are shifted to higher ppm relative to the corresponding signal (6.85 ppm) in the *m*-xylene starting material **299**. This shift to higher ppm is consistently observed upon introduction of a Bpin group into the arene substrates discussed in this thesis.

Due to the quadrupolar nature of boron, the signal for the carbon attached to it is broadened[31] and not typically visible in the ^{13}C NMR spectrum; this is consistent throughout all borylated products.

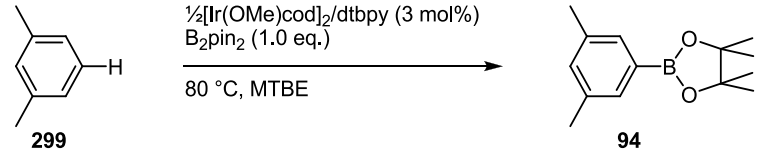

Figure 91 - C-H borylation of *m*-xylene under thermal conditions.

Graph 1 - Time/conversion plot for the thermal borylation of *m*-xylene.

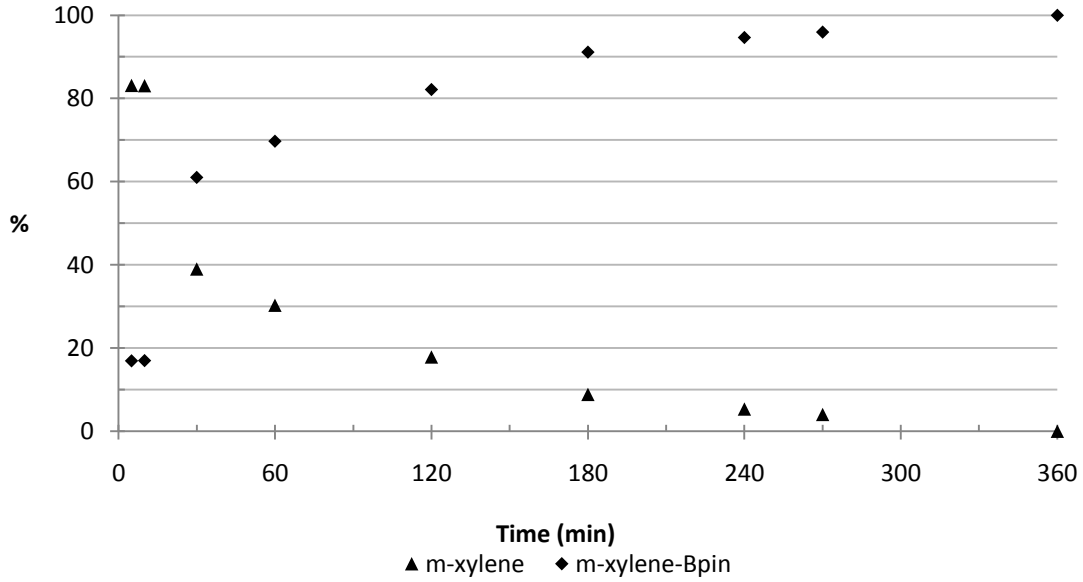

The same process was carried out for the C-H borylation of *m*-xylene under microwave conditions in order to determine the time required for complete reaction (***Graph 2***).

Graph 2 - Time/conversion plot for the microwave borylation of *m*-xylene.

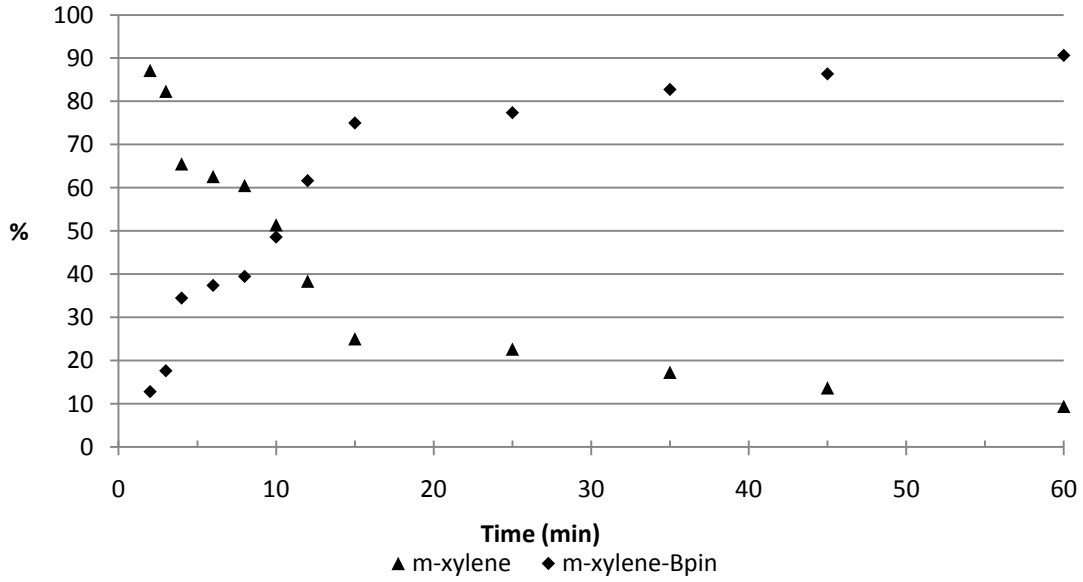

For the microwave borylation of *m*-xylene, the reaction was complete in 60 minutes affording an isolated yield of 96%, which equates to a 6 fold increase in the reaction rate compared with the reaction using conventional heating. This result was unexpected as the reactions were carried out at the same reaction temperature. Reflecting that a 10 °C increase in reaction temperature typically leads to a doubling in the reaction rate,[8] the majority of the literature reports of improved reaction times and conversions compared with reactions ran under standard thermal conditions are based on an increase in reaction temperature for the microwave reaction.[2,3] For reactions carried out at the same temperature, as in this case, there remains a lack of understanding of the cause of the observed accelerations.[2,3]

3.5.2 Cause of Microwave Acceleration Effect

Microwave reactions usually display rate accelerations due to an increased reaction temperature. However, the apparent reaction temperature in the experiments described above was the same in both thermal and microwave heating modes. As such, efforts were made to de-convolute the cause of the microwave acceleration.

Specific microwave effects could be due to different components within the reaction mixture strongly absorbing microwave irradiation. It is known that solvent, metal particles and strongly absorbing substrates can be involved in accelerating a reaction under microwave conditions.[2,10,19-22] Each of the possible contributors towards the observed acceleration effect will be discussed in turn in order to ascertain the key contributors to the observed acceleration effect. The first of the possible factors to be investigated is the effect of the substrate.

3.5.2.1 Investigation of Substrate Scope for the Microwave Accelerated C-H Borylation Reaction

The reaction procedure was applied to a range of substrates in order to assess whether the observed acceleration effect was generally applicable to a variety of carbocyclic and heterocyclic arenes. Substrates previously reported in the literature as being slow to borylate

under standard conditions were investigated as inherently fast reactions would not benefit from this technology.

The same reaction screening process was carried out for subsequent substrates as for *m*-xylene, by first undertaking a time/conversion profile for the standard thermal reaction followed by the microwave reaction. In each case assessing the point at which both reactions reach full conversion.

3.5.2.1.1 Carbocyclic Substrates

The first substrate investigated was *p*-xylene. The borylation of *p*-xylene was reported by Ishiyama and co-workers[29] utilising $[Ir(Cl)cod]_2$/bpy catalyst system at 3 mol% in neat arene with B_2pin_2. The reaction was heated for 16 hours at 80 °C to afford the desired product in 58% isolated yield. This moderate yield is due to the sterically hindered nature of all aromatic C-H bonds. However, due to the symmetry of the substrate a single borylation product would be formed, allowing simple identification and purification of the product.

Under standard heating condition (Δ), after a reaction time of 18 hours at 80 °C, the desired product was isolated in 55% yield. The formation of boronate **334** was confirmed by GC-MS analysis, which indicated a molecular ion of 232 *m/z*. Characteristic signals in the ^{1}H NMR spectrum at 7.57 (d, J = 1.6 Hz), 7.13 (dd, J = 1.6, 7.8 Hz) and 7.06 (d, J = 7.8 Hz) ppm consistent with a 1,2,4-trisubstituted aromatic C-H borylated product. It can again be observed that the peak adjacent to the installed Bpin group (7.57 ppm) is shifted to higher ppm relative to the other remaining protons (7.06, 7.13 ppm), as discussed previously. When the same transformation was conducted under microwave conditions over a 1 hour reaction time at 80 °C, aryl boronate **342** was isolated in 45% yield (***Figure 92***). This demonstrates that this microwave methodology can be very effective at facilitating the C-H borylation of sterically hindered substrates.

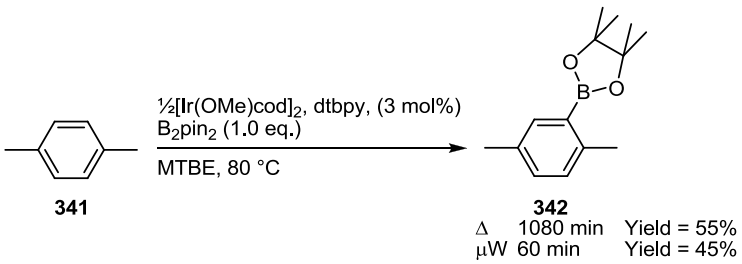

Figure 92 - C-H borylation of *p*-xylene under thermal and microwave conditions.

Although an improved yield relative to the previous literature or the thermal reaction could not be achieved, a reduction in reaction time to 1 hour makes this method of synthesis a significant improvement.

3.5.2.1.2 Pyridine and Quinoline Substrates

Pyridines have been shown to be effective substrates for C-H borylation, but examples in the literature have often required heating for times in the order of hours.[28,32]

For example, the borylation of 2,6-disubstituted pyridines has been previously reported by Smith and co-workers.[28,32] The borylation of 2,6-dimethylpyridine **343** was carried out using the Cp*Rh(η^5-C_6Me_6) **45** catalyst system at 2 mol% loading with HBpin in neat arene at 150 °C to yield the heteroarylboronate ester in 41% yield after 6 hours.[28]

Subsequently, Smith and co-workers[32] reported an improved procedure for the borylation of 2,6-dichloropyridine **57** using the [Ir(Ind)cod]/dppe catalyst system with HBpin in cyclohexane at 100 °C giving a 69% yield of product **58** after a 4 hour. Whilst literature reports show that moderate to good conversions can be achieved for these substrates, this work employed the more active [Ir(OMe)cod]$_2$/dtbpy catalyst system to improve the process. The substrates were subjected to the borylation methodology under standard heating and microwave conditions, effecting complete conversion in less than 30 minutes in all cases (***Figure 93***, ***Table 11***).

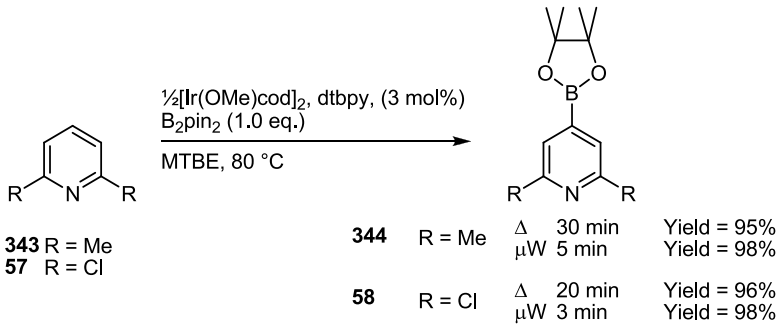

Figure 93 - C-H borylation of 2,6-substituted pyridines.

When borylated under standard thermal conditions, 2,6-dimethylpyridine required 30 minutes to achieve full conversion, resulting in a 95% isolated yield of the 4-borylated product. Under microwave conditions, an isolated yield of 98% was achieved after a reaction time of 5 minutes (***Table 11***, entry 1). Confirmation of the product was made by GC-MS analysis which showed a molecular ion of 233 *m/z*. The ^{1}H NMR spectrum contained a singlet at 7.31 ppm (s) for the aromatic protons, a singlet at 2.52 ppm for the equivalent methyl groups on the pyridine ring, along with a singlet at 1.35 ppm for the methyl groups of the pinacolate moiety.

The analogous borylation of 2,6-dichloropyridine afforded full conversion and 96% isolated yield after a reaction time of 20 minutes under thermal heating condition. Under microwave conditions, an isolated yield of 98% was achieved after a reaction time of 3 minutes (***Table 11***, entry 2). These reactions showed that the more electron deficient 2,6-dichloropyridine is borylated faster than the more electron rich 2,6-dimethyl substrate. As before, the product identity was confirmed via GC-MS analysis, which showed molecular ions 273, 274, 275 *m/z* in a 10:6:1 ratio, and the characteristic peaks observed at 7.59 ppm (s), for the equivalent aromatic protons, and 1.34 ppm (s) for the methyl groups of pinacolate moiety in the ^{1}H NMR spectrum.

Table 11 - C-H borylation of 2,6-disubstituted pyridines under thermal and microwave conditions.

Entry	R	Product	μW heating		standard heating	
			Time (min)	Yield[a]	Time (min)	Yield[a]
1	Me	**344**	5	98%	30	95%
2	Cl	**58**	3	98%	20	96%

The borylation of quinoline has been reported by Ishiyama, Hartwig and Miyaura.[33,34] In this case, a 10 fold excess of quinoline was used to ensure that a single borylated product was obtained. The reaction was run under standard heating conditions using the $[Ir(Cl)cod]_2$/dtbpy catalyst system at 100 °C for 16 hours to give the mono 3-borylated product in 84% yield (based on B_2pin_2) (***Figure 94***).

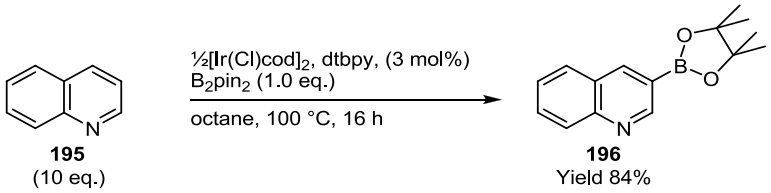

Figure 94 - C-H borylation of quinoline with the $[Ir(Cl)cod]_2$/dtbpy catalyst system.[33,34]

In order to assess if this reaction time could be reduced the microwave heating methodology was applied (***Figure 95***).

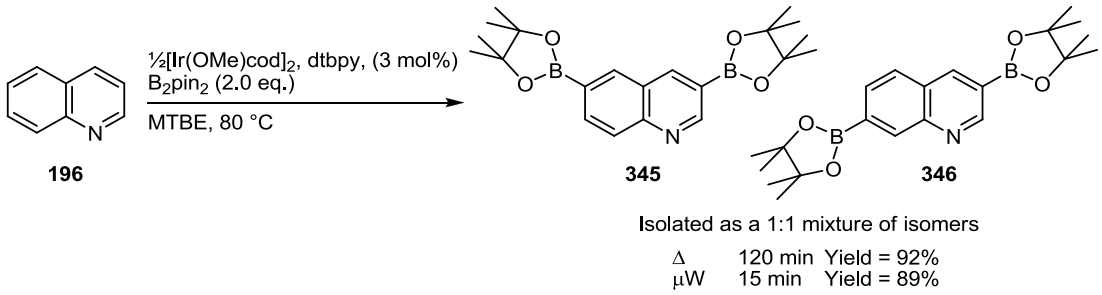

Figure 95 - C-H borylation of quinoline under thermal and microwave conditions.

When the thermal borylation of quinoline was undertaken with equimolar amounts of substrate and B_2pin_2, a mixture of 1 mono and 2 bis borylated products was formed as indicated by 3 peaks in the GC-MS total ion chromatogram giving molecular ions of 255, 381 and 381, respectively. Examination of the crude ^1H NMR spectrum showed the mono-borylated product to be 3-borylated quinoline by comparison with the literature chemical shift values for **196**. Formation of the mono-borylated product only was not possible due to the fact that the relative rates of borylation of quinoline and mono-borylated quinoline product are similar.

Consequently, to simplify analysis, the reaction was undertaken using 2.0 equivalents of B_2pin_2, forcing the reaction through to a 1:1 mixture of bis-borylated products.

The thermal reaction proceeded to completion in 2 hours to give a 92% overall yield of the two isomers. When carried out under microwave conditions, the borylation was accelerated; after heating for 15 minutes, an isolated yield of 89% as a 1:1 mixture of the two isomers was obtained.

The mixture of 3,6 and 3,7 borylated isomers formed from the reaction is analogous to the products of the borylation of naphthalene,[35] in which a mixture of the two isomers is formed. However, unlike naphthalene, quinoline is not symmetrical and as such the reaction also exhibits a preference for initial borylation on the more electron deficient pyridine ring at the C^3 position rather than adjacent to the quinoline nitrogen. This issue will be discussed in more detail in Chapter IV.

3.5.2.1.3 Pyrazine Substrates

Ishiyama, Hartwig and Miyaura have shown that the borylation of positions *ortho*- to pyridyl nitrogen atoms are challenging with their work on both quinoline and pyridine.[33,34] The reason for this difficulty is not fully understood, but some suggestions have been made that the active iridium catalyst can coordinate to the nitrogen blocking borylation at the 2 position.[33,34,36] Alternatively, it is feasible that the nitrogen lone pair could act as a steric blocking group for the 2 position. A further problem with boronates *ortho*- to N atoms is that they readily undergo proteodeboronation upon purification or subsequent reaction. However, the mechanism of such proteodeboronation remains to be established.

Such borylation has been shown to be viable by Marder and co-workers, who described borylation *ortho*- to nitrogen in both dtbpy and 2,3-dimethylpyrazine. In both cases, the regiochemistry was confirmed by X-ray crystallographic analysis following anhydrous Suzuki-Miyaura cross-coupling to yield 2-arylated products (***Figure 96***).[36]

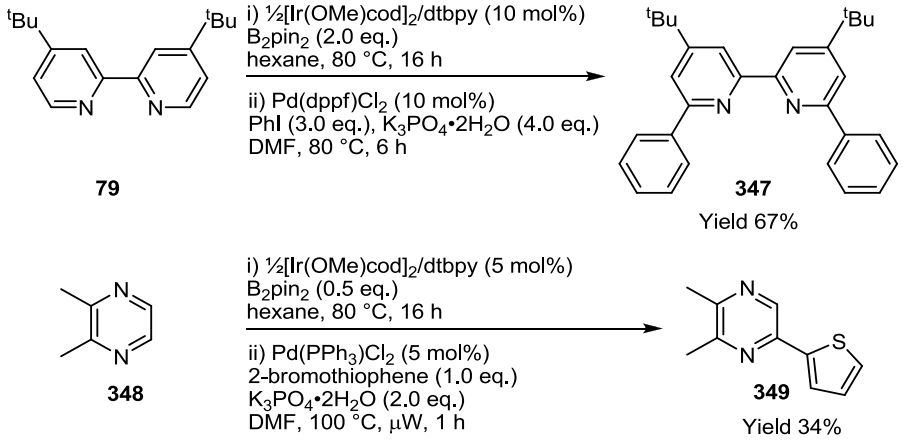

Figure 96 - C-H borylation of dtbpy and borylation/Suzuki-Miyaura cross-coupling of 2,3-dimethylpyrazine.

Building on these precedents, both 2,3- and 2,5-dimethylpyrazine were subjected to the borylation methodology (***Figure 97***, ***Table 12***).

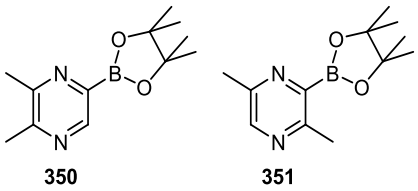

Figure 97 - Borylation products of 2,3- and 2,5-dimethyl pyrazine.

Table 12 - Thermal and microwave borylation of 2,3- and 2,5-dimethyl pyrazine.

Entry	arene	μW heating		standard heating	
		Time (min)	Yield[a]	Time (min)	Yield[a]
1	2,3-dimethyl pyrazine	15	100%	60	100%
2	2,5-dimethylpyrazine	60	48%	1080	35%

[a] GC-MS conversion

The borylation of 2,3-dimethyl pyrazine under thermal conditions proceeded in 60 minutes with a 100% GC-MS conversion. This same 100% conversion was achieved in only 15 minutes when the reaction was carried out under microwave conditions (***Table 12***, entry 1).

The reaction with 2,5-dimethylpyrazine was more challenging due to the sterically hindered nature of the substrate in analogy to *p*-xylene.[29] The thermal reaction was carried over a reaction time of 18 hours to give a GC-MS conversion of 35%. When the microwave conditions were applied, a 48% conversion (GC-MS) could be achieved in 1 hour (***Table 12***, entry 2). Reflecting the rapid proteodeboronation pathways, both the products were unstable to chromatography and as such could not be isolated in pure form.

3.5.2.1.4 5-Membered Heterocycles

Having considered electron deficient heterocycles, attention was then turned to the more electron rich 5-membered heterocycles. Unsubstituted 5-membered heteroarenes typically react rapidly to form 2- and 2,5-disubstituted products. The borylation of sterically hindered 2,5-substituted thiophenes has been shown to be viable by Smith and co-workers.[37] However, in some cases, the reactions are problematic due to the sterically hindered nature of the positions being borylated. The borylation of other 2,5-disubstituted 5-membered heterocycles have not been explored and thus appeared to be suitable for further study.

Examples already in the literature were borylated under the microwave conditions along with borylation of other of 2- and 2,5-disubstituted 5-membered heterocycles (***Table 13***).

Table 13 - Borylation of substituted 5 membered heterocycles.

Entry	arene	product	μW heating		standard heating	
			Time (mins)	Yield	Time (mins)	Yield
1	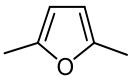 **352**	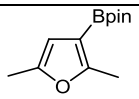 **353**	2	99%	5	98%
2	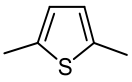 **354**	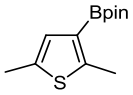 **355**	15	98%	120	99%
3	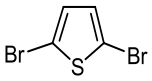 **356**	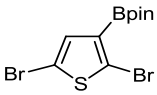 **357**	60	82%[a]	1080	84%[b]
4	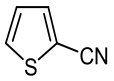 **358**	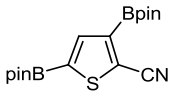 **359**	15	98%	120	96%

[a] 18% starting material recovered

[b] 16% starting material recovered

The borylation of 2,5-dimethylfuran was facile, even when carried out under thermal conditions, giving an isolated yield of 98% after a 5 minute reaction time. This reaction can still be accelerated by microwave irradiation as the required reaction time to reach full conversion and 99% isolated yield is reduced to 2 minutes of heating (***Table 13***, entry 1). Product identity was confirmed by GC-MS analysis showing a molecular ion 222 *m/z*, and by characteristic signals in the ^{1}H NMR spectrum at 6.02 ppm (s), for the remaining aromatic proton. Peaks at 2.41 (s) and 2.23 ppm (s) were consistent with the two inequivalent methyl groups and the peak at 1.29 ppm from the methyl groups of the pinacolate moiety.

Smith and co-workers[37] have previously reported the borylation of both 2,5-dimethyl and 2,5-dibromothiophene with moderate success. For example, when the borylation of 2,5-dimethylthiophene was attempted at room temperature, no product was formed. However, the use of [Ir(Ind)cod]/dmpe (2 mol%) at 150 °C enabled a 97% isolated yield to be achieved (***Figure 98***).

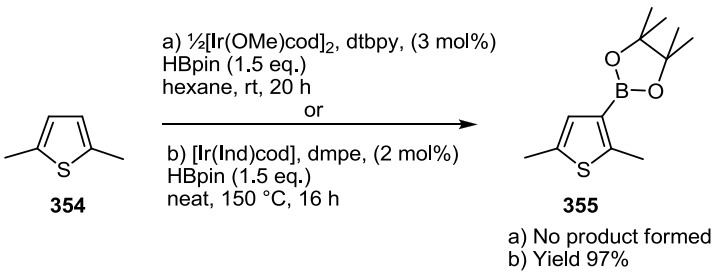

Figure 98 - Borylation of 2,5-dimethylthiophene by Smith and co-workers.

The application of both the thermal and microwave methodologies allowed borylation products to be isolated in excellent yields. Under thermal conditions, the reaction required heating for 2 hours affording a 99% isolated yield. When carried out under microwave conditions, the reaction was accelerated requiring a total reaction time of 15 minutes to afford a 98% isolated yield (***Table 13***, entry 2). The molecular ion of 238 *m/z* (GC-MS) confirmed the nature of the product. As before, the 1,2,5-trisubstituted 5-membered heteroaromatic product was characterised by singlets at 6.81, 2.59, 2.37 and 1.28 ppm in the ^{1}H NMR spectrum, corresponding to the remaining aromatic proton, the inequivalent methyl groups on the thiophene ring and the methyl groups of the pinacolate moiety.

Smith and co-workers[37] encountered similar problems for the borylation of 2,5-dibromothiophene as for the dimethyl analogue. They utilised [Ir(OMe)cod]$_2$/dtbpy at a total catalyst loading of 9 mol% with a total reaction time of 48 hours to give an isolated yield of 56%. This was achieved by an initial catalyst loading of 6 mol% with stirring for 36 hours at which point the reaction was deemed to have ceased. This was followed by loading of a further 3 mol% of catalyst and 1.0 equivalent of HBpin (***Figure 99***).

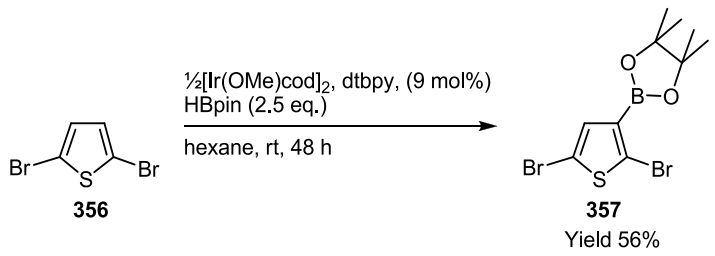

Figure 99 - Room temperature borylation of 2,5-dibromothiophene.

Again, using the thermal and microwave methodologies, 2,5-dibromothiophene was successfully borylated at the 3-position. Thermal borylation conditions required heating for 18 hours affording product in an 84% isolated yield. The reaction was carried out under microwave conditions reducing the reaction time to 1 hour with an isolated yield of 82%, (***Table 13***, entry 3). The product identity was confirmed GC-MS with molecular ions of 366, 368 and 370 *m/z* in a 1:2:1 ratio and the characteristic signals in the ^{1}H NMR spectrum at 7.11, 1.33 ppm, consistent with the remaining thiophene hydrogen and the pinacolate methyl groups respectively.

Finally, the borylation of 2-cyanothiophene was carried out under thermal conditions with 2.0 equivalents of B_2pin_2 in order to drive conversion to the bis borylated product as the reaction was unselective for monoborylation when carried out with 1.0 equivalent of B_2pin_2. Under thermal conditions, a reaction time of 2 hours was required to achieve a 96% isolated yield. When carried out under microwave conditions, the reaction required only 15 minutes of heating to yield 98% of the bis-borylated product (***Table 13***, entry 4). The bis-borylated product was identified by GC-MS, showing a molecular ion of 361 *m/z*, and by the characteristic signals in the ^{1}H NMR spectrum at 7.89 ppm (s), 1.33 ppm and 1.34 ppm for the thiophene proton and the methyl groups of the two pinacolate moieties.

Both the thermal and microwave methodologies showed improved reaction times and conversions compared to the previously published examples by Smith and co-workers.[37] However, Smith only utilised the $[Ir(OMe)cod]_2$/dtbpy catalyst system at room temperature which may be the cause of the lack of or poor conversions observed for 2,5-dimethylthiophene and 2,5-dibromothiophene, ***Figure 98*** and ***Figure 99***, respectively.

When the thermal reaction is compared to the microwave reaction for these more sterically hindered substrates, it can be observed that the methodology is particularly effective at accelerating the reaction of hindered substrates. This is particularly evident for 2,5-dibromothiophene, for which an 18 fold acceleration was achieved allowing excellent isolated yields for a substrate with C-H bonds that suffer from significant steric hindrance.

3.5.2.1.5 Indole Based Substrates

Smith and co-workers[38] have demonstrated the borylation of a range of 2-substituted indoles, which resulted in 7-borylated products due to a proposed coordinated directing effect of the indole nitrogen. One substrate which was found to be difficult to borylate was 1,2,3-tetrahydrocyclopenta[b]indole, with only 45% yield achieved over a 36 hour reaction time (***Figure 100***).

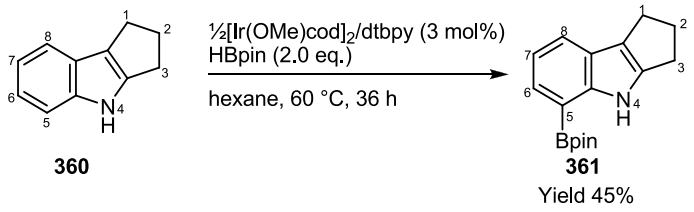

360 **361**
Yield 45%

Figure 100 - Borylation of 1,2,3-tetrahydrocyclopenta[b]indole with $[Ir(OMe)cod]_2$/dtbpy and HBpin.

Due to the moderate yield and long reaction time, it was considered that use of the microwave borylation methodology might lead to improvement in the process. As such, 1,2,3-tetrahydrocyclopenta[b]indole and a range of structurally similar indole derivatives were subjected to the methodology (***Table 14***).

Table 14 - Borylation of indole based substrates.

Entry	arene	product	μW heating		standard heating	
			Time (mins)	Yield	Time (mins)	Yield
1	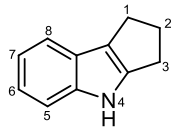 **360**	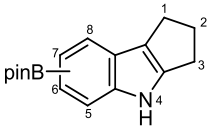 **361,362**	15	36%[a,b]	120	38%[a,b]
2	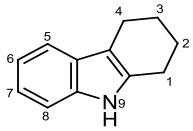 **363**	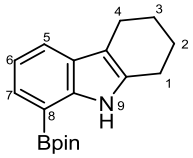 **364**	15	90%	120	89%
3	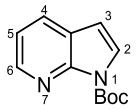 **365**	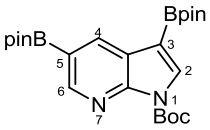 **172**	20	92%[c]	360	90%[c]

[a] 58% starting material recovered in both cases.

[b] 85:15 mixture of 5- and 7-pinacolboronate esters.

[c] 2.0 eq. of B_2pin_2 used to achieve complete bis-borylation of substrate.

Consistent with Smith's observations,[38] under the standard thermal heating conditions 1,2,3-tetrahydrocyclopenta[b]indole proved to be a difficult substrate to borylate giving only a 38% isolated yield of an 85:15 mixture of the 5- and 7- aryl boronate esters, respectively (**361**, **362**), after 2 hours at 80 °C. Interestingly, no 6-borylated product was formed. When the microwave methodology was applied to the substrate it was shown that the reaction time could be reduced to 15 minutes to afford a comparable 36% isolated yield of the same isomeric mixture (***Table 14***, entry 1). The structurally analogous 1,2,3,4-tetrahydro-9H-carbazole was borylated under standard thermal conditions over a reaction time of 2 hours to give an isolated yield of 89% of the 8-borylated isomer, selectively. A similar isolated yield of 90% was achieved when the reaction was carried out under microwave conditions with a reaction time of 15 minutes (***Table 14***, entry 2).

The difference in reactivity between 1,2,3-tetrahydrocyclopenta[b]indole and 1,2,3,4,-tetrahydro-9H-carbazole is remarkable considering the two compounds differ only in the size of the aliphatic ring. A reason for this difference in reactivity remains elusive.

The borylation of *N*-Boc protected 7-azaindole resulted in the 3,5-bis-borylated compounds as the sole product. Attempts to isolate the mono borylated product were successful as both mono isomers and the bis-substituted product formed simultaneously. Attempts to borylate the unprotected azaindole were not successful which could be attributed to the proximity of the two ring nitrogen atoms forming a strongly coordinating environment which sequesters the catalyst causing the reaction to fail. The strongly coordinating nature of pyridine nitrogen has been previously reported[33,34,36] and coordination of the indole nitrogen has been suggested.[38,39] Individually, each of these effects is sufficiently transient to allow effective conversion to products, but as a cooperative effect this may be too great to overcome and as such the reaction does not proceed.

The thermal borylation of *N*-Boc-7-azaindole proceeds in the presence of 2.0 equivalent of B_2pin_2 afforded a 90% yield of the 3,5-borylated product in a 6 hour reaction time. Under microwave conditions the reaction time was dramatically reduced to 20 minutes, giving a 92% isolated yield (***Table 14***, entry 3). This equates to a reaction acceleration of 18 times when carried out under microwave conditions. The product identities were confirmed by ^{1}H NMR spectroscopy. The signal at 8.84 ppm was consistent H^6, as its position at high ppm corresponds to a hydrogen adjacent to an azine nitrogen. A 4-bond-W coupling to (J = 1.6 Hz) confirms H^4 and thus the position of a Bpin group in the 5-position. A sharp singlet at 8.03 ppm corresponds to H^2 which shows a long range coupling to $C^{3'}$ in the HMBC spectrum. Coupling is not observed between H^4 and C^3 confirming the position of the Bpin group. X-ray crystallographic analysis confirmed the structure of **172** (***Figure 101***).

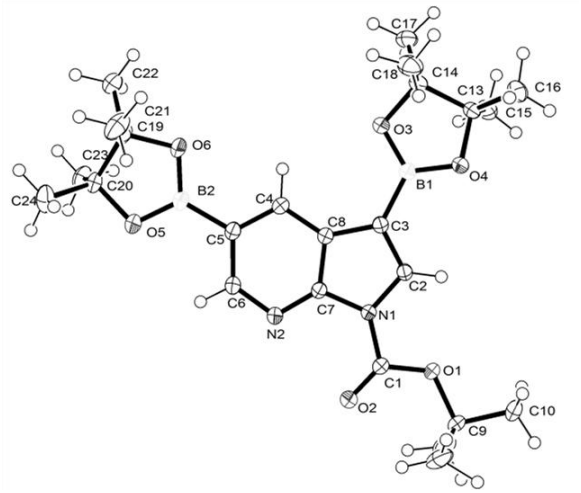

Figure 101 - Molecular structure of **172** (Thermal ellipsoids drawn at 50% probability).

Smith and co-workers[40] subsequently reported the synthesis of the 3,5-borylated *N*-Boc-7-azaindole using the $[Ir(OMe)cod]_2$/dtbpy catalyst system at 6 mol% loading with 3.5 equivalents of HBpin at room temperature over a reaction time of 96 hours. This highlights the advantages of the rapid synthesis of this molecule by microwave or thermal methods compared to the room temperature reaction which requires 4 days (***Figure 102***).

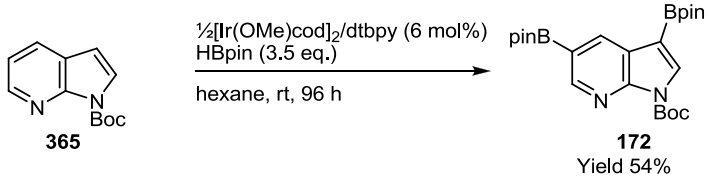

Figure 102 - C-H borylation of *N*-Boc-7-azaindole at room temperature by Smith.[40]

Whilst this work was in progress, Gaunt and co-workers[27] reported the borylation of *N*-Boc protected pyrrole using microwave irradiation (***Figure 103***). The reaction was carried out using the $[Ir(Cl)cod]_2$/dtbpy catalyst system (4 mol%) at 100 °C over a 1 hour reaction time. $[Ir(Cl)cod]_2$ has been shown to be a less effective catalyst precursor than the methoxy analogue.[41]

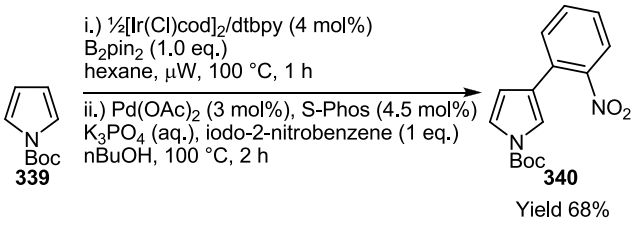

Figure 103 - Borylation and cross-coupling of *N*-Boc pyrrole.[27]

Smith and co-workers[40] also presented a synthesis of **366** utilising the $[Ir(OMe)cod]_2$/dtbpy catalyst system at 3 mol% loading with 1.5 equivalents of HBpin at 55 °C affording the desired product in 90% yield after 13 hours (***Figure 104***).

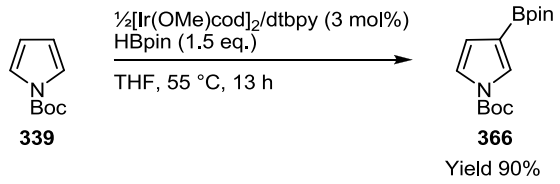

Figure 104 - Borylation of *N*-Boc pyrrole by Smith and co-workers.[40]

Our microwave methodology was applied to the borylation of this substrate. It was found that the reaction reached full conversion affording 98% isolated yield after 3 minutes at 80 °C (***Figure 105***). Product identity was confirmed by ^{1}H NMR spectroscopy and GC-MS with the molecular ion of 293 *m/z* being observed.

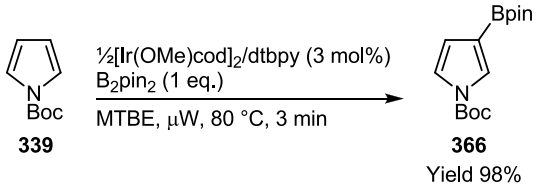

Figure 105 - Borylation of *N*-Boc pyrrole under microwave conditions.

3.5.2.1.6 Conclusions

The microwave accelerated synthesis of arylboronates has been shown to be a highly general process for carbocyclic aromatics, 5-membered heterocycles, pyridines, quinolines, and indole based substrates. The acceleration of the reaction was observed for all attempted examples.

However, the extent of the acceleration was dependent on the inherent reactivity of the substrate. This is exemplified by the reaction time of the very reactive 2,5-dimethylfuran being reduced from 5 minutes to 2 minutes, a 2.5 fold acceleration. This was compared to 2,5-dibromothiophene which is accelerated 18 fold, reducing reaction time from 18 hours to 1 hour. The trend of the most challenging substrates being accelerated to the greatest degree was consistent throughout the series of experiments.

The acceleration effect was observed across a wide range of substrate classes. If the substrate absorbing the microwave radiation were the key factor then it would be expected that more polar substrates would exhibit the largest effect. As both non-polar carbocyclic (e.g. *m*-xylene) and polar heterocyclic (e.g. 2,6-dichloro-pyridine) substrates were accelerated it can be reasonably concluded that a strongly microwave absorbing substrate is not the key to the observed acceleration.

3.5.2.2 Microwave Absorbing Solvents

The solvent, in which a microwave reaction is carried out, can have a dramatic effect on the efficiency of the heating achieved. This is due to the mode of action of microwave heating with solvents containing a large dipole aligning more efficiently with the electrical field applied and thus heating more efficiently.

The dielectric constant and loss tangent of a solvent are good measures of its microwave absorbing ability. Solvents with significant dipoles such as DMSO, ethylene glycol and pyridine absorb microwaves strongly and are thus heated to the desired temperature quickly with little energy input. Hydrocarbon solvents such as hexane and toluene absorb microwave irradiation very poorly.[10,11]

For the solvent to be the key to the acceleration effect observed it would be necessary for it to be a strong microwave absorber. However, MTBE is relatively poor at absorbing microwave irradiation due to its small dielectric constant of 2.2 which is similar to that of toluene and as such it seems that this factor may not be critical for the microwave acceleration of this reaction.

3.5.2.3 Nano-Particle Formation

As previously discussed in section 3.3, iridium nanoparticles have been shown to catalyse the C-H borylation reaction and metal nanoparticles are also known to be very strong microwave absorbers.[2,10,19-22] For these reasons it was considered possible that iridium nanoparticles might be formed during the reaction. In order to assess whether this was the case the formation of iridium nanoparticles was sought to see whether they were able to catalyse the C-H borylation reaction. A selection of iridium sources was explored including $IrCl_3$, $[Ir(OMe)cod]_2$, $[Ir(Cl)cod]_2$, and $[Ir(Cp^*)Cl_2]_2$, with each metal source being examined in the presence and absence of dtbpy. Reactions were carried out using 1 and 3 mol% Ir with, where used, 1.0 equiv (with respect to [Ir]) of dtbpy at 100 and 150 °C in MTBE with 1.0 equivalents of B_2pin_2 and *m*-xylene as substrate. The reactions were sampled by GC-MS in order observe any conversion to aryl boronate products. For all examples, no product was observed with only B_2pin_2 and arene visible in the GC-MS total ion chromatogram.

All attempts to find an alternative iridium source to carry out the same chemistry were unsuccessful suggesting that the microwave accelerated reaction occurs through the known iridium active species.

3.5.2.4 Origins of the Microwave Acceleration Effect

These experiments have been unsuccessful in finding the cause of the microwave acceleration, effect but phenomena such as microscopic hotspots in the reaction medium are possible. It is also possible that the iridium catalyst may strongly absorb microwave radiation.

3.5.3 Microwave Accelerated One-Pot C-H Borylation/Suzuki-Miyaura Cross-Coupling Sequence

With a method developed for the rapid synthesis of arylboronates from arenes using microwave irradiation, it was sought to improve the one-pot methodology described in chapter II by the application of these new findings.

The use of microwave heating for the Suzuki-Miyaura reaction has been well documented in the literature with many examples reported.[42] A range of arenes were subjected to C-H borylation over the reaction times developed through the work of this chapter. The Suzuki-Miyaura cross-coupling was the carried out in the same reaction tube over a standardised 5 minute reaction time for all examples (***Figure 106***).

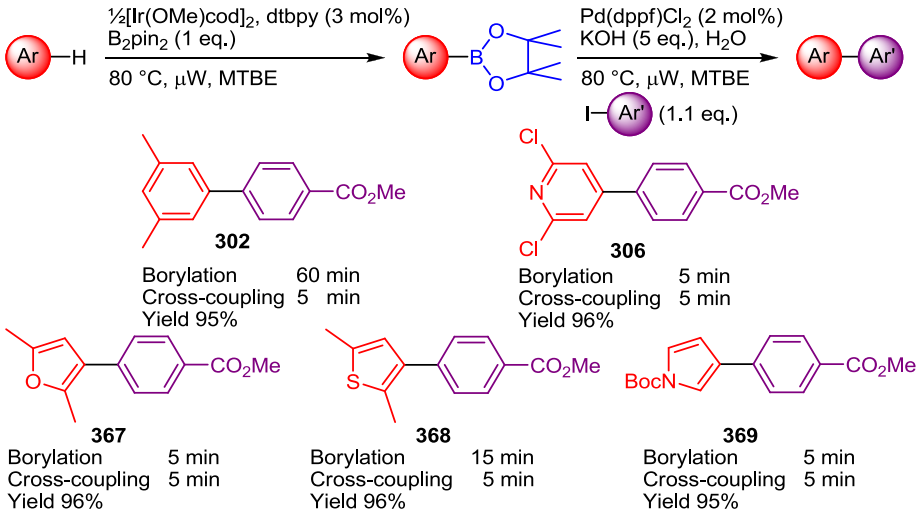

Figure 106 - Microwave accelerated one-pot, single solvent C-H borylation/Suzuki-Miyaura cross coupling sequence.

The sequence was successful for all examples affording quantitative conversions and 95 - 96% isolated yields as 2 mol% $Pd(dppf)Cl_2$ was used for the reaction and thus 4 mol% homocoupled biaryl was be formed by reduction of the Pd^{II} catalyst precursor to Pd^0.

3.6 Conclusions

This methodology has demonstrated a fast and efficient method for the synthesis of borylated arenes with dramatic acceleration of reactions both relative to the standard heating procedure, but also to previous literature reports for the synthesis of the compounds discussed.

The origin of the microwave effect has not been fully determined, but it is likely that a 'specific microwave effect' is the cause of the acceleration observed, with microscopic hotspots being a possible cause.

The one-pot, single solvent C-H borylation/Suzuki-Miyaura cross-coupling sequence has been successfully adapted to a microwave accelerated variant which now allows access to biaryl products from arenes plus aryl halides in reaction times of minutes.

The microwave accelerated C-H borylation methodology has been shown to be particularly effective for more sterically hindered or unreactive substrates. This is an area which will now be further discussed in chapter IV.

3.7 Chapter III - References

1 Mkhalid, I. A. I.; Barnard, J. H.; Marder, T. B.; Murphy, J. M.; Hartwig, J. F., *Chem. Rev.* **2010**, *110*, 890.

2 Kappe, C. O., *Chem. Soc. Rev.* **2008**, *37*, 1127.

3 Kappe, C. O., *Angew. Chem. Int. Ed.* **2004**, *43*, 6250.

4 Gedye, R.; Smith, F.; Westaway, K.; Ali, H.; Baldisera, L.; Laberge, L.; Rousell, J., *Tetrahedron Lett.* **1986**, *27*, 279.

5 Giguere, R. J.; Bray, T. L.; Duncan, S. M.; Majetich, G., *Tetrahedron Lett.* **1986**, *27*, 4945.

6 Scifinder search carried out on 3/11/2010 for 'Microwave Organic' returned 4225 results.

7 Kappe, C. O., *Angew. Chem. Int. Ed.* **2005**, *44*, 7666.

8 Baghurst, D. R.; Mingos, D. M. P., *Chem. Soc. Rev.* **1991**, *20*, 1.

9 Gabriel, C.; Gabriel, S.; Grant, E. H. ; Halstead, B. S. J. ; Mingos, D. M. P., *Chem. Soc. Rev.* **1998**, *27*, 213.

10 Loupy, A., *Microwaves in Organic Synthesis*. Wiley-VCH: Weinheim, 2002; p 499.

11 Tierney, J. P.; Lindström, P., *Microwave Assisted Organic Synthesis*. Blackwell: Oxford, 2004; p 280.

12 Schanche, J-S., *Mol. Diversity* **2003**, *7*, 293.

13 Kuhnert, N., *Angew. Chem. Int. Ed.* **2002**, *41*, 1863.

14 Langa, F.; de la Cruz, P.; de la Hoz, A.; Diaz-Ortiz, A.; Diez-Barra, E., *Contemp. Org. Synth.* **1997**, *4*, 373.

15 Perreux, L.; Loupy, A., *Tetrahedron* **2001**, *57*, 9199.

16 Strauss, C. R., *Angew. Chem. Int. Ed.* **2002**, *41*, 3589.

17 Baghurst, D. R.; Mingos, D. M. P., *J. Chem. Soc., Chem. Commun* **1992**, 674.

18 Saillard, R.; Poux, M.; Berlan, J.; Audhuy-Peaudecerf, M., *Tetrahedron* **1995**, *51*, 4033.

19 Kremsner, J. M.; Kappe, C. O., *J. Org. Chem.* **2006**, *71*, 4651.

20 Bogdal, D.; Lukasiewicz, M.; Pielichowski, J.; Miciak, A.; Bednarz, S., *Tetrahedron* **2003**, *59*, 649.

21 Lukasiewicz, M.; Bogdal, D.; Pielichowski, J., *Adv. Synth. Catal.* **2003**, *345*, 1269.

22 Appukkuttan, P.; Dehaen, W.; Van der Eycken, E., *Chem. Eur. J.* **2007**, *13*, 6452.

23 Strauss, C. R.; Trainor, R. W., *Aust. J. Chem.* **1995**, *48*, 1665.

24 Larhed, M.; Hallberg, A., *J. Org. Chem.* **1996**, *61*, 9582.

25 Glasnov, T. N.; Stadlbauer, W.; Kappe, C. O., *J. Org. Chem.* **2005**, *70*, 3864.

26 Yinghuai, Z.; Chenyan, K.; Peng, A. T.; Emi, A.; Monalisa, W.; Louis, L. K-J.; Hosmane, N. S.; Maguire, J. A., *Inorg. Chem.* **2008**, *47*, 5756.

27 Beck, E. M.; Hatley, R. ; Gaunt, M. J., *Angew. Chem. Int. Ed.* **2008**, *47*, 3004.

28 Cho, J. Y.; Iverson, C. N.; Smith, M. R., III., *J. Am. Chem. Soc.* **2000**, *122*, 12868.

29 Ishiyama, T.; Takagi, J.; Ishida, K.; Miyaura, N.; Anastasi, N. R.; Hartwig, J. F., *J. Am. Chem. Soc.* **2002**, *124*, 390.

30 Harrisson, P; Morris, J; Steel, P. G.; Marder, T. B., *Synlett* **2009**, *1*, 147.

31 Nöth, H.; Wrackmeyer, B., *Nuclear magnetic resonance spectroscopy of boron compounds.* Springer-Verlag: Berlin, New York, 1978.

32 Cho, J.; Tse, M. K.; Holmes, D.; Maleczka, R. E., Jr.; Smith, M. R., III., *Science* **2002**, *295*, 305

33 Ishiyama, T.; Miyaura, N., *J. Organomet. Chem.* **2003**, *680*, 3.

34 Takagi, J.; Sato, K.; Hartwig, J. F.; Ishiyama, T.; Miyaura, N., *Tetrahedron Lett.* **2002**, *43*, 5649.

35 Coventry, D. N.; Batsanov, A. S.; Goeta, A. E.; Howard, J. A. K.; Marder, T. B.; Perutz, R. N., *Chem. Commun.* **2005**, 2172.

36 Mkhalid, I. A. I.; Coventry, D. N.; Albesa-Jove, D.; Batsanov, A. S.; Howard, J. A. K.; Perutz, R. N.; Marder, T. B., *Angew. Chem. Int. Ed.* **2006**, *45*, 489.

37 Chotana, G. A.; Kallepalli, V. A.; Maleczka, Robert E. Jr.; Smith, Milton R. III., *Tetrahedron* **2008**, *64*, 6103.

38 Paul, S.; Chotana, G. A.; Holmes, D.; Reichle, R. C.; Maleczka, R. E., Jr.; Smith, M. R., III., *J. Am. Chem. Soc.* **2006**, *128*, 15552.

39 Lo, W. F.; Kaiser, H. M.; Spannenberg, A.; Beller, M.; Tse, M. K., *Tetrahedron Lett.* **2007**, *48*, 371.

40 Kallepalli, V. A.; Shi, F.; Paul, S.; Onyeozili, E. N.; Maleczka, R. E., Jr.; Smith, M. R., III., *J. Org. Chem.* **2009**, *74*, 9199.

41 Ishiyama, T.; Nobuta, Y.; Hartwig, J. F.; Miyaura, N., *Chem. Commun.* **2003**, 2924.

42 Larhed, M.; Moberg, C.; Hallberg, A., *Acc. Chem. Res* **2002**, *35*, 717.

CHAPTER IV- C-H BORYLATION OF SUBSTITUTED QUINOLINES

4.1 Introduction

The borylation of substrates which possess more than one sterically accessible position can result in multiple regioisomeric products being formed.[1,2] This is exemplified in the borylation of mono-substituted benzenes at 80 °C, which form an approximately statistical mixture (2:1) of *meta:para* borylated products.[3] As such, the majority of the work published exploring substrate scope has involved the use of steric blocking groups to limit the available sites for borylation.[4] This allows more facile purification and isolation of products.

The selectivity of the borylation reaction has been shown to be dominated by steric effects.[4] However, in heteroaromatic substrates, a more subtle electronic influence has been shown to be important. Borylation of 5-membered heterocycles occurs adjacent to the heteroatom,[2,5] whilst, borylation of pyridine substrates avoids positions adjacent to the heteroatom.[2] The electronic effects which have been observed are not fully understood.

In order to more fully explore the underlying cause of this electronic selectivity it is necessary to remove any steric influence on the selectivity of the reaction. The work described below seeks to deliver substrates which contain positions of steric equivalence but electronic inequivalence. The quinoline scaffold was chosen to carry out this study.

This chapter will provide an overview of existing methodologies used in both the synthesis and derivatisation of quinolines. The synthesis of borylated quinolines will be discussed. Efforts have also been made to understand the observed selectivity. Importantly, this work has provided an insight into the underlying electronic effects that impact upon the selectivity of the borylation process in aromatic and heteroaromatic systems. Along with the goal of understanding the causes of selectivity, this work also provides a method for the functionalisation of quinolines.

4.2 Uses of Quinoline Derivatives

The quinoline heterocyclic scaffold is an important class of molecules with applications in many areas of chemistry (***Figure 107***).[6-10] Reflecting their prevalence in natural products,[11-13] quinoline-containing compounds have been shown to be highly biologically active compounds with a diverse range of medical applications, e.g., treatment of malaria,[14,15] HIV,[16-19] and

tuberculosis. [6,20-22] In addition to this biological role, quinolines have found other diverse applications including those in molecular electronics (OLEDs)[23] and dye-stuffs.[10]

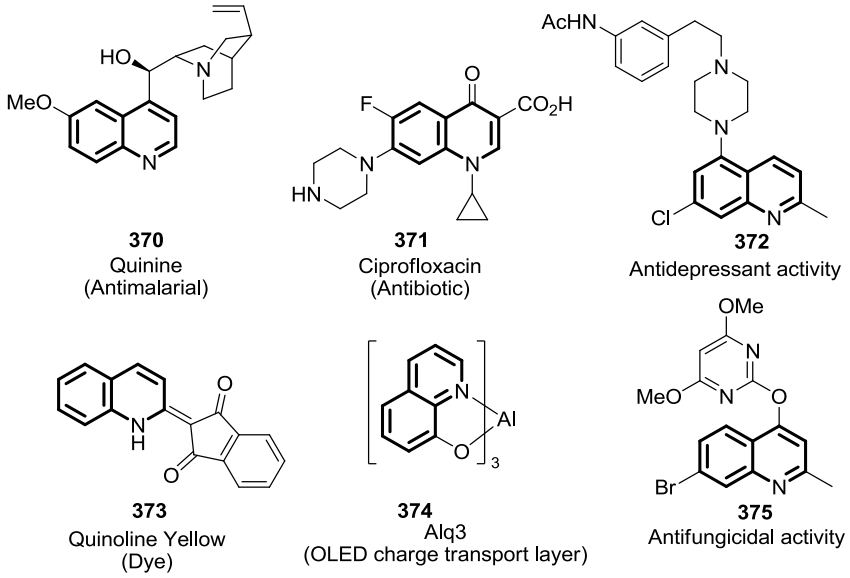

Figure 107 - Applications of quinolines.[6-10,24]

Due to the wide range of applications which quinolines have found, methods for their synthesis and derivatisation have become important. The following section will address the issues associated with these topics.

4.3 Quinoline Synthesis

Quinoline was first discovered in 1834 by extraction from coal tar.[25] Following its discovery, syntheses of the quinoline ring system[26,27] were developed by Skraup,[28-33] Döbner and Miller,[31-35] Combes,[36] and Friedländer.[37-39] These involve reactions of substituted anilines and can provide a wide range of substitution patterns. However, they typically require harsh conditions and often involve problematic purifications (***Figure 108***).[32,33,35]

Further discussion of both procedural and mechanistic issues associated with these reactions will be undertaken later in the chapter (Section 4.4.3.1), with particular focus on the Döbner-Miller reaction.

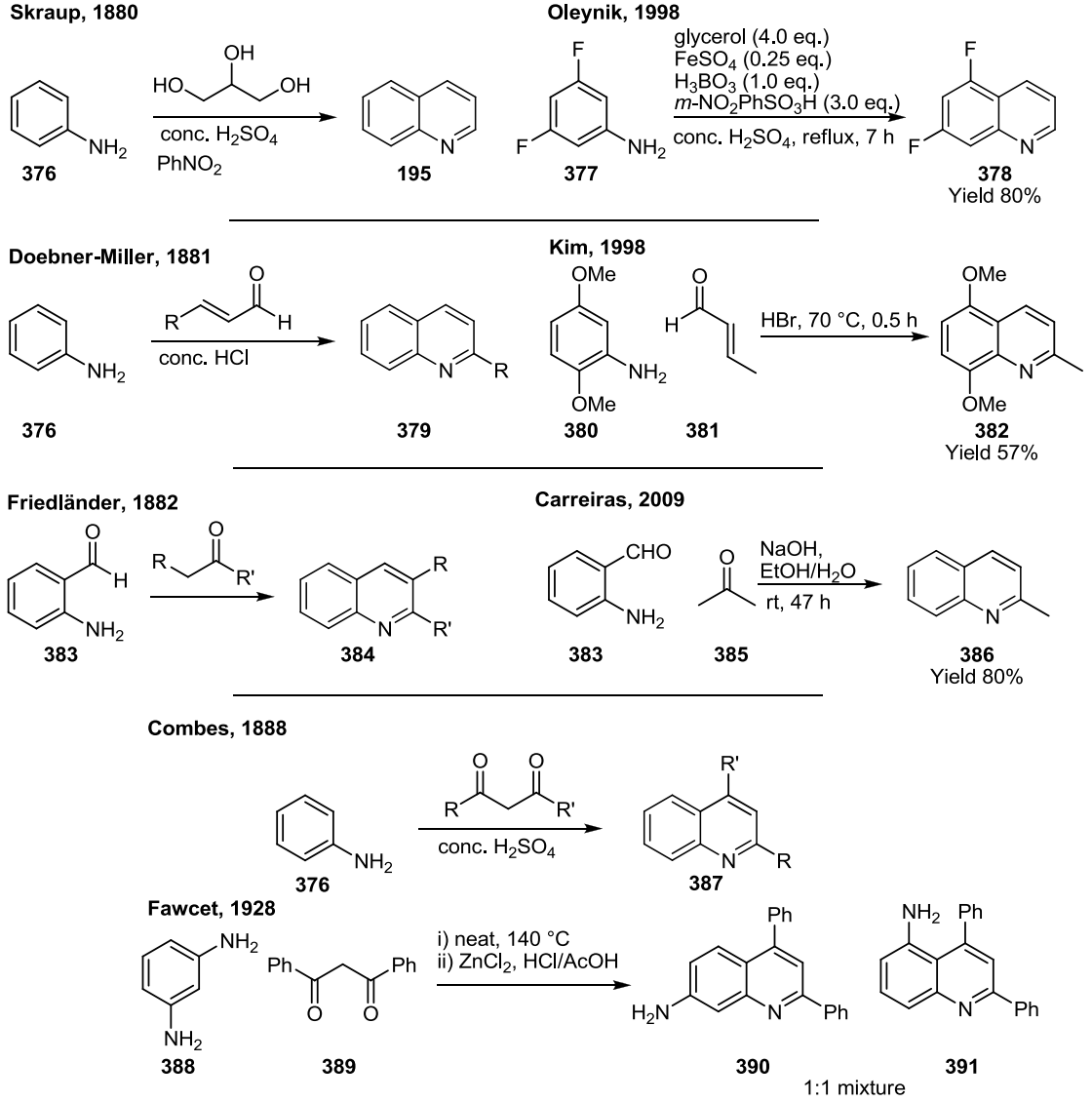

Figure 108 - Classical methods for the synthesis of quinolines.[40-42]

Following these initial discoveries, a wide range of new methods for synthesizing the heterocyclic core have been developed (***Figure 109***).[43-48] Similarly, these methods install all functionality at the start of the synthesis.

The majority of the new methods developed utilise a similar starting point for the reactions, namely substituted anilines. The major improvements are based on the higher selectivity for the desired product and easier product recovery compared to classical methods. Although these methods offer more selective routes to quinoline compounds many syntheses still require forcing conditions or strongly acidic work-up to afford the desired products. As such, the functional group tolerance of these reactions is not significantly improved when compared to

the classical methods. Due to these factors methods for derivatising preformed quinolines are thus desirable.

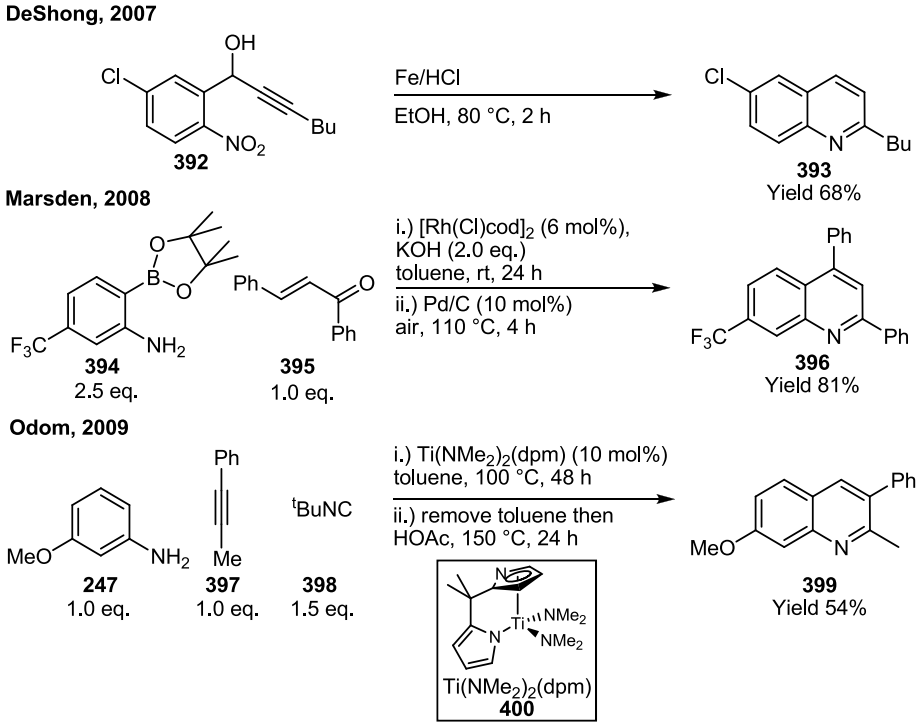

Figure 109 - Novel synthetic methodologies of quinoline scaffolds.[44-46]

4.3.1 Functionalisation of Quinolines

The late stage functionalisation of molecules has become a widely used strategy within drug development and library synthesis. Methods for the functionalisation of the preformed quinoline ring system are highly desirable. A common route to further functionalisation of quinolines is through the use of nucleophilic displacement reactions of halide groups installed on the quinoline ring (***Figure 110***). This concept will be discussed in more detail later in the chapter.

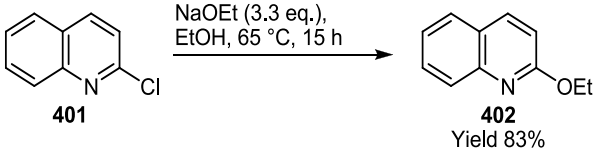

Figure 110 - Nucleophilic halide displacement with 2-chloroquinoline.[49,50]

Direct functionalisation of quinoline C-H bonds is also possible but, in many cases, regioselectivity is low. Electrophilic aromatic substitution of quinolines typically yields mixtures of 5- and 8-functionalised products with activation occurring on the more electron rich carbocyclic ring (***Figure 111***).

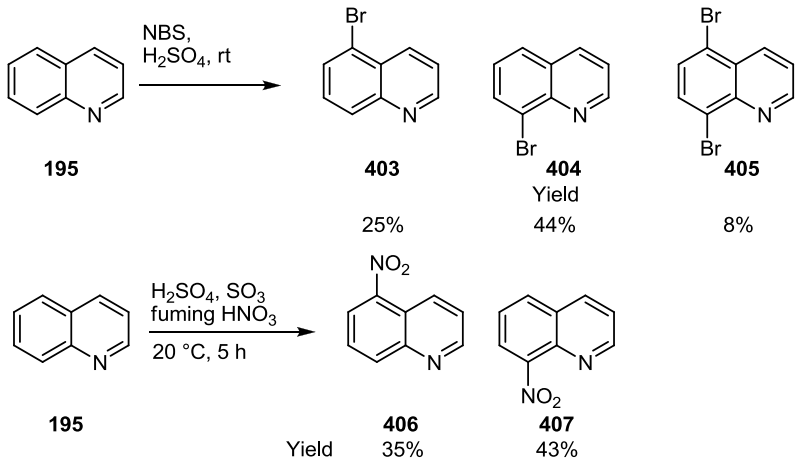

Figure 111 - Electrophilic bromination and nitration of quinoline.[51,52]

Nucleophilic aromatic substitution functionalises the more electron deficient heteroaromatic ring in the 2- and 4- positions (***Figure 112***); however, reactivity is typically low resulting in extended reaction times.

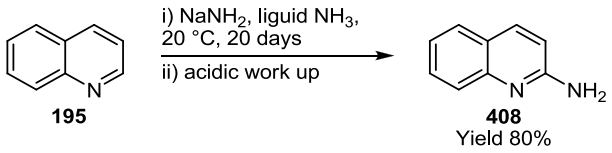

Figure 112 - Nucleophilic addition to quinoline.[53]

C-H activation of both quinoline and quinoline *N*-oxide typically afford the 2-substituted products (***Figure 113***). However, reactions typically require high reaction temperatures (130 - 150 °C) to afford high product yields.

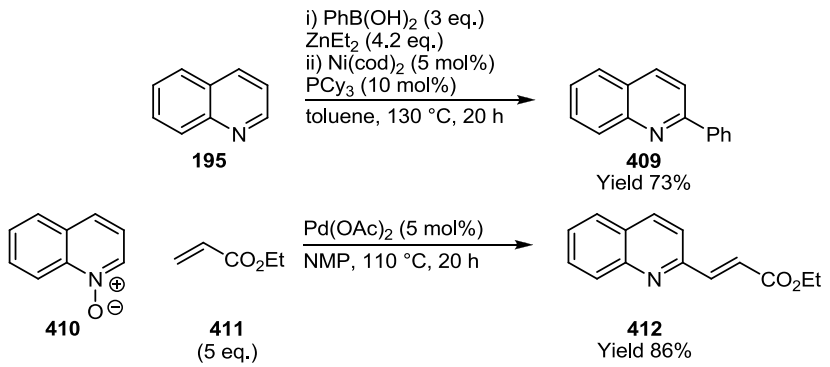

Figure 113 - Nickel catalysed direct arylations of quinoline and palladium catalysed oxidative Heck-coupling to quinoline *N*-Oxide.[54,55]

Knochel and co-workers[56] have developed an alternative strategy involving directed metalation chemistry. Coordination of the base complex to the pyridine nitrogen directs deprotonation to the 2-position. However, due to the strong bases and highly nucleophilic reaction conditions functional group compatibility is low (***Figure 114***).

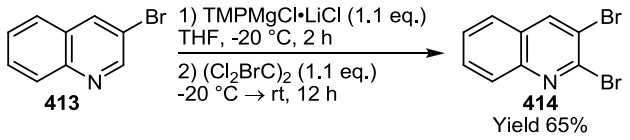

Figure 114 - *N*-directed magnesiation of 3-bromoquinoline.[56]

A wide variety of methods have been developed for the functionalisation and derivatisation of quinolines. However, the reactions employed typically require harsh reaction conditions. The following section will examine application of a milder C-H borylation strategy for the functionalisation of quinolines.

4.3.2 Selectivity of C-H Borylation in Analogous Systems to Quinoline

4.3.2.1 C-H Borylation of Quinoline

As discussed in chapter III, the C-H borylation of quinoline was first reported by Ishiyama and co-workers[57] using a 10 fold excess of quinoline to ensure that a single mono-borylated product was formed in 84% yield (based on B_2pin_2) (***Figure 94***).

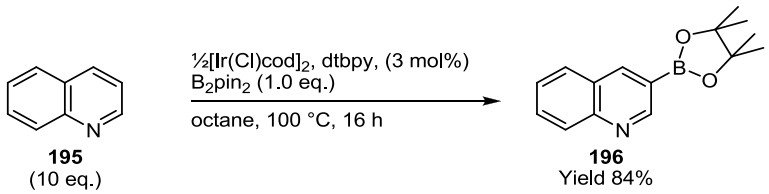

Figure 115 - C-H borylation of quinoline with $[Ir(Cl)cod]_2$/dtbpy catalyst system.[57]

As discussed in chapter III,[58] when quinoline was subjected to C-H borylation using equimolar quantities of arene and diboron reagent it was not possible to form the mono-borylated product in the absence of bis-borylated products. When the reaction was conducted with 2.0 equivalents of B_2pin_2 the reaction proceeded to give a 1:1 mixture of 3,6 and 3,7 bis-borylated products (***Figure 95***).

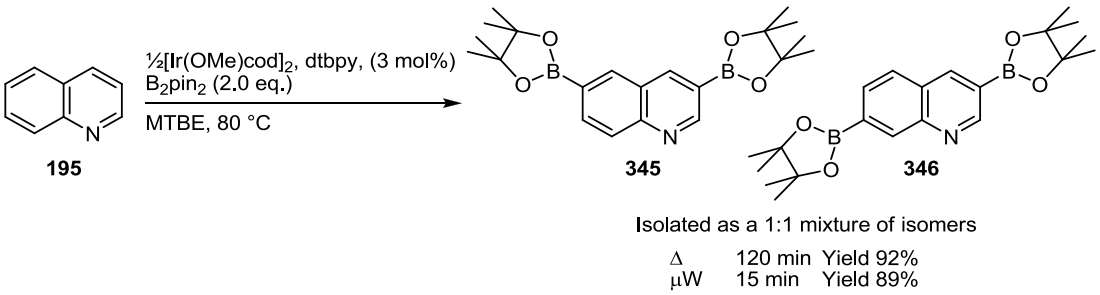

Figure 116 - C-H borylation of quinoline under thermal and microwave conditions.[58]

In this case, based on the precedent established by Ishiyama[57] it can be assumed that initial borylation occurs on the more reactive heteroaromatic ring. Borylation on the carbocyclic ring occurs subsequently. The formation of a 1:1 mixture of 3,6- and 3,7-bis-borylated products is due to the 6- and 7-positions being sterically equivalent. The borylation of quinoline is able to

provide interesting insights into the selectivity of the reaction but, due to the large excess of quinoline required to avoid multiple product formation, is of limited synthetic use.

4.3.2.2 Analogy to Naphthalene Borylation

The selectivity of the C-H borylation reaction with quinoline highlights that the regiochemistry of the reaction is dominated by steric effects. In general, borylation does not occur at positions *ortho* to a substituent or a ring junction. The selectivity observed for quinoline is therefore directly analogous to that seen with naphthalene. Initial reaction affords the 2-borylated product, as this is the only position non-adjacent to a ring junction. When excess B_2pin_2 is present, a second borylation occurs to give a 1:1 mixture of the 2,6 and 2,7 bis-borylated products (***Figure 117***).[59]

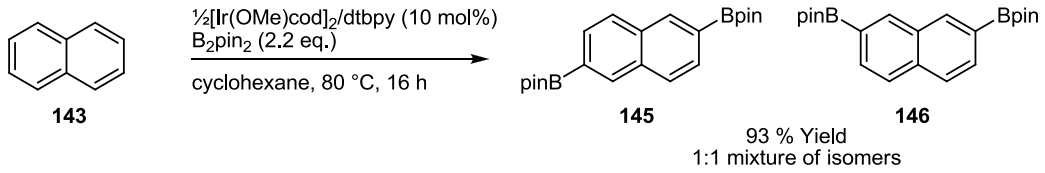

Figure 117 - C-H borylation of naphthalene using the $[Ir(OMe)cod]_2$/dtbpy catalyst system.

4.3.2.3 Analogy to Pyridine Borylation

Whilst the analogy of the borylation of quinoline to naphthalene addresses the issue of steric selectivity, it does not explain the electronic selectivity. Further parallels can be drawn with the borylation of pyridine.

Unsubstituted pyridine shows diminished reactivity, due to co-ordination of the substrate to the iridium catalyst thus blocking the site required for C-H activation.[2,57] A 2:1 mixture of *meta*:*para* products is obtained with no *ortho* product being formed (***Figure 118***).

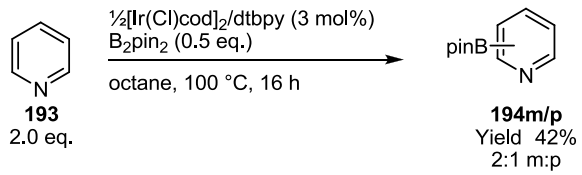

Figure 118 - C-H borylation of pyridine $[Ir(Cl)cod]_2$/dtbpy catalyst system.[2,57]

However, the introduction of groups in, either one or both of, the 2 and 6 positions block coordination to Ir allowing significantly improved reactivity. As discussed previously, heteroarenes exhibits higher reactivity than the carbocycles, c.f., quinoline. This is evident from a comparison of the borylation of 2,6-dimethylpyridine and *m*-xylene. The borylation of *m*-xylene required 6 hours to reach full conversion whist 2,6-dimethylpyridine required 30 minutes (***Figure 119***).

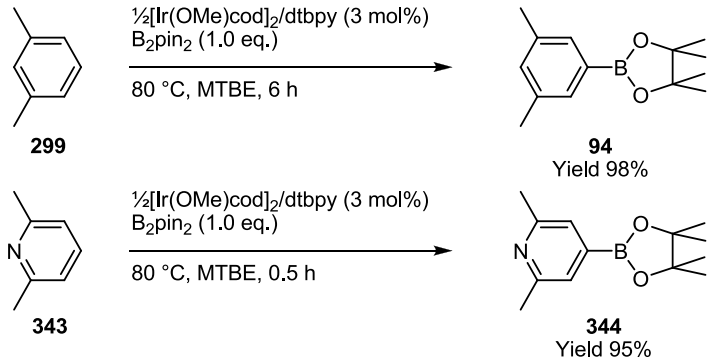

Figure 119 - Borylation of 2,6-dimethylpryride and *m*-xylene.[58]

The enhanced reactivity of pyridines is further demonstrated by the borylation of 2-phenylpyridine. Borylation occurs exclusively on the heterocyclic ring affording a 1:1 mixture of 4- and 5-borylated products (***Figure 120***).[1]

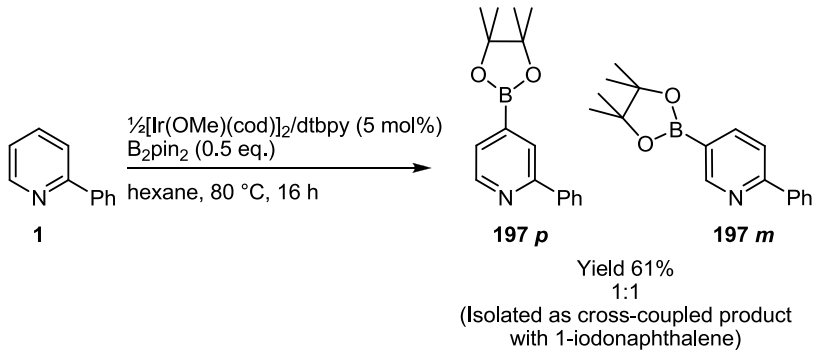

Figure 120 - Borylation of 2-phenylpyridine using the $[Ir(OMe)cod]_2$/dtbpy catalyst system.[1]

The introduction of substituents can force borylation to occur adjacent to the pyridine nitrogen; thus, 4,4′-^{t}Bu$_2$-2,2′-bipyridine is exclusively borylated *ortho*- to nitrogen[1] (***Figure 121***). As discussed in chapter I, pyridine borylation does not normally occur at the 2-position.[2] However, the borylation of dtbpy demonstrates that the 2-position is reactive if the remaining positions are sterically blocked.

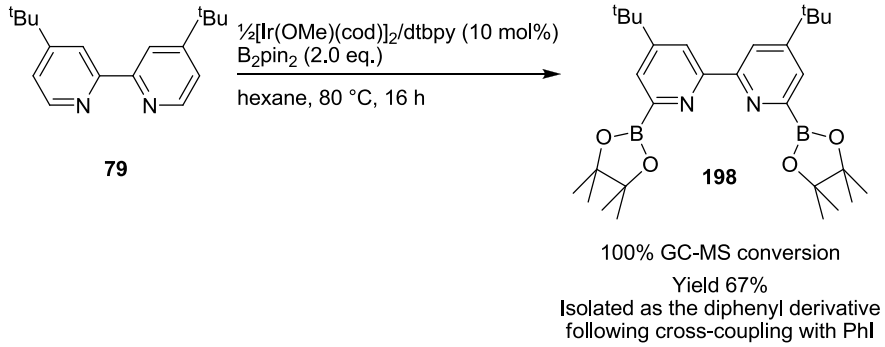

Figure 121 - Borylation of dtbpy using the $[Ir(OMe)cod]_2$/dtbpy catalyst system.[1]

Beyond the observations dealing with the reaction of the parent quinoline, there have been no reports describing the application of iridium catalysed borylation as a strategy for the preparation of functionalised quinolines.

4.4 Results and Discussion

Given the prevalence of quinoline derivatives within biological and materials applications, it was of interest to explore the effect of different substitution patterns on the regiochemical outcome of the borylation reaction; along with the interest in exploring the electronic selectivity of these systems.

4.4.1 Borylation of 2,6-Disubstituted Quinolines

The 2,6-disubstituted quinoline scaffold was chosen as the first substrate class to explore. This class of substrates contains C-H bonds which are either *ortho*- to a substituent or at a position adjacent to a ring junction. The substrates used for this study were all commercially available; however, derivatives can be prepared by the Döbner-Miller reaction, *vide infra*.

Each reaction was conducted as described in chapter III. This involved charging a crimp top microwave vial with substrate which was followed by sealing with a crimp top, purging with argon and addition of a catalyst stock solution ($[Ir(OMe)cod]_2$ (0.015 mmol), dtbpy (0.03 mmol) and B_2pin_2 (1.0 mmol)). The reactions were then heated in the microwave reactor for 1.5 hours at 100 °C. All reactions were monitored by GC-MS, products were purified by silica gel column chromatography and characterised NMR spectroscopy to confirm product identity (***Figure 122***, ***Table 15***).

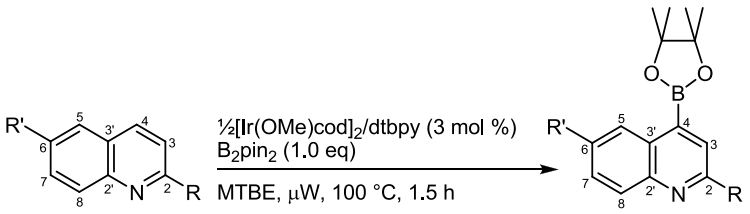

Figure 122- Borylation of 2,6-disubstituted quinolines.

Table 15 - Microwave assisted C-H borylation of 2,6-disubstituted quinolines.

Entry	R	R′	Substrate	Product	Temp (°C)	Time (h)	Isolated Yield (%)
1	Me	Me	**415**	**420**	100	1.5	72
2	Me	OMe	**416**	**421**	100	1.5	76
3	Me	Cl	**417**	**422**	100	1.5	79
4	Me	Br	**418**	**423**	100	1.5	84
5	CN	OMe	**419**	**424**	100	1.5	(98)[a]
6	CN	OMe	**419**	**424**	rt[b]	48	83

[a] GC-MS conversion to product, (85:15) mixture of 4-:3- isomers (confirmed by ^{1}H NMR analysis of crude reaction mixture)

[b] Reaction run at ambient temperature (no heating) which was monitored at ca. 22 - 25 °C

The borylation of 2,6-dimethylquinoline **415** will be discussed as a representative example (***Table 15***, entry 1). Upon completion of the reaction, the observation of a molecular ion of 283 *m/z* by GC-MS was consistent with a mono-borylated product **420**. The reaction mixture was subjected to silica gel column chromatography to give **420** in 72% isolated yield which was further analysed by ^{1}H, ^{13}C and ^{11}B NMR (for the ^{1}H NMR spectrum see ***Figure 123***).

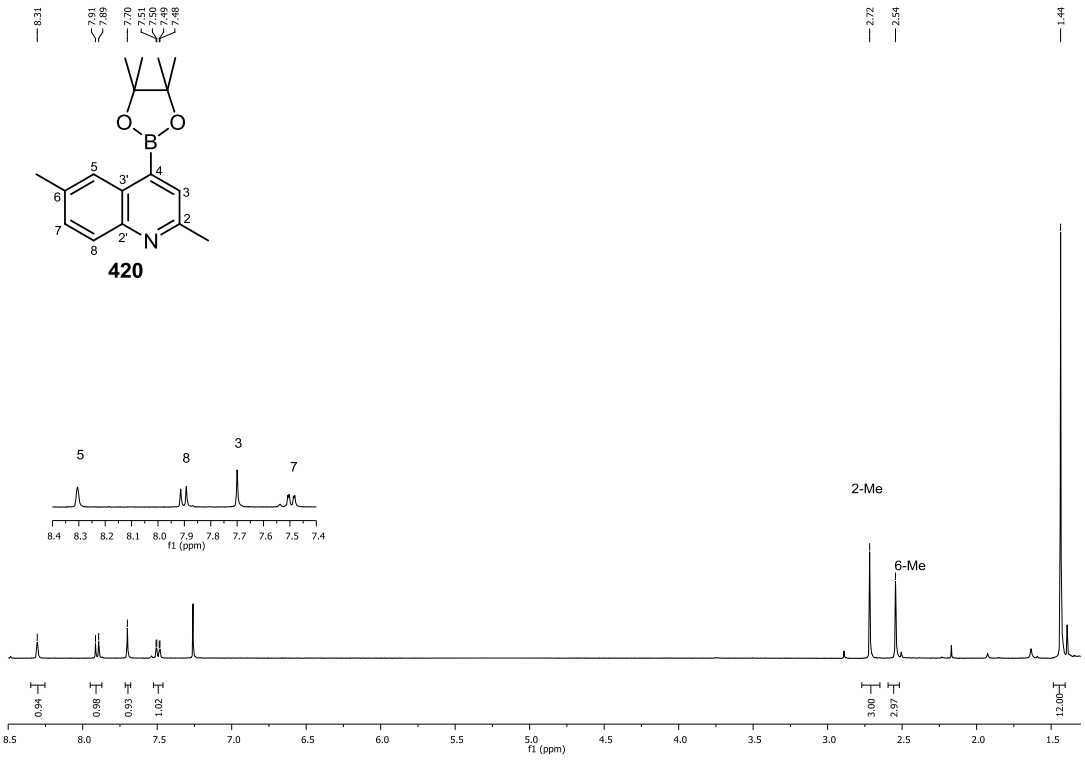

Figure 123 - ^{1}H NMR spectrum of 2,6-dimethyl-4-Bpin-quinoline (400 MHz, $CDCl_3$).

Product identity was confirmed by full assignment of ^{1}H and ^{13}C NMR spectra using COSY, HSQC and HMBC spectroscopic techniques. Analysis of the ^{1}H NMR spectrum confirmed the broad singlet at 8.31 ppm as H^5; however, coupling from H^5 to H^7 at 7.49 ppm could not be resolved. In contrast, the signal at 7.49 ppm (dd) showed 4-bond-W-coupling to H^5 (J =1.9 Hz), consistent with their *meta*- disposition. The signal at 7.70 ppm exhibited a 3-bond-*ortho*-coupling to the signal at 7.90 ppm (J = 8.5 Hz) consistent with their *ortho*- relationship. Both H^5 and H^7 showed long range correlations with the carbon of the methyl group at C^6 in the HMBC spectrum. The sharp singlet at 7.70 ppm was consistent with borylation on the heteroaromatic ring in either the 3- or 4- positions. Correlation in the HMBC spectrum between the C^2 methyl group and the signal at 7.70 ppm confirmed the position of the Bpin group to be at the C^4 position. As discussed in chapter II, the carbon attached to boron was not visible in the ^{13}C NMR spectrum due to line broadening caused by the quadrupolar boron nucleus. Signals for the hydrogens closest to the Bpin group (H^3 and H^5) are shifted to higher ppm, relative to the parent arene, whilst signals for H^7 and H^8 remained unchanged.

Similarly, all of the other 2,6-disubstituted quinolines gave the 4-borylated product, as detailed in ***Table 15***. All spectroscopic data, and thus, the resulting peak assignments, were consistent with the patterns described for **420**. The regioisomeric identities of the products formed were further confirmed by single crystal X-ray analyses of 6-chloro-2-methyl-4-Bpin-quinoline and 6-bromo-2-methyl-4-Bpin-quinoline (***Figure 124***).

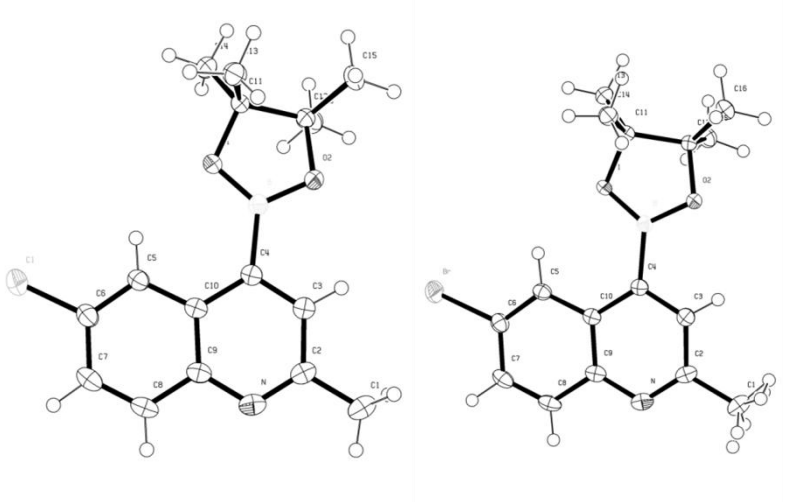

422 **423**

Figure 124 - Molecular structure of 2-methyl-6-chloro-4-Bpin-quinoline and 2-methyl-6-bromo-4-Bpin-quinoline (Thermal ellipsoids drawn at 50% probability).

Interestingly, when 2-cyano-6-methoxyquinoline **419** was subjected to borylation at 100 °C under microwave conditions, an 85:15 mixture of 4-borylated and 3-borylated products was formed, confirmed by ^{1}H NMR spectroscopic analysis of the crude reaction mixture.

When this reaction was carried out at room temperature, the 4-borylated product **424** was formed exclusively. The concept of reducing reaction temperature to improve selectivity is a common approach. Room temperature borylation reactions have been widely used in the case of highly reactive substrates, such as thiophene and furan, for which heating is not required to achieve rapid conversion to product (***Figure 125***).[3,5,60] However, specific studies of the influence of temperature on the selectivity of a borylation reaction have not been reported.

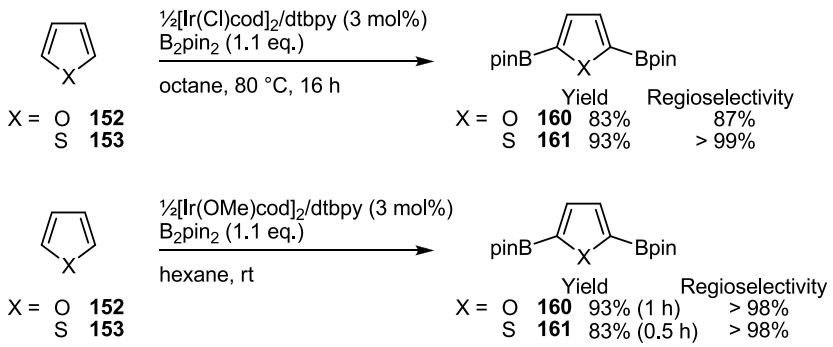

Figure 125 - Temperature dependent borylation of thiophene and furan.[3,5,60]

Thiophene and furan were reported to borylate with > 99% and 87% selectivity, respectively, for the 2,5-bisborylated product. The regioselectivity of the reaction with furan is likely due to an increased relative reactivity of the 3-position in this substrate. The two syntheses differ in the nature of the catalyst precursor employed, with the room temperature reaction utilising the more active $[Ir(OMe)cod]_2$/dtbpy catalyst system. However, it can be seen that the reduction in reaction temperature can provide higher regioselectivity.

The results using 2,6-disubstituted quinolines demonstrate the preference for borylation to occur at positions adjacent to ring junctions over positions adjacent to the substituents in these systems. The higher reactivity of the heteroaromatic ring is also demonstrated with a preference for the 4-position over the similar steric environment of the 8-position.

This preference may be purely due to the higher reactivity of the heteroarene or may suggest a steric influence of the nitrogen lone pair, suggesting that the steric bulk of a nitrogen lone pair is greater than that of a C-H bond. Such an inhibitory effect may also contribute to the lack of *ortho* borylation in analogous pyridine systems.[1,2]

4.4.2 Borylation of 4,7-Disubstituted Quinolines

Having demonstrated the regioselective borylation of 2,6-disubstituted quinolines, attention was turned to 4,7-disubstituted quinolines. This class of substrate offered a challenge due to all positions of the ring being sterically hindered, apart from the 2-position adjacent to the nitrogen in the heterocyclic ring. The 4,7-disubstituted quinoline scaffold was borylated as described in the previous section using microwave heating at 100 °C for 1.5 hours (***Figure 126***, ***Table 16***).

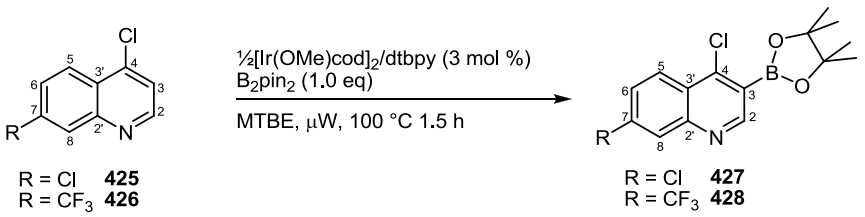

Figure 126- Borylation of 4,7-disubstituted quinolines.

Table 16 - C-H borylation of 4,7-disubstituted quinolines.

Entry	R	Starting Material	Product	Temp (°C)	GC-MS Conversion (%)	Yield (%)
1	Cl	**425**	**427**	100	> 95	81
2	CF_3	**426**	**428**	100	> 95	76

Substrates **425** and **426** are commercially available and thus formed the starting point for this work. Compounds **425** and **426** were subjected to the borylation reaction forming 3-functionalised products. Product identity was confirmed by full assignment of ^{1}H and ^{13}C NMR spectra using COSY, HSQC and HMBC spectroscopic techniques.

For example, for the borylation of 4,7-dichloroquinoline **425**, analysis of the product by GC-MS gave a molecular ions at 323, 324 and 325 *m/z* in a 10:6:1 ratio, consistent with a mono-borylated product **427**. A sharp singlet in the ^{1}H NMR spectrum at 9.03 ppm was assigned to H^2 with a position at high ppm consistent with a proton adjacent to an azine nitrogen. The H^2 signal was also shifted to higher ppm relative to the parent heterocycle due to the Bpin group in the C^3 position. The signal at 156.2 ppm at the ^{13}C NMR spectrum was assigned by HSQC correlation with H^2. The position of this signal is again consistent with the carbon adjacent to an azine nitrogen.

The remainder of the ^{1}H NMR spectrum revealed close analogy to the starting heterocycle; suggesting that the carbocyclic ring remained undisturbed during the reaction. Notably, Signals at 8.28 ppm (d) and 7.58 ppm (dd) in the ^{1}H NMR spectrum correspond to H^5 and H^6 respectively. A coupling constant of J = 9.0Hz is consistent with the *ortho*- relationship of these atoms. The signal at 7.58 ppm (dd) shows a 4-bond-W-coupling (J = 2.0 Hz) to the signal at 8.11 ppm (d) confirming the identity of the H^6 and H^8 signals respectively. The coupling

constants are consistent with the *meta*- relationship of H^6 and H^8. All spectroscopic data and atomic assignments for **428** were consistent with the patterns described for **427**.

The reaction selectively activates the 3-position in preference to the 2 and 6- positions. As discussed previously, borylation at the 2-position is challenging. Borylation *ortho*- to a substituent in preference over the 2-position is analogous to that observed in the borylation of 4,4′-OMe_2-2,2′-bipyridine, which preferentially reacts at the positions *ortho*- to the methoxy groups and not *ortho* to the pyridine nitrogen (***Figure 127***).[1]

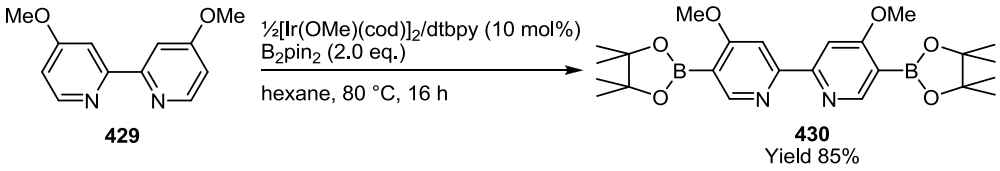

Figure 127 - Borylation of 4,4′-$(OMe)_2$-2,2′-bipyridine.

As discussed in Chapter I, selective borylation *ortho* to chlorine or methoxy substituents has been reported in the reactions of chlorobenzene and anisole using the Si-SMAP supported monodentate phosphine iridium catalyst system (***Figure 128***).[61,62]

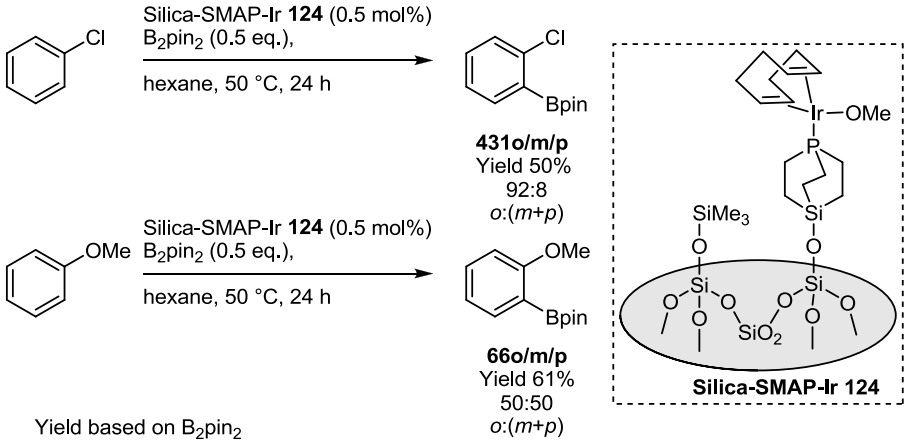

Figure 128 - *Ortho*-borylation of chlorobenzene and anisole with Si-SMAP-Ir catalyst system.[61,62]

However, in contrast to the dtbpy-ligated iridium catalyst the mono-phosphine based system presumably has an additional vacant site which would allow coordination via Cl or O of the

substrate to direct *ortho*-borylation. A measure of steric bulk was noted by Smith and co-workers,[63] in their studies of the borylation of 4-substituted benzonitriles. A scale of steric size ranged from smallest to largest in the following order F<CN<OMe<Cl<SMe<Me<Br<I.[63-65] This steric measure demonstrates that both OMe and Cl are relatively small substituents. It is, however, possible that the observed effect is not purely due to steric availability but also to an *ortho*-activating effect of the substituent.

In order to assess whether the presence of the 4-chloro group was necessary to achieve reaction, 4-methyl-7-trifluoromethyl quinoline **432** was prepared. A palladium catalysed procedure, analogous to that previously used for the methylation of 9-chloroanthracene **433** (***Figure 129***)[66] was applied to the formation of **432**.

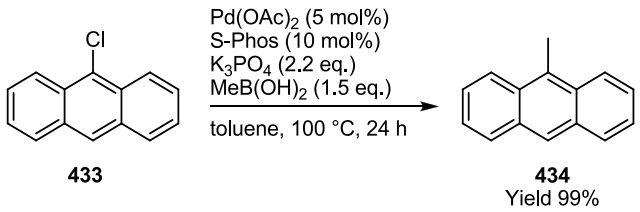

Figure 129 - Suzuki-Miyaura cross coupling of methyl boronic acid.[66]

Compound **426** was subjected to palladium catalysed Suzuki-Miyaura cross-coupling with methyl boronic acid affording **432** in 93% yield (***Figure 130***).

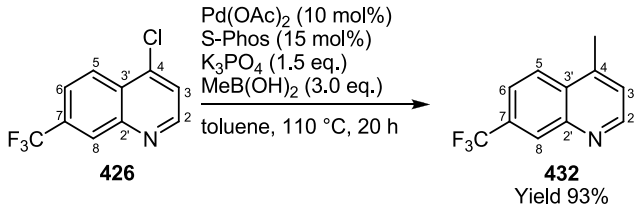

Figure 130 - Synthesis of **432** by palladium catalysed methylation of **426**.

Analysis by GC-MS showed a molecular ion of 211 *m/z*, consistent with **432**. Analysis of the ^{1}H NMR spectrum showed the signal at 8.87 ppm (d) which is consistent with a hydrogen adjacent to an azine nitrogen, H^2. H^2 showed an *ortho*-3-bond coupling (J = 4.2 Hz) to the signal 7.35 ppm (d) corresponding H^3. The peak pattern discussed for the carbocyclic ring of 4-

4,7-dichloroquinoline-3-Bpin **427** was present in the ^{1}H NMR spectrum confirming assignments of resonances for H^5, H^6 and H^8. Correlation in the HMBC spectrum between the C^4-methyl hydrogens at 2.75 ppm and the carbon at $C^{3'}$ (130.1 ppm) and C^3 (123.7 ppm) further confirm the regiochemistry of **432**.

432 was subjected to the borylation reaction conditions at 100 °C for 1.5 hours (***Figure 131***). However, analysis by GC-MS showed less than 5% conversion to multiple borylation products. The lack of reactivity of **432** is puzzling when compared to the borylation *ortho*- to nitrogen of dtbpy.[1] Based on the reaction of dtbpy, **432** would be expected to form the 2-borylated product but this was not observed. The reason for this is not understood.

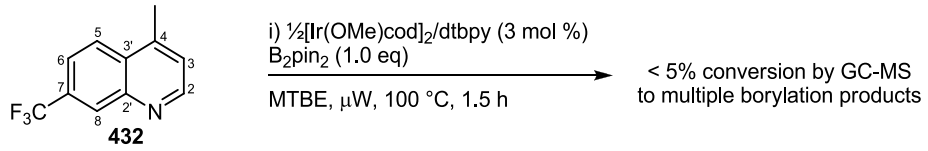

Figure 131 - Attempted C-H borylation of **432**.

The low reactivity of **432** relative to **426** and **427** suggests that chlorine substituent may provide an *ortho*-activating electronic effect. This concept will be discussed further later in the chapter.

4.4.3 2,7-Disubstituted Quinolines

Having demonstrated the regioselective borylation of 2,6- and 4,7-disubstituted quinolines, 2,7-disubstituted quinolines were examined. However, only 2,7-dimethyl and 2-methyl-7-chloro-quinoline were readily commercially available. The following section will describe efforts towards the synthesis of a series of 2-methyl-7-substituted quinolines via the Döbner-Miller reaction.

4.4.3.1 Synthesis of 2-Methyl-7-Substituted Quinolines

As discussed earlier in this chapter, a wide range of methods for the synthesis of quinolines have been developed.[28-39,43-48,67-69] The method most suited to the synthesis of 2-substituted quinolines is the Döbner-Miller[34] reaction.

4.4.3.1.1 The Döbner-Miller Reaction

The reaction utilises a substituted aniline and crotonaldehyde in concentrated acid to form the desired product. The reaction is classically carried out by addition of the aniline and crotonaldehyde to refluxing concentrated (6 M) hydrochloric acid, but many adaptations of the reaction have been described. The adaptations will be further discussed throughout this section. In order to understand the selectivity of the reaction, key points associated with its mechanism will now be highlighted.

4.4.3.1.1.1 Mechanism of the Döbner-Miller Reaction

The Döbner-Miller reaction is thought to proceed by initial condensation of crotonaldehyde with the aniline followed by conjugate addition of a second equivalent of aniline to the α,β-unsaturated imine forming a Schiff base, **435**. This then undergoes cyclisation followed by loss of the second aniline equivalent to give the dihydroquinoline **439.** Oxidation then leads to the quinoline product **440** (***Figure 132***).[31]

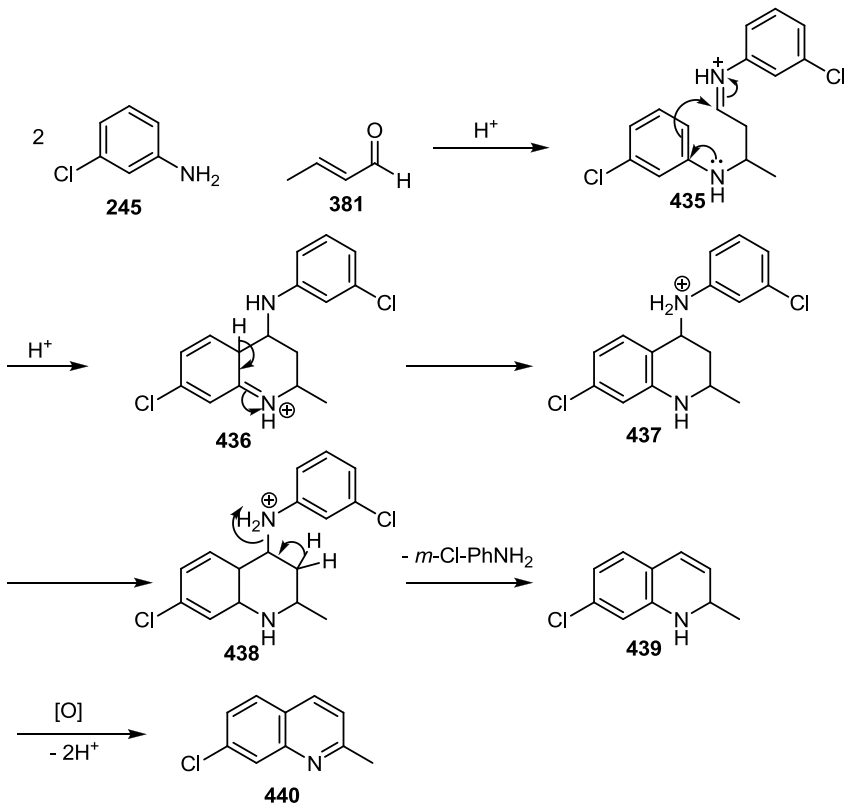

Figure 132 - Proposed mechanism for the formation of 2-methyl-7-chloroquinoline via the Döbner-Miller reaction.

Although procedurally simple, the reaction is affected by a number of problems. The synthesis of 2-methyl-6-substituted quinolines is typically facile due to the symmetrical nature of the starting aniline leading to only one cyclisation product being possible. As such the 6-substituted derivatives are readily commercially available. However, the reaction to form 7-substituted product is often affected by competing formation of the 5-substituted derivative. With the 3-substituted aniline **245** shown in ***Figure 132***, there is the possibility for the cyclisation to occur at two positions, both *ortho*- and *para*- to the chloro-substituent.[32]

The harsh reaction conditions typically cause significant decomposition of the intermediates, limiting the yield and complicating purification. Crotonaldehyde is unstable to acidic media and also suffers decomposition during the reaction.[70]

Finally, inefficient oxidation of the dihydroquinoline by air to complete the aromatisation to the desired quinoline can also result in reduced yield. These problems are exemplified by the

description of the Döbner-Miller reaction as the "worst 'witches brew' in heterocyclic synthesis".[10]

Due to the problems associated with the reaction a number of reports have detailed improvements to the methodology.[31-33,35] As discussed, a major problem with achieving a high yield for the reaction is the purification of the desired product. Leir[35] reported the use of zinc chloride in the purification step of the Döbner-Miller reaction (***Figure 133***).

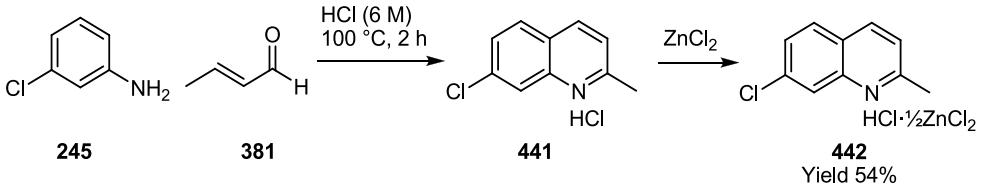

Figure 133 - Purification of 2-methyl-7-chloroquinoline with $ZnCl_2$.[35]

The complex **442** precipitates from the reaction medium at room temperature. Collection of the precipitate, followed by extensive washing with HCl, 2-propanol and diethyl ether affords the pure complex. The uncomplexed quinoline is accessed by washing with concentrated aqueous ammonia and extraction with organic solvents. Interestingly, this method extracts only the 7-substituted product from the reaction mixture in preference to the 5-substituted product, the reason for this selectivity is yet to be explained.

Matsugi and co-workers[70] have demonstrated the use of a two-phase solvent system to carry out the reaction. The use of toluene as a co-solvent with aqueous HCl decreases polymerisation of the aldehyde during the reaction (***Figure 134***).

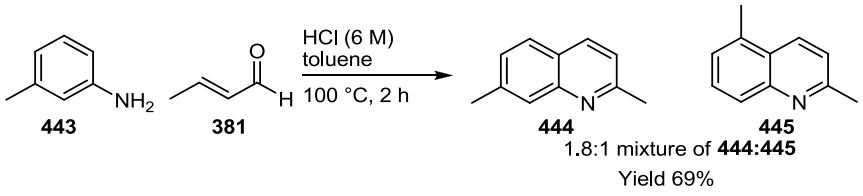

Figure 134 - Two-phase solvent system used in the Döbner-Miller reaction.[70]

Song and co-workers[33] demonstrated that the addition of a chemical oxidant and alcohol solvent facilitates the final oxidation step of the reaction. This, combined with the zinc chloride

purification method discussed earlier, afforded quinoline products in high yields (***Figure 135***). The method also uses slow addition of crotonaldehyde by syringe pump to prevent decomposition. The use of an external oxidant provides improved yields, but also adds complexity to the reaction procedure.

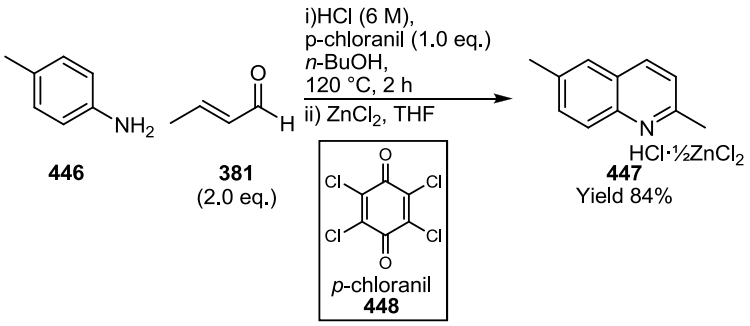

Figure 135 - Döbner-Miller reaction utilising *p*-chloranil as a chemical oxidant.[33]

4.4.3.1.2 Döbner-Miller Synthesis of 2-Methyl-7-Substituted Quinolines

The synthesis of 2-methyl-7-substituted quinoline derivatives bearing substituents with electron donating and withdrawing properties was attempted. The preparation of these derivatives will be described in the following section. A number of the procedural improvements which have been developed were incorporated into the method used.[32,70]

4.4.3.1.2.1 Synthesis of 2-Methyl-7-Bromoquinoline

The first 2-methyl-7-substituted quinoline to be synthesised was 2-methyl-7-bromoquinoline (***Figure 136***). Addition of HCl (6 M) to *m*-bromoaniline caused immediate precipitation of the aniline HCl salt. Toluene was added and the reaction was heated to reflux. Heating caused *ca.* 2/3 of the solid to be dissolved. Crotonaldehyde was added to the reaction as a solution in toluene via a syringe pump over 1 hour. Addition of the aldehyde caused the remaining solid to dissolve and a yellow solution to form due to the higher solubility of the Schiff base intermediate. The reaction was heated for 2 hours. Over this period the colour darkened from yellow to orange to a dark red brown.

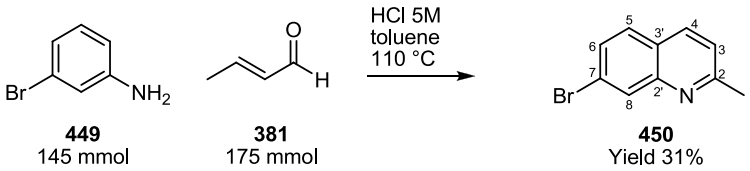

Figure 136 - Synthesis of 2-methyl-7-bromoquinoline.

The reaction was cooled to 60 °C and then $ZnCl_2$ was added as a 1:1 THF:acetone solution. Slow addition and efficient stirring were critical to allow a finely divided precipitate to form. If the addition of the zinc chloride was carried out at a lower temperature, the complex formed as a thick gum which made purification more challenging.

The precipitate was collected by filtration and washed with cold HCl (5 M), THF, isopropyl alcohol and diethyl ether resulting in a white solid. The solid was combined with hexane and aqueous concentrated ammonia to afford the uncomplexed quinoline in 31% yield. A molecular ion of 221 [M^+(^{79}Br)] *m/z* observed by GC-MS is consistent with **450**. Product identity was confirmed by full assignment of the ^{1}H and ^{13}C NMR spectra using COSY, HSQC and HMBC spectroscopic techniques. Correlation in the HMBC spectrum between the methyl group protons at 2.73 ppm and C^3 at 122.5 ppm allowed identification of H^3 at 7.28 ppm (d). Correlation in the COSY spectrum between H^3 and H^4 was confirmed by a coupling constant of J = 8.4 Hz consistent with their *ortho*-relationship.

The signal at 8.20 ppm in the ^{1}H NMR spectrum, consistent with H^8, was coupled (J = 1.8 Hz) to the signal at 7.55 ppm for H^6. This peak was also coupled to the signal at 7.62 ppm with a coupling constant of J = 8.6 Hz corresponding to H^5. All spectral data were consistent with literature reports.[71]

4.4.3.1.2.2 Synthesis of 2-Methyl-7-(Trifluoromethyl)quinoline

The procedure described above was applied to the synthesis of 2-methyl-7-(trifluoromethyl)quinoline (***Figure 137***). Analysis of the crude reaction mixture by GC-MS showed 2 major products with a molecular ion of 211 *m/z* consistent with the desired product, along with a large number of minor decomposition products. When the zinc chloride isolation method was attempted, no precipitate formed. The reaction mixture was then neutralised with

aqueous ammonia, extracted with ether and subjected to silica gel column chromatography. Silica gel flash column chromatography eluting with chloroform allowed for separation of the desired product from the complex mixture of decomposition products. GC-MS analysis of the purified product showed a molecular ion of 211 *m/z* which was consistent with **452**. Product identity was confirmed by full assignment of ^{1}H and ^{13}C NMR spectra using COSY, HSQC and HMBC spectroscopic techniques in the same manner as for **450**.

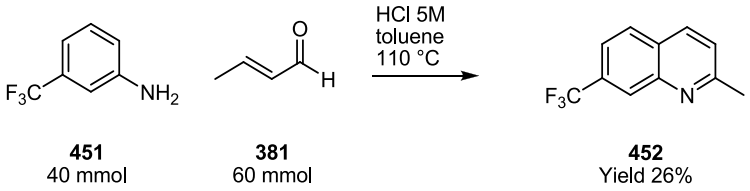

451 40 mmol **381** 60 mmol **452** Yield 26%

Figure 137 - Synthesis of 2-methyl-7-(trifluoromethyl)quinoline.

Attempts to synthesise of the 2-methyl-7-methoxy and 2-methyl-7-cyano quinolines using the described methodology were more problematic. The formation of the 2-methyl-7-methoxyquinoline **453** was observed by GC-MS analysis of the Döbner-Miller reaction which displayed a molecular ion of 173 *m/z*. However, attempts to purify the resulting product mixture were unsuccessful by either addition of zinc chloride or column chromatography.

Formation of the 7-cyanoquinaldine **454** was not observed by GC-MS with only starting aniline and crotonaldehyde visible in the GC-MS. The deactivating nature of the cyano substituent could potentially prevent the ring closing step from proceeding. Interestingly, this was not a problem with the trifluoromethyl-substituted analogue despite the similarity in directing effects. Due to these difficulties, a new approach towards the synthesis of **453** and **454** was required, and nucleophilic substitution of the halogen in 2-methyl-7-bromo-quinoline was attempted.

4.4.3.1.2.3 Synthesis of 7-Methoxy-2-Methylquinoline

Reports in the literature had detailed the conversion of aryl bromides to anisoles via a copper mediated reaction with sodium methoxide (***Figure 138***).[72,73]

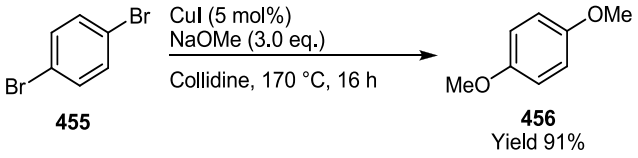

455 **456** Yield 91%

Figure 138 - Copper catalysed anisole synthesis.[73]

A modified literature procedure[72] was used for the reaction with 2-methyl-7-bromoquinoline (***Figure 139***). Sodium methoxide was generated *in situ* by addition of sodium metal to methanol. A high sodium methoxide concentration was reported to be required to achieve an efficient reaction,[72] so the methanol was removed to dryness by evaporation under reduced pressure. Addition of copper (I) bromide and aryl bromide in DMF was followed by heating for 45 minutes at 110 °C affording the desired product in 96% yield. GC-MS analysis showed a molecular ion of 173 *m/z* in the mass spectrum consistent with the desired product. In particular, the appearance of signals at 2.70 ppm in the ^{1}H NMR spectrum and 55.7 ppm in the ^{13}C NMR spectrum confirmed the introduction of the methoxy moiety.

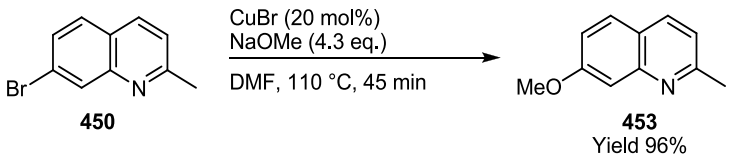

450 **453** Yield 96%

Figure 139 - Synthesis of 2-methyl-7-methoxyquinoline.

4.4.3.1.2.4 Synthesis of 7-Cyano-2-Methylquinoline

As for the previous example, 2-methyl-7-bromoquinoline was used to prepare the desired 7-cyano derivative **454**. This was achieved through the use of a microwave assisted route developed by Hallberg and co-workers.[74] The palladium catalysed reaction converts aryl bromides to nitriles utilising zinc (II) cyanide as the transmetalating agent following a classical cross-coupling mechanism (***Figure 140***).

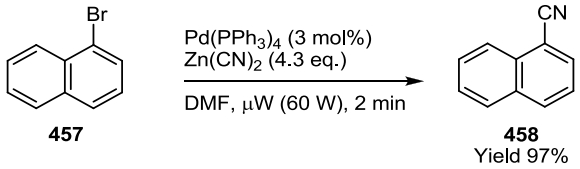

Figure 140 - Microwave assisted synthesis of aryl nitriles.[74]

The preparation of **454** was carried out using a modified literature procedure (***Figure 141***). The reaction was heated at 150 °C for 20 minutes in a microwave reactor, affording **454** in 84% yield. Analysis by GC-MS showed a molecular ion of 168 *m/z* consistent with the desired product. As with the other quinolines, the substitution pattern was confirmed by ^{1}H and ^{13}C NMR analysis using COSY, HSQC and HMBC spectroscopic techniques. Installation of the nitrile functionality was confirmed by a characteristic peak at 2231 cm^{-1} in the IR spectrum.

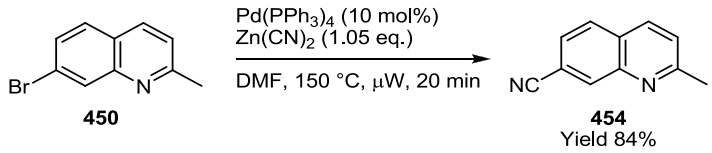

Figure 141 - Palladium catalysed synthesis of **454** from **450**.

4.4.3.1.2.5 Synthesis of 2-Methyl-7-(Trimethylsilyl)quinoline

Finally the synthesis of 2-methyl-7-(trimethylsilyl)quinoline was attempted *via* lithium-halogen exchange of the quinoline bromide followed by trapping with TMSCl. The quinoline bromide **450** was cooled to -78 °C and reacted with *n*-BuLi (1.0 eq.) for 10 minutes. Subsequent addition of TMSCl and warming to room temperature afforded the desired product **459** in 64% yield (***Figure 142***). Analysis by GC-MS showed molecular ion of 215 *m/z*, which is consistent with the mono-silylated product **459**. Further analysis by ^{1}H and ^{13}C NMR spectroscopy confirmed the regiochemistry of **459** in the same manner as described above. The peak at 0.37 ppm in the ^{1}H NMR spectrum was indicative of the presence of a TMS group in the molecule.

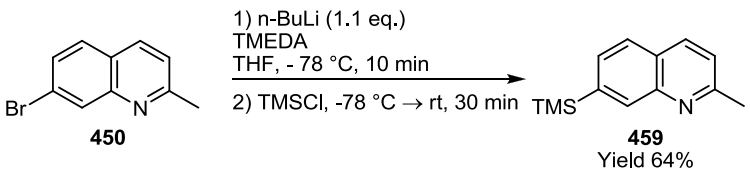

450 **459**
Yield 64%

Figure 142 - Synthesis of **459** by lithium-halogen exchange and trapping with a TMS electrophile.

In summary, although the Döbner-Miller synthesis of quinolines has a number of problems associated with low yields and purification of products, its use was able to provide sufficient examples for study of the borylation reaction.

4.4.3.2 Borylation of 2-Methyl-7-Substituted Quinolines

Prediction of the regiochemistry for borylation of 2,7-disubsttuted quinolines offered a significant challenge due to the fact that the 4- and 5- positions are sterically similar but electronically inequivalent. The borylation reactions were undertaken using the previously described method (***Figure 143***,***Table 17***).

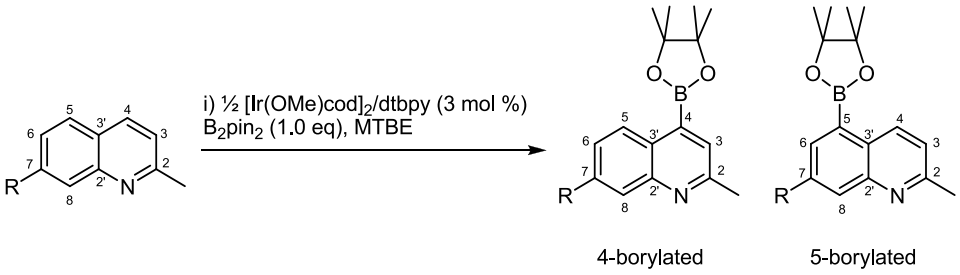

4-borylated 5-borylated

Figure 143 - C-H borylation of 2,7-disubstituted quinolines.

Table 17 - C-H borylation of 2,7-disubstituted quinolines.

Entry	R	Temp.[a]	Time (h)	GC-MS Conversion (%)	GC-MS ratio (%)			Yield%[b]
					4-	5-	other	
1	Me	100 °C	1	88	82	12	6[c]	-
2		rt	72	93	95	5	-	80
					460			
3	TMS	100 °C	1.5	85	70	20	10[d]	-
4		rt	72	91	85	10	5[d]	68
					461			
5	OMe	100 °C	1.5	>95	90	10	-	-
6		rt	48	89	95	5	-	73
					462			
7	CN	100 °C	0.25	>95	82	9	9[e]	-
8		rt	48	92	95	5	-	86
					463			
9	Cl	100 °C	1.5	> 95	5	95	-	81
						464		
10	Br	100 °C	1.5	80	65[f]	35[f]	-	-
11		rt	48	90	80	20	-	80[g]
					465	**466**		
12	CF_3	100 °C	1.5	>95	60	40	-	-
13		rt	20	94	70	30	-	92[h]
					467	**468**		

[a] 100 °C reactions run in a microwave reactor, rt reactions run at ambient temperature which was monitored at ca. 22 - 25 °C.

[b] Isolated yield of major isomer, unless otherwise stated.

[c] Isomer not isolable.

[d] Mono-borylated isomer; unable to isolate and confirm identity of minor isomer by ^{1}H NMR spectroscopic analysis.

[e] Bis-borylated isomer derived from the 4-monoborylated isomer.

[f] Isomer ratio determined by ^{1}H NMR spectroscopic analysis as GC-MS peaks unresolved.

[g] Major isomer isolated in 65% yield, minor isomer isolated in 15% yield.

[h] Major isomer isolated in 65% yield, minor isomer isolated in 27% yield.

The borylation of 2,7-dimethylquinoline **444** showed an overall preference for reaction at the heterocycle over the carbocycle, (***Table 17***,, entry 1). Analysis by GC-MS of the elevated temperature reaction showed peaks of 283 *m/z* consistent with three mono-borylated products (82:12:6). When the reaction was carried out at room temperature a higher regioselectivity of >95:5 with preference for the 4-borylated product **460** was observed, enabling isolation of the major product in 80% yield (***Table 17***, entry 2). The increased selectivity associated with

reduction in reaction temperature is consistent with the observation made for the borylation of 2-cyano-6-methoxyquinoline **419** (Section 4.4.1).

Product identity was confirmed by full assignment of ^{1}H and ^{13}C NMR spectra using COSY, HSQC and HMBC spectroscopic techniques and comparison to the parent arene chemical shifts (***Figure 144***).

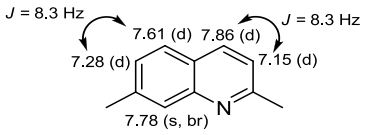

Figure 144 - ^{1}H NMR chemical shifts of 2,7-dimethylquinoline (400 MHz, $CDCl_3$).

The retention of the peak pattern, from the parent heterocycles, on the carbocyclic ring confirmed that borylation had taken place on the heterocyclic ring. The broad singlet at 7.79 ppm is consistent with H^8, assigned through HMBC correlation to C^6 (128.32 ppm) and $C^{3'}$ (127.4 ppm). The signal at 7.34 ppm (dd) showed coupling constants of J = 1.7, 8.4 Hz, these values consistent with *ortho* and *meta* couplings. This, along with HMBC correlations to C^8, $C^{3'}$ and the methyl group of at C^7, confirm its identity as H^6. The signal at 8.46 ppm (d) couples (J = 8.4 Hz) to the signal for H^6; therefore, the signal corresponds to H^5.

Confirmation of the site of borylation was made by identification of the signal at 158.1 ppm in the ^{13}C NMR spectrum as C^2. The position of this signal is consistent with a carbon adjacent to an azine nitrogen. Correlation in the HMBC spectrum between C^2 and the peak at 2.72 ppm in the ^{1}H NMR spectrum confirms this peak as the methyl group attached to C^2. The sharp singlet in the ^{1}H NMR spectrum at 7.67 ppm was correlated by HMBC to the carbon of the C^2 methyl group, confirming its identity as H^3. As discussed previously, signals for protons closest to the installed Bpin group (H^5 and H^3) are shifted to higher ppm. This shift in signals and coupling constant pattern in the ^{1}H NMR spectrum is consistent throughout all 4-borylated-2,7-disubstituted quinolines (***Figure 145***).

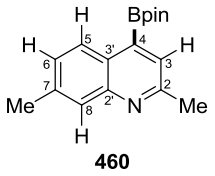

460

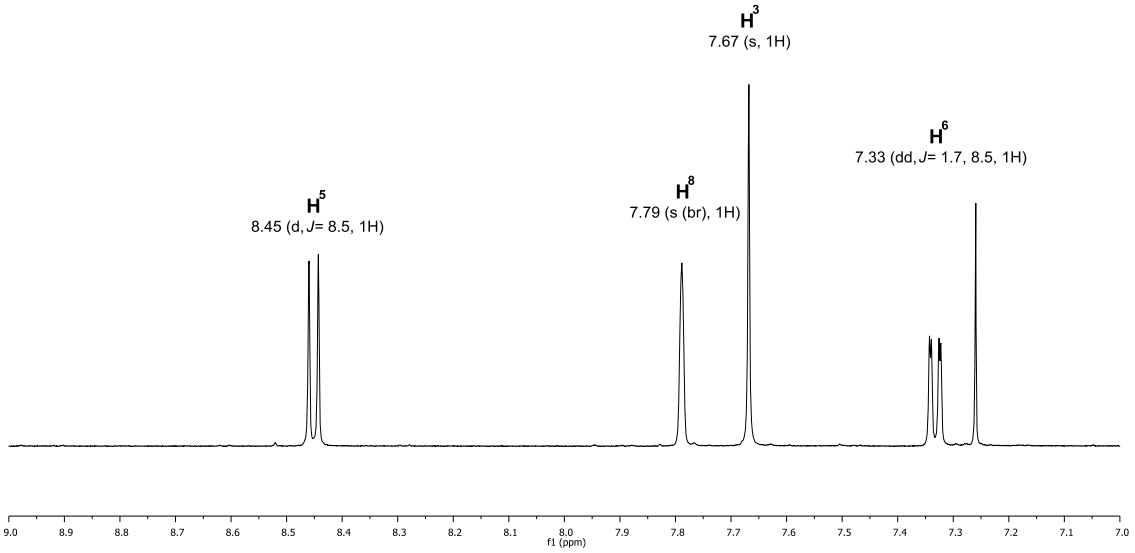

Figure 145 - Aromatic region of ^{1}H NMR spectrum of **460.**

This preference for the 4-borylated isomer was similarly observed when the 7-substituent was changed to TMS **459**, OMe **453** and CN **454** (***Table 17***, entries 4-9) with all examples showing an improvement in selectivity towards the major 4-isomer upon reduction of the reaction temperature.

However, when the borylation of 7-chloro-2-methyl-quinoline **440** was attempted at 100 °C over a 1.5 hour reaction time, a 95:5 mixture of two borylation products was observed. The major component was isolated by column chromatography in 81% yield. Full assignment of ^{1}H and ^{13}C NMR spectra using COSY, HSQC and HMBC spectroscopic techniques confirmed that borylation took place at the 5- position rather than the 4-position affording **464**.

The ^{1}H NMR spectrum contained a pair of doublets at 8.93 ppm and 7.30 ppm (J = 8.7 Hz) and a pair at 8.09 ppm and 8.01 ppm (J = 2.5 Hz) (***Figure 146***). This pattern is consistent with a product containing *meta* and *ortho* coupling patterns. HMBC correlation between the signals at 7.30 ppm (J = 8.7 Hz) in the ^{1}H NMR spectrum and 25.5 ppm in the ^{13}C NMR spectrum confirmed the former as H^3. The signal at 8.93 ppm (J = 8.7 Hz) was therefore confirmed as H^4

by comparison of coupling constants and correlation in the COSY spectrum. Correlation in the HMBC spectrum between the signal at 8.09 ppm with C^{8} and $C^{3'}$ confirm its identity as H^{6}. The peak at 8.01 ppm correlates to C^{6}, $C^{3'}$ and weakly to $C^{2'}$ which enables the signal to be assigned to H^{8}. As with all borylated quinolines described, the characteristic shift of protons closest to Bpin is again observed for H^{4} and H^{6}.

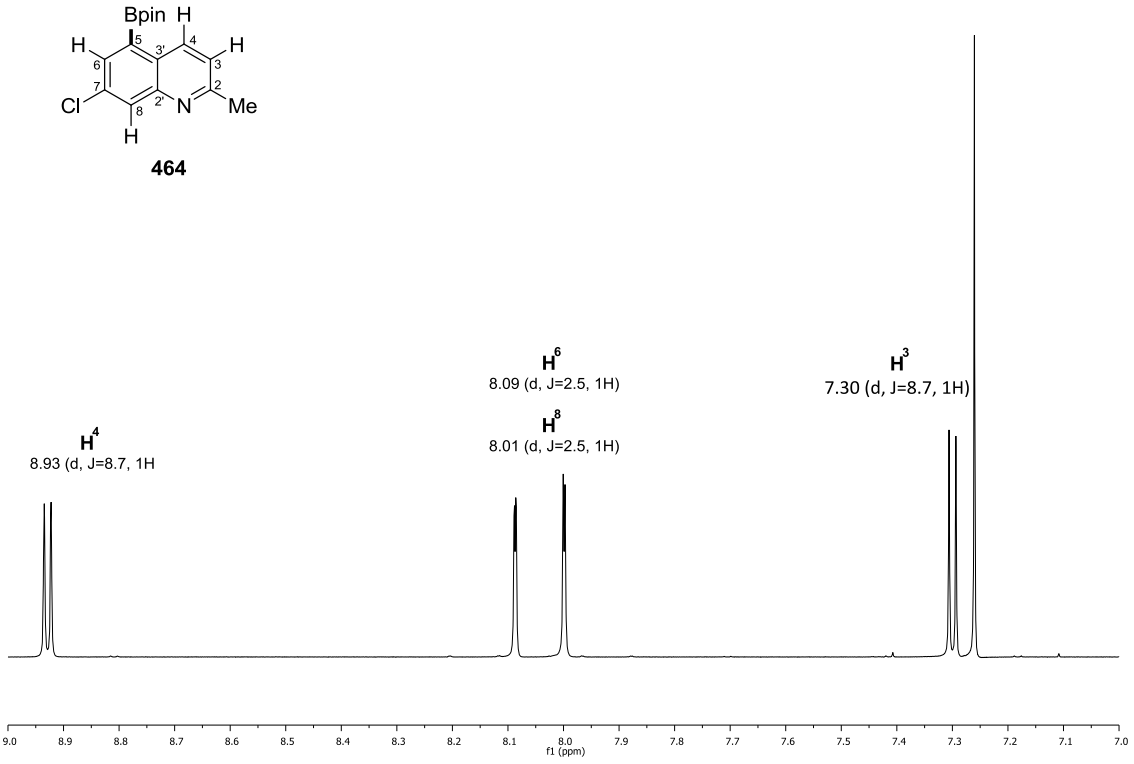

Figure 146 - Aromatic region of ^{1}H NMR spectra of **464.**

The regiochemistry of the two product classes was further confirmed by single crystal X-ray analyses, of 2,7-dimethyl-4-Bpin-quinoline and 2-methyl-7-chloro-5-Bpin quinoline (***Figure 147***).

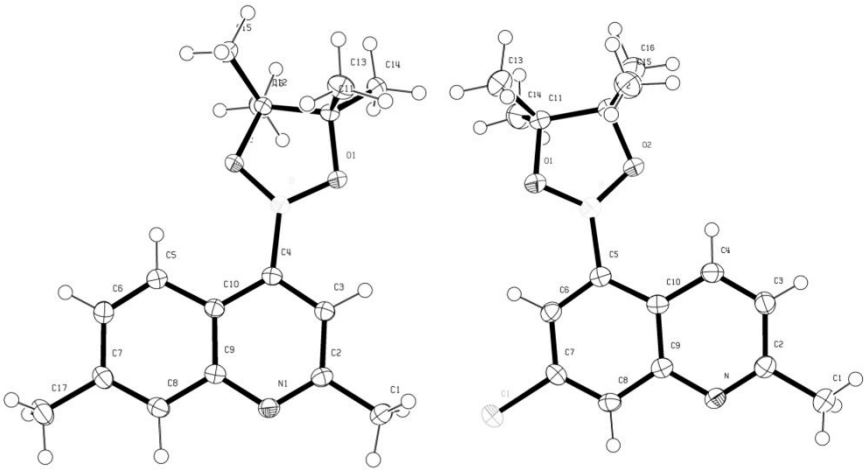

460 **464**

Figure 147 - Molecular structures of 2,7-dimethyl-4-Bpin-quinoline and 2-methyl-7-chloro-5-Bpin quinoline (Thermal ellipsoids drawn at 50% probability).

The borylation of 2-methyl-7-bromo-quinoline **450** and 2-methyl-7-trifluoromethyl-quinoline **452** showed a preference for the 4-borylated product. However, the major isomer was not formed exclusively even when the reaction temperature was reduced to room temperature. The borylation of 2-methyl-7-bromo-quinoline 450 (Table 17, entries 10 & 11) gave a 65:35 mixture of the 4:5 products (**465**:**466**) at 100 °C, which was improved to 80:20 when carried out at room temperature. Analysis by GC-MS showed molecular ions 347, 349 *m/z* in a 1:1 ratio, which was consistent with the described products. The mixture of products from the room temperature reaction of **450** (***Table 17***, entry 11) was separable by silica gel column chromatography affording the 4-borylated isomer **465** in 65% yield and the 5-borylated isomer **466** in 15% yield (***Figure 148***).

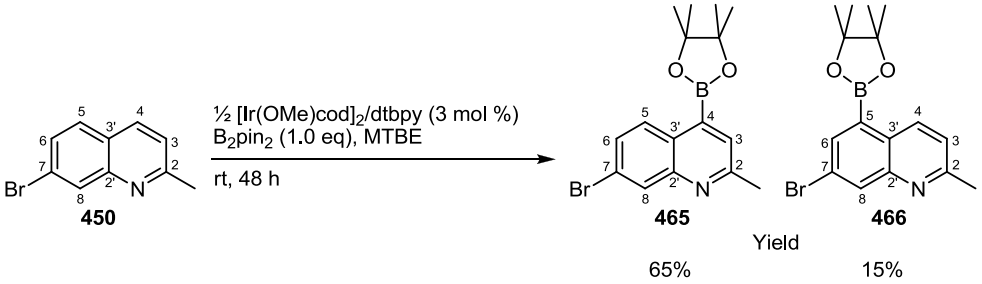

Figure 148 - Room temperature borylation of **450**.

Similarly, the borylation of 2-methyl-7-(trifluoromethyl)quinoline **452** (***Table 17***, entries 12 & 13) resulted in a 60:40 mixture of the 4:5 products at 100 °C. Borylation at room temperature afforded a 70:30 mixture of the 4- and 5- borylated products (**467**:**468**). GC-MS analysis showed molecular ion of 337 *m/z*, which was consistent with the products described.

The mixture of products from the room temperature reaction of **452** (***Table 17***, entry 11) was again separable by silica gel column chromatography affording the 4-borylated product **467** in 65% yield and the 5-borylated product **468** in 27% yield (***Figure 149***).

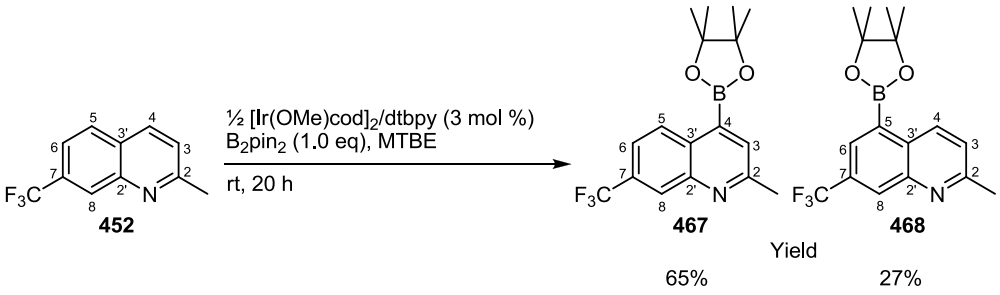

Figure 149 - Room temperature borylation of **452**.

As before, full assignment of ^{1}H and ^{13}C NMR spectra using COSY, HSQC and HMBC spectroscopic techniques permitted the identity of both reaction products to be unambiguously confirmed. Peak patterns, coupling constants and other 2D correlations were completely consistent with the examples discussed in the previous section.

From the reactions with a 7-chloro **440**, 7-bromo **450** and 7-trifluoromethyl **452** substituted derivatives it can be seen that there is an electronic effect causing borylation in the normally disfavoured carbocyclic ring. This effect is most strongly exhibited by the chloro derivative and, to a lesser extent, by the bromo and trifluoromethyl derivatives.

The electronic directing effects observed through the borylation of substituted quinoline substrates gives insight into the factors which affect the site selectivity of the reaction.

Although electronic factors are influential in determining selectivity, steric factors remain the dominant directing effect within the borylation system. The greater reactivity of the heteroaromatic ring compared to the carbocyclic ring has again been highlighted.

This work has shown that the introduction of a strong activating group, Cl, is able to alter this inherent reactivity. The preferential avoidance of borylation at the 2- and 8-positions is highlighted in the reactions of 2,6-disubstituted and 4,7-disubstituted quinolines. Avoidance of the 8-position can be explained by the higher reactivity of the heteroaromatic ring, but a steric effect of the quinoline nitrogen lone pair may also make activation at this position unfavourable. This is highlighted in the comparison between the borylation of 2-methyl-6-chloroquinoline and 2-methyl-7-chloroquinoline (***Figure 150***).

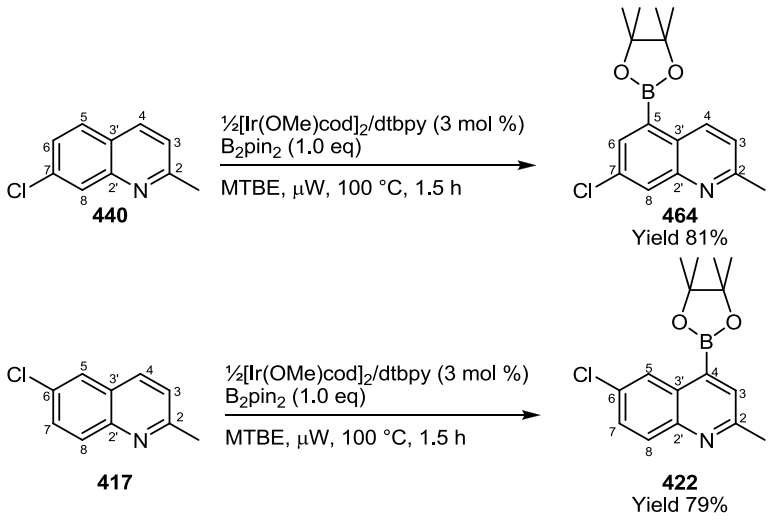

Figure 150 - Borylation reaction with 2-methyl-6-chloro- and 2-methyl-7-chloro-quinoline.

The introduction of a chloro substituent into the 7-position of the carbocyclic ring of **440** forces borylation to occur on that ring, whilst a chloro substituent in the 6-position in **417** does not switch borylation to the carbocyclic ring. The two peri positions, i.e. the 5-position in **440** and the 8-position in **417**, differ sterically by their proximity to either a C-H bond or a nitrogen lone pair. This could imply the steric bulk on a nitrogen lone pair is greater than that of a peri C-H bond. However, this argument does not consider relative influence of the heteroatom on the two positions. Finally, this work highlights the use of reduced temperature to improve the regiochemical distribution of products in substrates where multiple borylation isomers can form.

4.4.4 Conclusions

The regioselective direct C-H borylation of a range of substituted quinolines has been demonstrated. With careful control of substituents, highly regioselective reactions can be obtained. The borylation of 2,7-substituted quinolines has highlighted an interesting electronic selectivity which has not previously been reported. This electronic selectivity may be enhanced by undertaking reactions at lower temperatures. This temperature dependence has allowed unselective reactions at elevated temperatures to become regioselective at room temperature.

The electronic selectivity observed in the quinoline systems reported in this chapter is not fully understood. However, one possibility is that relative C-H acidities within molecules could determine the regioisomeric identity of the product formed.

4.4.5 Investigation of Electronic Effects in the Borylation Reaction

This section will highlight attempts made to understand the electronic selectivity observed in the borylation of substituted quinolines. The acidity of C-H bonds has been suggested as a possible explanation of selectivity in systems which are controlled by electronic factors.[75] This section will highlight work on the calculation of pK_a values for the quinoline substrates by an established DFT method.[76] Attempts to correlate selectivity and C-H acidity will be discussed. In order to put the work into context, previous observations and conclusions will be highlighted.

4.4.5.1 Borylation of Heteroaromatic Substrates

Substrates which clearly exemplify the electronic effects of the borylation reaction are heteroarenes. This electronic influence can be observed in the borylation of 5-membered heterocycles which are selective for the 2-position in preference to the 3-position. Similarly, the borylation of unsubstituted quinoline is selective for the 3-position in preference to the sterically equivalent 2, 6 and 7 positions (***Figure 151***).

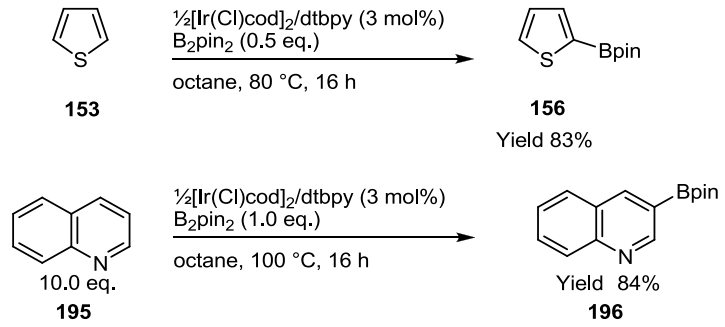

Figure 151 - Borylation of thiophene and quinoline.

Interestingly, when compared to pK_a values calculated by established DFT methods,[76] (***Figure 152***) a distinct correlation can be observed between the most acidic positions and those activated.

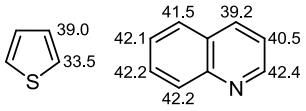

Figure 152 - Calculated pK_a values for thiophene and quinoline.[76]

The correlation between selectivity and acidity is observed for these simple substrates. In the case of quinoline, the most acidic position is not activated; however, this can be attributed to the greater steric hindrance around the 4-position. Of the sterically equivalent 2, 3, 6 and 7 positions, the 3-position has the lowest pK_a and this is the site of borylation.

Smith and co-workers,[75] recently reported the *ortho*-borylation of benzodioxole using an isolable iridium catalyst (***Figure 153***).

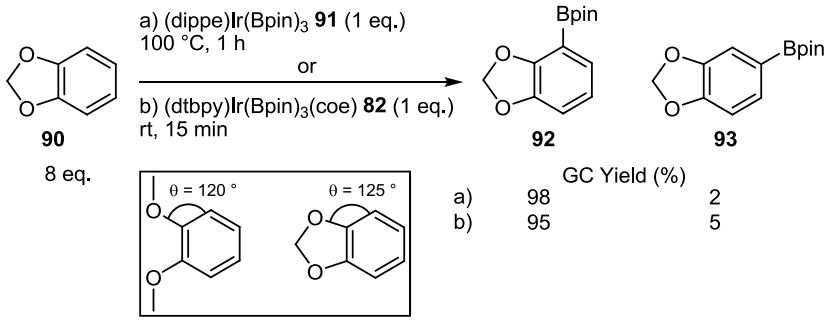

Figure 153 - The *ortho*-borylation of benzodioxole.

The report also included theoretical studies of transition states for the catalytic reaction. These calculations support a transition state for the C-H activation step which is consistent with a proton transfer process (***Figure 154***). This finding supports the suggestion that C-H acidity may be important in determining the regioselectivity of the reaction.

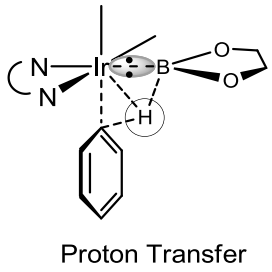

Figure 154 - Proton transfer in the transition state for C-H borylation reaction.

These results, along with reports from Hall and Hartwig[77] and Lin and Marder,[78] support a transition state in which boryl nucleophilicity facilitates C-H borylation. The possible role of boryl group in deprotonation of the C-H bond is similar to the ligand assisted deprotonation suggested for palladium catalysed direct C-H arylations (***Figure 155***).[79] In these direct arylation systems, C-H acidity has also been suggested as the selectivity determining factor.[79]

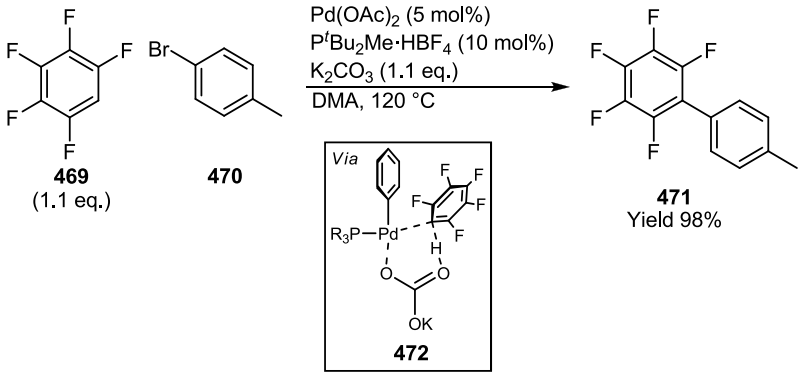

Figure 155 - Direct arylations via the ligand assisted deprotonation pathway.[79]

In order to gain further insight into the role of C-H acidity in determining regioselectivity, a computational study was undertaken. This utilised methodology developed by Guo and co-

workers[76] to calculate pK_a values for the positions of interest. The method was applied to the substituted quinolines discussed earlier in this chapter.

4.4.5.2 DFT method for the Calculation of pK_a Values in Aromatic Systems

The determination of pK_a values for all C-H bonds within an aromatic system would not be possible using experimental methods. However, an *in silico* approach allows values for all positions to be determined. Guo and co-workers[76] have developed a method to allow the C-H acidities of aromatic C-H bonds to be calculated and plotted on a pK_a scale. This method provides values for pK_a in the solution phase by utilising a DMSO polarised continuum solvent model. The calculated values have been compared to those determined experimentally and were found to provide results within 1.1 pK_a units of the experimental data. The methodology uses a proton exchange reaction to calculate acidities of the constituent species (***Figure 156***).

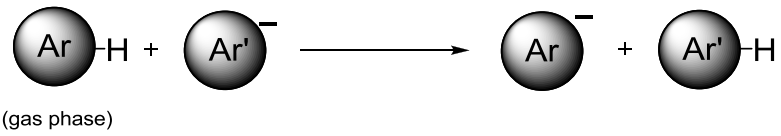

Figure 156 - Proton exchange reaction used as the basis for pK_a calculations.

Gas phase optimisation and frequency calculations are performed on the parent arene and the carbanions at the positions for which pK_a values are required. Gaussian 03 was used for all DFT calculations.[80] Optimisation calculations were conducted using B3LYP/6-31G(d), whilst, frequency calculations utilised B3LYP/6-311++G(2df,2p). The IEF-PCM solvation model was used to calculate solvation free energies which were performed using B3LYP/6-311++G(2df,2p) (tsnum=60, tsare=0.4, radii=bondi, alpha=1.20). The use of diffuse functions in the basis set is necessary to describe accurately the anions being calculated.[81]

The methodology calculates the sum of electronic and thermal free energies in the gas phase (G_{gas}) for each species. The term $\Delta G_{(gas)}$ is calculated and represents the gas phase Gibbs energies for the exchange reaction in the gas phase (***Figure 157***). This forms the gas phase portion of the calculation.

$$\Delta G_{(gas)} = \sum_{products} G_{(gas)} - \sum_{reactants} G_{(gas)}$$

Figure 157 - Calculation of $\Delta G_{(gas)}$.

The solvation Gibbs free energy ($\Delta_{(solv)}G$) is calculated for each species in the exchange reaction (**Figure 158**). This requires the total energy of each species in the gas phase (E) and PCM energy (E_{PCM}) generated from the solution phase calculation of each species. The total change in solvation Gibbs free energy for the reaction (Total $\Delta_{(solv)}G$) is then calculated.

$$\Delta_{(solv)}G = E_{PCM} - E$$

$$Total\ \Delta_{(solv)}G = \sum_{products} \Delta_{(solv)}G - \sum_{reactants} \Delta_{(solv)}G$$

Figure 158 - Equation for the calculation of $\Delta_{(solv)}G$ and Total $\Delta_{(solv)}G$.

From the gas and solution phase calculations the change in Gibbs free energy for the solution phase exchange reaction ($\Delta G_{(exchange)}$) is calculated (***Figure 159***).

$$\Delta G_{exchange} = \Delta G_{(gas)} + \text{Total}\ \Delta_{\text{solv}}G$$

Figure 159 - Calculation of $\Delta G_{(exchange)}$.

In order for this method to provide values on a pK_a scale, a reference is used, in this case furan. The pK_a of C(2)-H in furan has been determined experimentally to be 35.0.[76] Calculation of $\Delta G_{(gas)}$ and $\Delta_{(solv)}G$ for furan and furan mono-anion allow $\Delta G_{(exchange)}$ to be calculated using the arene of interest as the other reaction partner. From the calculation of $\Delta G_{(exchange)}$, the pK_a of the target arene C-H bond can be calculated (***Figure 160***).

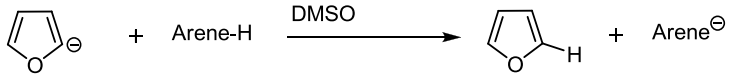

$$pK_a\ (\text{Arene-H}) = pK_a\ (\text{furan}) + \frac{\Delta G_{exchange}}{2.303 \times RT}$$

$$pK_a\ (\text{Arene-H}) = 35.0 + \frac{\Delta G_{exchange}}{2.303 \times RT}$$

Figure 160 - Theoretical proton exchange reaction with furan and calculation of target arene pK_a.

The above method has been shown to provide accurate pK_a values when compared to values determined experimentally. It was decided to apply the method to the substituted quinoline substrates. Although the method provides values of pK_a in a DMSO solution, rather than the less polar solvents required for the Ir catalysed C-H borylation process, it was felt that the solution state model was more appropriate than simple gas phase acidity calculations, as values were referenced to a pK_a scale. The method had also been demonstrated as an accurate method for obtaining pK_a values for quinoline substrates.[76] The following section will discuss the application of the method described above to the calculation of pK_a values for substituted quinolines.

4.4.5.2.1 pK_a of Substituted Quinolines

The DFT method was used to calculate pKa values for the substituted quinolines discussed earlier in the chapter. The calculated values were then compared with the experimental selectivities to derive correlations between the data. The first class of substrates to be examined were the 2,7-disubstituted quinolines.

4.4.5.3 Calculated pK_a Values for substituted quinolines

The methodology was applied to the 4- and 5-positions of the 2-methyl-7-substituted quinolines (***Figure 161***). The other positions were not calculated as the aim of the study was to determine the reasons behind regioselectivity for the two positions. The calculated pK_a values demonstrate a correlation between the most acidic position and the site of preferred borylation.

The model successfully predicts the site of borylation for **444**, **453**, **454** and **459.** The values observed for **440**, **450** and **452** less closely fit the model.

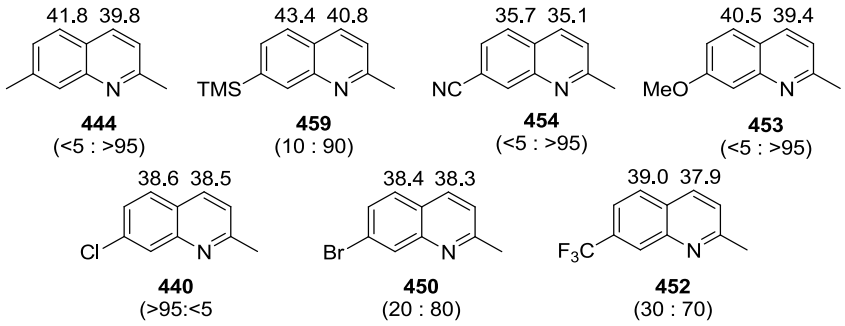

Figure 161 - pK_a values and observed selectivities for 2,7-disubstituted quinolines.

Analysis of **424** in the same manner reveals that the acidity of the 3-position is higher than that of the 4-position (***Figure 162***). However, the selectivity at room temperature is exclusively the formation of the 4-borylated product. At elevated temperature reaction affords a 25:75 mixture of 3- and 4- isomers. The pKa calculations suggest that the 3-position should be more reactive. This suggests that the steric environment around the 3-position is more hindered than the 4-position.

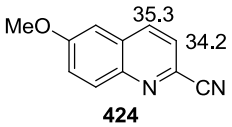

Figure 162 - Calculated pK_a values for **424.**

Calculations performed on **425**, **426** and **434** demonstrate the acidity enhancing effect to positions *ortho*- to a chloro group (***Figure 163***). The calculations also demonstrate the low acidity of the 2-position in all examples.

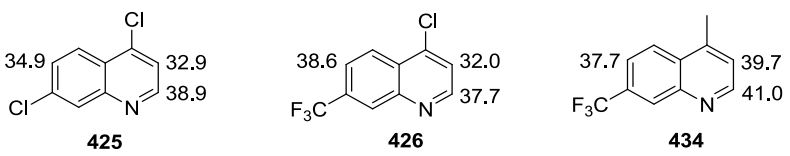

Figure 163 - Calculated pK_a values for **425**, **426**, **434.**

4.5 Conclusions

The methodology has demonstrated the regioselective borylation of a range of substituted quinolines in high yield. Borylation of 4-chloro-7-substituted quinolines has demonstrated an *ortho*-chlorine effect which allows borylation of these sterically hindered systems. The borylation of 2,7-disubstituted quinolines has highlighted interesting electronic selectivity associated with the ring system. Variation of the substituents on the carbocyclic ring has enabled the inherent selectivity of the ring system to be altered.

DFT studies of the pK_a of the aromatic C-H bonds have demonstrated the importance of C-H acidity in the selectivity of the reaction. However, the model does not fully explain the observed selectivity.

4.6 Chapter IV - References

1 Mkhalid, I. A. I.; Coventry, D. N.; Albesa-Jove, D.; Batsanov, A. S.; Howard, J. A. K.; Perutz, R. N.; Marder, T. B., *Angew. Chem. Int. Ed.* **2006**, *45*, 489.

2 Takagi, J.; Sato, K.; Hartwig, J. F.; Ishiyama, T.; Miyaura, N., *Tetrahedron Lett.* **2002**, *43*, 5649.

3 Ishiyama, T.; Takagi, J.; Ishida, K.; Miyaura, N.; Anastasi, N. R.; Hartwig, J. F., *J. Am. Chem. Soc.* **2002**, *124*, 390.

4 Mkhalid, I. A. I.; Barnard, J. H.; Marder, T. B.; Murphy, J. M.; Hartwig, J. F., *Chem. Rev.* **2010**, *110*, 890.

5 Ishiyama, T.; Takagi, J.; Yonekawa, Y.; Hartwig, J. F.; Miyaura, N., *Adv. Synth. Catal.* **2003**, *345*, 1103.

6 Joule, J. A.; Mills, K., *Heterocyclic Chemistry*. Fourth ed.; Wiley-Blackwell: London, 2000; p 589.

7 Jones, G., *The Chemistry Of Heterocyclic Compounds - Quinolines Part I*. John Wiley & Sons Inc: New York, 1977; p 898.

8 Coffey, S., *Heterocyclic Compounds - Part F*. Second ed.; Elsevier: New York, 1976; Vol. IV, p 485.

9 Elderfield, R. C., *Quinoline, Isoquinoline and Their Benzo Derivatives*. John Wiley & Sons Inc.: New York, 1952; Vol. 4, p 661.

10 Keller, P. A.; Katritzky, A. R.; Ramsden, C. A.; Scriven, E. F. V.; Taylor, R. J. K., *Comprehensive Heterocyclic Chemistry III*. Elsevier: Oxford, 2008; Vol. 7, p 1066.

11 Michael, J. P., *Nat. Prod. Rep.* **2008**, *25*, 166.

12 Michael, J. P., *Nat. Prod. Rep.* **2005**, *22*, 627.

13 Wada, Y.; Fujioka, H.; Kita, Y., *Mar. Drugs.* **2010**, *8*, 1394.

14 LaMontagne, M. P.; Blumbergs, P.; Strube, R. E., *J. Med. Chem.* **1982**, *25*, 1094.

15 Nasveld, P.; Kitchener, S., *Trans. R. Soc. Trop. Med. Hyg.* **2005**, *99*, 2.

16 Mouscadet, J.-F.; Desmaële, D., *Molecules* **2010** *15*, 3048.

17 Normand-Bayle, M.; Bénard, C.; Zouhiri, F.; Mouscadet, J.-F.; Leh, H.; Thomas, C-M.; Mbemba, G.; Desmaële, D.; d'Angelo, J., *Bioorg. Med. Chem. Lett.* **2005**, *15*, 4019.

18 Polanski, J.; Zouhiri, F.; Jeanson, L.; Desmaële, D.; d'Angelo, J.; Mouscadet, J.-F.; Gieleciak, R.; Gasteiger, J.; Bret, M. L., *J. Med. Chem.* **2002**, *45*, 4647.

19 Zouhiri, F.; Danet, M.; Bénard, C.; Normand-Bayle, M.; Mouscadet, J.-F.; Leh, H.; Thomas, C. M.; Mbemba, G.; d'Angelo, J.; Desmaële, D., *Tetrahedron Lett.* **2005**, *46*, 2201.

20 Upadhayaya, R. S.; Vandavasi, J. K.; Kardile, R. A.; Lahore, S. V.; Dixit, S. S.; Deokar, H. S.; Shinde, P. D.; Sarmah, M. P.; Chattopadhyaya, J., *Eur. J. Med. Chem.* **2010**, *45*, 1854.

21 Eswaran, S.; Adhikari, A. V.; Chowdhury, I. H.; Pal, N. K.; Thomas, K. D., *Eur. J. Med. Chem.* **2010**, *45*, 3374.

22 Nakamoto, K.; Tsukada, I.; Tanaka, K.; Matsukura, M.; Haneda, T.; Inoue, S.; N.Murai; Abe, S.; Ueda, N.; Miyazaki, M.; Watanabe, N.; Asada, M.; Yoshimatsu, K.; Hata, K., *Bioorg. Med. Chem. Lett.* **2010**, *20*, 4624.

23 Tang, C. W.; VanSlyke, S. A., *App. Phys. Lett.* **1987**, *51*, 913.

24 Bergauer, M.; Bertani, B.; Biagetti, M.; Bromidge, S. M.; Falchi, A.; Leslie, C. P.; Merlo, G.; Pizzi, D. A.; Rinaldi, M.; Stasi, L. P.; Tibasco, J.; Vong, A. K. K.; Ward, S. E. 2005.

25 Runge, F., *Pogg. Ann.* **1834**, *31*, 68.

26 Manske, R. H., *Chem. Rev.* **1942**, *30*, 1683.

27 Bergstrom, F. W., *Chem. Rev*. **1944**, *35*, 77.

28 Skraup, Z. H., *Monatsh. Chem.* **1880**, *1*, 316.

29 Skraup, Z. H., *Monatsh. Chem.* **1881**, *2*, 139.

30 Skraup, Z. H., *Ber. Dtsh. Chem. Ges.* **1882**, *15*, 897.

31 Yamashkin, S. A.; Oreshkina, E. A., *Chem. Heterocycl. Compd.* **2006**, *42*, 701.

32 Denmark, S. E.; Venkatraman, S., *J. Org. Chem.* **2006**, *71*, 1668.

33 Song, Z.; Mertzman, M.; Hughes, D. L., *J. Heterocycl. Chem.* **1993**, *30*, 17.

34 Döbner, O.; Miller, W. V., *Ber. Dtsh. Chem. Ges.* **1881**, *14*, 2812.

35 Leir, C. M., *J. Org. Chem.* **1977**, *42*, 911.

36 Combes, A., *Bull. Chim. Soc. France* **1888**, *49*, 89.

37 Marco-Contelles, J.; Pérez-Mayoral, E.; Samadi, A.; Carreiras, M. do Carmo; Soriano, E., *Chem. Rev.* **2009**, *109*, 2652.

38 Friedländer, P., *Chem. Ber.* **1882**, *15*, 2572.

39 Cheng, C-C.; Yan, S-J., *The Friedländer Synthesis of Quinolines*. John Wiley & Sons, Inc.: New York, 2004.

40 Oleynik, I. I.; Shteingarts, V. D., *J. Fluorine Chem.* **1998**, *91*, 25.

41 Choi, H-Y.; Lee, B. S.; Chi, D-Y.; Kim, D-J., *Heterocycles* **1998**, *48*, 2647.

42 Fawcett, R. C.; Robinson, R. J., *J. Chem. Soc.* **1927**, 2254.

43 Wang, Y.; X. Xin; Y. Liang; Y. Lin; R. Zhang; D. Dong, *Eur. J. Org. Chem.* **2009**, 4165.

44 Majumder, S.; Gipson, K. R.; Odom, A. L., *Org. Lett.* **2009**, *11*, 4720.

45 Horn, J.; Marsden, S. P.; Nelson, A.; House, D.; Weingarten, G. G., *Org. Lett.* **2008**, *10*, 4117.

46 Sandelier, M. J.; DeShong, P., *Org. Lett.* **2007**, *9*, 3209.

47 Arcadi, A.; Aschi, M.; Marinelli, F.; Verdecchia, M., *Tetrahedron* **2008**, *64*, 5354.

48 Yi, C. S.; Yun, S. Y.; Guzei, I. A., *J. Am. Chem. Soc.* **2005**, *127*, 5782.

49 Friedländer, P.; Ostermaier, H., *Chemische Berichte* **1882**, *15*, 332.

50 Broch, S.; Aboab, B.; Anizon, F.; Moreau, P., *Eur. J. Med. Chem* **2010**, *45*, 1657.

51 Tochilkin, A. I.; Kovel'man, I. R.; Prokof'ev, E. P.; Gracheva, I. N.; Levinskii, M. V., *Chem. Heterocycl. Compd.* **1988**, *24*, 892.

52 Königs, W., *Chem. Ber.* **1879**, *12*, 448.

53 Tschitschibabin, A. E.; Witkovsky, D. P.; Lapschin, M. I., *Chem. Ber.* **1925**, *58*, 803.

54 Tobisu, M.; Hyodo, I.; Chatani, N., *J. Am. Chem. Soc.* **2009**, *131*, 12070.

55 Wu, J.; Cui, X.; Chen, L.; Jiang, G.; Wu, Y., *J. Am. Chem. Soc.* **2009**, *131*, 13888.

56 Boudet, N.; Lachs, J. R.; Knochel, P., *Org. Lett.* **2007**, *9*, 5525.

57 Ishiyama, T.; Miyaura, N., *J. Organomet. Chem.* **2003**, *680*, 3.

58 Harrisson, P.; Morris, J.; Marder, T. B.; Steel, P. G., *Org. Lett.* **2009**, *11*, 3586.

59 Coventry, D. N.; Batsanov, A. S.; Goeta, A. E.; Howard, J. A. K.; Marder, T. B.; Perutz, R. N., *Chem. Commun.* **2005**, 2172.

60 Ishiyama, T.; Takagi, J.; Hartwig, J. F.; Miyaura, N., *Angew. Chem. Int. Ed.* **2002**, *41*, 3056.

61 Yamazaki, K.; Kawamorita, S.; Ohmiya, H.; Sawamura, M., *Org. Lett.* **2010**, *12*, 3978.

62 Kawamorita, S.; Ohmiya, H.; Hara, K.; Fukuoka, A.; Sawamura, M., *J. Am. Chem. Soc.* **2009**, *131*, 5058.

63 Chotana, G. A.; Rak, M. A.; Smith, M. R. III., *J. Am. Chem. Soc.* **2005**, *127*, 10539.

64 Sotomatsu, T.; Murata, Y.; Fujita, T., *J. Comput. Chem.* **1991**, *12*, 135.

65 Sotomatsu, T.; Fujita, T., *J. Org. Chem.* **1989**, *54*, 4443.

66 Walker, S. D.; Barder, T. E.; Martinelli, J. R.; Buchwald, S. L., *Angew. Chem. Int. Ed.* **2004**, *43*, 1871.

67 Conrad, M.; Limpach, L., *Chem. Ber.* **1887**, *20*, 944.

68 Conrad, M.; Limpach, L., *Chem. Ber.* **1891**, *24*, 2990.

69 Reitsema, R. H., *Chem. Rev.* **1948**, *43*, 43.

70 Matsugi, M.; Tabusa, F.; Minamikawa, J-I., *Tetrahedron Lett.* **2000**, *41*, 8525.

71 von Sprecher, A.; Gerspacher, M.; Beck, A.; Kimmel, S.; Wiestner, H.; Anderson, G. P.; Niederhauser, U.; Subramanian, N.; Bray, M. A., *Bioorg. Med. Chem. Lett.* **1998**, *8*, 965.

72 Aalten, H. L.; van Koten, G.; Grove, D. M.; Kuilman, T.; Piekstra, O. G.; Hulshof, L. A.; Sheldon, R. A., *Tetrahedron* **1989**, *45*, 5565.

73 Bacon, R. G. R.; Rennison, S. C., *J. Chem. Soc., C.* **1969**, 312.

74 Alterman, M.; Hallberg, A., *J. Org. Chem.* **2000**, *65*, 7984.

75 Vanchura, I. I. B. A.; Preshlock, S. M.; Roosen, P.C.; Kallepalli, V. A.; Staples, R.J.; Maleczka, R. E., Jr.; Singleton, D. A.; Smith, M. R., III., *Chem. Commun.* **2010**, *46*, 7724.

76 Shen, K.; Fu, Y.; Li, J-N.; Liu, L.; Guo, Q-X., *Tetrahedron* **2007**, *63*, 1568.

77 Webster, C. E.; Fan, Y.; Hall, M. B.; Kunz, D.; Hartwig, J. F., *J. Am. Chem. Soc.* **2003**, *125*, 858.

78 Dang, L.; Lin, Z.; Marder, T. B., *Chem. Commun.* **2009**, 3987.

79 Lafrance, M.; Rowley, C. N.; Woo, T. K.; Fagnou, K., *J. Am. Chem. Soc.* **2006**, *128*, 8754.

80 Gaussian 03, Revision E.01, Frisch, M. J. ; Trucks, G. W.; Schlegel, H. B.; Scuseria, G. E.; Robb, M. A.; Cheeseman, J. R.; Montgomery, J. A., Jr.; Vreven, T.; Kudin, K. N.; Burant, J. C.; Millam, J. M.; Iyengar, S. S.; Tomasi, J.; Barone, V.; Mennucci, B.; Cossi, M.; Scalmani, G.; Rega, N.; Petersson, G. A.; Nakatsuji, H.; Hada, M.; Ehara, M.; Toyota, K.; Fukuda, R.; Hasegawa, J.; Ishida, M.; Nakajima, T.; Honda, Y.; Kitao, O.; Nakai, H.; Klene, M.; Li, X.; Knox, J. E.; Hratchian, H. P.; Cross, J. B.; Bakken, V.; Adamo, C.; Jaramillo, J.; Gomperts, R.; Stratmann, R. E.; Yazyev, O.; Austin, A. J.; Cammi, R.; Pomelli, C.; Ochterski, J. W.; Ayala, P. Y.; Morokuma, K.; Voth, G. A.; Salvador, P.; Dannenberg, J. J.; Zakrzewski, V. G.; Dapprich, S.; Daniels, A. D.; Strain, M. C.; Farkas, O.; Malick, D. K.; Rabuck, A. D.; Raghavachari, K.; Foresman, J. B.; Ortiz, J. V.; Cui, Q.; Baboul, A. G.; Clifford, S.; Cioslowski, J.; Stefanov, B. B.; Liu, G.; Liashenko, A.; Piskorz, P.; Komaromi, I.; Martin, R. L.; Fox, D. J.; Keith, T.; Al-aham, M. A.; Peng, C. Y.; Nanayakkara, A.; Challacombe, M.; Gill, P. M. W.; Johnson, B.; Chen, W.; Wong, M. W.; Gonzalez, C.; Pople, J. A. Gaussian, Inc., Wallingford CT 2004.

81 Matulis, V. E.; Halauko, Y. S.; Ivashkevich, O. A.; Gaponik, P. N., *Theochem* **2009**, *909*, 19.

CHAPTER V - AZAINDOLE PROTECTION AND BORYLATION

5.1 Introduction

Azaindole is a polyaromatic heterocycle analogous to the indole nucleus, where one of the carbon atoms at the 4 - 7 positions is replaced by a nitrogen atom to give the 4-, 5-, 6- and 7-azaindoles, respectively (***Figure 164***).[1,2]

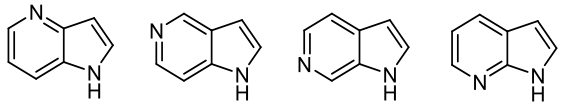

Figure 164 - Structures of 4- , 5- , 6- and 7- azaindole.[1,2]

The azaindole nucleus has received much interest in the literature, which can be attributed to its utility in a number of areas of chemistry. Azaindole compounds represent key building blocks in pharmaceutical, agrochemical, and natural product synthesis.[1,2] In biological systems, azaindoles act as a biostere for the indole and purine ring systems, which has sparked interest in the derivative chemistry of the system. There are numerous examples of biologically active azaindole derivatives in the literature (***Figure 165***).[1,2]

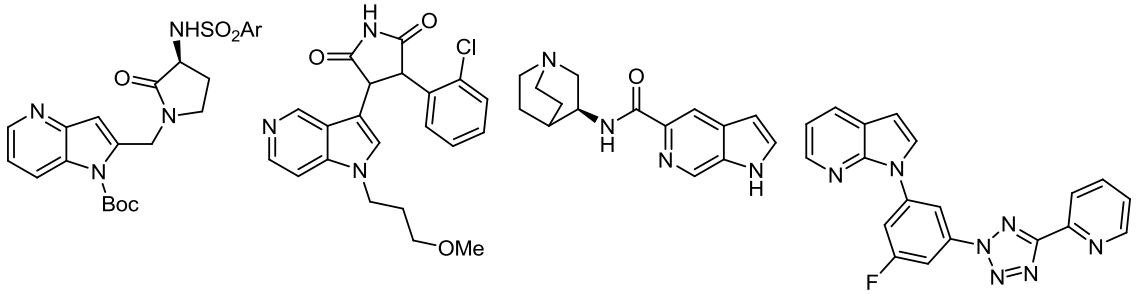

Figure 165 - Selected Biologically active 4-, 5-, 6- and 7-azaindoles.[1,2]

The prevalence of the azaindole scaffold in the literature makes methods for the functionalisation of this class of heterocycle important. Upon commencing the work described, the C-H borylation of the azaindole scaffold had yet to be reported. Initial studies focussed on

the 7-azaindole scaffold due to the commercial availability of this compound. The potential for selective borylation of the electronically distinct ring systems was also of interest.

5.2 C-H Borylation of 7-Azaindoles

The C-H borylation of 7-azaindole was attempted with ½[Ir(OMe)cod]$_2$/dtbpy (3 mol%), catalyst system over a 16 hour reaction period (***Figure 166***). Analysis of the crude reaction mixture by GC-MS revealed two peaks with molecular ions of 239 and 118 *m/z*, corresponding to B_2pin_2 and 7-azaindole, respectively.

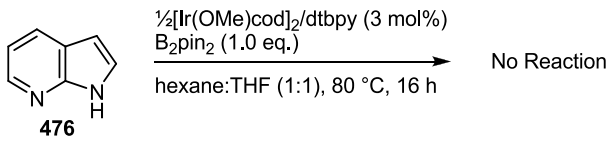

Figure 166 - Attempted C-H borylation of 7-azaindole.

The lack of reactivity was attributed to strong binding of the catalyst by both the pyridyl and pyrole N atoms. Borylation of the parent pyridine and pyrole have been demonstrated and as such the coordination is sufficiently transient to allow the reaction to proceed (***Figure 167***).[3]

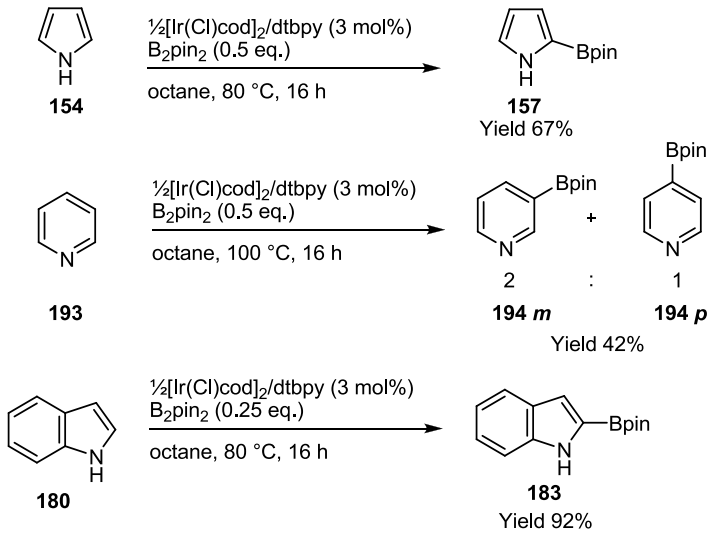

Figure 167 - C-H borylation of pyridine, indole and pyrole.[3]

However, in the case of 7-azaindole **476** the cooperative effect of the two binding regions is sufficient to strongly coordinate to the catalyst rendering it unable to perform the reaction. With

this theory in mind it was decided to synthesise a series of *N*-protected 7-azaindoles. By protection of the azaindole, the coordinating environment would be sterically blocked and borylation was predicted to occur.

5.2.1 Synthesis of *N*-Protected 7-Azaindoles

Protecting groups with a range of steric and electronic properties were chosen in order to give insight into the reactivity and selectivity of the borylation reaction.

Initial efforts focussed on the installation of simple alkyl protecting group, with the preparation of *N*-methyl-7-azaindole. Deprotonation of the azaindole NH was carried out by addition of sodium hydride at 0 °C followed reaction with methyl iodide to afford the desired product **481** in 48% yield (***Figure 168***). The product identity was confirmed with molecular ion of 133 *m/z* $(M+H)^+$ in the MS (ES^+) and characteristic signal at 3.87 ppm in the ^1H NMR spectrum for the *N*-methyl group. The positioning and coupling pattern of the aromatic signals for the azaindole core in the ^1H NMR spectrum remained consistent with the unprotected parent arene.

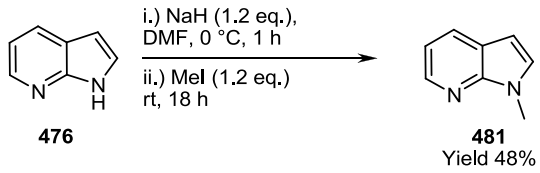

Figure 168 - Synthesis of *N*-methyl-7-azaindole.

A similar strategy was applied to the synthesis of *N*-benzyl-7-azaindole and *N*-acyl-7-azaindole. Deprotonation and subsequent reaction with benzyl bromide or acetyl chloride afforded the desired product **482** and **483** in 82% and 58% yield respectively. Confirmation of product identity was carried out by MS (ES^+) and ^1H NMR spectroscopic analysis. **482** showed a molecular ion of 209 *m/z* $(M+H)^+$ and characteristic signal for the benzyl CH_2 at 5.53 ppm in the ^1H NMR spectrum. **483** was confirmed by presence of a molecular ion of 161 *m/z* $(M+H)^+$ in MS (ES^+) spectrum and characteristic signal at 3.05 ppm in the ^1H NMR spectrum for the

methyl of the *N*-Acyl group. The structures were further confirmed by X-ray crystallographic analysis (***Figure 169***).

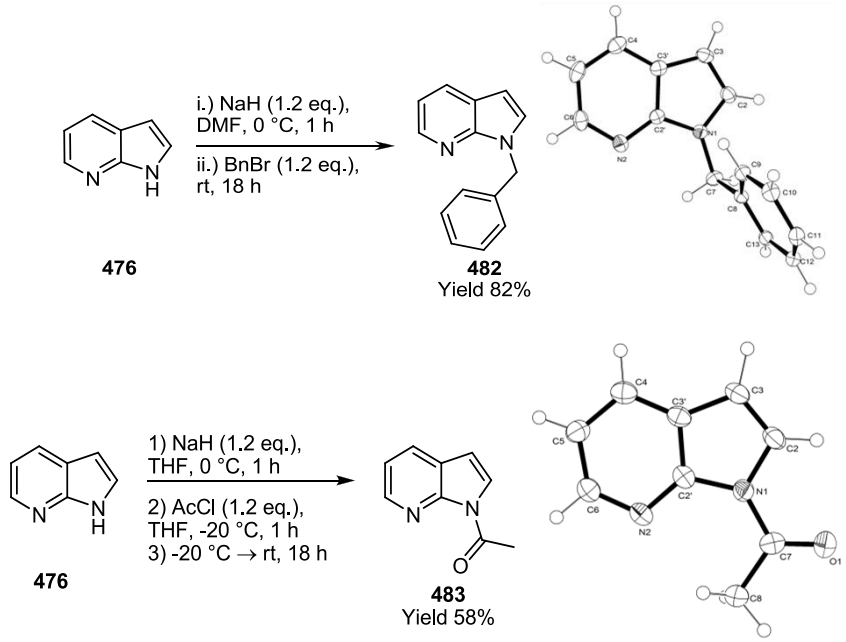

Figure 169 - Synthesis and molecular structure of **482** and **483** (Thermal ellipsoids drawn at 50% probability).

The synthesis of *N*-Boc-7-azaindole was carried out by addition of DMAP followed by addition of Boc-anhydride affording full conversion within 3 minutes and a 98% yield of **365**.

As previously, product identity was confirmed by MS (ES^+) analysis with a molecular ion of 218 *m/z* $(M+H)^+$ and characteristic signal at 1.69 ppm in the ^1H NMR spectrum consistent with the *tert*-butyl of the *N*-Boc group. X-ray crystallographic analysis provided further confirmation of the structure of **365** (***Figure 170***). The reaction required slow addition of Boc_2O due to the vigorous evolution of CO_2 from the reaction.

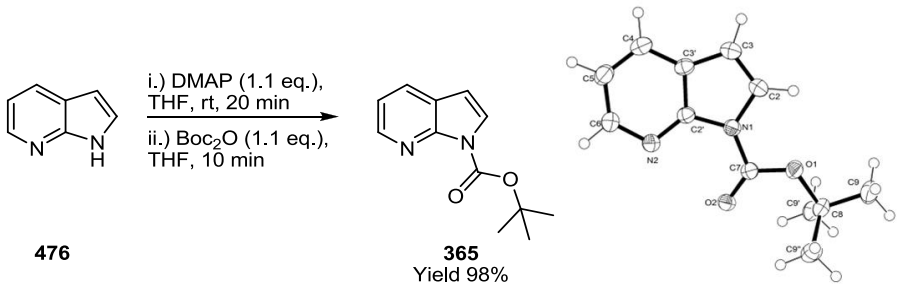

Figure 170 - Synthesis and molecular structure of **365** (Thermal ellipsoids drawn at 50% probability).

Deprotonation of **476** with sodium hydride followed by reaction with DMAP and mesyl chloride afforded the product **484** in an 82% yield. MS (ES^+) analysis showed a molecular ion of 197 *m/z*, consistent with **484**. Further confirmation was provided by a signal for SO_2Me at 3.56 ppm in the ^1H NMR spectrum and X-ray crystallographic analysis of the product (***Figure 171***).

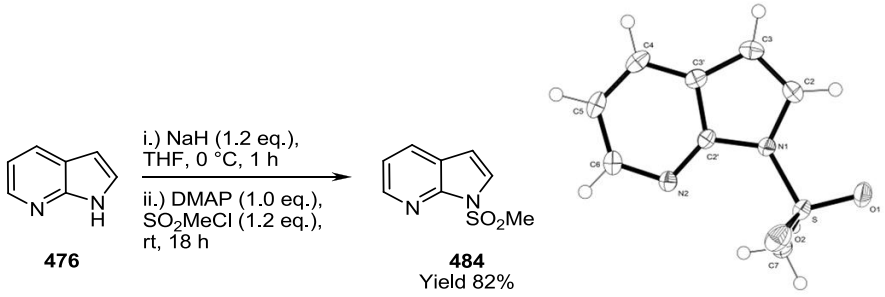

Figure 171 - Synthesis and molecular structure of **484** (Thermal ellipsoids drawn at 50% probability).

Following the synthesis of simple alkyl, acyl and sulfonyl protected azaindoles, the introduction of a silicon protecting group was explored. Initial deprotonation of the azaindole with sodium hydride was followed by reaction with trimethylsilylchloride afforded TMS protected 7-azaindole. Analysis by MS (ES^+) showed a molecular ion of 190 *m/z* $(M+H)^+$ confirming that the product had formed. However, the product was unstable to chromatography and resulted in recovery of azaindole starting material.

As such *N*-TIPS-7-azaindole was synthesised by the same route but utilising TIPSCl as the silylating reagent. This resulted in the desired product **485** in 70% yield. MS (ES^+) and ^1H NMR spectroscopy confirmed the product identity with molecular ion of 274 *m/z* $(M+H)^+$ and characteristic peak at 0.95 ppm isopropyl group of *N*-TIPS. As previously the product was confirmed by X-ray crystallographic analysis (***Figure 172***).

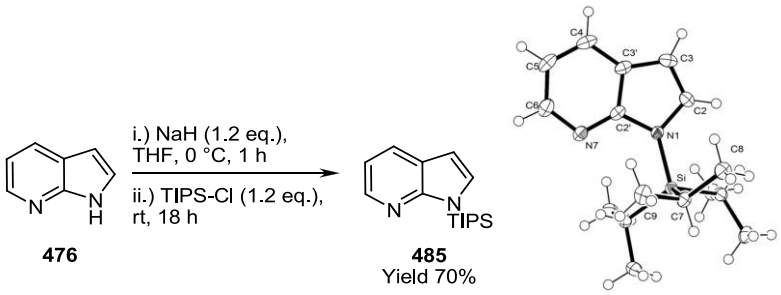

Figure 172 - Synthesis and molecular structure of **485** (Thermal ellipsoids drawn at 50% probability).

5.2.2 C-H Borylation of *N*-protected 7-Azaindoles

Having successfully accessed a range of protected azaindoles the compounds were subjected to C-H borylation (***Figure 173***). All reactions were monitored by GC-MS to assess conversion. Samples of the crude reaction mixture were submitted for ^{1}H NMR spectroscopy to attempt to assign the regiochemistry of the products formed.

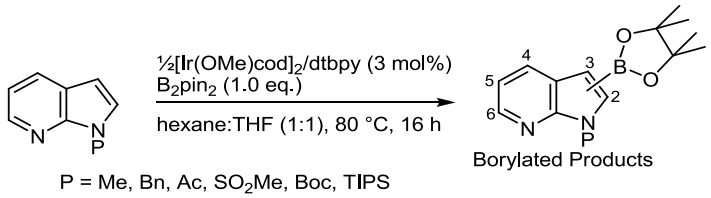

Figure 173 - C-H borylation of protected azaindole.

Table 18 - C-H borylation of protected azaindoles.

Entry	Protecting Group	GC-MS Conversion (%)	Isomers formed	Product Identity
1	Me	100%	1 mono (60%) 3 bis (40% 25:50:25)	Unable to assign complex mixture
2	Bn	100%	4 mono (30%) 7 bis (70%)	Unable to assign Complex mixture
3	Ac	100%	2 mono (60% 85:15) 1 bis (40%)	mono C^3 (major) mono C^5 (minor) bis C^3-C^5
4	SO_2Me	100%	2 mono (75:25)	mono C^3 (major) mono C^5 (minor) bis C^3-C^5
5	Boc	100%	2 mono (95% 90:10) 1 bis (5%)	mono C^3 (major) mono C^5 (minor) bis C^3-C^5
6	TIPS	80%	2 mono (60% 80:20) 1 bis (40%)	mono C^3 (major) mono C^5 (minor) bis C^3-C^5

Borylation was successful with all of the protected azaindoles (***Table 18***). However, multiple borylation products were observed. Borylation of methyl and benzyl protected azaindoles (***Table 18***, entries 1 & 2) afforded a complex mixture of products. This was especially true for the borylation of the benzyl protected derivative (***Table 18***, entry 2) which formed a total of 11 different borylated products.

Borylation of **383** and **384** (***Table 18***, entries 3 & 4) were more selective but still resulted in multiple borylated products. Borylation of Boc protected derivative **365** (***Table 18***, entries 5) provided 2 mono borylated products in a 9:1 ratio with a small amount of bis-borylated product.

The borylation of **485** was also relatively selective (***Table 18***, entry 2) with a 8:2 mixture of mono-borylated products; however, the reaction also formed a large quantity of bis borylated product and did not reach full conversion.

Due to the highly complex nature of the product mixtures formed from the borylation of protected azaindoles, it was decided to concentrate on a single substrate in order to gain further understanding of the ring systems reactivity.

Due to the ease of starting material preparation and high selectivity towards borylation, *N*-Boc-7-azaindole was chosen for further study. Borylation of *N*-Boc azaindole **365** afforded two mono-borylated products in a 9:1 ratio with activation in the C^3 and C^5 position along with a small amount of bis borylated product, determined by ^{1}H NMR spectroscopy (***Figure 174***).

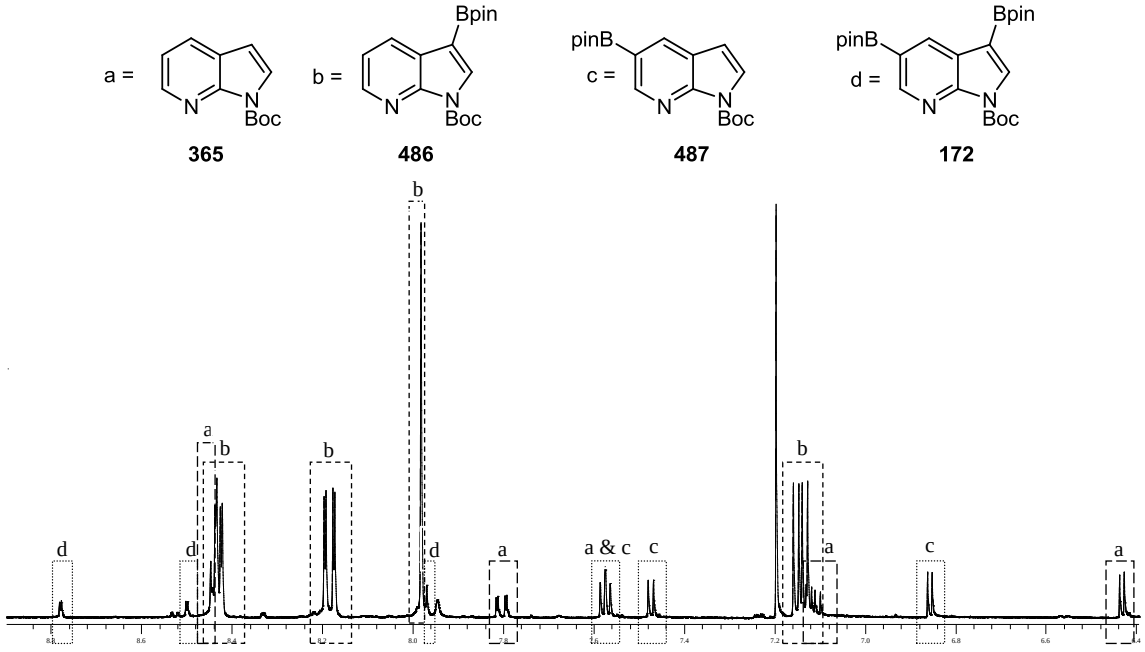

Figure 174 - ^{1}H NMR spectrum of 1-*N*-Boc-7-azaindole borylation products.

At the time of this work, there had been little work carried out to attempt to improve the methodology associated with the borylation reaction. The classical reaction conditions utilised a narrow range of reaction solvent (octane, hexane, THF).[4,5] Reactions had previously only been carried out in sealed reaction vessels with standard reaction heating methods employed.

In order to gain further insight into the reactivity of the ring system and the effect of changes to the reaction methodology, systematic variations were made to the reaction components. A series of test experiments were carried out in order to asses any potential benefits of procedural alteration. These variations will be discussed in the following section.

5.2.3 *N*-Boc-7-Azaindole Borylation Study

5.2.3.1 Variation of B_2pin_2 Stoichiometry for the Borylation of *N*-Boc-7-Azaindole

The consumption B_2pin_2 in the borylation catalytic cycle has been shown to operate as a two stage process.[6] The first stage is the fast consumption of B_2pin_2 followed by the slower consumption of the HBpin with the release of H_2.[7] When the reaction is carried out in a sealed vessel the H_2 released causes a pressure build up. It is possible that the increased pressure of H_2 may inhibit or even totally shutdown the second cycle where HBpin is consumed.

To assess the effect of releasing this pressure build up, the reaction was carried out under a flow of nitrogen. The borylation procedure used was the same as for the initial studies. Reactions were carried out with 0.5 and 1.0 equivalents of B_2pin_2 to asses if the reaction progressed into the second HBpin cycle (***Figure 175***, ***Table 19***). The reaction was conducted in a round bottom flask equipped with a condenser and nitrogen inlet. The products formed were monitored by ^{1}H NMR spectroscopy of the crude product mixture.

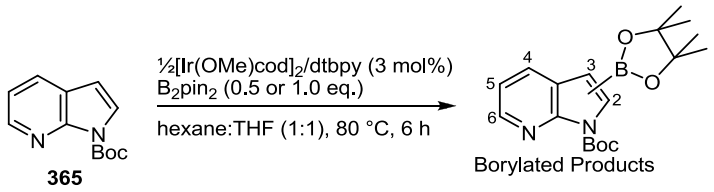

Figure 175 **-** Open borylation of **365.**

Table 19 **-** Open borylation reaction of **365**.

Entry	Conditions	B_2pin_2	^{1}H NMR Conversion%			
			SM	Mono - C_3	Mono-C_5	Bis C_3-C_5
			365	**486**	**487**	**172**
1	Open	0.5	46	37	10	7
2	Open	1.0	10	64	15	11

The reaction with 0.5 equivalents of B_2pin_2 (***Table 19***, entry 1) afforded 54% conversion with 61% of the boron in the reaction consumed by formation of 37% mono-C^3, 10% mono-C^5, and 7% of the bis-borylated product. The reaction with 1.0 equivalents of B_2pin_2 (***Table 19***, entry 2) afforded 90% conversion with 50% of the boron in the reaction consumed. These results suggest that the second HBpin cycle is not taking place to any significant degree. It is possible that loss of HBpin from the reaction in the N_2 stream may lead to the low conversion.

Carrying out the reaction in an open system was unable to give the desired levels of conversion for the reaction. As such it was decided to conduct further studies in the classical sealed system.

5.2.3.2 Variation of Reaction Solvent for the Borylation of *N*-Boc-7-Azaindole

As discussed previously, the range of reaction solvents which the borylation reaction is carried out in is very limited. As such a screen of some other solvents was conducted. The reaction has been demonstrated to work most successfully in non-polar solvents. Literature reports also suggest that highly polar solvents not suitable for the reaction.[4,8] The C-H borylation reaction is typically carried out in hexane. Due to the highly non-polar nature of this solvent there was little scope to investigate more non polar systems. THF has been used as a solvent in the C-H borylation reaction; however, the reactivity of THF systems is lower than the more non-polar solvent systems.[5]

It was postulated that heteroatom coordination may be the cause of lower reactivity in borylation reaction where THF has been used as a solvent.[5] As such ether based solvents containing a steric blocking group adjacent to the heteroatom were sought.

The solvents to be examined were DMF, THF, 2-Me-THF and MTBE. DMF and THF were included in order to confirm literature reports associated with the activity of systems containing them. The choice of 2-Me-THF and MTBE was made due to the hindered nature of the heteroatom in the solvents which should prevent coordination to the metal centre affording higher reactivity than THF.

The borylation reaction was carried out using the same procedure as for the previous reaction in this chapter with both 0.5 and 1.0 equivalent of B_2pin_2 (***Figure 176***, ***Table 20***).

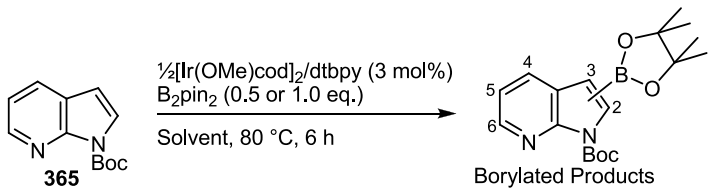

Figure 176 - Solvent screen for C-H borylation of *N*-Boc-7-azaindole.

Table 20 - Solvent screen for C-H borylation of *N*-Boc-7-azaindole.

			^{1}H NMR Conversion%			
Entry	Solvent	B_2pin_2	SM	Mono-C_3	Mono-C_5	Bis C_3-C_5
			365	**486**	**487**	**172**
1	DMF	0.5	100	0	0	0
2	THF	0.5	38	45	13	4
3	THF	1.0	5	32	14	50
4	2-Me-THF	0.5	39	45	11	5
5	2-Me-THF	1.0	0	32	16	52
6	MTBE	0.5	14	63	15	8
7	MTBE	1.0	6	20	10	64

As predicted DMF was ineffective as a borylation solvent (***Table 20***, entry 1) resulting in 0% conversion. Similarly, as predicted, THF was efficient at effecting the transformation affording 62% and 95% conversion with 0.5 and 1.0 equivalents of B_2pin_2, respectively. The reactions with 2-MeTHF (***Table 20***, entries 4 and 5) afforded a similar conversion and product distribution to the THF reaction.

The reactions carried out with MTBE offered higher conversion than all other solvents for reactions with both the 0.5 and 1.0 equivalents of B_2pin_2 (***Table 20***, entry 6 and 7). This higher relative reactivity of this sterically hindered solvent suggests that solvent coordination is a problem within the C-H borylation reaction. MTBE showed the highest conversion from starting material with 86% conversion to products with 94% of the available boron consumed for the reaction with 0.5 equivalents of B_2pin_2. The solvent screen was able to identify MTBE as a highly suitable solvent for the C-H borylation reaction.

5.2.3.3 Application of Microwave Heating to the Borylation of *N*-Boc-7-Azaindole

Another goal of this chapter was to attempt the use of different processing techniques for carrying out the borylation reaction. As such microwave irradiation was used to facilitate the heating of the reaction. The reaction was again conducted in the same manner as previously. Reactions were the heated to 80 °C and 140 °C for 5 and 30 minutes. The reactions were monitored by ^{1}H NMR spectroscopy (***Table 21***) of the crude product mixture.

Table 21 - Microwave heating for C-H borylation of *N*-Boc-7-azaindole.

Entry	Temp	Time	B_2pin_2	^{1}H NMR conversion%			
				SM	Mono - C_3	Mono-C_5	Bis C_3-C_5
				365	**486**	**487**	**172**
1	80 °C	5 min	0.5	37	46	11	5
2	80 °C	30 min	0.5	37	46	13	4
3	80 °C	5 min	1.0	0	63	17	20
4	80 °C	30 min	1.0	0	68	14	18
5	140 °C	5min	0.5	35	46	12	7
6	140 °C	30 min	0.5	36	44	15	5
7	140 °C	5min	1.0	0	67	13	20
8	140 °C	30 min	1.0	0	67	13	20

At the time this work was carried out, there had been no reports of using microwave irradiation to facilitate the C-H borylation reaction. Reactions carried out with 0.5 equivalent of B_2pin_2 reached 63 - 65% conversion irrespective of reaction time or temperature (***Table 21***, entries 1, 2, 5 and 6). Similarly, the reactions conducted with 1.0 equivalent of B_2pin_2 afforded full conversion of starting material, again, independent of reaction time and temperature.

These results highlight maximum conversion for each set of conditions is achieved within 5 minutes at 80 °C. This represents a significant acceleration of the reaction relative to the standard heating conditions. This methodology and the implications of the use of microwave

irradiation formed the contents of the microwave accelerated protocol discussed earlier in this thesis in chapter III.

5.3 Conclusions

The work described in this chapter formed the basis of methodologies developed for the one-pot C-H borylation/Suzuki-Miyaura cross-coupling sequence (Chapter II) and the microwave accelerated C-H borylation protocol (Chapter III).

Due the implications of the findings of this work, time was directed towards these areas. However, this chapter forms the basis of interesting discoveries into the borylation of protected azaindole. The predominant product in all protected systems was the 3-borylated isomer. This highlights the higher reactivity of the electron rich 5-membered ring over the electron deficient 6-membered ring. This is in contrast to reactions of carbocyclic arenes where electron deficient arenes are more reactive. However, as discussed in chapter IV, the reasons associated with regiocontrol in heteroaromatic systems are not fully understood. C-H acidity may be able to further explain the observed reactivity.

5.4 Chapter V - References

1 Popowycz, F.; Merour, J-Y.; Joseph, B., *Tetrahedron* **2007**, *63*, 8689.

2 Popowycz, F.; Routier, S.; Joseph, B.; Merour, J-Y., *Tetrahedron* **2007**, *63*, 1031.

3 Takagi, J.; Sato, K.; Hartwig, J. F.; Ishiyama, T.; Miyaura, N., *Tetrahedron Lett.* **2002**, *43*, 5649.

4 Ishiyama, T.; Takagi, J.; Hartwig, J. F.; Miyaura, N., *Angew. Chem. Int. Ed.* **2002**, *41*, 3056.

5 Murphy, J. M.; Liao, X.; Hartwig, J. F., *J. Am. Chem. Soc.* **2007**, *129*, 15434.

6 Tamura, H.; Yamazaki, H.; Sato, H.; Sakaki, S., *J. Am. Chem. Soc.* **2003**, *125*, 16114.

7 Cho, J.; Tse, M. K.; Holmes, D.; Maleczka, R. E., Jr.; Smith, M. R., III., *Science* **2002**, *295*, 305

8 Ishiyama, T.; Isou, H.; Kikuchi, T.; Miyaura, N., *Chem. Commun.* **2010**, *46*, 159.

CHAPTER VI - *IPSO*-TRIFLUOROMETHYLATION OF ARYL BORONATES

6.1 Introduction

The presence of the trifluoromethyl group within a molecule is able to dramatically affect its pharmacological properties.[1] The group has been shown to have a profound effect on lipophilicity, metabolic stability and bioavailability of molecules. Due to these effects the trifluoromethyl group has been utilised in a wide variety of biologically active compounds, with uses in active pharmaceutical and agrochemical agents (***Figure 177***).[2]

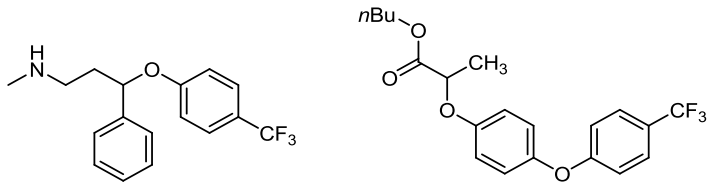

488
Active ingrediant in **Prozac**
(Eli Lilly antidepressant)

489
Active ingrediant in **Fusilade**
(Syngenta herbicide)

Figure 177 - CF_3 containing active pharmaceutical and agrochemical compounds.[2]

Due to these factors, methods for the introduction of trifluoromethyl groups into organic molecules have become increasingly important. At the time this work was carried out the conversion of aryl boronates to trifluoromethyl arenes had not been reported. The aim of this work was to develop a method to facilitate this transformation. This chapter will discuss preliminary work into the development of a copper mediated process for the introduction of trifluoromethyl groups into arenes. A proposed strategy involved reaction of aryl boronates with a copper (I) salts followed by addition of an electrophilic trifluoromethyl source could afford the trifluoromethylated arene.

The findings detailed in the remainder of this chapter are only preliminary due to the report detailed in chapter II of a similar method to facilitate the desired transformation.[3] In order to place the work in context, the following section will detail classical methods for the introduction of trifluoromethyl groups into arenes.

6.2 Classical Methods

Swart and co-workers reported the use of SbF_3 in the synthesis of trifluoromethyl groups through reaction with $ArCCl_3$ compounds. The trichlorotoluene requires synthesis from the corresponding toluene derivative by radical chlorination.[4]

Due to the harsh conditions required for the reactions, functional group tolerance is low. These limitations make this methodology unsuitable for the late stage introduction of the trifluoromethyl group into advanced intermediates. Recently a number of techniques have been developed to allow conversion of ArX (X= Cl, Br, I) to $ArCF_3$ via metal catalysed and mediated processes. This section will now discuss these developments in turn.

6.3 Metal Mediated Conversion of ArX to $ArCF_3$

6.3.1 Copper Mediated Trifluoromethylation

A series of copper mediated reactions have reported the *ipso*-trifluoromethylation of aryl halides.[5-9] The early reports by Fuchikami[5] and Schlosser[6] utilised trialkylsilyltrifluoromethyl reagents with copper (I) salts and potassium fluoride to afford the transformation (***Figure 178***). Increased reactivity is observed with electron deficient arenes, due to the nucleophilic role of CF_3^- in the reaction mechanism. The reaction with the pyridine substrate exemplifies the higher reactivity of electron deficient aryl halides. The reactivity of the system is limited to aryl iodide and bromides; however, the reaction with aryl bromides affords significantly lower yields.

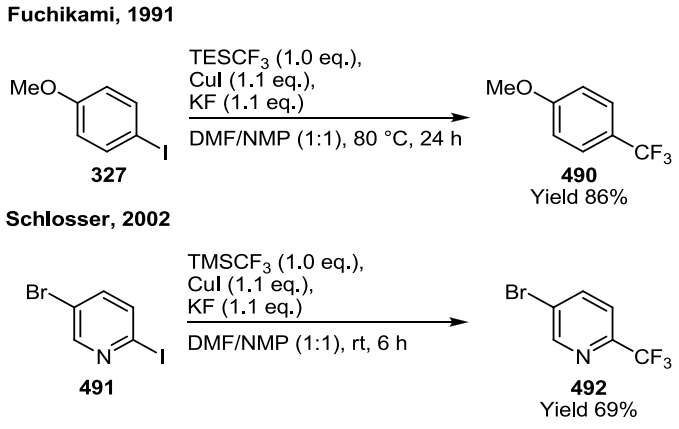

Figure 178 - Copper (I) mediated trifluoromethylation.[5,6]

More recently, Vicic and co-workers,[7,8] have utilised a NHC ligated copper system to pre-form a copper-CF_3 reagent to carry out the transformation (***Figure 179***). The reactivity is again mainly limited to aryl iodides.

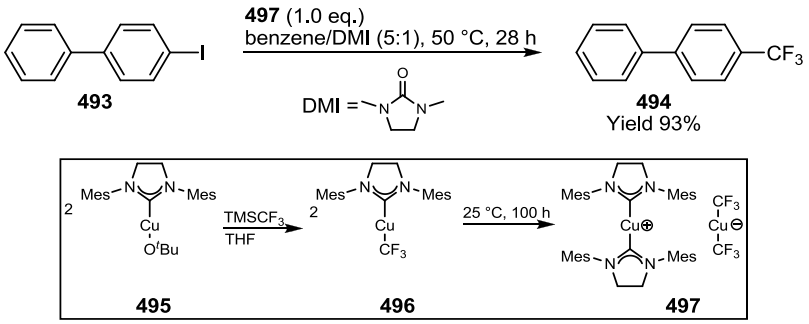

Figure 179 - Copper NHC mediated trifluoromethylation.

The use of cheap copper sources for the stoichiometric reactions discussed to date makes them more applicable to large scale synthesis. However, the use of stoichiometric NHC ligands in the reactions reported by Vicic,[7,8] along with extended reaction times is likely to limit their use.

The first catalytic copper system was reported by Amii and co-workers.[9] In a similar fashion, to the reactions discussed earlier in this section, a ligated copper (I) systems was reacted with a nucleophilic CF_3 source to form a copper-CF_3 reagent (***Figure 180***).

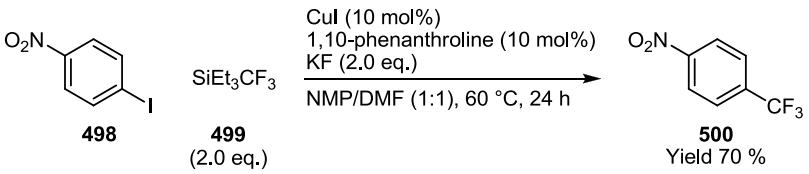

Figure 180 - Copper catalysed trifluoromethylation of aryl iodides.

The reaction proceeds via initial complexation of the CuI by 1,10-phenanthroline. This species undergoes nucleophilic attack from CF_3^- generated by fluoride mediated displacement of TES. The ligated-copper-CF_3 species generated reacts with the aryl iodide to form $ArCF_3$ and ligated copper iodide. The latter is then able to re-enter the catalytic cycle. The presence of the diamine ligand increases the electron density on the metal centre which increases the

nucleophilicity of the Cu-CF_3 reagent and stabilises the ligated-copper iodide intermediate allowing regeneration of the Cu-CF_3 active species.

Although this method is catalytic in copper, the reaction times required to facilitate the transformation are long. The limited substrate scope, only aryl iodides, is also a limitation of this methodology. Although the field of copper mediated trifluoromethylation has seen a number of important reports the major drawback of the methodology is due to the limited substrate scope.

6.4 Palladium Catalysed Trifluoromethylation

The application of palladium catalysts towards trifluoromethylation has been limited by the high activation barrier for reductive elimination of aryl trifluoromethyl products from palladium.[10,11] Fast reductive elimination of trifluoromethyl arene from palladium (II) was reported by Grushin and co-workers (***Figure 181***).[12]

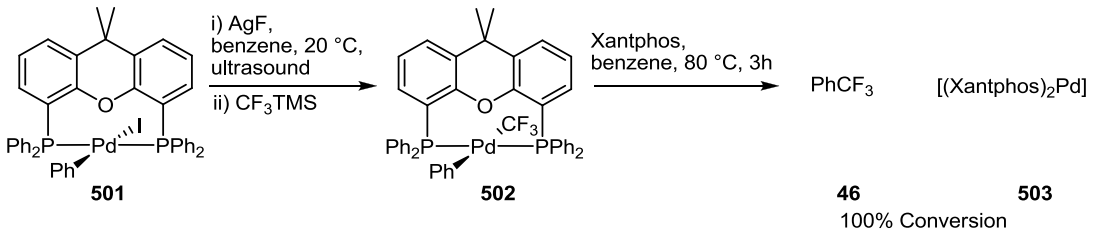

Figure 181 - Reductive elimination of $PhCF_3$ from Pd^{II}.

The role of Xantphos was crucial in the reaction, as replacement with other mono and bidentate ligands failed to affect the conversion to trifluoromethyl arene. This unique reactivity is attributed to the ability of Xantphos to change the conformation of its binding angle forcing reductive elimination of the product.[12]

As discussed on chapter II for the Suzuki-Miyaura reaction, a wide variety of electron rich bulky biaryl phosphine ligands have been developed. Their electron donating properties enable oxidative addition of their palladium complexes to less reactive aryl chlorides. The steric bulk associated with the ligand also acts to facilitate fast reductive elimination. This role of inducing reductive elimination is reminiscent of the previous example (***Figure 181***).

Buchwald and co-workers[11] reported the use of biaryl phosphine ligands to affect the palladium catalysed trifluoromethylation of aryl chlorides (***Figure 182***). Although only aryl chloride examples are reported, oxidative addition of aryl bromides and iodides is more facile and as such the reaction should be transferable to these substrate classes.[13]

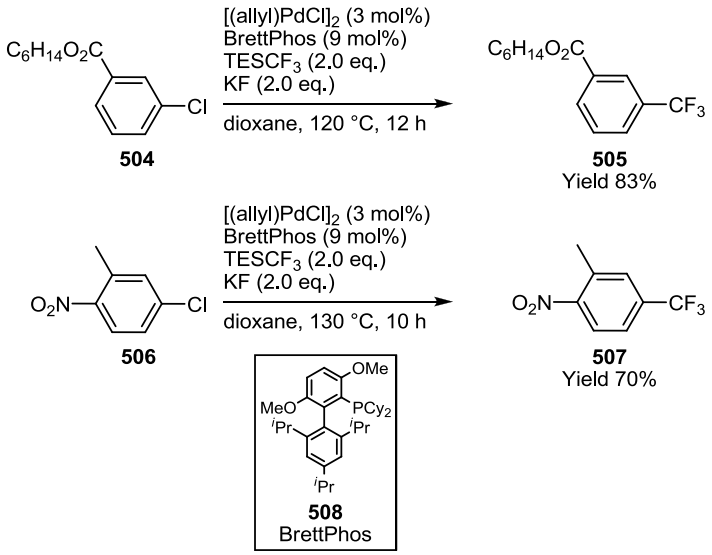

Figure 182 **-** Palladium catalysed trifluoromethylation of aryl chlorides.

The reaction functions well with both electron rich and electron poor arenes, although, the majority of the examples reported contain electron donating groups. Oxidative addition of electron rich aryl halides is typically more challenging due to their role as the electrophilic reaction partner.

The examples discussed in the previous section form the 'state of the art' in terms of introducing trifluoromethyl groups into arenes. At the time this work was carried out *ipso*-trifluoromethylation of aryl boronates was not known. This would be a desirable transformation, considering the wealth of other conversions which have been developed, as discussed in Chapter II. Copper was identified as a possible catalyst due to a number of reactions of aryl boronates utilising copper (I) salts. The following section will highlight aspects of the reactivity of copper (I) salts with aryl boronates

6.5 Reactions of Cu^{I} and Ag^{I} Salts with Aryl Boronates

A number of transformations of aryl boronates have utilised copper group metals. Copper itself has been shown to afford functionalised products via Cu^{I} and Cu^{II} catalysed and mediated reactions, as discussed in Chapter II. The reactivity of copper (II) salts, has been widely studied in the context of the Chan-Lam-Evans heteroatom cross-coupling reactions.[14-17]

The reactions of copper (I) salts typically proceed by formation of a copper-aryl intermediate which reacts with an electrophile. A number of groups have been able to isolate and characterise these intermediates which has given significant insight into how the reaction proceed. Hou and co-workers,[18] demonstrated a copper catalysed *ipso*-carboxylation of aryl boronates (***Figure 183***). The stoichiometric reaction demonstrates the ligated copper-aryl intermediate **512**, which is reacted with CO_2 as an electrophile.

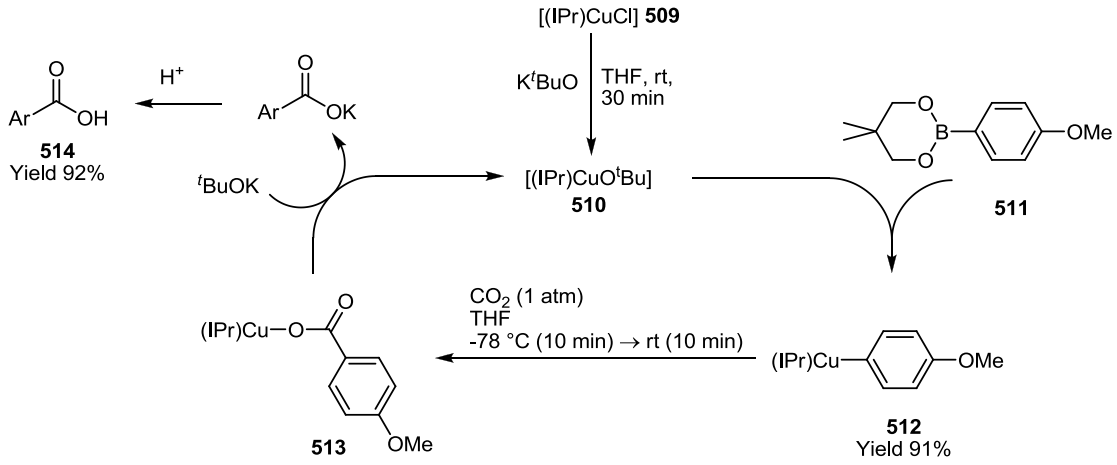

Figure 183 - Copper catalysed *ipso*-carboxylation of aryl boronates.

Burgey and co-workers[19] utilised copper (I) salts to perform a similar role with their use as a transmetalating agent for the Suzuki-Miyaura cross-coupling of 2-pyridyl boronates. These 2-pyridyl boronates are typically unstable under the reaction conditions of the Suzuki-Miyaura reaction, due to fast proteodeboronation. However, the report suggests that copper is able to transmetalate the pyridyl boronates faster than proteodeboronation. As for the previous example, an aryl copper species is suggested as being crucial for this reaction (***Figure 184***).

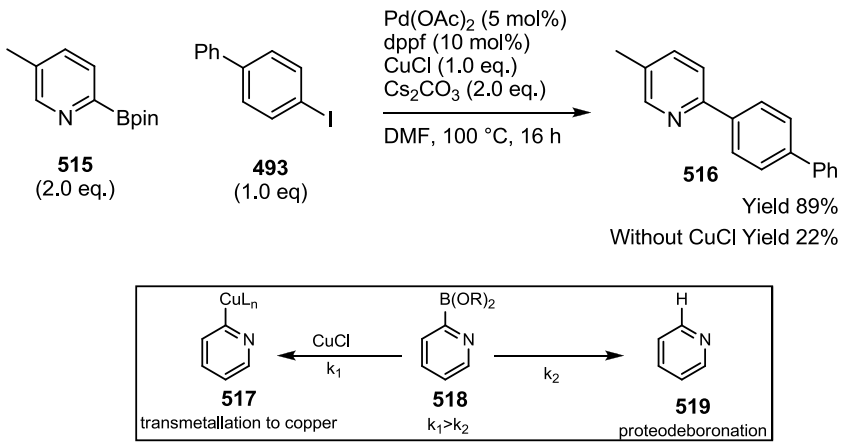

Figure 184 - Copper mediated Suzuki-Miyaura cross coupling.

Finally, in a related system, Ritter and co-workers demonstrated the silver (I) mediated fluorination of aryl boronates. The reaction requires performing of a silver-aryl species **520**, which then reacts with Selectfluor® as a source of F^+ (***Figure 185***).

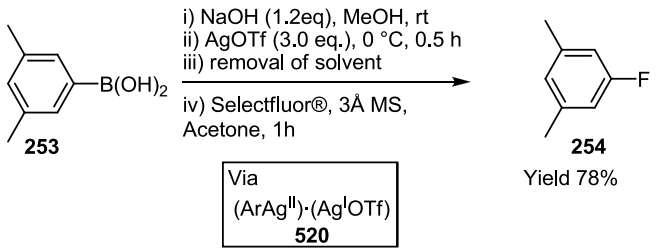

Figure 185 - Silver mediated fluorination of aryl boronates.

The three examples discussed in this section proceed via highly related metal aryl species which in some cases are isolable as with **512** and the commercially available mesitylcopper (Cu-2,4,6-Me(C_6H_2). The ability for aryl boronates to form these aryl metal species and their subsequent reactions with electrophiles resulted in the postulation that an analogous system could be developed for the introduction of trifluoromethyl groups. For the reaction to be viable a suitable CF_3^+ source was required.

6.5.1 Electrophilic Trifluoromethylating Reagents

Several electrophilic trifluoromethylating reagents have been described in the literature (***Figure 186***).[20-25] The application of electrophilic trifluoromethylation has been limited due to the challenging preparation of reagents such as **523**. However, the use of hypervalent iodine reagents has become more widely applied due to the easy preparation of **521** and **522** from 2-iodobenzoic acid.

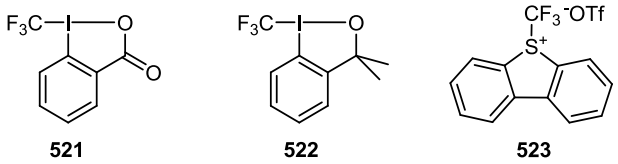

521 **522** **523**

Figure 186 - Electrophilic trifluoromethylating reagents.[20-25]

Hypervalent iodine reagents have been applied to reactions with nucleophiles such as α-nitro esters, β-keto esters, affording α-trifluoromethylated products.[21] Use of metal additives enable synthesis of trifluoromethylethers with aliphatic alcohols.[22] Aromatic trifluoromethylation is limited to substrates containing electron donating activating groups and can encounter problems of multiple product formation[24] (***Figure 187***).

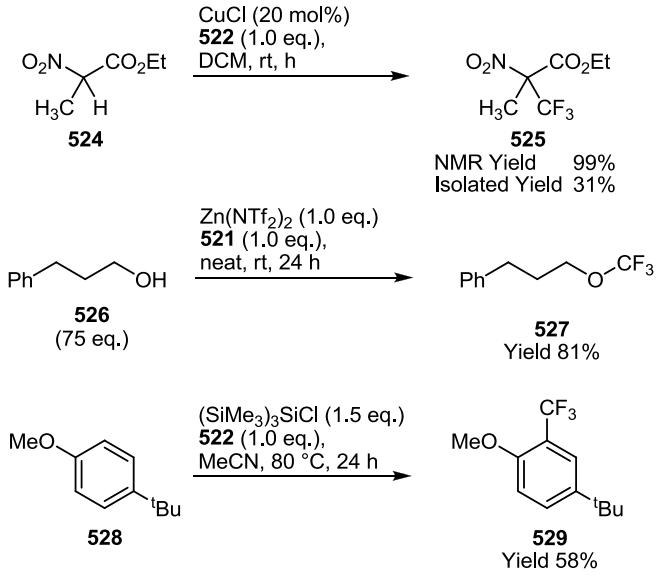

Figure 187 - Application of hypervalent iodine trifluoromethylating reagents.[21,22,24]

The previous sections have explored the ability of copper (I) salts to form aryl metal species with aryl boronates and their subsequent reaction with electrophiles. The role of hypervalent iodine reagents in the generation of electrophilic CF_3 has been discussed. The following section will describe the preliminary efforts made towards combining these two areas to form a system which will carry out a copper mediated trifluoromethylation of aryl boronates.

6.6 Results and Discussion

Synthesis of an electrophilic trifluoromethylating reagent was required before the proposed reaction could be attempted. The reagent chosen was **521**, due to the ease of synthesis from simple starting materials. A literature procedure[23] for the synthesis of **521** from 2-iodobenzoic acid **530** was followed. Initial oxidation with sodium periodate to form **531**, was followed by exchange of the OH group with acetic anhydride in acetic acid to afford **532** in quantitative yield. Subsequent reaction of **532** with $TMSCF_3$ and catalytic KF afforded **521** in 76% overall yield (***Figure 188***). Product identity was confirmed by comparison of literature vales for the ^1H and ^{13}C NMR chemical shifts. A signal at -34.2 ppm in the ^{19}F NMR spectrum was consistent with an I-CF_3 group.

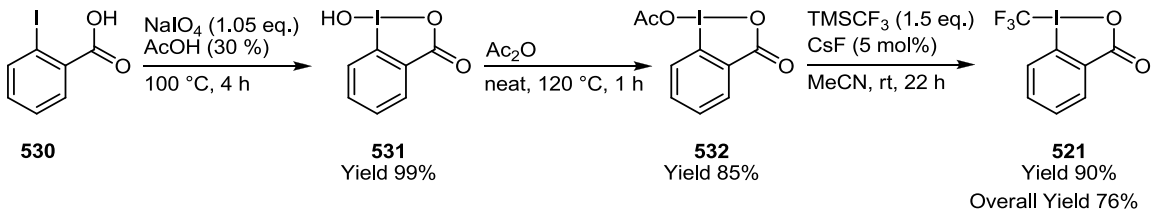

Figure 188 - Synthesis of **521.**

With the preparation of the **521** complete a series of reactions were conducted in order to ascertain whether the proposed conversion of aryl boronate to aryl trifluoromethyl was viable.

6.6.1 Trifluoromethylation of Aryl boronates

A model substrate was chosen to carry out test reactions, with initial studies utilising 4-biphenylboronic acid **533**. The high molecular weight, compared to simple mono-aryl systems, was desirable to enable easier purification of the product by reducing volatility.

In the proposed reaction, it was postulated a two step process would occur. Initial formation of a copper aryl species would be followed by reaction with the electrophilic trifluoromethyl source **521**.

A test reaction was conducted using stoichiometric amounts of copper (I) bromide in DMF which was stirred for 30 minutes to form the proposed aryl metal species, followed by addition of **521** (***Figure 189***). The initial reaction afforded the desired product **494** in 45% yield. GC-MS analysis gave a molecular ion of 222 *m/z*, consistent with **494**. Characterisation of the product by ^{1}H, and ^{19}F NMR provided chemical shift values consistent with those reported for **494** in the literature with a signal at 63.5 ppm in the ^{19}F NMR spectrum. A pale green solution formed on addition of CuBr and **533** to DMF, this colouration remained for the duration of the first step of the reaction. Upon addition of **521** as a solution in DMF, an immediate change in colour to a bright green-blue was observed. This change in colour is indicative of oxidation of from Cu^{I} to $Cu^{II/III}$. This oxidation of copper is unsurprising as hypervalent iodine reagents are known to act as oxidising reagents, with commercial reagents such as IBX.[26]

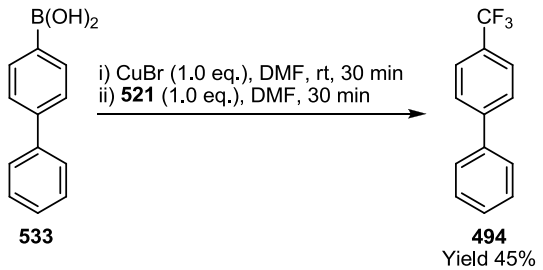

Figure 189 - Copper mediated trifluoromethylation test reaction.

Attempts to reproduce or improve upon the success of this initial reaction were more troublesome. Employing the same conditions failed to afford the same product yield, with yields of between 18 - 20% being achieved. In order to probe capricious nature of the reaction, the

order of reagent addition was investigated. Purification and isolation of each reaction was not feasible for the screening of reaction conditions. It was not possible to monitor the reaction by GC-MS as the boronic acid was not visible. The reaction progress was monitored by ^{19}F NMR by introduction of hexafluorobenzene as a standard to measure conversion against.

When the reaction was carried out in the absence of copper, no reaction occurred and all starting materials appeared unchanged. No colour change was observed, with the reaction remaining colourless throughout. Premixing of aryl boronic acid with copper bromide in DMF followed by addition of **521** after 30 minutes afforded an average of 18% yield over 3 reactions. The characteristic pale green to dark blue-green colour change occurred upon addition of **521**. Disappearance of the signal at -34 ppm in the ^{19}F NMR spectrum confirms consumption of **521**.

Addition of copper bromide, boronic acid and **521** to a dry reaction vessel, followed by addition of DMF afforded an average yield of 11% over 3 reactions. As previously the characteristic colour change was observed, along with, the signal for **521** being lost from the ^{19}F NMR spectrum.

Finally, copper bromide was mixed with **521** in DMF, followed by addition of aryl boronic acid. The first stage of the procedure afforded the colour change with the reaction failing to afford the desired product. Analysis by ^{19}F NMR spectroscopy shows loss of the signal for **521**.

This series of reactions suggests that the combination of **521** and copper (I) salts causes oxidation of the copper and degradation of **521**. However, the role of copper with regards to the aryl boronic acids is not clear as product is formed with both premixing and when all reagents are combined at the same time.

One possibility for the inconsistency in yields afforded could be due to the low solubility of copper (I) salts. A screen of copper (I) salts was conducted in order to investigate whether improved yield could be achieved.

6.6.2 Copper (I) Source Screen

The reaction was conducted with 30 minutes pre-stirring of the metal in the presence of 4-biphenylboronic acid, followed by addition of **521** and an additional 30 minutes of stirring (***Figure 190***, ***Table 22***). The reaction again was monitored by ^{19}F NMR spectroscopy.

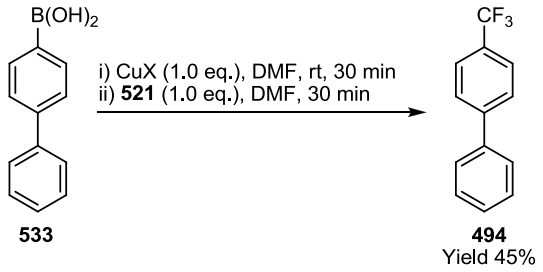

Figure 190 - Copper (I) salt screen.

Table 22 - Copper (I) salt screen.

Entry	Copper source	Solubility	NMR Yield
1	CuBr	partially soluble	18%
2	CuCl	partially soluble	12%
3	CuI	insoluble	No Conversion
4	Cu_2O	insoluble	No Conversion
5	$Cu(OTf)•(MeCN)_4$	soluble	25%

Variatin of the copper (I) salt used to perform the reaction was unable to improve the yield of **494** significantly. The use of $Cu(OTf)•(MeCN)_4$ (***Table 22***, entry 5) was able to achieve a slightly higher conversion that the other catalyst sources. $Cu(OTf)•(MeCN)_4$ was soluble in the reaction solvent where as all other copper sources were either partially or totally insoluble. The higher solubility of $Cu(OTf)•(MeCN)_4$ may be why a higher product yield is achievable.

Although an efficient procedure for the synthesis of aryl-CF_3 products from aryl boronates has not been developed, this work represents a starting point for further study. While this work was in progress Qing and co-workers[3] reported a copper mediated system for the conversion of aryl boronate to trifluoromethyl groups (***Figure 191***).

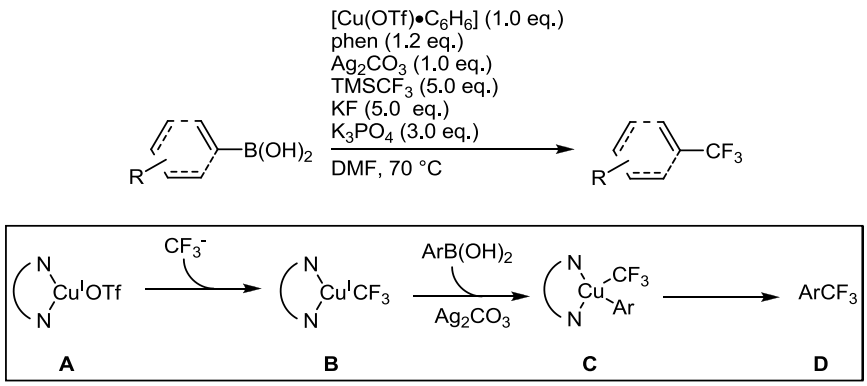

Figure 191 - Oxidative trifluoromethylation of aryl boronic acids.

The reaction utilises a ligated copper (I) salt, which is proposed to react with CF_3^- followed by transmetalation of aryl boronate and oxidation of copper by silver carbonate. Reductive elimination affords the product.

The reaction described in this chapter could proceed via a similar reaction pathway. Aryl boronate could transmetalate to copper (I), as discussed earlier in this chapter, followed by addition of CF_3 and oxidation of copper by **521**. This could then undergo reductive elimination of the product.

The method developed by Qing and co-workers is high yielding with a broad substrate scope. However, the reaction contains stoichiometric or super stoichiometric quantities of all reagents. The method described in this chapter has the potential to offer a simplified system to facilitate the reaction. However, due to this report and time pressures this work was not pursued further. The future outlook for this work was considered and will now be discussed.

6.7 Future Outlook and Conclusion

A full study of the reaction could not be carried out due to time pressures. However, areas of possible future success have been considered. The use of ligands in the reaction could offer advantageous effects. Firstly, ligated copper (I) species are more soluble than the free metal salts. Higher solubility of the catalyst should increase reactivity. Along with increased solubility the ligand may provide increased stability of the aryl metal system, once formed. This is evident from the copper carboxylation system discussed earlier in this chapter, where the copper aryl

species is isolable. However, addition of stoichiometric NHC ligands, as in this example, would make the method unsuitable for large scale synthesis (***Figure 183***).[18] The use of electron rich alkyl phosphine or diamine ligands (e.g. dtbpy, 1,10-phenanthroline) would be a possible alternatives.

Use of base to aid transmetalation of the aryl boronate is another area which could be explored. This strategy was employed by Ritter and co-workers[27] in the fluorination of aryl boronates (***Figure 185***). However, transmetalation of aryl boronates to copper has been shown to be effective without the need for base (***Figure 184***).

From the initial observations, this reaction has potential to be developed into an effective system for trifluoromethylation. However, at present, significant further work is required to achieve this goal. The reaction has facilitated the transformation of aryl boronates to aryl trifluoromethyl groups in a low yield. However, the highly capricious nature of the reaction and irreproducibility are areas which require further insight to be gained.

Most recently, concurrently with the preparation of this thesis, Liu and co-workers[28] described a directly analogous procedure to the one detailed in this chapter for the electrophilic trifluoromethylation of boronic acids. The suggested mechanism proceeds via a metal aryl species followed by addition of the CF_3^+ (***Figure 192***).

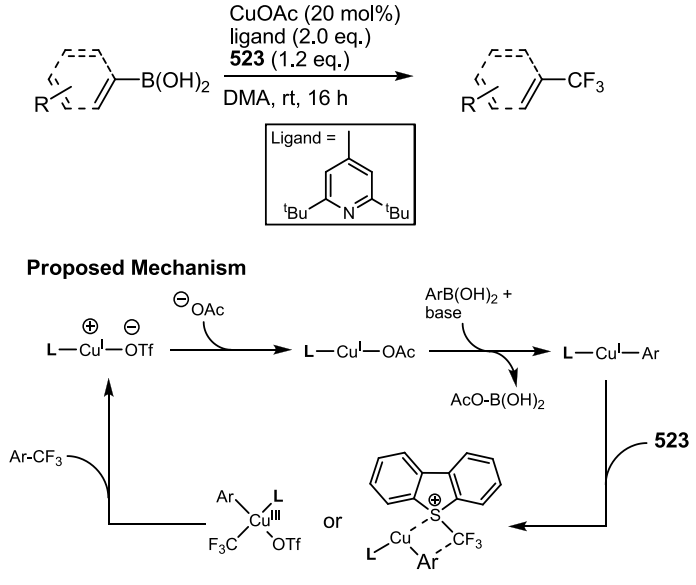

Figure 192 - Electrophilic trifluoromethylation of aryl boronic acids.

This report highlights the potential of the work discussed in this chapter as a route to trifluoromethylated arenes.

6.8 Chapter VI - References

1 Banks, R. E.; Smart, B. E.; Tatlow, J. C., *Organofluorine Chemistry*. Plenum: New York, 1994.

2 Quadbeck-Seeger, H.-J.; Faust, R.; Knaus, G.; Siemeling, U., *World Records in Chemistry*. Wiley-VCH: Weinheim, Germany, 1999.

3 Chu, L.; Qing, F-L., *Org. Lett.* **2010**, *12*, 5060.

4 Swarts, F., *Bull. Soc. Chim. Belg.* **1982**, *24*, 309.

5 Urata, H.; Fuchikami, T., *Tetrahedron Lett.* **1991**, *32*, 91.

6 Cottet, F.; Schlosser, M., *Eur. J. Org. Chem.* **2002**, 327.

7 Dubinina, G. G.; Ogikubo, J.; Vicic, D. A., *Organometallics* **2008**, *27*, 6233.

8 Dubinina, G. G.; Furutachi, H.; Vicic, D. A., *J. Am. Chem. Soc.* **2008**, *130*, 8600.

9 Oishi, M.; Kondo, H.; Amii, H., *Chem. Commun.* **2009**, 1909.

10 Wang, X.; Truesdale, L.; Yu, J-Q., *J. Am. Chem. Soc.* **2010**, *132*, 3642.

11 Cho, E. J.; Senecal, T. D.; Kinzel, T.; Zhang, Y.; Watson, D. A.; Buchwald, S. L., *Science* **2010**, *328*, 1679.

12 Grushin, V. V.; Marshall, W. J., *J. Am. Chem. Soc.* **2006**, *128*, 12644.

13 Miyaura, N.; Suzuki, A., *Chem. Rev.* **1995**, *95*, 2457.

14 Chan, D. M. T.; Monaco, K. L.; Wang, R-P.; Winters, M. P., *Tetrahedron Lett.* **1998**, *39*, 2933.

15 Chan, D. M. T.; Monaco, K. L.; Li, R.; Bonne, D.; Clark, C. G.; Lam, P. Y. S., *Tetrahedron Lett.* **2003**, *44*, 3863.

16 Lam, W. H.; Lin, Z., *Organometallics* **2003**, *22*, 473.

17 Evans, D. A.; Katz, J. L.; West, T. R., *Tetrahedron Lett.* **1998**, *39*, 2937.

18 Ohishi, T.; Nishiura, M.; Hou, Z., *Angew. Chem. Int. Ed.* **2008**, *47*, 5792.

19 Deng, J. Z.; Paone, D. V.; Ginnetti, A. T.; Kurihara, H.; Dreher, S. D.; Weissman, S. A.; Stauffer, S. R.; Burgey, C. S., *Org. Lett.* **2009**, *11*, 345.

20 Eisenberger, P.; Gischig, S.; Togni, A., *Chem. Eur. J.* **2006**, *12*, 2579.

21 Kieltsch, I.; Eisenberger, P.; Togni, A., *Angew. Chem. Int. Ed.* **2007**, *46*, 754.

22 Koller, R.; Stanek, K.; Stolz, D.; Aardoom, R.; Niedermann, K.; Togni, A., *Angew. Chem. Int. Ed.* **2009**, *48*, 4332.

23 Stanek, K.; Koller, R.; Togni, A., *J. Org. Chem.* **2008**, *73*, 7678.

24 Wiehn, M. S.; Vinogradova, E. V.; Togni, A., *J. Fluorine Chem.* **2010**, *131*, 951.

25 Umemoto, T., *Chem. Rev.* **1996**, *96*, 1757.

26 Magdziak, D.; Rodriguez, A. A.; Van De Water, R. W.; Pettus, T. R. R., *Org. Lett.* **2002**, *4*, 285.

27 Furuya, T.; Ritter, T., *Org. Lett.* **2009**, *11*, 2860.

28 Xu, J.; Luo, D-F.; Xiao, B.; Liu, Z-J.; Gong, T-J.; Fu, Y.; Liu, L., *Chem. Commun.* **2011**, *47*, 4300.

CHAPTER VII - CONCLUSIONS AND FUTURE WORK

7.1 Conclusions

The work set out in this thesis has successfully addressed some of the key problems associated with iridium catalysed C-H borylation and its related transformations.

Solvent incompatibility within one-pot reaction sequences remains to be a key problem for the sustainable application of the methodologies. The single solvent C-H borylation/Suzuki-Miyaura cross-coupling sequence provided a simple and efficient method for the synthesis of biaryls by addressing the issue of solvent incompatibility. Moreover, the discovery of a new reaction solvent for the C-H borylation reaction is significant due to the limited options available at present.

Further development of the C-H borylation methodology has been achieved through the application of microwave heating. The microwave accelerated C-H borylation reaction has enabled the synthesis of borylated arenes and heteroarenes in reaction times of minutes, compared to the hours typically required when standard heating methods are used.

The use of microwave heating has been further developed by application to a microwave accelerated single solvent, one-pot C-H borylation/Suzuki-Miyaura cross-coupling sequence. This allows access to cross-coupled biaryls from arenes plus aryl halides in total reaction times of minutes.

Further work should be conducted in order to gain insight into the mode of action of the microwave accelerated C-H borylation reaction. Initial studies were unable to pinpoint the cause of the acceleration observed within the reactions.

The borylation of substituted quinolines has revealed an interesting electronic selectivity. The site of borylation can be directed dependent on the identity of the substituents. This work has provided insight into the role of electronics in the C-H borylation reaction.

Theoretical pK_a calculations have attempted to provide further insight into the origins of the observed selectivity. The calculations have provided a method to predict the site of C-H borylation based on the acidity of the C-H bond being activated. However, the model does not provide a full explanation of the selectivity observed.

7.2 Future Work

Although this thesis has addressed some key issues associated with the C-H borylation reaction, there are several areas in which initial experiments have been conducted which should be further studied.

The area of electronic selectivity within the C-H borylation reaction is of interest. Utilisation of naphthryidine and naphthalene systems analogous to the 2,6- and 2,7-disubstituted quinolines (***Figure 193***) may provide further information to be gathered on the influence of different substituents on the site of borylation.

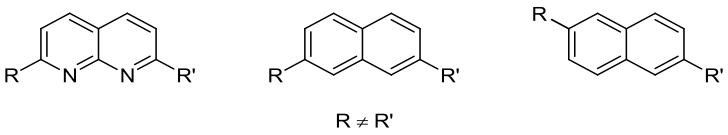

Figure 193 - Potential substrates to probe electronic selectivity of C-H borylation reaction.

The borylation of protected and substituted azaindoles would also be of interest. The work in this area showed an inherent selectivity for the 2-positions in the arene. Application of room temperature borylation may be able to afford a more selective reaction, in a similar manner to that of quinoline. However, there are very few examples in the literature of azaindoles containing different substitution patterns. One issue in pursuing this work would concern substrate synthesis.

An initial experiment was conducted on the conversion of aryl boronates to trifluoromethyl groups via a copper mediated method utilising hypervalent iodine CF_3 reagents. Further work in this area could progress this interesting but capricious observation into an efficient process. Further work is required to better understand the mechanism of this reaction as to date the mode of action is only postulated. In analogy to many of the other copper mediated reaction of aryl boronates the addition of electron donating ligands (pyridines, NHC's) may provide a more stable and reactive catalyst system.

CHAPTER VIII - EXPERIMENTAL DETAILS

8.1 General Experimental Considerations

Solvents

40-60 Petroleum ether was redistilled before use and refers to the fraction of light petroleum ether boiling in the range 40-60 °C. MTBE was purchased from Sigma Aldrich as anhydrous 99.8% and used as received. All other solvents were obtained dried from Innovative Technology Solvent Purification System (SPS).

Reagents

All reagents were purchased from Alfa-Aesar, Acros, Sigma Aldrich or Lancaster, and were checked for purity by GC-MS and/or ^{1}H NMR spectroscopy and used as received. B_2pin_2 was kindly provided by AllylChem. Co. Ltd. (Dalian, China).

Chromatography

Analytical thin layer chromatography (TLC) was performed using commercially available aluminium-backed plates coated with silica gel 60 F_{254} (UV_{254}) and visualised under ultra-violet light (at 254 nm). Flash column chromatography was carried out using 200-400 mesh silica gel 40-63 μm.

NMR Spectroscopy

^{1}H, ^{13}C, ^{19}F, and ^{11}B NMR spectra were recorded in $CDCl_3$ (unless otherwise stated) on Varian Mercury-200 (^{1}H), Varian Mercury-400 (^{1}H, ^{13}C, ^{19}F), Bruker Avance-400 (^{1}H, ^{13}C, ^{11}B) , Varian Inova-500 (^{1}H, ^{13}C) or Varian VNMRS-700 (^{1}H, ^{13}C) spectrometers and reported as follows: chemical shift δ (ppm) (multiplicity, coupling constant *J* (Hz), number of protons, assignment). All ^{13}C NMR spectra were proton decoupled. The chemical shifts are reported using the residual signal of $CHCl_3$ as the internal reference (δH = 7.26 ppm; δC = 77.16 ppm). All chemical shifts are quoted in parts per million relative to tetramethylsilane (δH = 0.00 ppm) and coupling constants are given in hertz. Assignment of spectra was carried out using COSY, HSQC, and HMBC experiments.

Mass spectrometry

GC-MS analyses were performed using an Agilent 6890N gas chromatograph (column: HP-5MS, 10 m, Ø 0.25 mm, film 0.25 μm; injector: 250 °C; oven: 70 °C (2 min), 70 °C to 250 °C (20 °C min^{-1}), 250 °C (5 min); carrier gas: He (1.6 mL min^{-1})) equipped with an Agilent 5973 inert mass selective detector operating in EI mode and a custom built Anatune liquid handling system functioning as autosampler/injector. Electrospray mass spectra (ES) were obtained on a Micromass LCT Mass Spectrometer. High resolution mass spectra were obtained using a Thermo-Finnigan LTQFT mass spectrometer or Xevo QToF mass spectrometer (Waters UK, Ltd) by Durham University Mass Spectrometry service, or performed by the EPSRC National Mass Spectrometry Service Centre, University of Wales, Swansea.

Melting point

Melting points were determined a using Thermo Scientific 9100 melting point apparatus and are uncorrected.

Microwave

Microwave experiments were carried out using a Personal Chemistry Emrys Optimizer microwave reactor.

IR spectroscopy

Infrared spectra were recorded as a solution in chloroform via transmission IR cells on a Perkin-Elmer FTIR 1600 spectrometer.

Dry Loading

Reaction solvent is removed under reduced pressure to afford the crude product. To the flask silica gel (0.4 g per 0.1 g crude product) and $CHCl_3$ (5 mL per 0.1 g crude product) were added. The solvent was removed under reduced pressure to dryness. The resulting powder was added to a silica gel flash column and purified as stated.

8.2 General Procedures

General Procedure A - One-pot, C-H Borylation/Suzuki-Miyaura Cross-Coupling Sequence with Methyl 4-Iodobenzoate

Under N_2, a catalyst stock solution was prepared by weighing $[Ir(OMe)cod]_2$ (131 mg, 0.4 mmol Ir), dtbpy (105 mg, 0.4 mmol) and B_2pin_2 (713 mg, 2.75 mmol) into a sealable vial, followed by addition of MTBE (26.4 mL). The vial was fitted with a rubber septum and then shaken to develop a deep red colour. Under N_2, a Youngs tap tube was charged with B_2pin_2 (200 mg, 0.79 mmol) followed by the corresponding arene (1.0 mmol). MTBE (0.4 mL) was added followed by 2.0 mL of the catalyst stock solution (catalyst loading = 3 mol%, 1.0 mmol B_2pin_2). The reaction was heated for 6 hours at 80 °C in an aluminium heating block. Upon completion, the reaction placed under an N_2 atmosphere and degassed water (1.0 mL) was added. The reaction was left for 1 minute to allow effervescence to cease before addition of the subsequent reagents. Upon completion, $Pd(dppf)Cl_2$ (21 mg, 3 mol%), KOH (280 mg, 5.0 mmol) and methyl 4-iodobenzoate (314 mg, 1.2 mmol) were added. The reaction was sealed and heated for 3 hours at 80 °C in an aluminium, heating block. After the reaction was complete, the biphasic solvent mixture cooled and passed through a plug of Celite. The solids washed with DCM (200 mL) and the filtrate was concentrated under reduced pressure to afford the crude product. This was purified by silica flash-column chromatography as described for each compound.

General Procedure B - One-pot, C-H Borylation/Suzuki-Miyaura Cross-Coupling Sequence with Aryl Halides (as detailed)

Under N_2, a catalyst stock solution was prepared by weighing $[Ir(OMe)cod]_2$ (131 mg, 0.4 mmol Ir), dtbpy (105 mg, 0.4 mmol) and B_2pin_2 (713 mg, 2.75 mmol) into a sealable vial, followed by addition of MTBE (26.4 mL). The vial was fitted with a rubber septum and then shaken to develop a deep red colour. Under N_2, a Youngs tap tube was charged with B_2pin_2 (200 mg, 0.79 mmol) followed by *m*-xylene (106 mg, 120 μL, 1.0 mmol). MTBE (0.4 mL) was added followed by 2.0 mL of the catalyst stock solution (catalyst loading = 3 mol%, B_2pin_2 (1.0 mmol)). The reaction was then heated for 6 hours at 80 °C in an aluminium heating block. Upon completion, the reaction placed under an N_2 atmosphere and degassed water (1.0 mL) was

added. The reaction was left for 1 minute to allow effervescence to cease before addition of the subsequent reagents. $Pd(dppf)Cl_2$ (21 mg, 3 mol%), KOH (280 mg, 5.0 mmol) and the corresponding aryl halide (1.2 mmol) were added. The reaction was sealed and heated for 3 hours at 80 °C in an aluminium, heating block. After the reaction was complete, the biphasic solvent mixture cooled and passed through a plug of Celite. The solids washed with DCM (200 mL) and the filtrate was concentrated under reduced pressure to afford the crude product. This was purified by silica flash-column chromatography as described for each compound.

General Procedure C - C-H Borylation (Standard Heating Conditions)

Under N_2, a catalyst stock solution was prepared by weighing $[Ir(OMe)cod]_2$ (104 mg, 0.156 mmol Ir), dtbpy (84 mg, 0.312 mmol) and B_2pin_2 (2644 mg, 10.40 mmol) into a sealable volumetric flask, followed by addition of MTBE to make up a 25 mL solution. The flask was sealed with a crimp top septum cap and shaken to develop a deep red colour. Under N_2, a thick walled microwave synthesis vial (max volume 5 mL) was charged with the corresponding substrate (1.0 mmol) and sealed with a crimp top septum cap. The catalyst stock solution (2.4 mL) (catalyst loading (3 mol%), B_2pin_2 (1.0 mmol)) was added and the reaction was heated for the time stated at 80 °C in an aluminium heating block. Upon completion, the reaction was cooled to room temperature and volatiles were removed under reduced pressure to afford the crude product. This was purified by silica flash-column chromatography as described for each compound.

General Procedure D - C-H Borylation (Microwave Heating Conditions)

Under N_2, a catalyst stock solution was prepared by weighing $[Ir(OMe)cod]_2$ (104 mg, 0.156 mmol Ir), dtbpy (84 mg, 0.312 mmol) and B_2pin_2 (2644 mg, 10.40 mmol) into a sealable volumetric flask, followed by addition of MTBE to make up a 25 mL solution. The flask was sealed with a crimp top septum cap and shaken to develop a deep red colour. Under N_2, a thick walled microwave synthesis vial (max volume 5 mL) was charged with the corresponding substrate (1.0 mmol) and sealed with a crimp top septum cap. The catalyst stock solution (2.4 mL) (catalyst loading (3 mol%), B_2pin_2 (1.0 mmol)) was added and the reaction was heated for the time stated at 80 °C in a microwave reactor. Upon completion, the reaction was cooled to

room temperature and volatiles were removed under reduced pressure to afford the crude product. This was purified by silica flash-column chromatography as described for each compound.

General Procedure E - One-pot, C-H Borylation/Suzuki-Miyaura Cross-Coupling Sequence with Methyl 4-Iodobenzoate (Microwave Accelerated)

Under N_2, a catalyst stock solution was prepared by weighing $[Ir(OMe)cod]_2$ (104 mg, 0.156 mmol Ir), dtbpy (84 mg, 0.312 mmol) and B_2pin_2 (2644 mg, 10.40 mmol) into a sealable volumetric flask, followed by addition of MTBE to make up a 25 mL solution. The flask was sealed with a crimp top septum cap and shaken to develop a deep red colour. Under N_2, a thick walled microwave synthesis vial (max volume 5 mL) was charged with the corresponding substrate (1.0 mmol) and sealed with a crimp top septum cap. The catalyst stock solution (2.4 mL) (catalyst loading (3 mol%), B_2pin_2 (1.0 mmol)) was added and the reaction was heated for the time stated at 80 °C in a microwave reactor. Upon completion, the reaction placed under an N_2 atmosphere and degassed water (1.0 mL) was added. The reaction was left for 1 minute to allow effervescence to cease before addition of the subsequent reagents. Upon completion, $Pd(dppf)Cl_2$ (14 mg, 2 mol%), KOH (280 mg, 5.0 mmol) and methyl 4-iodobenzoate (288 mg, 1.1 mmol) were added and the tube was resealed. The reaction was heated for 5 minutes at 80 °C in a microwave reactor. After the reaction was complete, the biphasic solvent mixture cooled and passed through a plug of Celite. The solids washed with DCM (150 mL) and the filtrate was concentrated under reduced pressure to afford the crude product. This was purified by silica flash-column chromatography as described for each compound.

General Procedure F - C-H Borylation of Quinolines (Microwave Heating Conditions)

Under N_2, a catalyst stock solution was prepared by weighing $[Ir(OMe)cod]_2$ (104 mg, 0.156 mmol Ir), dtbpy (84 mg, 0.312 mmol) and B_2pin_2 (2644 mg, 10.40 mmol) into a sealable volumetric flask, followed by addition of MTBE to make up a 25 mL solution. The flask was sealed with a crimp top septum cap and shaken to develop a deep red colour. Under N_2, a thick walled microwave synthesis vial (max volume 5 mL) was charged with the corresponding substrate (1.0 mmol) and sealed with a crimp top septum cap. The catalyst stock solution (2.4

mL) (catalyst loading (3 mol%), B_2pin_2 (1.0 mmol)) was added and the reaction was heated for the time stated at 100 °C for 1.5 hours in a microwave reactor. Upon completion, the reaction was cooled to room temperature and volatiles were removed under reduced pressure to afford the crude product. This was dry loaded on to silica gel and purified by silica gel flash-column chromatography with gradient elution of solvents, unless otherwise stated.

General Procedure G - C-H Borylation of Quinolines (Room Temperature Reaction)

Under N_2, a catalyst stock solution was prepared by weighing $[Ir(OMe)cod]_2$ (104 mg, 0.156 mmol Ir), dtbpy (84 mg, 0.312 mmol) and B_2pin_2 (2644 mg, 10.40 mmol) into a sealable volumetric flask, followed by addition of MTBE to make up a 25 mL solution. The flask was sealed with a crimp top septum cap and shaken to develop a deep red colour. Under N_2, a thick walled microwave synthesis vial (max volume 5 mL) was charged with the corresponding substrate (1.0 mmol) and sealed with a crimp top septum cap. The catalyst stock solution (2.4 mL) (catalyst loading (3 mol%), B_2pin_2 (1.0 mmol)) was added and the reaction was stirred for the time stated at room temperature on a magnetic stirring block. Upon completion, the volatiles were removed under reduced pressure to afford the crude product. This was dry loaded on to silica gel and purified by silica gel flash-column chromatography with gradient elution of solvents, unless otherwise stated.

Catalyst Preparation

Preparation of $[Ir(Cl)cod]_2$

A 1L 2-necked round bottom flask was charged with $IrCl_3$ (5.0g, 17 mmol), Water (150 mL) and propan-2-ol (250 mL). To the dark purple/black solution, excess 1,5-cyclooctadiene (25 mL) was added. The flask was fitted with a reflux condenser and heated using a heating mantle to reflux for 4 hours. Upon completion the solution was a bright clear red-orange colour. The reaction was cooled and fitted with distillation apparatus. The reaction was then heated and solvent removed (200 mL) by distillation. The reaction mixture was left to cool to room temperature for 2 hours allowing a red crystalline solid to form. The solid was filtered and washed with cold methanol (3 × 50 mL) and dried under reduced pressure to afford $[Ir(Cl)cod]_2$ (7.98g, 71%)

Preparation of $[Ir(OMe)cod]_2$

A 500 mL round bottom flask was charged with $[Ir(Cl)cod]_2$ (5g, 7.5 mmol) and KOH (1g, 18 mmol). The flask was purged with nitrogen and degassed methanol (150 mL) was added. The reaction was stirred at room temperature for 3 hours under nitrogen, with a continuous flow of nitrogen bubbling through the reaction solvent. Upon completion no orange/red solid remained and a pale yellow precipitate had formed. Degassed water (200 mL) was added to the reaction mixture and the vessel was cooled to 0 °C for 1 hour. The yellow solid was filtered and washed with water (6 × 50 mL) and cold methanol (3 × 25 mL). The solid was transferred to a round bottom flask and placed under reduced pressure. The flask was heated to 40 °C in a water bath for 2 hours followed by drying under reduced pressure for a further 12 hours affording $[Ir(OMe)cod]_2$ (3.1g, 63 %) as a fine free flowing yellow powder.

2-(3′,5′-dimethylphenyl)-4,4,5,5-tetramethyl-1,3,2-dioxaborolane, 94[1]

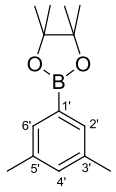

Under N_2, a catalyst stock solution was prepared by weighing $[Ir(OMe)cod]_2$ (131 mg, 0.4 mmol Ir), dtbpy (105 mg, 0.4 mmol) and B_2pin_2 (713 mg, 2.75 mmol) into a sealable vial, followed by addition of MTBE (26.4 mL). The vial was fitted with a rubber septum and then shaken to develop a deep red colour. Under N_2, a Youngs tap tube was charged with B_2pin_2 (200 mg, 0.79 mmol) followed *m*-xylene (106 mg, 120 μL, 1.0 mmol). MTBE (0.4 mL) was added followed by 2.0 mL of the catalyst stock solution (catalyst loading = 3 mol%, B_2pin_2 (1.0 mmol)). The reaction was then heated for 6 h at 80 °C in an aluminium heating block.

The solvent was then removed under reduced pressure and the resulting oil was purified by silica flash column chromatography eluting with 5% EtOAc:hexane to afford 2-(3′,5′-dimethylphenyl)-4,4,5,5-tetramethyl-1,3,2-dioxaborolane as a white crystalline solid (223 mg, 96%); m.p. 90 - 91 °C (from hexane); ν_{max} ($CHCl_3$) 2991, 2976, 1599, 1420, 1356, 1240, 1139, 964, 849, 711 cm^{-1}; ^{1}H NMR (400 MHz, $CDCl_3$) δ 7.45 (s, br, 2H, 2′,6′-***H***), 7.11 (s, br, 1H, 4′-***H***), 2.32 (s, 6H, 3′,5′-***CH₃***), 1.34 (s, 12H, pin***CH₃***); ^{13}C NMR (101 MHz, $CDCl_3$) δ 137.4 (***C***-3′, ***C***-5′), 133.2 (***C***-2′, ***C***-6′), 132.6 (***C***-4′), 83.9 (pin-***C***-$(CH_3)_2$), 25.1 (pin-C-***C****H*$_3$), 21.4; ^{11}B NMR (128 MHz, $CDCl_3$) δ 31.1; *m/z* (GC-MS, EI) 232 (52%, M^+), 217 (42%, M^+-CH_3), 190 (8%, M^+-$C(CH_3)_2$), 175 (14%), 159 (5%), 146 (94%, M^+-$C_2(CH_3)_4$), 133 (100%, M^+-$C(CH_3)_2C(CH_3)_2O$).

94 was also prepared by general procedure C using *m*-xylene (106 mg, 120 μL, 1.0 mmol) which was heated for 6 hours to afford **94** as a white crystalline solid (227 mg, 98%).

94 was also prepared by general procedure D using *m*-xylene (106 mg, 120 μL, 1.0 mmol) which was heated for 1 hour to afford **94** as a white crystalline solid (223 mg, 96%).

methyl 3′,5′-dimethylbiphenyl-4-carboxylate, 302[2]

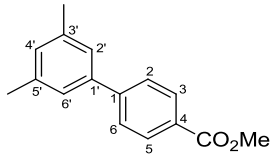

General procedure A was applied to *m*-xylene (106 mg, 120 μL, 1.0 mmol). Purification by silica gel flash column chromatography eluting with 5% EtOAc:hexane afforded methyl 3′,5′-dimethylbiphenyl-4-carboxylate as a white crystalline solid (216 mg, 90%); m.p. 68 - 71 °C (from hexane); ν_{max} ($CHCl_3$) 3016, 1719 (C=O), 1608, 1512, 1436, 1283, 1226, 1204, 797, 721 cm^{-1}; ^{1}H NMR (700 MHz, $CDCl_3$) δ 8.08 (d, *J* = 8.5, 2H, 3,5-***H***), 7.64 (d, *J* = 8.5, 2H, 2,6-***H***), 7.23 (s, br, 2H, 2′,6′-***H***′), 7.03 (s, br, 1H, 4-***H***), 3.93 (s, 3H, CO_2***CH*****$_3$**), 2.38 (s, 6H, 3′,5′-***CH*****$_3$**); ^{13}C NMR (176 MHz, $CDCl_3$) δ 167.3 (***C***O_2Me), 146.1 (***C***-1′), 140.2 (***C***-1), 138.7 (***C***-3′,5′), 130.2 (***C***-3,5), 130.0 (***C***-4′), 128.9 (***C***-4), 127.3 (***C***-2,6), 125.4 (***C***-2′,6′), 52.3 (Ar-CO_2***CH*****$_3$**), 21.6 (3′,5′-***CH*****$_3$**); *m/z* (GC-MS, EI) 240 (88%, M^+), 209 (100%, M^+-OCH_3), 165 (45%, M^+ -Me,CO_2CH_3).

302 was also prepared by general procedure B using methyl-4-bromobenzoate (258 mg, 1.2 mmol) affording **302** as a white crystalline solid (221 mg, 92%).

302 was also prepared by general procedure E using *m*-xylene (106 mg, 120 μL, 1.0 mmol). The borylation reaction was heated for 1 hour. After cross-coupling the reaction afforded **302** as a white crystalline solid (228 mg, 95%).

methyl 3′,5′-dichlorobiphenyl-4-carboxylate, 298[3]

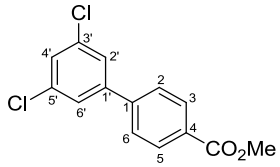

General procedure A was applied to 1,3-dichlorobenzene (147 mg, 114 μL, 1.0 mmol). Purification by silica flash-column chromatography using 5% EtOAc: hexane afforded methyl 3′,5′-dichlorobiphenyl-4-carboxylate (259 mg, 92%); m.p. 114 - 115 °C (from hexane); Anal. found C, 59.75; H, 3.7%; Calcd. for $C_{16}H_{10}Cl_2O_2$ C, 59.8; H, 3.6%; ν_{max} (CH_2Cl_2) 3054, 2985,

1721 (C=O), 1562, 1427, 1275, 1258, 1112, 895, 768, 694 cm^{-1}; ^{1}H NMR (700 MHz, $CDCl_3$) δ 8.11 (d, *J* = 8.5, 2H, 3,5-***H***), 7.60 (d, *J* = 8.5, 2H, 2,6-***H***)), 7.48 (d, *J* = 1.8, 2H, 2′,6′-***H***), 7.38 (t, *J* = 1.8, 1H, 4′-***H***), 3.95 (s, 3H, CO_2***CH₃***); ^{13}C NMR (176 MHz, $CDCl_3$) δ 166.8 (***C***O_2CH_3), 143.2 (Ar-***C***), 143.0 (Ar-***C***), 135.7 (***C***-3′,5′), 130.5 (***C***-3,5), 130.3 (***C***-4), 128.2 (***C***-4′), 127.3 (***C***-2,6), 126.0 (***C***-2′,6′), 52.5 (CO_2***CH₃***); *m/z* (GC-MS, EI) 282 (35%, $M^+(^{37}Cl^{37}Cl)$), 281 (8%, $M^+(^{35}Cl^{37}Cl)$), 280 (55%, $M^+(^{35}Cl^{35}Cl)$), 251 (64%, $M^+(^{37}Cl^{37}Cl)$ -OCH_3), 250 (15%, $M^+(^{35}Cl^{37}Cl)$ -OCH_3), 249 (100%, $M^+(^{35}Cl^{35}Cl)$ -OCH_3), 188 (23%, $M^+(^{35}Cl)$ -Cl,CO_2CH_3), 186 (71%, $M^+(^{35}Cl)$ -Cl,CO_2CH_3), 150 (25%, M^+ -2Cl,CO_2CH_3), 124 (13%), 93 (28%).

methyl 3′,5′-dibromobiphenyl-4-carboxylate, 303[4]

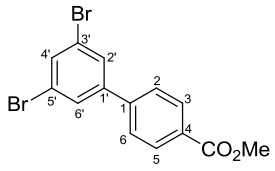

General procedure A was applied to 1,3-dibromobenzene (236 mg, 120 μL, 1.0 mmol). Purification by silica flash-column chromatography using 5% EtOAc: hexane afforded methyl 3′,5′-dibromobiphenyl-4-carboxylate (348 mg, 94%); m.p. 115 - 116 °C (from hexane); Anal. found C, 45.2; H, 2.7%; Calcd. for $C_{14}H_{10}Br_2O_2$ C, 45.4; H, 2.7%; ν_{max} (CH_2Cl_2) 3054, 2985, 1721 (C=O), 1547, 1428, 1258, 1111, 895, 768 cm^{-1}; ^{1}H NMR (700 MHz, $CDCl_3$) δ 8.10 (d, *J* = 8.5, 2H, 3,5-***H***), 7.67 (s, 3H, 2′,4′,6′-***H***), 7.58 (d, *J* = 8.5, 2H, 2,6-***H***), 3.94 (s, 3H, CO_2***CH₃***); ^{13}C NMR (176 MHz, $CDCl_3$) δ 166.8 (***C***O_2CH_3), 143.7 (Ar-***C***), 142.8 (Ar-***C***), 133.6 (Ar-***C***), 130.5 (***C***-3,5), 130.2 (Ar-***C***), 129.3 (***C***-4), 127.3 (***C***-2,6), 123.7 (***C***-3′,5′), 52.5 (CO_2***CH₃***); *m/z* (GC-MS, EI) 372 (40%, $M^+(^{81}Br^{81}Br)$) , 370 (83%, $M^+(^{79}Br^{81}Br)$) 368 (41%, $M^+(^{79}Br^{79}Br)$), 341 (49%, $M^+(^{81}Br^{81}Br)$ -OMe), 339 (100%, $M^+(^{79}Br^{81}Br)$ -OMe), 337 (50%, $M^+(^{79}Br^{79}Br)$ -OMe), 232 (48%, $M^+(^{81}Br)$ -Br,CO_2Me)), 230 (49%, $M^+(^{79}Br)$ -Br,CO_2Me)) 151 (58%, M^+- 2Br,CO_2Me,), 115 (24%).

methyl 3′-chloro-5′-methylbiphenyl-4-carboxylate, 304

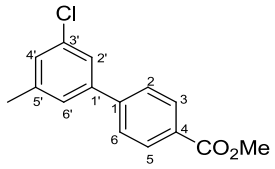

General procedure A was applied to 1-chloro-3-methylbenzene (127 mg, 118 μL, 1.0 mmol). Purification by silica flash-column chromatography using 5% EtOAc: hexane afforded methyl 3′-chloro-5′-methylbiphenyl-4-carboxylate as a white solid (242 mg, 93%); m.p. 69 - 70 °C (from hexane); Anal. found C, 69.4; H, 5.1%; Calcd. for $C_{15}H_{13}ClO_2$ C, 69.1; H, 5.0%; ν_{max} (CH_2Cl_2) 3054, 2985, 1720 (C=O), 1607, 1428, 1272, 1112, 895, 767 cm^{-1}; ^1H NMR (500 MHz, $CDCl_3$) δ 8.10 (d, *J* = 8.6, 2H, 3,5-***H***), 7.62 (d, *J* = 8.6, 2H, 2,6-***H***), 7.40 (s, br, 1H, 2′-***H***), 7.30 (s, 1H, 6′-***H***), 7.20 (s, br, 1H, 4′-***H***), 3.94 (s, 3H, CO_2***C*H*₃***), 2.41 (s, 3H, 5′-***CH₃***); ^{13}C NMR (126 MHz, $CDCl_3$) δ 167.1 (***C***O_2CH_3), 144.6 (**C**-1), 141.8 (***C***-1′), 140.6 (***C*** -5′), 134.8 (***C***-3′), 130.43 (***C***-3,5), 129.6 (***C***-4), 129.0 (***C***-4′), 127.3 (***C***-2,6), 126.5 (***C***-6′), 124.7 (***C***-2′), 52.4 (CO_2***C*H*₃***), 21.5 (5′-***CH₃***); *m/z* (GC-MS, EI) 262 (24%, $M^+(^{37}Cl)$), 260 (75%, $M^+(^{35}Cl)$), 231 (32%, $M^+(^{37}Cl)$ -OCH_3) 229 (100%, $M^+(^{35}Cl)$ -OCH_3), 166 (55%, M^+-Cl,CO_2CH_3); HRMS (ASAP) *m/z* found $(M+H)^+$ 261.0671, $C_{15}H_{14}{}^{35}ClO_2$ requires *M* 261.0682.

methyl 3′-bromo-5′-cyanobiphenyl-4-carboxylate, 305

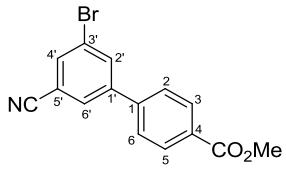

General procedure A was applied to 3-bromobenzonitrile (182 mg, 116 μL, 1.0 mmol). Purification by silica flash-column chromatography using 5% EtOAc: hexane afforded methyl 3′-bromo-5′-cyanobiphenyl-4-carboxylate as an white crystalline solid (291 mg, 92%); m.p. 165 - 166 °C (from hexane); Anal. found: C, 56.8; H, 3.3; N, 4.4%; Calcd. for $C_{15}H_{10}BrNO_2$ C, 57.0; H, 3.2; N, 4.4%; ν_{max} (CH_2Cl_2) 3055, 2985, 2187 (C≡N), 1722 (C=O), 1558, 1427, 1275, 1259, 1113, 895, 768 cm^{-1}; ^1H NMR (700 MHz, $CDCl_3$) δ 8.15 (d, *J* = 8.5, 2H, 3,5-***H***), 7.98 (s, 1H, 4′-***H***), 7.82 (s, 1H, 2′-***H***), 7.80 (s, 1H, 6′-***H***), 7.61 (d, *J* = 8.5, 2H, 2,6-***H***), 3.96 (s, 3H, CO_2***C*H*₃***); ^{13}C NMR (176 MHz, $CDCl_3$) δ 166.4 (***C***O_2CH_3***)***, 143.1 (***C***-1***)***, 141.6 (***C***-1′***)***, 134.7 (***C***-2′), 133.8

(***C***-4′), 130.6 (***C***-6′***)***, 130.5 (***C***-3,5***)***, 129.4 (***C***-4***)***, 127.1 (***C***-2,6***)***, 123.5 (***C***-3′***)***, 117.1 (***CN)***, 114.7 (***C***-5′***)***, 52.3 (CO_2***C*H$_3$*)**; *m/z* (GC-MS, EI) 317 (42%, M^+(^{81}Br)), 315 (43%, M^+(^{79}Br)), 286 (85%, M^+(^{81}Br) -OCH_3), 284 (85%, M^+(^{81}Br) -OCH_3), 205 (4%, M+ -Br,OCH_3), 177 (100%, M^+-Br,CO_2CH_3), 150 (22%, M^+- Br,CN,CO_2CH_3)), 88 (20%); HRMS (ASAP) *m/z* found $(M+H)^+$ 315.9974, $C_{15}H_{11}{}^{79}BrNO_2$ requires *M* 315.9973.

methyl 4-(2′,6′-dichloropyridin-4′-yl)benzoate, 306

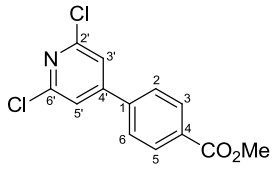

General procedure A was applied to 2,6-dichloropyridine (147 mg, 1.0 mmol). Purification by silica flash-column chromatography using 5% EtOAc: hexane to afforded methyl 4-(2′,6′-dichloropyridin-4′-yl)benzoate as a pale pink solid (265 mg, 94%); m.p. 162 -163 °C (from hexane); Anal. found: C, 55.6; H, 3.4; N, 4.9%; Calcd. for $C_{13}H_9Cl_2NO_2$ C, 55.3; H, 3.2; N, 5.0%; ν_{max} 3010, 1723 (C=O), 1587, 1530, 1423, 1226, 1195, 936, 808, 724, 676 cm^{-1}; ^{1}H NMR (400 MHz, $CDCl_3$) δ 8.17 (d, *J* = 8.6, 2H, 3,5-***H***), 7.66 (d, *J* = 8.6, 2H, 2,6-***H***), 7.50 (s, 2H, 3′,5′-***H***), 3.96 (s, 3H, CO_2***CH*$_3$***)**; ^{13}C NMR (101 MHz, $CDCl_3$) δ 166.4 (***C***O_2CH_3), 153.0 (***C***-4′), 151.5 (***C***-2′,6′), 140.1 (***C***-1), 131.9 (***C***-4), 130.8 (***C***-3,5), 127.4 (***C***-2,6), 121.2 (***C***-3′,5′), 52.7 (CO_2***CH*$_3$***)**; *m/z* (GC-MS, EI) 283 (28%, M^+(^{37}Cl^{37}Cl)), 282 (6%, M^+(^{35}Cl^{37}Cl)), 281 (44%, M^+(^{35}Cl^{35}Cl)), 252 (64%, M^+(^{37}Cl^{37}Cl) -OCH_3), 251 (14%, M^+(^{35}Cl^{37}Cl) -OCH_3), 250 (100%, M^+(^{35}Cl^{35}Cl) -OCH_3), 224 (6%, M^+(^{37}Cl^{37}Cl) -CO_2CH_3), 222 (10%, M^+(^{35}Cl^{35}Cl) -CO_2CH_3), 189 (11%, M^+(^{37}Cl^{37}Cl) - Cl,CO_2CH_3), 187 (33%, M^+(^{35}Cl^{35}Cl) -Cl,CO_2CH_3), 151 (15%, M^+ -2Cl,CO_2CH_3)), 126 (15%); HRMS (ESI) *m/z* found 282.0085, $C_{13}H_{10}{}^{35}Cl_2NO_2$ requires *M* 282.0083.

306 was also prepared by general procedure E using 2,6-dichloropyridine (147 mg, 1.0 mmol). The borylation reaction was heated for 5 minutes. **306** was isolated as pale pink solid (270 mg, 96%).

methyl 3′-cyano-5′-(trifluoromethyl)biphenyl-4-carboxylate, 307

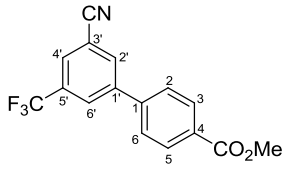

General procedure A was applied to 3-(trifluoromethyl)benzonitriles (171 mg, 133 μL, 1.0 mmol). Purification by silica flash-column chromatography using 5% EtOAc: hexane to afforded methyl 3′-cyano-5′-(trifluoromethyl)biphenyl-4-carboxylate as a white crystalline solid (265 mg, 87%); m.p. 129 - 130 °C (from hexane); Anal. found C, 62.6; H, 3.4; N, 4.6%; Calcd. for $C_{16}H_{10}F_3NO_4$ C, 62.9; H, 3.3; N, 4.6%; ν_{max} ($CHCl_3$) 3076, 2225(C≡N), 1753 (C=O), 1650, 1524, 1314, 1134, 1040, 894, 772 cm^{-1}; ^{1}H NMR (700 MHz, $CDCl_3$) δ 8.18 (d, *J* = 8.4, 2H, 3,5-***CH*₃**), 8.07 (s, br, 2H, 2′,6′-***H***), 7.93 (s, 1H, 4′-***H***), 7.66 (d, *J* = 8.4, 2H, 2,6-***H***), 3.97 (s, 3H, CO_2***CH*₃**); ^{13}C NMR (176 MHz, $CDCl_3$) δ 166.6 (***C***O_2CH_3), 142.8 (Ar-***C***), 141.8 (Ar-***C***), 134.1 (***C***-2′), 133.0 (q, $^2J_{C\text{-}F}$ = 33.9, ***C***-5′), 131.1 (***C***-4), 130.9 (***C***-3,5), 128.4 (q, $^3J_{C\text{-}F}$ = 3.5, ***C***-6′), 128.3 (q, $^3J_{C\text{-}F}$ = 3.8, ***C***-4′), 127.4 (***C***-2,6), 123.0 (q, $^1J_{C\text{-}F}$ = 274.0, 5′-***CF*₃**), 117.4 (3′-***C***N), 114.5 (***C***-3′), 52.6 (CO_2***CH*₃**); ^{19}F NMR (376 MHz, $CDCl_3$) δ -63.47; *m/z* (GC-MS, EI) 305 (41%, M^+), 286 (5%, M^+-F), 274 (100%, M^+-OCH_3), 246 (6%, M^+-CO_2CH_3), 226 (26%), 177 (15%); HRMS (ASAP) *m/z* found $(M)^+$ 305.0664, $C_{16}H_{10}F_3NO_2$ requires *M* 305.0660.

methyl 3′-chloro-5′-(trifluoromethyl)biphenyl-4-carboxylate, 308

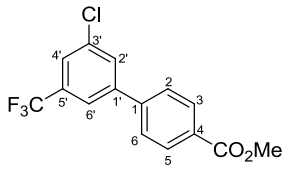

General procedure A was applied to 1-chloro-3-(trifluoromethyl)benzene (181 mg, 135 μL, 1.0 mmol). Purification by silica flash-column chromatography using 5% EtOAc: hexane afforded methyl 3′-chloro-5′-(trifluoromethyl)biphenyl-4-carboxylate as an off-white solid (295 mg, 94%); m.p. 79 - 80 °C (from hexane); Anal. found C, 57.3; H, 3.3%; Calcd. for $C_{15}H_{10}{}^{35}ClF_3O_2$ C, 57.25; H, 3.2%; ν_{max} (CH_2Cl_2) 3055, 2986, 1721 (C=O), 1588, 1434, 1331, 1275, 1176, 1134, 1058, 893, 766 cm^{-1}; ^{1}H NMR (500 MHz, $CDCl_3$) δ 8.15 (d, *J* = 8.4, 2H, 3,5-***H***), 7.78 (s, br, 1H, Ar-***H***), 7.74 (s, br, 1H, Ar-***H***), 7.68 - 7.61 (m, 3H, 2,6-***H***/Ar-***H***), 3.96 (s, 3H, CO_2C***H*₃**); ^{13}C

NMR (126 MHz, $CDCl_3$) δ 166.8 (***C***O_2CH_3), 142.9 (Ar-***C***), 142.8 (Ar-***C***), 135.8 (***C***-3′), 133.1 (q, $^2J_{C\text{-}F}$ = 33.5, ***C***-5′), 130.9 (***C***-2′), 130.6 (***C***-3,5), 130.5 (***C***-4), 127.4 (***C***-2,6), 125.2 (q, $^3J_{C\text{-}F}$ = 3.8, Ar-***C***), 123.4 (q, $^1J_{C\text{-}F}$ = 273.2, 5′-***C*****F_3**), 122.6 (q, $^3J_{C\text{-}F}$ = 3.8, Ar-***C***), 52.6 (CO_2***C*****H_3**); ^{19}F NMR (376 MHz, $CDCl_3$) δ -62.70; *m/z* (GC-MS, EI) 316 (13%, $M^+(^{37}Cl)$, 314 (43%, $M^+(^{35}Cl)$, 285 (32%, $M^+(^{37}Cl)$ -OCH_3), 283 (100%, $M^+(^{35}Cl)$ -OCH_3), 220 (41%, M^+- Cl,CO_2CH_3); HRMS (ASAP) *m/z* found $(M+H)^+$ 315.0405, $C_{15}H_{11}{}^{35}ClF_3O_2$ requires *M* 315.0400.

methyl 3′-bromo-5′-(trifluoromethyl)biphenyl-4-carboxylate, 309

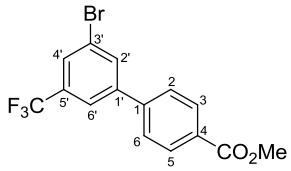

General procedure A was applied to 1-bromo-3-(trifluoromethyl)benzene (225 mg, 140 μL, 1.0 mmol). Purification by silica flash-column chromatography using 5% EtOAc: hexane afforded methyl 3′-bromo-5′-(trifluoromethyl)biphenyl-4-carboxylate as a white crystalline solid (337 mg, 94%); m.p. 90 - 91 °C (from hexane); Anal. found C, 50.5; H, 2.8%; for $C_{15}H_{10}BrF_3O_2$ C, 50.2; H, 2.8%; ν_{max} (CH_2Cl_2) 3054, 2985, 1721 (C=O), 1427, 1328, 1274, 1258, 1175, 1135, 895, 768 cm^{-1}; ^{1}H NMR (700 MHz, $CDCl_3$) δ 8.14 (d, *J* = 8.2, 2H, 3,5-***H***), 7.92 (s, br, 1H, 2′-***H***), 7.77 (s, br, 2H, 4′-***H***, 6′-***H***), 7.63 (d, *J* = 8.2, 2H, 2,6-***H***), 3.95 (s, 3H, CO_2***C*****H_3**); ^{13}C NMR (176 MHz, $CDCl_3$) δ 166.7 (***C***O_2CH_3), 143.1 (Ar-***C***), 142.7 (Ar-***C***), 133.8 (***C***-2′), 133.2 (q, $^2J_{C\text{-}F}$ = 33.0, ***C***-5′), 130.6 (***C***-3,5), 130.5 (***C***-4), 128.0 (q, $^3J_{C\text{-}F}$ = 3.8, Ar-***C***), 127.4 (***C***-2,6), 123.5 (***C***-3′), 123.3 (q, $^1J_{C\text{-}F}$ = 272.5, 5′-***C*****F_3**), 123.0 (q, $^3J_{C\text{-}F}$ = 3.7, Ar-***C***), 52.5 (CO_2***C*****H_3**); ^{19}F NMR (376 MHz, $CDCl_3$) δ -63.20; *m/z* (GC-MS, EI) 360 (57%, $M^+(^{81}Br)$), 358 (58%, $M^+(^{81}Br)$), 329 (99%, $M^+(^{81}Br)$-OCH_3), 327 (100%, $M^+(^{79}Br)$-OCH_3), 220 (98%, M^+- Br,CO_2CH_3); HRMS (ASAP) *m/z* found $(M+H)^+$ 358.9880, $C_{15}H_{11}{}^{79}BrF_3O_2$ requires *M* 358.9895.

methyl 3′,5′-bis(trifluoromethyl)biphenyl-4-carboxylate, 310[5]

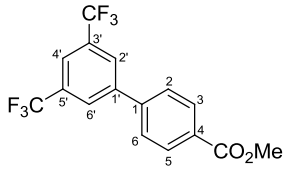

General procedure A was applied to 1,3-bis(trifluoromethyl)benzene (214 mg, 156 μL, 1.0 mmol). Purification by silica flash-column chromatography using 5% EtOAc:hexane to afforded methyl 4-(3′,5′-bis(trifluoromethyl)-phenyl)benzoate as a pale yellow solid (329 mg, 94%); m.p. 103 - 104 °C (from hexane); Anal. found C, 55.3; H, 2.9%; Calcd. for $C_{16}H_{10}F_6O_2$ C, 55.2; H, 2.9%; ν_{max} (CH_2Cl_2) 3054, 2986, 1721 (C=O), 1611, 1426, 1382, 1275, 1180, 896, 766, 696 cm^{-1}; ^{1}H NMR (700 MHz, $CDCl_3$) δ 8.19 (d, 2H, *J* = 8.2 Hz, 3,5-***H***), 8.04 (s, 2H, 2′,6′-***H***), 7.92 (s, 1H, 4′-***H***), 7.69 (d, 2H, *J* = 8.2 Hz, 2,6-***H***), 3.95 (s, 3H, CO_2***CH*****$_3$**); ^{13}C NMR (176 MHz, $CDCl_3$) δ 166.7 (***C***O_2CH_3), 142.6 (Ar-***C***), 142.5 (Ar-***C***), 132.6 (q, $^2J_{C\text{-}F}$ = 33.7, ***C***-3′,5′), 130.7 (***C***-4), 127.61 (***C***-2,6), 127.60 (q, $^3J_{C\text{-}F}$ = 3.5, ***C***-2′,6′), 127.5 (***C***-3,5), 123.2 (q, $^1J_{C\text{-}F}$ = 274.7, 3′,5′-***CF*****$_3$**), 121.7 (q, $^3J_{C\text{-}F}$ = 3.7, ***C***-4′), 52.6 (CO_2***CH*****$_3$**); ^{19}F NMR (376 MHz, $CDCl_3$) δ -63.22; *m/z* (GC-MS, EI) 347 (64%, M^+), 316 (100%, M^+- OCH_3), 269 (55%), 220 (20%, M^+- CF_3,CO_2CH_3).

methyl 3′-bromo-5′-methoxybiphenyl-4-carboxylate, 311

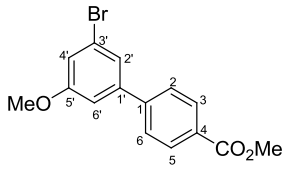

General procedure A was applied to 1-bromo-3-methoxybenzene (187 mg, 127 μL, 1.0 mmol). Purification by silica flash-column chromatography using 5% EtOAc: hexane to afforded methyl 3′-chloro-5′-methoxybiphenyl-4-carboxylate as an off-white solid (298 mg, 93%); m.p. 107 - 108 °C (from hexane); Anal. found C, 56.1; H, 4.1%; Calcd. for $C_{15}H_{13}BrO_3$ C, 56.1; H, 4.1%; ν_{max} (CH_2Cl_2) 3054, 2985, 1720 (C=O), 1600, 1558, 1428, 1276, 1112, 1033, 895, 768 cm^{-1}; ^{1}H NMR (700 MHz, $CDCl_3$) δ 8.09 (d, *J* = 8.5, 2H, 3,5-***H***), 7.59 (d, *J* = 8.5, 2H, 2,6-***H***), 7.33 (t, *J* = 1.5, 1H, Ar-***H***), 7.07 (t, *J* = 2.1, 1H, Ar-***H***), 7.04 (dd, *J* = 1.5, 2.1, 1H, Ar-***H***), 3.94 (s, 3H, CO_2***CH*****$_3$**), 3.84 (s, 3H, 5′-O***CH*****$_3$**); ^{13}C NMR (176 MHz, $CDCl_3$) δ 166.9 (***C***O_2CH_3), 160.8 (***C***-5′), 144.2 (Ar-***C***), 143.0 (Ar-***C***), 130.3 (***C***-3,5), 129.8 (***C***-4), 127.2 (***C***-2,6), 123.5 (Ar-***C***),

123.0 (Ar-***C***), 116.7 (***C***-4′), 112.5 (Ar-***C***), 55.8 (5′-O***CH₃***), 52.4 (ArCO₂***CH₃***); *m/z* (GC-MS, EI) 322 (99%, $M^+(^{81}Br)$), 320 (100%, $M^+(^{79}Br)$), 290 (85%, $M^+(^{81}Br)$-OCH_3), 288 (86%, $M^+(^{79}Br)$-OCH_3), 182 (46%, M^+- Br,CO_2CH_3), 139 (64%); HRMS (ASAP) *m/z* found $(M+H)^+$ 321.0133, $C_{15}H_{14}{}^{79}BrO_3$ requires *M* 321.0126.

methyl 3′-chloro-5′-methoxybiphenyl-4-carboxylate, 312

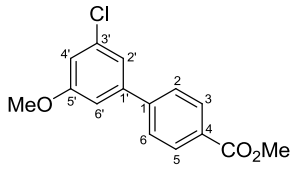

General procedure A was applied to 1-chloro-3-methoxybenzene (143 mg, 123 μL, 1.0 mmol). Purification by silica flash-column chromatography using 5% EtOAc:hexane afforded methyl 3′-chloro-5′-methoxybiphenyl-4-carboxylate as an off-white solid (251 mg, 91%); m.p. 103 - 104 °C (from hexane); Anal. found C, 64.7; H, 4.8%; Calcd. for $C_{15}H_{13}ClO_3$ C, 65.1; H, 4.8%; ν_{max} (CH_2Cl_2) 3054, 2985, 1720 (C=O), 1596, 1428, 1277, 1259, 1111, 1038, 895, 843, 766, 686 cm^{-1}; ^{1}H NMR (700 MHz, $CDCl_3$) δ 8.09 (d, *J* = 8.5, 2H, 3,5-***H***), 7.60 (d, *J* = 8.5, 2H, 2,6-***H***), 7.18 (s, 1H, 2′-***H***), 7.01 (s, 1H, 6′-***H***), 6.91 (s, 1H, 4′-***H***), 3.93 (s, 3H, CO_2***CH₃***), 3.85 (s, 3H, 5′-O***CH₃***); ^{13}C NMR (176 MHz, $CHCl_3$) δ 167.0 (***C***O_2CH_3), 160.9 (***C***-5′), 144.4 (Ar-***C***), 142.8 (Ar-***C***), 135.6 (***C***-3′), 130.4 (***C***-3,5), 129.8(***C***-4), 127.3 (***C***-2,6), 120.1 (***C***-2′), 113.8 (***C***-4′), 112.1 (***C***-6′), 55.9 (5′-O***CH₃***), 52.4 (CO_2***CH₃***); *m/z* (GC-MS, EI) 278 (30%, $M^+(^{37}Cl)$), 276 (95%, $M^+(^{35}Cl)$), 247 (32%, $M^+(^{37}Cl)$ -OCH_3), 245 (100%, $M^+(^{35}Cl)$ -OCH_3), 182 (37%, M^+-Cl,CO_2CH_3), 139 (45%); HRMS (ASAP) *m/z* found $(M+H)^+$ 277.0616, $C_{15}H_{14}{}^{35}ClO_3$ requires *M* 277.0631.

methyl 3′,5′-dimethoxybiphenyl-4-carboxylate, 313[6]

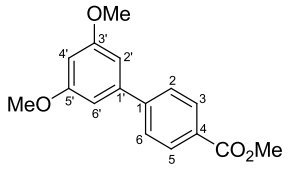

General procedure A was applied to 1,3-dimethoxybenzene (138 mg, 132 μL, 1.0 mmol). Purification by silica flash-column chromatography using 5% EtOAc: hexane afforded methyl 3′-chloro-5′-methoxybiphenyl-4-carboxylate as an off-white crystalline solid (251 mg, 91%); m.p. 80 - 81 °C (from hexane); Anal. found C, 70.4; H, 6.0%; Calcd. for $C_{16}H_{16}O_4$ C, 70.6; H, 5.9%; ν_{max} (CH_2Cl_2) 3066, 2980, 1720 (C=O), 1594, 1442, 1276, 1252, 894, 772 cm^{-1}; ^1H NMR (700 MHz, $CDCl_3$) δ 8.09 (d, *J* = 8.2, 2H, 3,5-***H***), 7.64 (d, *J* = 8.2, 2H, 2,6-***H***), 6.75 (s, 2H, 2′,6′-***H***′), 6.51 (s, 1H, 4′-***H***), 3.94 (s, 3H, CO_2***CH₃***), 3.85 (s, 6H, 3′,5′-O***CH₃***); ^{13}C NMR (176 MHz, $CDCl_3$) δ 167.1 (***C***O_2CH_3), 161.2 (***C***-3′,5′), 145.9 (***C***-1), 142.5 (***C***-1′), 130.2 (***C***-3,5), 129.16 (***C***-4), 127.3 (***C***-2,6), 105.75 (***C***-2′,6′), 100.17 (***C***-4′), 55.7 (3,′5′-O***CH₃***), 55.6 (CO_2***CH₃***); *m/z* (GC-MS, EI) 272 (100%, M^+), 241 (39%), 211 (10%).

methyl 3′-methoxy-5′-methylbiphenyl-4-carboxylate, 314

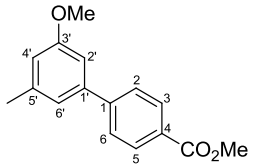

General procedure A was applied to 1-methoxy-3-methylbenzene (126 mg, 122 μL, 1.0 mmol). Purification by silica flash-column chromatography using 5% EtOAc:hexane afforded methyl 3′-methoxy-5′-methylbiphenyl-4-carboxylate as a white solid (236 mg, 92%); m.p. 56 - 57 °C (from hexane); Anal. found C, 74.95; H, 6.4%; Calcd. for $C_{16}H_{16}O_3$ C, 75.0; H, 6.3%; ν_{max} (CH_2Cl_2) 3054, 2985, 1718 (C=O), 1598, 1429, 1275, 1257, 1159, 1112, 895, 767 cm^{-1}; ^1H NMR (500 MHz, $CDCl_3$) δ 8.09 (d, *J* = 8.2, 2H, 3,5-***H***), 7.64 (d, *J* = 8.2, 2H, 2,6-***H***), 7.03 (s, 1H, 6′-***H***), 6.95 (s, 1H, 2′-***H***), 6.77 (s, 1H, 4′-***H***), 3.94 (s, 3H, CO_2***CH₃***), 3.86 (s, 3H, 3′-O***CH₃***), 2.41 (s, 3H, 5′-***CH₃***); ^{13}C NMR (126 MHz, $CDCl_3$) δ 167.2 (***C***O_2CH_3), 160.3 (***C***-3′), 145.9 (***C***-1), 141.5 (***C***-1′), 140.2 (***C***-5′), 130.2 (***C***-3,5), 129.1 (***C***-4), 127.3 (***C***-2,6), 120.9 (***C***-6′), 114.6 (***C***-4′), 110.3 (***C***-2′), 55.6 (3′-O***CH₃***), 52.4 (CO_2***CH₃***), 21.9 (5′-***CH₃***); *m/z* (GC-MS, EI) 256 (100%,

M^+), 241 (2%, M^+-CH_3), 225 (57%, M^+-OCH_3), 182 (35%, M^+- CH_3,CO_2CH_3), 152 (15%); HRMS (ASAP) *m/z* found $(M+H)^+$ 257.1164, $C_{16}H_{17}O_3$ requires $(M+H)^+$ 257.1178.

3,5-dimethyl-4′-(trifluoromethyl)biphenyl, 316[7]

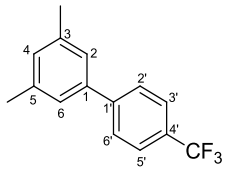

General procedure B was applied using 1-iodo-4-(trifluoromethyl)benzene (326 mg, 176 μL, 1.2 mmol). Purification by silica flash-column chromatography using 5% EtOAc:hexane to afforded 3,5-dimethyl-4′-(trifluoromethyl)biphenyl as a colourless oil (228 mg, 91%); ν_{max} ($CHCl_3$) 3042, 1614, 1344, 1211, 1182, 1092, 1035, 855 cm^{-1}; ^1H NMR (500 MHz, $CDCl_3$) δ 7.69 (s, 4H, 2′,3′,5′,6′-***H***), 7.24 (s, 2H, 2,6-***H***), 7.08 (s, 1H, 4-***H***), 2.42 (s, 6H, 3,5-***CH₃***); ^{13}C NMR (126 MHz, $CDCl_3$) δ 145.2 (Ar-1′-***C***), 140.0 (***C***-1), 138.8 (Ar-***C***), 130.0 (Ar-***C***), 129.4 (q, $^2J_{C\text{-}F}$ = 32.4, ***C***-4′), 127.6 (Ar-C), 125.8 (q, $^3J_{C\text{-}F}$ = 3.8, ***C***-3′,5′), 125.4 (Ar-***C***), 124.6 (q, $^1J_{C\text{-}F}$ = 271.5, 4′-***CF₃***), 21.6 (3,5-***CH₃***); ^{19}F NMR (376 MHz, $CDCl_3$) δ -62.8; *m/z* (GC-MS, EI) 250 (100%, M^+), 235 (44%, M^+-CH_3), 215 (6%), 181 (15%, M^+-CF_3), 165 (26%, M^+-CH_3,CF_3).

4′-methoxy-3,5-dimethylbiphenyl, 317[8]

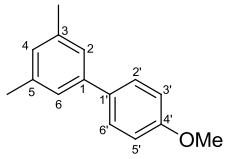

General procedure B was applied using 1-iodo-4-methoxybenzene (281 mg, 1.2 mmol).Purification by silica flash-column chromatography using 5% EtOAc:hexane afforded 4′-methoxy-3,5-dimethylbiphenyl as colourless oil (191 mg, 90%); ν_{max} ($CHCl_3$) 3024, 1672, 1567, 1528, 1297, 1213, 1074, 854 cm^{-1}; ^1H NMR (400 MHz, $CDCl_3$) δ 7.62 (d, *J* = 7.6 Hz, 2H, 2′,6′-***H***), 7.29 (s, 2H, 2,6-***H***), 7.05 - 7.07 (m, 3H, 4, 3′,5′-***H***), 3.92 (s, 3H, 4′-O***CH₃***), 2.48 (s, 6H, 3,5-***CH₃***); ^{13}C NMR (101 MHz, $CDCl_3$) δ 159.2 (***C***-4′), 141.0 (Ar-***C***), 138.3 (***C***-3,5), 134.2 (Ar-***C***), 128.5 (Ar-***C***), 128.3 (Ar-***C***), 124.8 (Ar-***C***), 114.2 (***C***-3′,5′), 55.4 (4′-O***CH₃***), 21.5 (3,5-***CH₃***); *m/z*

(GC-MS, EI) 212 (100%, M^+), 197 (70%, M^+-CH_3), 169 (30%), 153 (20%, M^+-CH_3,CH_3,OCH_3).

3,5-dimethyl-4′-nitrobiphenyl, 318[9]

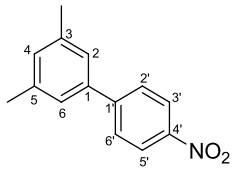

General procedure B was applied using iodo-4-nitrobenzene (299 mg, 1.2 mmol).Purification by silica flash-column chromatography using 5% EtOAc:hexane to afforded 3,5-dimethyl-4′-nitrobiphenyl as an off-white crystalline solid (211 mg, 93%); m.p. 120 - 121 °C; ν_{max} ($CHCl_3$) 3044, 1656, 1608, 1531 (N=O), 1394, 1139, 886, 766, 707 cm^{-1}; ^1H NMR (400 MHz, $CDCl_3$) δ 8.15 (d, *J* = 9.0, 2H, 3′,5′-***H***), 7.59 (d, *J* = 9.0, 2H, 2′,6′-***H***), 7.12 (s, 2H, 2,6-***H***), 6.98 (s, 1H, 4-***H***), 2.30 (s, 6H, 3,5-***CH₃***); ^{13}C NMR (101 MHz, $CDCl_3$) δ 148.0 (***C***-4′), 147.2 (Ar-***C***), 138.8 (***C***-3,5), 130.4 (***C***-4), 127.8 (Ar-***C***), 125.4 (***C***-2,6-***C***), 123.8 (Ar-***C***), 21.3 (3,5-***CH₃***); *m/z* (GC-MS, EI) 227 (100%, M^+), 212 (8%), 165 (75%).

3′,5′-dimethylbiphenyl-4-carbonitrile, 319[10]

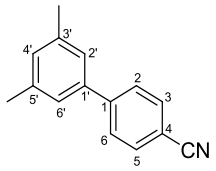

General procedure B was applied using 4-bromobenzonitrile (218 mg, 1.2 mmol). Purification by silica flash-column chromatography using 5% EtOAc:hexane to afforded 3′,5′-dimethylbiphenyl-4-carbonitrile as a pale yellow solid (190 mg, 92%); m.p. 58 - 59 °C; ν_{max} 2918, 2230 (C≡N), 1608, 1510, 1460, 1396, 1180, 1334, 859 cm^{-1}; ^1H NMR (400 MHz, $CDCl_3$) δ 7.69 (m, 4H, 2,3,5,6-***H***), 7.21 (s, 2H, 2′,6′-***H***), 7.07 (s, 1H, 4-***H***), 2.40 (s, 6H, 3′,5′-***CH₃***); ^{13}C NMR (101 MHz, $CDCl_3$) δ 146.1 (***C***-1), 139.3 (***C***-1′), 138.8 (***C***-3′,5′), 132.6 (***C***-3,5), 130.4 (***C***-4′), 127.8 (***C***-2,6), 125.2 (***C***-2′,6′), 119.2 (4-***CN***), 110.8 (***C***-4), 21.5 (3′,5′-***CH₃***); *m/z* (GC-MS, EI) 207 (100%, M^+), 192 (49%, M^+-CH_3), 177 (6%, M^+-$2CH_3$), 165 (15%, M^+-CH_3,CN).

319 also prepared by General procedure B using 4-chlorobenzonitrile (164 mg, 1.2 mmol). Purification by silica flash-column chromatography using 5% EtOAc:hexane to afforded 3′,5′-dimethylbiphenyl-4-carbonitrile (104 mg, 50%). Further elution afforded aryl boronate **94** (102 mg, 44%).

N,N,3′,5′-tetramethylbiphenyl-4-amine, 320[11]

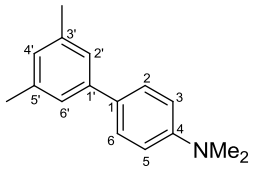

General procedure B was applied using 1-bromo-4-N, *N*-dimethylanaline (240 mg, 1.2 mmol). Purification by silica flash-column chromatography using 5% EtOAc:hexane to afforded N,N,3′,5′-tetramethylbiphenyl-4-amine as a pale yellow crystalline solid (189 mg, 92%); ν_{max} (CH_2Cl_2) 3054, 2985, 1605, 1513, 1425, 1275, 1254, 1179, 1033, 895, 768 cm^{-1}; ^{1}H NMR (400 MHz, $CDCl_3$) δ 7.50 (d, *J* = 8.5, 2H, 2,6-***H***), 7.19 (s, 2H, 2′,6′-***H***), 6.92 (s, 1H, 4′-***H***), 6.80 (d, *J* =8.5, 2H, 3,5-***H***), 3.06 (s, 6H, 4-***N(CH$_3$)$_2$***), 2.34 (s, 6H, 3′,5′-***CH$_3$***); ^{13}C NMR (101 MHz, $CDCl_3$) δ 154.2 (***C***-4), 141.2 (***C***-1′), 138.8 (***C***-3′,5′), 130.3 (***C***-1), 129.8 (***C***-4′), 128.8 (***C***-2,6), 125.5 (***C***-2′,6′), 112.7 (***C***-3,5), 41.3 (4-***N(CH$_3$)$_2$***), 21.9 (3′,5′-***CH$_3$***); *m/z* (GC-MS, EI) 225 (100%, M^+), 210 (14%, M^+-CH_3), 193 (4%, M^+-2CH_3), 165 (17%, M^+-CH_3,NMe_2), 152 (5%), 113 (6%), 105 (10%).

2-(2′, 5′-dimethylphenyl)-4, 4, 5, 5-tetramethyl-1, 3, 2-dioxaborolane, 342[12]

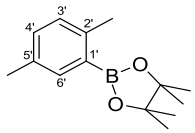

General procedure C was applied to *p*-xylene (106 mg, 123 μL, 1.0 mmol). The reaction was heated for 18 hours. Purification by silica flash-column chromatography eluting with 5% EtOAc:hexane afforded 2-(2′,5′-dimethylphenyl)-4,4,5,5-tetramethyl-1,3,2-dioxaborolane as a white crystalline solid (105 mg, 45%); m.p. 89 - 90 °C (from hexane); ν_{max} ($CHCl_3$) 2994, 2974, 2342, 1608, 1415, 1344, 1247, 1130, 975, 856, 708 cm^{-1}; ^1H NMR (400 MHz, $CDCl_3$) δ 7.57 (d, *J* = 1.6, 1H, Ar-6′-***H***), 7.13 (dd, *J* = 1.6, 7.8, 1H, 4′-***H***), 7.06 (d, *J* = 7.8, 1H, 3′-***H***), 2.49 (s, 3H, Ar-***CH₃***), 2.30 (s, 3H, Ar-***CH₃***), 1.34 (s, 12H, pin-***CH₃***); ^{13}C NMR (101 MHz, $CDCl_3$) δ 141.9 (Ar-***C***), 136.6 (Ar-***C***), 134.1 (Ar-***C***), 131.8 (Ar-***C***), 130.0 (Ar-***C***), 83.6 (pin-***C***$(CH_3)_2$), 25.1 (pin-***CH₃***), 21.9 (Ar-***CH₃***), 21.0 (Ar-***CH₃***); ^{11}B NMR (128 MHz, $CDCl_3$) δ 31.71; *m/z* (GC-MS, EI) 232 (38%, M^+), 217 (19%, M^+-CH_3), 175 (100%, M^+-CH_3,$C(CH_3)_2$), 132 (80%, M^+-$C(CH_3)_2C(CH_3)_2O$).

342 was also prepared by general procedure D using *p*-xylene (106 mg, 123 μL, 1.0 mmol) and heating for 1 hour. Purification by silica flash-column chromatography eluting with 5% EtOAc:hexane afforded **342** as a white crystalline solid (127 mg, 55%).

2,6-dimethyl-4-(4′,4′,5′,5′-tetramethyl-1′,3′,2′-dioxaborolan-2′-yl)pyridine, 344[1]

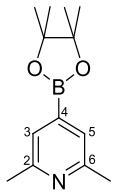

General procedure C was applied to 2,6-lutidine (107 mg, 115 μL, 1.0 mmol) which was heated for 30 minutes. Purification by silica flash-column chromatography eluting with 2% MeOH/DCM afforded 2,6-dimethyl-4-(4′,4′,5′,5′-tetramethyl-1′,3′,2′-dioxaborolan-2′-yl)pyridine as an off-white crystalline solid (221 mg, 95%); m.p. 82 - 83 °C (from hexane); ν_{max} ($CHCl_3$) 3020, 2982, 1521, 1472, 1392, 1366, 1251, 1142, 849, 719 cm^{-1}; ^1H NMR (400 MHz,

CDCl3) δ 7.31 (s, 2H, 3,5-***H***), 2.52 (s, 6H, 2,6-***CH₃***), 1.35 (s, 12H, pin-***CH₃***); ^{13}C NMR (101 MHz, $CDCl_3$) δ 157.1 (***C***-2,6), 125.2 (***C***-3,5), 84.4 (pin-***C***$(CH_3)_2$), 24.9 (pin-***CH₃***), 24.3 (2,6-***CH₃***); ^{11}B NMR (128 MHz, $CDCl_3$) δ 31.24; *m/z* (GC-MS, EI) 233 (76%, M^+), 218 (45%, M^+-CH_3), 190 (9%, M^+-$3CH_3$), 176 (18%, M^+- CH_3,$C(CH_3)_2$), 160 (5%), 147 (100%, $2CH_3$, $C(CH_3)_2O$), 133 (66%, M^+-$3CH_3$, $C(CH_3)_2O$).

344 was also prepared by general procedure D using 2,6-lutidine (107 mg, 115 μL, 1.0 mmol) and heating for 5 minutes. Purification by silica flash-column chromatography eluting with 2% MeOH/DCM afforded **344** as an off-white crystalline solid (229 mg, 98%).

2,6-dichloro-4-(4′,4′,5′,5′-tetramethyl-1′,3′,2′-dioxaborolan-2′-yl)pyridine, 58[13]

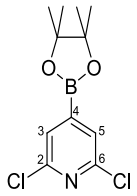

General procedure C was applied to 2,6-dichloropyridine (147 mg, 1.0 mmol) which was heated for 20 minutes. The reaction was heated for 20 minutes. Purification by silica flash-column chromatography eluting with 100% DCM afforded 2,6-dichloro-4-(4′,4′,5′,5′-tetramethyl-1′,3′,2′-dioxaborolan-2′-yl)pyridine as a pale pink solid (263 mg, 96%); m.p. 118 - 119 °C (from hexane); Anal. found C, 48.4; H, 5.2; N, 5.0%; Calcd. for $C_{11}H_{14}BCl_2NO_2$ C, 48.2; H, 5.15; N, 5.1%; ν_{max} ($CHCl_3$) 2984, 1515, 1422, 1358, 1337, 1161, 1141, 965, 873, 802, 674 cm^{-1}; ^{1}H NMR (400 MHz, $CDCl_3$) δ 7.59 (s, 2H, 3,5-***H***), 1.34 (s, 12H, pin-***CH₃***); ^{13}C NMR (126 MHz, $CDCl_3$) δ 150.6 (***C***-2,6), 128.0 (***C***-3,5), 85.4 (pin-***C***$(CH_3)_2$), 25.0 (pin-***CH₃***); ^{11}B NMR (128 MHz, $CDCl_3$) δ 29.58; *m/z* (GC-MS, EI) 275 (27%, $M^+(^{37}Cl^{37}Cl)$), 274 (12%, $M^+(^{35}Cl^{37}Cl)$), 273 (41%, $M^+(^{35}Cl^{35}Cl)$, 260 (58%, $M^+(^{37}Cl^{37}Cl)$ -CH_3), 259 (24%, $M^+(^{35}Cl^{37}Cl)$ -CH_3), 258 (91%, $M^+(^{35}Cl^{35}Cl)$ -CH_3), 233 (7%, $M^+(^{37}Cl^{37}Cl)$ -$C(CH_3)_2$), 231 (12%, $M^+(^{35}Cl^{37}Cl)$ -$C(CH_3)_2$), 230 (4%, $M^+(^{35}Cl^{35}Cl)$ -$C(CH_3)_2$), 191 (64%, $M^+(^{37}Cl^{37}Cl)$-$C(CH_3)_2C(CH_3)_2$), 189 (100%, $M^+(^{35}Cl^{37}Cl)$ -$C(CH_3)_2C(CH_3)_2$), 188 (25%, $M^+(^{35}Cl^{35}Cl)$-$C(CH_3)_2C(CH_3)_2$), 174 (19%), 152 (19%).

58 was also prepared by general procedure D using 2,6-dichloropyridine (147 mg, 1.0 mmol) which was heated for 3 minutes. Purification by silica flash-column chromatography eluting with 100% DCM afforded **58** as a pale pink solid (268 mg, 98%).

3,6-bis(4′,4′,5′,5′-tetramethyl-1′,3′,2′-dioxaborolan-2′-yl)quinoline 345 and

3,7-bis(4′,4′,5′,5′-tetramethyl-1′,3′,2′-dioxaborolan-2′-yl)quinoline 346

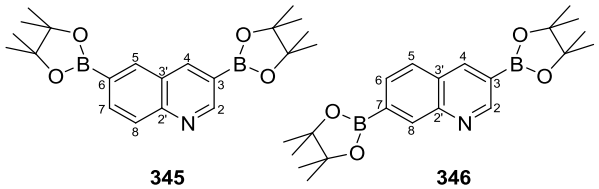

345 **346**

General procedure C was applied to quinoline (129 mg, 118 μL, 1.0 mmol) with an additional 1.0 equivalents of B_2pin_2 (254 mg) which was heated for 2 hours. Purification by silica flash-column chromatography eluting with 10% MeOH/DCM afforded a 1:1 mixture of 3,6-bis(4′,4′,5′,5′-tetramethyl-1′,3′,2′-dioxaborolan-2′-yl)quinoline **345** and 3,7-bis(4′,4′,5′,5′-tetramethyl-1′,3′,2′-dioxaborolan-2′-yl)quinoline **346** as a yellow solid (350 mg, 92%); m.p. 96 - 97 °C; ν_{max} ($CHCl_3$) 2997, 2981, 1622, 1600, 1442, 1417, 1307, 1226, 1140, 1089, 794, 673 cm^{-1}; ^1H NMR (400 MHz, $CDCl_3$) δ 9.21 (s, 1H, **345**-2-***H***), 9.20 (s, 1H, **346**-2-***H***), 8.65 - 8.61 (m, 3H, **345**-4,5-***H*** & **346**-4-***H***), 8.35 (s, 1H, **346**-8-***H***), 8.11 (d, *J* = 1.3, 8.6, 1H, **346**-6-***H***), 8.07 (d, *J* = 8.6, 1H, **346**-5-***H***)), 7.88 (d, *J* = 8.1, 1H, **345**-8-***H***), 7.80 (d, *J* = 8.1, 1H, **345**-7-***H***), 1.35 - 1.27 (m, 48H, pin-$\boldsymbol{CH_3}$); ^{13}C NMR (101 MHz, $CDCl_3$) δ 156.0 (**346**-***C***-2), 155.0 (**345**-***C***-2), 149.0 (**345**-***C***-2′), 148.2 (**346**-***C***-2′), 145.1 (**345**-***C***-4), 144.2 (**346**-***C***-4), 137.4 (**345**-***C***-5), 137.0 (**346**-***C***-5), 135.6 (**346**-***C***-6), 131.2 (**345**-***C***-8), 129.3 (**345**-***C***-3′), 128.6 (**346**-**C**-3′), 127.7 (**345**-***C***-7), 127.2 (**345**-***C***-8), 84.6 (pin-$\boldsymbol{C}(CH_3)_2$), 84.52 (pin-$\boldsymbol{C}(CH_3)_2$), 84.47 (pin-$\boldsymbol{C}(CH_3)_2$), 84.3 (pin-$\boldsymbol{C}(CH_3)_2$), 25.13 (pin-$\boldsymbol{CH_3}$), 25.08 (pin-$\boldsymbol{CH_3}$), 24.8 (pin-$\boldsymbol{CH_3}$), 24.3 (pin-$\boldsymbol{CH_3}$); ^{11}B NMR (128 MHz, $CDCl_3$) δ 32.12; *m/z* (GC-MS, EI) 381 (100%, M^+), 366 (26%), 322 (10%), 295 (23%), 281 (28%), 238 (77%), 181 (40%); HRMS (ASAP) *m/z* found $(M+H)^+$ 380.2431, $C_{21}H_{30}{}^{10}B_2NO_4$ requires *M* 380.2428.

Recrystallisation of the mixture of **345** and **346** in hexane afforded pure pale yellow crystals of 3,6-bis(4′,4′,5′,5′-tetramethyl-1′,3′,2′-dioxaborolan-2′-yl)quinoline **345**; ^{1}H NMR (500 MHz, $CDCl_3$) δ 9.21 (s, 1H, 2-***H***), 8.60 (s, 2H, 4,5-***H***), 7.88 (d, *J* = 8.1, 1H, 8-***H***), 7.81 (d, *J* = 8.1, 1H, 7-***H***), 1.39 (s, 12H, pin-***CH₃***), 1.38 (s, 12H, pin-***CH₃***); ^{13}C NMR (126 MHz, $CDCl_3$) δ 155.0 (***C***-2), 149.0 (***C***-2′), 144.2 (***C***-4), 137.4 (***C***-5), 131.2 (***C***-8), 129.4 (***C***-3′), 127.7 (***C***-7), 84.6 (pin-***C***$(CH_3)_2$), 84.4 (pin-***C***$(CH_3)_2$), 25.2 (pin-***CH₃***), 24.8 (pin-***CH₃***); ^{11}B NMR (128 MHz, $CDCl_3$) δ 32.10; *m/z* (GC-MS, EI) 381 (100%, M^+), 366 (26%), 322 (10%), 295 (23%), 281 (28%), 238 (77%), 181 (40%).

345 and **346** were also prepared by general procedure D using quinoline (129 mg, 118 μL, 1.0 mmol) with an additional 1.0 equivalents of B_2pin_2 (254 mg) which was heated for 15 minutes. Purification by silica flash-column chromatography eluting with 10% MeOH/DCM afforded a 1:1 mixture of **345** and **346** (337 mg, 89%).

2-(2′,5′-dimethylfuran-3′-yl)-4,4,5,5-tetramethyl-1,3,2-dioxaborolane, 353

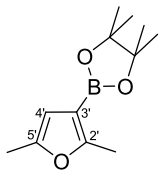

General procedure C was applied to 2,5-dimethylfuran (96 mg, 106 μL, 1.0 mmol) which was heated for 5 minutes. Purification by silica gel flash column chromatography eluting with 100% DCM afforded 2-(2,5-dimethylfuran-3-yl)-4,4,5,5-tetramethyl-1,3,2-dioxaborolane as a colourless oil (217 mg, 98%); ν_{max} ($CHCl_3$) 2977, 2923, 1579, 1471, 1371, 1308, 1143, 1051, 837 cm^{-1}; ^{1}H NMR (400 MHz, $CDCl_3$) δ 6.02 (s, 1H, 4′-***H***), 2.41 (s, 3H, ***CH₃***), 2.23 (s, 3H, ***CH₃***), 1.29 (s, 12H, pin-***CH₃***); ^{13}C NMR (101 MHz, $CDCl_3$) δ 161.1 (***C***-5′), 150.5 (***C***-2′), 110.0 (***C***-4′), 83.4 (pin-***C***$(CH_3)_2$), 25.3 (pin-***CH₃***), 14.4 (Ar-***CH₃***), 13.6 (Ar-***CH₃***); ^{11}B NMR (128 MHz, $CDCl_3$) δ 30.07; *m/z* (GC-MS, EI) 222 (60%, M^+), 207 (16%), 165 (40%),137 (20%), 122 (100%); HRMS (EI) *m/z* found $(M)^+$ 221.1458, requires $C_{12}H_{19}{}^{10}BO_3$ *M* 221.1458.

353 was also prepared by general procedure D using 2,5-dimethylfuran (96 mg, 106 μL, 1.0 mmol) which was heated for 2 minutes. Purification by silica gel flash column chromatography eluting with 100% DCM afforded 2-(2,5-dimethylfuran-3-yl)-4,4,5,5-tetramethyl-1,3,2-dioxaborolane as a colourless oil (220 mg, 99%).

2-(2′,5′-dimethylthiophen-3′-yl)-4,4,5,5-tetramethyl-1,3,2-dioxaborolane, 355[14]

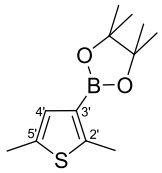

General procedure C was applied to 2,5-dimethylthiophene (114 mg, 112 μL, 1.0 mmol) with 2 hours of heating. Purification by silica gel flash column chromatography eluting with 100% DCM to afforded 2-(2′,5′-dimethylthiophen-3′-yl)-4,4,5,5-tetramethyl-1,3,2-dioxaborolane as a colourless oil (236 mg, 99%); ν_{max} ($CHCl_3$) 2976, 2919, 1490, 1389, 1301, 1262, 1141, 866 cm^{-1}; ^1H NMR (400 MHz, $CDCl_3$) δ 6.81 (s, 1H, 4-***H***), 2.59 (s, 3H, Ar-***CH₃***), 2.37 (s, 3H, Ar-***CH₃***), 1.28 (s, 12H, pin-***CH₃***); ^{13}C NMR (101 MHz, $CDCl_3$) δ 150.9 (***C***-4′), 136.2 (Ar-***C***), 130.8 (Ar-***C***), 83.1 (pin-***C***$(CH_3)_2$), 24.9 (pin-***CH₃***), 15.7 (***CH₃***), 14.8 (***CH₃***); ^{11}B NMR (128 MHz, $CDCl_3$) δ 29.25; *m/z* (GC-MS, EI) 238 (100%, M^+), 223 (7%), 181 (42%).

355 was also prepared by general procedure D using 2,5-dimethylthiophene (114 mg, 112 μL, 1.0 mmol) with 15 minutes of heating. Purification by silica gel flash column chromatography eluting with 100% DCM to afforded 2-(2′,5′-dimethylthiophen-3′-yl)-4,4,5,5-tetramethyl-1,3,2-dioxaborolane as a colourless oil (233 mg, 98%)

2-(2′,5′-dibromothiophen-3′-yl)-4,4,5,5-tetramethyl-1,3,2-dioxaborolane, 357[14]

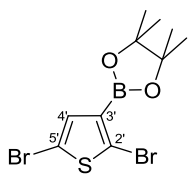

General procedure C was applied to 2,5-dibromothiophene (242 mg, 1.0 mmol) which was heated for 18 hours. Purification by silica gel flash column chromatography eluting initially

with 100% hexane to remove remaining 2,5-dibromothiophene followed by elution with 100% DCM to afford 2-(2′,5′-dibromothiophen-3′-yl)-4,4,5,5-tetramethyl-1,3,2-dioxaborolane as an off-white solid (310 mg, 84%); m.p. 73.2 - 73.9 °C; Anal. found C, 33.0; H, 3.6%; Calcd. for $C_{10}H_{13}BBr_2O_2S$ C, 32.7; H, 3.6%; ν_{max} ($CHCl_3$) 2977, 2908, 1518, 1418, 1364, 1303, 1244, 995, 960, 879, 846, 688 cm^{-1}; ^1H NMR (500 MHz, $CDCl_3$) δ 7.11 (s, 1H, 4-***H***), 1.33 (s, 12H, pin-***CH₃***); ^{13}C NMR (126 MHz, $CDCl_3$) δ 136.1 (***C***-4′), 122.2 (***C***-2′), 111.2 (***C***-5′), 84.4 (pin-***C***$(CH_3)_2$), 25.0 (pin-***CH₃***); ^{11}B NMR (128 MHz, $CDCl_3$) δ 28.27; *m/z* (GC-MS, EI) 370 (49%, $M^+(^{81}Br^{81}Br)$), 368 (100%, $M^+(^{79}Br^{81}Br)$), 366 (50%, $M^+(^{79}Br^{79}Br)$), 355 (7%, $M^+(^{81}Br^{81}Br)$ - CH_3, 353 (14%, $M^+(^{79}Br^{81}Br)$ -CH_3), 351(7%, $M^+(^{79}Br^{79}Br)$ -CH_3), 289 (60%, $M^+(^{81}Br)$ -Br), 289 (60%, $M^+(^{79}Br)$ -Br), 208 (75%, M^+ -2Br), 166 (65%).

357 was also prepared by general procedure D using 2,5-dibromothiophene (242 mg, 1.0 mmol) which was heated for 1 hour. Purification by silica gel flash column chromatography eluting initially with 100% hexane to remove remaining 2,5-dibromothiophene followed by elution with 100% DCM afforded 2-(2′,5′-dibromothiophen-3′-yl)-4,4,5,5-tetramethyl-1,3,2-dioxaborolane as an off-white solid (301 mg, 82%).

3,5-bis(4′,4′,5′,5′-tetramethyl-1′,3′,2′-dioxaborolan-2′-yl)thiophene-2-carbonitrile, 359[15]

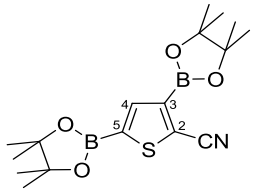

General procedure C was applied to 2-cyanothiophene (109 mg, 93 μL, 1.0 mmol) with an additional 0.5 equivalents of B_2pin_2 (127 mg) which was heated for 2 hours. Purification by silica flash-column chromatography eluting with 100% DCM afforded 3,5-bis(4′,4′,5′,5′-tetramethyl-1′,3′,2′-dioxaborolan-2′-yl)thiophene-2-carbonitrile as a white crystalline solid (345 mg, 96%); m.p. 132 - 133 °C; ν_{max} ($CHCl_3$) 2988, 2931, 2217 (C≡N), 1532, 1455, 1374, 1316, 1138, 969, 847, 669 cm^{-1}; ^1H NMR (500 MHz, $CDCl_3$) δ 7.89 (s, 1H, 4-***H***), 1.34 (s, 12H, pin-***CH₃***), 1.33 (s, 12H, pin-***CH₃***); ^{13}C NMR (126 MHz, $CDCl_3$) δ 143.38 (***C***-4), 123.4 (***C***-2), 114.6

(2-***C*N**), 85.1 (pin-***C***$(CH_3)_2$), 84.9 (pin-***C***$(CH_3)_2$), 25.04 (pin-***CH*$_3$**), 24.98 (pin-***CH*$_3$**); ^{11}B NMR (128 MHz, $CDCl_3$) δ 28.77; *m/z* (GC-MS, EI) 361 (55%, M^+), 346 (44%, M^+-CH_3), 331 (8%, M^+-$2CH_3$), 319 (100%, M^+-$C(CH_3)_2$), 303 (55%), 275 (20%), 262 (39%), 246 (13%).

359 was also prepared by general procedure D using 2-cyanothiophene (109 mg, 93 μL, 1.0 mmol) with an additional 0.5 equivalents of B_2pin_2 (127 mg) which was heated for 15 minutes. Purification by silica flash-column chromatography eluting with 100% DCM afforded 3,5-bis(4′,4′,5′,5′-tetramethyl-1′,3′,2′-dioxaborolan-2′-yl)thiophene-2-carbonitrile as a white crystalline solid (354 mg, 98%).

5-(4′,4′,5′,5′-tetramethyl-1′,3′,2′-dioxaborolan-2′-yl)-1,2,3-tetrahydrocyclopenta[b]indole, 361[16]

7-(4′,4′,5′,5′-tetramethyl-1′,3′,2′-dioxaborolan-2′-yl)-1,2,3-tetrahydrocyclopenta[b]indole, 362

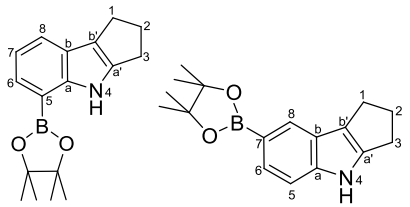

General procedure C was applied to 1,2,3-tetrahydrocyclopenta[b]indole (157 mg, 1.0 mmol) which was heated for 2 hours. Purification by silica flash-column chromatography eluting with 5% EtOAc:hexane afforded 5-(4′,4′,5′,5′-tetramethyl-1′,3′,2′-dioxaborolan-2′-yl)-1,2,3-tetrahydrocyclopenta [b]indole as a pale yellow solid (88 mg, 31%); m.p. 134 - 135 °C; ν_{max} ($CHCl_3$) 2997, 1422, 1257, 1219, 1140, 935, 848, 768 cm^{-1}; ^{1}H NMR (400 MHz, $CDCl_3$) δ 8.94 (s, 1H, *N*-***H***), 7.57-7.53 (m, 2H, 6,8-***H***), 7.09 (t, *J* = 7.3, 1H, 7-***H***), 2.94 - 2.90 (m, 2H, ***CH*$_2$**), 2.85 - 2.82 (m, 2H, ***CH*$_2$**), 2.64 - 2.42 (m, 2H, ***CH*$_2$**), 1.40 (s, 12H, pin-***CH*$_3$**); ^{13}C NMR (101 MHz, $CDCl_3$) δ 146.6 (***C***-a), 143.9 (***C***-a′), 127.8 (***C***-b), 123.9 (***C***-7), 122.1 (***C***-6), 119.2 (***C***-8), 119.1 (***C***-b′), 83.9 (pin-***C***$(CH_3)_2$), 29.0 (***CH*$_2$**), 26.3 (***CH*$_2$**), 25.2 (pin-***CH*$_3$**), 24.7 (***CH*$_2$**); ^{11}B NMR (128 MHz, $CDCl_3$) δ 31.27; *m/z* (GC-MS, EI) 283 (100%, M^+), 226 (25%, M^+-$CO(CH_3)_3$), 183 (35%, M^+- $C(CH_3)_2C(CH_3)_2O$).

Further elution afforded 7-(4′,4′,5′,5′-tetramethyl-1′,3′,2′-dioxaborolan-2′-yl)-1,2,3-tetrahydrocyclopenta[b]indole as a white solid (14 mg, 5%); m.p. 134 - 135 °C; ν_{max} ($CHCl_3$) 3447, 3007, 2997, 1421, 1260, 1219, 1140, 937, 849, 767, 669 cm^{-1}; ^1H NMR (400 MHz, $CDCl_3$) δ 7.97 (s, 1H, ***N-H***), 7.88 (s, 1H, Ar-8-***H***), 7.55 (d, *J* = 8.2, 1H, 6-***H***), 7.29 (d, *J* = 8.2, 1H, 5-***H***), 2.92 - 2.73 (m, 4H, ***CH₂***), 2.58 - 2.45 (m, 2H, ***CH₂***), 1.37 (s, 12H, pin-***CH₃***); ^{13}C NMR (126 MHz, $CDCl_3$) δ 143.8 (***C***-a), 143.3 (***C***-a′), 127.0 (***C***-b), 126.4 (***C***-8), 124.7 (***C***-6), 120.6 (***C***-b′), 111.0 (***C***-5), 83.6 (pin-***C***$(CH_3)_2$), 28.8 (***CH₂***), 26.1 (***CH₂***), 25.1 (pin-***CH₃***), 24.7 (***CH₂***); ^{11}B NMR (128 MHz, $CDCl_3$) δ 31.35; *m/z* (GC-MS, EI) 283 (100%, M^+), 226 (25%, M^+-$CO(CH_3)_3$), 183 (35%, M^+- $C(CH_3)_2C(CH_3)_2O$); HRMS (ASAP) *m/z* found $(M+H)^+$ 283.1857, $C_{17}H_{22}{}^{10}BNO_2$ requires *M* 283.1853.

361 and **362** were also prepared by general procedure D using 1,2,3-tetrahydrocyclopenta[b]indole (157 mg, 1.0 mmol) which was heated for 15 minutes. Purification by silica flash-column chromatography eluting with 5% EtOAc:hexane afforded 5-(4′,4′,5′,5′-tetramethyl-1′,3′,2′-dioxaborolan-2′-yl)-1,2,3-tetrahydrocyclopenta[b]indole as a pale yellow solid (91 mg, 32%). Further elution afforded 7-(4′,4′,5′,5′-tetramethyl-1′,3′,2′-dioxaborolan-2′-yl)-1,2,3-tetrahydrocyclopenta [b]indole as a white solid (17 mg, 6%).

8-(4′,4′,5′,5′-tetramethyl-1′,3′,2′-dioxaborolan-2′-yl)-1,2,3,4-tetrahydro-9H-carbazole, 364

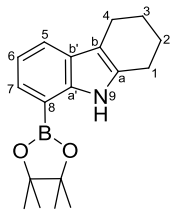

General procedure C was applied to 1,2,3,4-tetrahydro-9H-carbazole (171 mg, 1.0 mmol) which was heated for 2 hours. Purification by silica flash-column chromatography eluting with 5% EtOAc:hexanes afforded 8-(4′,4′,5′,5′-tetramethyl-1′,3′,2′-dioxaborolan-2′-yl)-1,2,3,4-tetrahydro-9H-carbazole (264 mg, 89%); m.p. 152 - 154 °C; ν_{max} ($CHCl_3$) 3023, 2399, 1521, 1423, 1226, 1203, 905, 793, 715, 674 cm^{-1}; ^1H NMR (400 MHz, $CDCl_3$) δ 8.71 (s, 1H, ***N-H***), 7.60 (d, *J* = 7.7, 1H, Ar-5-***H***), 7.58 (d, *J* = 7.2, 1H, Ar-7-***H***), 7.10 (dd, *J* = 7.2, 7.7, 1H, Ar-6-***H***),

2.81 (t, *J* = 5.9, 2H, ***CH₂***), 2.73 (t, *J* = 5.9, 2H, ***CH₂***), 2.00 - 1.83 (m, 4H, ***CH₂***), 1.41 (s, 12H, pin-***CH₃***); ^{13}C NMR (126 MHz, $CDCl_3$) δ 141.1 (***C***-a′), 134.2 (***C***-b′), 128.3 (***C***-7), 126.9 (***C***-b), 121.4 (***C***-5), 118.7 (***C***-6), 109.7 (***C***-a), 83.9 (pin-***C***$(CH_3)_2$), 25.2 (pin-***CH₃***), 23.6 (***CH₂***), 23.6 (***CH₂***), 23.5 (***CH₂***), 21.1 (***CH₂***); ^{11}B NMR (128 MHz, $CDCl_3$) δ 31.07; *m/z* (GC-MS, EI) 297 (100%, M^+), 269 (30%, M^+-C_2H_4), 254 (7%), 214 (31%), 196 (16%), 187 (29%), 169 (23%), 143 (32%); HRMS (ASAP) *m/z* found $(M+H)^+$ 297.2015, $C_{18}H_{25}{}^{10}BNO_5$ requires *M* 297.2009.

364 was also prepared by general procedure D using 1,2,3,4-tetrahydro-9H-carbazole (171 mg, 1.0 mmol) which was heated for 15 minutes. Purification by silica flash-column chromatography eluting with 5% EtOAc:hexanes to afford 8-(4′,4′,5′,5′-tetramethyl-1′,3′,2′-dioxaborolan-2′-yl)-1,2,3,4-tetrahydro-9H-carbazole (268 mg, 90%).

tert-butyl 3,5-bis(4′,4′,5′,5′-tetramethyl-1′,3′,2′-dioxaborolan-2′-yl)-1H-pyrrolo[b]pyridine-1-carboxylate, 172

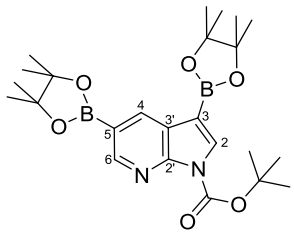

General procedure C was applied to tert-butyl 1H-pyrrolo[b]pyridine-1-carboxylate (218 mg, 1.0 mmol) which was heated for 6 hours. Purification by silica flash-column chromatography eluting with 5% EtOAc:hexanes afforded tert-butyl 3,5-bis(4′,4′,5′,5′-tetramethyl-1′,3′,2′-dioxaborolan-2′-yl)-1H-pyrrolo[b]pyridine-1-carboxylate (423 mg, 90%); m.p. 177 - 178 °C (from methanol); Anal. Calcd. for $C_{24}H_{36}B_2N_2O_6$: C, 61.2; H, 7.7; N, 6.0 found: C, 60.9; H, 7.7; N, 5.8%; ν_{max} 3027, 2988, 1755 (C=O), 1609, 1534, 1482, 1416, 1235, 1138, 1068, 934, 711 cm^{-1}; ^{1}H NMR (400 MHz, $CDCl_3$) 8.84 (d, *J* = 1.6, 1H, Ar-6-***H***), 8.56 (d, *J* = 1.6, 1H, Ar-4-***H***), 8.03 (s, 1H, Ar-2-***H***), 1.65 (s, 9H, ^{t}Bu-***CH₃***), 1.25 (s, 24H, pin-***CH₃***); ^{13}C NMR (126 MHz, $CDCl_3$) δ 151.7 (***C***$O_2{}^t$Bu), 151.3 (***C***-2′), 147.7 (***C***-6), 137.6 (***C***-4), 135.9 (***C***-3′), 125.4 (***C***-2), 84.6 (pin-***C***$(CH_3)_2$), 84.1 (pin-***C***$(CH_3)_2$), 83.8 (^{t}Bu-***C***$(CH_3)_3$), 28.3 (^{t}Bu-***CH₃***), 25.1 (pin-***CH₃***); ^{11}B NMR (128 MHz, $CDCl_3$) δ 30.22; *m/z* (GC-MS, EI) 470 (20%, M^+) (100%, M^+-

$CO_2C(CH_3)_3$), 355 (10%), 313 (10%), 285 (42%), 171 (10%); HRMS (ASAP) *m/z* found $(M+H)^+$ 471.2830, $C_{24}H_{37}B_2N_2O_6$ requires *M* 471.2833.

172 was also prepared by general procedure D using tert-butyl 1H-pyrrolo[b]pyridine-1-carboxylate (218 mg, 1.0 mmol) which was heated for 20 minutes. Purification by silica flash-column chromatography eluting with 5% EtOAc:hexanes afforded tert-butyl 3,5-bis(4′,4′,5′,5′-tetramethyl-1′,3′,2′-dioxaborolan-2′-yl)-1H-pyrrolo[b]pyridine-1-carboxylate (433 mg, 92%)

tert-butyl 3-(4′,4′,5′,5′-tetramethyl-1′,3′,2′-dioxaborolan-2′-yl)-1H-pyrrole-1-carboxylate, 366[17]

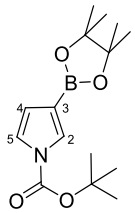

General procedure D was applied to tert-butyl 1H-pyrrole-1-carboxylate (167 mg, 1.0 mmol) which was heated for 3 minutes. Purification by silica flash-column chromatography eluting with 100% DCM afforded tert-butyl 3-(4′,4′,5′,5′-tetramethyl-1′,3′,2′-dioxaborolan-2′-yl)-1H-pyrrole-1-carboxylate as a white solid (287 mg, 98%); m.p. 76 - 77 °C; ν_{max} ($CHCl_3$) 2983, 1731 (C=O), 1560, 1487, 1376, 1323, 1287, 1134, 968, 755, 689 cm^{-1}; ^1H NMR (400 MHz, CD_3OD) δ 7.55 (t, *J* = 1.6, 1H, Ar-5-***H***), 7.23 (dd, *J* = 1.6, 3.1, 1H, Ar-4-***H***), 6.39 (dd, *J* = 1.6, 3.1, 1H), 1.61 (s, 9H), 1.31 (s, 12H); ^{13}C NMR (101 MHz, $CDCl_3$) δ 148.8 (***C***O_2Me), 129.0 (***C***-2), 121.0 (***C***-5), 116.4 (***C***-4), 84.1 (pin-***C***$(CH_3)_2$), 83.5 (^{t}Bu-***C***$(CH_3)_3$), 28.2 (^{t}Bu-***CH₃***), 25.0 (pin-***CH₃***); ^{11}B NMR (128 MHz, $CDCl_3$) δ 29.45; *m/z* (GC-MS, EI) 293 (17%, M^+), 278 (4%, M^+-CH_3), 237 (72%, M^+-^{t}Bu), 222 (16%, M^+-^{t}BuO), 193 (37%, M^+-$CO_2{}^t$Bu), 178 (53%), 138 (23%), 107 (69%), 93 (32%), 57 (100%, ^{t}Bu).

methyl 4-(2′,5′-dimethylfuran-3′-yl)benzoate, 367

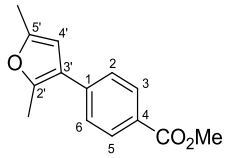

General procedure E was applied to 2,5-dimethylfuran (96 mg, 106 μL, 1.0 mmol). The borylation reaction was heated for 5 minutes. Purification by silica flash-column chromatography eluting with 5% EtOAc:hexanes afforded methyl 4-(2′,5′-dimethylfuran-3′-yl)benzoate (220 mg, 96%); m.p. 88 - 89 °C; ν_{max} ($CHCl_3$) 2977, 1708 (C=O), 1600, 1438, 1364, 1240, 1033, 845, 710 cm^{-1}; ^1H NMR (700 MHz, $CDCl_3$) δ 8.04 (d, *J* = 8.5, 2H, 3,5-***H***), 7.43 (d, *J* = 8.5, 2H, 2,6-***H***), 6.15 (s, 1H, 3′-***H***), 3.92 (s, 3H, O***CH₃***), 2.44 (s, 3H, C***H₃***), 2.30 (s, 3H, C***H₃***); ^{13}C NMR (176 MHz, $CDCl_3$) δ 167.2 (***C***O_2CH_3), 150.4 (***C***-5′), 147.2 (***C***-2′), 139.5 (***C***-1), 130.1 (***C***-4), 127.8 (***C***-2,6), 127.2 (***C***-3,5), 121.0 (***C***-3′), 106.8 (***C***-4′), 52.3 (O***CH₃***), 13.6 (***CH₃***), 13.5 (***CH₃***); GC-MS (EI) - (M^+) 230 (100%, M^+), 199 (38%), 171 (10%); HRMS (ASAP) *m/z* found $(M+H)^+$ 231.1017, $C_{14}H_{15}O_3$ requires *M* 231.1016.

methyl 4-(2′,5′-dimethylthiophen-3-yl)benzoate, 368

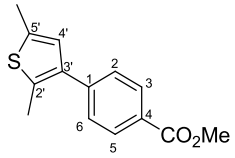

General procedure E was applied to 2,5-dimethylthiophene (114 mg, 112 μL, 1.0 mmol). The borylation reaction was heated for 5 minutes. Purification by silica flash-column chromatography eluting with 5% EtOAc:hexanes to afford methyl 4-(2′,5′-dimethylthiophen-3′-yl)benzoate (236 mg, 96%); m.p. 93 - 94 °C ; ν_{max} ($CHCl_3$) 2975, 1706 (C=O), 1600, 1431, 1355, 1240, 1139, 1113, 863, 849, 710 cm^{-1}; ^1H NMR (500 MHz, $CDCl_3$) δ 8.06 (d, *J* = 8.3, 2H, 3,5-***H***), 7.43 (d, *J* = 8.3, 2H, 2,6-***H***), 6.73 (s, 1H, 3′-***H***), 3.93 (s, 3H, O***CH₃***), 2.45 (s, 6H, C***H₃***); ^{13}C NMR (126 MHz, $CDCl_3$) δ 167.2 (***C***O_2CH_3), 141.8 (***C***-5′), 137.4 (***C***-1), 136.3 (***C***-3′), 133.3 (***C***-2′), 129.9 (***C***-2,6), 128.6 (***C***-3,5), 128.2 (***C***-1), 127.1 (***C***-4′), 52.3 (O***CH₃***), 15.3 (***CH₃***), 14.5 (***CH₃***); GC-MS (EI) - (M^+) 246 (100%, M^+), 231 (10%), 215 (28%), 187 (17%), 171 (11%); HRMS (ASAP) *m/z* found $(M+H)^+$ 247.0790, $C_{14}H_{15}O_2S$ requires *M* 247.0787.

tert-butyl 3-(4′-(methoxycarbonyl)phenyl)-1H-pyrrole-1-carboxylate, 369

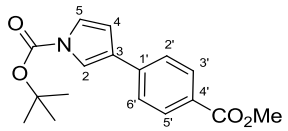

General procedure E was applied to tert-butyl 1H-pyrrole-1-carboxylate (167 mg, 1.0 mmol). The borylation reaction was heated for 5 minutes. Purification by silica flash-column chromatography eluting with 5% EtOAc:hexanes to afford tert-butyl 3-(4′-(methoxycarbonyl)phenyl)-1H-pyrrole-1-carboxylate (285 mg, 95%); m.p. 98 - 99 °C (from hexane); ν_{max} ($CHCl_3$) 2908, 1733 (C=O), 1706 (C=O), 1607, 1560, 1508, 1406, 1269, 1193, 970, 764, 685 cm^{-1}; ^1H NMR (500 MHz, $CDCl_3$) δ 8.07 - 7.99 (m, 2H, 3′,5′-H), 7.65 - 7.56 (m, 3H, 2′,6′-***H***, 5-***H***), 7.32 (s, 1H, 2-***H***), 6.60 (dd, *J* = 1.8, 3.3, 1H, 4-***H***), 3.94 (s, 3H, O***CH₃***), 1.64 (s, 9H, C***(CH₃)₃***); ^{13}C NMR (126 MHz, $CDCl_3$) δ 167.2 (***C***O_2Me), 148.9 (*N*-***C***$O_2{}^t$Bu), 139.1 (***C***-1′), 130.4 (***C***-2′,6′), 128.2 (***C***-4′), 127.0 (***C***-3), 125.4 (***C***-3′,5′), 121.6 (***C***-5), 117.1 (***C***-2), 110.5 (***C***-4), 84.5 (***C***$(CH_3)_3$), 52.3 (CO_2***CH₃***), 28.2 (C***(CH₃)₃***); *m/z* GC-MS (EI) - (M^+) 301 (12%, M^+), 245 (100%), 201 (57%), 170 (42%); HRMS (ASAP) *m/z* found $(M+H)^+$ 302.1390, $C_{17}H_{20}O_4N$ requires *M* 302.1387.

2,6-dimethyl-5-(4′,4′,5′,5′-tetramethyl-1′,3′,2′-dioxaborolan-2′-yl)quinoline, 420

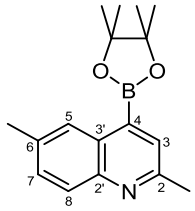

General procedure F was applied to 2,6-dimethylquinoline (157 mg, 1.0 mmol). Purification by flash-column chromatography on neutral alumina with gradient elution of MeOH/DCM from 0.5 - 5% over 25 column volumes, affording 2,6-dimethyl-5-(4′,4′,5′,5′-tetramethyl-1′,3′,2′-dioxaborolan-2′-yl)quinoline as a white solid (203 mg, 72%); m.p. 96 - 97 °C; ν_{max} ($CHCl_3$) 3021, 1519, 1474, 1423, 1381, 1364, 1331, 1225, 1141, 1016, 928, 849, 793 cm^{-1}; ^1H NMR (500 MHz, $CDCl_3$) δ 8.31 (s, br, 1H, 5-***H***), 7.90 (d, *J* = 8.5, 1H (8-***H***), 7.70 (s, 1H, 3-***H***), 7.49 (dd, *J* = 1.9, 8.5, 1H, 7-***H***), 2.72 (s, 3H, 2-***CH₃***), 2.54 (s, 3H, 6-***CH₃***), 1.43 (s, 12H, pin-***CH₃***); ^{13}C NMR (126 MHz, CDCl3) δ 157.2 (***C***-2), 146.4 (***C***-2′), 135.8 (***C***-6), 131.4 (***C***-7), 129.9 (***C***-3), 129.4 (***C***-3′), 128.9 (***C***-8), 127.1 (***C***-5), 84.6 (pin-***C***$(CH_3)_2$, 25.3 (6-***CH₃***), 25.2 (pin-***CH₃***), 22.1 (2-***CH₃***); ^{11}B NMR (128 MHz, $CDCl_3$) δ 31.32; *m/z* (GC-MS, EI) 283 (100%, M^+), 268 (15%, M^+-CH_3) , 240 (10%, M^+-$C(CH_3)_2$), 226 (5%, M^+-$CO(CH_3)_2$), 210 (19%), 197 (17%), 183 (78%, M^+-$CO(CH_3)_2C(CH_3)_2$); HRMS (ASAP) *m/z* found $(M)^+$ 282.1769, requires $C_{17}H_{22}{}^{10}BNO_2$ *M* 282.1780.

6-methoxy-2-methyl-4-(4′,4′,5′,5′-tetramethyl-1′,3′,2′-dioxaborolan-2′-yl)quinoline, 421

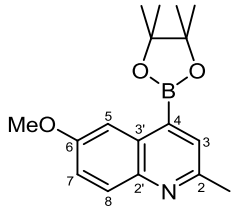

General procedure F was applied to 2-methyl-6-methoxyquinoline (173 mg, 1.0 mmol). Purification by silica gel flash-column chromatography with gradient elution of MeOH/DCM from 0.5 - 12.5% over 25 column volumes, affording 6-methoxy-2-methyl-4-(4′,4′,5′,5′-tetramethyl-1′,3′,2′-dioxaborolan-2′-yl)quinoline as an off-white solid (227 mg, 76%); m.p. 121 - 122 °C; ν_{max} ($CHCl_3$) 3020, 1620, 1519, 1475, 1420, 1382, 1364, 1332, 1225, 1142, 963, 928,

849, 718, 666 cm^{-1}; ^{1}H NMR (500 MHz, $CDCl_3$) δ 8.00 (d, *J* = 2.8, 1H, 5-***H***), 7.92 (d, *J* = 9.2, 1H, 8-***H***), 7.70 (s, 1H, 3-***H***), 7.33 (dd, *J* = 2.8, 9.2, 1H, 7-***H***), 3.93 (s, 3H, 6-O***CH₃***), 2.70 (s, 3H, 2-***CH₃***), 1.43 (s, 12H, pin-***CH₃***); ^{13}C NMR (126 MHz, $CDCl_3$) δ 157.5 (***C***-2), 155.6 (***C***-2′), 143.9 (***C***-6), 130.5 (***C***-3′), 130.4 (***C***-8), 130.1 (***C***-3), 121.3 (***C***-7), 106.7 (***C***-5), 84.6 (pin-***C***$(CH_3)_2$), 55.5 (6-O***CH₃***), 25.2 (pin-***CH₃***), 25.0 (2-***CH₃***); ^{11}B NMR (128 MHz, $CDCl_3$) δ 31.09; *m/z* (GC-MS, EI) 299 (100%, M^+), 284 (5%, M^+- CH_3), 226 (21%), 199 (25%, M^+- $CO(CH_3)_2C(CH_3)_2$), 184 (5%), 156 (11%); HRMS (ASAP) *m/z* found $(M+H)^+$ 299.1805, $C_{17}H_{23}{}^{10}BNO_3$ requires *M* 299.1807.

6-chloro-2-methyl-4-(4′,4′,5′,5′-tetramethyl-1′,3′,2′-dioxaborolan-2′-yl)quinoline, 422

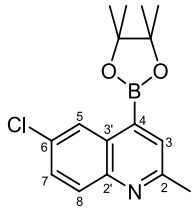

General procedure F was applied to 2-methyl-6-chloroquinoline (177 mg, 1.0 mmol). Purification by silica gel flash-column chromatography with gradient elution of MeOH/DCM from 0.5 - 12.5% over 25 column volumes, affording 6-chloro-2-methyl-4-(4′,4′,5′,5′-tetramethyl-1′,3′,2′-dioxaborolan-2′-yl)quinoline as a white solid (239 mg, 79%); m.p. 105 - 106 °C; ν_{max} ($CHCl_3$) 3019, 1504, 1473, 1426, 1362, 1225, 1016, 928, 793, 666 cm^{-1}; ^{1}H NMR (700 MHz, $CDCl_3$) δ 8.59 (d, *J* = 2.3, 1H, Ar-5-***H***), 7.94 (d, *J* = 8.9, 1H, Ar-8-***H***), 7.77 (s, 1H, Ar-3-***H***), 7.60 (dd, *J* = 2.3, 8.9, 1H, Ar-7-***H***), 2.73 (s, 3H, Ar-***CH₃***), 1.43 (s, 12H, pin-***CH₃***); ^{13}C NMR (176 MHz, $CDCl_3$) δ 158.3 (Ar-2-***C***), 146.1 (Ar-2′-***C***), 131.6 (Ar-6-***C***), 130.6 (Ar-3-***C***), 130.4 (Ar-8-***C***), 129.81 (Ar-3′-***C***), 129.78 (Ar-7-***C***), 127.0 (Ar-5-***C***), 84.6 (pin-***C***$(CH_3)_2$), 24.9 (Ar-***CH₃***), 24.6 (pin-***CH₃***); ^{11}B NMR (128 MHz, $CDCl_3$) δ 30.60; *m/z* (GC-MS, EI) 305 (34%, $M^+(^{37}Cl)$), 303 (100%, $M^+(^{35}Cl)$), 290 (7%, $M^+(^{37}Cl)$ -CH_3), 288 (23%, $M^+(^{35}Cl)$ -CH_3), 245 (6%, $M^+(^{35}Cl)$ -$CO(CH_3)_2$), 221 (43%, $M^+(^{37}Cl)$ -$C(CH_3)_2C(CH_3)_2$), 219 (15%, $M^+(^{35}Cl)$ -$C(CH_3)_2C(CH_3)_2$), 205 (24%, $M^+(^{37}Cl)$ -$CO(CH_3)_2C(CH_3)_2$), 203 (76%, $M^+(^{35}Cl)$ -$CO(CH_3)_2C(CH_3)_2$), 184 (27%, M^+ -Cl,$C(CH_3)_2C(CH_3)_2$), 141 (9%); HRMS (ASAP) *m/z* found $(M)^+$ 303.1299, $C_{16}H_{19}{}^{10}BNO_2{}^{35}Cl$ requires *M* 303.1312.

6-bromo-2-methyl-4-(4′,4′,5′,5′-tetramethyl-1′,3′,2′-dioxaborolan-2′-yl)quinoline, 423

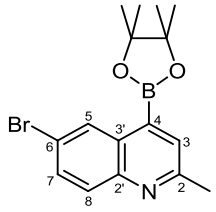

General procedure F was applied to 2-methyl-6-bromoquinoline (222 mg, 1.0 mmol). Purification by silica gel flash-column chromatography with gradient elution of MeOH/DCM from 0.5 - 12.5% over 25 column volumes, affording 6-bromo-2-methyl-4-(4′,4′,5′,5′-tetramethyl-1′,3′,2′-dioxaborolan-2′-yl)quinoline as a white solid (292 mg, 84%); m.p. 124 - 125 °C; Anal. found C, 55.0; H, 5.5; N, 4.1%; Calcd. for $C_{16}H_{19}BBrNO_2$ C, 55.2; H, 5.5; N, 4.0%; ν_{max} ($CHCl_3$) 3020, 1601, 1520, 1475, 1423, 1390, 1364, 1332, 1304, 1228, 1141, 1017, 928, 848, 718 cm^{-1}; ^1H NMR (500 MHz, $CDCl_3$) δ 8.75 (d, *J* = 2.2, 1H, Ar-5-***H***), 7.87 (d, *J* = 8.9, 1H, Ar-8-***H***), 7.76 (s, 1H, Ar-3-***H***), 7.73 (dd, *J* = 2.2, 8.9, 1H, Ar-7-***H***), 2.72 (s, 3H, Ar-***CH₃***), 1.43 (s, 12H, pin-***CH₃***); ^{13}C NMR (126 MHz, CDCl3) δ 158.6 (Ar-2-***C***), 146.4 (Ar-2′-***C***), 132.5 (Ar-***C***), 130.8 (Ar-***C***), 130.7 (Ar-***C***), 130.48 (Ar-***C***), 130.46 (Ar-***C***), 120.1 (Ar-7-***C***), 84.8 (pin-***C***$(CH_3)_2$), 25.3 (Ar-***CH₃***), 25.1 (pin-***CH₃***); ^{11}B NMR (128 MHz, $CDCl_3$) δ 31.19; *m/z* (GC-MS, EI) 349 (98%, $M^+(^{81}Br)$), 347 (100%, $M^+(^{79}Br)$), 334 (17%, $M^+(^{81}Br)$ -CH_3), 332 (17%, $M^+(^{79}Br)$ -CH_3), 291 (6%, $M^+(^{81}Br)$ -$CO(CH_3)_2$), 289 (6%, $M^+(^{79}Br)$ -$CO(CH_3)_2$), 249 (59%, $M^+(^{81}Br)$ -$CO(CH_3)_2C(CH_3)_2$), 247 (59%, $M^+(^{79}Br)$ -$CO(CH_3)_2C(CH_3)_2$), 226 (18%, M^+ -Br, $CO(CH_3)_2C(CH_3)_2$), 211 (29%, -Br, $C(CH_3)_2$,CH_3), 181 (33%, M^+ -Br,$CO(CH_3)_2C(CH_3)_2$), 169 (17%), 141 (20%); HRMS (ASAP) *m/z* found $(M)^+$ 346.0715, $C_{16}H_{19}{}^{10}BBrNO_2$ requires *M* 346.0729.

6-methoxy-4-(4′,4′,5′,5′-tetramethyl-1′,3′,2′-dioxaborolan-2′-yl)quinoline-2-carbonitrile, 424

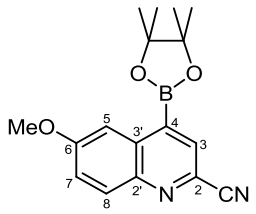

General procedure G was applied to 6-methoxyquinoline-2-carbonitrile (184 mg, 1.0 mmol). The reaction was stirred at room temperature for 18 hours. Upon completion, volatiles were removed under reduced pressure and the remaining residue was purified by silica gel flash-column chromatography with gradient elution of MeOH/DCM from 0.5 - 12.5% over 25 column volumes, affording 6-methoxy-4-(4′,4′,5′,5′-tetramethyl-1′,3′,2′-dioxaborolan-2′-yl)quinoline-2-carbonitrile as a off-white solid (270 mg, 87%); m.p. 230 - 231 °C; Anal. Calcd. for $C_{17}H_{19}BN_2O_3$: C, 65.8; H, 6.2; N, 9.0 found: C, 65.3; H, 6.1; N, 8.8%; ν_{max} ($CHCl_3$) 3019, 2216, 1619, 1477, 1415, 1372, 1336, 1218, 1140, 1028, 963, 928, 848, 689 cm^{-1}; ^1H NMR (500 MHz, $CDCl_3$) δ 8.12 (s, 1H, Ar-3-***H***), 8.08 (d, *J* = 2.7, 1H, Ar-5-***H***), 8.06 (d, *J* = 9.3, 1H, Ar-8-***H***), 7.48 (dd, *J* = 2.8, 9.3, 1H, Ar-7-***H***), 4.00 (s, 3H, Ar-O***CH₃***), 1.46 (s, 12H, pin-***CH₃***); ^{13}C NMR (126 MHz, $CDCl_3$) δ 160.4 (Ar-6-***C***), 144.6 (Ar-2′-***C***), 133.8 (Ar-3′-***C***), 131.9 (Ar-8-***C***), 131.4 (Ar-3-***C***), 130.3 (Ar-2-***C***), 124.1 (Ar-7-***C***), 118.2 (Ar-***CN***), 106.2 (Ar-5-***C***) , 85.2 (pin-***C***$(CH_3)_2$), 55.8 (Ar-O***CH₃***), 25.3 (pin-***CH₃***); ^{11}B NMR (128 MHz, $CDCl_3$) δ 30.64; *m/z* (GC-MS, EI) 310 (100%, M^+), 295 (19%, M^+-CH_3), 253 (7%, M^+-$CO(CH_3)_2$), 237 (26%), 224 (40%), 210 (64%, M^+-$CO(CH_3)_2C(CH_3)_2$), 180 (11%), 167 (15%); HRMS (ASAP) *m/z* found $(M)^+$ 310.1590, $C_{17}H_{19}{}^{10}BNO_3$ requires *M* 310.1603.

4,7-dichloro-3-(4′,4′,5′,5′-tetramethyl-1′,3′,2′-dioxaborolan-2′-yl)quinoline, 427

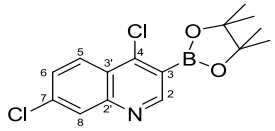

General procedure F was applied to 4,7-dichloroquinoline (196 mg, 1.0 mmol). Purification by recrystallisation from acetonitrile, afforded 4,7-dichloro-3-(4′,4′,5′,5′-tetramethyl-1′,3′,2′-

dioxaborolan-2′-yl)quinoline as a pale yellow crystalline solid (258 mg, 81%); m.p. 127 - 128 °C; ν_{max} ($CHCl_3$) 3020, 1604, 1474, 1422, 1375, 1225, 1016, 928, 849, 793 cm^{-1}; ^1H NMR (400 MHz, $CDCl_3$) δ 9.03 (s. 1H, 2-***H***), 8.28 (d, *J* = 9.0, 1H, 5-***H***), 8.11 (d, *J* = 2.0, 1H, 8-***H***), 7.58 (dd, *J* = 2.0, 9.0, 1H, 6-***H***), 1.41 (s, 12H, pin-***CH₃***); ^{13}C NMR (126 MHz, $CDCl_3$) δ 156.2 (***C***-2), 150.4 (***C***-2′), 150.0 (Ar-***C***), 149.9 (Ar-***C***), 137.5 (***C***-4), 128.8 (***C***-6), 126.7 (***C***-5), 125.2 (Ar-***C***), 85.0 (pin-***C***$(CH_3)_2$), 25.1 (pin-***CH₃***); ^{11}B NMR (128 MHz, $CDCl_3$) δ 30.32; *m/z* (GC-MS, EI) 325 (40%, $M^+(^{37}Cl^{37}Cl)$), 324 (20%, $M^+(^{35}Cl^{37}Cl)$), 323 (62%, $M^+(^{35}Cl^{35}Cl)$), 310 (20%, $M^+(^{37}Cl^{37}Cl)$-CH_3), 309 (10%, $M^+(^{35}Cl^{37}Cl)$-CH_3), 308 (30%, $M^+(^{35}Cl^{35}Cl)$-CH_3), 290 (22%, $M^+(^{37}Cl)$ -Cl), 287 (65%, $M^+(^{35}Cl)$ -Cl), 267 (26%, $M^+(^{37}Cl^{37}Cl)$-$CO(CH_3)_2$) 266 (11%, $M^+(^{35}Cl^{37}Cl)$-$CO(CH_3)_2$), 265 (40%, $M^+(^{35}Cl^{35}Cl)$-$CO(CH_3)_2$), 245 (15%, $M^+(^{37}Cl)$ -Cl, $3CH_3$), 243 (47%, $M^+(^{35}Cl)$ -Cl, $3CH_3$), 225 (64%, $M^+(^{37}Cl^{37}Cl)$ -$CO(CH_3)_2C(CH_3)_2$), 224 (25%, $M^+(^{35}Cl^{37}Cl)$ -$CO(CH_3)_2C(CH_3)_2$), 223 (100%, $M^+(^{35}Cl^{35}Cl)$ -$CO(CH_3)_2C(CH_3)_2$), 190 (15%, $M^+(^{37}Cl)$ -Cl, $CO(CH_3)_2C(CH_3)_2$), 188 (46%, $M^+(^{35}Cl)$ -Cl, $CO(CH_3)_2C(CH_3)_2$); HRMS (ASAP) *m/z* found $(M)^+$ 323.0771, $C_{15}H_{16}{}^{10}B^{35}Cl_2NO_2$ requires *M* 323.0766.

4-chloro-3-(4,4,5,5-tetramethyl-1,3,2-dioxaborolan-2-yl)-7-(trifluoromethyl)quinoline, 428

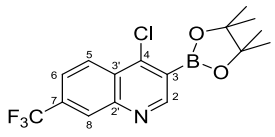

General procedure F was applied to 4-chloro-7-(trifluoromethyl)quinoline (231 mg, 1.0 mmol). Purification by recrystallisation from acetonitrile, affordied 4-chloro-3-(4,4,5,5-tetramethyl-1,3,2-dioxaborolan-2-yl)-7-(trifluormethyl)quinoline as a white solid (289 mg, 81%); m.p. 93 - 94 °C; Anal. found C, 54.0; H, 4.6; N, 3.7%; Calcd. for $C_{16}H_{16}BClF_3NO_2$ C, 53.7; H, 4.5; N, 3.9%; ν_{max} ($CHCl_3$) 3019, 1520, 1475, 1422, 1225, 1140, 928, 849, 792 cm^{-1}; ^1H NMR (500 MHz, $CDCl_3$) δ 9.12 (s, 1H, 2-***H***), 8.47 (d, *J* = 8.8, 1H, 5-***H***), 8.42 (s, br, 1H, 8-***H***), 7.80 (dd, *J* = 1.6, 8.8, 1H, 6-***H***), 1.43 (s, 12H, pin-***CH₃***); ^{13}C NMR (176 MHz, $CDCl_3$) δ 156.2 (***C***-2), 149.5 (***C***-2′), 149.0 (Ar-***C***), 132.6 (q, $^2J_{C\text{-}F}$ = 32.9, ***C***-7), 127.9 (Ar-***C***), 127.5 (***C***-8), 126.4 (***C***-5), 123.7 (q, $^1J_{C\text{-}F}$ = 272.8, 7-***CF₃***), 123.1 (***C***-6), 84.9 (pin-***C***$(CH_3)_2$), 24.9 (pin-***CH₃***); ^{11}B NMR (128 MHz, $CDCl_3$) δ 30.78; ^{19}F NMR (376 MHz, $CDCl_3$) δ -62.88; *m/z* (GC-MS, EI) 359 (12%, $M^+(^{37}Cl)$),

357 (38%, $M^+(^{35}Cl)$), 344 (11%, $M^+(^{37}Cl)$ -CH_3), 342 (34%, $M^+(^{35}Cl)$ -CH_3), 322 (100%, M^+-Cl), 301 (15%, $M^+(^{37}Cl)$ -$CO(CH_3)_2$), 299 (48%, $M^+(^{35}Cl)$ -$CO(CH_3)_2$), 280 (62%, M^+ -Cl, $C(CH_3)_2$), 259 (22%, $M^+(^{37}Cl)$ -$CO(CH_3)_2C(CH_3)_2$), 257 (68%, $M^+(^{35}Cl)$ -$CO(CH_3)_2C(CH_3)_2$), 222 (48%, M^+ -Cl, $CO(CH_3)_2C(CH_3)_2$); HRMS (ASAP) *m/z* found $(M+H)^+$ 357.1027, $C_{16}H_{16}{}^{10}B^{35}ClF_3NO_2$ requires *M* 357.1029.

4-methyl-7-(trifluoromethyl)quinoline, 434

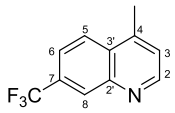

A 50 mL round bottomed flask was charged with 4-chloro-7-(trifluoromethyl)quinoline (723 mg, 3.13 mmol), methylboronic acid (562 mg, 9.4 mmol), palladium (II) acetate (67mg, 0.3 mmol), S-Phos (192 mg, 0.5 mmol) and K_3PO_4 (1.0g, 4.5 mmol). Degassed toluene (20 mL) was added and the reaction mixture then heated in an oil bath at 110 °C for 20 hours. The reaction was then cooled to room temperature and diluted with EtOAc (50 mL). The organic layer was washed with water. The combined aqueous washings were then back extracted with EtOAc (3 x 50 mL). The combined organics were washed with brine (3 x 20 mL), dried over $MgSO_4$ and filtered. The solvent was evaporated under reduced pressure and the remaining oil was purified by silica gel flash column chromatography with 40% EtOAc/hexane affording 4-methyl-7-(trifluoromethyl)quinoline as an off white solid (614 mg, 93%); m.p. 67 - 68 °C; Anal. Calcd. for $C_{11}H_8F_3N$: C, 62.6; H, 3.8; N, 6.6 found: C, 62.0; H, 3.9; N, 6.6%; ν_{max} ($CHCl_3$) 3018, 1599, 1519, 1475, 1457, 1423, 1329, 1303, 1225, 1160, 1133, 1088, 839, 847, 666 cm^{-1}; ^1H NMR (700 MHz, $CDCl_3$) δ 8.87 (d, *J* = 4.2, 1H, 2-***H***), 8.41 (s, br, 1H, 8-***H***), 8.13 (d, *J* = 8.7, 1H, 5-***H***), 7.74 (dd, *J* = 1.5, 8.7, 1H, 6-***H***), 7.35 (d, *J* = 4.2, 1H, 3-***H***), 2.75 (s, 3H, 4-***CH₃***); ^{13}C NMR (176 MHz, $CDCl_3$) δ 151.8 (***C***-2), 147.4 (***C***-2′), 144.6 (***C***-4), 131.2 (q, $^2J_{C-F}$ = 32.6, (***C***-7)), 130.1 (***C***-3′), 128.1 (q, $^3J_{C-F}$ = 4.4, ***C***-8), 125.4 (***C***-5), 124.2 (q, $^1J_{C-F}$ = 272.8, 7-***CF₃***), 123.7 (***C***-3), 122.2 (q, $^3J_{C-F}$ = 3.2, (***C***-6)), 18.9 (4-***CH₃***); ^{19}F NMR (376 MHz, $CDCl_3$) δ -62.63; *m/z* (GC-MS, EI) 211 (100%, M^+), 192 (6%, M^+-F), 172 (4%, M^+-2F), 142 (8%, M^+-CF_3), 115 (9%); HRMS (ASAP) *m/z* found $(M)^+$ 211.0583, $C_{11}H_8NF_3$ requires *M* 211.0609.

7-bromo-2-methylquinoline, 450[18]

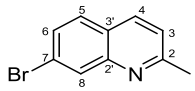

3-bromoaniline (25 g, 145 mmol, 15.82 mL) was added to a 250 mL two-necked round bottom flask fitted with a condenser and a septum. Hydrochloric acid 5 M (100 mL) was added and the resultant mixture heated to 110 °C. Crotonaldehyde (12.22 g, 174 mmol, 14.45 mL) was then added as a solution in toluene (10 mL) over a period of 1 hour using a syringe pump. Upon complete addition of the aldehyde the reaction was heated for a further 1 hour and the solution was allowed to cool to 60 °C. To this hot solution, $ZnCl_2$ (19.72 g, 145 mmol) was added slowly as a solution in THF/acetone (50 mL, 1:1), causing a precipitate to form. The reaction vessel was then allowed to cool to room temperature and then cooled in an ice bath for 1 hour. The solid was filtered, washed with cold HCl (5 M) (200 mL), THF (200 mL), isopropyl alcohol (200 mL) and diethyl ether (200 mL).The resultant white solid dissolved in a mixture of hexane (100 mL) and aqueous ammonia (29%, 50 mL) and stirred until complete dissolution had been achieved. The organic layer was separated and the aqueous layer extracted with diethyl ether (3 x 50 mL). The combined organics were dried over $MgSO_4$, filtered and evaporated under reduced pressure. The resulting solid was purified by silica gel flash column chromatography (hexane:Ethyl acetate, 8:2) affording 7-bromo-2-methylquinoline as a white solid (10.04 g, 31%); m.p. 77 - 78 °C; Anal. found C, 54.1; H, 3.6; N, 6.3%; Calcd. for $C_{10}H_8BrN$ C, 54.1; H, 3.6; N, 6.3%; ν_{max} ($CHCl_3$) 3021, 1525, 1423, 1225, 1016, 928, 669 cm^{-1}; ^1H NMR (700 MHz, $CDCl_3$) δ 8.20 (d, *J* = 1.8, 1H, 8-***H***), 7.99 (d, *J* = 8.4, 1H, 4-***H***), 7.62 (d, *J* = 8.6, 1H, 5-***H***), 7.55 (dd, *J* = 1.8, 8.6, 1H, 6-***H***), 7.28 (d, *J* = 8.4, 1H, 3-***H***), 2.73 (s, 3H, 2-$\boldsymbol{CH_3}$); ^{13}C NMR (176 MHz, $CDCl_3$) δ 160.4 (***C***-2), 148.7 (***C***-2′), 136.1 (***C***-4), 131.4 (***C***-8), 129.4 (***C***-6), 128.9 (***C***-5), 125.3 (***C***-3′), 123.6 (***C***-7), 122.5 (***C***-3), 25.6 (2-$\boldsymbol{CH_3}$); *m/z* (GC-MS, EI) 223 (98%, $M^+(^{81}Br)$), 221 (100%, $M^+(^{79}Br)$), 208 (5%, $M^+(^{81}Br)$ -CH_3), 206 (5%, $M^+(^{79}Br)$ -CH_3), 142 (18%, M^+ -Br), 127 (7%, M^+ -Br,CH_3), 115 (28%); HRMS (ASAP) *m/z* found $(M)^+$ 220.9840, $C_{10}H_8N^{79}Br$ requires *M* 220.9832.

2-methyl-7-(trifluoromethyl)quinoline, 452[19]

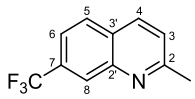

3-(Trifluoromethyl)aniline (6.44 g, 40 mmol, 5.0 mL) was added to a 100 mL two-necked round bottom flask fitted with a condenser and a septum. Hydrochloric acid 5 M (20 mL) was added and the mixture heated to 110 °C. Crotonaldehyde (4.21 g, 60 mmol, 4.90 mL) was then added as a solution in toluene (5 mL) over a period of 1 hour using a syringe pump. Upon complete addition of the aldehyde the reaction was heated for a further 1 hour, the solution was then allowed to cool to room temperature. The aqueous reaction mixture was extracted with diethyl ether (3 x 50 mL) and the combined organic extracts were washed with brine (3 x 25 mL) and dried over $MgSO_4$ and filtered. The solvent was removed under reduced pressure and the resulting oil was purified by silica gel flash column chromatography eluted with $CHCl_3$ to give 2-methyl-7-(trifluoromethyl)quinoline as a pale yellow crystalline solid (2.16 g, 26%); m.p. 54 - 55 °C; Anal. Calcd. for $C_{11}H_8F_3N$: C, 62.6; H, 3.8; N, 6.6 found: C, 62.4; H, 3.9; N, 6.6%; ν_{max} ($CHCl_3$) 3020, 1610, 1518, 1475, 1423, 1375, 1349, 1319, 1281, 1168, 1062, 1016, 905, 792 cm^{-1}; ^1H NMR (500 MHz, $CDCl_3$) δ 8.34 (s, br, 1H, Ar-8-***H***), 8.10 (d, *J* = 8.4, 1H, 4-***H***), 7.89 (d, *J* = 8.4, 1H, 5-***H***), 7.66 (d, *J* = 8.4, 1H, 6-***H***), 7.41 (d, *J* = 8.4, 1H, 3-***H***), 2.78 (s, 3H, 3-***CH₃***); ^{13}C NMR (126 MHz, $CDCl_3$) δ 160.9 (***C***-2), 147.1 (***C***-2′), 136.2 (***C***-4), 131.4 (q, $^2J_{C\text{-}F}$ = 32.6, ***C***-7), 128.9 (***C***-5), 128.2 (***C***-3′), 126.8 (q, $^3J_{C\text{-}F}$ = 4.4, ***C***-8), 124.3 (q, $^1J_{C\text{-}F}$ = 272.6, 7-***CF₃***), 124.2 (***C***-3), 121.6 (q, $^3J_{C\text{-}F}$ = 3.2, ***C***-6), 25.7 (2-***CH₃***); ^{19}F NMR (188 MHz, $CDCl_3$) δ -62.22; *m/z* (GC-MS, EI) 211 (100%, M^+), 196 (10%, M^+-CH_3), 142 (4%, M^+-CF_3); HRMS (ASAP) *m/z* found $(M)^+$ 211.0634, $C_{11}H_8F_3N$ *M* 211.0609.

7-methoxy-2-methylquinoline, 453[20]

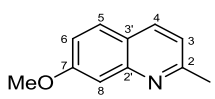

In a 50 mL two-necked round bottom flask, equipped with a condenser, sodium (1.0 g, 43.5 mmol) was added to MeOH (5 mL, 123 mmol) to form sodium methoxide *in situ*. Once all of the sodium had reacted the methanol solvent was removed under reduced pressure, 7-bromo-2-

methylquinoline (2.22 g, 10.0 mmol) was added along with DMF (5 mL). The reaction vessel was heated to 110 °C. Once at the reaction temperature, CuBr (285 mg, 2.0 mmol) was added as a solution in DMF (1.0 mL). The reaction was heated at 110 °C for a further 45 minutes. The reaction was then transferred to a separating funnel and water (100 mL) was added. The layers were separated abd the aqueous layer was extracted with DCM (3 × 50 mL). The combined organic layers were dried over $MgSO_4$, filtered, and concentrated. The resulting oil was purified by silica gel flash column chromatography eluted with 60% EtOAc/hexane yielding 7-methoxy-2-methylquinoline as a pale yellow oil (1.66 g, 96%); ν_{max} ($CHCl_3$) 3019, 2973, 1621, 1603, 1511, 1459, 1419, 1340, 1211, 1174, 1029, 928, 846, 785, 669 cm^{-1}; ^1H NMR (700 MHz, $CDCl_3$) δ 7.93 (d, *J* = 8.2, 1H, 4-***H***), 7.62 (d, *J* = 8.9, 1H, 5-***H***), 7.35 (d, *J* = 2.3, 1H, 8-***H***), 7.15 - 7.10 (m, 2H, 3,6-***H***), 3.92 (s, 3H, 7-O***CH₃***), 2.70 (s, 3H, 2-***CH₃***); ^{13}C NMR (176 MHz, $CDCl_3$) δ 160.9 (***C***-2′), 159.4 (***C***-2), 149.8 (***C***-3′), 136.0 (***C***-4), 128.7 (***C***-5), 121.8 (***C***-7), 119.9 (***C***-3), 118.9 (***C***-6), 107.1 (***C***-8), 55.7 (7-O***CH₃***), 25.5 (2-***CH₃***); *m/z* (GC-MS, EI) 173 (100%, M^+), 158 (4%, M^+-CH_3), 142 (16%, M^+-OCH_3), 130 (43%), 115 (6%), 103 (11%); HRMS (ASAP) *m/z* found $(M)^+$ 173.0852, $C_{11}H_{11}NO$ requires *M* 173.0841.

2-methylquinoline-7-carbonitrile, 454

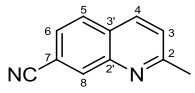

2-methyl-7-bromoquinoline (2.2g, 10 mmol), $Pd(PPh_3)_4$ (115 mg, 1 mol%) and $Zn(CN)_2$ (1.23g, 10.5 mmol) were added to a 20 mL microwave vial. The vial was equipped with a magnetic stirrer bar and sealed with a PTFE crimp top. After purging the reaction with argon, dry DMF (15 mL) was added and the reaction heated at 150 °C for 25 minutes in a microwave reactor. The reaction mixture was then cooled to room temperature before being opened and transferred to a separating funnel. Water (100 mL) was added, the layers separated, extracted with EtOAc (4 × 100 mL) and DCM (2 × 100 mL). The combined organic layers were dried over $MgSO_4$, filtered and the solvent removed under reduced pressure to give a dark brown solid.

The crude product was added to hexane (50 mL) and heated to reflux. The solution was the filtered hot to remove the insoluble impurities. The solute was cooled fin a freezer to afford off-

white crystals. The resulting crystals were filtered and washed with cold hexane yielding the product as a white crystalline solid (1.4 g, 84%); m.p. 99 - 100 °C; Anal. found C, 78.2; H, 4.8; N, 16.6%; Calcd. for $C_{11}H_8N_2$ C, 78.6; H, 4.8; N, 16.7%; ν_{max} ($CHCl_3$) 3018, 2231 (C≡N), 1605, 1526, 1475, 1422, 1225, 1016, 928, 846 cm^{-1}; ^1H NMR (700 MHz, $CDCl_3$) δ 8.37 (s, br, 1H, 8-***H***), 8.09 (d, *J* = 8.4, 1H, 4-***H***), 7.86 (d, *J* = 8.3, 1H, 5-***H***), 7.64 (dd, *J* = 1.5, 8.3, 1H, 6-***H***), 7.43 (d, *J* = 8.4, 1H, 3-***H***), 2.78 (s, 3H, 2-***CH₃***); ^{13}C NMR (176 MHz, $CDCl_3$) δ 161.6 (***C***-2), 147.0 (***C***-2′), 136.1 (***C***-4), 134.8 (***C***-8), 129.1 (***C***-5), 128.8 (***C***-3′), 126.8 (***C***-6), 124.8 (***C***-3), 118.9 (7-***CN***), 113.0 (***C***-7), 25.7 (2-***CH₃***); *m/z* (GC-MS, EI) 168 (100%, M^+), 153 (11%, M^+-CH_3), 142 (11%, M^+-CN); HRMS (ASAP) *m/z* found $(M)^+$ 168.0696; $C_{11}H_8N_2$ requires *M* 168.0687.

2-methyl-7-(trimethylsilyl)quinoline, 459

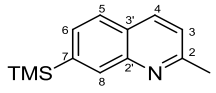

To an oven dried flask purged with argon, 7-bromo-2-methylquinoline (1.1g, 5.0 mmol) was added. To the flask, dry THF (15 mL) and TMEDA (1.0 mL) were added and the resulting solution cooled to -78 °C. *n*-BuLi (1.6M in hexanes) (3.4 mL, 5.5 mmol) was added and stirred for 5 minutes, forming a red coloured solution. TMSCl (1.4 mL, 12 mmol) was then added and the reaction was allowed to stir at -78 C for 10 minutes and then removed from the cold bath and warmed to room temperature. After 30 minutes, water (2.0 mL) was added to quench the reaction. The reaction mixture was extracted with EtOAc (3 × 20 mL) and washed with brine (3 × 20 mL). The combined organics were dried over $MgSO_4$ and the solvent evaporated under reduced pressure. The resulting oil was purified by silica gel flash column chromatography eluting with 20% EtOAc/hexane affording **2-**methyl-7-(trimethylsilyl)quinoline as a colourless oil (692 mg, 64%); ν_{max} ($CHCl_3$) 3019, 2957, 1503, 1475, 1422, 1225, 1084, 927, 840, 665 cm^{-1}; ^1H NMR (500 MHz, $CDCl_3$) δ 8.22 (s, br, 1H, 8-***H***), 8.04 (d, *J* = 8.4, 1H, 4-***H***), 7.77 (d, *J* = 8.0, 1H, 5-***H***), 7.62 (dd, *J* = 0.9, 8.0, 1H, 6-***H***), 7.30 (d, *J* = 8.4, 1H, 3-***H***), 2.77 (s, 3H, 2-***CH₃***), 0.37 (s, 9H, 7-Si***(CH₃)₃***); ^{13}C NMR (126 MHz, $CDCl_3$) δ 159.2 (***C***-2), 147.5 (***C***-2′), 142.8 (***C***-3′), 136.3 (***C***-4), 134.6 (***C***-8), 129.9 (***C***-6), 126.83 (***C***-7), 126.75 (***C***-5), 122.5(***C***-3), 25.7 (2-***CH₃***), -1.0 (7-***Si(CH₃)₃***); *m/z* (GC-MS, EI) 215 (24%, M^+), 200 (100%, M^+-CH_3), 185 (6%, M^+-$2CH_3$),

170 (10%, M^+-3CH_3); HRMS (ASAP) *m/z* found $(M+H)^+$ 216.1207; $C_{13}H_{18}NSi$ requires *M* 216.1209.

2,7-dimethyl-4-(4′,4′,5′,5′-tetramethyl-1′,3′,2′-dioxaborolan-2′-yl)quinoline, 460

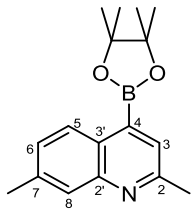

General procedure G was applied to 2,7-dimethylquinoline (157 mg, 1.0 mmol). The reaction was stirred at room temperature (25 °C) for 72 hours. Analysis by GC-MS showed a 95:5 mixture of 2 mono-borylated products. Volatiles were removed from the reaction under reduced pressure and the remaining residue was purified by silica gel flash-column chromatography with gradient elution of MeOH/DCM from 0.5 - 12.5% over 25 column volumes, affording the major isomer, 2,7-dimethyl-4-(4′,4′,5′,5′-tetramethyl-1′,3′,2′-dioxaborolan-2′-yl)quinoline, as an off-white solid (226 mg, 80%); m.p. 108 - 109 °C (from MeCN); ν_{max} ($CHCl_3$) 3020, 1519, 1475, 1422, 1225, 1016, 928, 849, 718, 666 cm^{-1}; ^1H NMR (400 MHz, $CDCl_3$) δ 8.46 (d, *J* = 8.4 Hz, 1H, 5-***H***), 7.79 (s, br, 1H, 8-***H***), 7.67 (s, 1H, 3-***H***), 7.34 (dd, *J* = 8.4, 1.7 Hz, 1H, 6-***H***), 2.72 (s, 3H, 2-***CH₃***), 2.54 (s, 3H, 7-***CH₃***), 1.43 (s, 12H, pin-***CH₃***); ^{13}C NMR (126 MHz, $CDCl_3$) δ 158.1 (***C***-2), 148.1 (***C***-2′), 139.3 (***C***-7), 129.1 (***C***-3), 128.32 (***C***-6), 128.28 (***C***-8), 127.9 (***C***-5), 127.4 (***C***-3′), 84.6 (pin-***C***$(CH_3)_2$), 25.2 (2-***CH₃***), 25.1 (pin-***CH₃***), 22.0 (7-***CH₃***); ^{11}B NMR (128 MHz, $CDCl_3$) δ 31.34; *m/z* (GC-MS, EI) 283 (100%, M^+), 268 (16%, M^+-CH_3), 225 (18%, M^+-$CO(CH_3)_2$), 210 (47%), 197 (30%), 183 (74%, M^+-$CO(CH_3)_2C(CH_3)_2$); HRMS (ASAP) *m/z* found $(M+H)^+$ 283.1851; $C_{17}H_{23}{}^{10}BNO_2$ requires *M* 283.1858.

Application of general procedure F with 2,7-dimethylquinoline (157 mg, 1.0 mmol) afforded a mixture of 3 mono-borylated products in a 82:12:6 ratio, as determined by GC-MS.

2-methyl-4-(4′,4′,5′,5′-tetramethyl-1′,3′,2′-dioxaborolan-2′-yl)-7-(trimethylsilyl)quinoline, 461

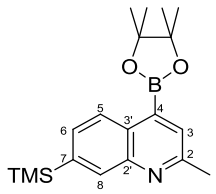

General procedure G was applied to 2-methyl-7-(trimethylsilyl)quinoline (215 mg, 1.0 mmol). The reaction was stirred at room temperature for 48 hours affording a mixture of mono-borylated products in an 85:10:5 ratio by GC-MS. Volatiles were removed under reduced pressure and the remaining residue was purified by silica gel flash-column chromatography with gradient elution of MeOH/DCM from 0.5 - 12.5% over 25 column volumes, affording only the major 2-methyl-4-(4′,4′,5′,5′-tetramethyl-1′,3′,2′-dioxaborolan-2′-yl)-7-(trimethylsilyl)quinoline product as a white solid (231 mg, 68%); m.p. 110 - 111 °C; ν_{max} ($CHCl_3$) 3016, 1522, 1476, 1423, 1212, 1016, 928, 849, 795 cm^{-1}; ^1H NMR (500 MHz, $CDCl_3$) δ 8.56 (d, *J* = 8.2, 1H, 5-***H***), 8.20 (s, br, 1H, 8-***H***), 7.74 (s, 1H, 3-***H***), 7.64 (dd, *J* = 1.1, 8.2, 1H, 6-***H***), 2.74 (s, 3H, Ar-***CH₃***), 1.42 (s, 12H, pin-***CH₃***), 0.34 (s, 9H, Si***(CH₃)₃***; ^{13}C NMR (126 MHz, $CDCl_3$) δ 158.2 (***C***-2), 147.1 (***C***-2′), 142.1 (***C***-6), 134.9 (***C***-8), 130.2 (***C***-6), 130.1 (***C***-3), 129.5 (***C***-3′), 127.2 (***C***-5), 84.6 (pin-***C***$(CH_3)_2$), 25.4 (Ar-***CH₃***), 25.2 (pin-***CH₃***), -1.00 (Ar-Si***(CH₃)₃***); ^{11}B NMR (128 MHz, $CDCl_3$) δ 31.82; *m/z* (GC-MS, EI) 341 (22%, M^+), 326 (100%, M^+-CH_3), 226 (12%, M^+-CH_3,$CO(CH_3)_2C(CH_3)_2$); HRMS (ASAP) *m/z* found $(M)^+$ 341.2096; $C_{19}H_{29}{}^{10}BNO_2Si$ requires *M* 341.2097.

Application of general procedure F with 2-methyl-7-(trimethylsilyl)quinoline (215 mg, 1.0 mmol) afforded a mixture of 3 mono-borylated products in a 70:20:10 ratio, as determined by GC-MS.

7-methoxy-2-methyl-4-(4′,4′,5′,5′-tetramethyl-1′,3′,2′-dioxaborolan-2′-yl)quinoline, 462

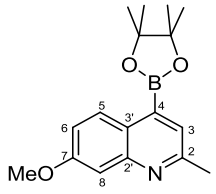

General procedure G was applied to 7-methoxy-2-methylquinoline (173 mg, 1.0 mmol). The reaction was stirred at room temperature for 48 hours affording a 95:5 mixture of 2 mono-borylated products as determined by GC-MS. Volatiles were removed under reduced pressure and the remaining residue was purified by silica gel flash-column chromatography with gradient elution of MeOH/DCM from 0.5 - 12.5% over 25 column volumes, affording the major 7-methoxy-2-methyl-4-(4′,4′,5′,5′-tetramethyl-1′,3′,2′-dioxaborolan-2′-yl)quinoline product as a pale yellow solid (218 mg, 73%); m.p. 87 - 88 °C; ν_{max} ($CHCl_3$) 2982, 1604, 1557, 1495, 1331, 1306, 1266, 1204, 1141, 1083, 987, 792 cm^{-1}; ^1H NMR (700 MHz, $CDCl_3$) δ 8.47 (d, *J* = 9.1, 1H, 5-***H***), 7.61 (s, 1H, 3-***H***), 7.36 (d, *J* = 2.6, 1H, 8-***H***), 7.16 (dd, *J* = 2.6, 9.1, 1H, 6-***H***), 3.94 (s, 3H, 7-O***CH₃***), 2.71 (s, 3H, 2-***CH₃***), 1.42 (s, 12H, pin-***CH₃***); ^{13}C NMR (176 MHz, $CDCl_3$) δ 160.2 (***C***-7), 158.2 (***C***-2), 149.4 (***C***-2′), 129.1 (***C***-5), 127.3 (***C***-3), 124.4 (***C***-3′), 118.7 (***C***-6), 107.1 (***C***-8), 84.4 (pin-***C***$(CH_3)_2$), 55.4 (7-O***CH₃***), 25.0 (2-***CH₃***), 24.9 (pin-***CH₃***); ^{11}B NMR (128 MHz, $CDCl_3$) δ 30.95; *m/z* (GC-MS, EI) 299 (100%, M^+), 284 (8%, M^+-CH_3), 242 (6%, M^+-$CO(CH_3)_2$), 226 (28%), 213 (13%), 199 (41%, M^+-$CO(CH_3)_2C(CH_3)_2$); HRMS (ASAP) *m/z* found $(M)^+$ 298.1749; $C_{17}H_{22}{}^{10}BNO_3$ requires *M* 298.1729.

Application of general procedure F with 7-methoxy-2-methylquinoline (173 mg, 1.0 mmol) afforded a mixture of 3 mono-borylated products in a 90:10 ratio, as determined by GC-MS.

2-methyl-4-(4′,4′,5′,5′-tetramethyl-1′,3′,2′-dioxaborolan-2′-yl)quinoline-7-carbonitrile, 463

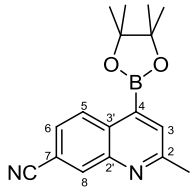

General procedure G was applied to 2-methyl-quinoline-7-carbonitrile (168 mg, 1.0 mmol). The reaction was stirred at room temperature (25 °C) for 48 hours affording a 95:5 mixture of mono-borylated products. Volatiles were removed under reduced pressure and the remaining residue was purified by recrystallisation from acetonitrile, affording only 7-methoxy-2-methyl-4-(4′,4′,5′,5′-tetramethyl-1′,3′,2′-dioxaborolan-2′-yl)quinoline as a white solid (252 mg, 86%); m.p. 149 - 150 °C; Anal. found C, 69.1; H, 6.5; N, 9.4%; Calcd. for $C_{17}H_{19}BN_2O_2$ C, 69.4; H, 6.5; N, 9.5%; ν_{max} ($CHCl_3$) 3021, 2230 (C≡N), 1520, 1475, 1423, 1359, 1335, 1225, 1141, 1016, 928, 850 cm^{-1}; ^1H NMR (500 MHz, $CDCl_3$) δ 8.71 (d, *J* = 8.6, 1H, 5-***H***), 8.36 (d, *J* = 1.5, 1H, 8-***H***), 7.87 (s, 1H, 3-***H***), 7.64 (dd, *J* = 1.5, 8.6, 1H, 6-***H***), 2.76 (s, 3H, 7-***CH₃***), 1.43 (s, 12H, pin-***CH₃***); ^{13}C NMR (126 MHz, $CDCl_3$) δ 160.5 (***C***-2), 146.8 (***C***-2′), 135.0 (***C***-8), 132.6 (***C***-3), 131.7 (***C***-3′), 130.0 (***C***-5), 126.9 (***C***-6), 119.2 (7-***CN***), 112.5 (***C***-7), 85.1 (pin-***C***$(CH_3)_2$), 25.5 (pin-***CH₃***), 25.2 (2-***CH₃***); ^{11}B NMR (128 MHz, $CDCl_3$) δ 30.60; *m/z* (GC-MS, EI) 294 (62%, M^+), 279 (36%, M^+-CH_3), 250 (5%), 237 (7%, M^+-$CO(CH_3)_2$), 221 (14%), 208 (100%), 194 (59%, M^+-$CO(CH_3)_2C(CH_3)_2$); HRMS (ASAP) *m/z* found $(M+H)^+$ 294.1648; $C_{17}H_{20}{}^{10}BNO_2$ requires *M* 294.1654.

Application of general procedure F with 2-methyl-quinoline-7-carbonitrile (168 mg, 1.0 mmol) afforded a mixture of 2 mono-borylated and 1 bis-borylated products in an 89:9:9 ratio, as determined by GC-MS.

7-chloro-2-methyl-5-(4′,4′,5′, 5′-tetramethyl-1′,3′,2′-dioxaborolan-2′-yl)quinoline, 464

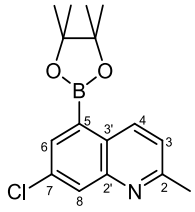

General procedure F was applied to 7-chloro-2-methylquinoline (177 mg. 1.0 mmol). The reaction afforded a 95:5 mixture of 2 mono-borylated products as determined by GC-MS. Purification by silica gel flash-column chromatography with gradient elution of MeOH/DCM from 0.5 - 12.5% over 25 column volumes, afforded 7-chloro-2-methyl-4-(4′,4′,5′,5′-tetramethyl-1′,3′,2′-dioxaborolan-2′-yl)quinoline as a white crystalline solid (245 mg, 81%); m.p. 149 - 150 °C (from MeCN); ν_{max} ($CHCl_3$) 3020, 1475, 1362, 1226, 1016, 928, 793 cm^{-1}; ^1H NMR (700 MHz, $CDCl_3$) δ 8.93 (d, *J* = 8.6, 1H, 4-***H***), 8.09 (d, *J* = 2.2, 1H, 6-***H***), 8.00 (d, *J* = 2.2, 1H, 8-***H***), 7.30 (d, *J* = 8.6, 1H, 3-***H***), 2.72 (s, 3H, 2-***CH₃***), 1.41 (s, 12H, pin-***CH₃***); ^{13}C NMR (176 MHz, $CDCl_3$) δ 159.9 (***C***-2), 148.6 (***C***-2′), 136.9 (***C***-4), 135.7 (***C***-8), 134.8 (***C***-7), 131.1 (***C***-6), 128.8 (***C***-3′), 122.6 (***C***-3), 84.5 (pin-***C***$(CH_3)_2$), 25.5 (2-***CH₃***), 25.2 (pin-***CH₃***); ^{11}B NMR (128 MHz, $CDCl_3$) δ 30.64; *m/z* (GC-MS, EI) 305 (30%, $M^+(^{37}Cl)$), 303 (91%, $M^+(^{35}Cl)$), 290 (10%, $M^+(^{37}Cl)$ -CH_3), 288 (31%, $M^+(^{35}Cl)$ -CH_3), 247 (3%, $M^+(^{37}Cl)$ -$CO(CH_3)_2$), 245 (9%, $M^+(^{35}Cl)$ -$CO(CH_3)_2$), 221 (24%, $M^+(^{37}Cl)$ -$C(CH_3)_2C(CH_3)_2$), 219 (78%, $M^+(^{35}Cl)$ -$C(CH_3)_2C(CH_3)_2$), 205 (32%, $M^+(^{37}Cl)$ -$CO(CH_3)_2C(CH_3)_2$), 203 (100%, $M^+(^{35}Cl)$ -$CO(CH_3)_2C(CH_3)_2$), 141 (11%); HRMS (ASAP) *m/z* found $(M)^+$ 302.1222; $C_{16}H_{19}{}^{10}BClNO_2$ requires *M* 302.1234.

7-bromo-2-methyl-4-(4′,4′,5′,5′-tetramethyl-1′,3′,2′-dioxaborolan-2′-yl)quinoline, 465

7-bromo-2-methyl-5-(4′,4′,5′,5′-tetramethyl-1′,3′,2′-dioxaborolan-2′-yl)quinoline, 466

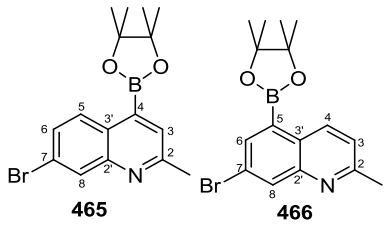

General procedure G was applied to 7-bromo-2-methylquinoline (221 mg, 1.0 mmol). The reaction was stirred at room temperature for 48 hours to afford a mixture of 2 mono-borylated isomers in a 65:35 ratio. Purification by silica gel flash-column chromatography with gradient elution of MeOH/DCM from 0.5 - 12.5% over 25 column volumes, afforded the major product, (*r.f.* 0.1) 7-bromo-2-methyl-4-(4′,4′,5′,5′-tetramethyl-1′,3′,2′-dioxaborolan-2′-yl)quinoline, as a white solid (225 mg, 65%); m.p. 149 - 150 °C; Anal. found C, 55.0; H, 5.5; N, 3.8%; Calcd. for $C_{16}H_{19}BBrNO_2$ C, 55.2; H, 5.5; N, 4.0%; ν_{max} ($CHCl_3$) 3018, 1609, 1515, 1475, 1339, 1225, 1011, 935, 838, 709, cm^{-1}; ^1H NMR (500 MHz, $CDCl_3$) δ 8.46 (d, *J* = 8.9, 1H, 5-***H***), 8.20 (d, *J* = 2.0, 1H, 8-***H***), 7.75 (s, 1H, 3-***H***), 7.57 (dd, *J* = 2.0, 8.9, 1H, 6-***H***), 2.72 (s, 3H, 2-***CH₃***), 1.42 (s, 12H, pin-***CH₃***); ^{13}C NMR (126 MHz, $CDCl_3$) δ 159.3 (***C***-2), 148.5 (***C***-2′), 131.4 (***C***-8), 130.3 (***C***-6), 129.8 (***C***-5), 129.5 (***C***-3′), 128.1 (***C***-7), 123.3 (***C***-3), 84.8 (pin-***C***$(CH_3)_2$), 25.3 (2-***CH₃***), 25.2 (pin-***CH₃***); ^{11}B NMR (128 MHz, $CDCl_3$) δ 30.88; *m/z* (GC-MS, EI) 349 (98%, $M^+(^{81}Br)$), 347 (100%, $M^+(^{79}Br)$), 334 (24%, $M^+(^{81}Br)$ $-CH_3$), 332 (24%, $M^+(^{79}Br)$ $-CH_3$), 291 (9%, $M^+(^{81}Br)$ $-CO(CH_3)_2$), 289 (9%, $M^+(^{79}Br)$ $-CO(CH_3)_2$), 265 (57%, $M^+(^{81}Br)$ $-C(CH_3)_2C(CH_3)_2$), 263 (58%, $M^+(^{81}Br)$ $-C(CH_3)_2C(CH_3)_2$), 249 (72%, $M^+(^{81}Br)$ $-CO(CH_3)_2C(CH_3)_2$), 247 (73%, $M^+(^{79}Br)$ $-CO(CH_3)_2C(CH_3)_2$), 226 (78%, M^+ -Br,$CO(CH_3)_2C(CH_3)_2$), 211 (7%, -Br, $C(CH_3)_2$,CH_3), 181 (9%, M^+ -Br,$CO(CH_3)_2C(CH_3)_2$), 168 (14%), 141 (22%); HRMS (ASAP) *m/z* found $(M)^+$ 346.0727; $C_{16}H_{19}{}^{10}BNO_2{}^{79}Br$ requires *M* 346.0729.

Further elution afforded (*r.f.* 0.05) 7-bromo-2-methyl-5-(4′,4′,5′,5′-tetramethyl-1′,3′,2′-dioxaborolan-2′-yl)quinoline a white solid (52 mg, 15%); m.p. 151 - 152 °C; ν_{max} ($CHCl_3$) 3020, 1602, 1539, 1520, 1475, 1422, 1225, 1016, 928, 848, 718 cm^{-1}; ^1H NMR (500 MHz, $CDCl_3$) δ 8.92 (d, *J* = 8.7, 1H, 4-***H***), 8.28 (d, *J* = 1.9, 1H, 6-***H***), 8.13 (d, *J* = 1.9, 1H, 8-***H***), 7.32 (d, *J* = 8.7,

1H, 3-***H***), 2.73 (s, 3H, 2-***CH₃***), 1.41 (s, 12H, pin-***CH₃***); ^{13}C NMR (126 MHz, $CDCl_3$) δ 159.8 (***C***-2), 148.7 (***C***-2′), 138.2 (***C***-8), 137.0 (***C***-4), 134.5 (***C***-6), 129.1 (***C***-3′), 123.3 (***C***-7), 122.8 (***C***-3), 84.5 (pin-***C***$(CH_3)_2$), 25.5 (2-***CH₃***), 25.2 (pin-***CH₃***); ^{11}B NMR (128 MHz, $CDCl_3$) δ 30.73; *m/z* (GC-MS, EI) 349 (98%, $M^+(^{81}Br)$), 347 (100%, $M^+(^{79}Br)$), 334 (22%, $M^+(^{81}Br)$ -CH_3), 332 (22%, $M^+(^{79}Br)$ -CH_3), 291 (8%, $M^+(^{81}Br)$ -$CO(CH_3)_2$), 289 (8%, $M^+(^{79}Br)$ -$CO(CH_3)_2$), 265 (50%, $M^+(^{81}Br)$ -$C(CH_3)_2C(CH_3)_2$), 263 (51%, $M^+(^{81}Br)$ -$C(CH_3)_2C(CH_3)_2$), 249 (74%, $M^+(^{81}Br)$ -$CO(CH_3)_2C(CH_3)_2$), 247 (75%, $M^+(^{79}Br)$ -$CO(CH_3)_2C(CH_3)_2$), 226 (80%, M^+ -Br, $CO(CH_3)_2C(CH_3)_2$), 211 (7%, -Br, $C(CH_3)_2$,CH_3), 181 (9%, M^+ -Br,$CO(CH_3)_2C(CH_3)_2$), 168 (11%), 141 (22%); HRMS (ASAP) *m/z* found $(M+H)^+$ 347.0825; $C_{16}H_{20}{}^{10}BNO_2{}^{79}Br$ requires *M* 347.0807.

Application of general procedure F with 7-bromo-2-methylquinoline (221 mg, 1.0 mmol) afforded a mixture of 2 mono-borylated products in a 80:20 ratio, as determined by GC-MS.

2-methyl-4-(4′,4′,5′,5′-tetramethyl-1′,3′,2′-dioxaborolan-2′-yl)-7-(trifluoromethyl) quinoline, 467

2-methyl-5-(4′,4′,5′,5′-tetramethyl-1′,3′,2′-dioxaborolan-2′-yl)-7-(trifluoromethyl) quinoline, 468

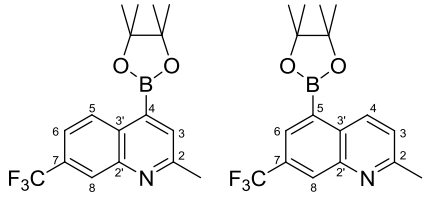

467 **468**

General procedure G was applied to 2-methyl-7-(trifluoromethyl)quinoline (211 mg, 1.0 mmol). The reaction was stirred at room temperature for 72 hours affording 2 mono-borylated products in a 70:30 ratio. Volatiles were removed under reduced pressure and the remaining residue was purified by silica gel flash-column chromatography with gradient elution of EtOAc/hexane from 20 - 75% over 15 column volumes, to afford with the major isomer (*r.f.* 0.15) 2-methyl-4-(4′,4′,5′,5′-tetramethyl-1′,3′,2′-dioxaborolan-2′-yl)-7-(trifluoromethyl)quinoline as a white crystalline solid (219 mg, 65%); m.p. 109 - 110 °C; ν_{max} ($CHCl_3$) 3019, 1524, 1476, 1423, 1204,

1016, 928, 849, 786, 662, 626, 492 cm^{-1}; ^{1}H NMR (500 MHz, $CDCl_3$) δ 8.73 (d, *J* = 8.7, 1H, 5-***H***), 8.32 (s, br, 1H, 8-***H***), 7.86 (s, 1H, 3-***H***), 7.68 (dd, *J* = 1.6, 8.7, 1H, 6-***H***), 2.77 (s, 3H, 2-***CH₃***), 1.44 (s, 12H, pin-***CH₃***); ^{13}C NMR (126 MHz, $CDCl_3$) δ 159.9 (***C***-2), 146.9 (***C***-2′), 131.9 (***C***-3), 130.9 (***C***-3′), 130.86 (q, $^{2}J_{C-F}$ = 31.5, ***C***-7), 129.6 (***C***-5), 126.9 (q, $^{3}J_{C-F}$ = 4.5, ***C***-8), 124.4 (q, $^{1}J_{C-F}$ = 272.4, 7-***CF₃***), 121.7 (q, $^{3}J_{C-F}$ = 3.0, ***C***-6), 85.0 (pin-***C***$(CH_3)_2$), 25.4 (2-***CH₃***), 25.2 (pin-***CH₃***); ^{11}B NMR (128 MHz, $CDCl_3$) δ 31.02; ^{19}F NMR (376 MHz, $CDCl_3$) δ -62.66; *m/z* (GC-MS, EI) 337 (65%, M^+), 322 (41%, M^+-CH_3), 280 (6%, M^+-$CO(CH_3)_2$), 264 (5%), 251 (79%), 237 (100%, M^+-$CO(CH_3)_2C(CH_3)_2$); HRMS (ASAP) *m/z* found $(M)^+$ 336.1500; $C_{17}H_{19}{}^{10}BF_3NO_2$ *M* 336.1497.

Further elution afforded (*r.f.* 0.1) 2-methyl-5-(4′,4′,5′,5′-tetramethyl-1′,3′,2′-dioxaborolan-2′-yl)-7-(trifluoromethyl)quinoline as an off-white solid (91 mg, 27%); m.p. 99 - 100 °C; Anal. found C, 60.2; H, 5.7; N, 4.1%;Calcd. for $C_{17}H_{19}BF_3NO_2$ C, 60.6; H, 5.7; N, 4.2%; ν_{max} ($CHCl_3$) 3022, 1520, 1476, 1421, 1195, 1018, 928, 853, 772 cm^{-1}; ^{1}H NMR (700 MHz, $CDCl_3$) δ 9.03 (d, *J* = 8.7, 1H, 4-***H***), 8.40 (s, br, 1H, 6-***H***), 8.23 (d, *J* = 1.3, 1H, 8-***H***), 7.41 (d, *J* = 8.7, 1H, 3-***H***), 2.76 (s, 3H, 2-***CH₃***), 1.43 (s, 12H, pin-***CH₃***); ^{13}C NMR (126 MHz, $CDCl_3$) δ 160.2 (***C***-2), 146.8 (***C***-2′), 136.9 (***C***-4), 132.0 (***C***-3′), 130.5 (q, $^{3}J_{C-F}$ = 3.1, ***C***-6), 130.45 (q, $^{2}J_{C-F}$ = 32.4, ***C***-7), 129.8 (q, $^{3}J_{C-F}$ = 4.3, ***C***-8), 124.14 (***C***-3), 124.14 (q, $^{1}J_{C-F}$ = 273.0, 7-***CF₃***), 84.5 (pin-***C***$(CH_3)_2$), 25.4 (2-***CH₃***), 25.1 (pin-***CH₃***); ^{11}B NMR (128 MHz, $CDCl_3$) δ 30.45; ^{19}F NMR (658 MHz, $CDCl_3$) δ -62.66; *m/z* (GC-MS, EI) 337 (65%, M^+), 322 (41%, M^+-CH_3), 280 (6%, M^+-$CO(CH_3)_2$), 264 (5%), 251 (79%), 237 (100%, M^+-$CO(CH_3)_2C(CH_3)_2$); HRMS (ASAP) *m/z* found $(M)^+$ 336.1494 $C_{17}H_{19}{}^{10}BF_3NO_2$ requires *M* 336.1497.

Application of general procedure F to 2-methyl-7-(trifluoromethyl)quinoline (211 mg, 1.0 mmol) afforded 2 mono-borylated products as a 60:40 ratio.

1-methyl-1H-pyrrolo[2,3-b]pyridine, 481[21]

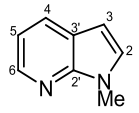

A flask was charged with 7-azaindole (500 mg, 4.24 mmol) and 60% NaH (204 mg, 5.09 mmol). The flask was purged with argon and cooled to 0°C. Once cool, DMF (20 mL) was added, and the reaction mixture was allowed to stir 1 hour until the evolution of H_2 was complete. Methyl iodide (0.4 mL, 5.09 mmol) was added drop wise and the reaction was slowly allowed to come to room temperature, and stirred for 18 hours in total. Upon completion, water was added to the reaction mixture, and the aqueous layer was extracted with Et_2O (3 × 50 mL). The combined organics were dried over $MgSO_4$, filtered and then concentrated under reduced pressure. The resulting oil was purified by flash column chromatography on silica-gel (hexane:EtOAc, 4:1) to **481** as a yellow oil (268 mg, 48% yield). ν_{max} ($CHCl_3$) 2925, 2850, 1732, 1598, 1468, 1345, 1121 cm^{-1}; ^1H NMR (500 MHz, $CDCl_3$) δ 8.34 (dd, *J* = 4.7, 1.4 Hz, 1H, 6-***H***), 7.90 (dd, *J* = 7.8, 1.4 Hz, 1H, 4-***H***), 7.17 (d, *J* = 3.4 Hz, 1H, 2-***H***), 7.05 (dd, *J* = 7.8, 4.7 Hz, 1H, 5-***H***), 6.44 (d, *J* = 3.4 Hz, 1H, 3-***H***), 3.89 (s, 3H, *N*-***CH₃***); ^{13}C NMR (126 MHz, $CDCl_3$) δ 148.0 (***C***-2′), 143.0 (***C***-6), 129.5 (***C***-4), 129.0 (***C***-2), 120.8 (***C***-3′), 115.7 (***C***-5), 99.5 (***C***-3), 31.5 (*N*-***CH₃***); *m/z* (ES^+) 133.1 (M^++H).

1-benzyl-1H-pyrrolo[2,3-b]pyridine, 482[22]

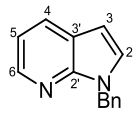

A flask was charged with 7-azaindole (500 mg, 4.24 mmol) and 60% NaH (204 mg, 5.09 mmol) and purged with argon. Dry DMF (20mL) was added and allowed to stir for 1 hour until the evolution of H_2 was complete. Benzyl Bromide (0.4 mL, 5.09 mmol) was added to the reaction mixture and stirred for 18h. Upon completion the reaction was quenched with water (150 mL) and extracted with Et_2O (3 × 50 mL). The combined organics were dried over $MgSO_4$, filtered and then concentrated under reduced pressure. The resulting yellow oil was purified by silica-gel flash column chromatography eluting with (hexane:EtOAc, 4:1) to afford **482** as a white

crystalline solid (721 mg, 82% yield); m.p. 60 - 62 °C; ν_{max} ($CHCl_3$) 3010, 2423, 1962, 1720, 1420, 1304, 1031, 890, 722 cm^{-1}; ^1H NMR (500 MHz, $CDCl_3$) δ 8.41 (s, br, 1H, 6-***H***), 7.97 (d, *J* = 7.8 Hz, 1H, 4-***H***), 7.37 - 7.23 (m, 5H, Bn-***H***), 7.22 (d, *J* = 3.4 Hz, 1H, 2-***H***), 7.13 (dd, *J* = 7.8, 4.7 Hz, 1H, 5-***H***), 6.53 (d, *J* = 3.4 Hz, 1H, 3-***H***), 5.56 (s, 2H, Bn-C***H₂***); ^{13}C NMR (126 MHz, $CDCl_3$) δ 147.8 (Ar-2′-***C***), 143.11 (Ar-6-C), 137.9 (Bn-***C***-CH_2), 128.9 (Ar-4-***C***), 128.8 (Bn-***C***), 128.0 (Bn-***C***), 127.7 (Bn-***C***), 127.5 (Ar-2-***C***), 120.6 (Ar-3′-C), 116.0 (Ar-5-***C***), 100.2 (Ar-3-***C***), 47.85 (Bn-*C*H_2); *m/z* (ES^+) 209.0 (M^++H).

1-(1H-pyrrolo[2,3-b]pyridin-1′-yl)ethanone, 483[23]

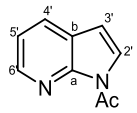

A flask was charged with 7-azaindole (500 mg, 4.24 mmol) and 60% NaH (204 mg, 5.09 mmol). The flask was purged with argon and cooled to 0°C. Once cool, THF (20 mL) was added, and the reaction mixture was allowed to stir 1 hour until the evolution of H_2 was complete. The reaction mixture was cooled to - 20°C and Acetyl Chloride (0.4 mL, 5.09 mmol) was added as a solution in THF (10mL) drop wise to the reaction mixture and stirred for 18 hours. Water was added to the reaction mixture, and the aqueous layer was extracted with EtOAc (3 × 50 mL). The combined organics were dried over $MgSO_4$, filtered and then concentrated under reduced pressure. The resulting solid was purified by flash column chromatography on silica-gel (hexane:EtOAc, 4:1) to give **483** as a white crystalline solid (393 mg, 58% yield); m.p. 58 - 60 °C; ν_{max}($CHCl_3$) 3010, 1704 (C=O), 1578, 1528, 1307, 1232, 1042 cm^{-1}; ^1H NMR (500 MHz, $CDCl_3$) δ 8.34 (d, *J* = 4.9 Hz, 1H, 6′-***H***), 7.96 (d, *J* = 3.9 Hz, 1H, 2′-***H***), 7.85 (d, *J* = 7.6 Hz, 1H, 4′-***H***), 7.17 (dd, *J* = 7.6, 4.9 Hz, 1H, 5′-***H***), 6.57 (d, *J* = 3.9 Hz, 1H, 3′-***H***), 3.04 (s, 3H, Ac-***CH₃***); ^{13}C NMR (126 MHz, $CDCl_3$) δ 169.4 (*N*-***C***OCH_3), 148.0 (***C***-a), 144.0 (***C***-6′), 129.5 (***C***-4′), 125.6 (***C***-2′), 124.0 (***C***-b), 118.9 (***C***-5′), 106.0 (***C***-3′), 26.1 (*N*-CO***C***H_3); *m/z* (ES^+) 161.0 (M^++H).

tert-butyl 1H-pyrrolo[2,3-b]pyridine-1-carboxylate, 365[24]

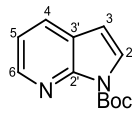

A flask was charged with 7-azaindole (500 mg, 4.24 mmol) and 4-dimethyl-amino-pyridine (DMAP) (569 mg, 4.66 mmol) and purged with argon. Dry THF (20mL) was added via cannula and the resulting solution was allowed to stir of 20 minutes in order to dissolve the reagents. After stirring, di-tert-butyl-dicarbonate (1017mg, 4.66 mmol) was added as a solution in dry THF (10 mL) via a cannula. The reaction mix was allowed to stir for 30 minutes. Upon completion the THF was removed under reduced pressure and the remaining semi-solid was re-dissolved in ethyl acetate. The organic layer was washed with a solution of saturate ammonium chloride solution (3 × 50mL) to remove the DMAP, and then washed with water (3 × 50 mL). The organic layer was dried over $MgSO_4$, filtered and concentrated. The resulting yellow oil was passing through a silica gel plug (hexane:EtOAc, 3:2) to give **365** as white crystalline solid (905 mg, 98%); m.p. 51-52 °C; ν_{max} ($CHCl_3$) 2975, 1730 (C=O), 1525, 1435, 1311, 1137, 1099, 768 cm^{-1}; ^1H NMR (500 MHz, $CDCl_3$) δ 8.45 (d, *J* = 4.8 Hz, 1H, 6-***H***), 7.80 (d, *J* = 7.8 Hz, 1H, 4-***H***), 7.57 (d, *J* = 4.0 Hz, 1H, 2-***H***), 7.11 (dd, *J* = 7.8, 4.8 Hz, 1H, 5-***H***), 6.43 (d, *J* = 4.0 Hz, 1H, 3-***H***), 1.61 (s, 9H, Boc-(C***H*****$_3$**)$_3$); ^{13}C NMR (126 MHz, $CDCl_3$) δ 148.5 (***C***O_2Me), 148.1 (***C***-2′), 145.2 (***C***-6), 129.3 (***C***-4), 126.7 (***C***-2), 123.2 (***C***-3′), 118.7 (***C***-5), 104.7 (***C***-3), 84.2 (^{t}Bu-***C***$(CH_3)_3$), 28.3 (^{t}Bu-C(***CH*****$_3$**)$_3$); *m/z* (ES^+) 219.1 (M^++H).

1-(methylsulfonyl)-1H-pyrrolo[2,3-b]pyridine, 484

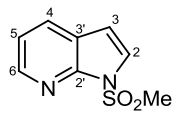

A flask was charged with 7-azaindole (500 mg, 4.24 mmol) and 60% NaH (204 mg, 5.09 mmol) the flask was purged with argon and cooled to 0°C. Dry THF (20 mL) was added and the reaction mixture was stirred at room temperature for 1.0h. DMAP (673 mg, 5.53 mmol) was added to THF (10 mL) and allowed to dissolve. The DMAP solution was transferred via cannula to the 7-azaindole solution. Mesyl chloride (0.4 mL, 5.09 mmol) was then added to the

reaction mixture and stirred for 18h. Water was added to the reaction mixture, and the aqueous layer was extracted with EtOAc (3 × 50 mL). The combined organics were dried over $MgSO_4$, filtered and then concentrated under reduced pressure. The resulting oil was purified by flash column chromatography on silica-gel (hexane:EtOAc, 4:1) to afford **484** as a yellow oil (688 mg, 82% yield); m.p. 63 -65 °C; $\nu_{max}(CHCl_3)$ 2922, 1579, 1348, 1150, 995 cm^{-1}; ^1H NMR (500 MHz, $CDCl_3$) δ 8.45 (dd, *J* = 4.7, 1.2 Hz, 1H, 6-***C***), 7.92 (dd, *J* = 7.9, 1.2 Hz, 1H, 4-***H***), 7.60 (d, *J* = 4.0 Hz, 1H, 2-***H***), 7.24 (dd, *J* = 7.9, 4.7 Hz, 1H, 5-***H***), 6.60 (d, *J* = 4.0 Hz, 1H, 3-***H***), 3.56 (s, 3H, *N*-Boc-C(**C*H*$_3$)$_3$); ^{13}C NMR (126 MHz, $CDCl_3$) δ 147.2 (***C***-2′), 144.9 (***C***-6), 130.0 (***C***-4), 125.8 (***C***-2), 123.0 (***C***-3′), 119.07 (***C***-5), 104.8 (***C***-3), 42.1 (*N*-SO_2***C***H_3); *m/z* (ES^+) 197.04(M^++H); HRMS (ESI) *m/z* found 197.0380; $C_8H_9N_2O_2S$ requires *M* 197.3079.

1-(triisopropylsilyl)-1H-pyrrolo[2,3-b]pyridine,485

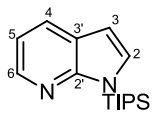

To a solution of 7-azaindole (500 mg, 4.24 mmol) in THF (20 mL) was added NaH (204 mg, 5.09 mmol) at 0°C under argon, the reaction mixture was stirred at room temperature for 1.0h. TIPSCl (1.1 mL, 5.09 mmol) was added to the reaction mixture and stirred for 18h. Water was added to the reaction mixture, and the aqueous layer was extracted with EtOAc (3 × 50 mL). The combined organics were dried over $MgSO_4$, filtered and then concentrated under reduced pressure. The resulting oil was purified by silica-gel flash column chromatography eluting with hexane (100%) to afford **485** as a white crystalline solid (807 mg, 70% yield); m.p. 62 - 63 °C; ^1H NMR (400 MHz, $CDCl_3$) δ 8.28 (d, *J* = 4.4 Hz, 1H, 6-***H***), 7.88 (d, *J* = 7.8 Hz, 1H, 4-***H***), 7.33 (d, *J* = 3.4 Hz, 1H, 2-***H***), 7.04 (dd, *J* = 7.7, 4.4 Hz, 1H, 5-***H***), 6.57 (dd, *J* = 3.4 Hz, 1H, 3-***H***), 1.95 - 1.85 (m, 3H, C***H***$(CH_3)_2$), 1.20 - 1.12 (m, 18H, CH***(CH$_3$)$_2$***); ^{13}C NMR (101 MHz, $CDCl_3$) δ 154.0 (***C***-2′), 142.4 (***C***-6), 131.2 (***C***-4), 127.9 (***C***-2), 122.4 (***C***-3′), 116.0 (***C***-5), 103.0 (***C***-3), 18.3 (***C***H$(CH_3)_2$), 12.4 (CH***(CH$_3$)$_2$***); *m/z* (ES^+) 275.1 (M^++H); HRMS (ESI) *m/z* found (M^++H) 275.1939; $C_{16}H_{27}N_2Si$ requires *M* 275.1938.

1-Trifluoromethyl-1,2-benziodoxol-3-(1H)-one, 521[25]

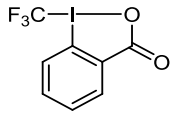

$NaIO_4$ (2.25 g, 10.5 mmol, 1.05 eq.) and 2-iodobenzoic acid (2.48 g, 10.0 mmol, 1.00 eq.) were added to aqueous AcOH (30%) (50 mL). The mixture heated to reflux with efficient stirring for 4 hours. The reaction was diluted with cold water (100 mL) and cooled to room temperature to crystallise the product. After 1 hour the precipitate was collected by filtration. The solids were washed with cold water (3 × 25 mL) and acetone (3 × 25 mL). The solid was air dried to afford **531** (2.61 g, 99%) as a white crystalline sold; ^{1}H NMR (400 MHz, DMSO) δ 8.05 - 7.91 (m, 1H), 7.86 - 7.80 (m, 1H), 7.72 - 7.65 (m, 1H). **531** (2.61 g, 9.90 mmol) was immediately added to acetic anhydride (20 mL) and heated to reflux for 15 minutes. After this time a clear yellow solution had formed. The reaction was cooled to - 20 °C to induce crystallisation of the product. After 2 hours, the solvent was decanted and the remaining solid was dried under reduced pressure for 12 hours to afford 1-acetoxy-1,2-benziodoxol-3-(1H)-one 532 (2.56 g, 85%). A 50 mL round bottomed flask was charged with **532** (1.98 g, 5.65 mmol). The flask was purged with argon and MeCN (15 mL) was added. CsF (85 mg, 0.56 mmol) and TMSCF3 (1.3 mL, 8.5 mmol) and the reaction was stirred for 22 hours at room temperature. After this time, the solvent was removed under reduced pressure and the resulting solid was purified by silica gel flash column chromatography eluting with 5% MeOH/DCM to afford 1-Trifluoromethyl-1,2-benziodoxol-3-(1H)-one **521** (2.5 g, 76%); m.p. 124 - 125 °C (lit. 122 °C)[25]; ^{1}H NMR (400 MHz, DMSO) δ 8.24 - 8.18 (m, 1H, Ar-H), 7.95 - 7.88 (m, 1H, Ar-H), 7.86 - 7.79 (m, 2H, Ar-H); ^{19}F NMR (376 MHz, $CDCl_3$) δ -33.1.

4-(trifluoromethyl)biphenyl, 494[26]

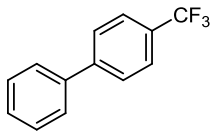

A round bottomed flask was charged with 4-biphenylboronic acid (198 mg, 1.0 mmol) and copper (I) bromide (mg, 1.0 mmol). The flask was purged with argon followed by addition of

DMF (2.0 mL). The reaction was stirred at room temperature for 1 hour. A solution **521** (330 mg, 1.0 mmol) in DMF (1.0 mL) was added and stirred for 30 minutes. Water (20 mL) was added to the reaction which was extracted with Et_2O (3 × 15 mL). The combined organics were washed with brine (3 × 15 mL), dried over $MgSO_4$ and filtered. The solvent was removed under reduced pressure to afford the crude product. The crude material was purified by silica gel flash column chromatography eluting with 100% hexane to afford 4-(trifluoromethyl)biphenyl (100 mg, 45%); m.p. 68-70 °C; ^{1}H NMR (400 MHz, $CDCl_3$) 7.79 (s, br, 4H, Ar-***H***), 7.50-7.64 (m, 4H, Ar-***H***), 7.38 (t, 1H, *J* = 8.0 Hz, Ar-***H***); ^{19}F NMR (376 MHz, $CDCl_3$) δ - 62.5; *m/z* GC-MS 222 (M^+, 100%), 201 (11%, M^+ -F), 152 (28%, M^+ -CF_3).

8.3 Experimental Details - References

1 Cho, J. Y.; Iverson, C. N.; Smith, M. R., III., *J. Am. Chem. Soc.* **2000**, *122*, 12868.

2 Guan, B-T.; Wang, Y.; Li, B-J.; Yu, D-G.; Shi, Z-J. , *J. Am. Chem. Soc.* **2008**, *130*, 14468.

3 Ishiyama, T.; Nobuta, Y.; Hartwig, J. F.; Miyaura, N., *Chem. Commun.* **2003**, 2924.

4 Feirong, L. L. F.; Rehder, K. S.; Campbell, M. G.; Viscardi, C. P. ; Strachem, J-P. WO2004016592, February 26, 2004.

5 Anthony, N. J.; Stokker, G. E.; Gomez, R. P.; Solinsky, K. M.; Waj, J. S.; Williams, T. M.; Young, S. D. WO9736875, April 1, 1997.

6 Percec, V.; Holerca, M. N.; Nummelin, S.; Morrison, J. J.; Glodde, M.; Smidrkal, J.; Peterca, M.; Rosen, B. M.; Uchida, S.; Balagurusamy, V. S. K.; Sienkowska, M. J.; Heiney, P. A. , *Chem. Eur. J.* **2006**, *12*, 6216.

7 So, C. M.; Lee, H. W.; Lau, C. P. ; Kwong, F. Y., *Org. Lett.* **2009**, *11*, 317.

8 Oh, C. H.; Lim, Y. M; You, C. H., *Tetrahedron Lett.* **2002**, *43*, 4645.

9 Macé, Y.; Raymondeau, B.; Pradet, C.; Blazejewski, J-C.; Maginer, E., *Eur. J. Org. Chem.* **2009**, *9*, 1390.

10 Martin, R.; Buchwald, S. L., *J. Am. Chem. Soc.* **2007**, *129*, 3844.

11 Köbrich, G., *Angew. Chem.* **1960**, *72*, 348.

12 Ishiyama, T.; Takagi, J.; Ishida, K.; Miyaura, N.; Anastasi, N. R.; Hartwig, J. F., *J. Am. Chem. Soc.* **2002**, *124*, 390.

13 Cho, J.; Tse, M. K.; Holmes, D.; Maleczka, R. E., Jr.; Smith, M. R., III., *Science* **2002**, *295*, 305

14 Chotana, G. A.; Kallepalli, V. A.; Maleczka, R. E., Jr.; Smith, M. R., III., *Tetrahedron* **2008**, *64*, 6103.

15 Smith, M. R., III.; Maleczka, R. E., Jr.; Chotana, G. A. 7514563 August 6, 2006.

16 Paul, S.; Chotana, G. A.; Holmes, D.; Reichle, R. C.; Maleczka, R. E., Jr.; Smith, M. R., III., *J. Am. Chem. Soc.* **2006**, *128*, 15552.

17 Billingsley, K. L.; Buchwald, S. L., *J. Am. Chem. Soc.* **2007**, *129*, 3358.

18 von Sprecher, A.; Gerspacher, M.; Beck, A.; Kimmel, S.; Wiestner, H.; Anderson, G. P.; Niederhauser, U.; Subramanian, N.; Bray, M. A., *Bioorg. Med. Chem. Lett.* **1998**, *8*, 965.

19 Polanski, J.; Zouhiri, F.; Jeanson, L.; Desmaële, D.; d'Angelo, J.; Mouscadet, J.-F.; Gieleciak, R.; Gasteiger, J.; Bret, M. Le, *J. Med. Chem.* **2002**, *45*, 4647.

20 Spaeth, B., *Chem. Ber.* **1924**, *57*, 1246.

21 Lane, B. S.; Brown, M. A.; Sames, D., *J. Am. Chem. Soc.* **2007**, *129*, 241.

22 Tatsugi, J.; Zhiwei, T.; Amano, T.; Izawa, Y., *Heterocycles* **2000**, *53*, 1145.

23 Helgen, C.; Bochet, C. G., *Heterocycles* **2006**, *67*, 797.

24 Clark, R. D.; Muchowski, J. M.; Fisher, L.E.; Flippin, L. A.; Repke, D. B.; Souchet, M., *Synthesis* **1991**, *10*, 871.

25 Eisenberger, P.; Gischig, S.; Togni, A., *Chem. Eur. J.* **2006**, *12*, 2579.

26 Bandari, R.; Höche, T.; Prager, A.; Dirnberger, K.; Buchmeiser, M. R., *Chem. Eur. J.* **2010**, *16*, 4650.

APPENDIX I - NMR SPECTRA

^{1}H and ^{13}C NMR spectra for compound 94

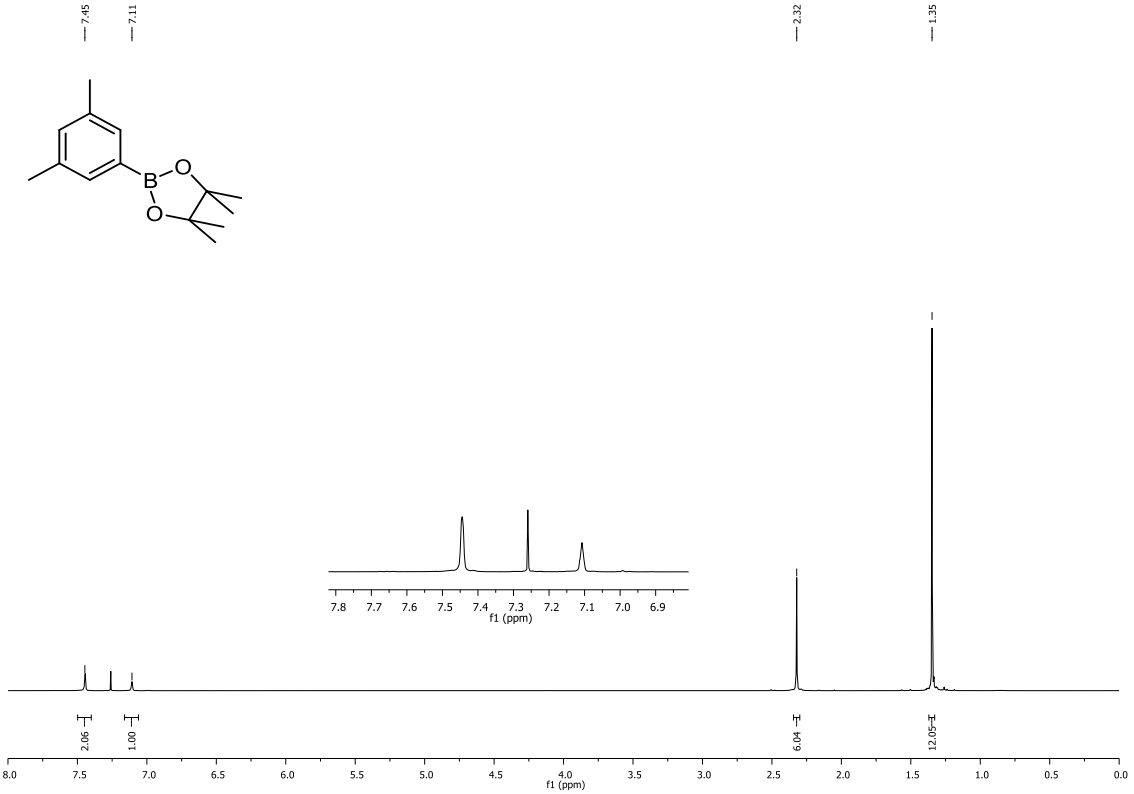

^{1}H NMR (400 MHz, $CDCl_3$)

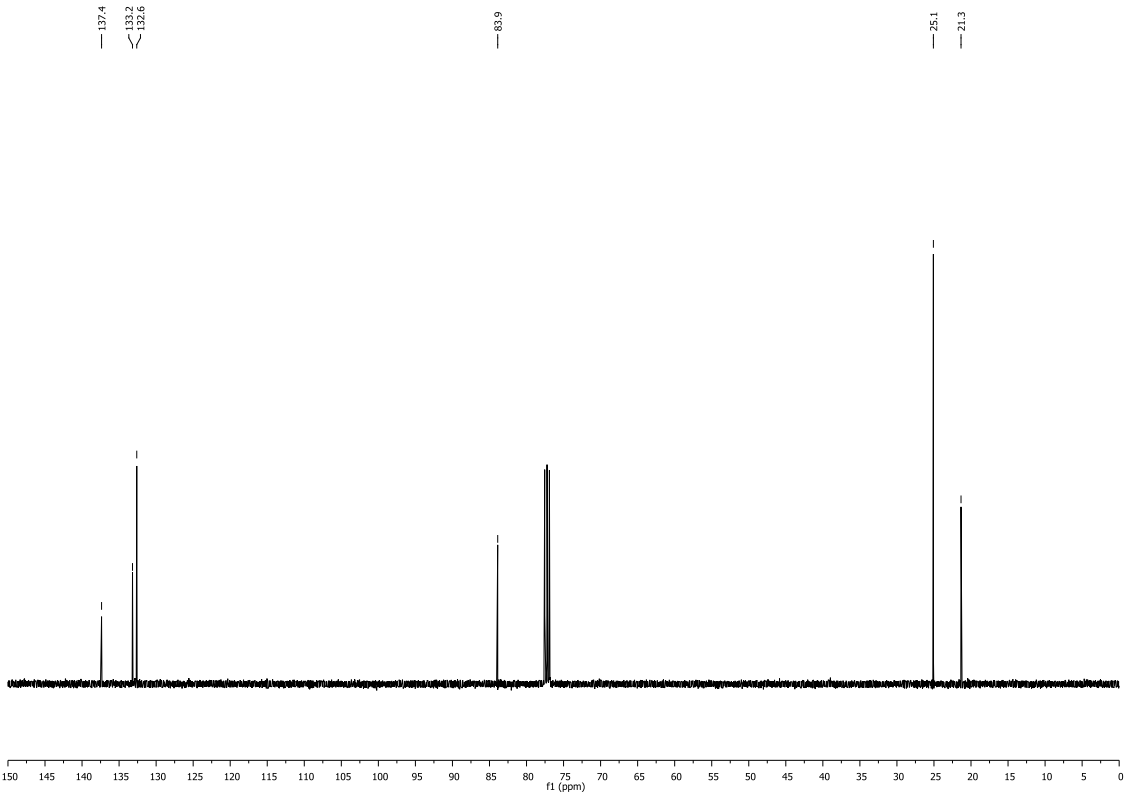

^{13}C NMR (101 MHz, $CDCl_3$)

^{1}H and ^{13}C NMR spectra for compound 302

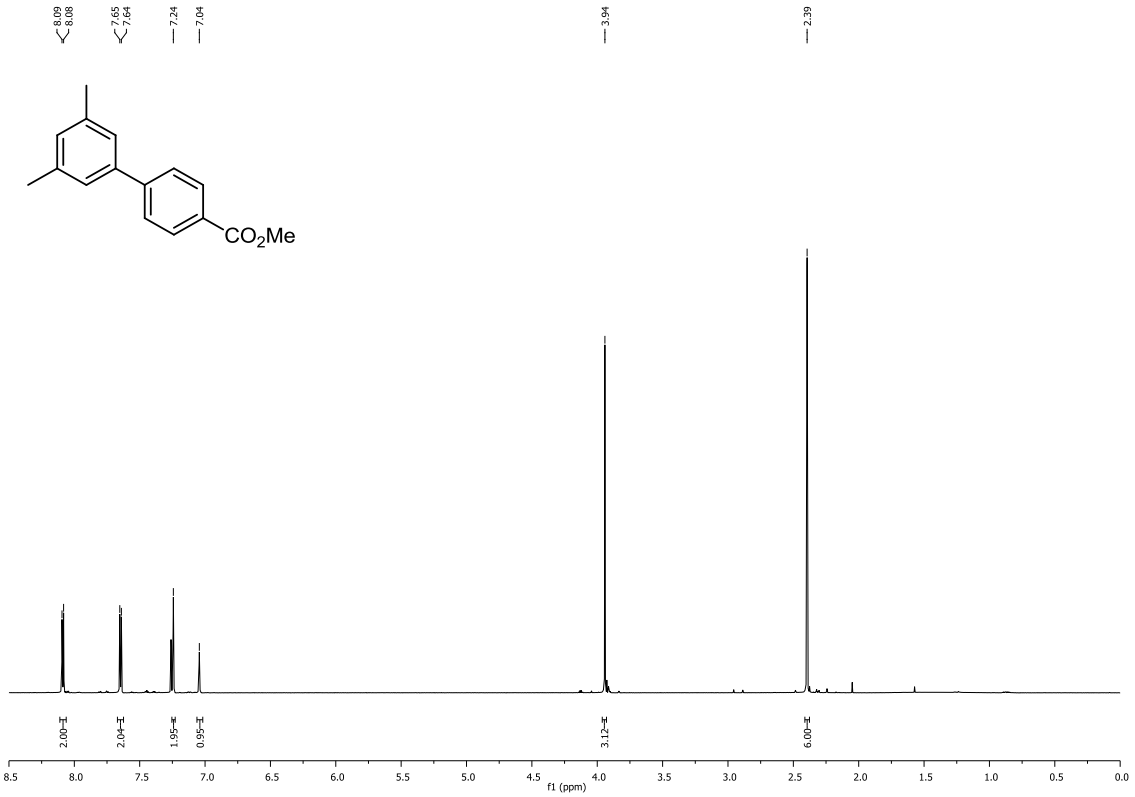

^{1}H NMR (700 MHz, $CDCl_3$)

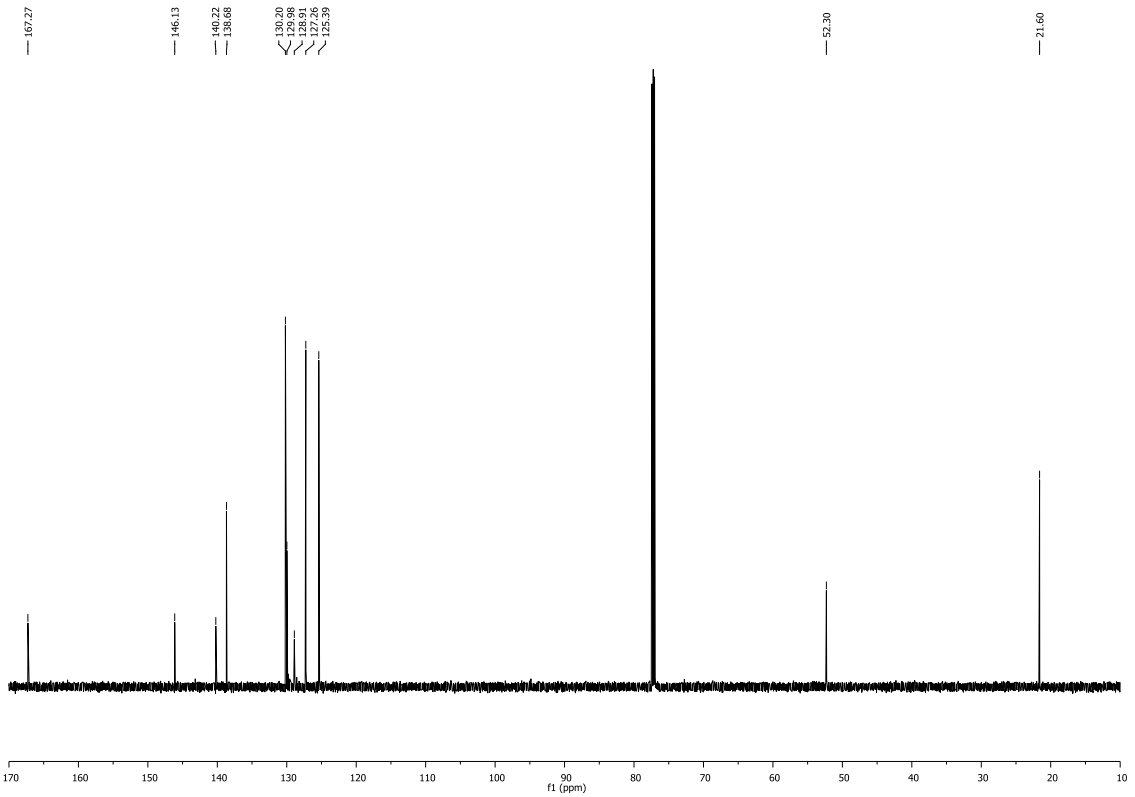

^{13}C NMR (176 MHz, $CDCl_3$)

^{1}H and ^{13}C NMR spectra for compound 298

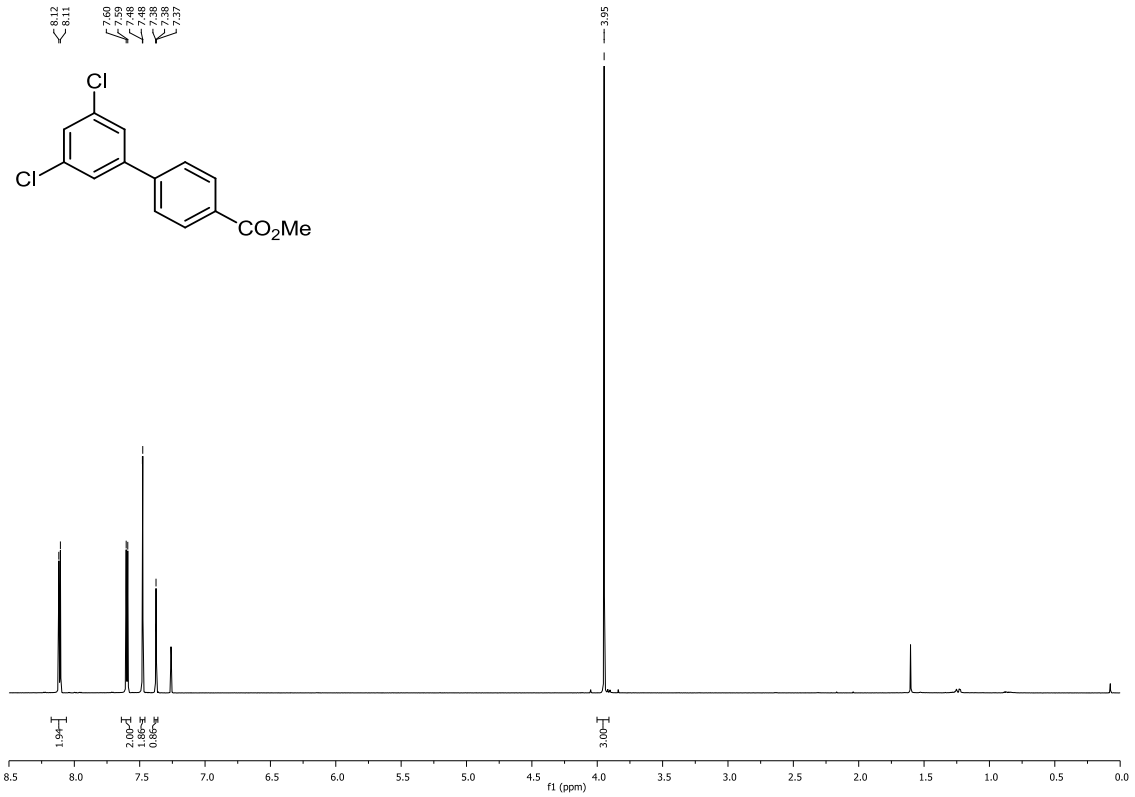

^{1}H NMR (700 MHz, $CDCl_3$)

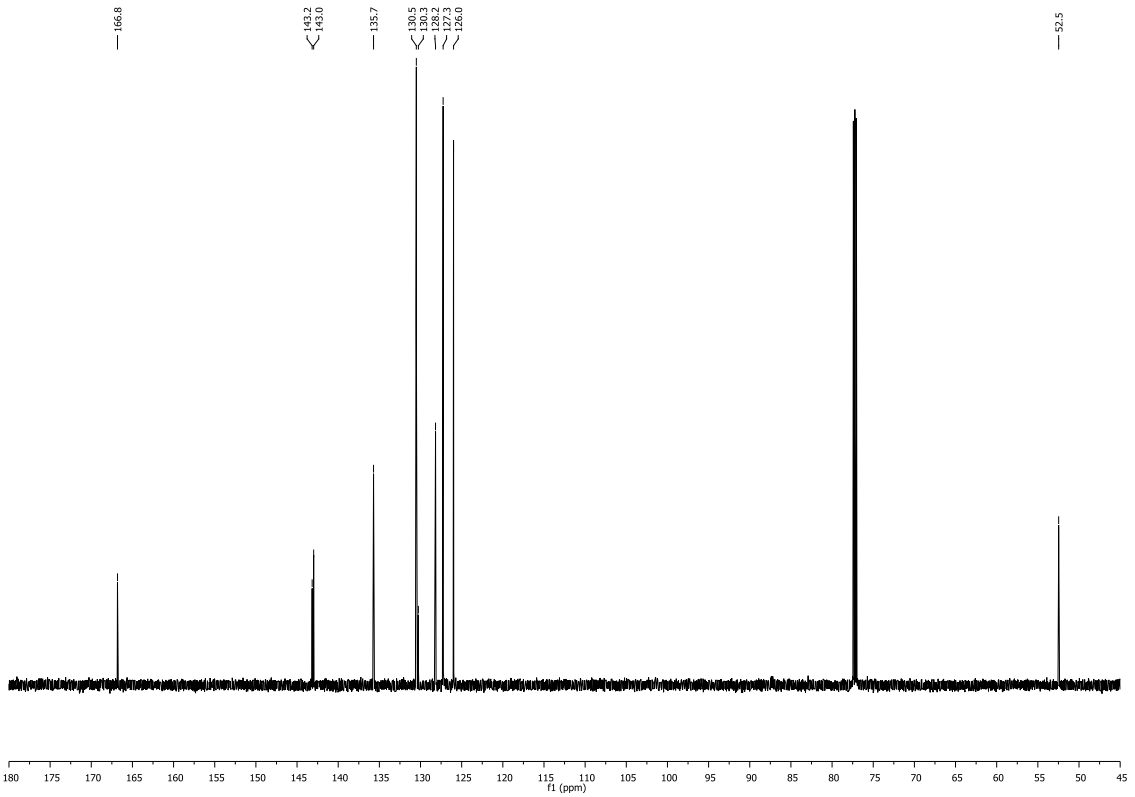

^{13}C NMR (176 MHz, $CDCl_3$)

^{1}H and ^{13}C NMR spectra for compound 303

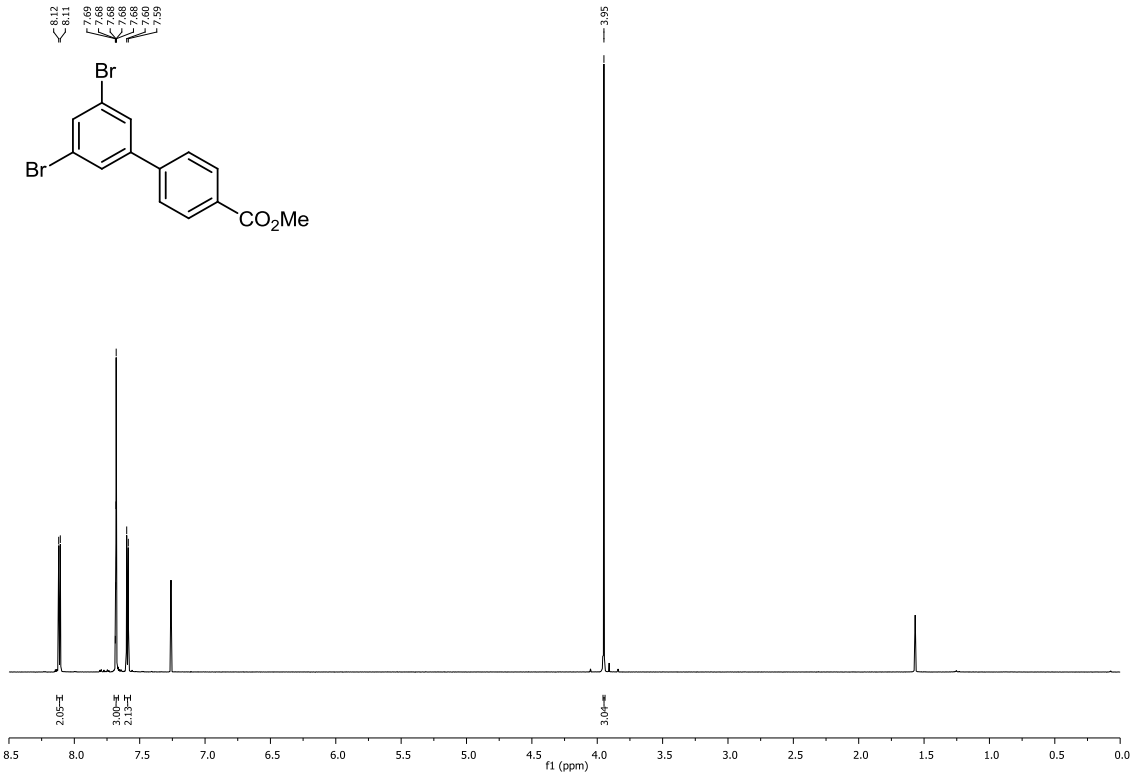

^{1}H NMR (700 MHz, $CDCl_3$)

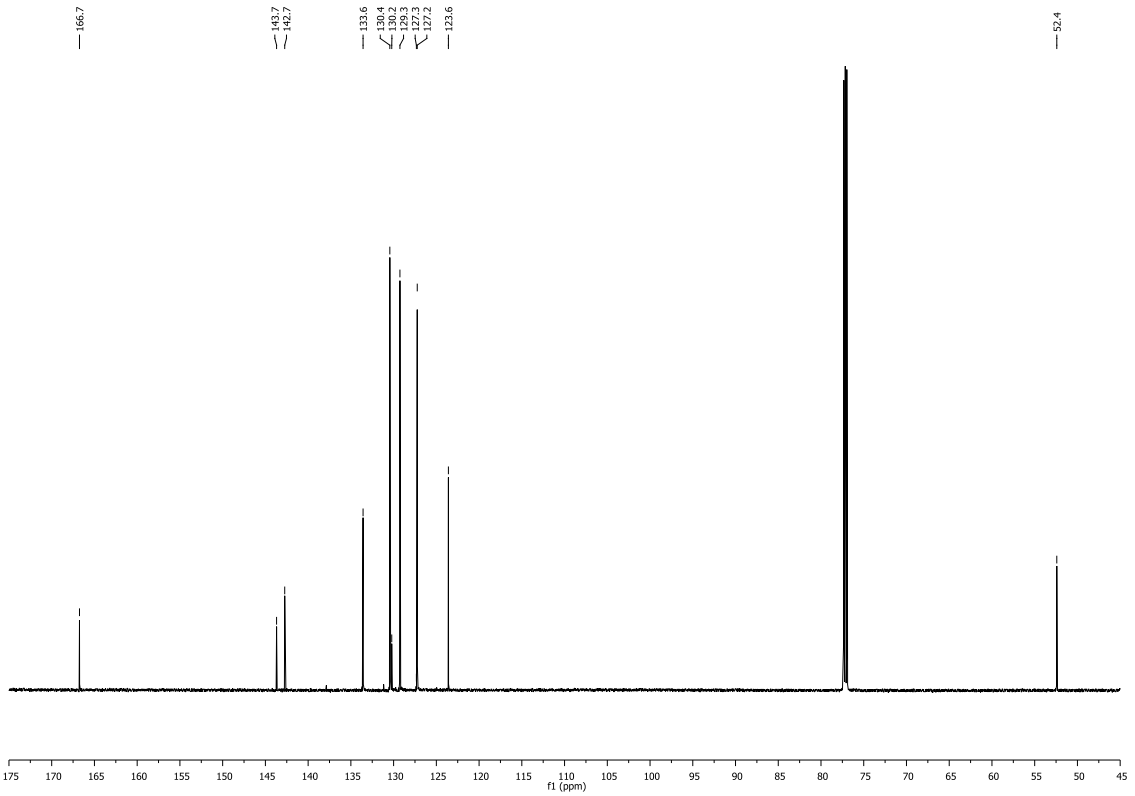

^{13}C NMR (176 MHz, $CDCl_3$)

^{1}H and ^{13}C NMR spectra for compound 304

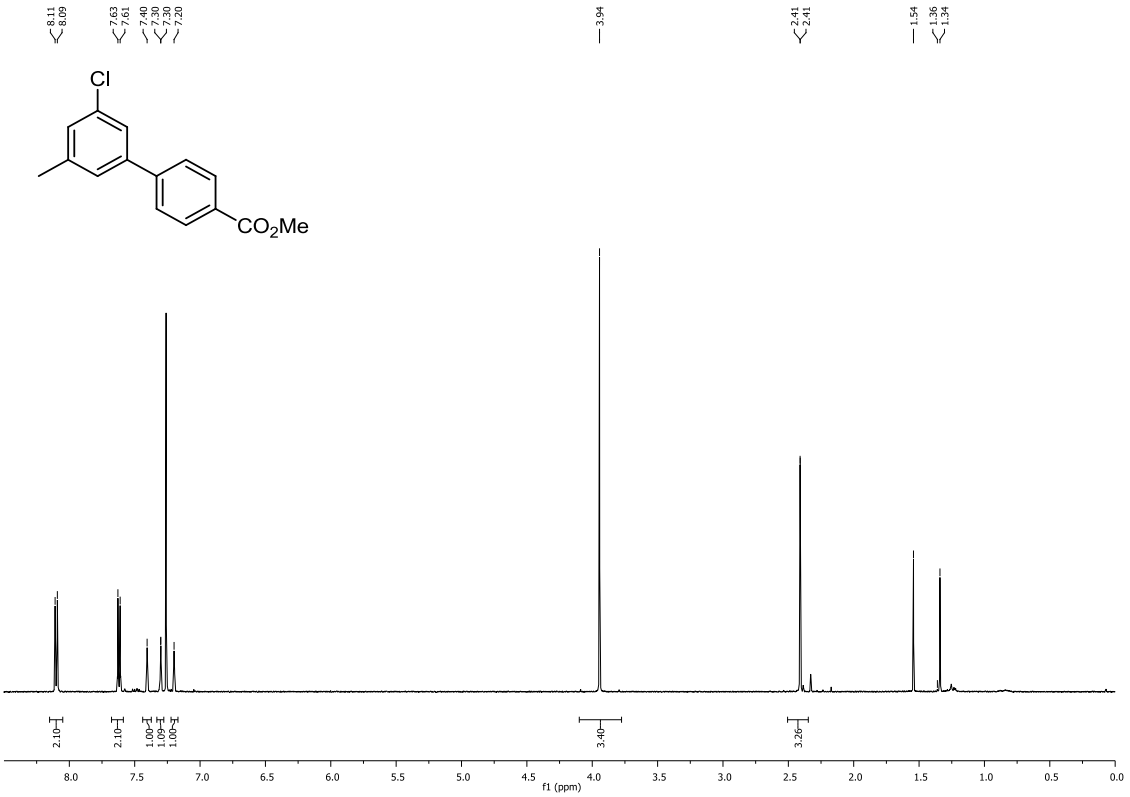

^{1}H NMR (500 MHz, $CDCl_3$)

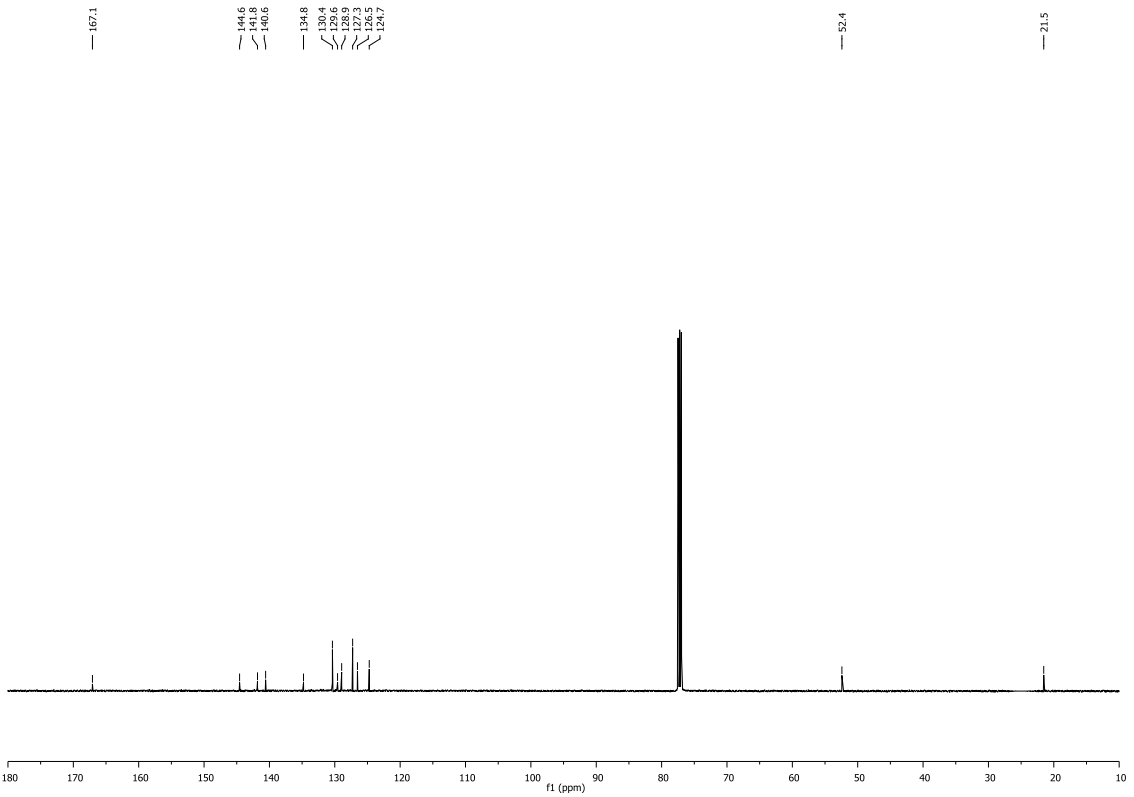

^{13}C NMR (126 MHz, $CDCl_3$)

^{1}H and ^{13}C NMR spectra for compound 305

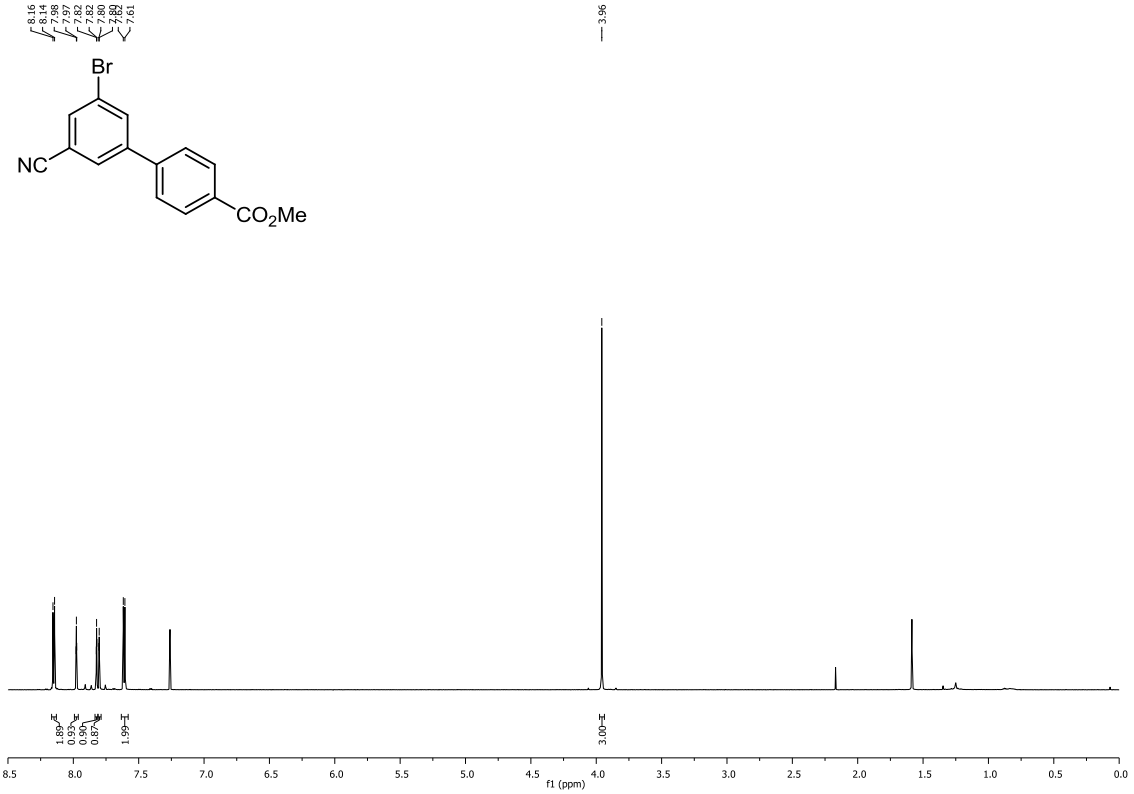

^{1}H NMR (700 MHz, $CDCl_3$)

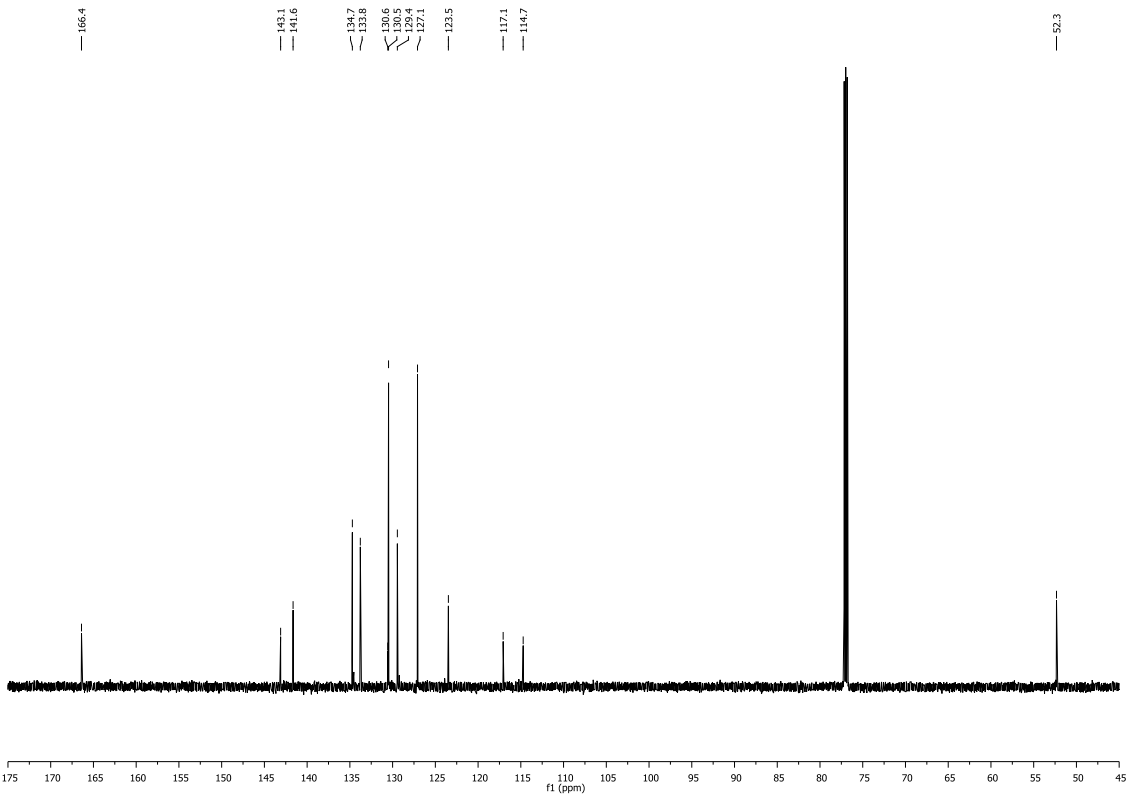

^{13}C NMR (176 MHz, $CDCl_3$)

^{1}H and ^{13}C NMR spectra for compound 306

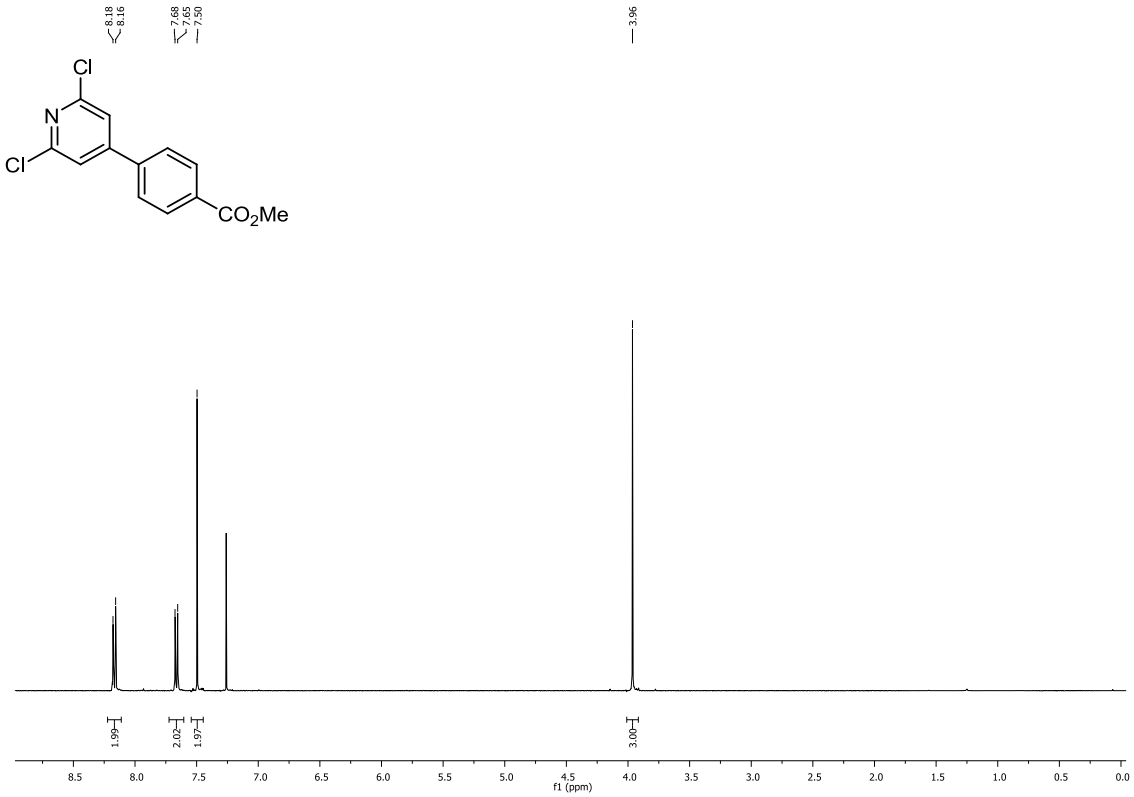

^{1}H NMR (400 MHz, $CDCl_3$)

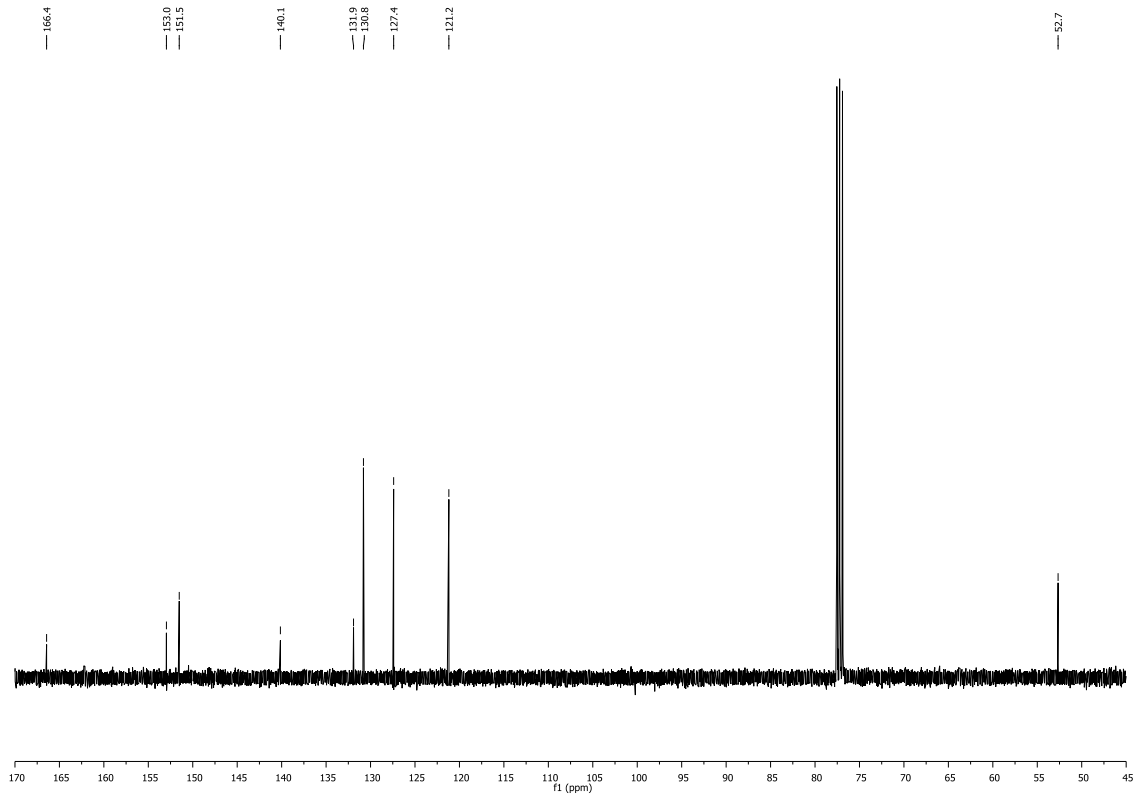

^{13}C NMR (101 MHz, $CDCl_3$)

^{1}H and ^{13}C NMR spectra for compound 307

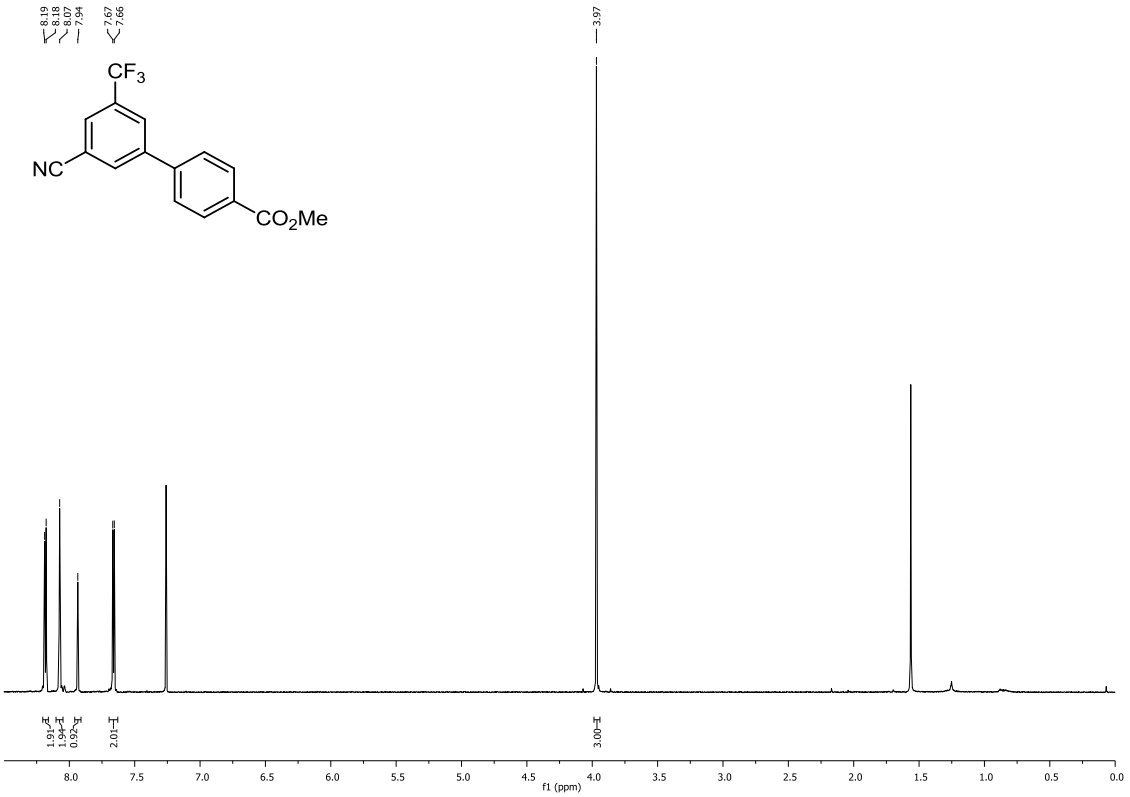

^{1}H NMR (700 MHz, $CDCl_3$)

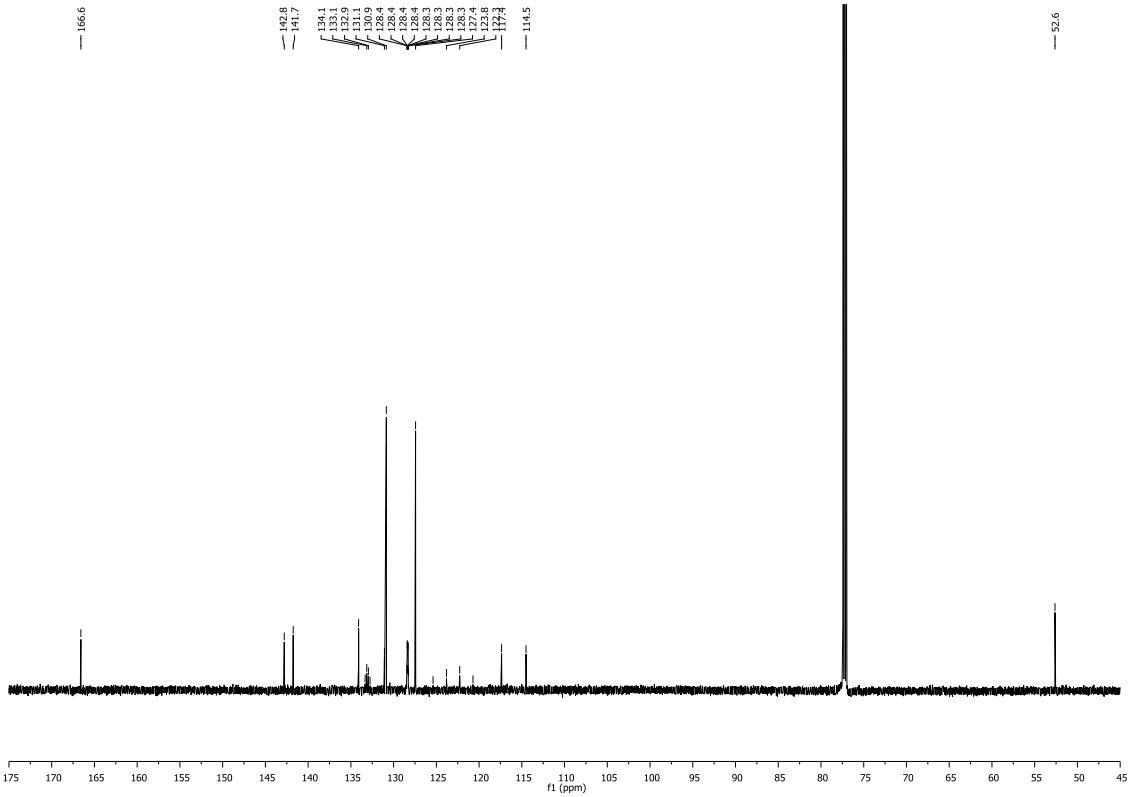

^{13}C NMR (176 MHz, $CDCl_3$)

^{1}H and ^{13}C NMR spectra for compound 308

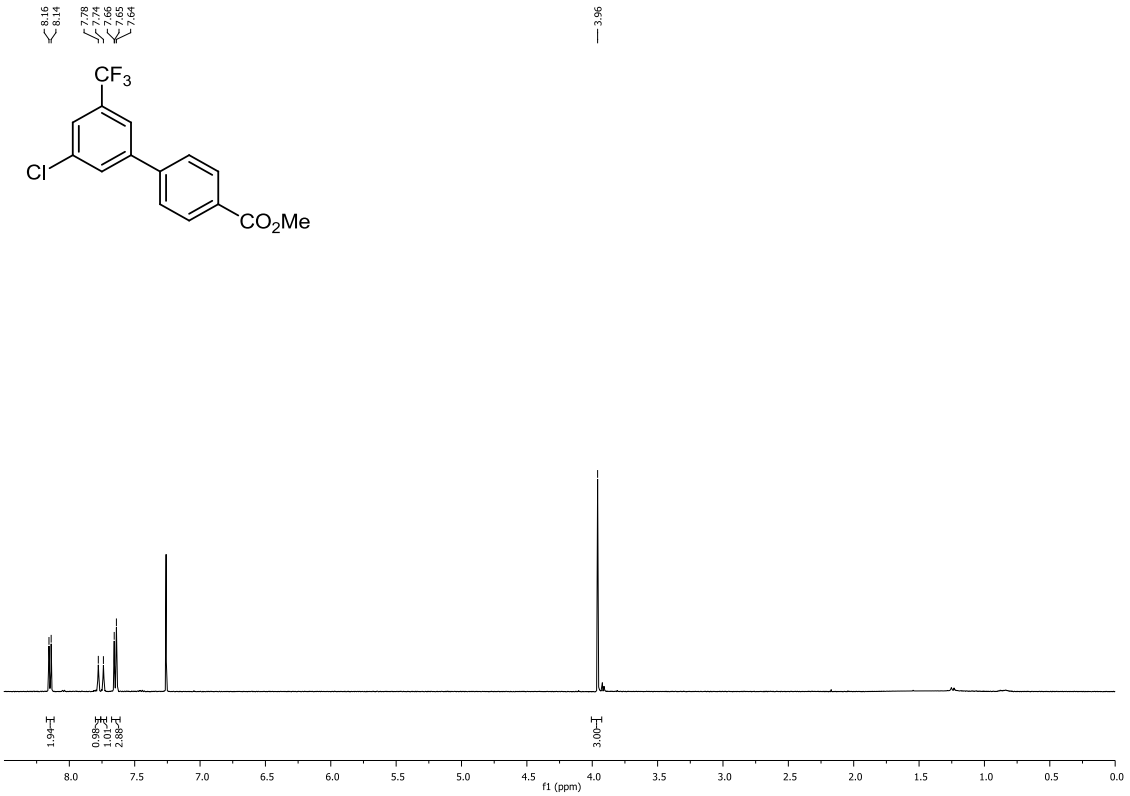

^{1}H NMR (500 MHz, $CDCl_3$)

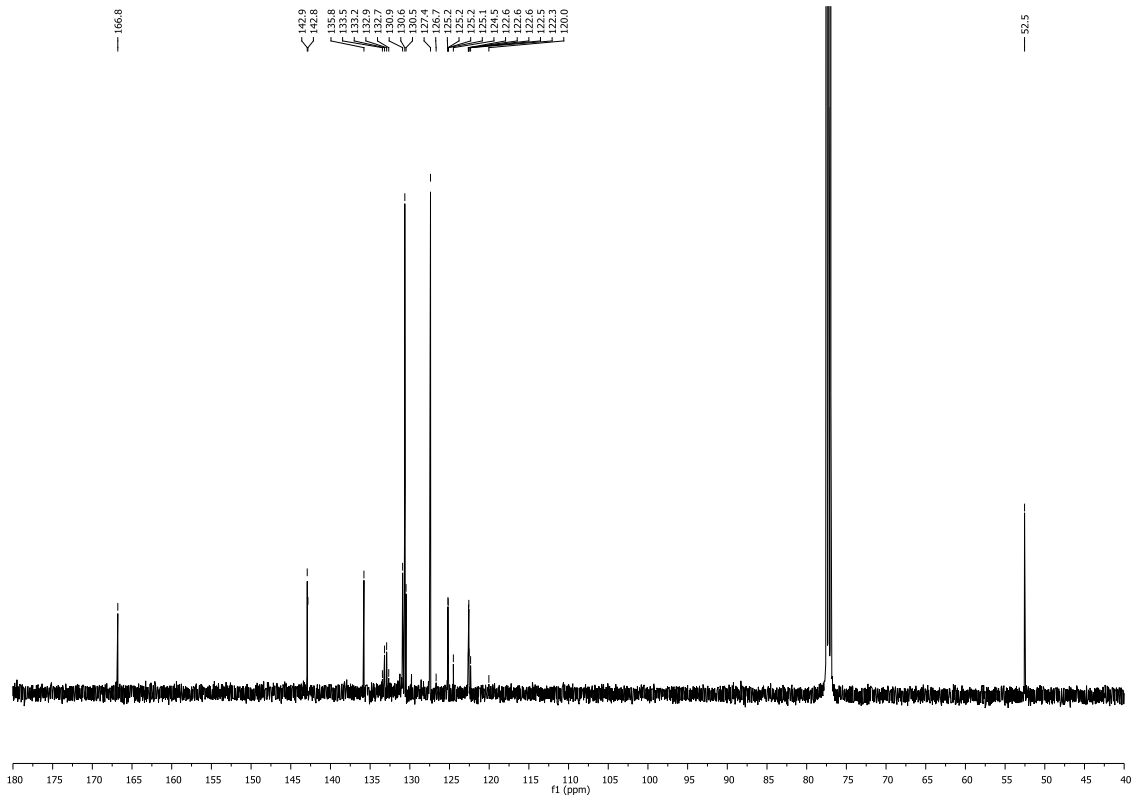

^{13}C NMR (126 MHz, $CDCl_3$)

^{1}H and ^{13}C NMR spectra for compound 309

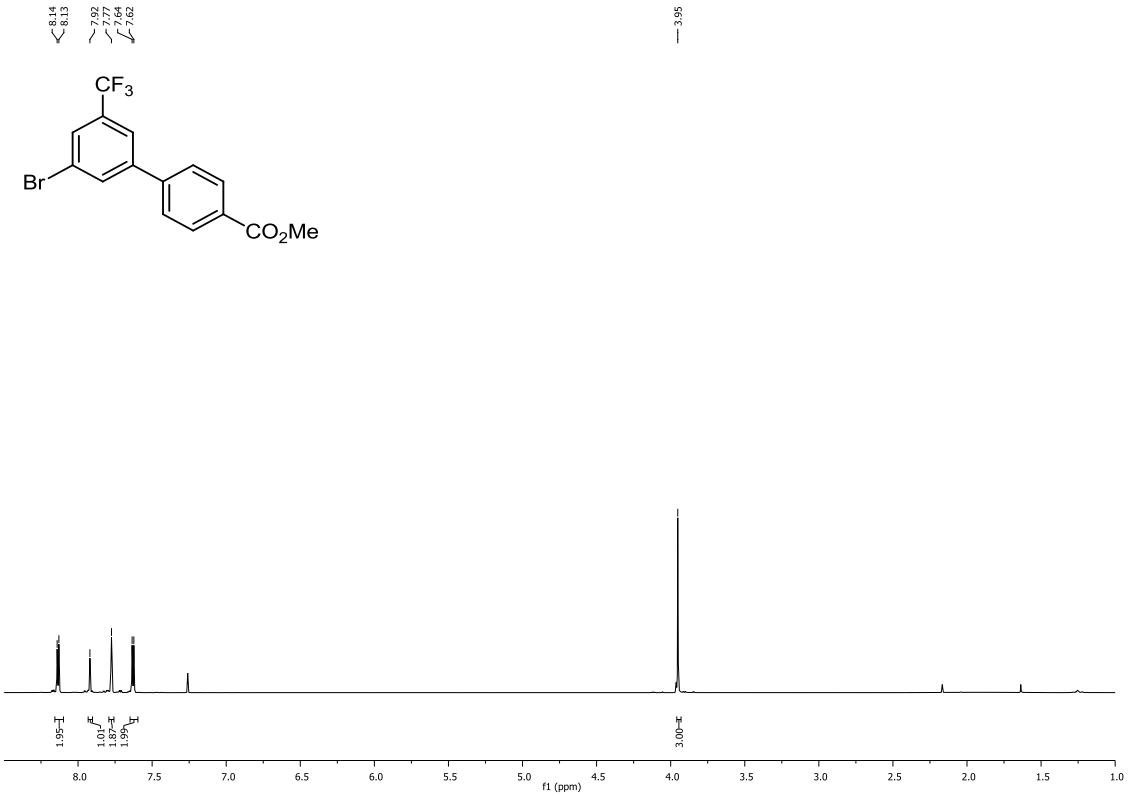

^{1}H NMR (700 MHz, $CDCl_3$)

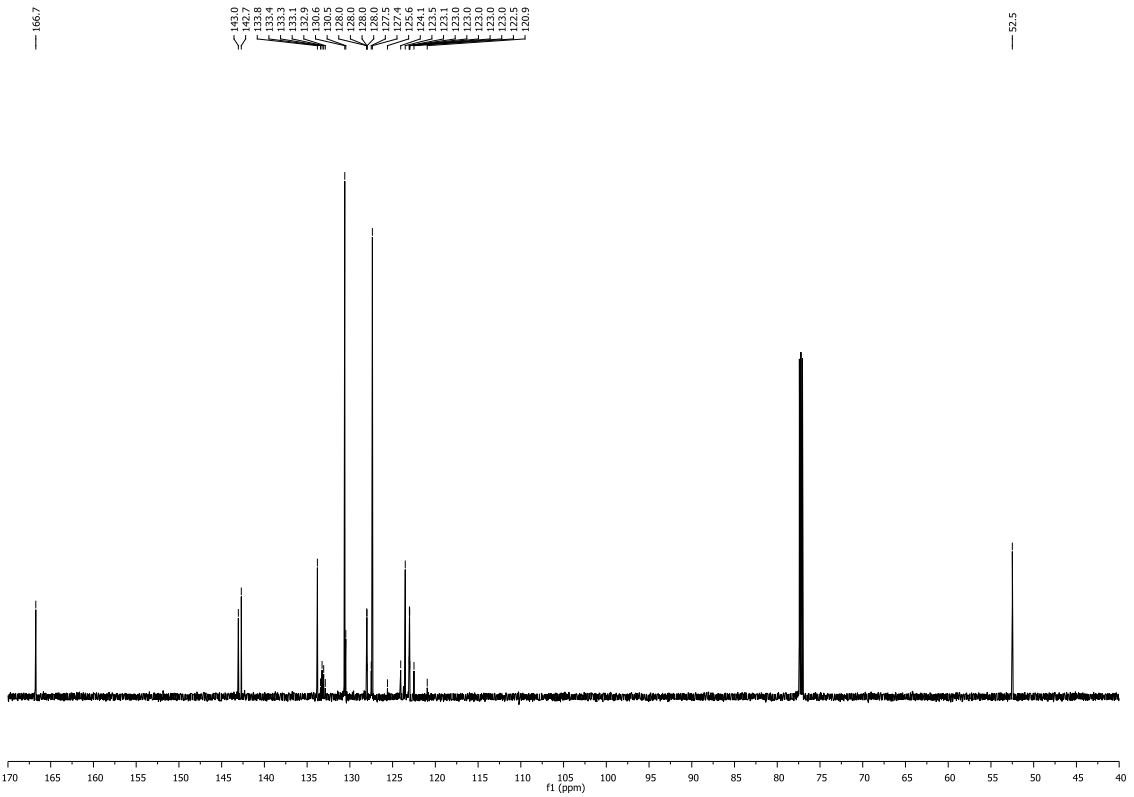

^{13}C NMR (176 MHz, $CDCl_3$)

^{1}H and ^{13}C NMR spectra for compound 310

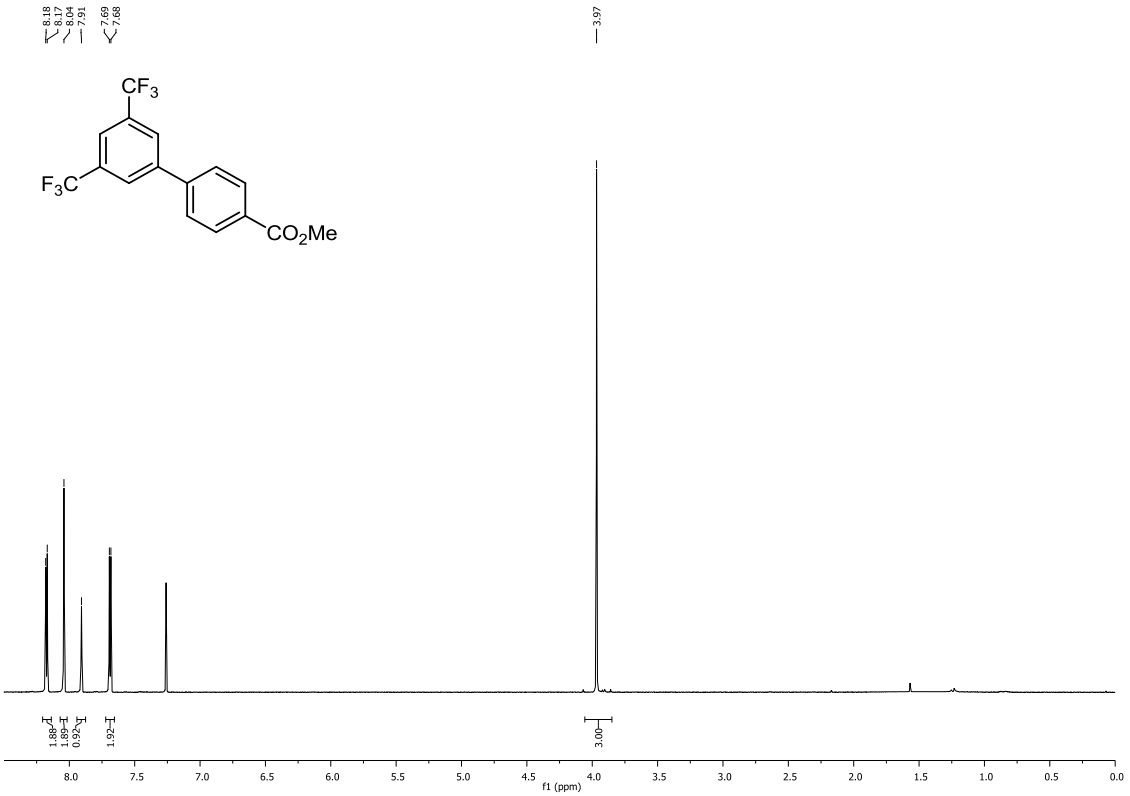

^{1}H NMR (700 MHz, $CDCl_3$)

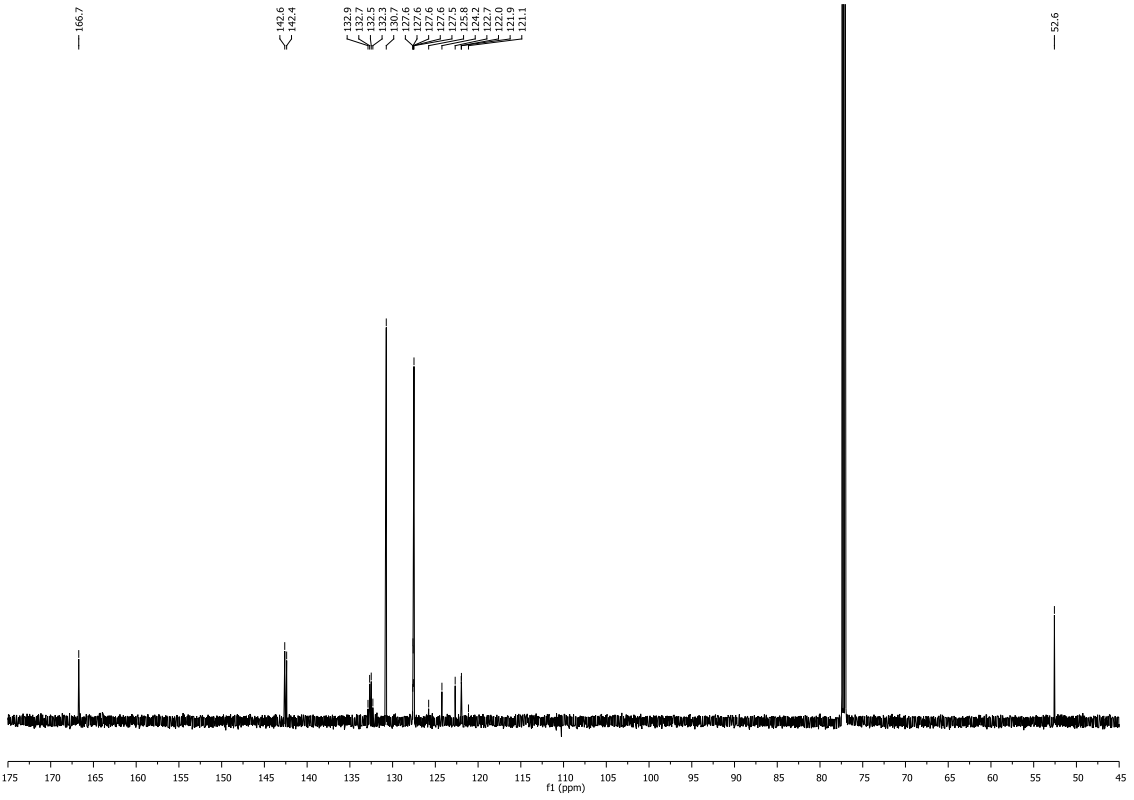

^{13}C NMR (176 MHz, $CDCl_3$)

^{1}H and ^{13}C NMR spectra for compound 311

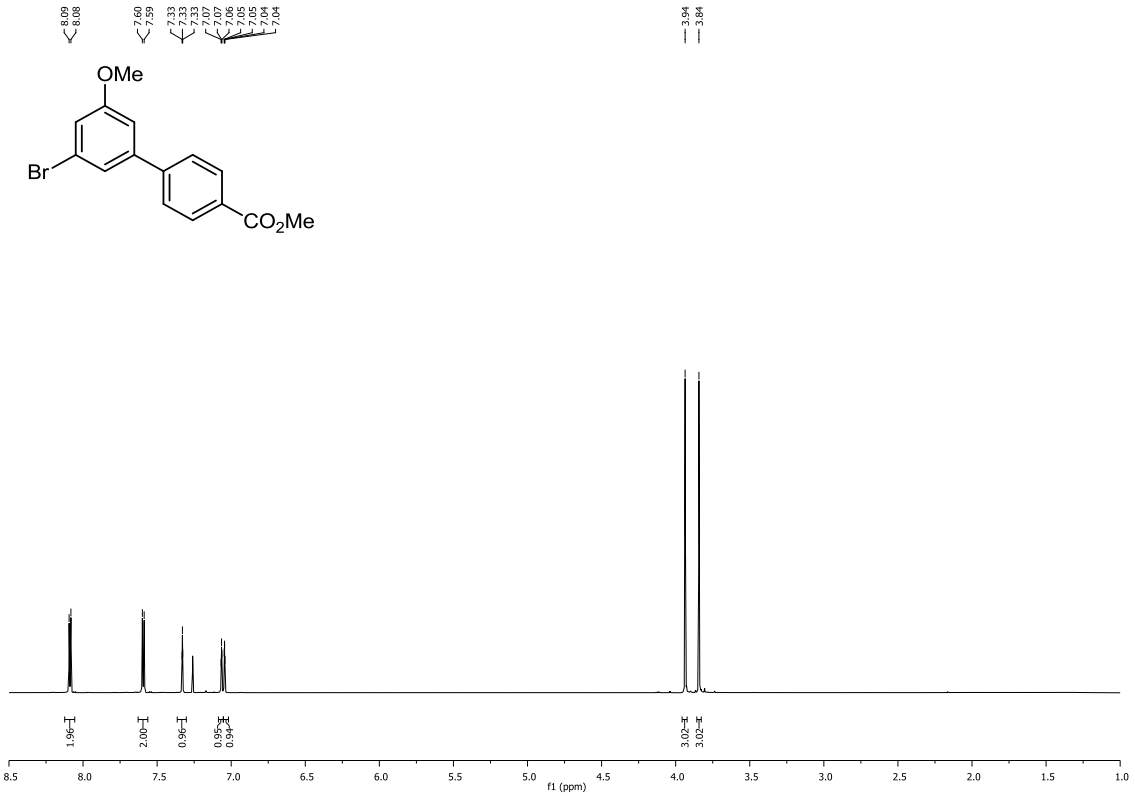

^{1}H NMR (700 MHz, $CDCl_3$)

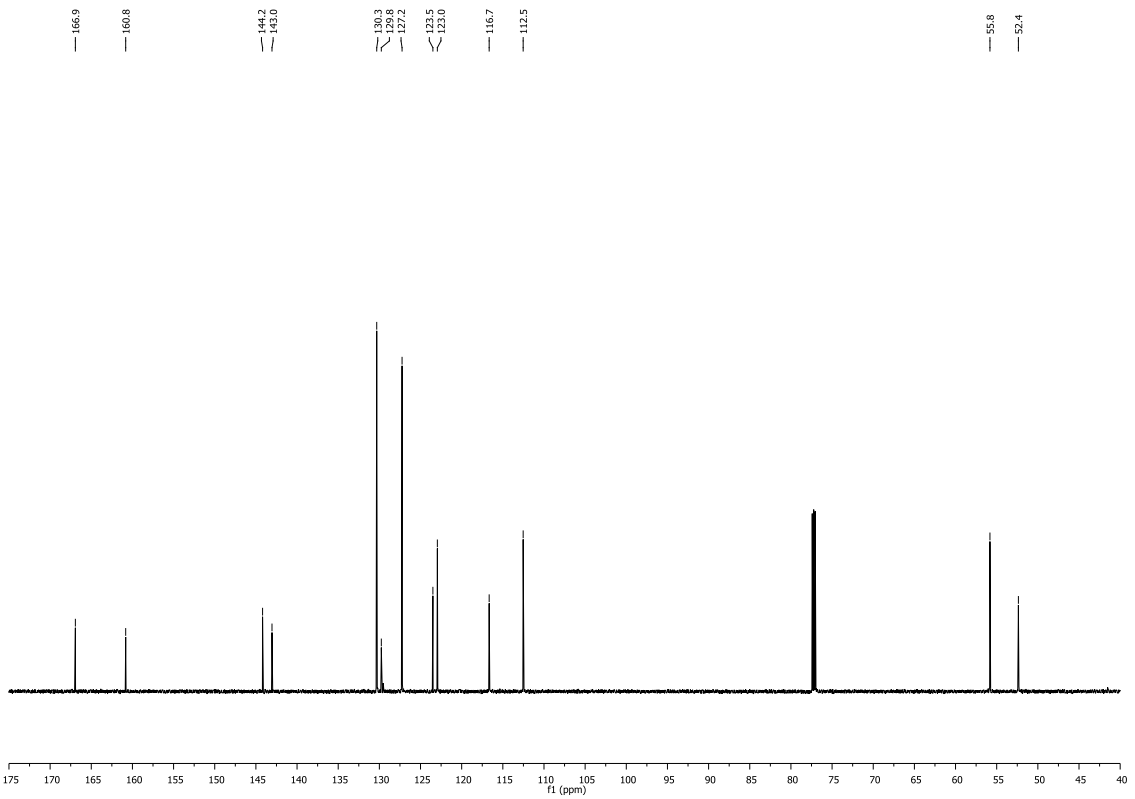

^{13}C NMR (176 MHz, $CDCl_3$)

^{1}H and ^{13}C NMR spectra for compound 312

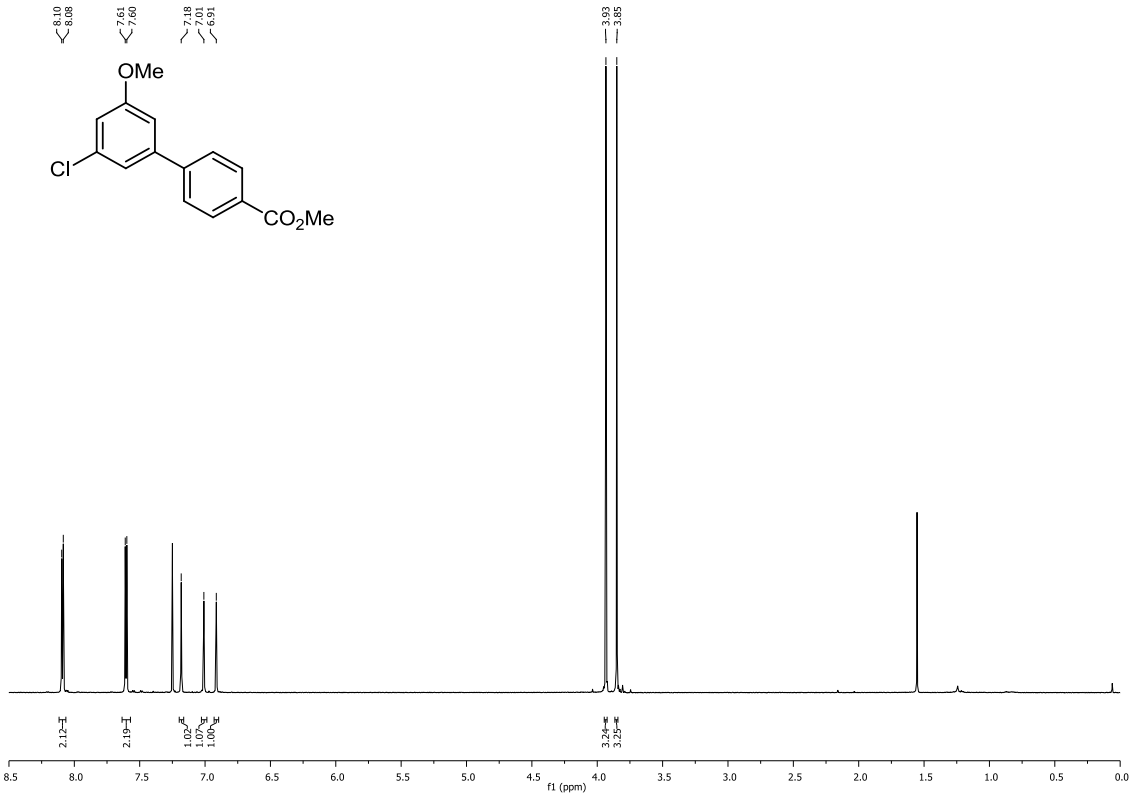

^{1}H NMR (700 MHz, $CDCl_3$)

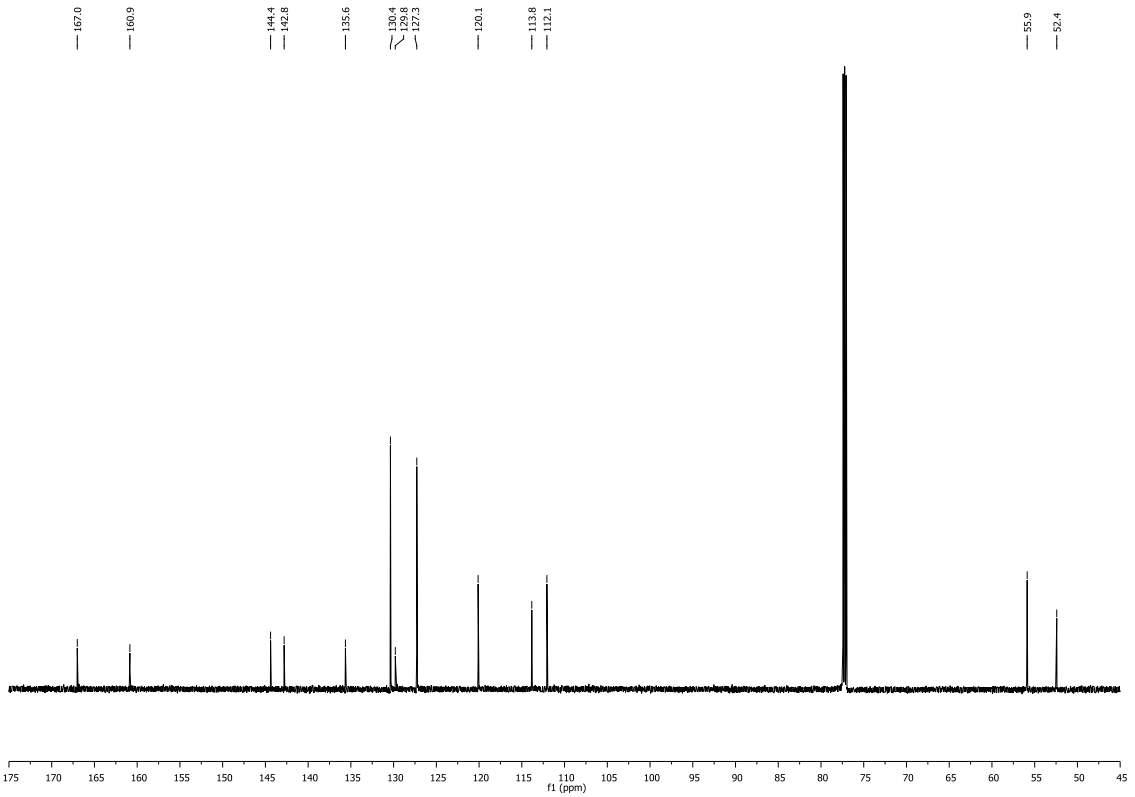

^{13}C NMR (176 MHz, $CHCl_3$)

^{1}H and ^{13}C NMR spectra for compound 313

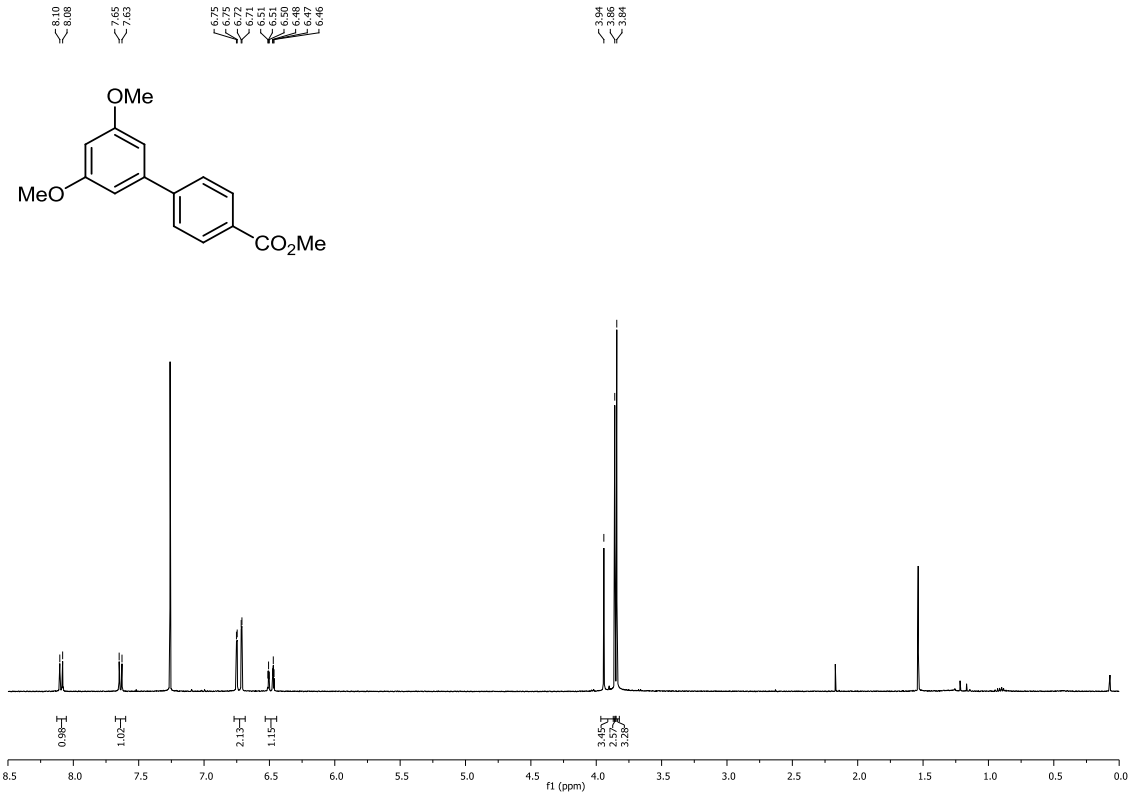

^{1}H NMR (400 MHz, $CDCl_3$)

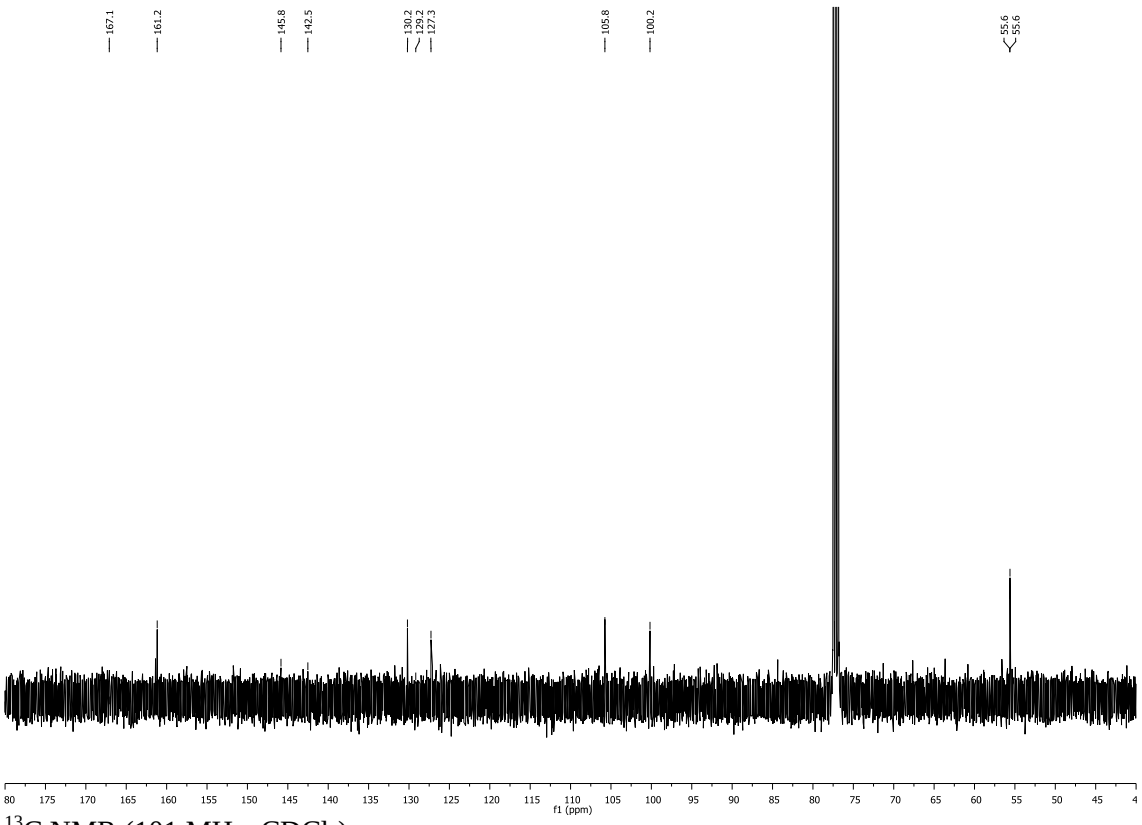

^{13}C NMR (101 MHz, $CDCl_3$)

^{1}H and ^{13}C NMR spectra for compound 314

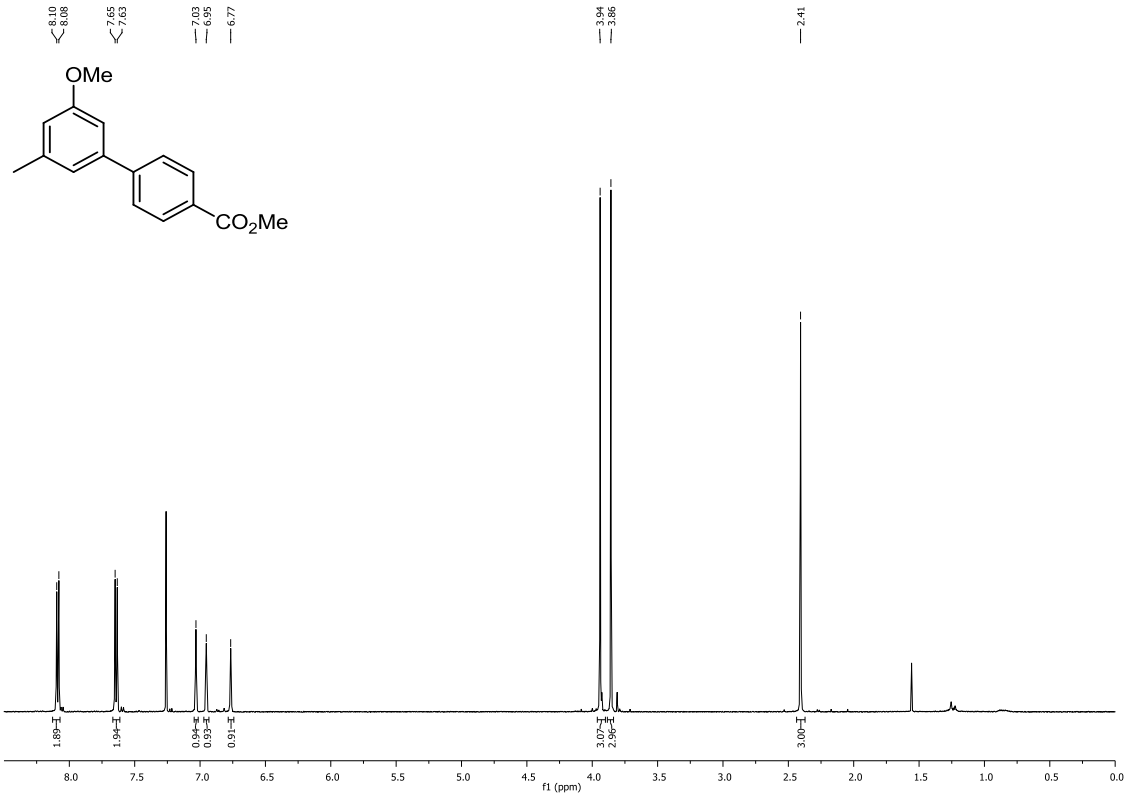

^{1}H NMR (500 MHz, $CDCl_3$)

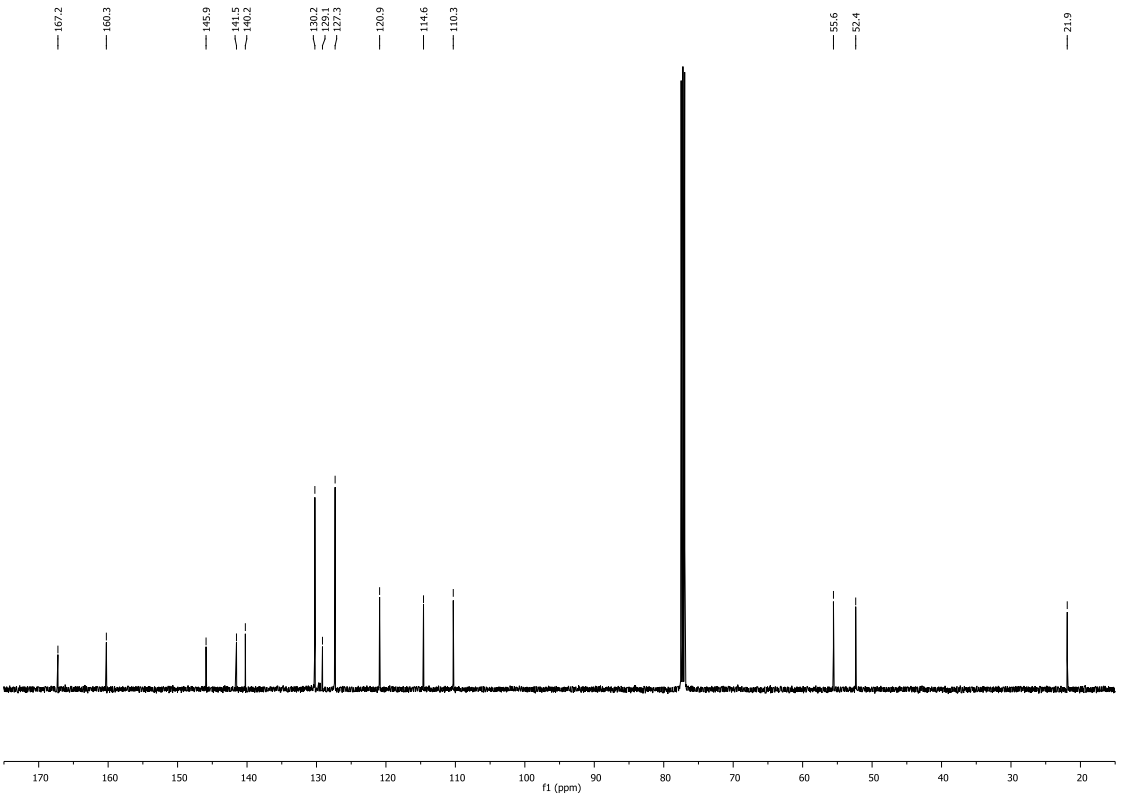

^{13}C NMR (126 MHz, $CDCl_3$)

^{1}H and ^{13}C NMR spectra for compound 316

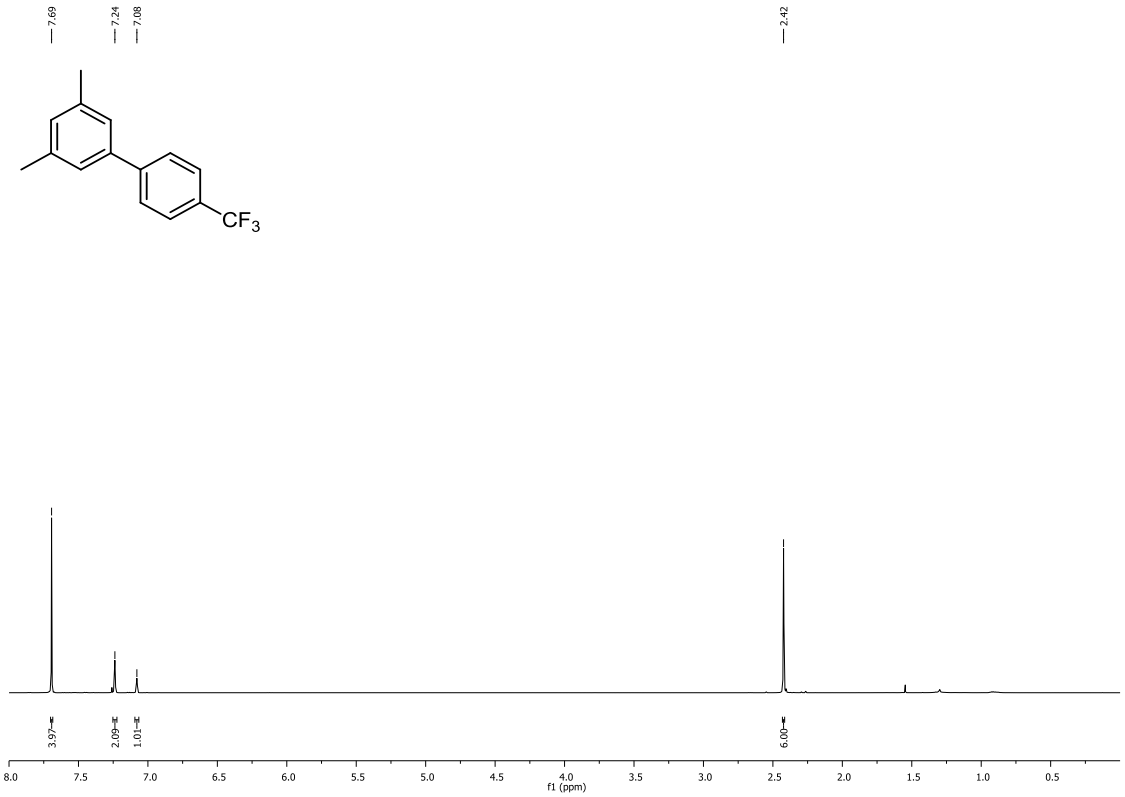

^{1}H NMR (500 MHz, $CDCl_3$)

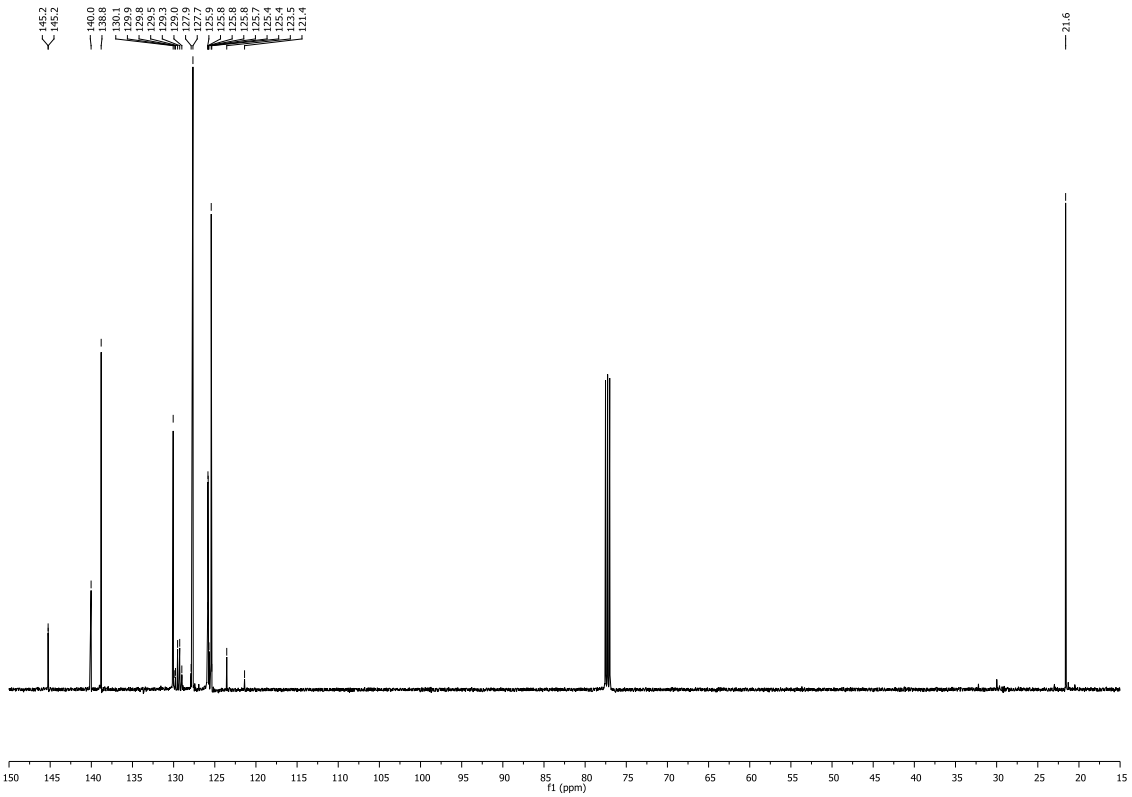

^{13}C NMR (126 MHz, $CDCl_3$)

^{1}H and ^{13}C NMR spectra for compound 317

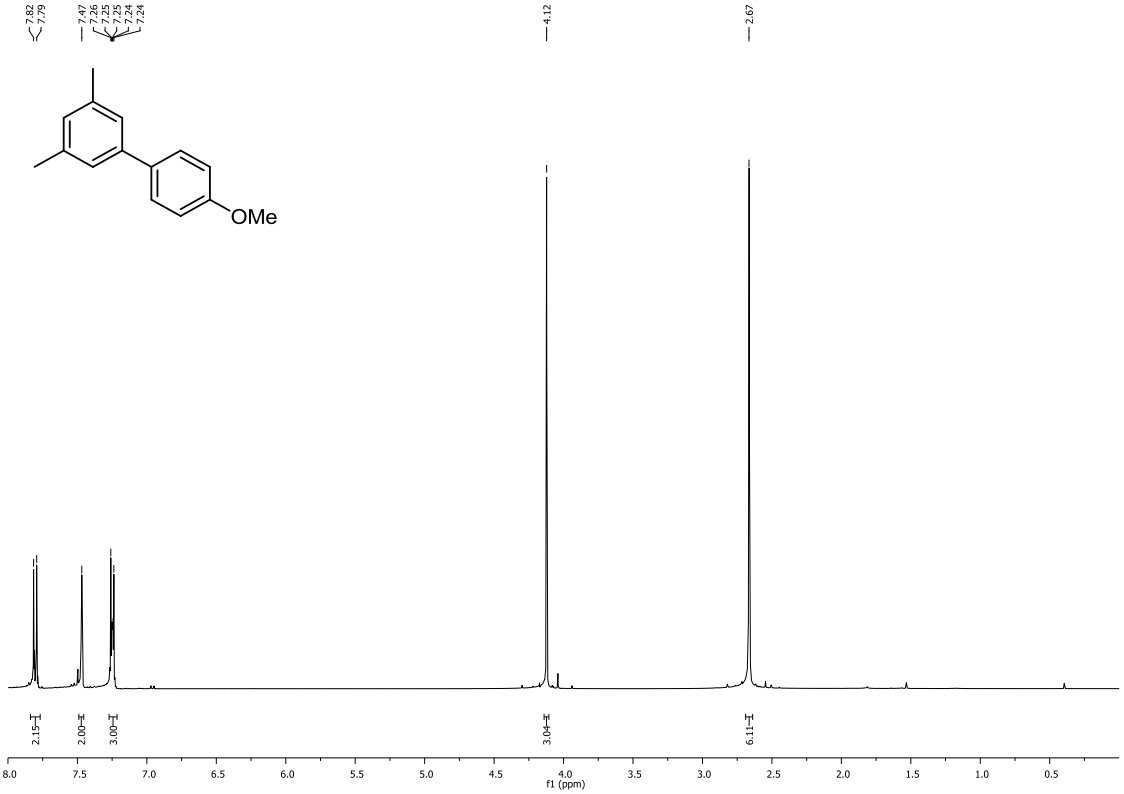

^{1}H NMR (400 MHz, $CDCl_3$)

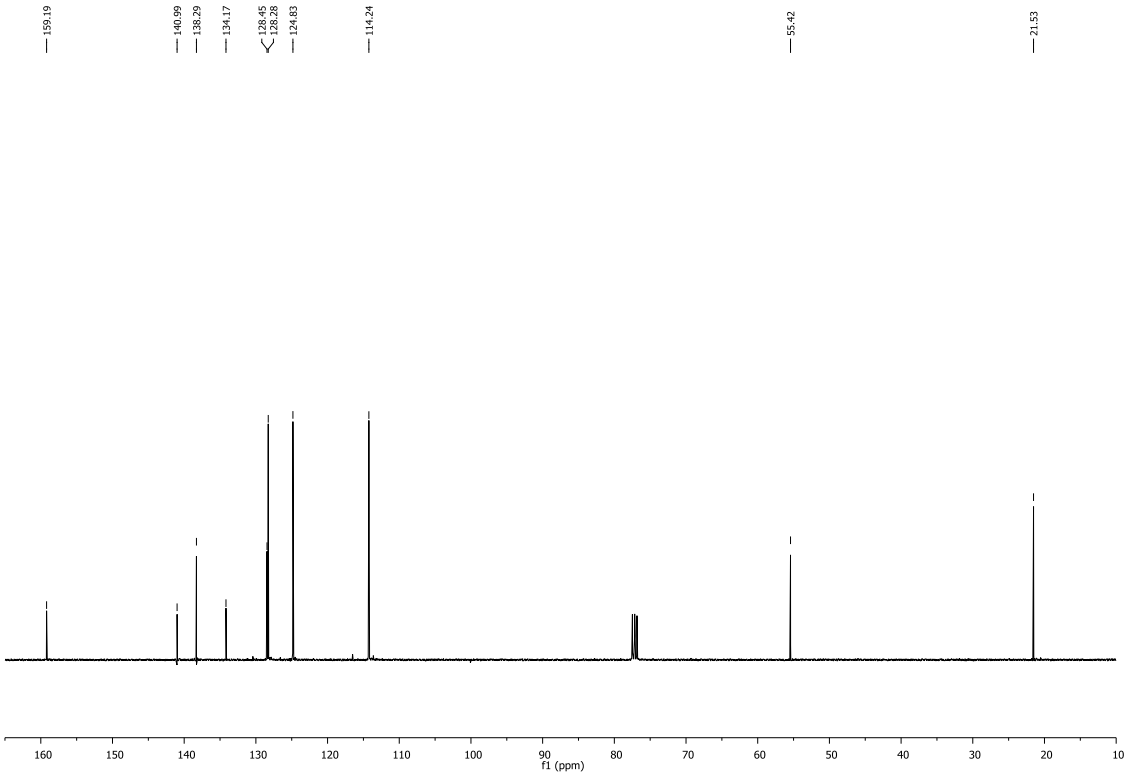

^{13}C NMR (101 MHz, $CDCl_3$)

^{1}H and ^{13}C NMR spectra for compound 318

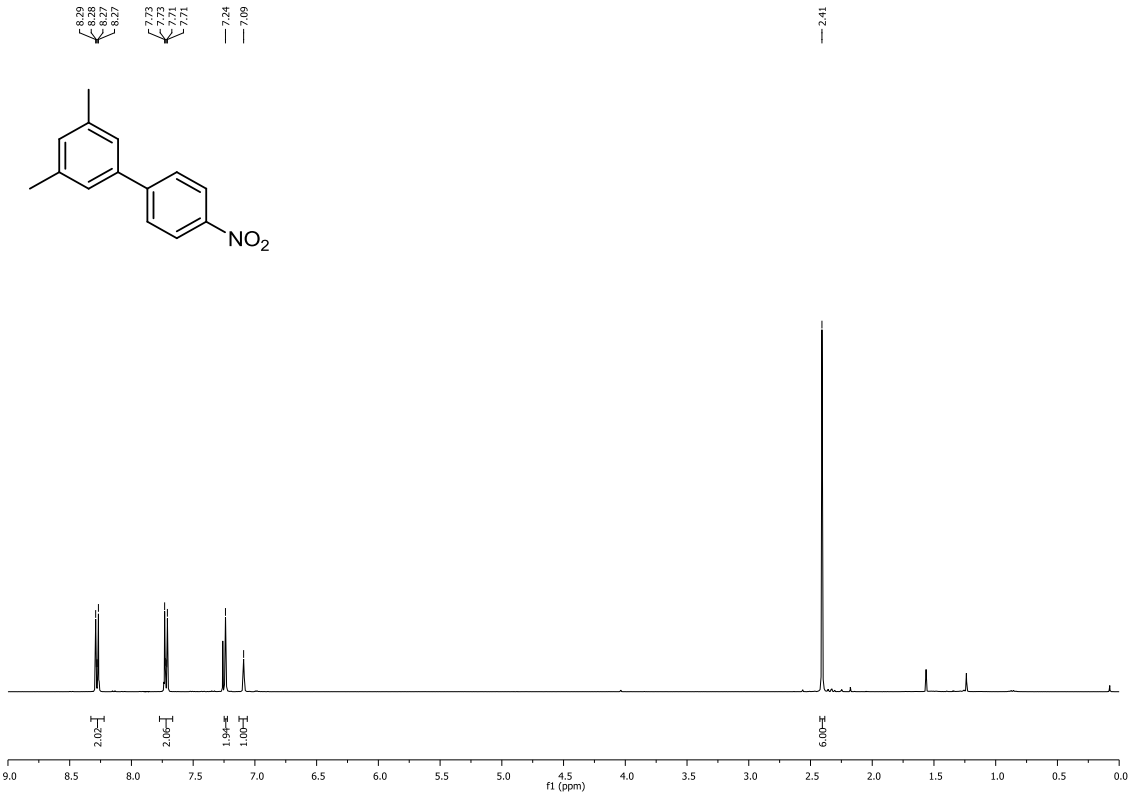

^{1}H NMR (400 MHz, $CDCl_3$)

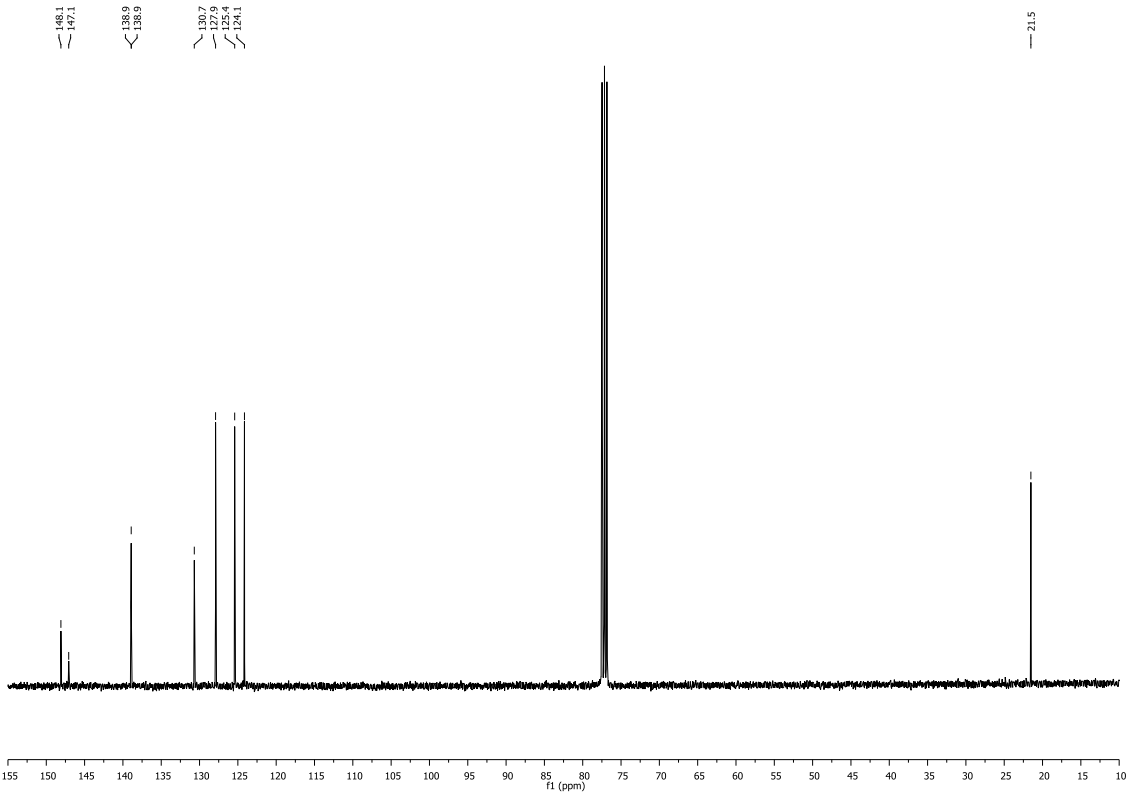

^{13}C NMR (101 MHz, $CDCl_3$)

^{1}H and ^{13}C NMR spectra for compound 319

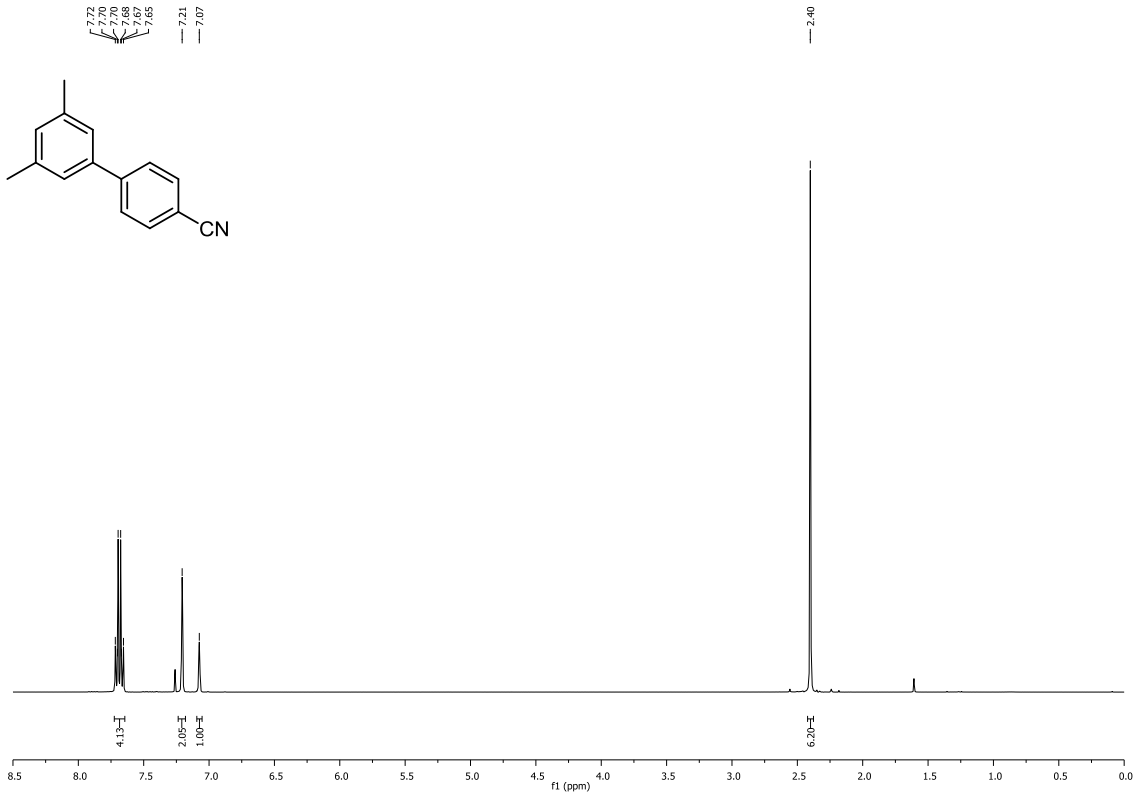

^{1}H NMR (400 MHz, $CDCl_3$)

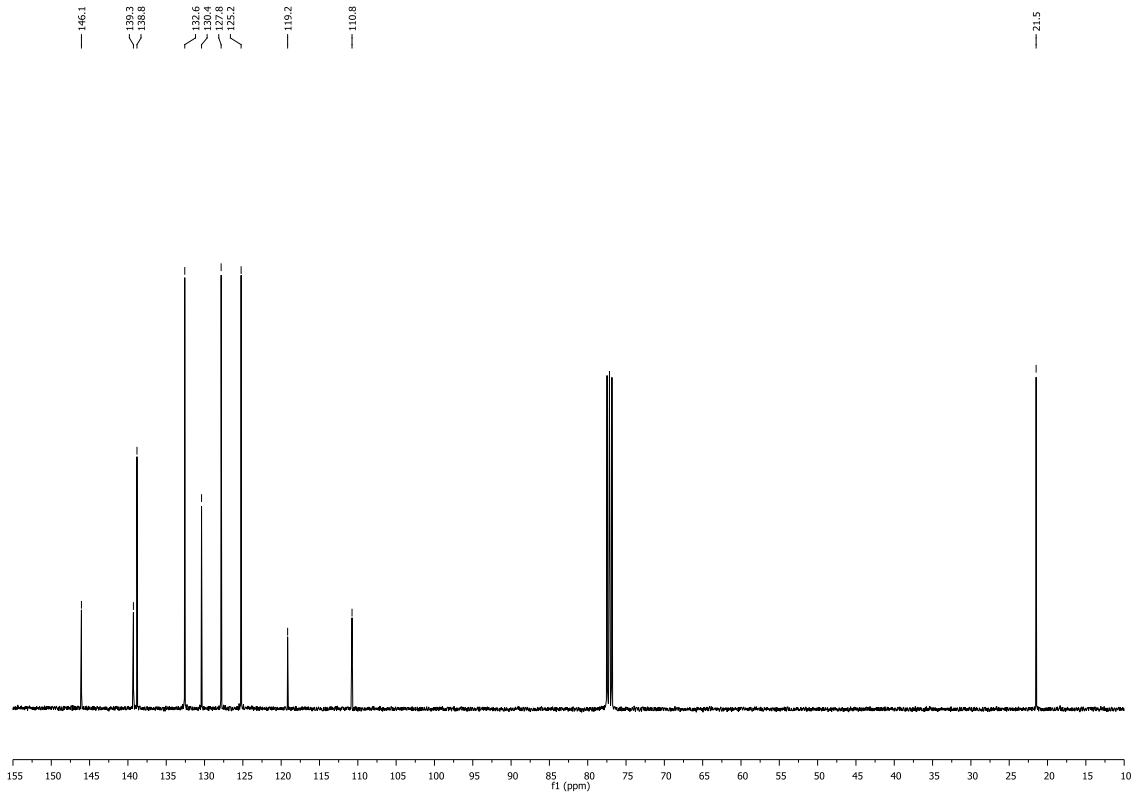

^{13}C NMR (101 MHz, $CDCl_3$)

^{1}H and ^{13}C NMR spectra for compound 320

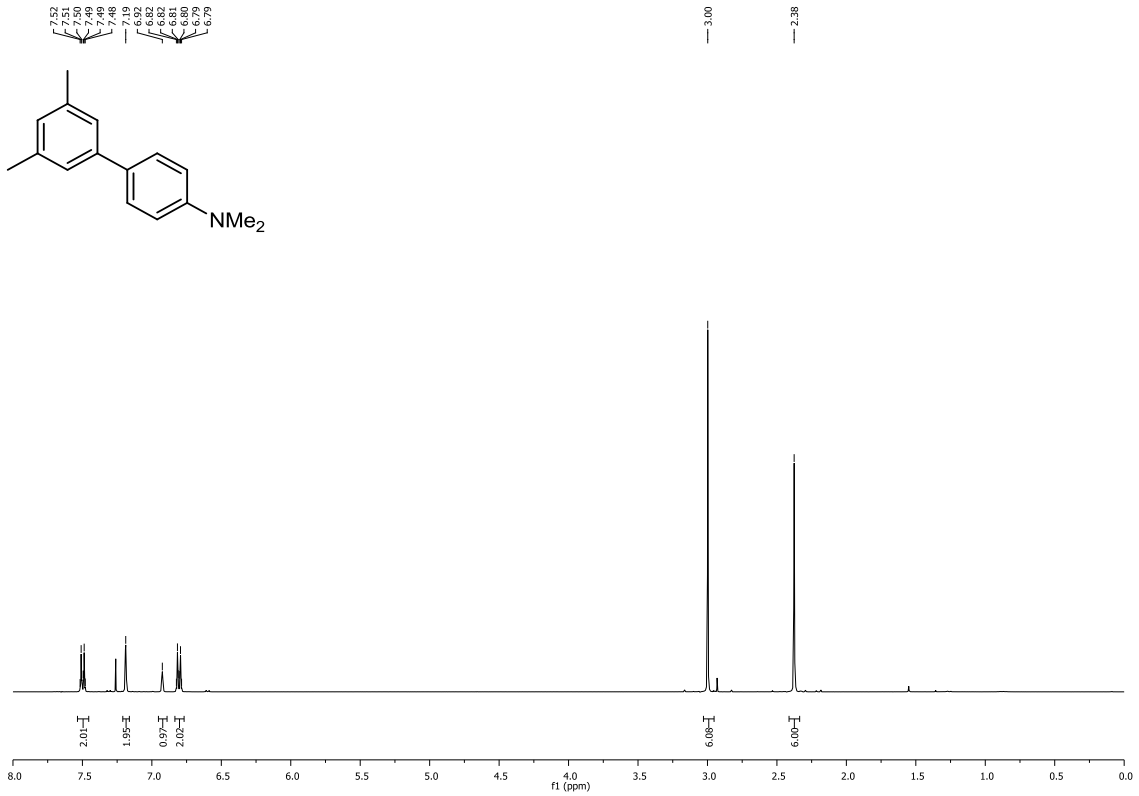

^{1}H NMR (400 MHz, $CDCl_3$)

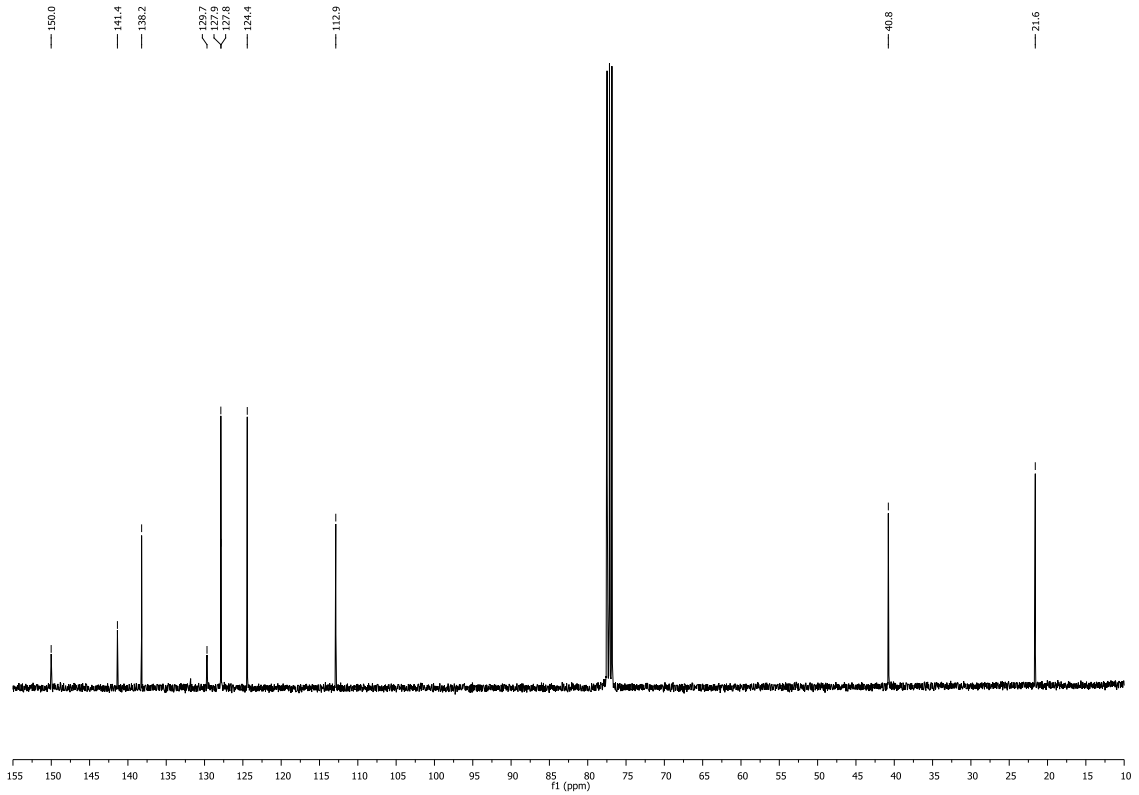

^{13}C NMR (101 MHz, $CDCl_3$)

^{1}H and ^{13}C NMR spectra for compound 342

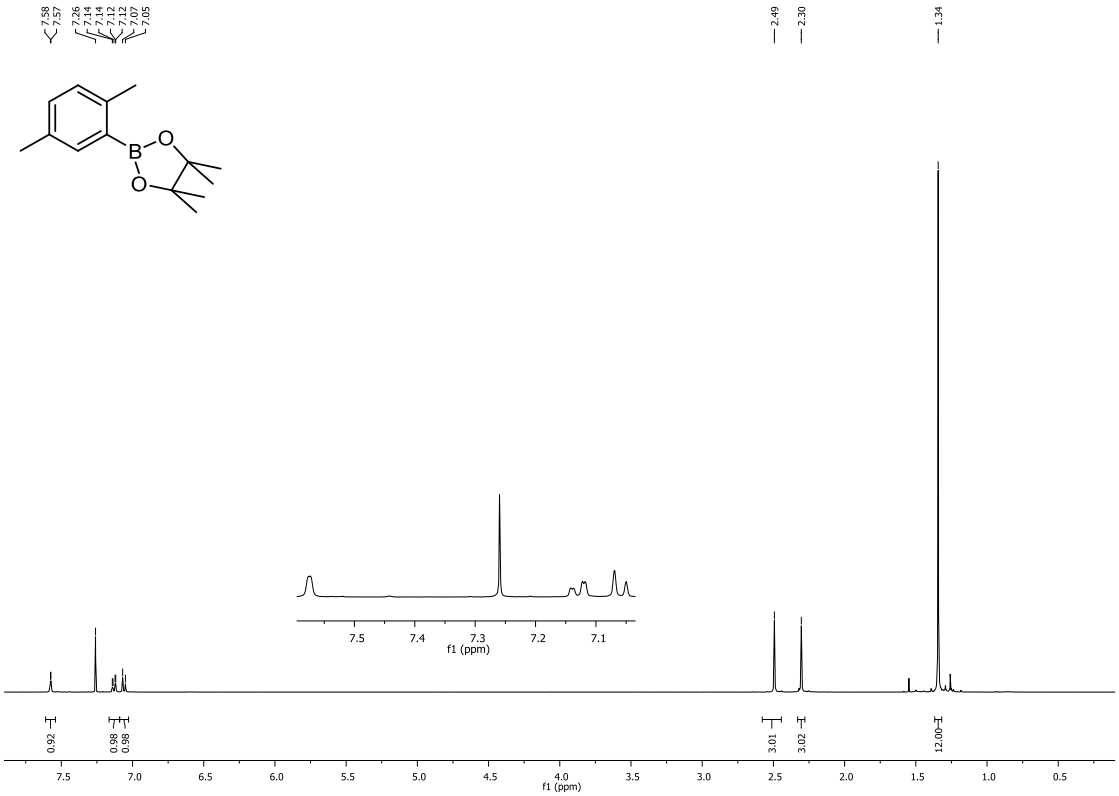

^{1}H NMR (400 MHz, $CDCl_3$)

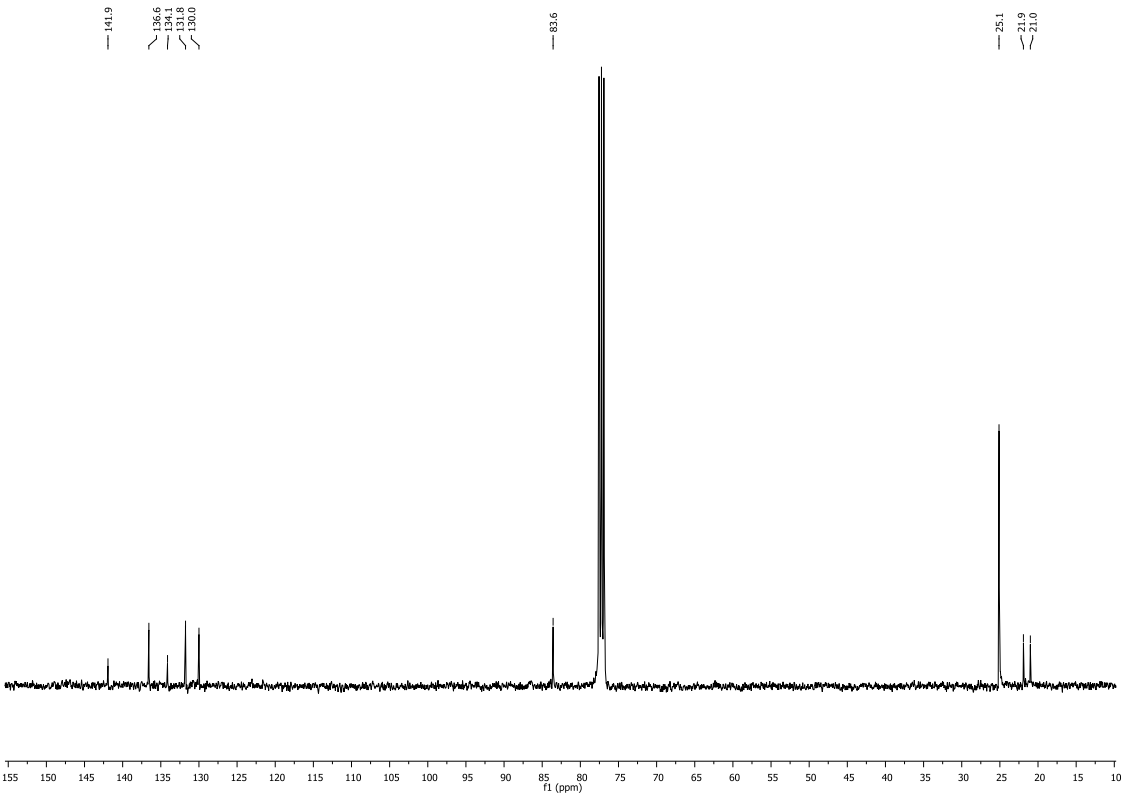

^{13}C NMR (101 MHz, $CDCl_3$)

^{1}H and ^{13}C NMR spectra for compound 344

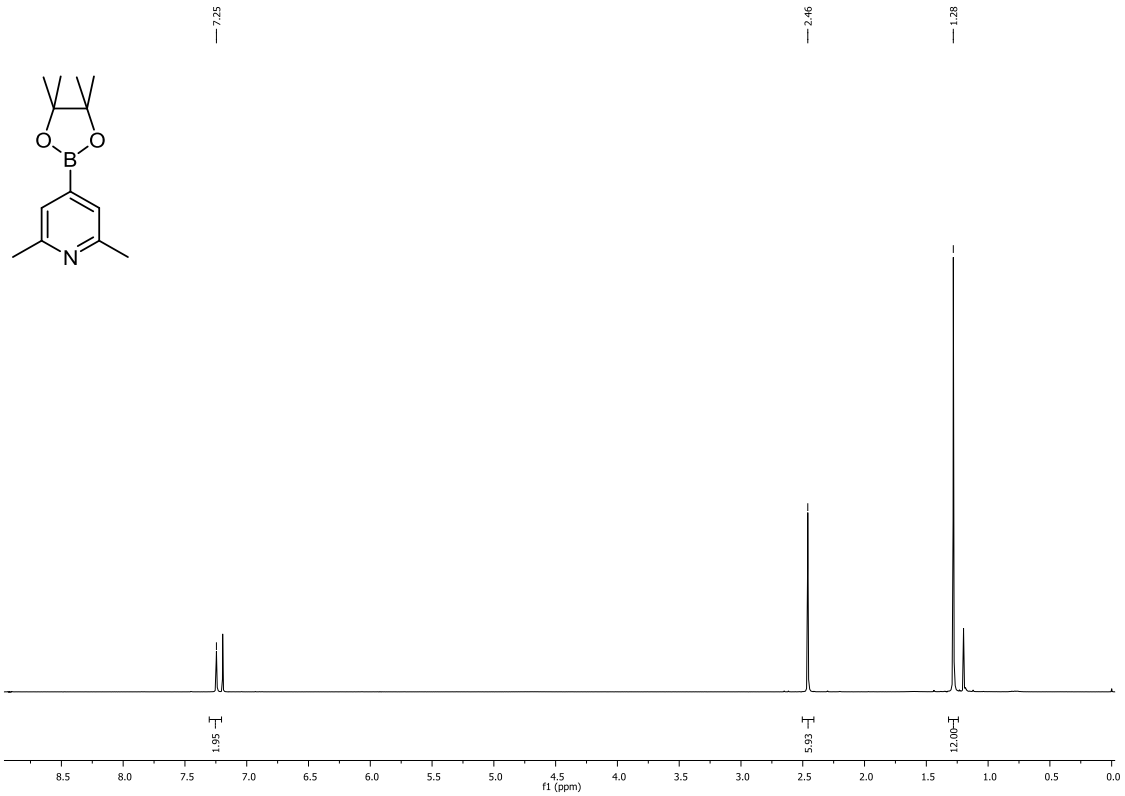

^{1}H NMR (400 MHz, $CDCl_3$)

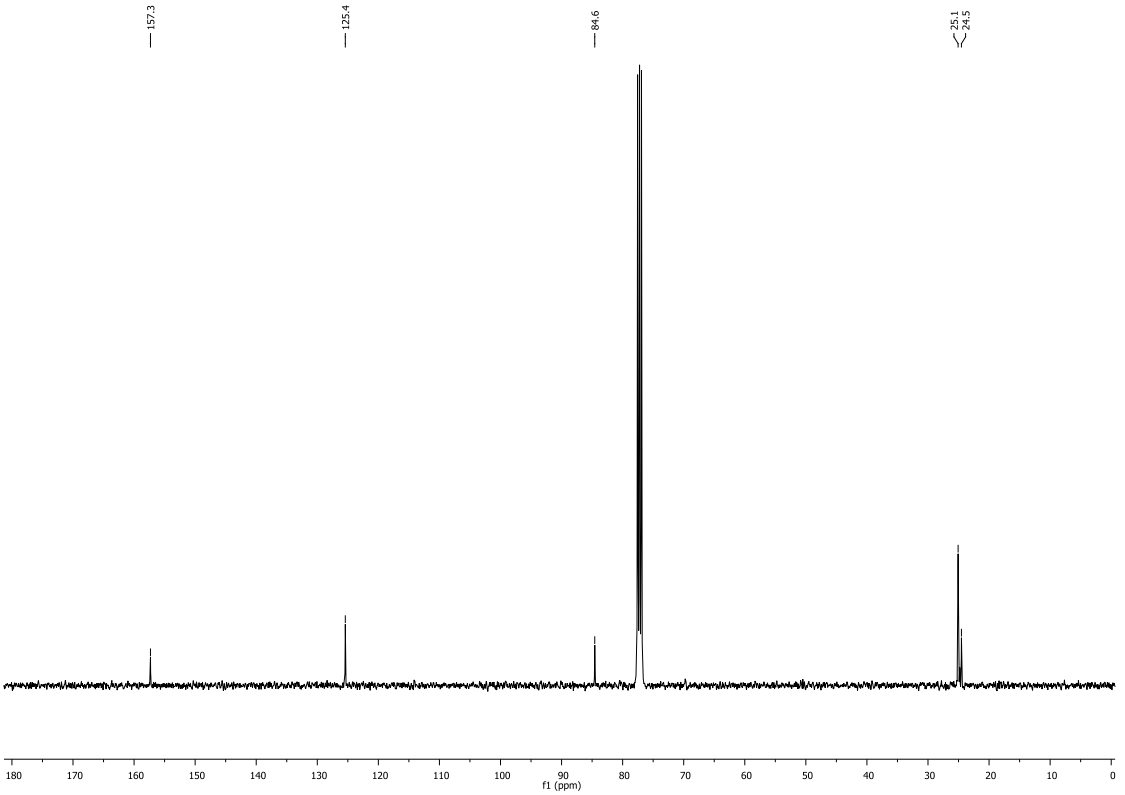

^{13}C NMR (101 MHz, $CDCl_3$)

^{1}H and ^{13}C NMR spectra for compound 58

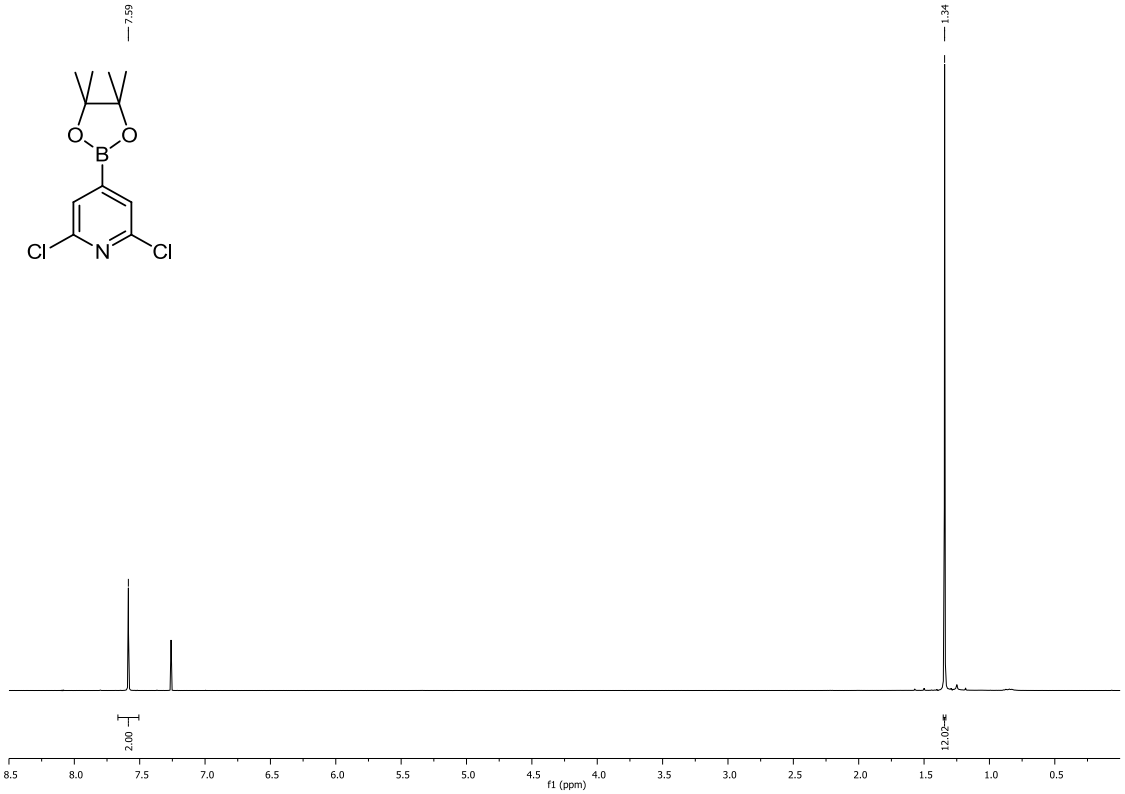

^{1}H NMR (400 MHz, $CDCl_3$)

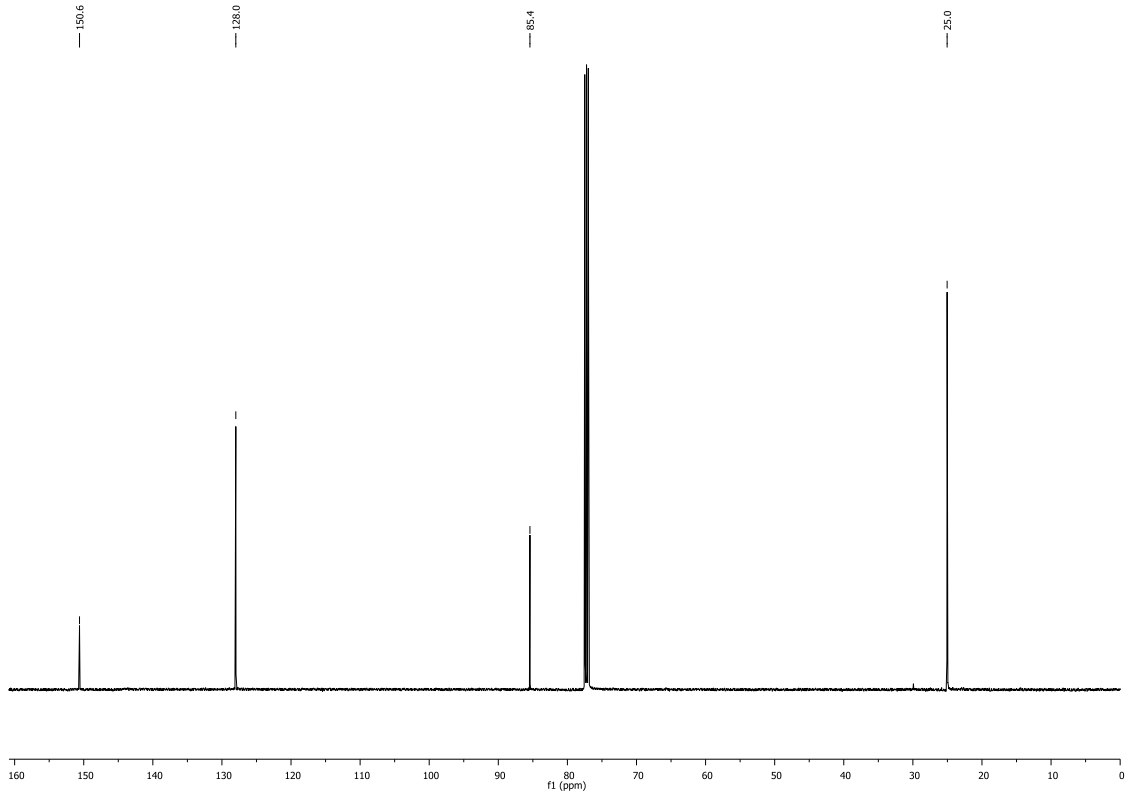

^{13}C NMR (101 MHz, $CDCl_3$)

^{1}H and ^{13}C NMR spectra for compound 345, 346

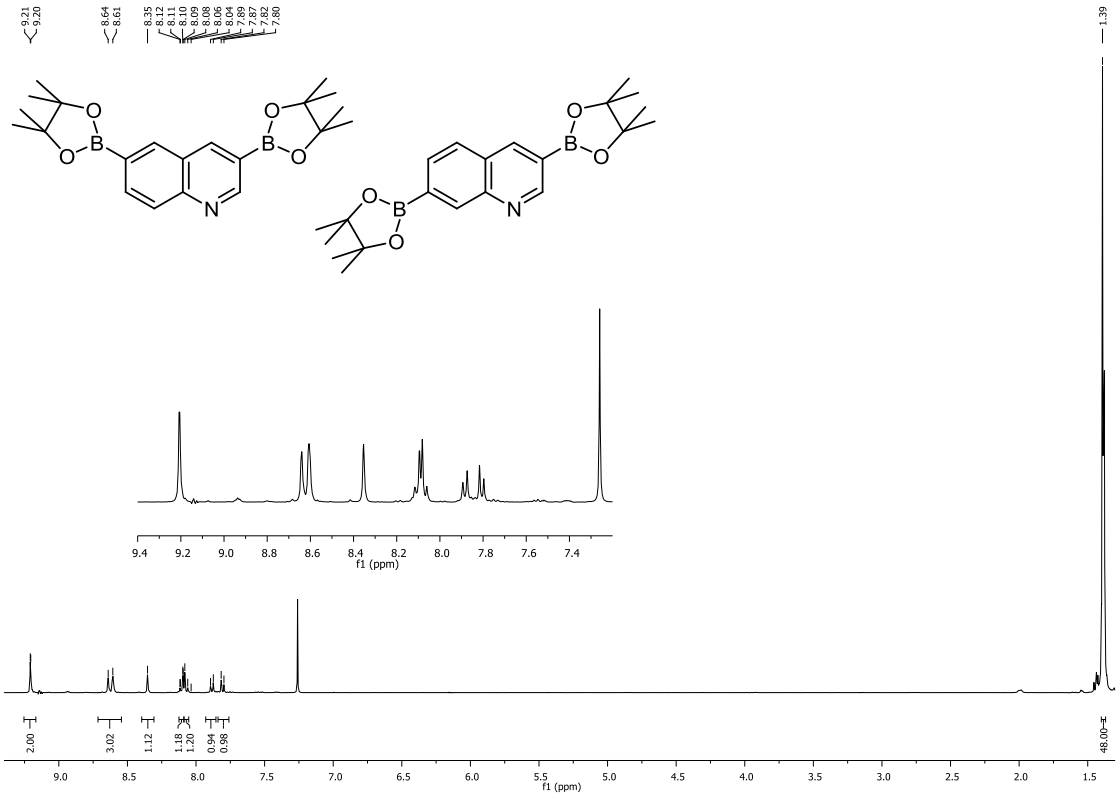

^{1}H NMR (400 MHz, $CDCl_3$)

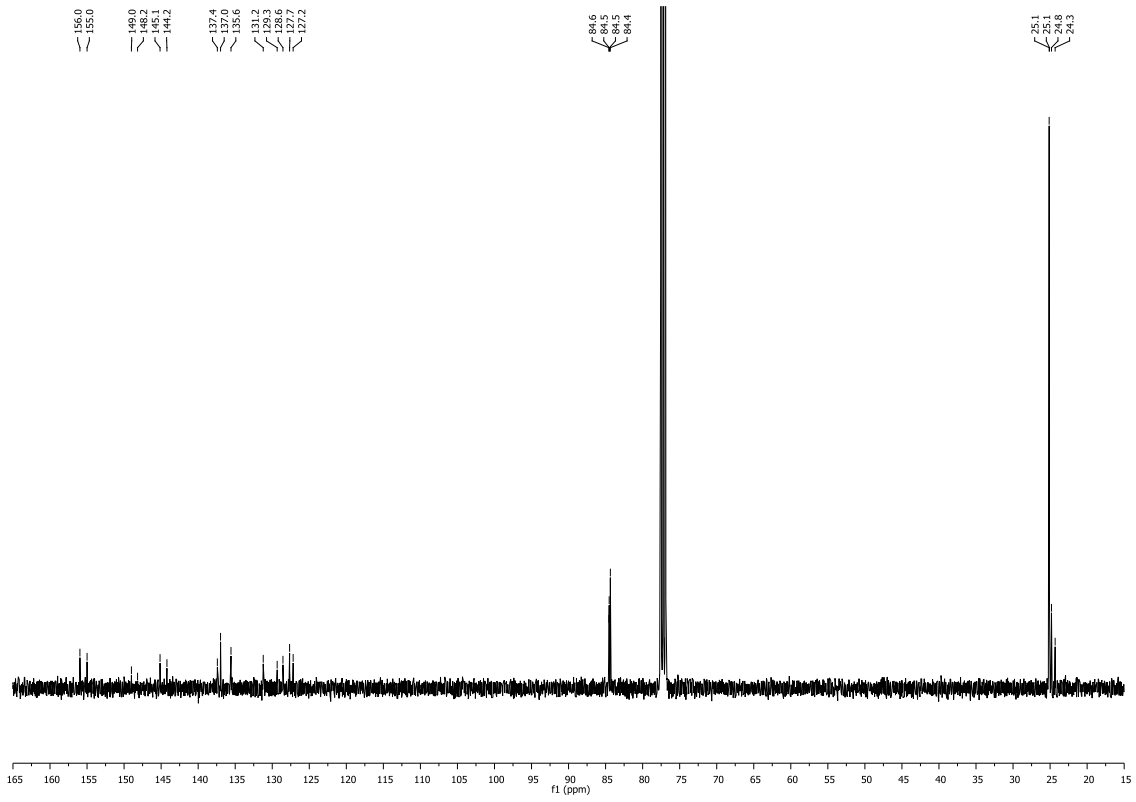

^{13}C NMR (101 MHz, $CDCl_3$)

^{1}H and ^{13}C NMR spectra for compound 345

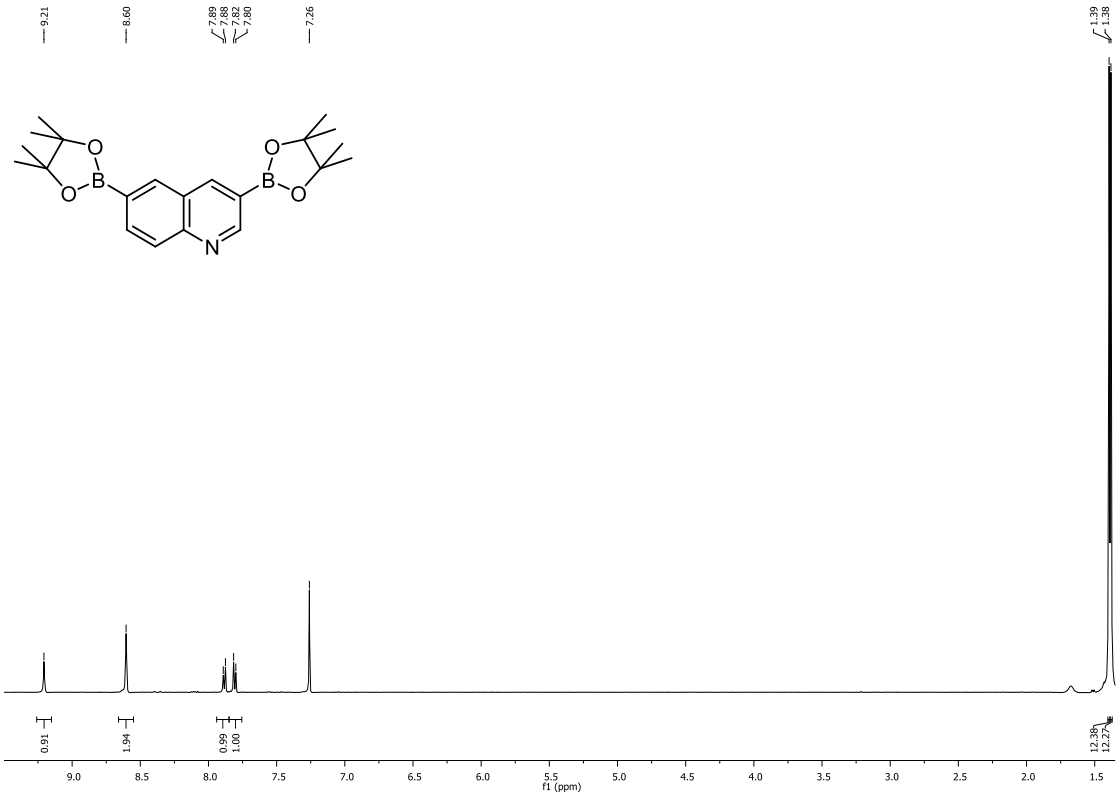

^{1}H NMR (500 MHz, $CDCl_3$)

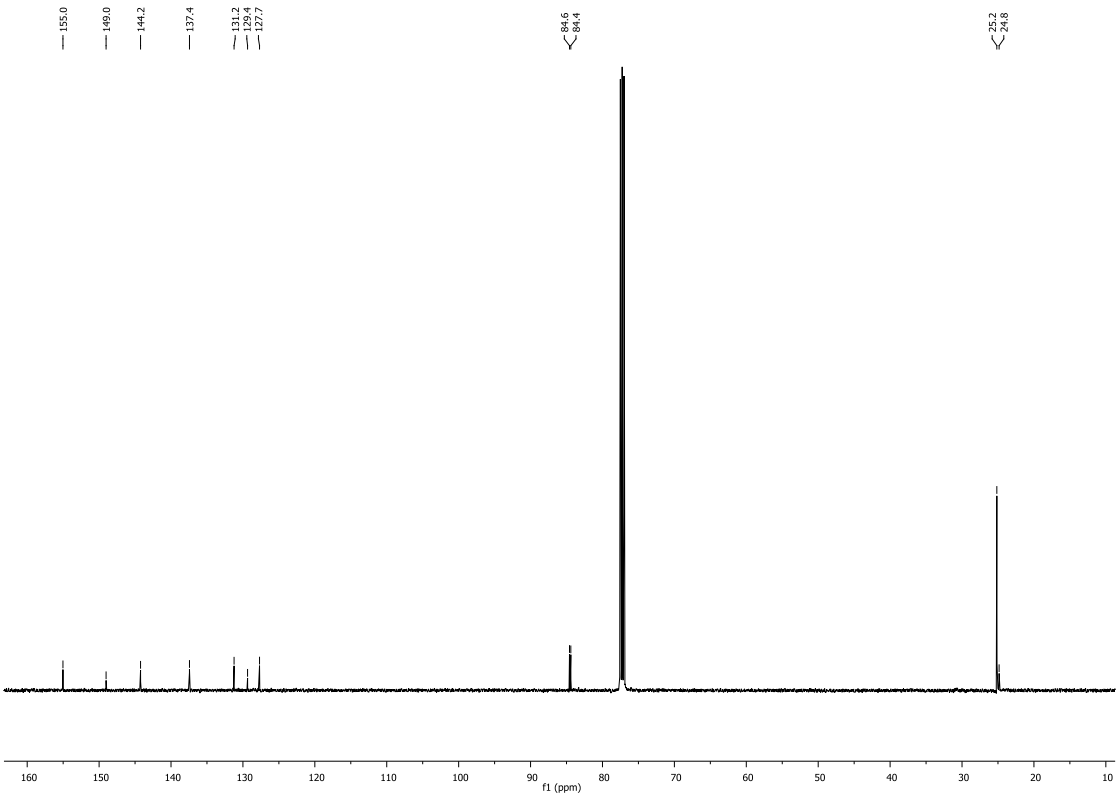

^{13}C NMR (126 MHz, $CDCl_3$)

^{1}H and ^{13}C NMR spectra for compound 353

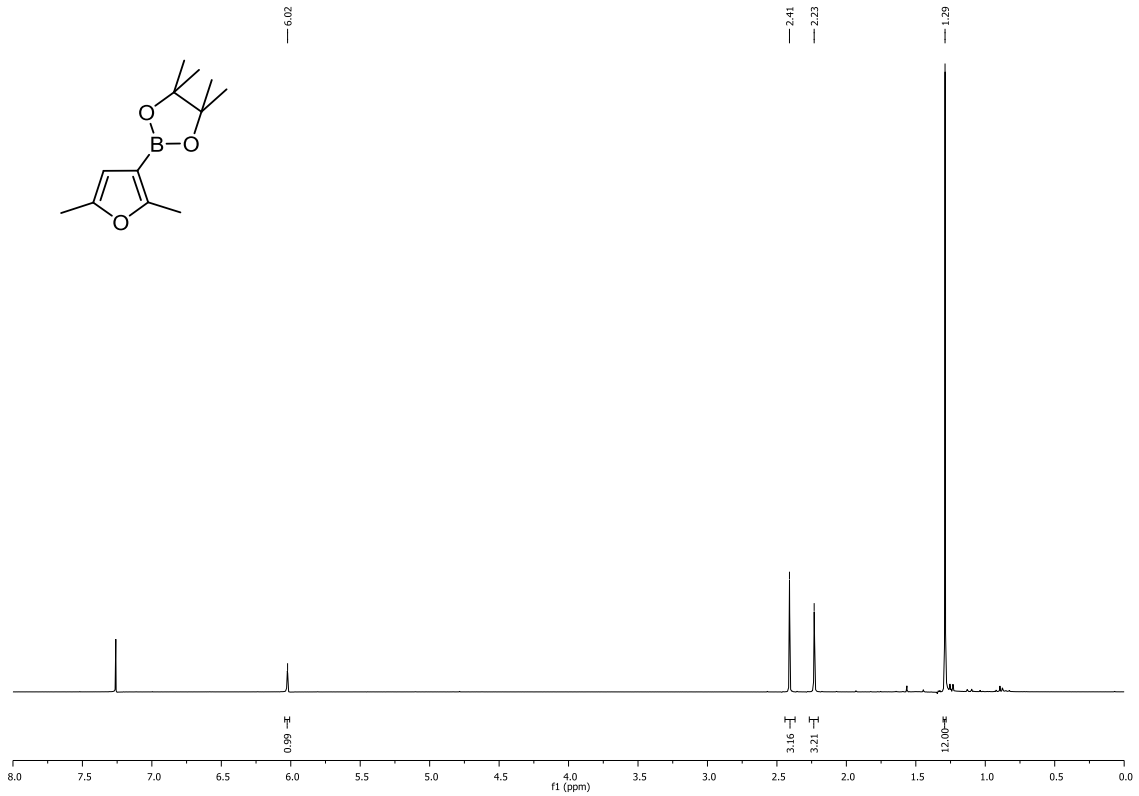

^{1}H NMR (400 MHz, $CDCl_3$)

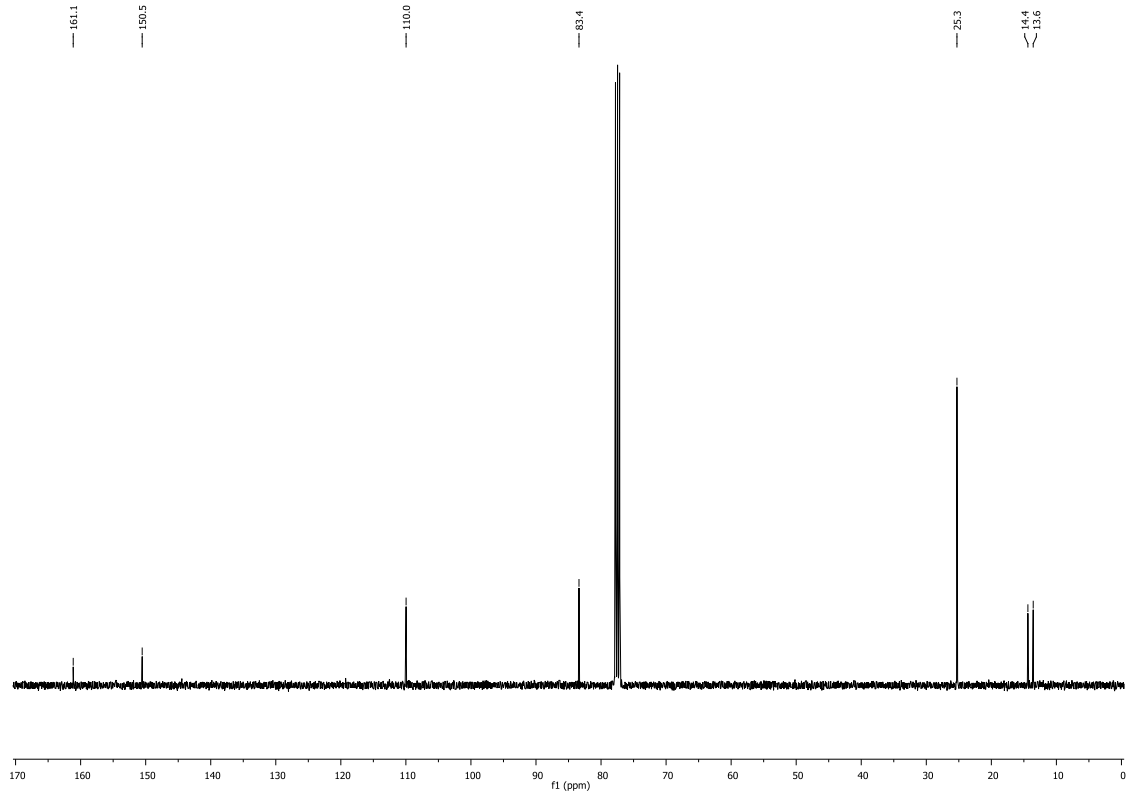

^{13}C NMR (101 MHz, $CDCl_3$)

^{1}H and ^{13}C NMR spectra for compound 355

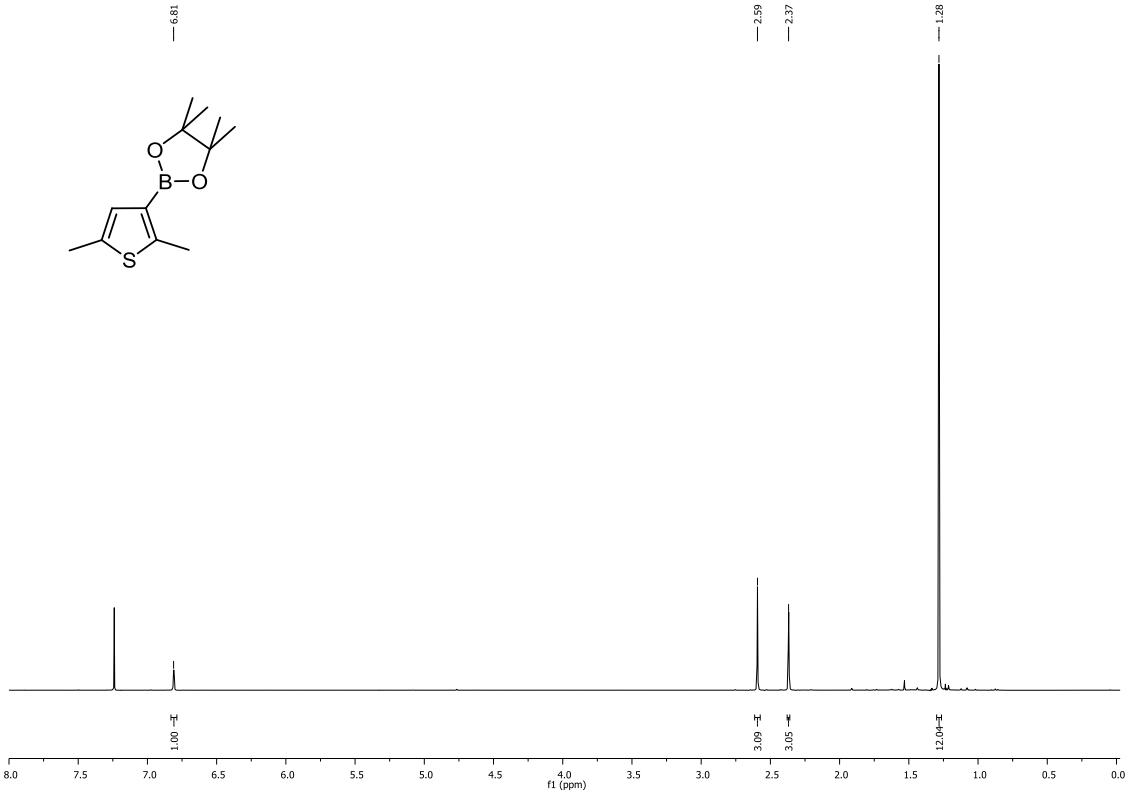

^{1}H NMR (400 MHz, $CDCl_3$)

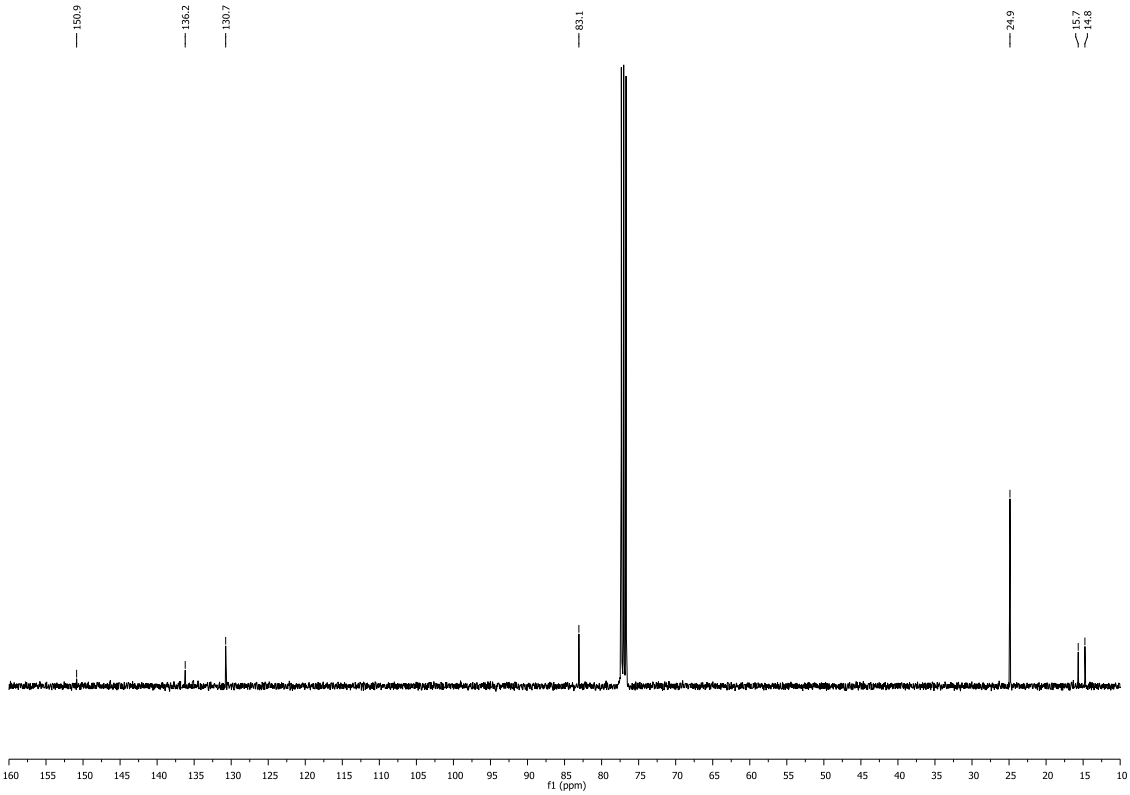

^{13}C NMR (101 MHz, $CDCl_3$)

^{1}H and ^{13}C NMR spectra for compound 357

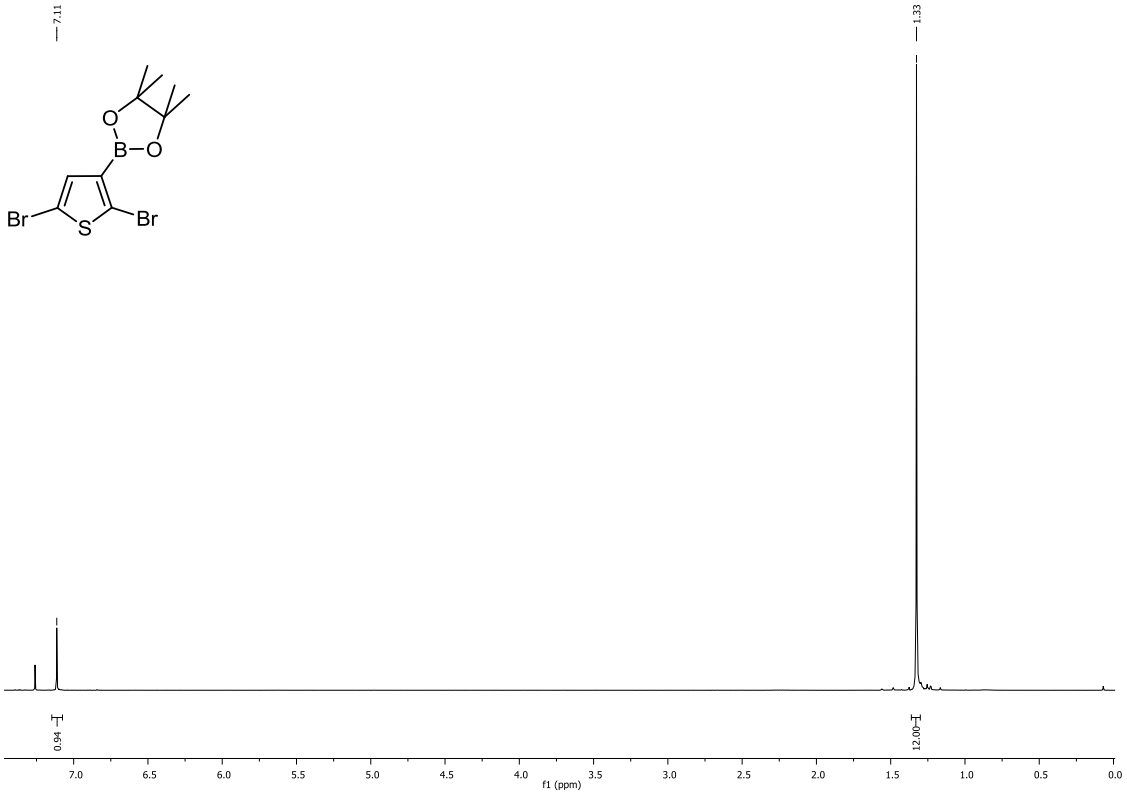

^{1}H NMR (500 MHz, $CDCl_3$)

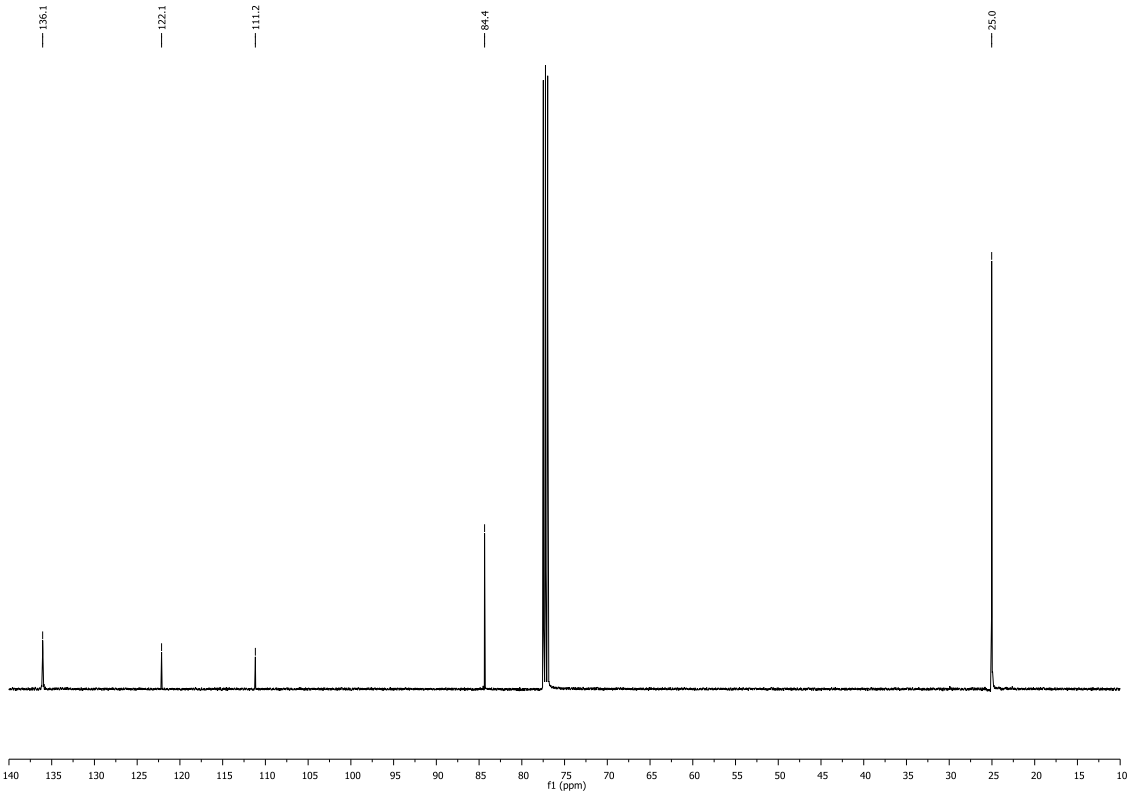

^{13}C NMR (126 MHz, $CDCl_3$)

^{1}H and ^{13}C NMR spectra for compound 359

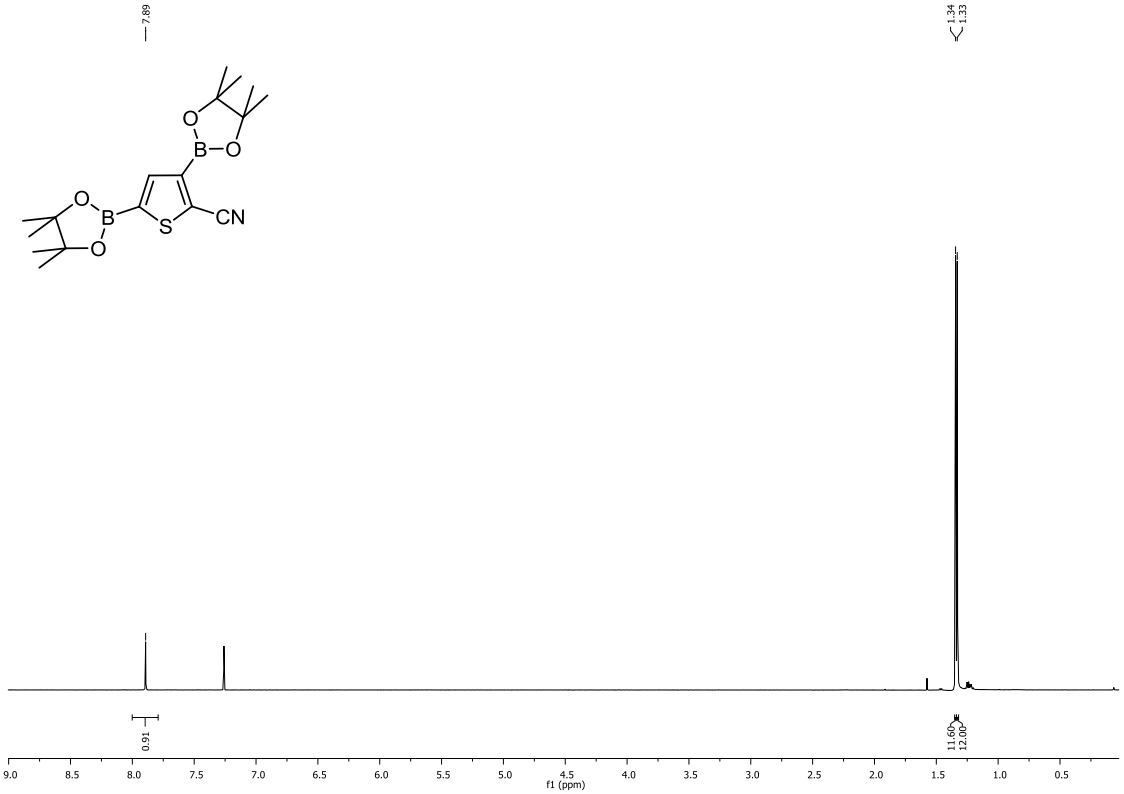

^{1}H NMR (500 MHz, $CDCl_3$)

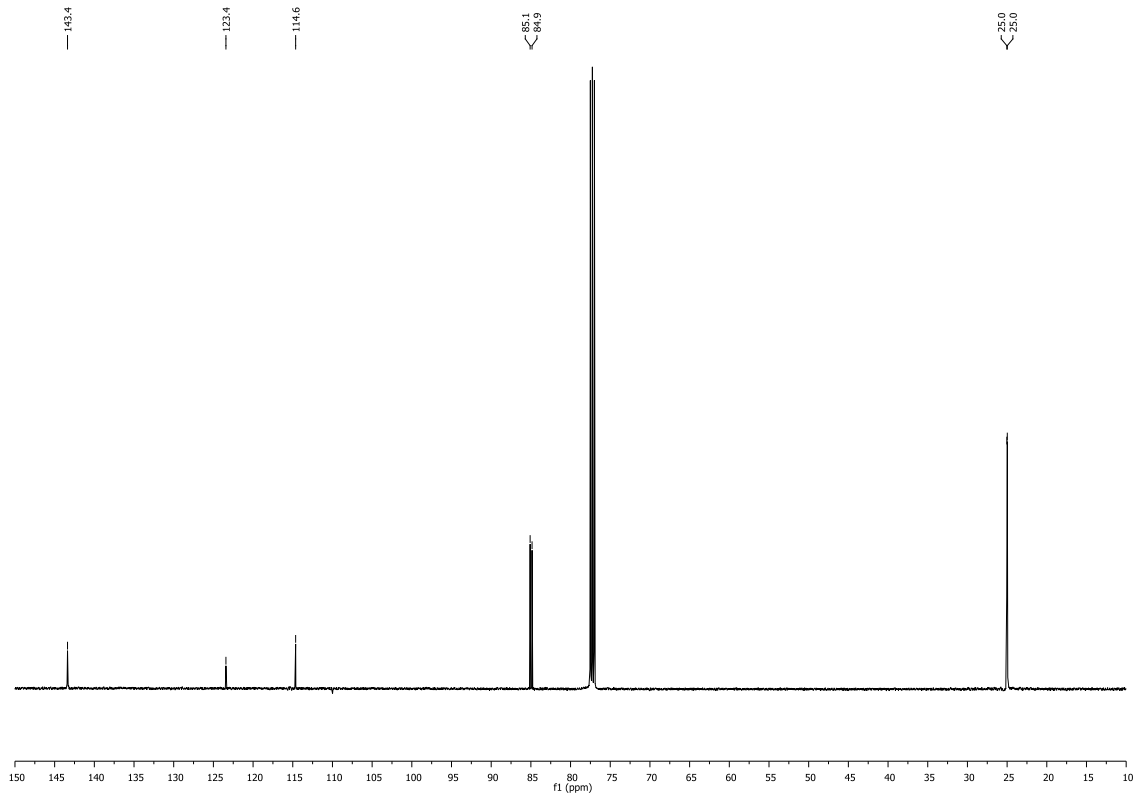

^{13}C NMR (126 MHz, $CDCl_3$)

^{1}H and ^{13}C NMR spectra for compound 361

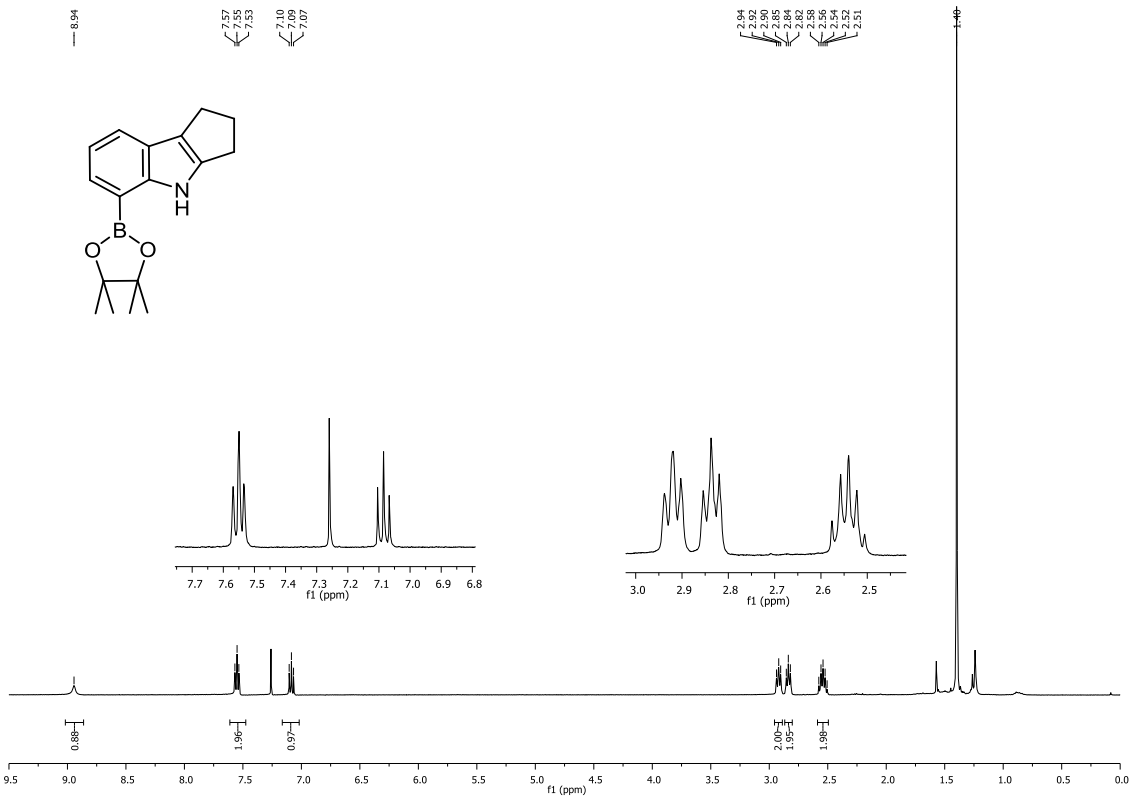

^{1}H NMR (400 MHz, $CDCl_3$)

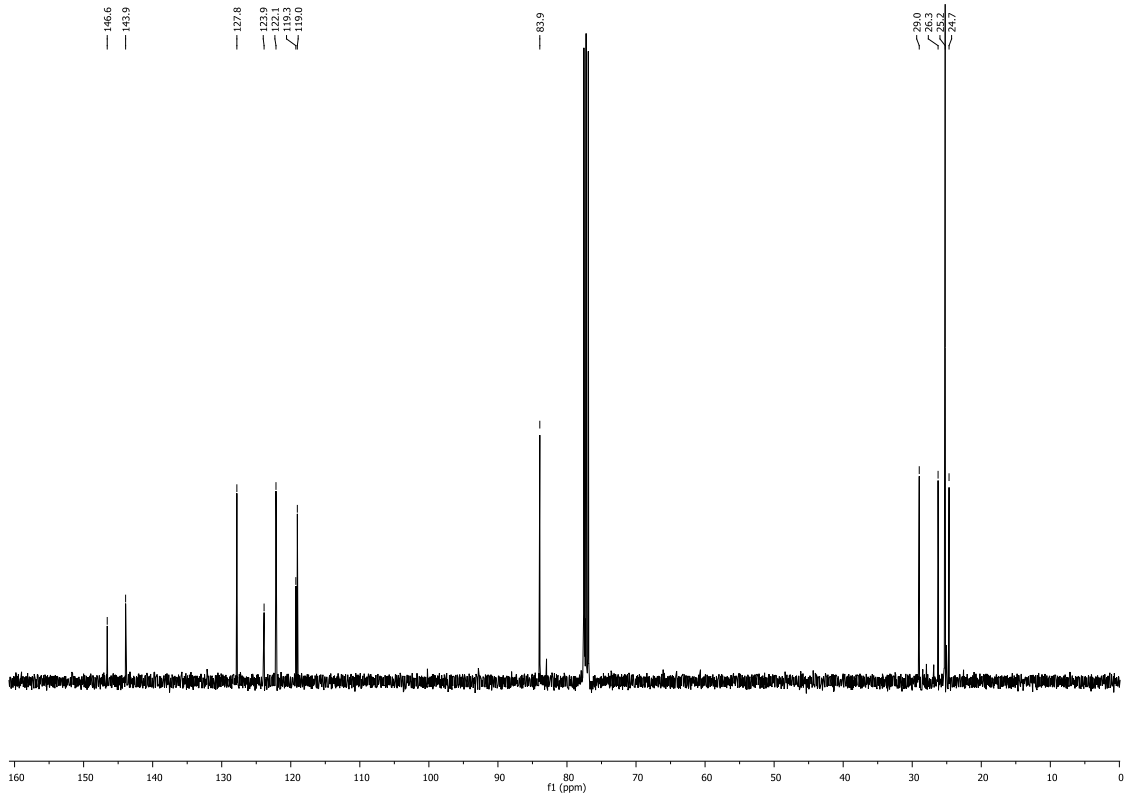

^{13}C NMR (101 MHz, $CDCl_3$)

^{1}H and ^{13}C NMR spectra for compound 362

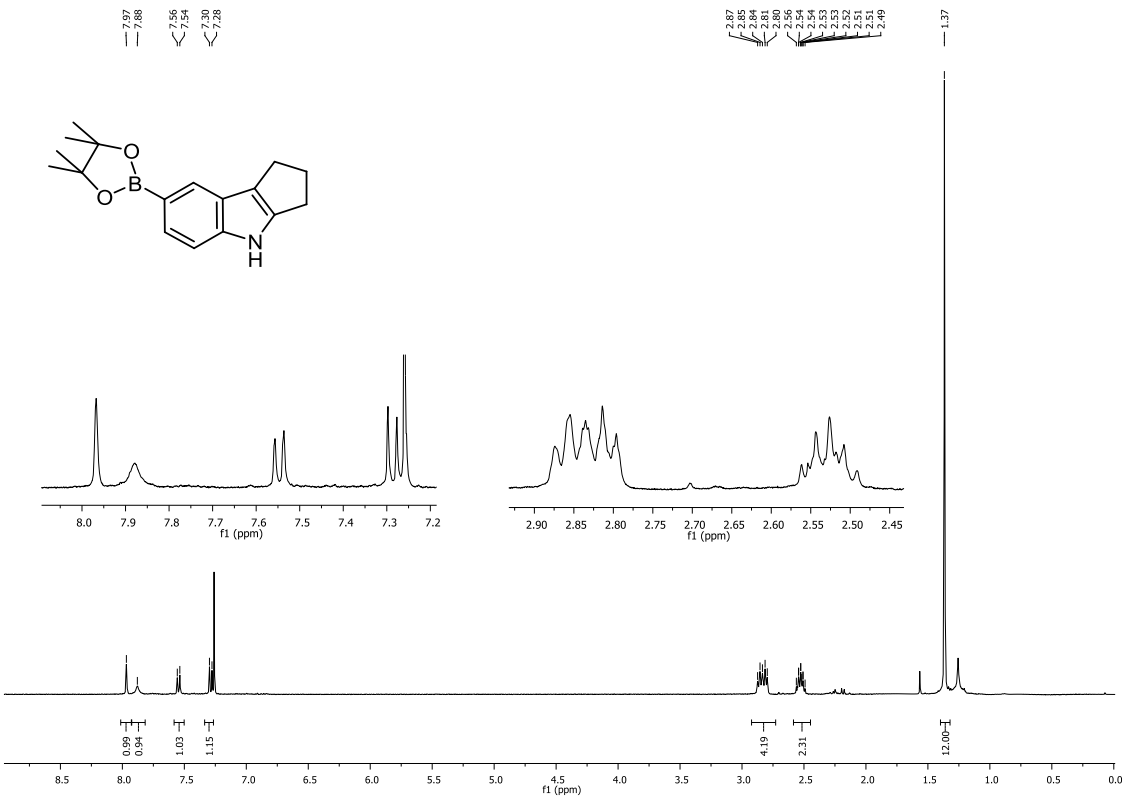

^{1}H NMR (400 MHz, $CDCl_3$)

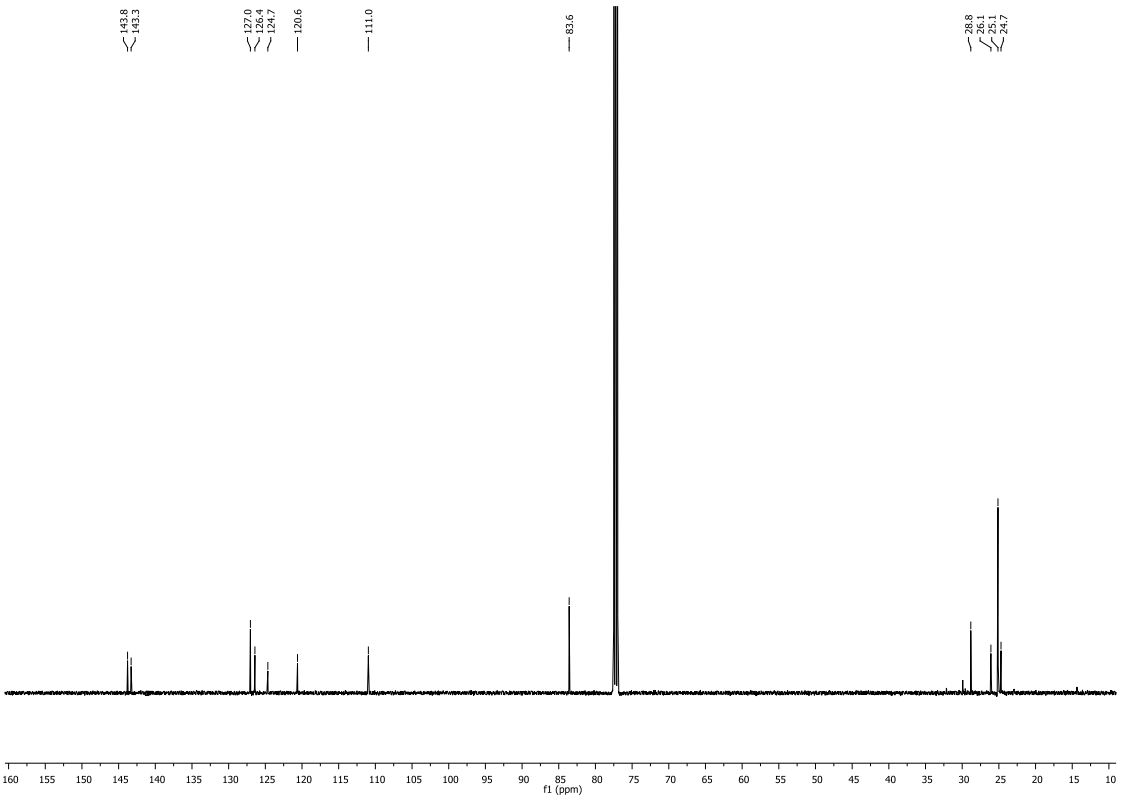

^{13}C NMR (126 MHz, $CDCl_3$)

^{1}H and ^{13}C NMR spectra for compound 364

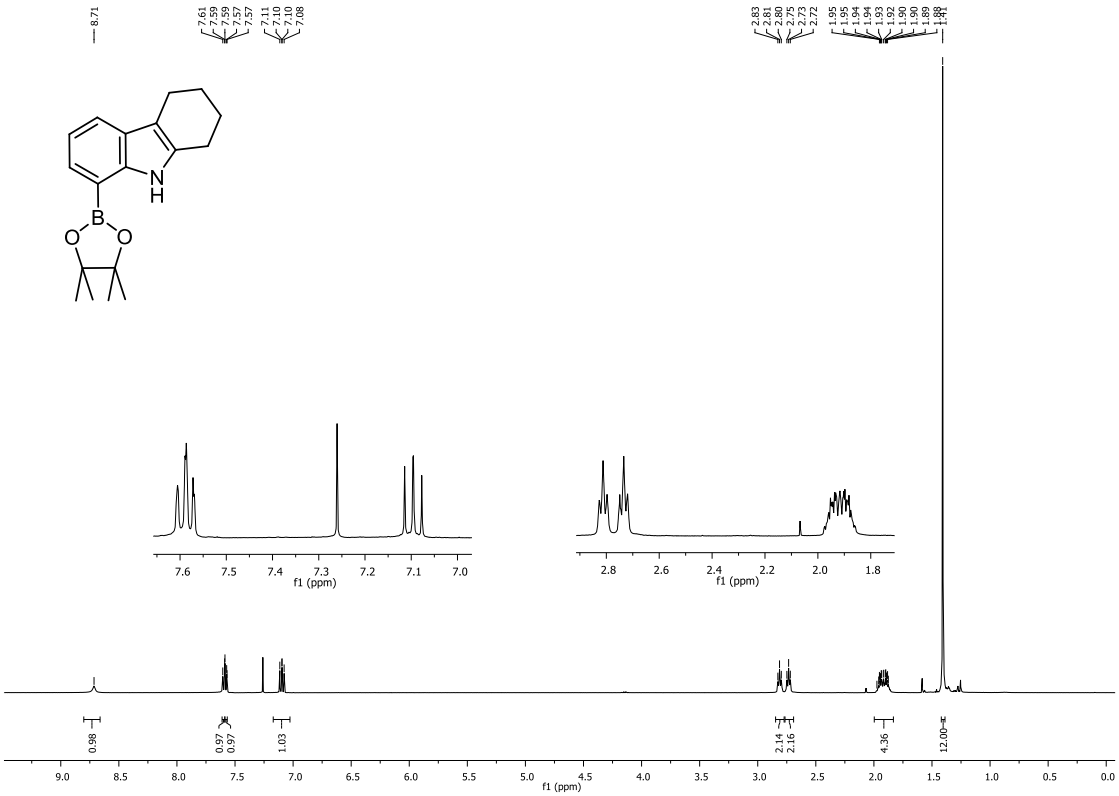

^{1}H NMR (400 MHz, $CDCl_3$)

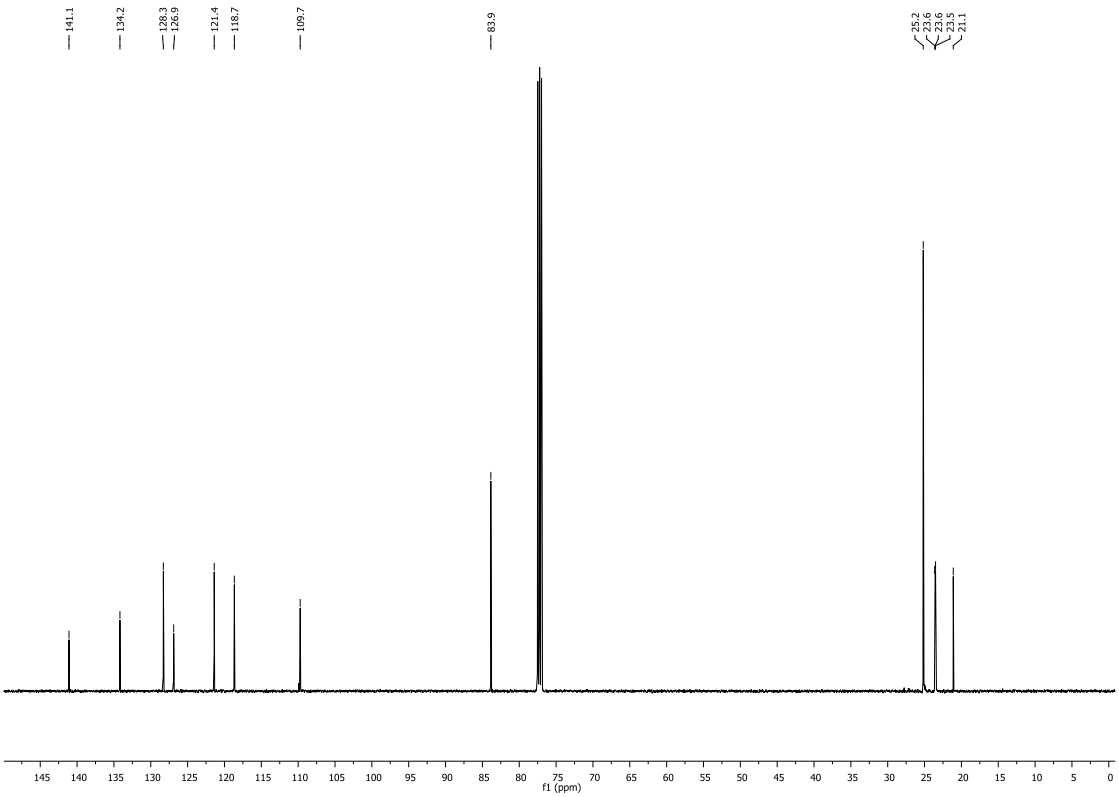

^{13}C NMR (126 MHz, $CDCl_3$)

^{1}H and ^{13}C NMR spectra for compound 172

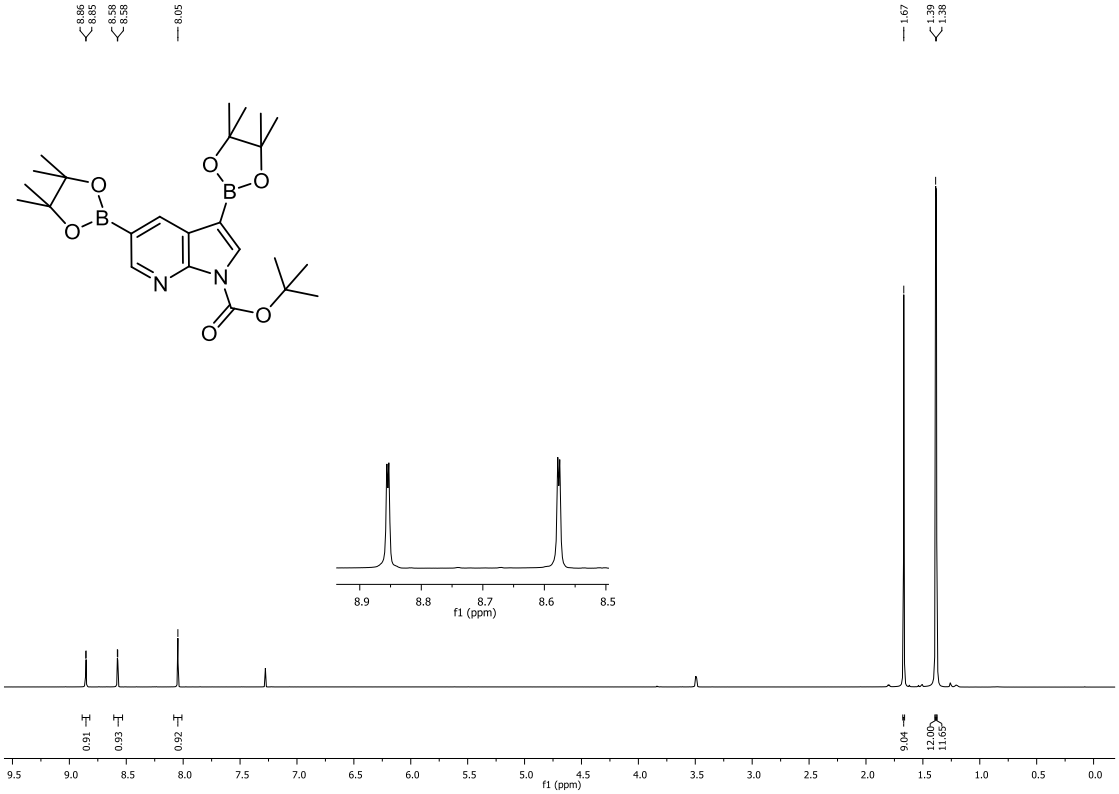

^{1}H NMR (500 MHz, $CDCl_3$)

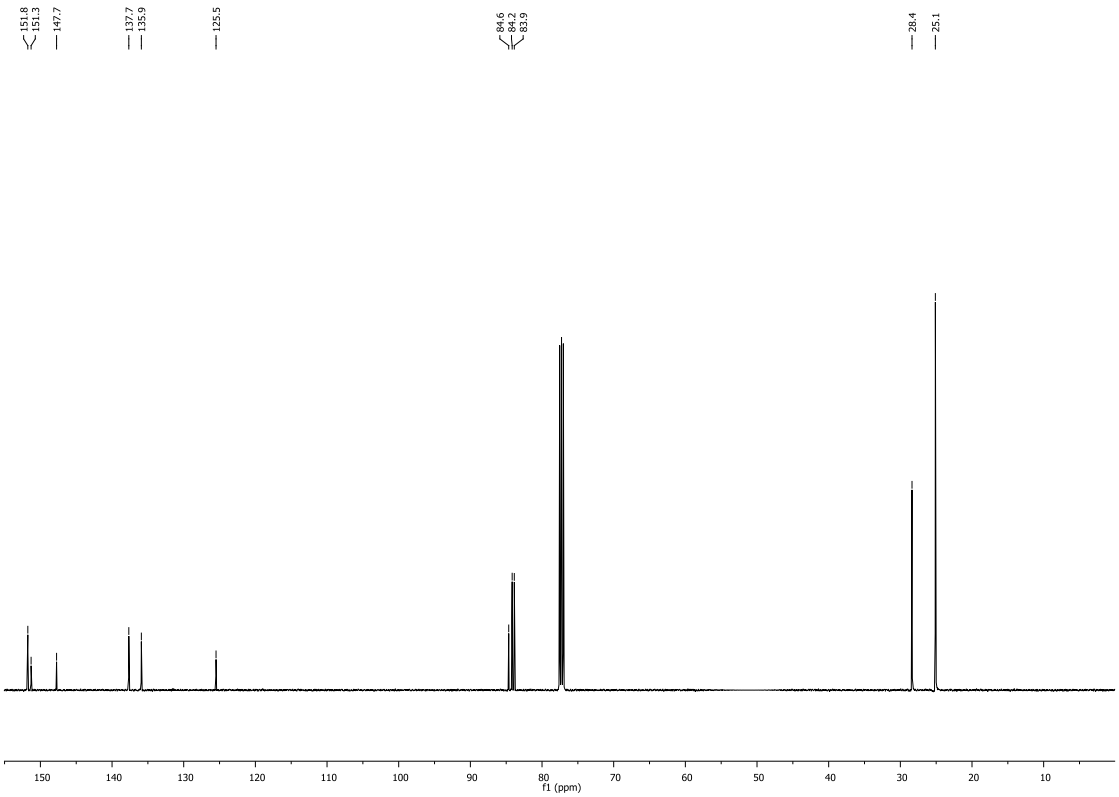

^{13}C NMR (126 MHz, $CDCl_3$)

^{1}H and ^{13}C NMR spectra for compound 366

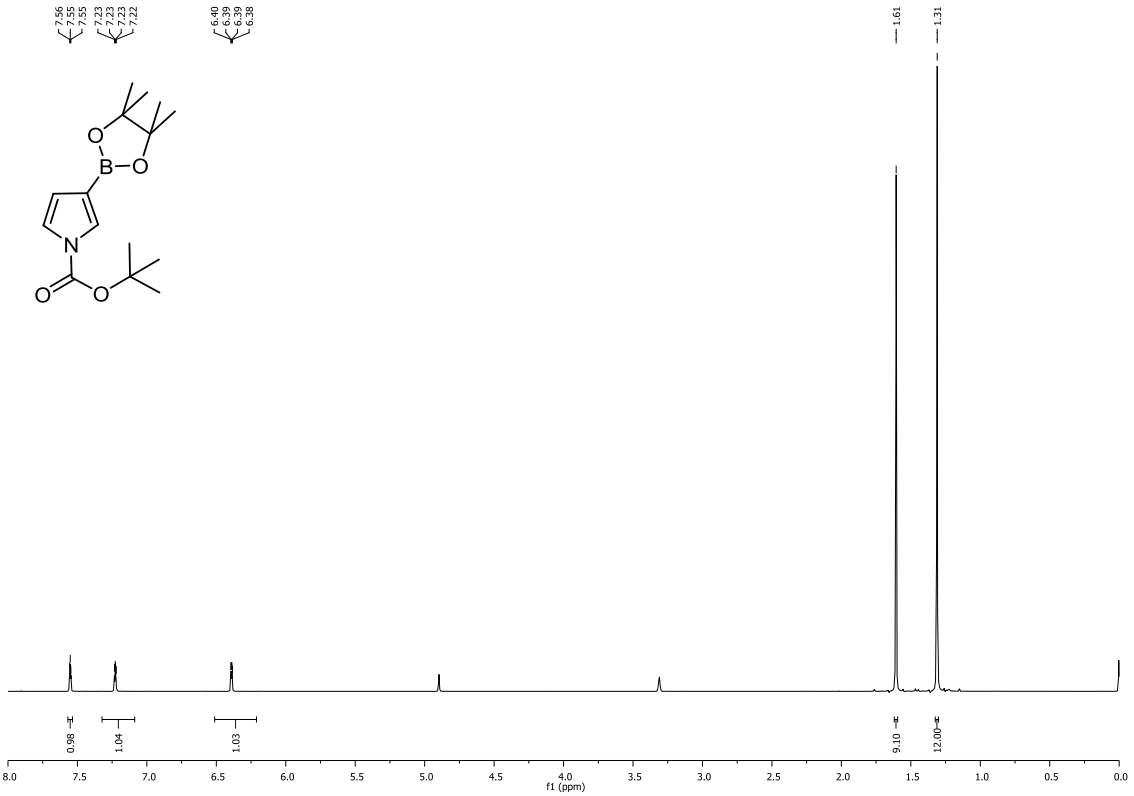

^{1}H NMR (400 MHz, CD_3OD)

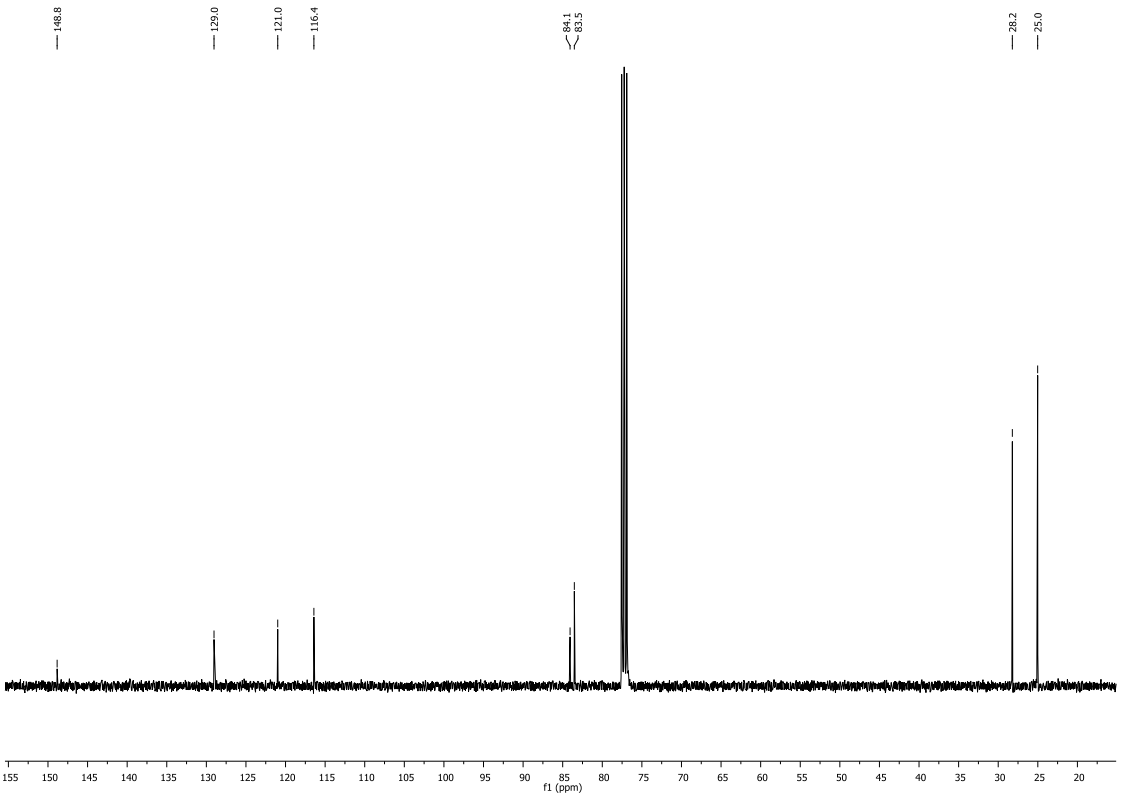

^{13}C NMR (101 MHz, $CDCl_3$)

^{1}H and ^{13}C NMR spectra for compound 367

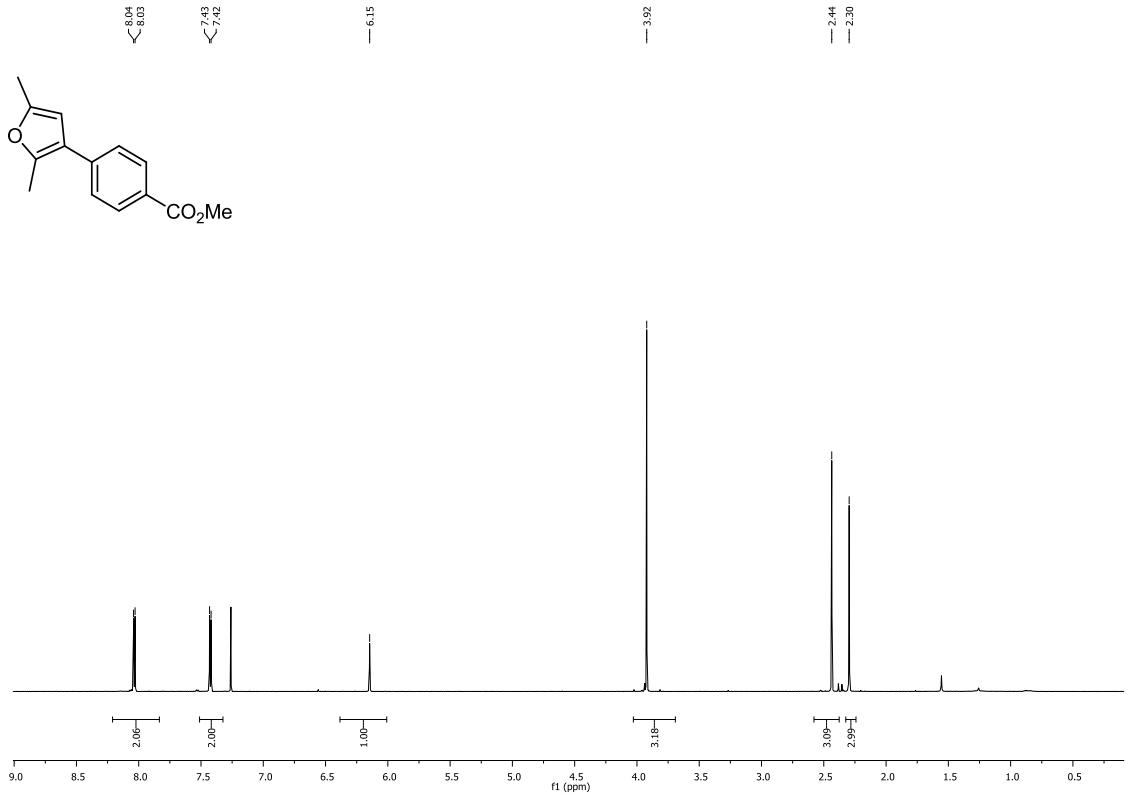

^{1}H NMR (700 MHz, $CDCl_3$)

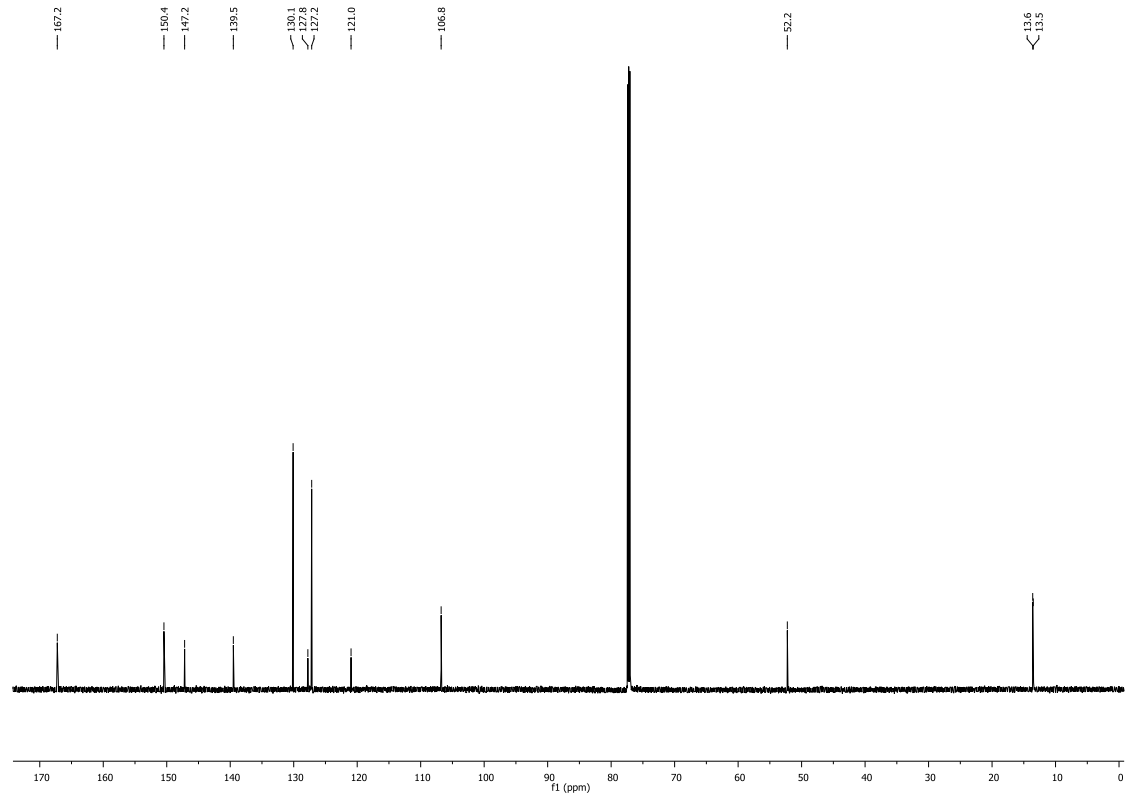

^{13}C NMR (176 MHz, $CDCl_3$)

^{1}H and ^{13}C NMR spectra for compound 368

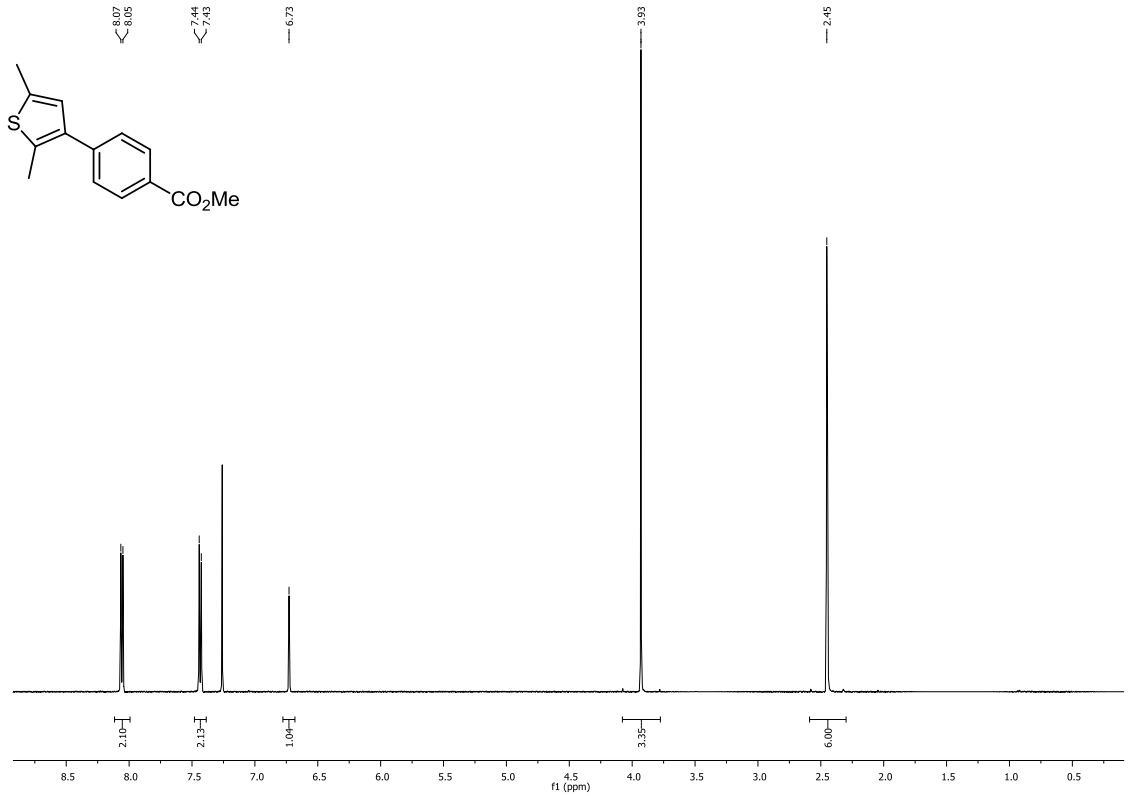

^{1}H NMR (500 MHz, $CDCl_3$)

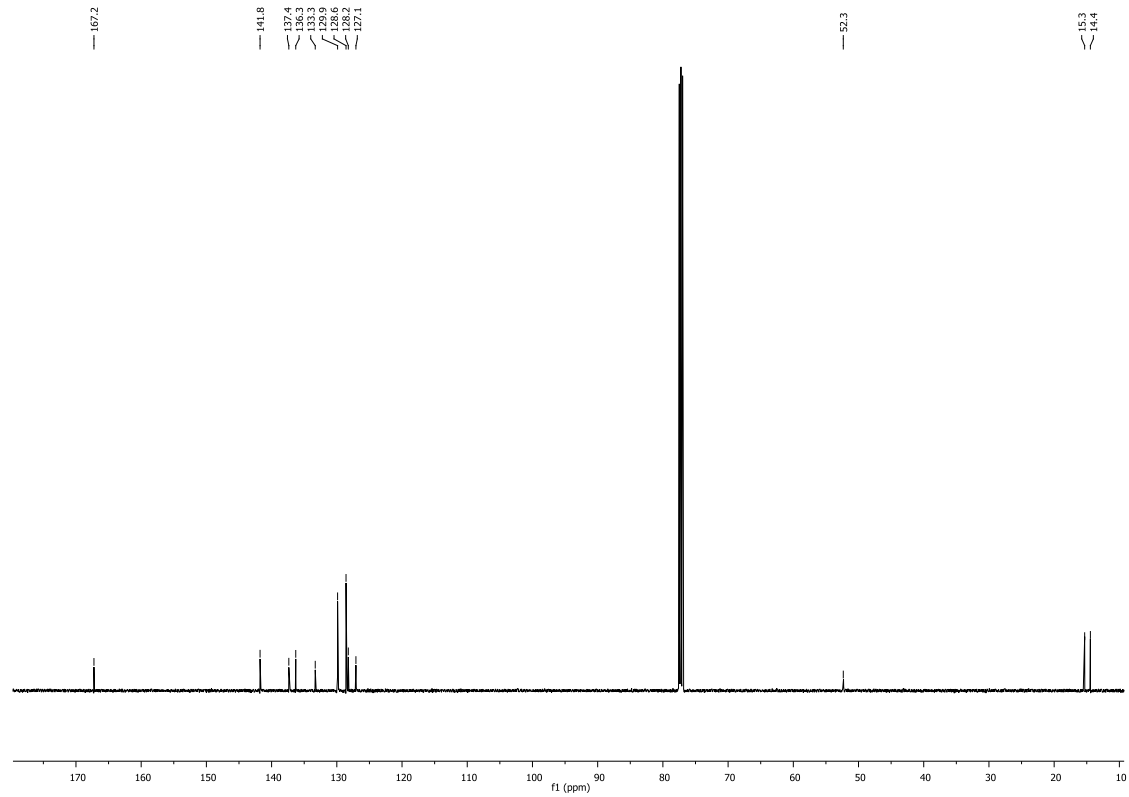

^{13}C NMR (126 MHz, $CDCl_3$)

^{1}H and ^{13}C NMR spectra for compound 369

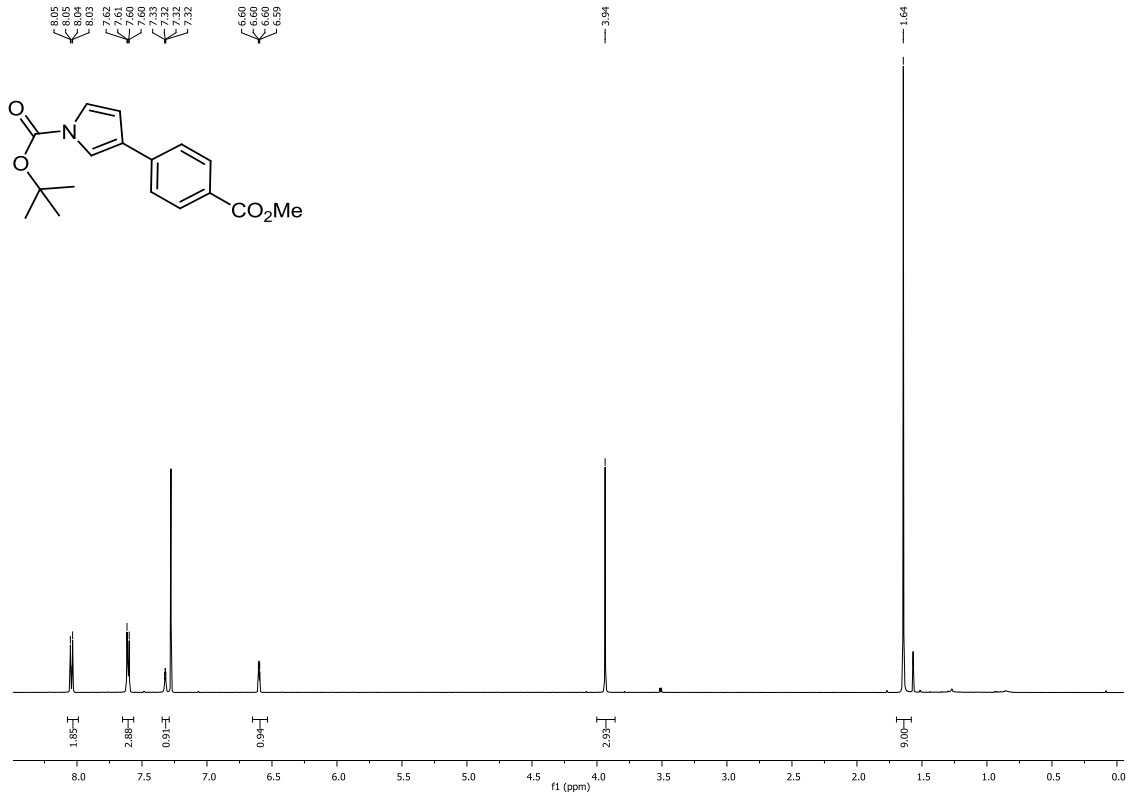

^{1}H NMR (500 MHz, $CDCl_3$)

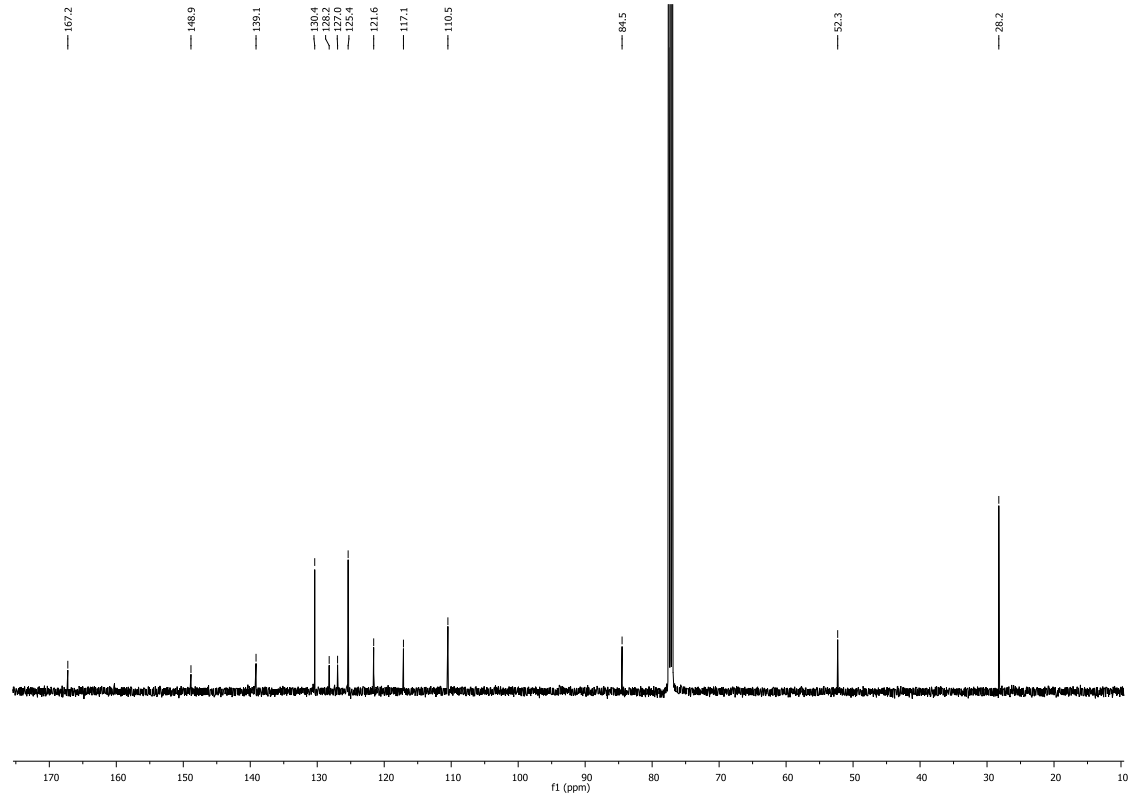

^{13}C NMR (126 MHz, $CDCl_3$)

^{1}H and ^{13}C NMR spectra for compound 420

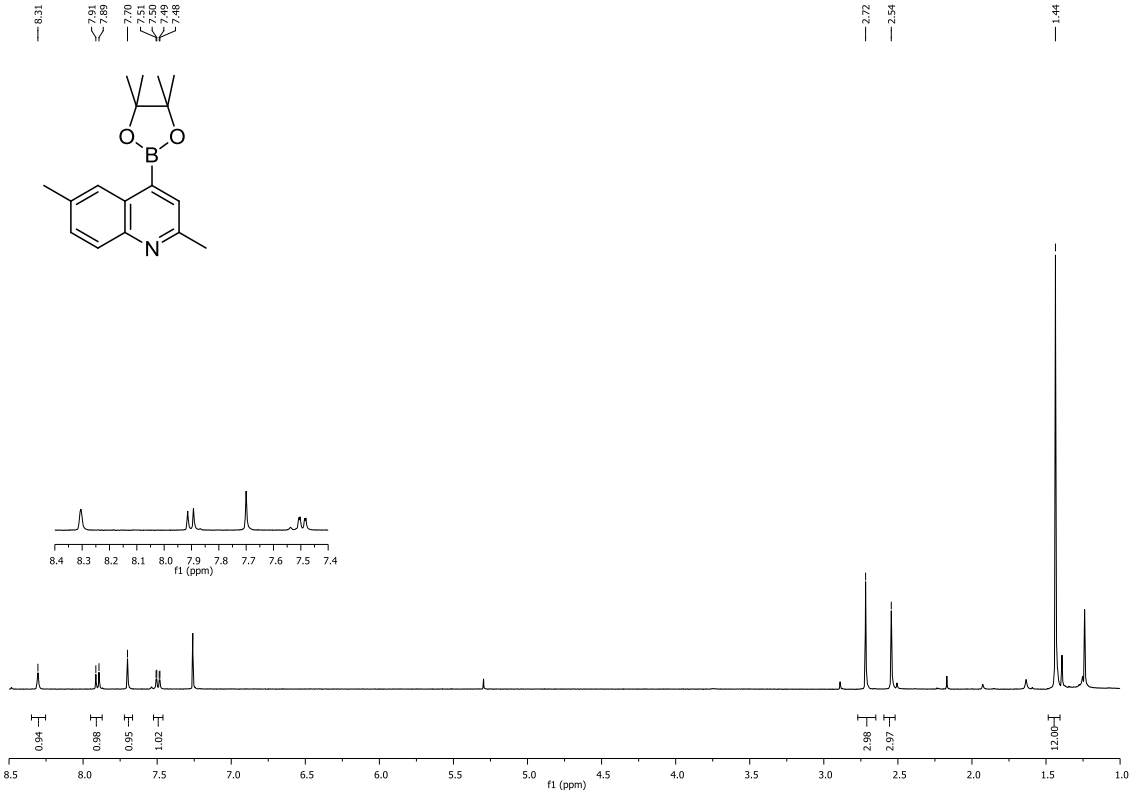

^{1}H NMR (500 MHz, $CDCl_3$)

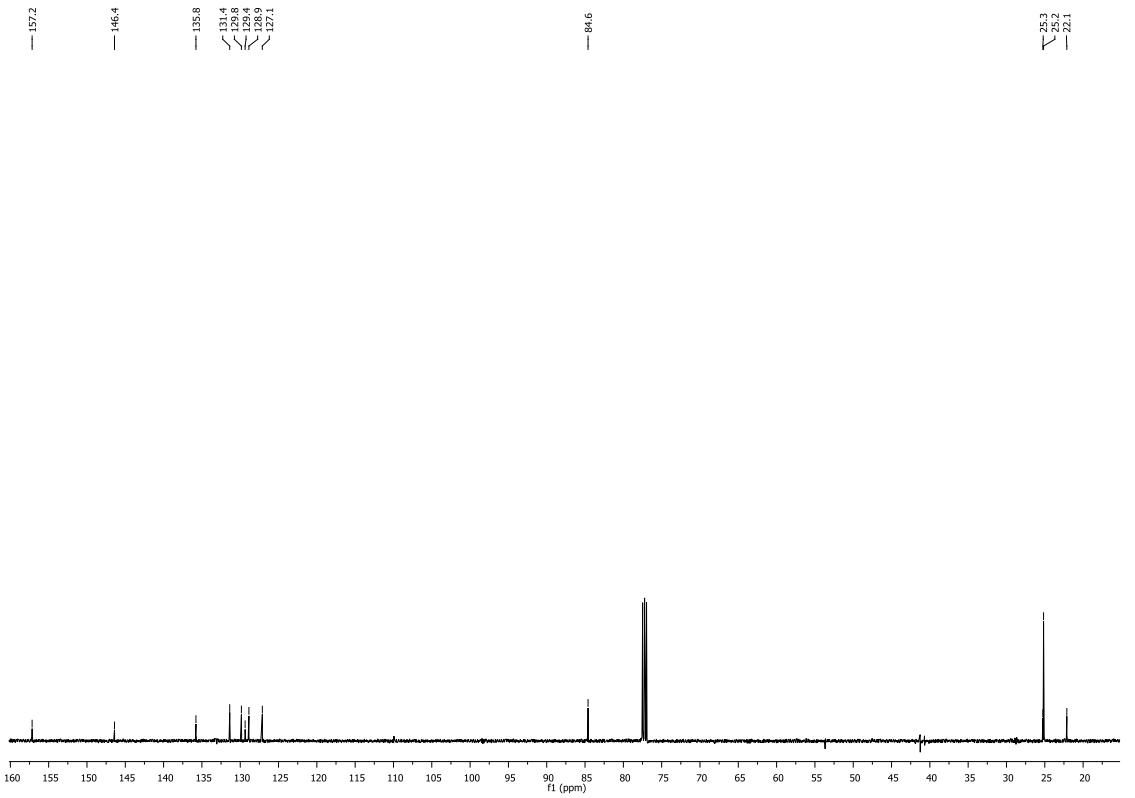

^{13}C NMR (126 MHz, $CDCl_3$)

^{1}H and ^{13}C NMR spectra for compound 421

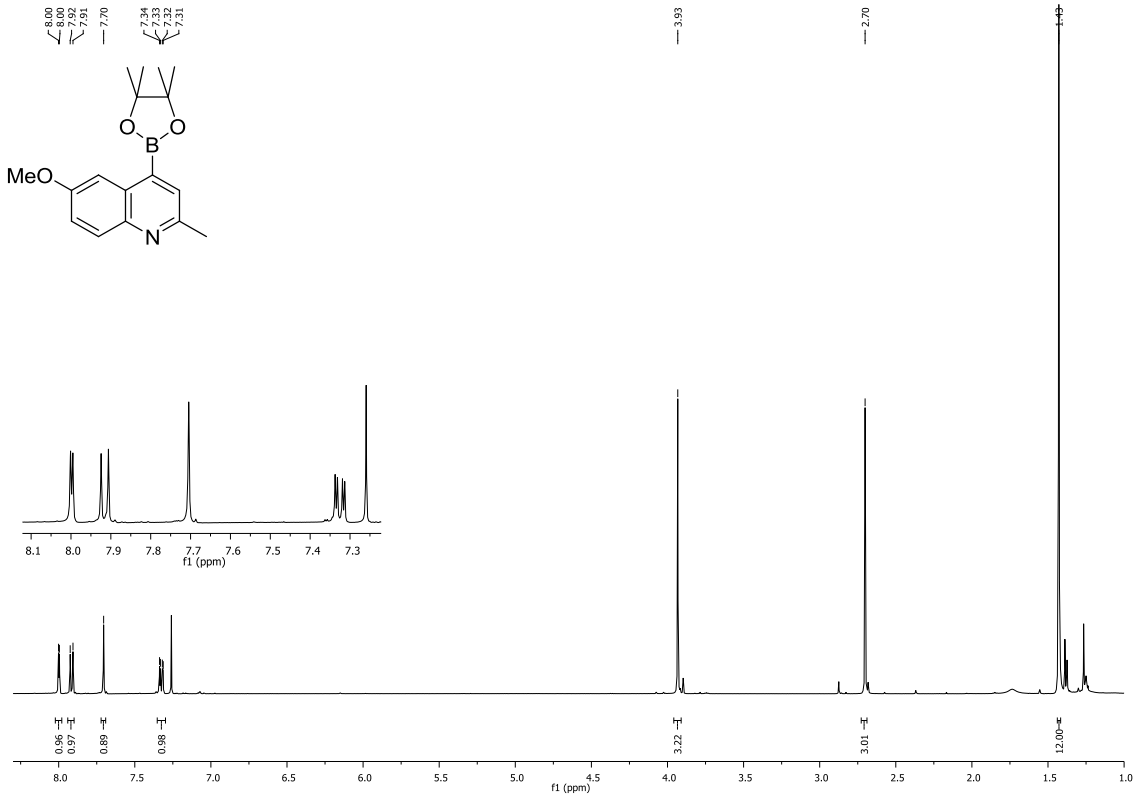

^{1}H NMR (500 MHz, $CDCl_3$)

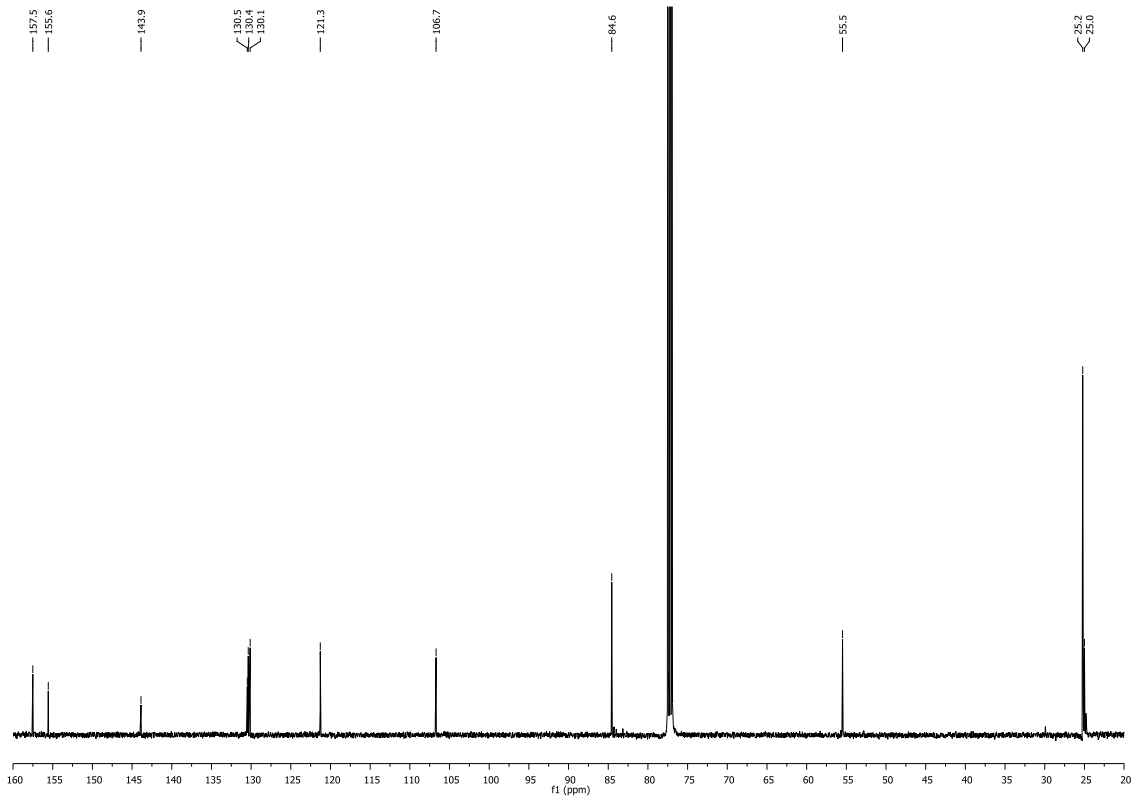

^{13}C NMR (126 MHz, $CDCl_3$)

^{1}H and ^{13}C NMR spectra for compound 422

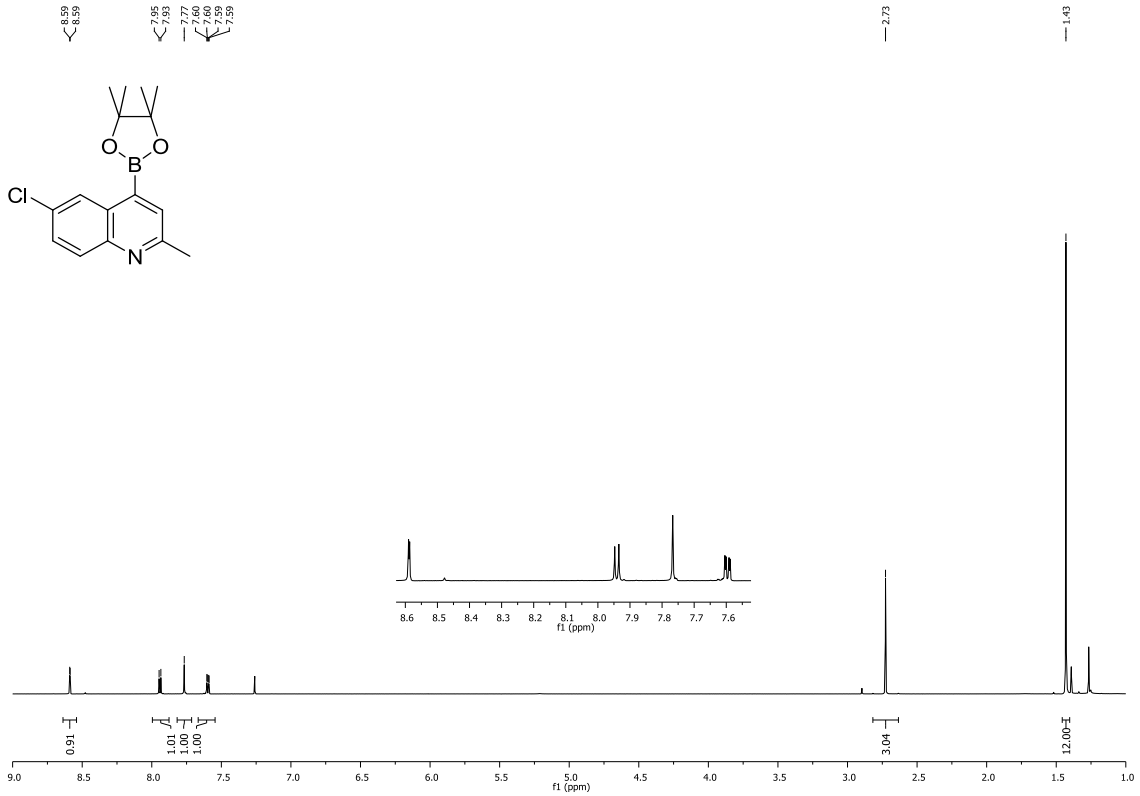

^{1}H NMR (700 MHz, $CDCl_3$)

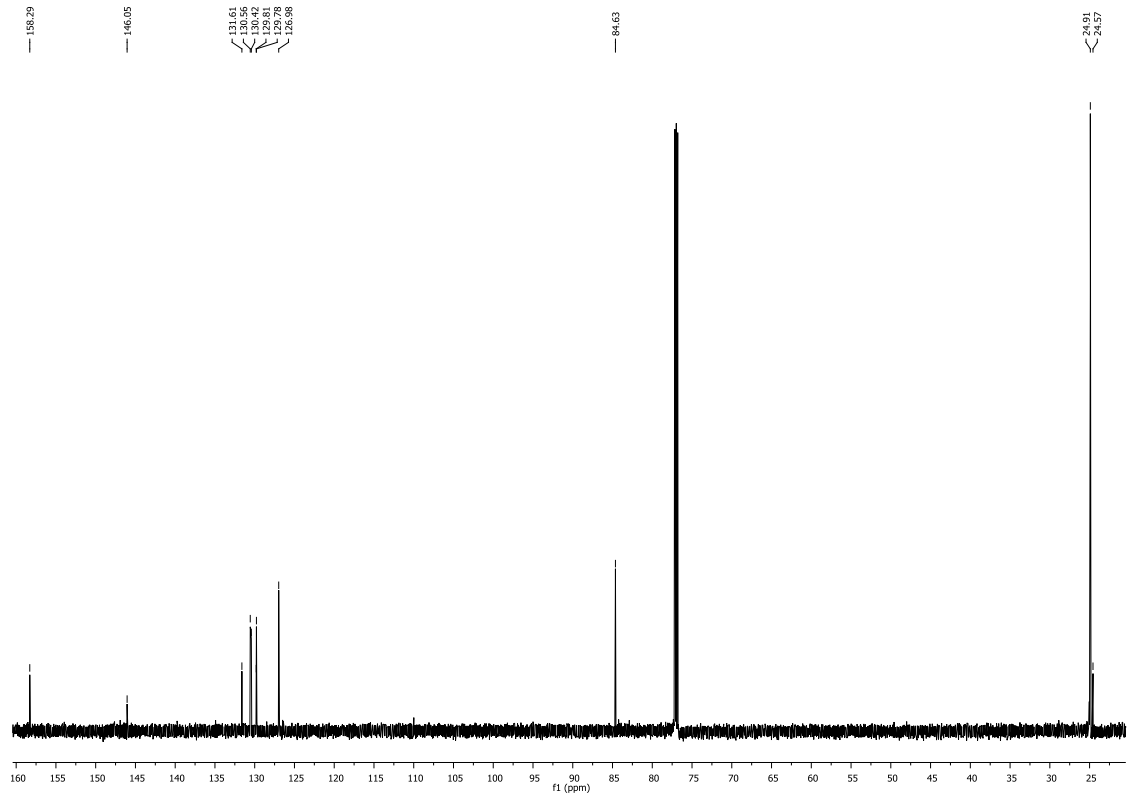

^{13}C NMR (176 MHz, $CDCl_3$)

^{1}H and ^{13}C NMR spectra for compound 423

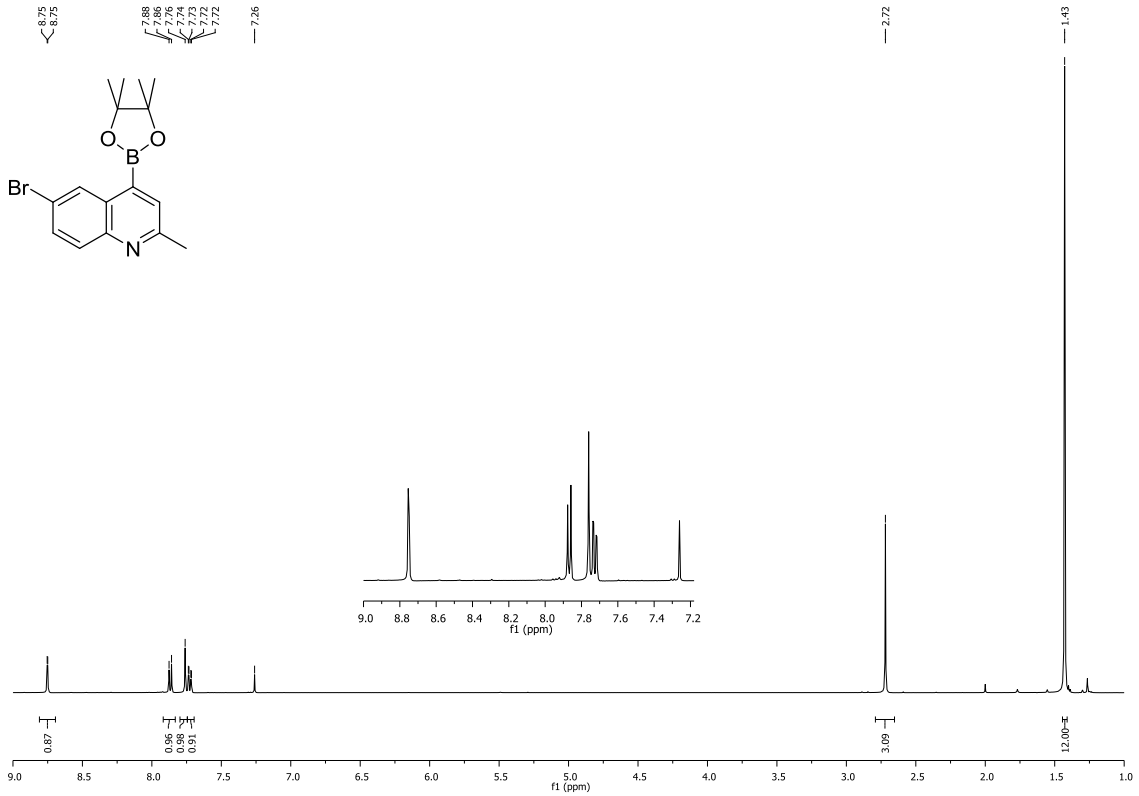

^{1}H NMR (500 MHz, $CDCl_3$)

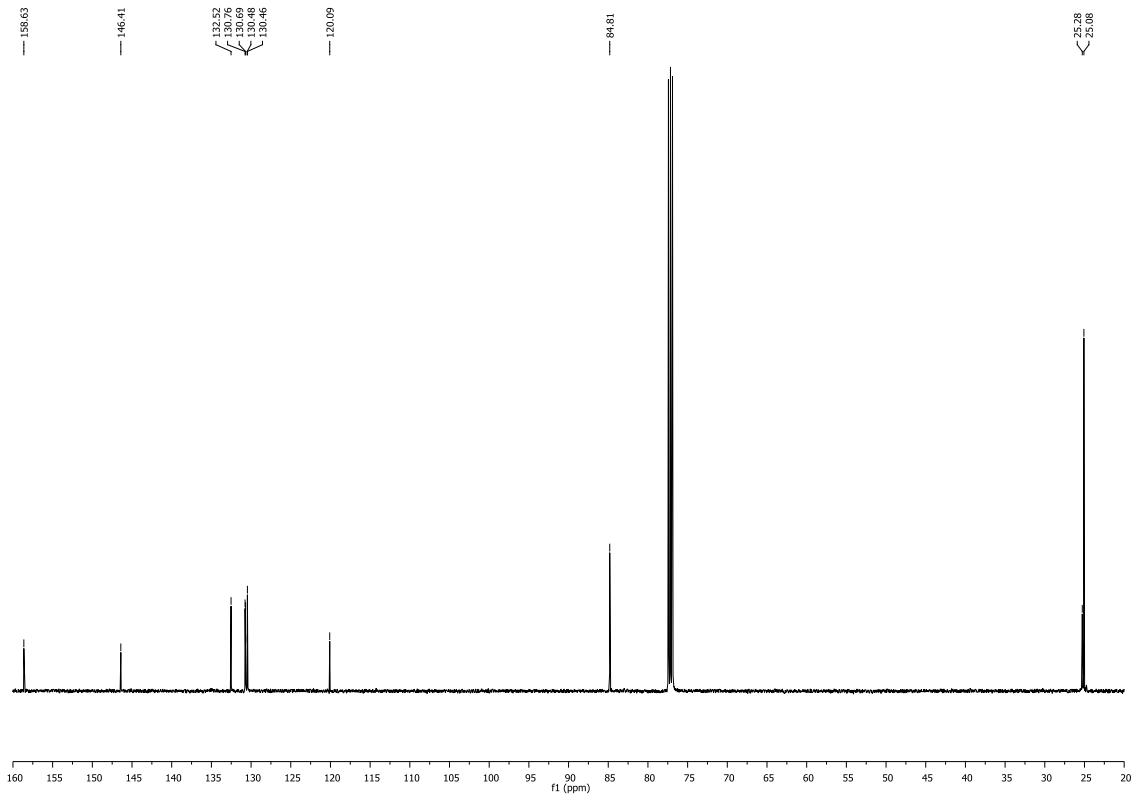

^{13}C NMR (126 MHz, $CDCl_3$)

^{1}H and ^{13}C NMR spectra for compound 424

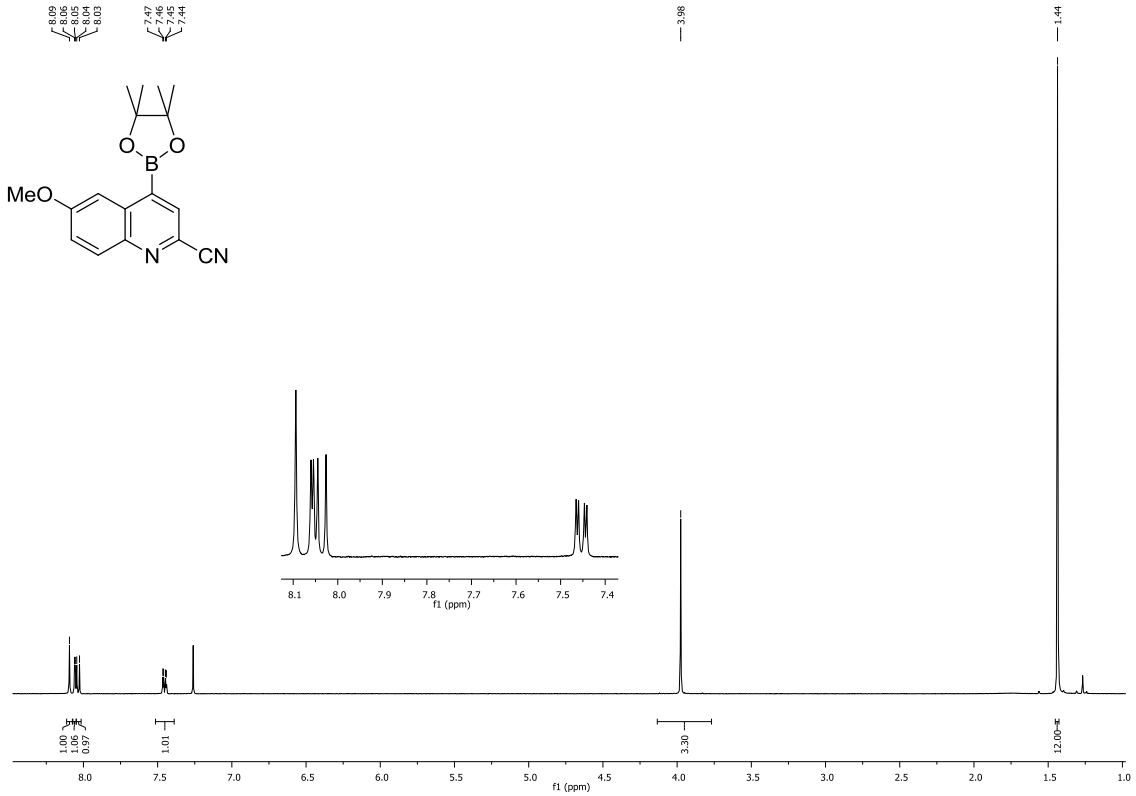

^{1}H NMR (500 MHz, $CDCl_3$)

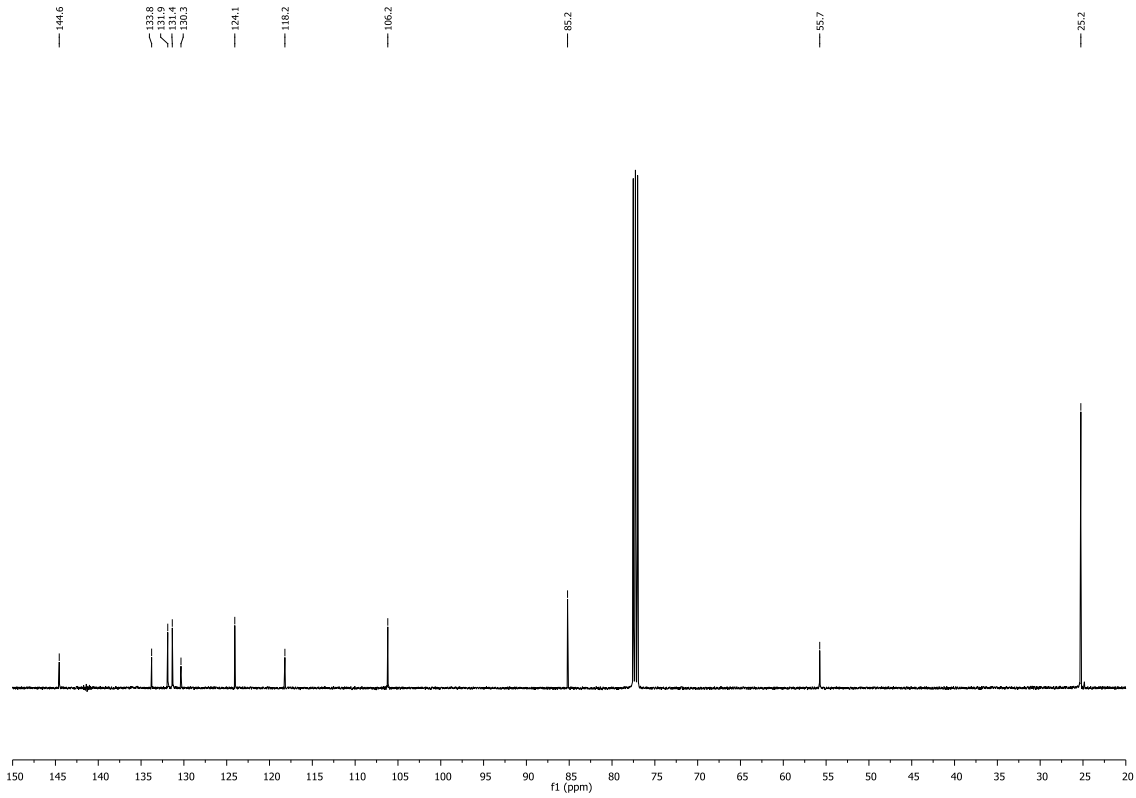

^{13}C NMR (126 MHz, $CDCl_3$)

^{1}H and ^{13}C NMR spectra for compound 427

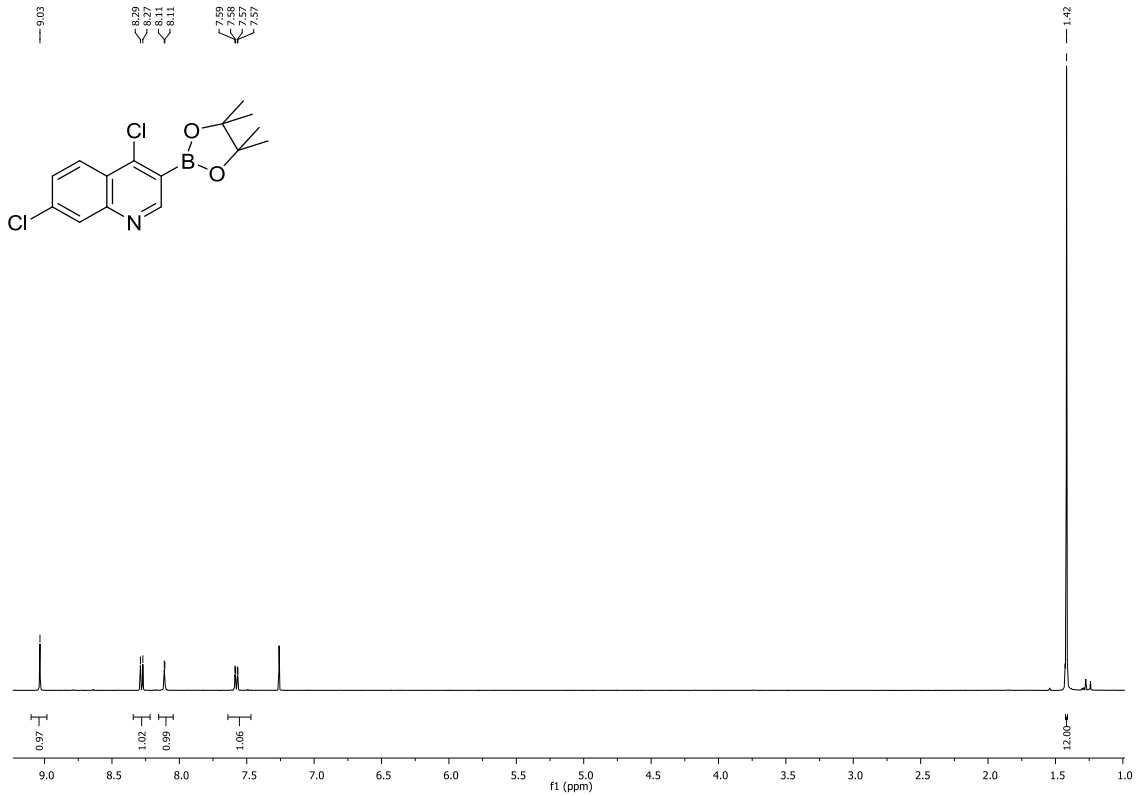

^{1}H NMR (500 MHz, $CDCl_3$)

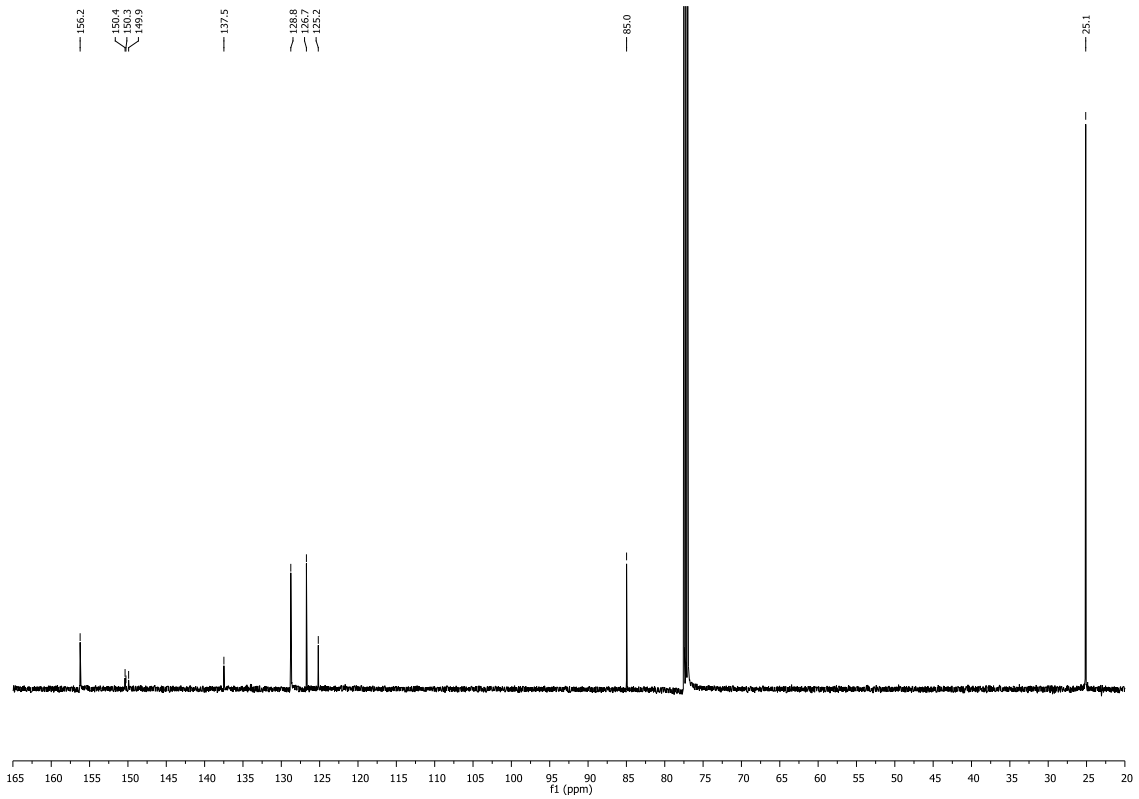

^{13}C NMR (126 MHz, $CDCl_3$)

^{1}H and ^{13}C NMR spectra for compound 428

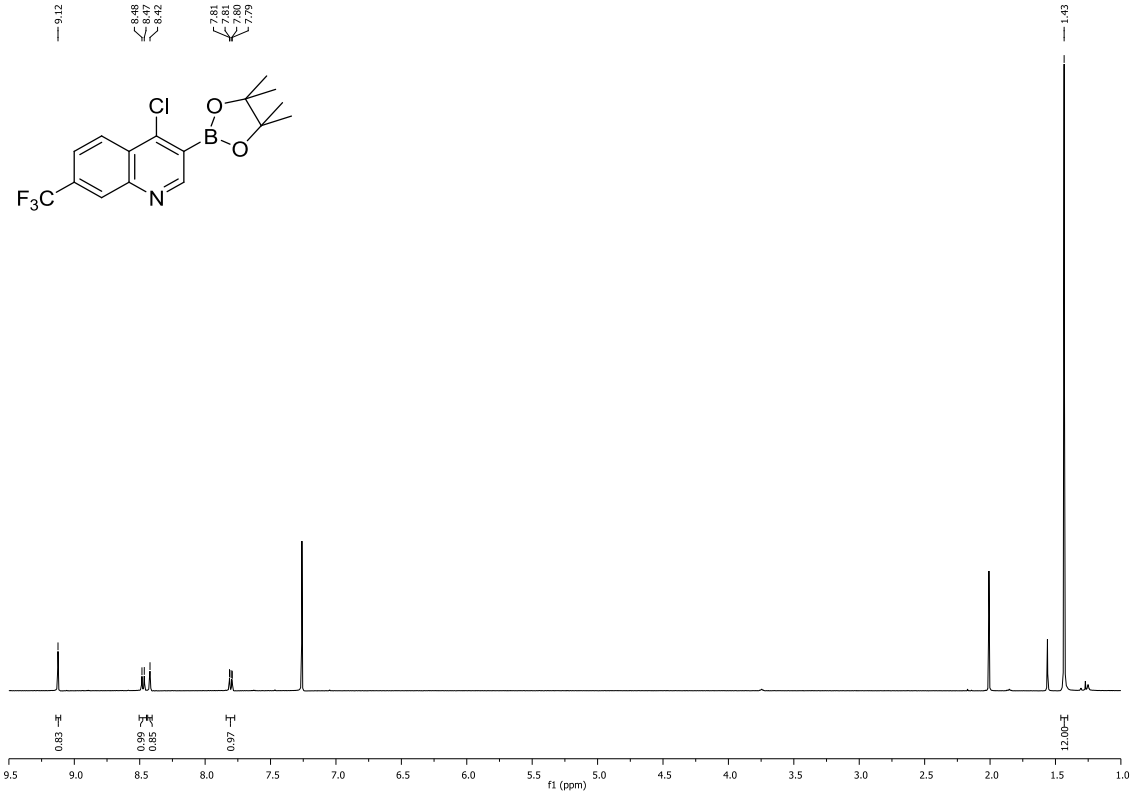

^{1}H NMR (500 MHz, $CDCl_3$)

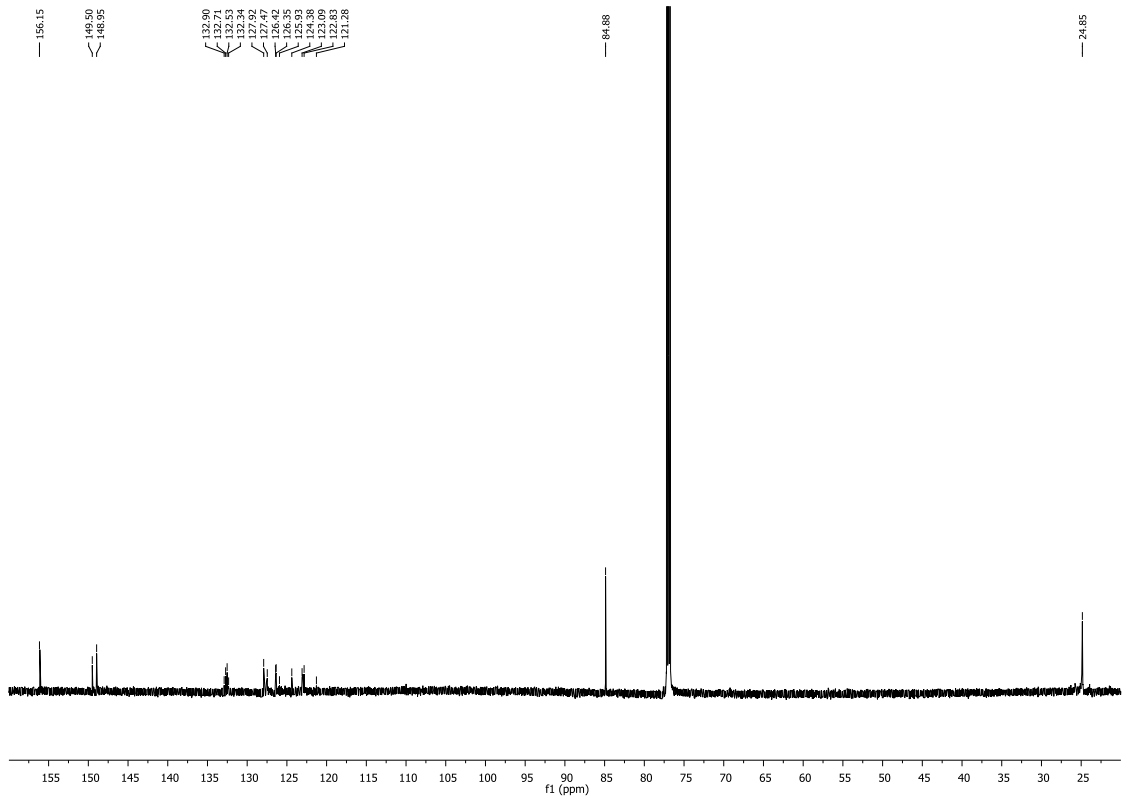

^{13}C NMR (176 MHz, $CDCl_3$)

^{1}H and ^{13}C NMR spectra for compound 434

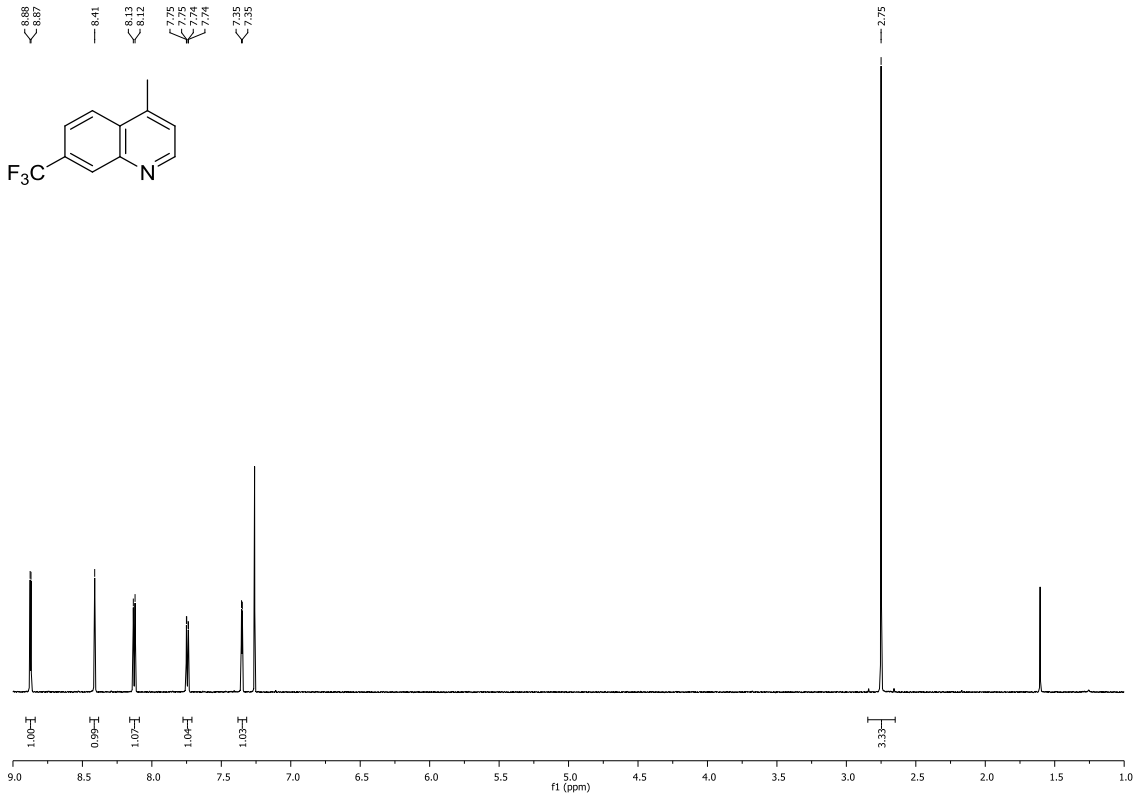

^{1}H NMR (700 MHz, $CDCl_3$)

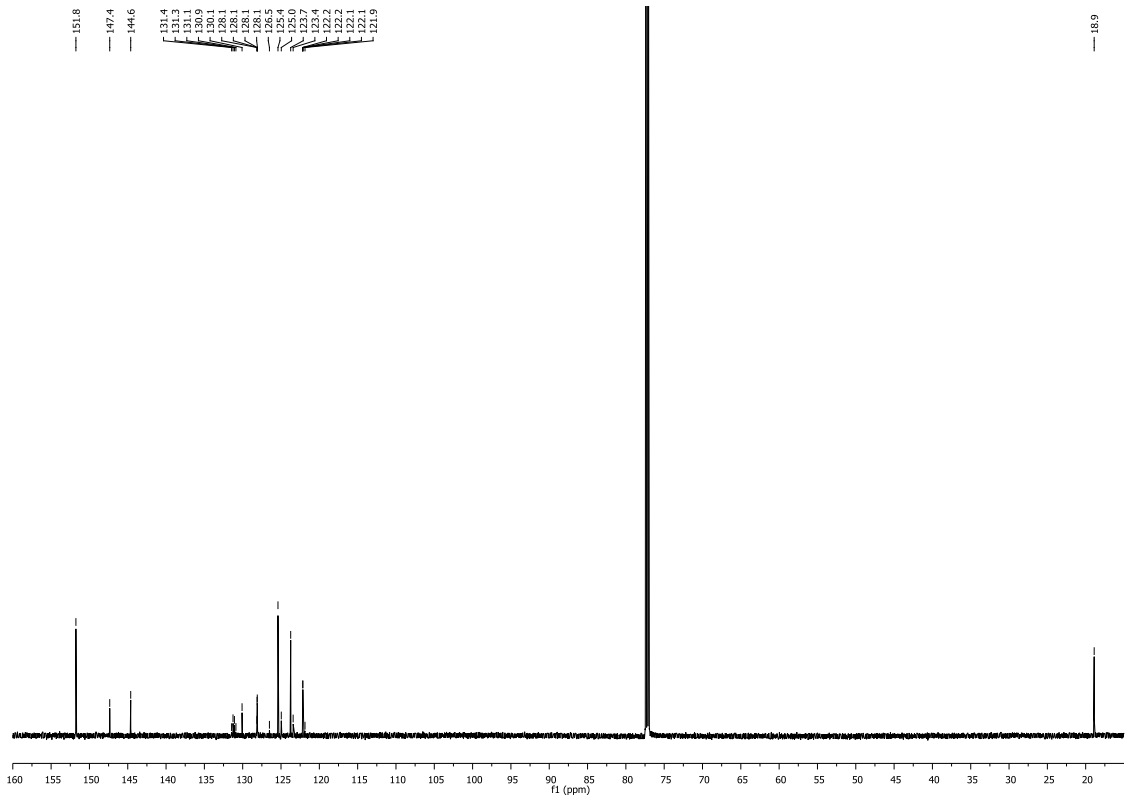

^{13}C NMR (176 MHz, $CDCl_3$)

^{1}H and ^{13}C NMR spectra for compound 450

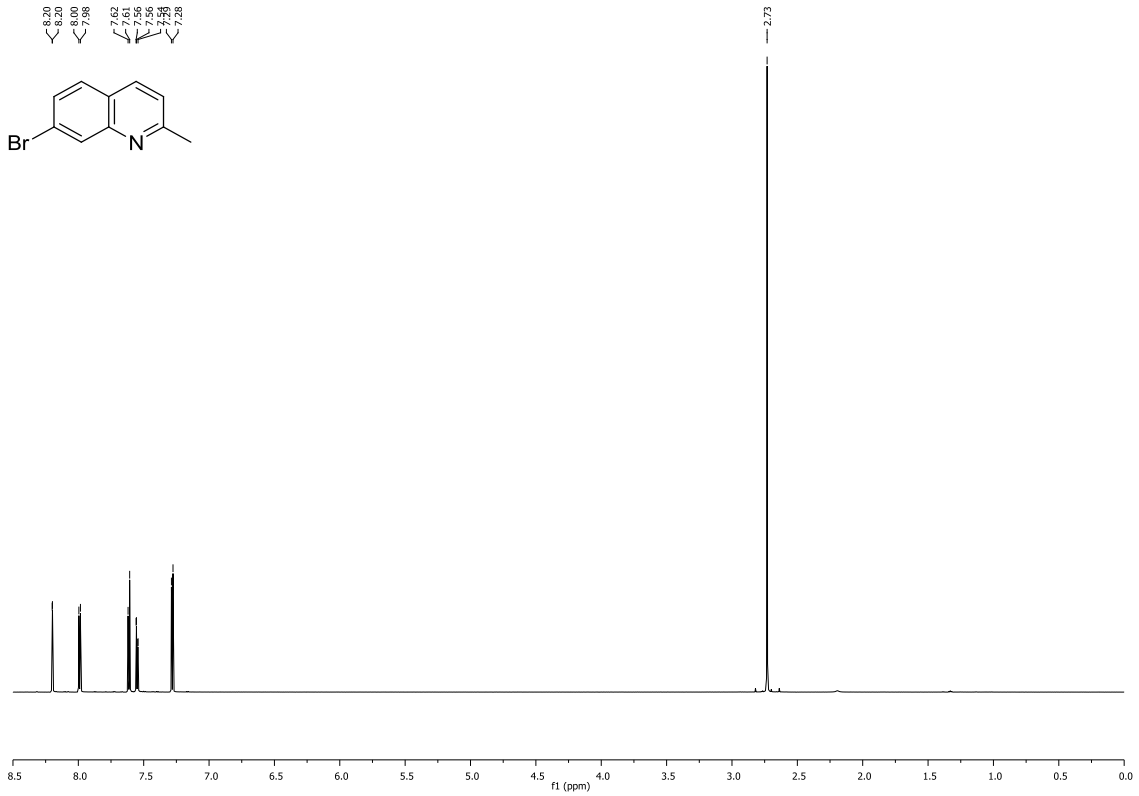

^{1}H NMR (700 MHz, $CDCl_3$)

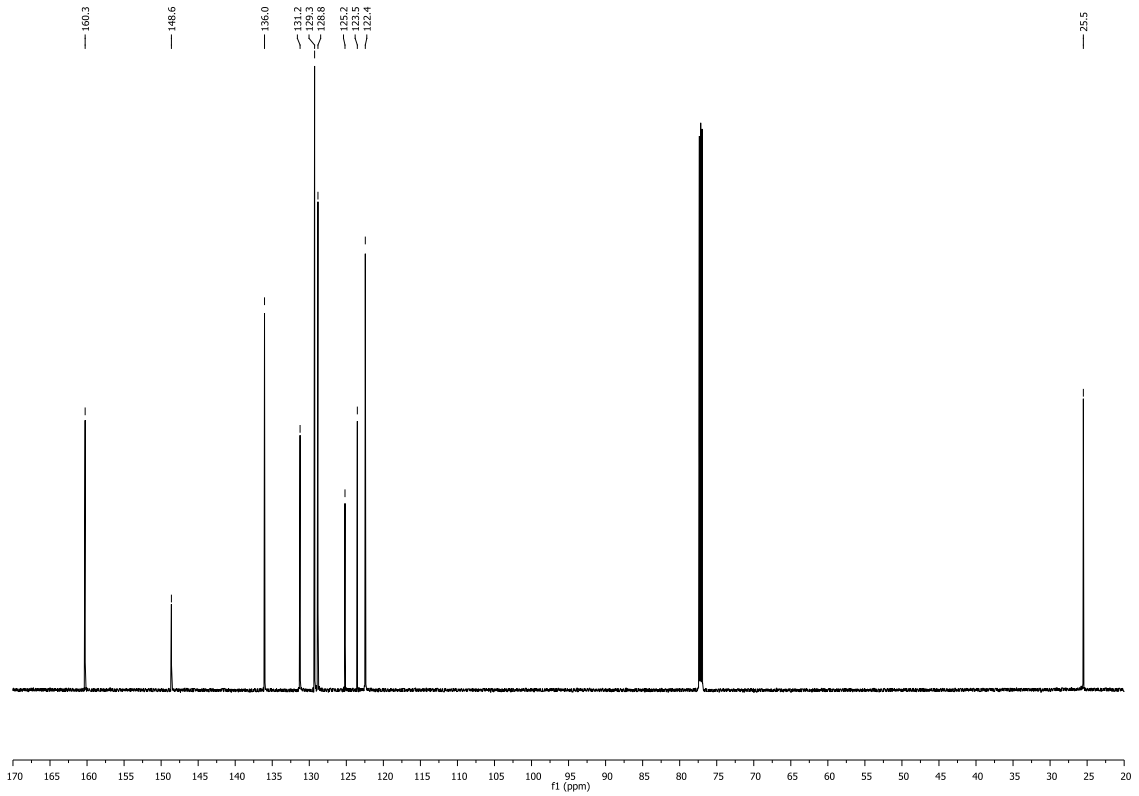

^{13}C NMR (176 MHz, $CDCl_3$)

^{1}H and ^{13}C NMR spectra for compound 452

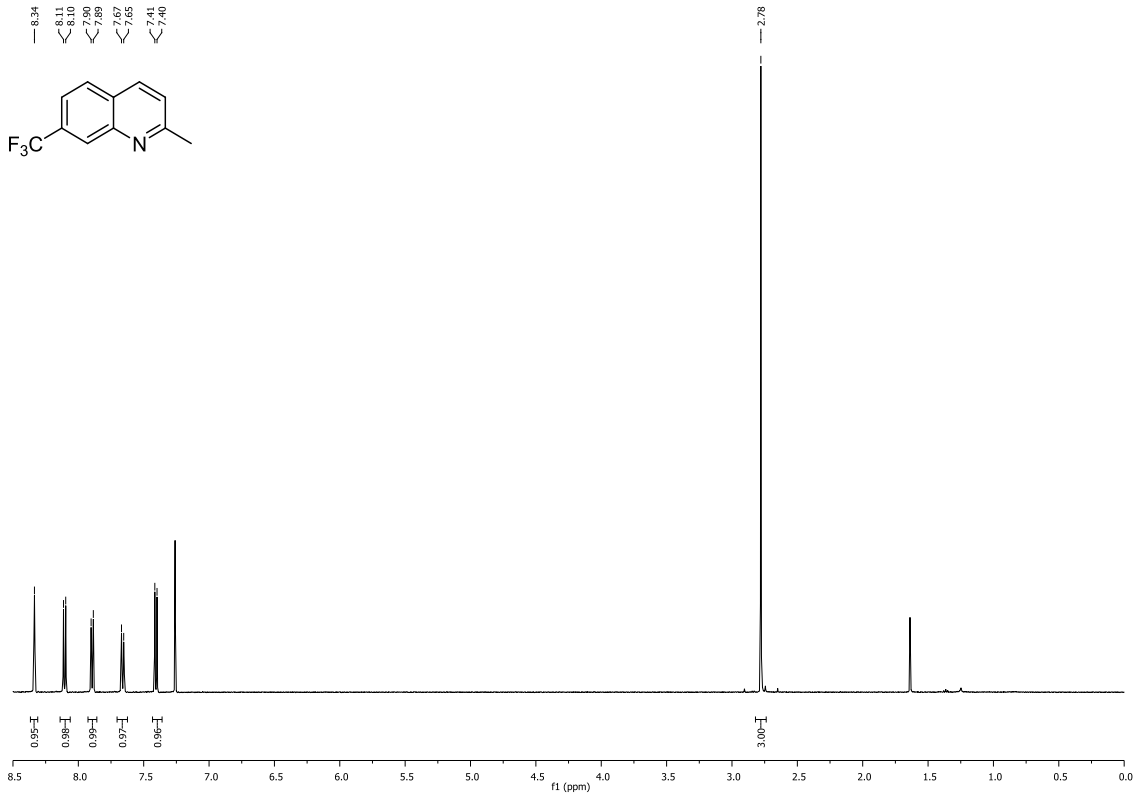

^{1}H NMR (500 MHz, $CDCl_3$)

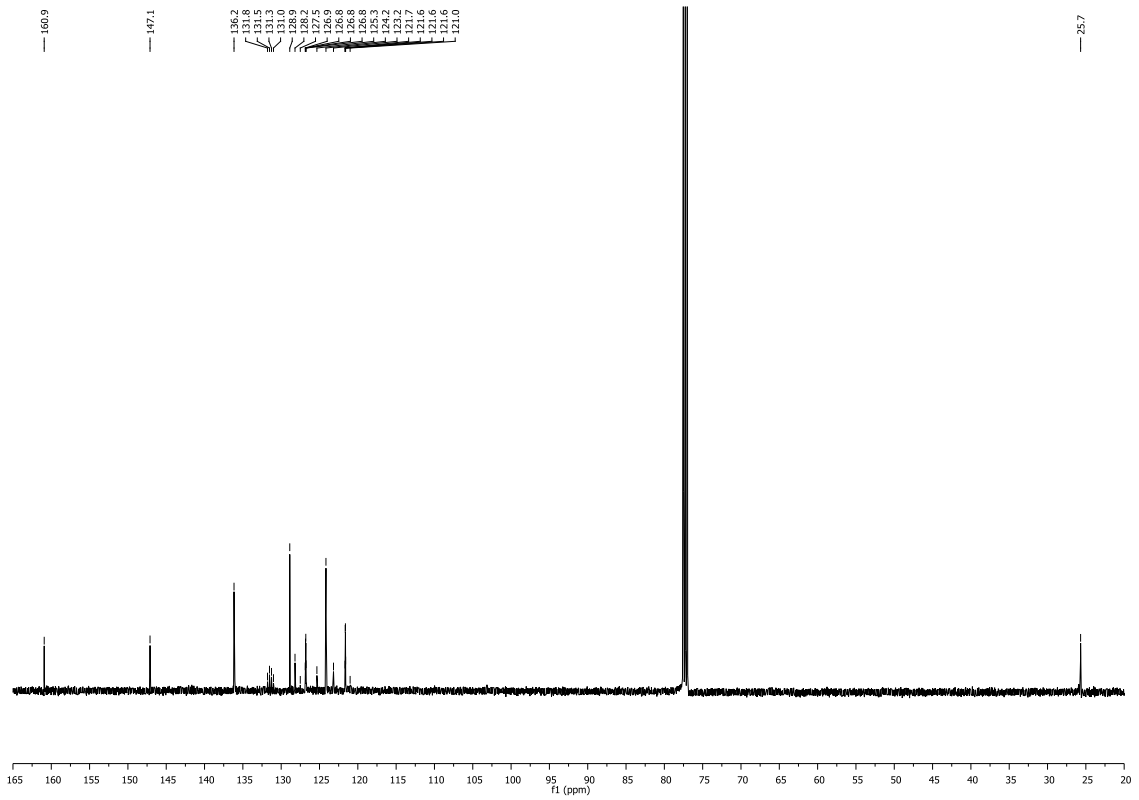

^{13}C NMR (126 MHz, $CDCl_3$)

^{1}H and ^{13}C NMR spectra for compound 453

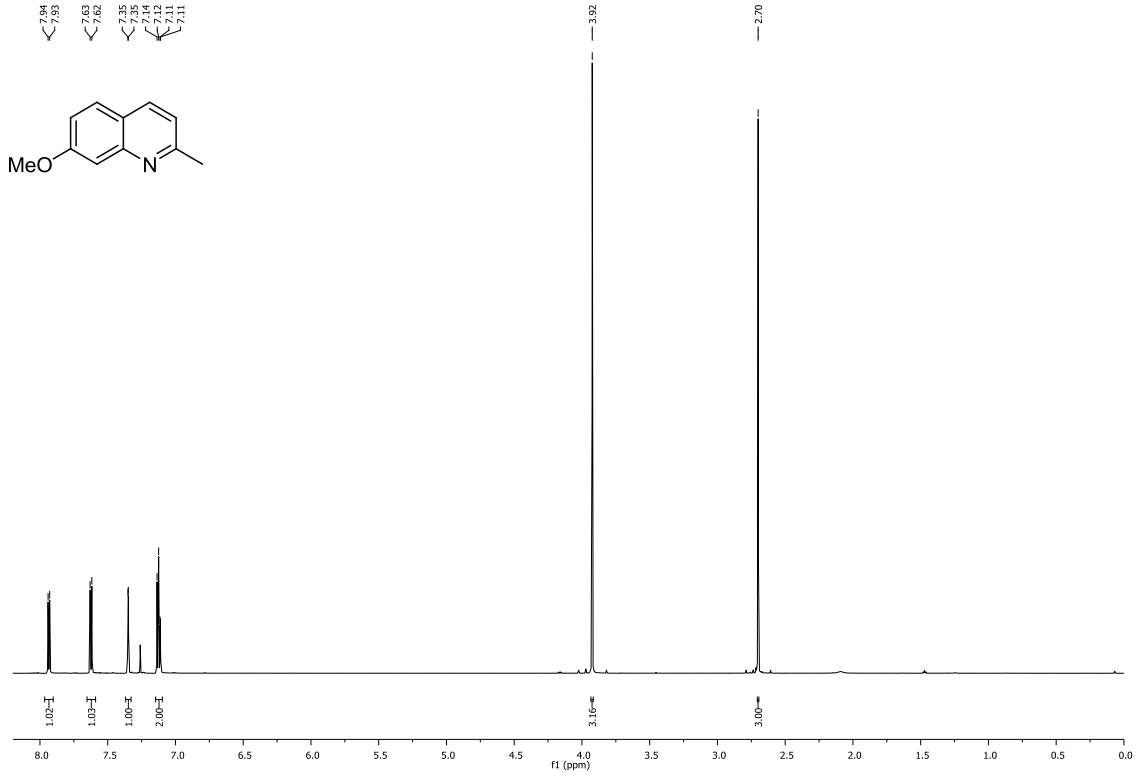

^{1}H NMR (700 MHz, $CDCl_3$)

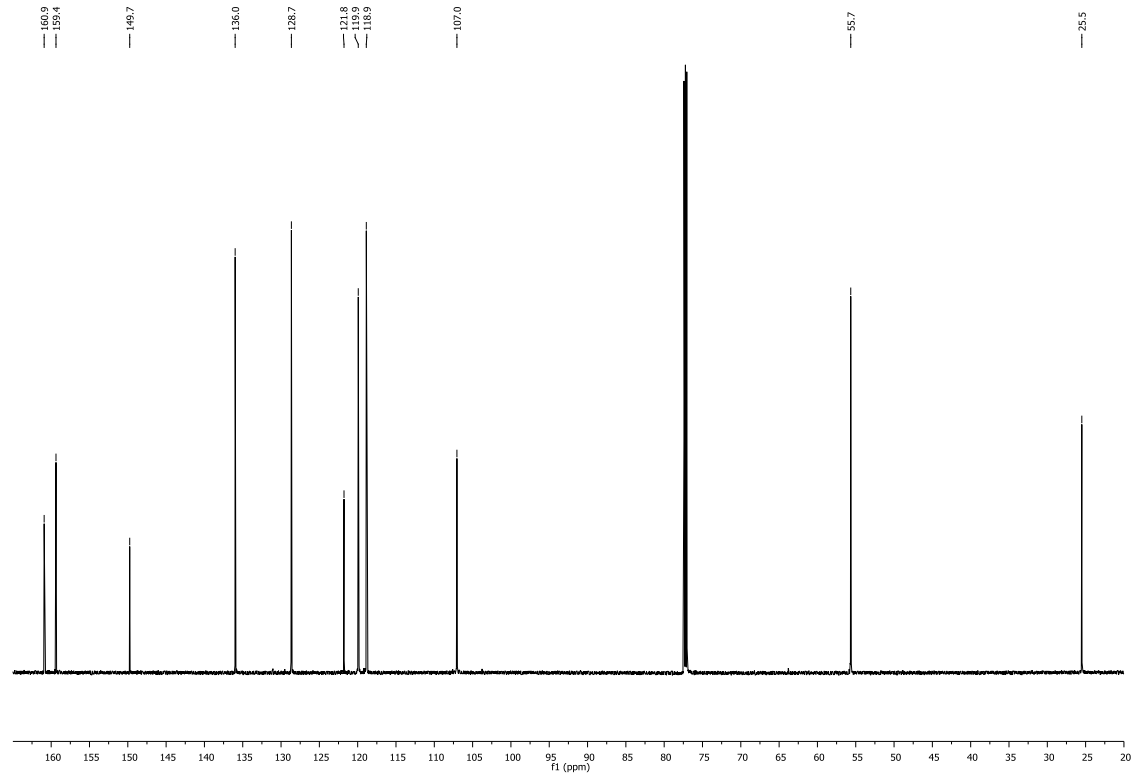

^{13}C NMR (176 MHz, $CDCl_3$)

^{1}H and ^{13}C NMR spectra for compound 454

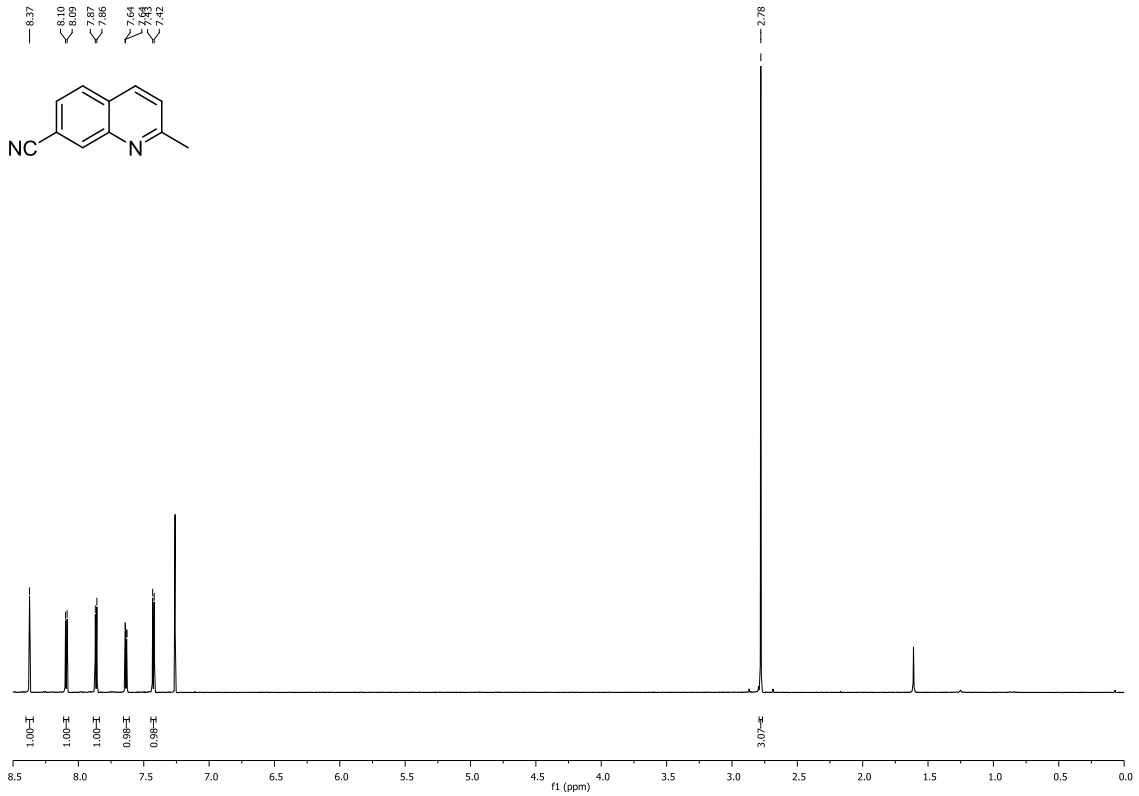

^{1}H NMR (700 MHz, $CDCl_3$)

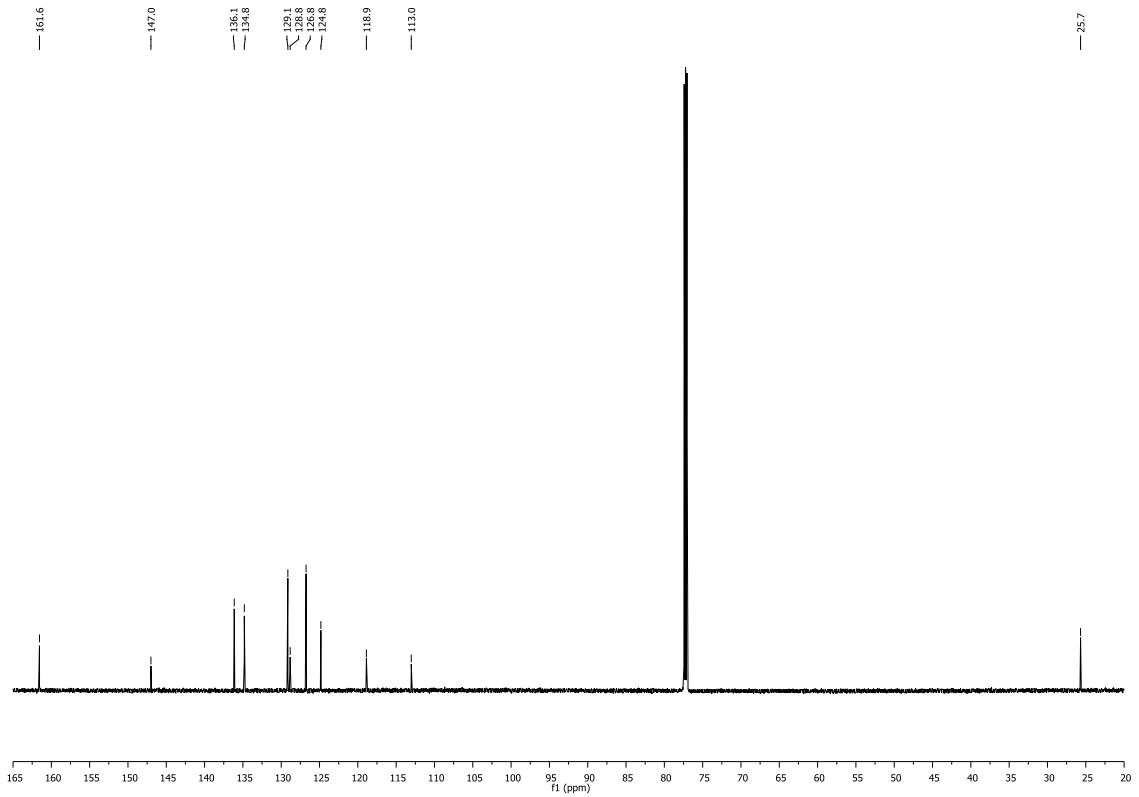

^{13}C NMR (176 MHz, $CDCl_3$)

^{1}H and ^{13}C NMR spectra for compound 459

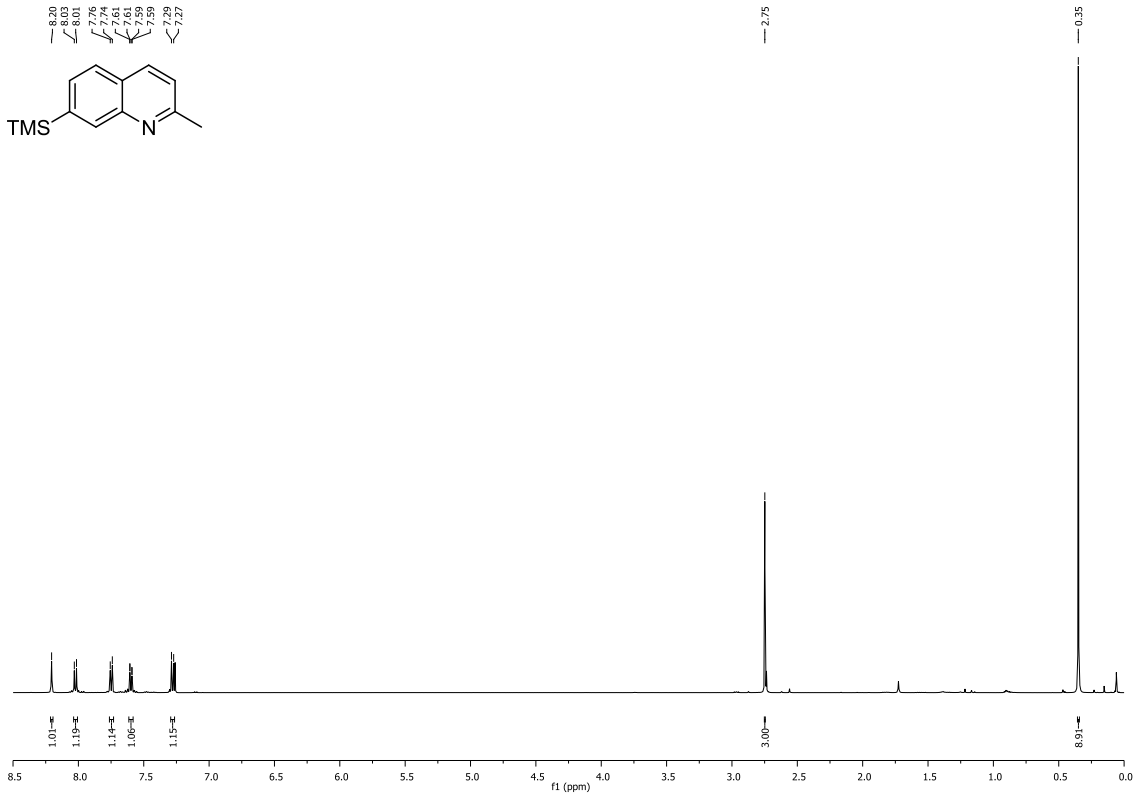

^{1}H NMR (500 MHz, $CDCl_3$)

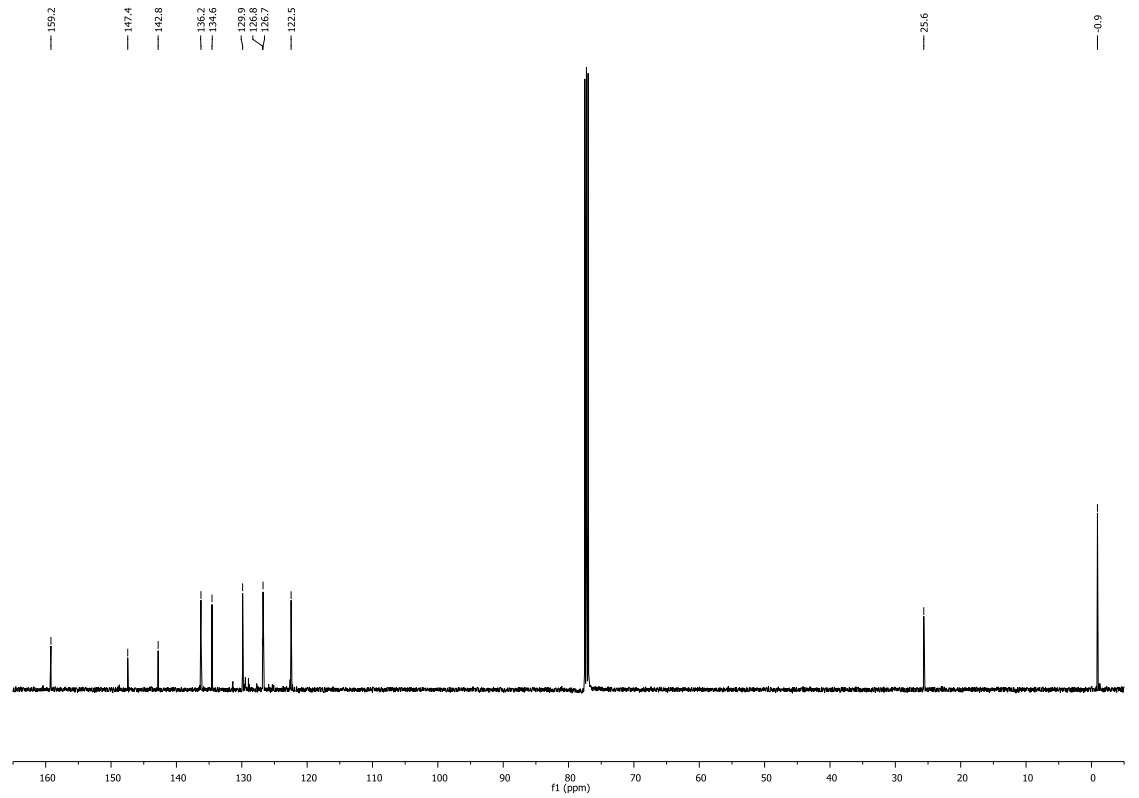

^{13}C NMR (126 MHz, $CDCl_3$)

^{1}H and ^{13}C NMR spectra for compound 460

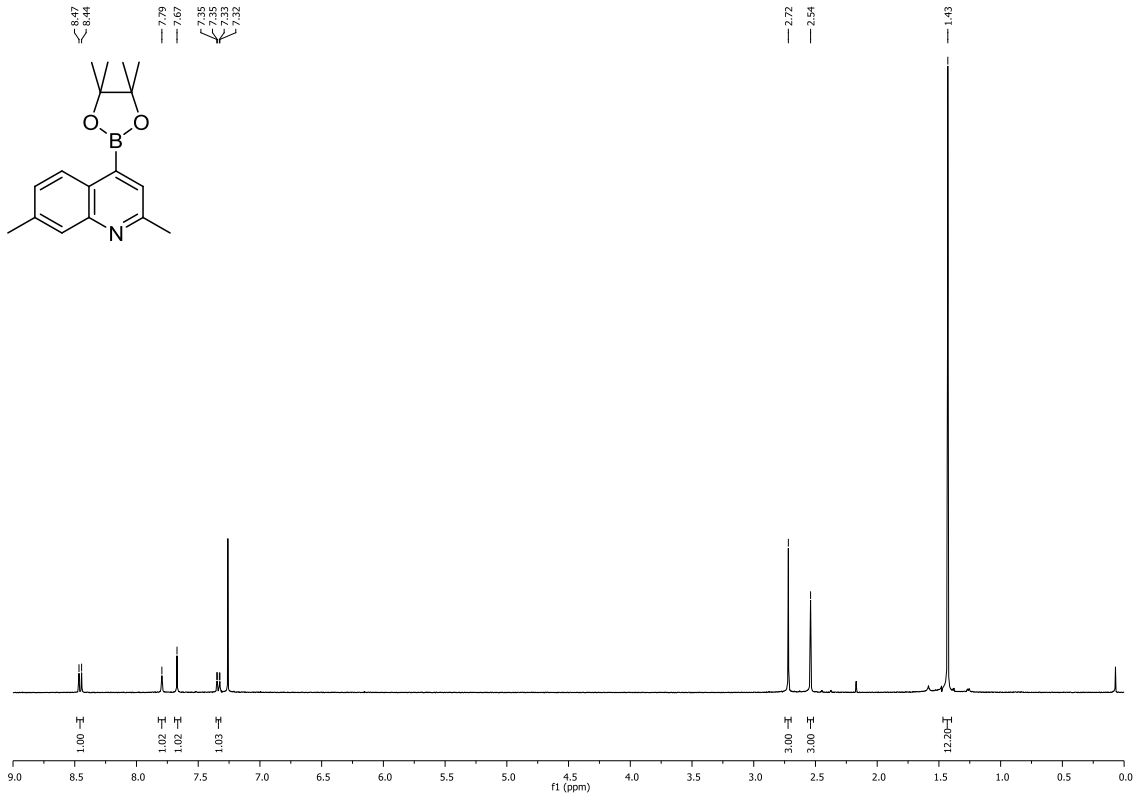

^{1}H NMR (400 MHz, $CDCl_3$)

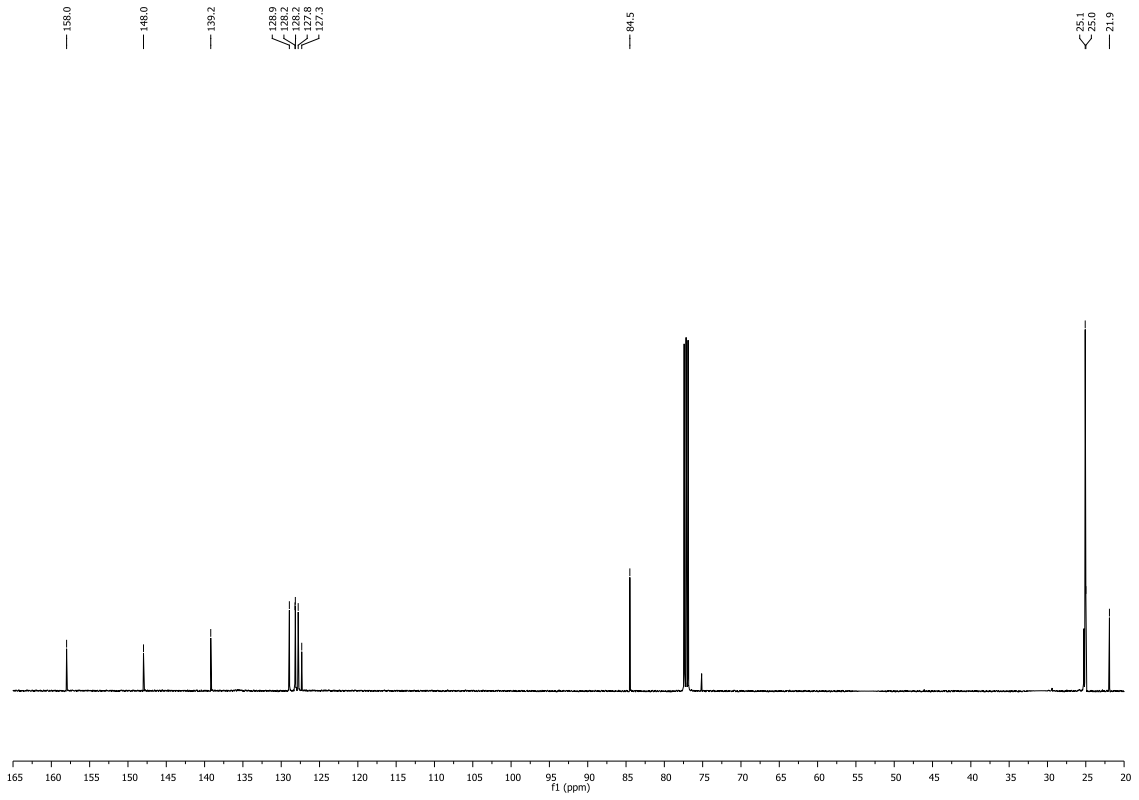

^{13}C NMR (176 MHz, $CDCl_3$)

^{1}H and ^{13}C NMR spectra for compound 461

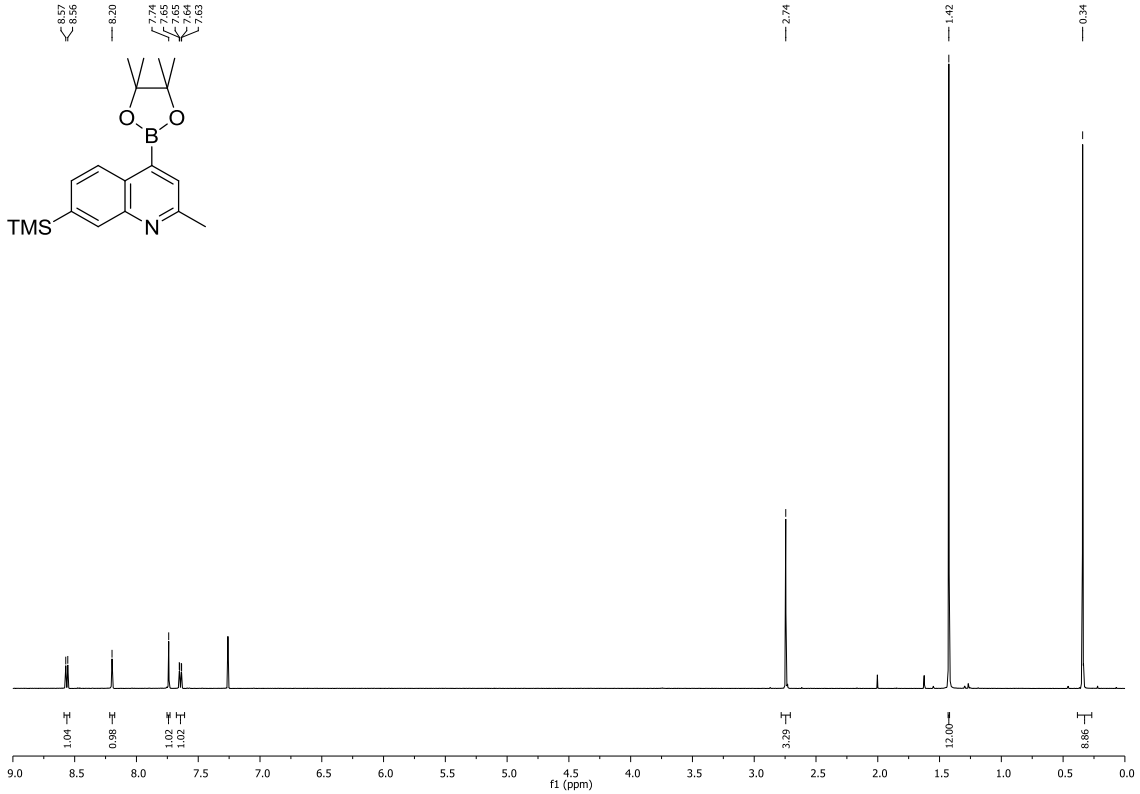

^{1}H NMR (500 MHz, $CDCl_3$)

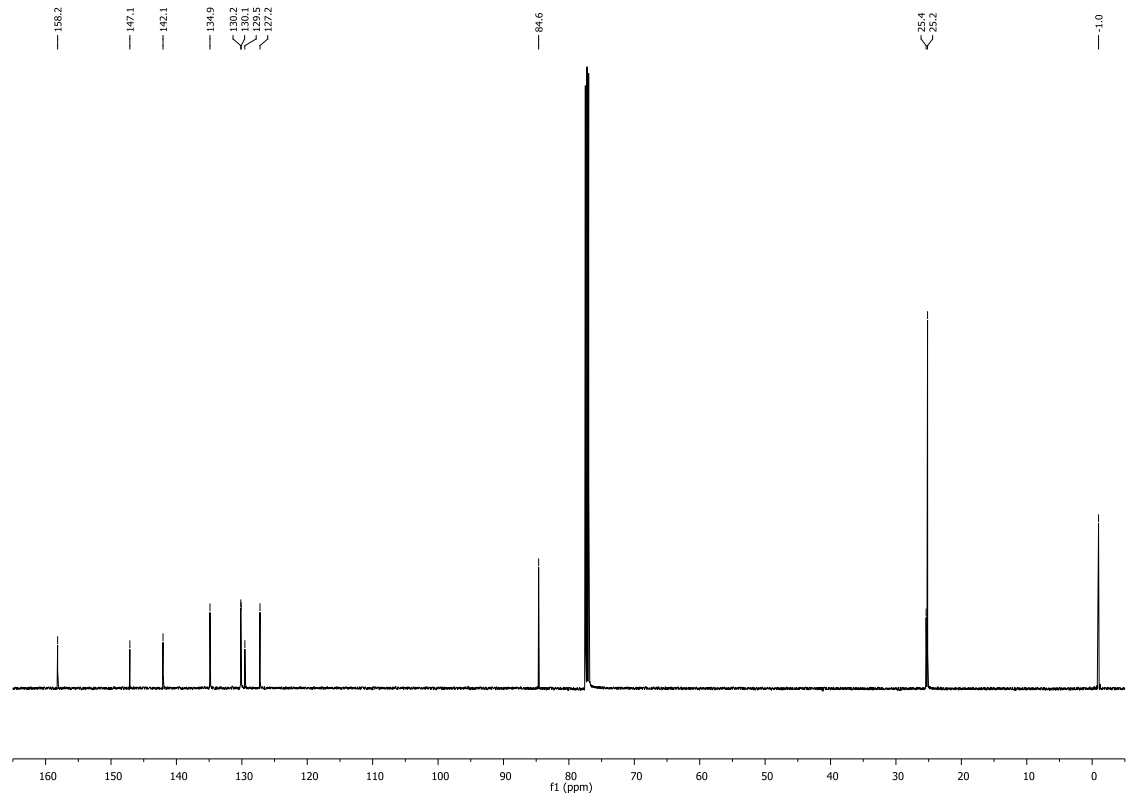

^{13}C NMR (126 MHz, $CDCl_3$)

^{1}H and ^{13}C NMR spectra for compound 462

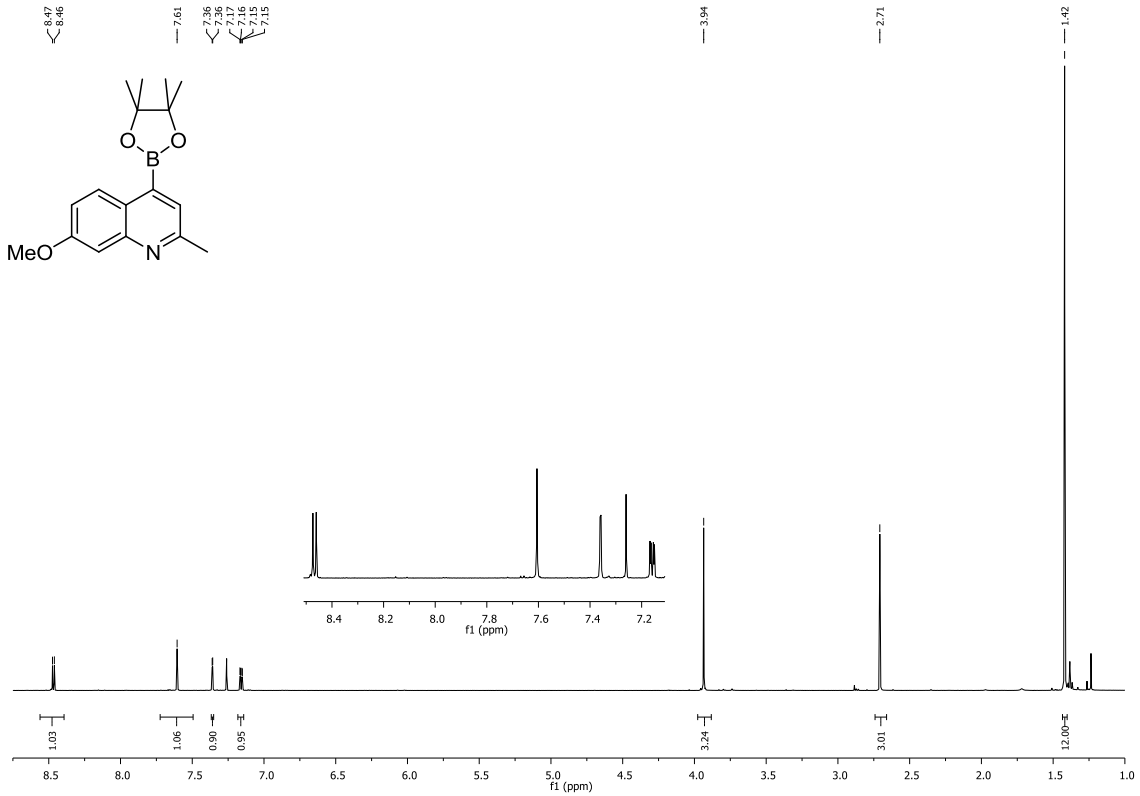

^{1}H NMR (700 MHz, $CDCl_3$)

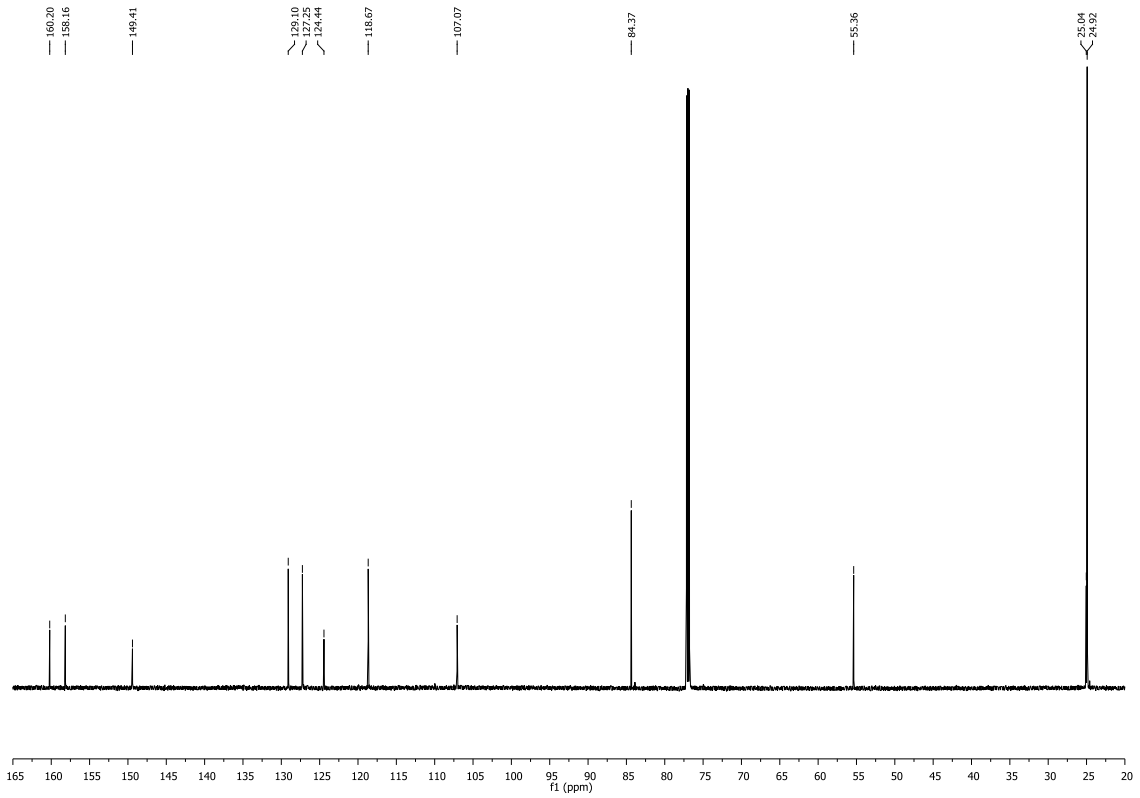

^{13}C NMR (176 MHz, $CDCl_3$)

^{1}H and ^{13}C NMR spectra for compound 463

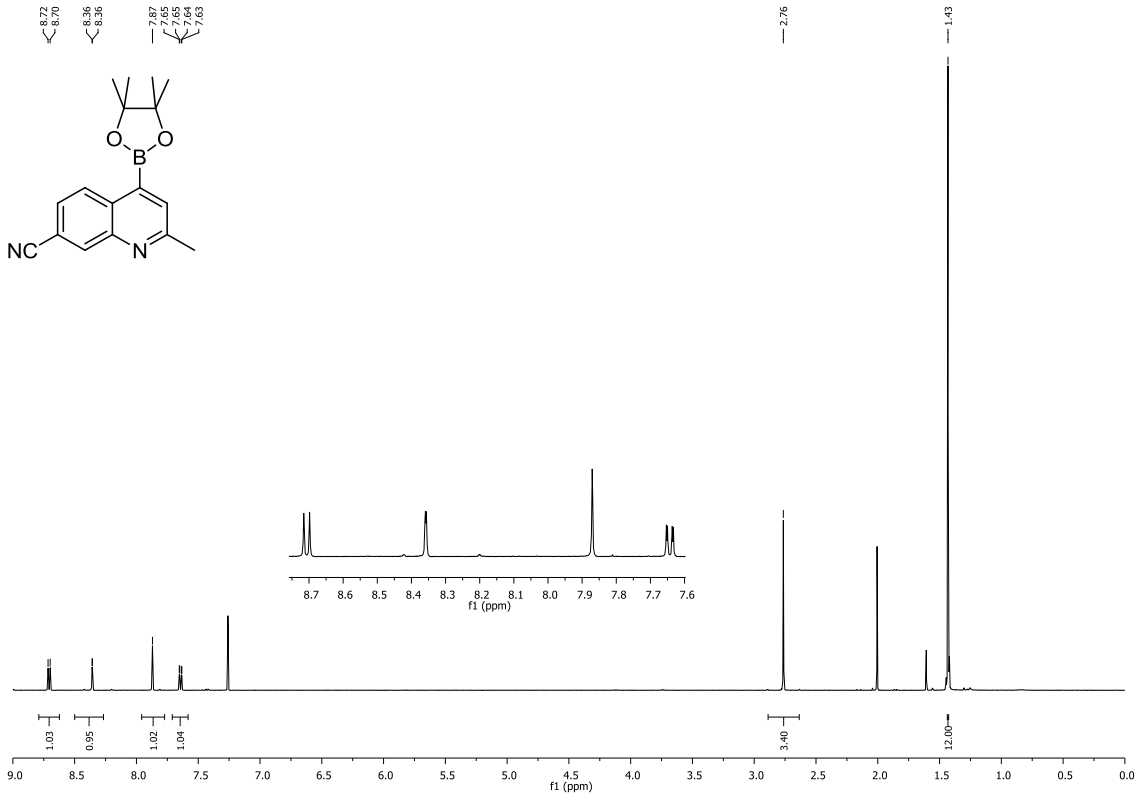

^{1}H NMR (500 MHz, $CDCl_3$)

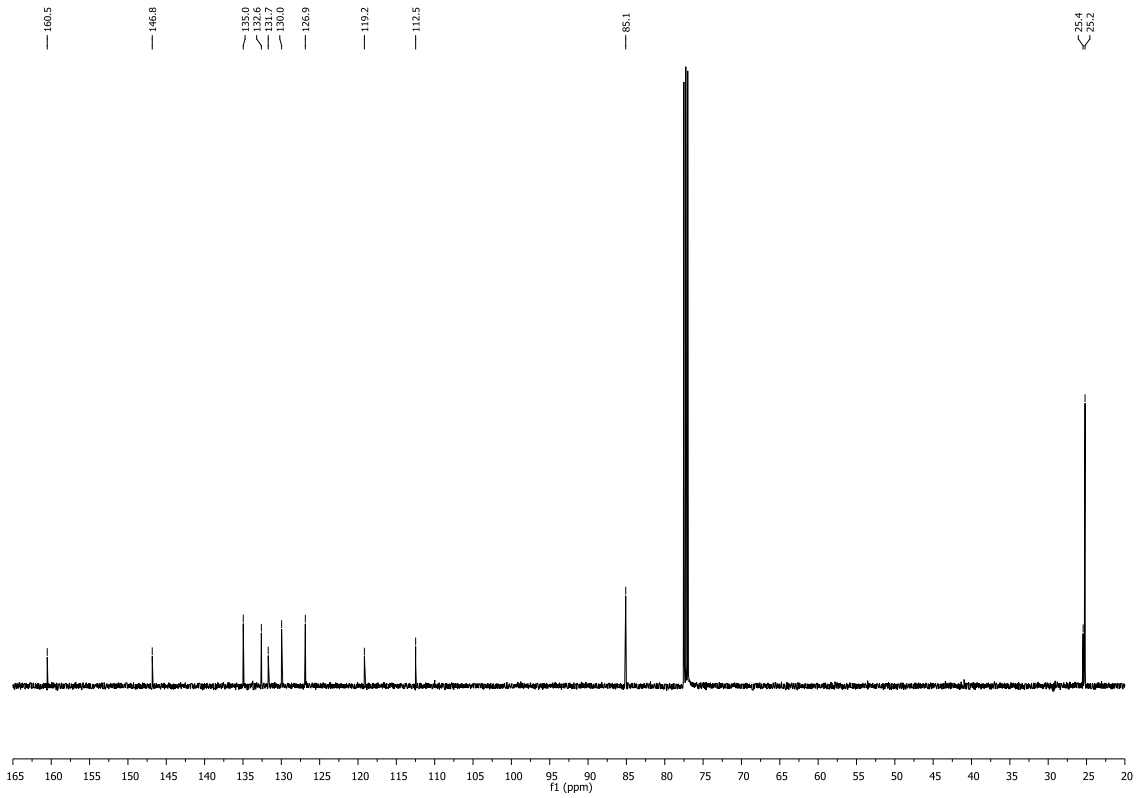

^{13}C NMR (126 MHz, $CDCl_3$)

^{1}H and ^{13}C NMR spectra for compound 464

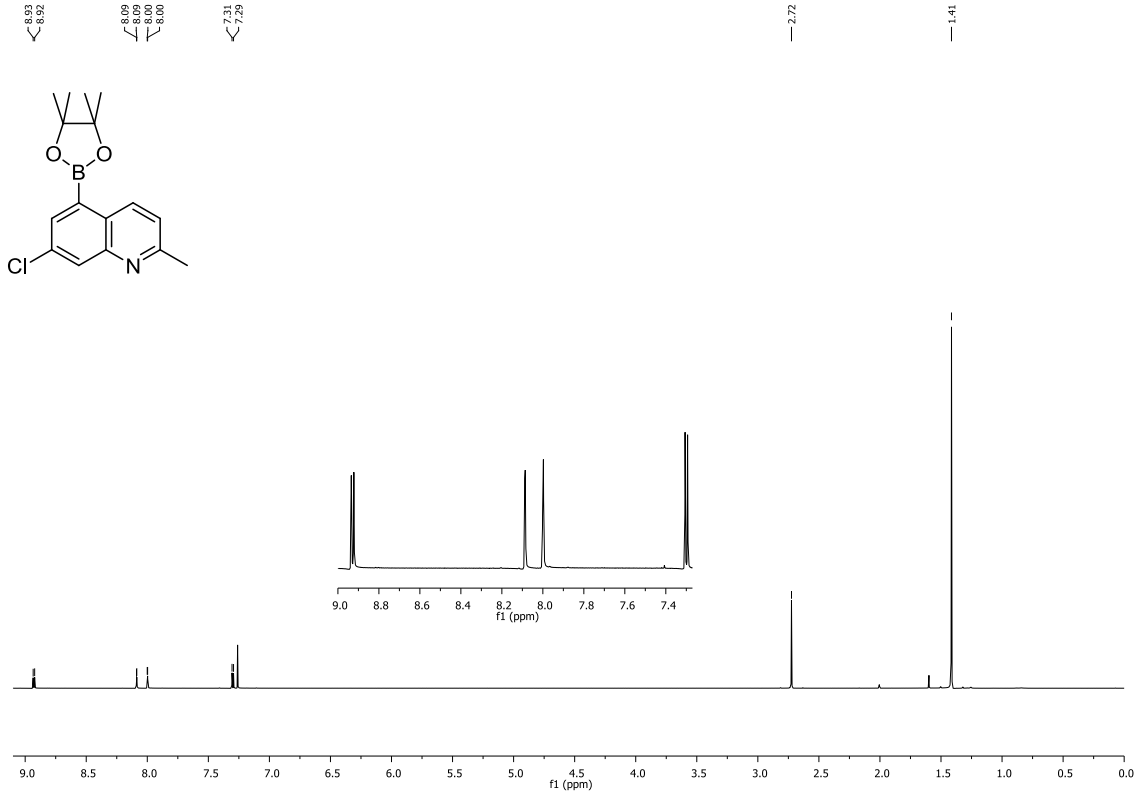

^{1}H NMR (700 MHz, $CDCl_3$)

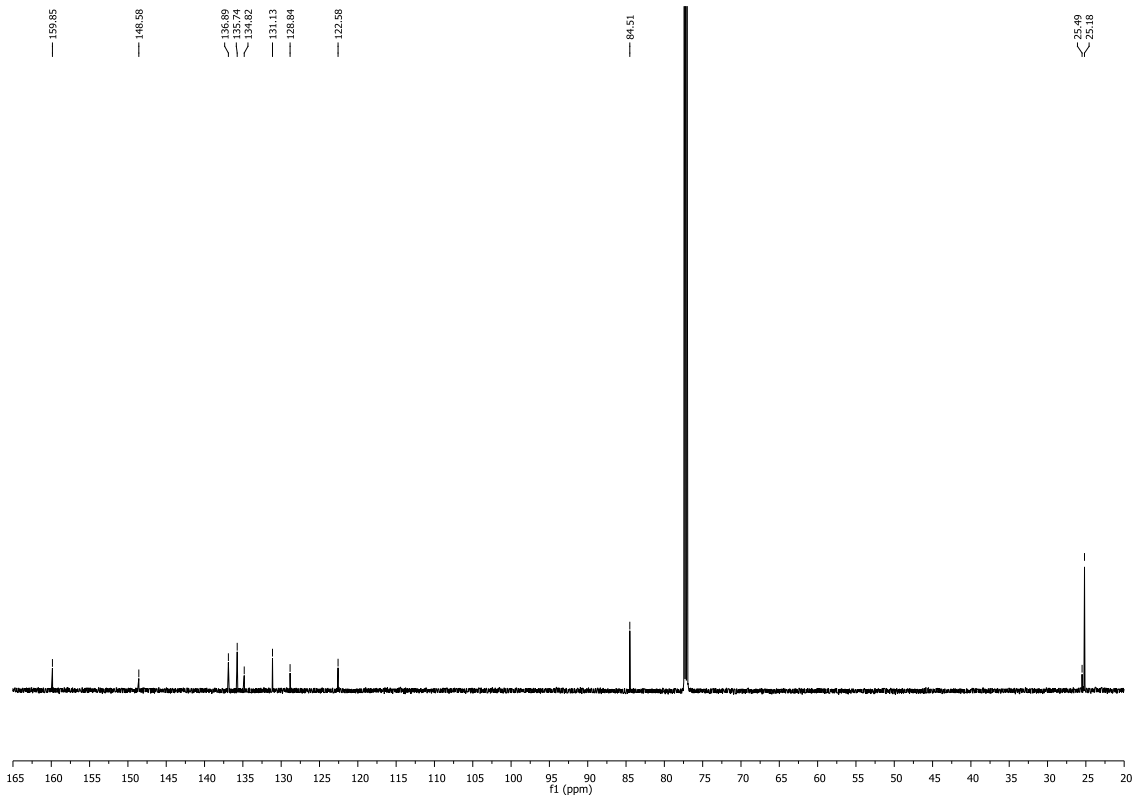

^{13}C NMR (176 MHz, $CDCl_3$)

^{1}H and ^{13}C NMR spectra for compound 465

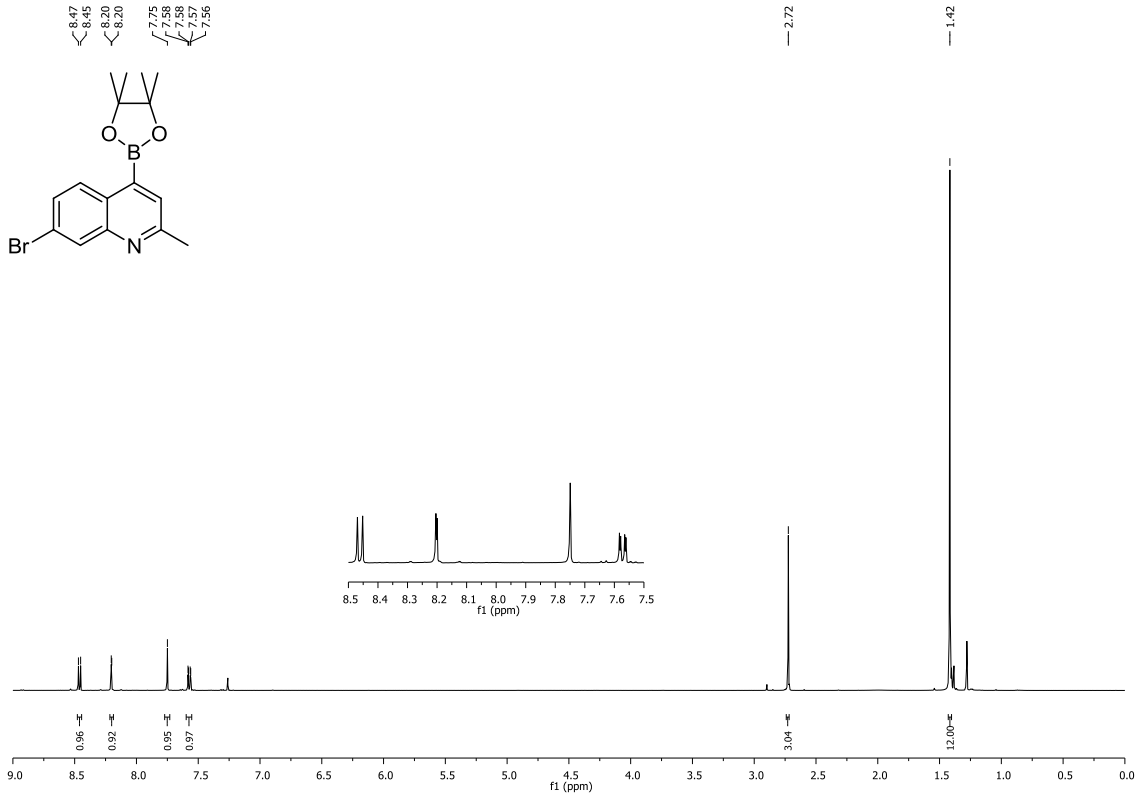

^{1}H NMR (500 MHz, $CDCl_3$)

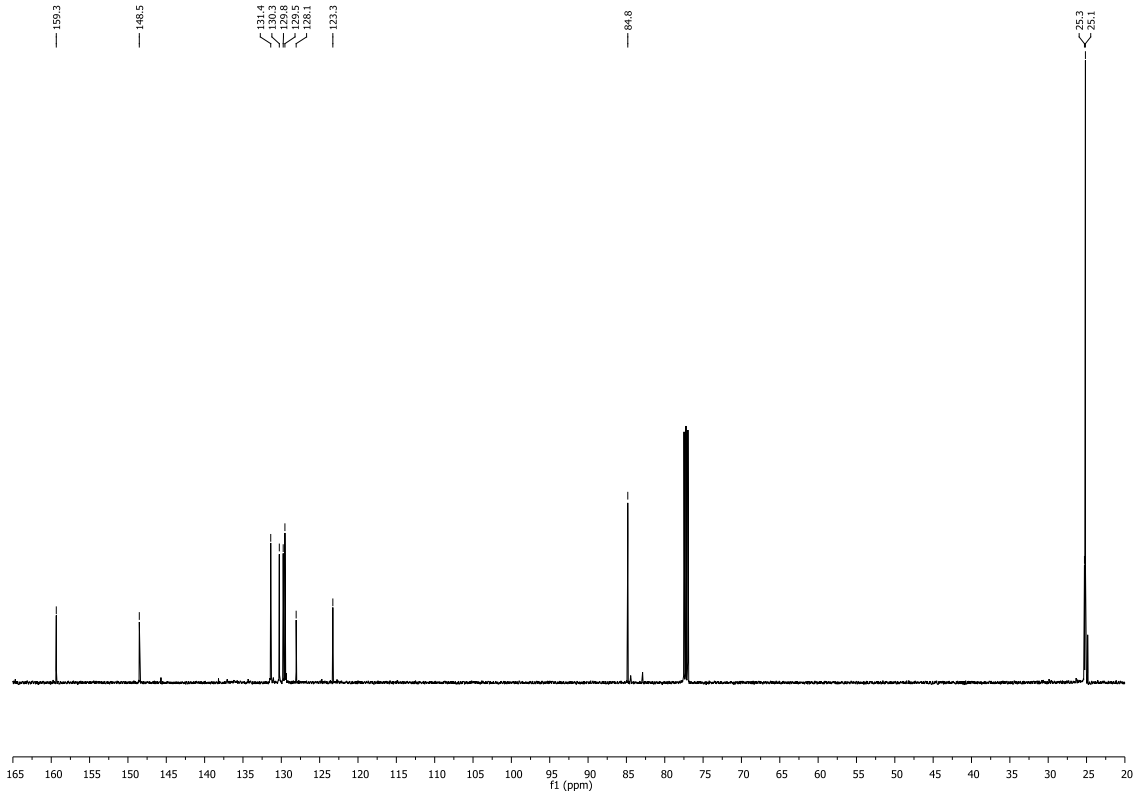

^{13}C NMR (126 MHz, $CDCl_3$)

^{1}H and ^{13}C NMR spectra for compound 466

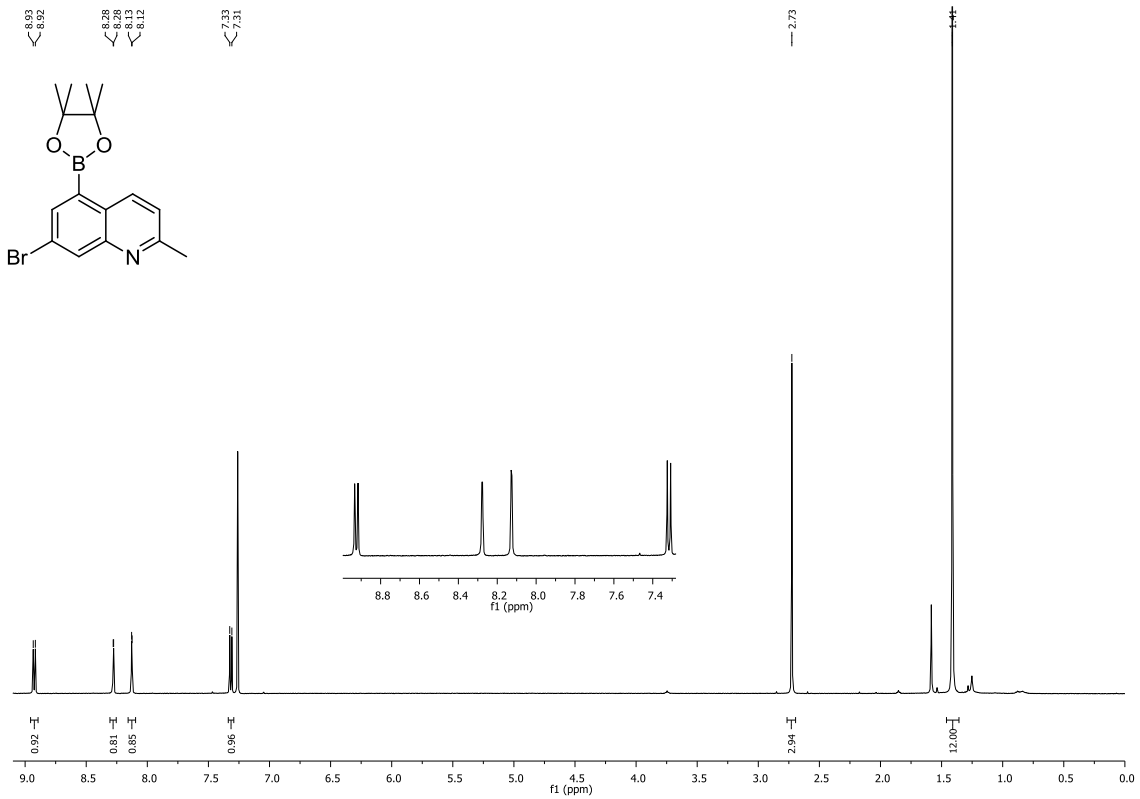

^{1}H NMR (500 MHz, $CDCl_3$)

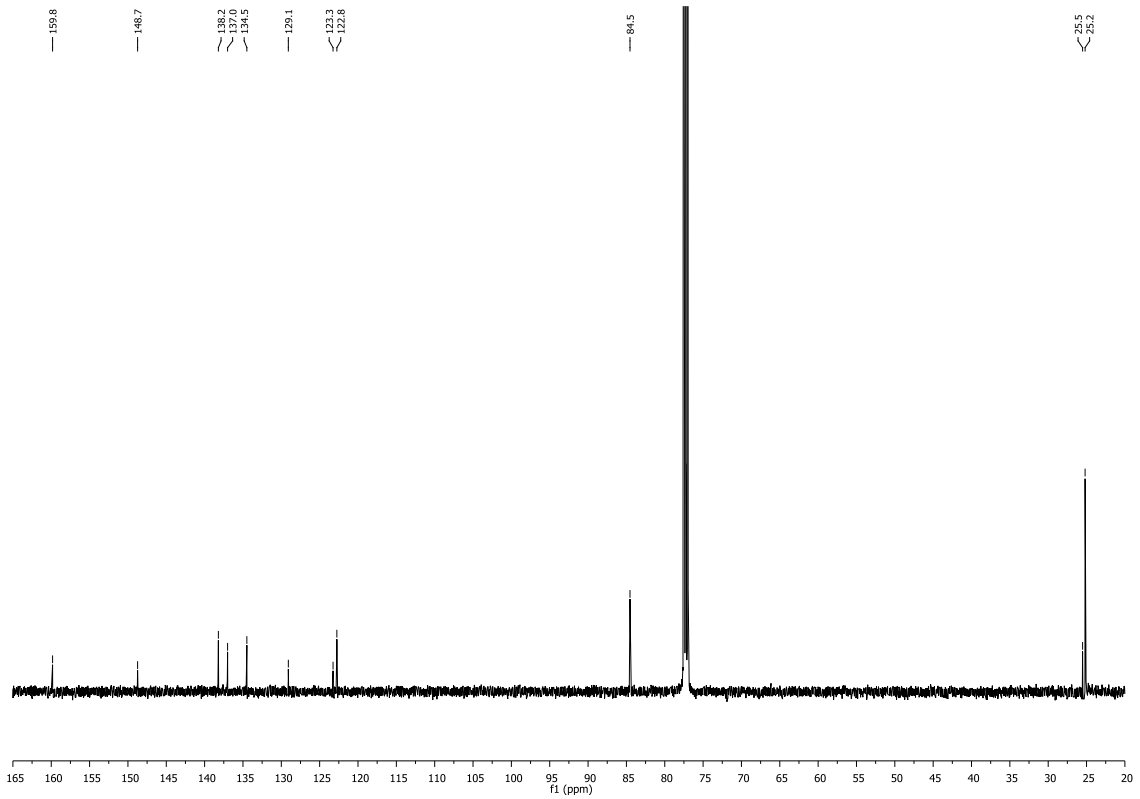

^{13}C NMR (126 MHz, $CDCl_3$)

^{1}H and ^{13}C NMR spectra for compound 467

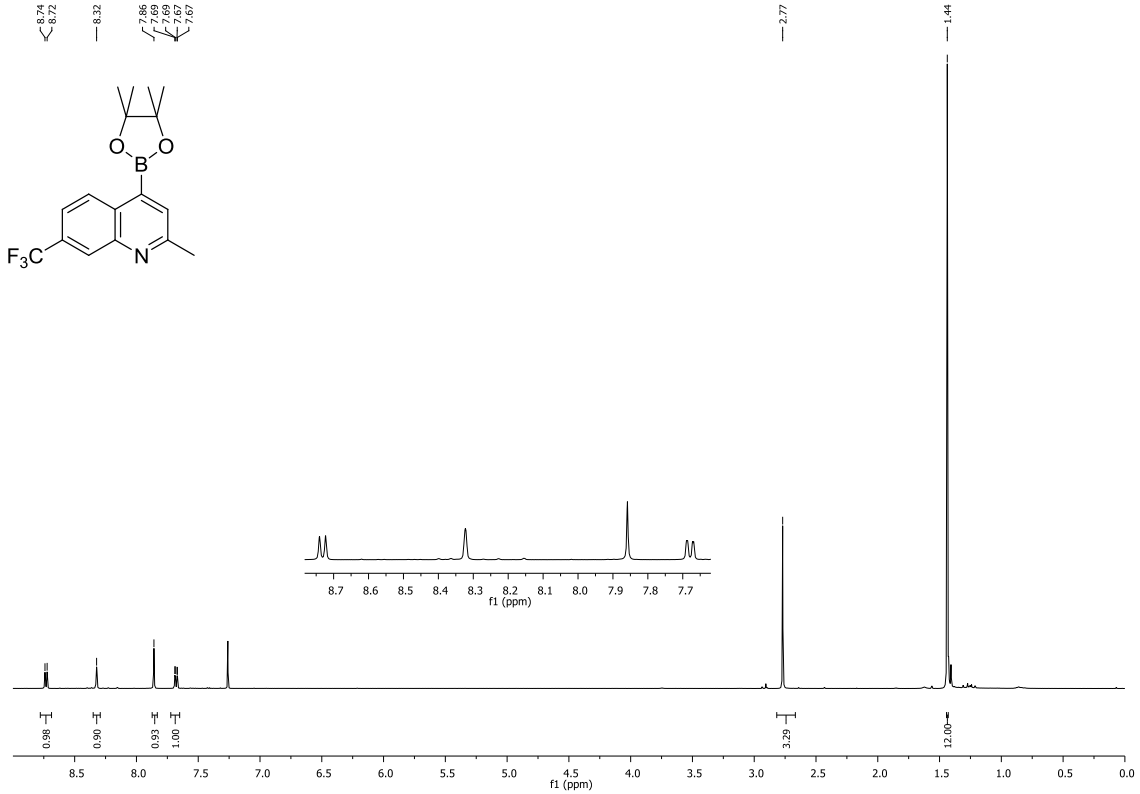

^{1}H NMR (500 MHz, $CDCl_3$)

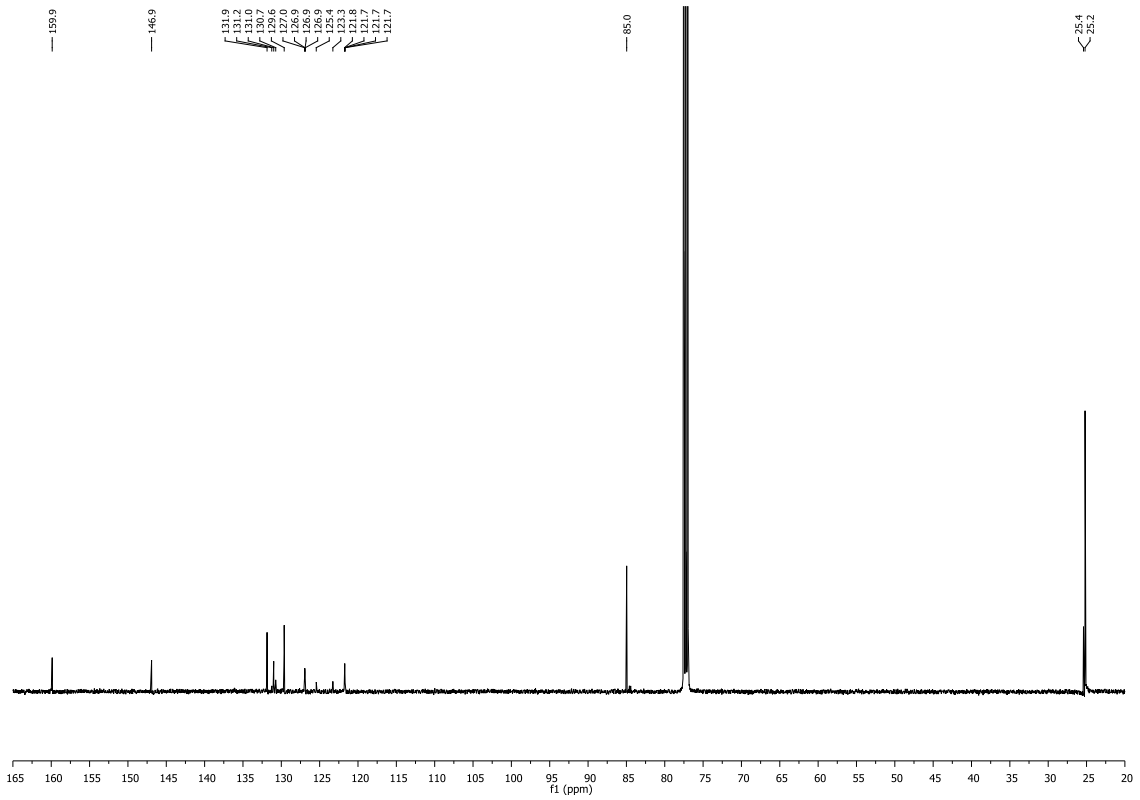

^{13}C NMR (126 MHz, $CDCl_3$)

^{1}H and ^{13}C NMR spectra for compound 468

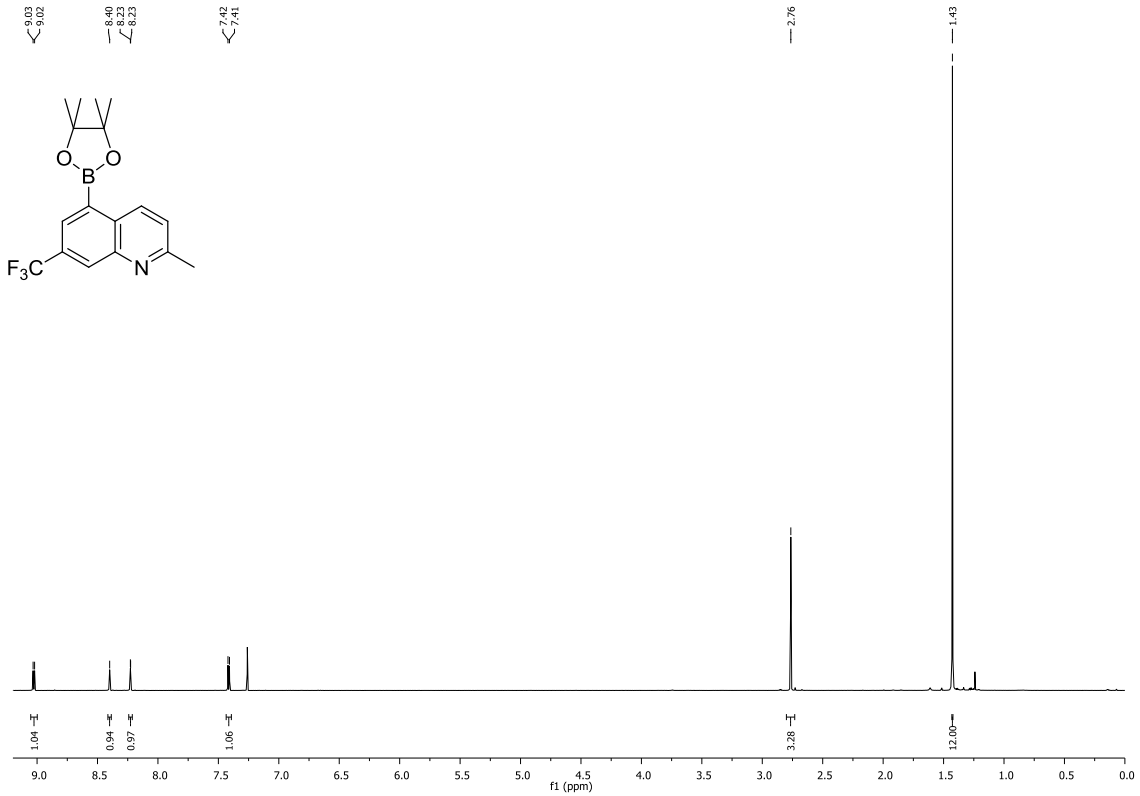

^{1}H NMR (700 MHz, $CDCl_3$)

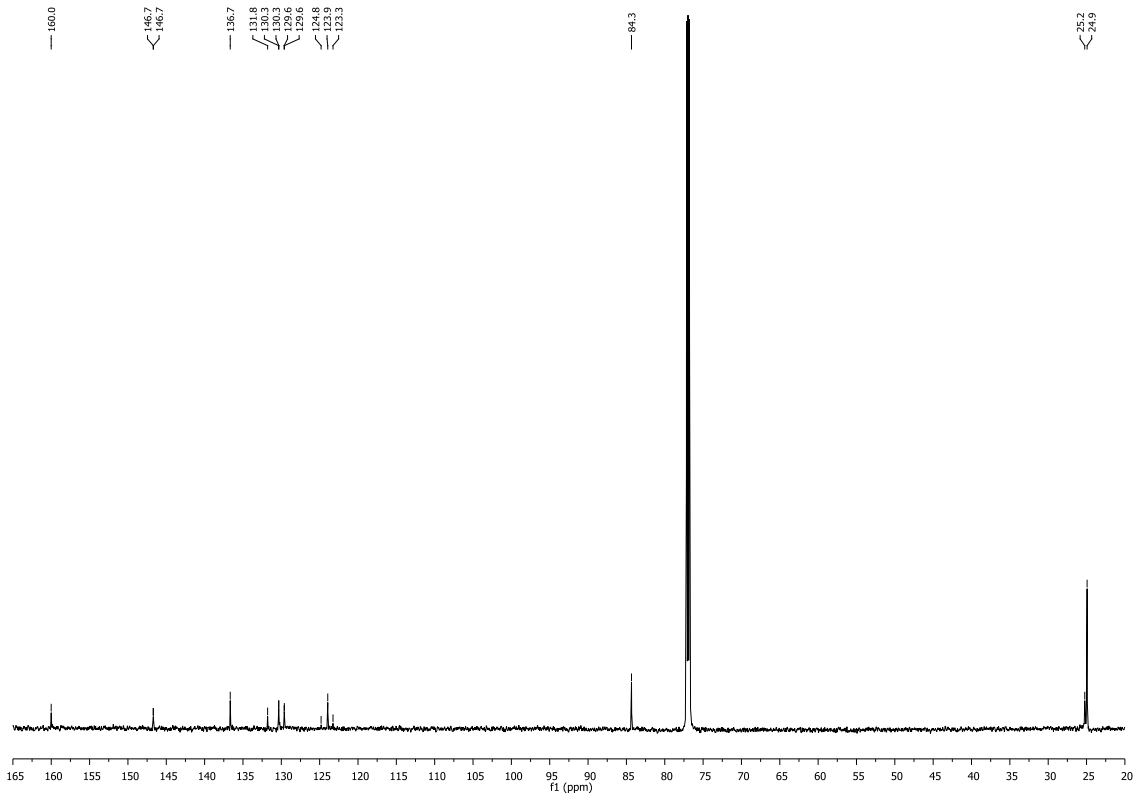

^{13}C NMR (126 MHz, $CDCl_3$)

^{1}H and ^{13}C NMR spectra for compound 481

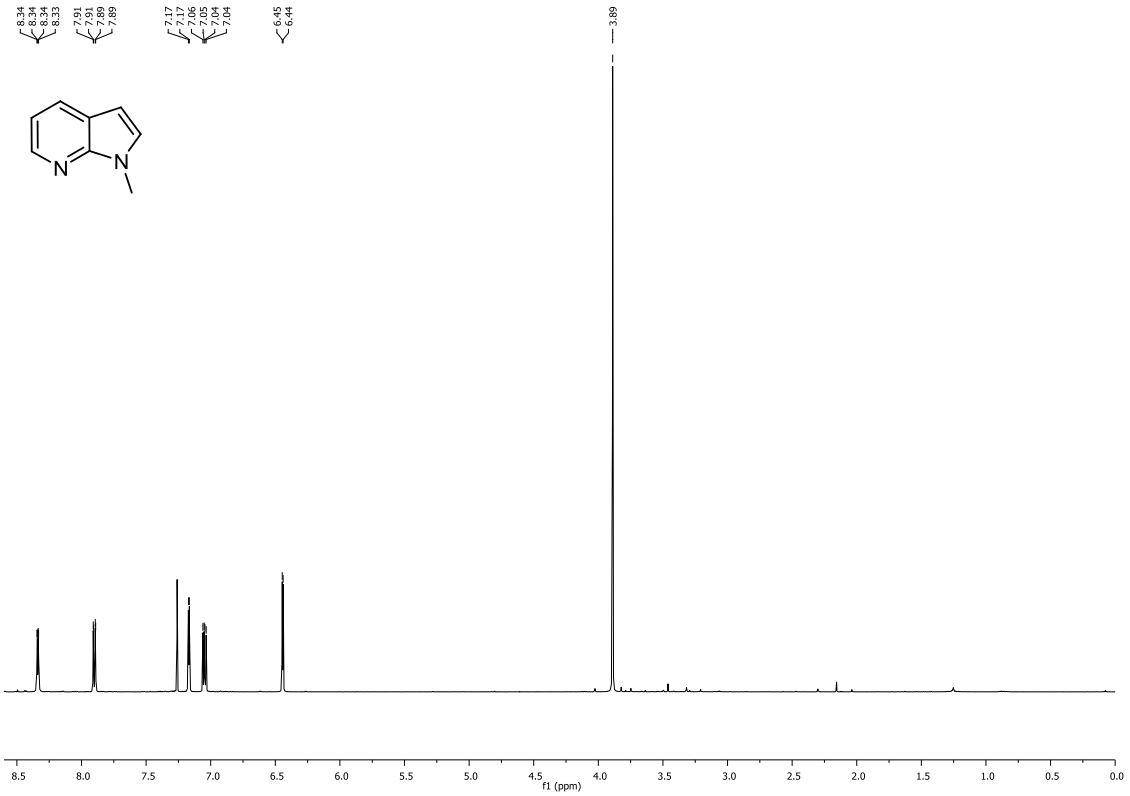

^{1}H NMR (500 MHz, $CDCl_3$)

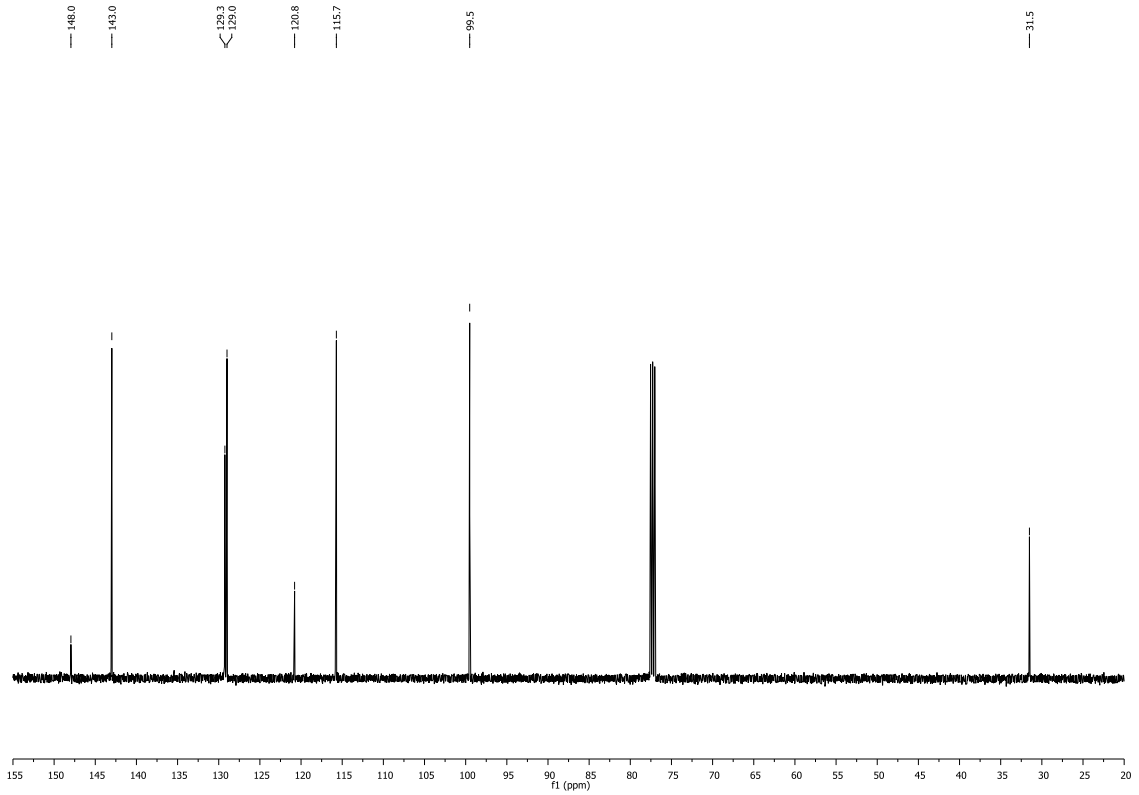

^{13}C NMR (126 MHz, $CDCl_3$)

^{1}H and ^{13}C NMR spectra for compound 482

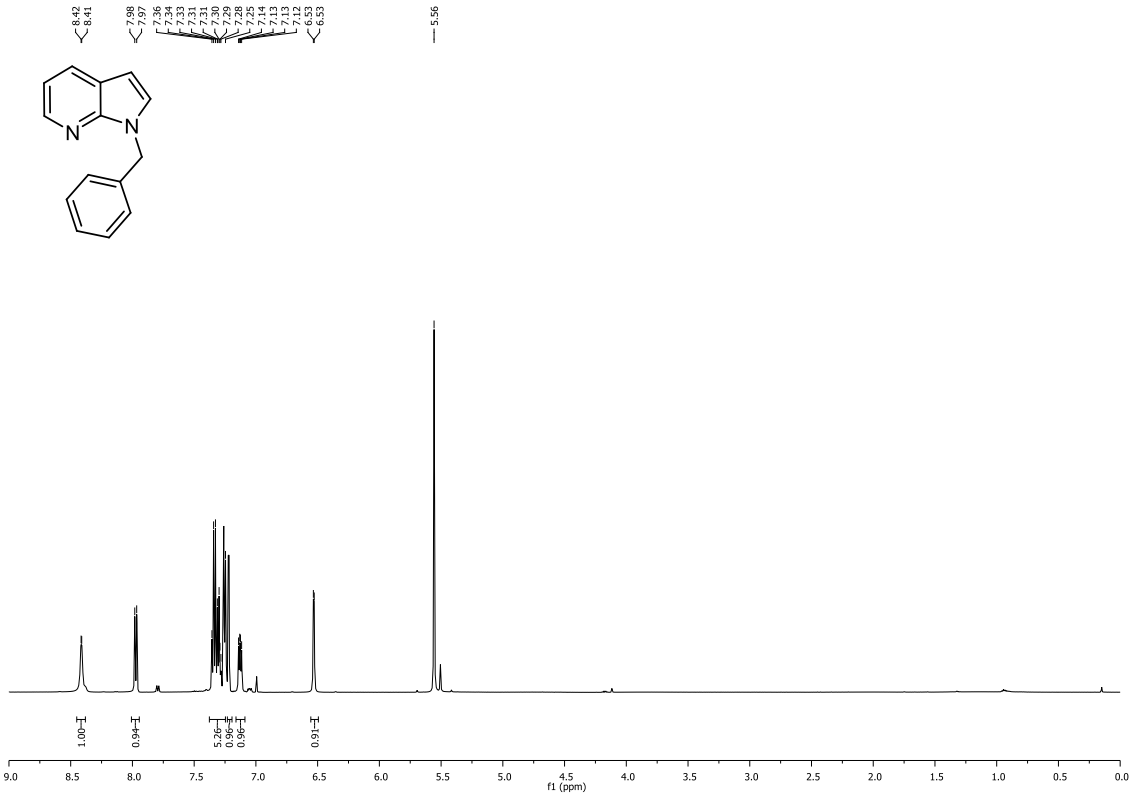

^{1}H NMR (500 MHz, $CDCl_3$)

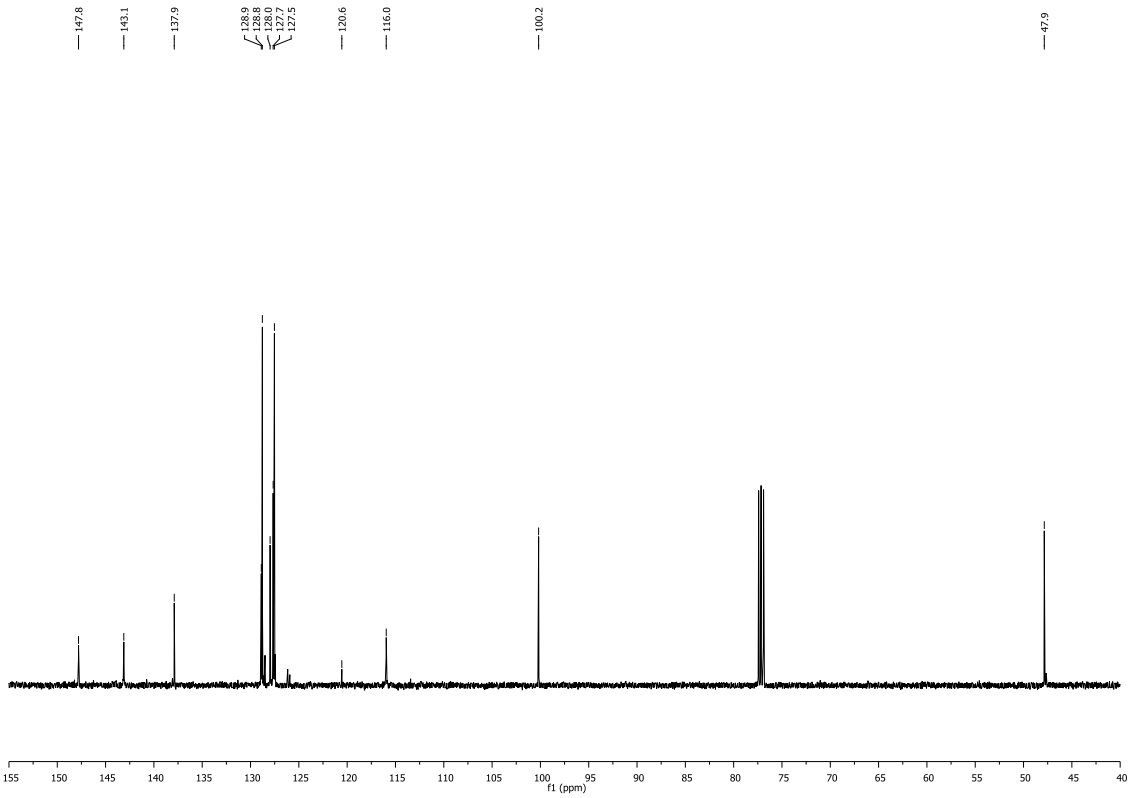

^{13}C NMR (126 MHz, $CDCl_3$)

^{1}H and ^{13}C NMR spectra for compound 483

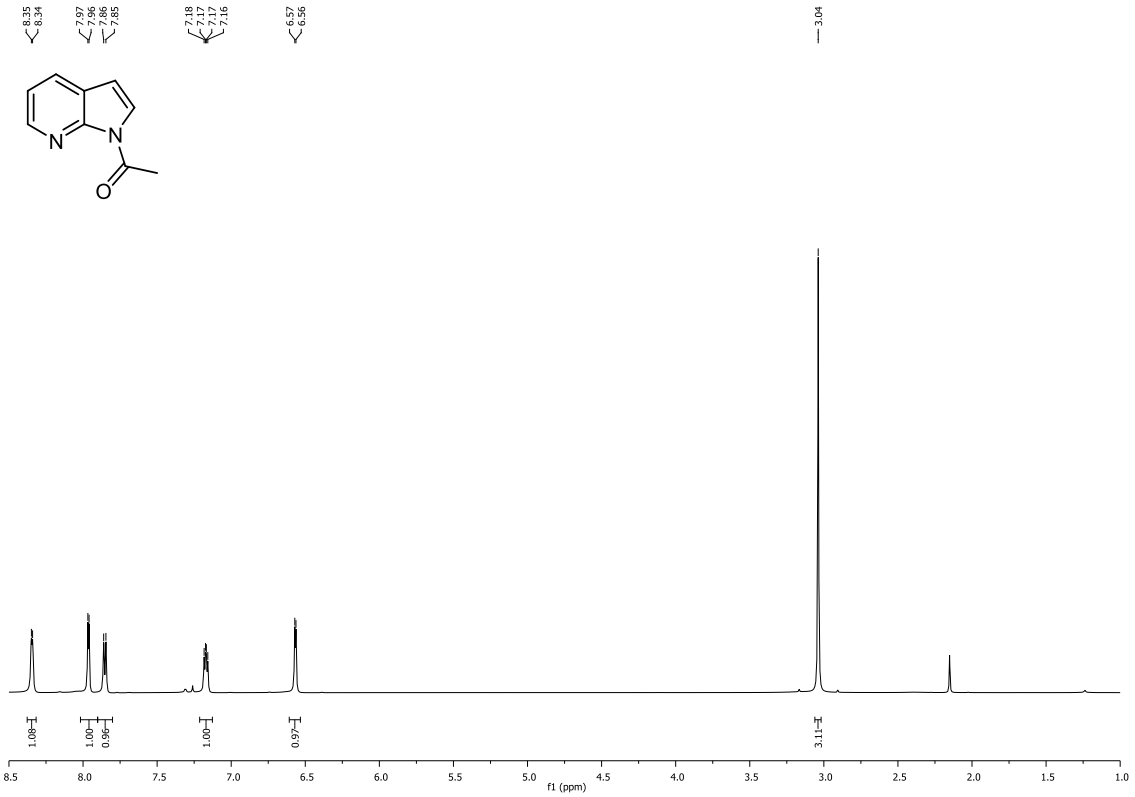

^{1}H NMR (500 MHz, $CDCl_3$)

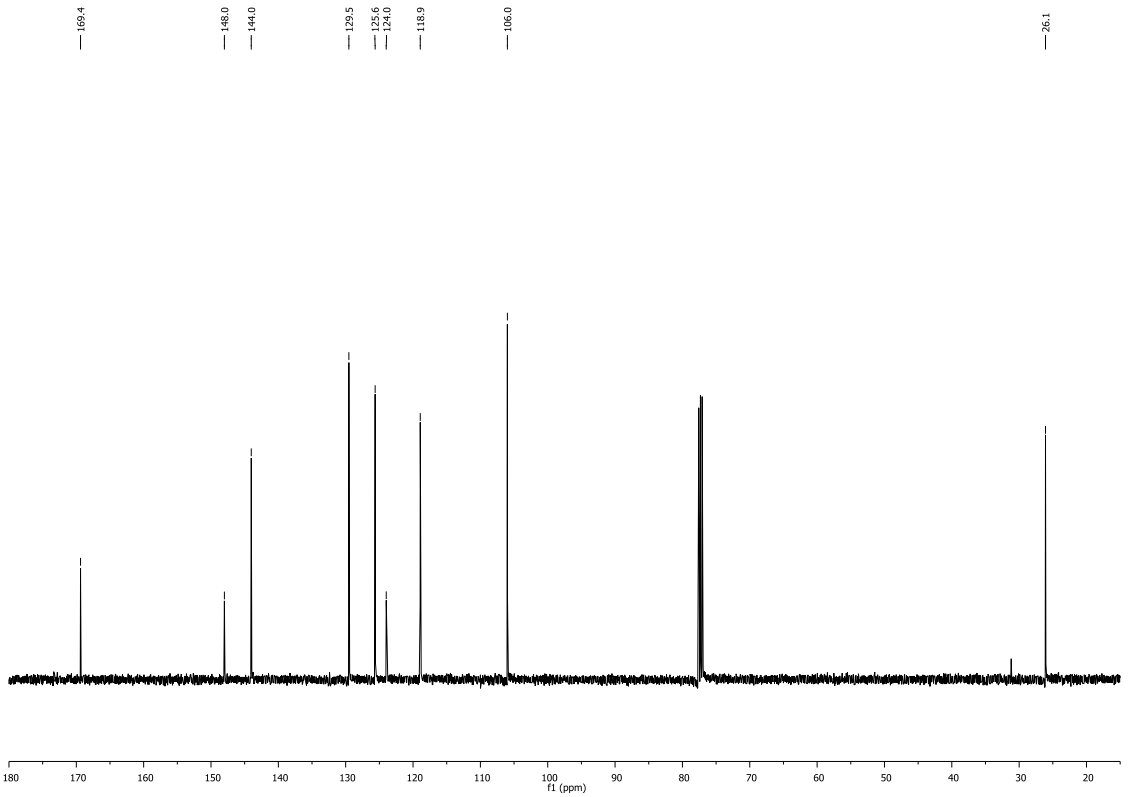

^{13}C NMR (126 MHz, $CDCl_3$)

^{1}H and ^{13}C NMR spectra for compound 365

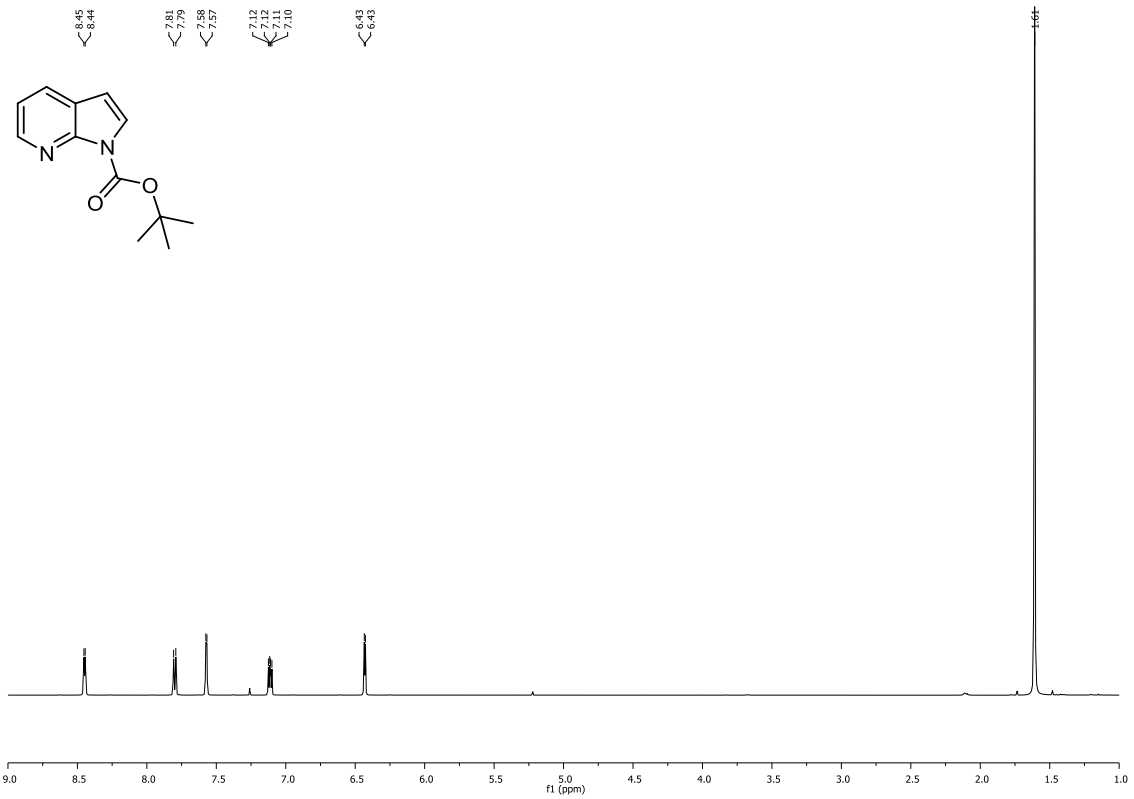

^{1}H NMR (500 MHz, $CDCl_3$)

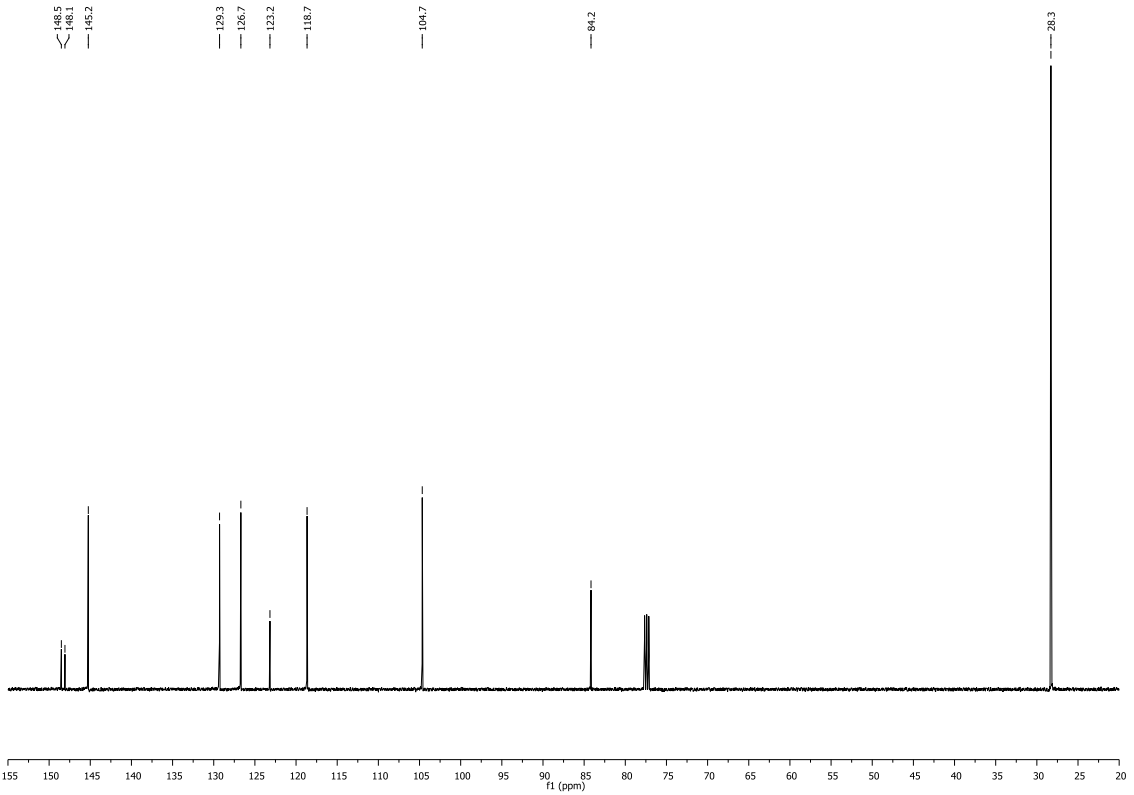

^{13}C NMR (126 MHz, $CDCl_3$)

^{1}H and ^{13}C NMR spectra for compound 484

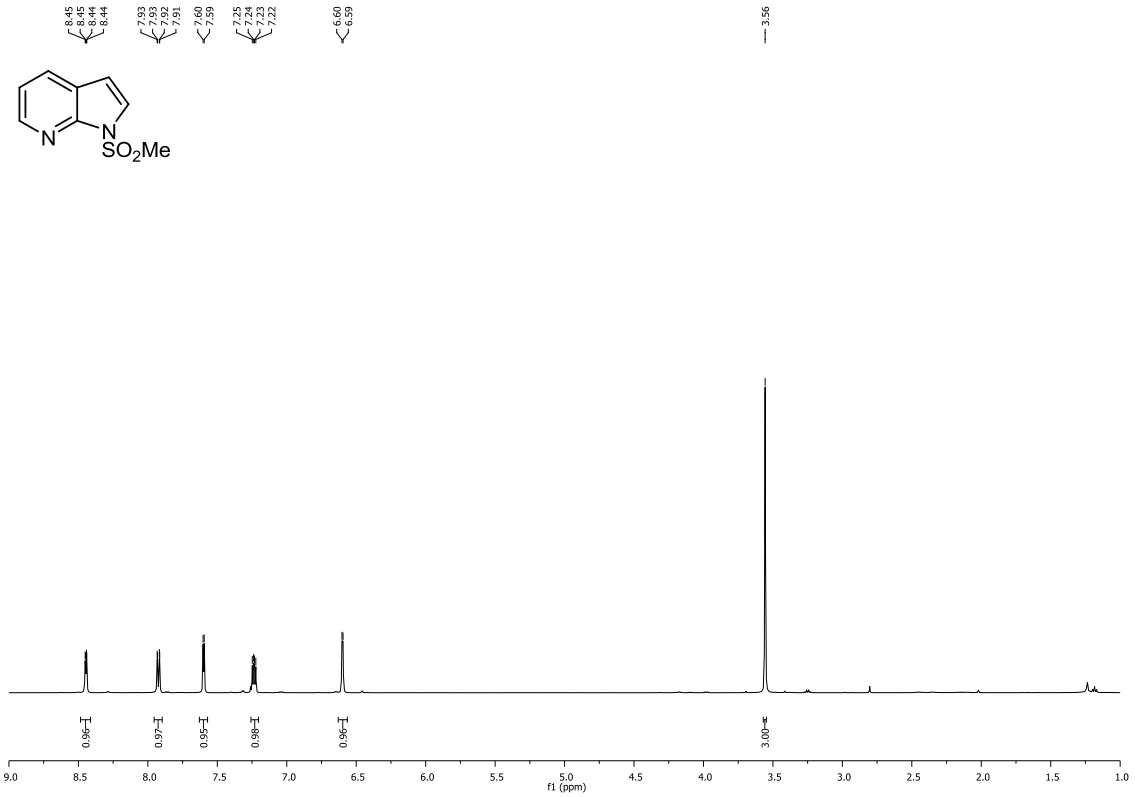

^{1}H NMR (500 MHz, $CDCl_3$)

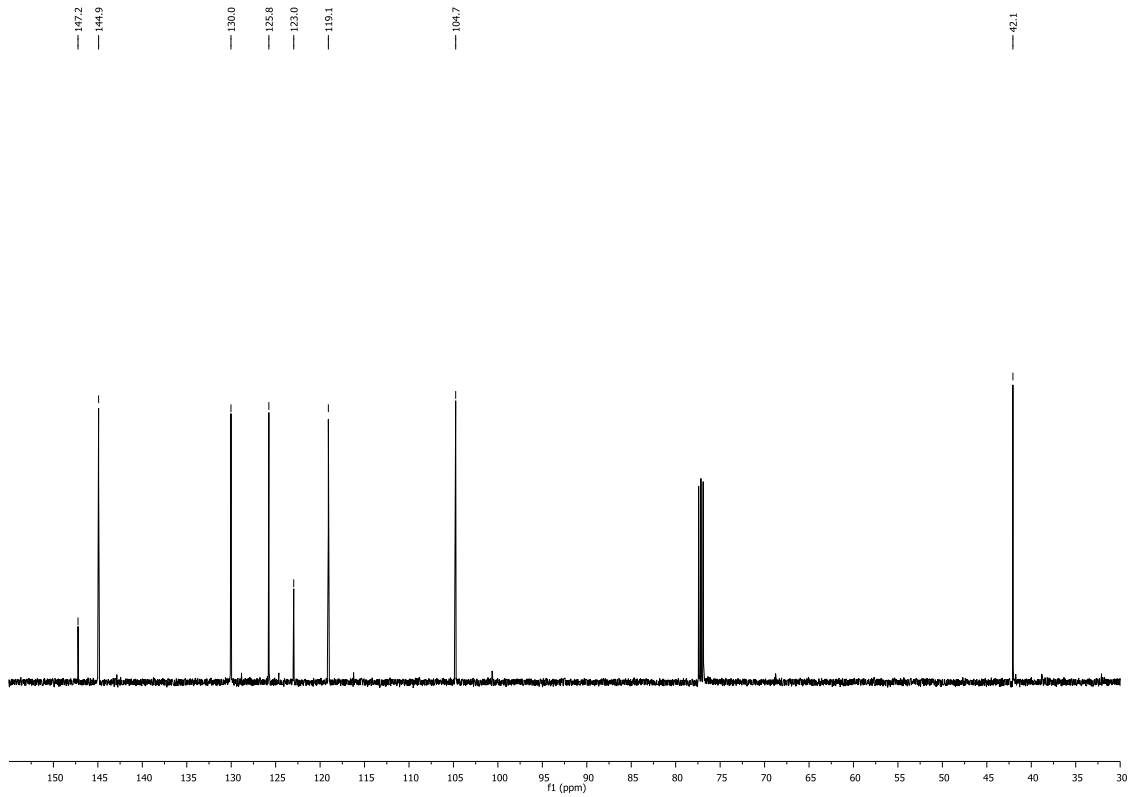

^{13}C NMR (126 MHz, $CDCl_3$)

^{1}H and ^{13}C NMR spectra for compound 485

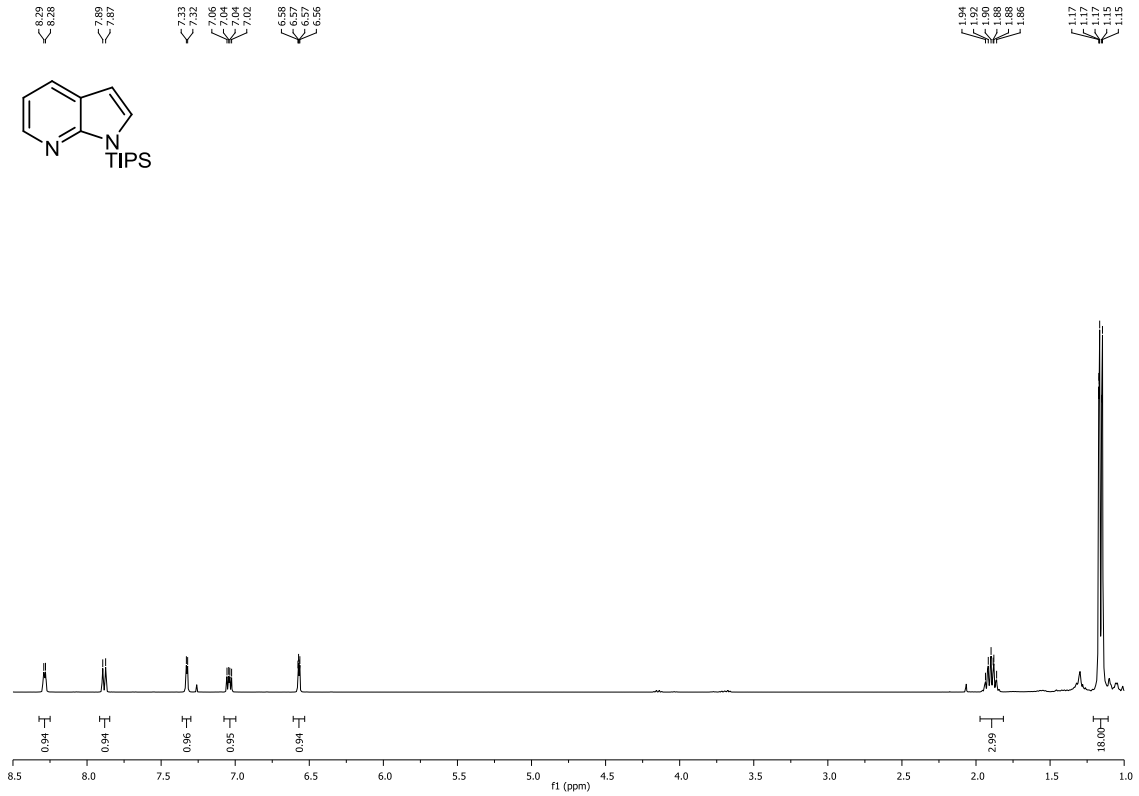

^{1}H NMR (400 MHz, $CDCl_3$)

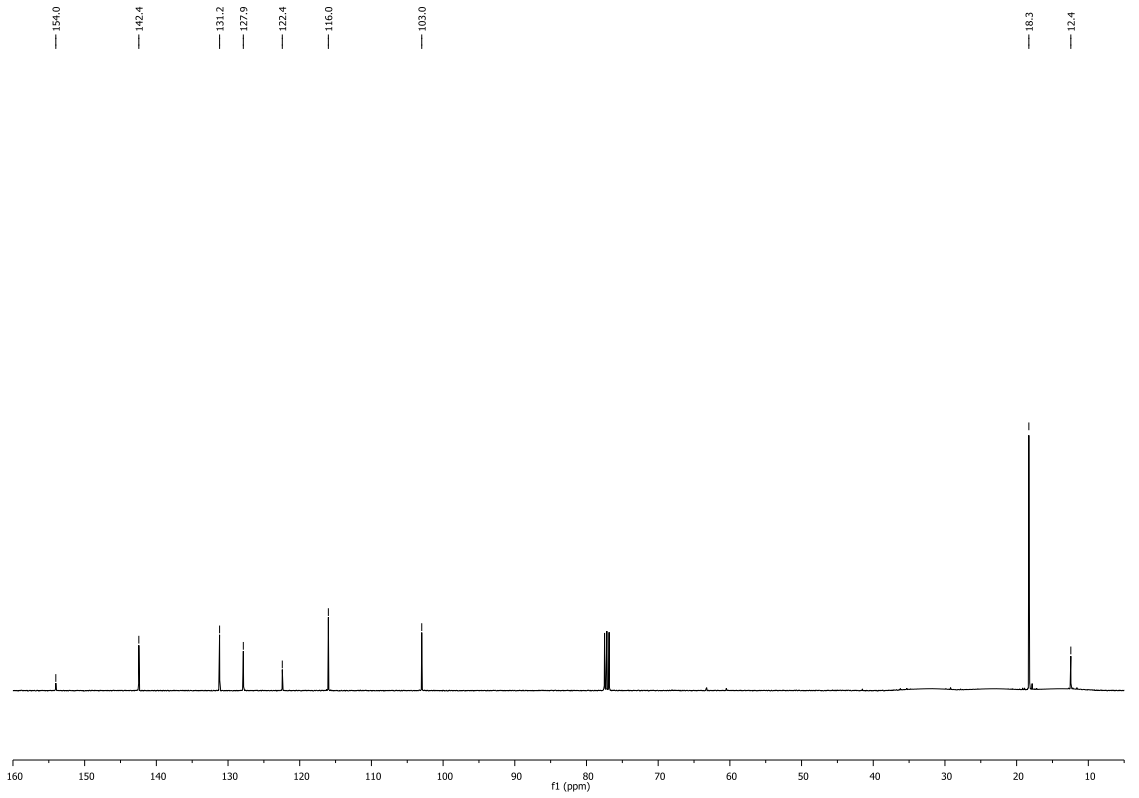

^{13}C NMR (101 MHz, $CDCl_3$)

APPENDIX II - X-RAY CRYSTAL STRUCTURES & DATA TABLES

General Crystallographic Procedures

Single-crystal diffraction experiments (Section 4.0) were carried out on Bruker 3-circle diffractometers with CCD area detectors SMART 1000 or PLATINUM135 using graphite-monochromated K_a radiation from a sealed Mo-anode tube ($\bar{\lambda}$ = 0.71073 Å) Crystals were cooled using Cryostream (Oxford Cryosystems) open-flow N_2 cryostats. The structures were solved by direct methods and refined by full-matrix least squares against F^2 of all data, using SHELXTL[1] and Olex2[2] software. Molecular structures are drawn with thermal ellipsoids at 50% probability.

Compound	08srv145	08srv132	08srv269	08srv130
Empirical formula	$C_9H_8N_2O$	$C_{14}H_{12}N_2$	$C_{12}H_{14}N_2O_2$	$C_8H_8N_2O_2S$
Formula weight	160.17	208.26	218.25	196.22
Temperature, K	393(2)	393(2)	393(2)	393(2)
Crystal system	Monoclinic	Monoclinic	orthorhombic	orthorhombic
Space group (no.)	Cc (# 9)	$P2_1$ (# 4)	$P2_12_12_1$ (# 19)	Pbca (# 61)
a, Å	6.9072(6)	9.4546 (13)	8.9587(10)	8.6022(9)
b, Å	16.6049(12)	5.6810 (8)	10.4836(11)	13.6368(13)
c, Å	6.7441(6)	10.0979 (14)	12.2873(13)	14.7729(14)
α, º	90.00	90.00	90.00	90.00
β, º	101.88(2),	100.52(2),	90.00	90.00
γ, º	90.00	90.00	90.00	90.00
V, Å^3	756.93(11)	533.25(13)	1154.0(2)	1733.0(3)
Z	4	2	4	8
ρ (calc.), g/cm^3	1.406	1.297	1.256	1.504
μ, mm^{-1}	0.095	0.078	0.087	0.338
Refls collected	3182	6566	13082	15179
Unique reflections	1060	1638	1910	2301
Reflections I>2σ (I)	691	1526	1646	1771
R_{int} ,%	4.54	3.22	3.50	3.43
Refined parameters	141	193	202	150
R(F) [I>2σ (I)]	0.045	0.0322	0.0350	0.0343
wR(F^2) [all data],%	0.0955	0.0877	0.0862	0.0905

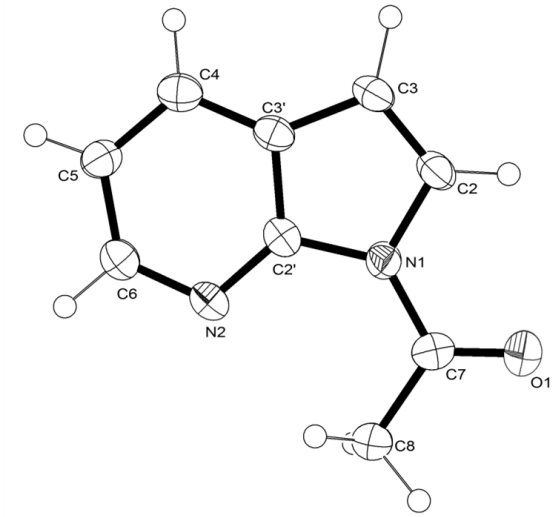

08srv145

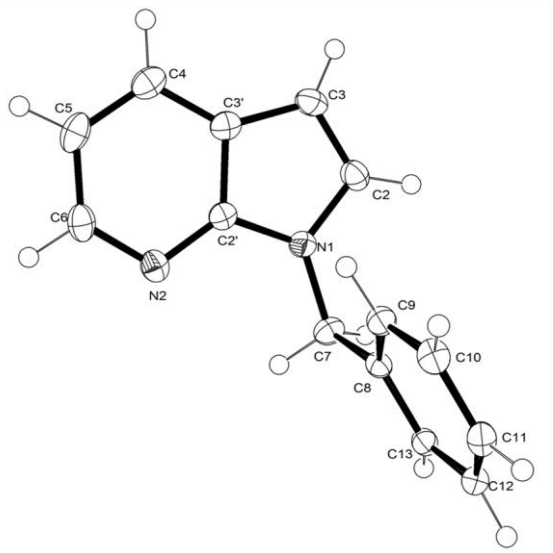

08srv132

08srv145	Coordinates (Å)		
Atom	x	y	z
O1	0.9348 (4)	0.25018 (14)	0.5168 (4)
N1	1.1612 (4)	0.00868 (16)	0.5146 (4)
N2	0.9142 (4)	0.11529 (16)	0.4709 (4)
H5	0.8276 (5)	−0.0971 (2)	0.4479 (5)
C2	0.708 (6)	−0.131 (3)	0.417 (6)
C9	1.0221 (5)	−0.1257 (2)	0.4846 (5)
H2	1.047 (5)	−0.182 (2)	0.487 (5)
H9-1	1.1787 (5)	−0.07160 (19)	0.5155 (5)
C1	1.317 (5)	−0.0915 (19)	0.539 (5)
H9-2	0.9759 (5)	0.0341 (2)	0.4787 (5)
H9-3	0.8041 (5)	−0.01409 (18)	0.4447 (5)
C8	1.0221 (5)	0.1874 (2)	0.5097 (5)
C7	1.2424 (5)	0.1820 (2)	0.5389 (6)
C4	1.293 (6)	0.237 (2)	0.607 (6)
H1	1.283 (7)	0.137 (3)	0.623 (8)
H4	1.277 (7)	0.174 (2)	0.416 (7)
C6	0.7054 (5)	0.1155 (2)	0.4303 (5)
C3	0.639 (5)	0.168 (2)	0.421 (5)
C5	0.6356 (5)	0.0398 (2)	0.4138 (5)
H3	0.486 (4)	0.0203 (18)	0.380 (4)

08srv132	Coordinates (Å)		
Atom	x	y	z
N1	0.12179 (12)	0.2580 (3)	0.17052 (12)
C2	0.03966 (15)	0.0651 (3)	0.17370 (17)
H2	−0.013 (2)	0.008 (4)	0.08700 (2)
C3	0.02472 (16)	−0.0557 (3)	0.29154 (19)
H3	−0.040 (2)	−0.186 (5)	0.28500 (2)
C4	0.09891 (16)	0.0186 (3)	0.41556 (17)
H4	0.092 (2)	−0.069 (5)	0.49800 (2)
C5	0.27961 (16)	0.3505 (3)	0.51797 (15)
H5	0.300 (2)	0.328 (4)	0.61000 (2)
C6	0.33540 (16)	0.5284 (3)	0.45236 (15)
H6	0.402 (2)	0.647 (4)	0.485 (2)
N7	0.28258 (12)	0.5160 (2)	0.31531 (12)
C8	0.19191 (14)	0.3248 (3)	0.29175 (14)
C9	0.18693 (14)	0.2164 (3)	0.41761 (14)
C10	0.32868 (16)	0.6633 (3)	0.21372 (16)
H11	0.332 (2)	0.826 (5)	0.244 (2)
H10	0.2551 (18)	0.651 (4)	0.1310 (17)
C11	0.47805 (14)	0.6019 (3)	0.18836 (13)
C12	0.54715 (14)	0.7612 (3)	0.11658 (13)
H12	0.498 (2)	0.917 (4)	0.088 (2)
C13	0.68350 (15)	0.7114 (3)	0.08987 (15)
H13	0.731 (2)	0.819 (4)	0.0377 (19)
C14	0.75259 (15)	0.5027 (3)	0.13636 (15)
H14	0.851 (2)	0.470 (4)	0.1159 (19)
C15	0.68471 (16)	0.3438 (3)	0.20853 (15)
H15	0.734 (2)	0.205 (4)	0.239 (2)
C16	0.54740 (15)	0.3922 (3)	0.23369 (14)
H16	0.5002 (19)	0.274 (4)	0.2792 (17)

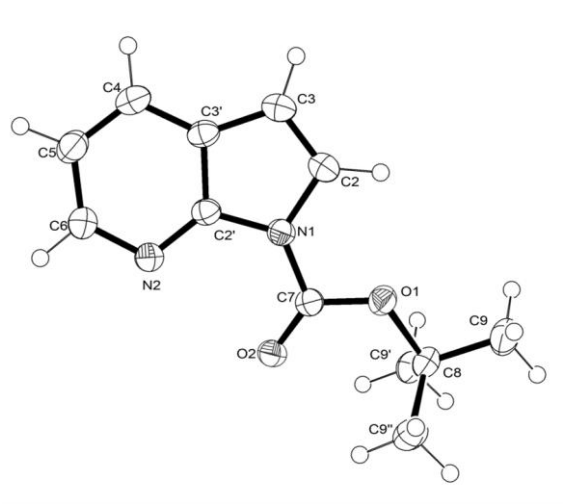

08srv269

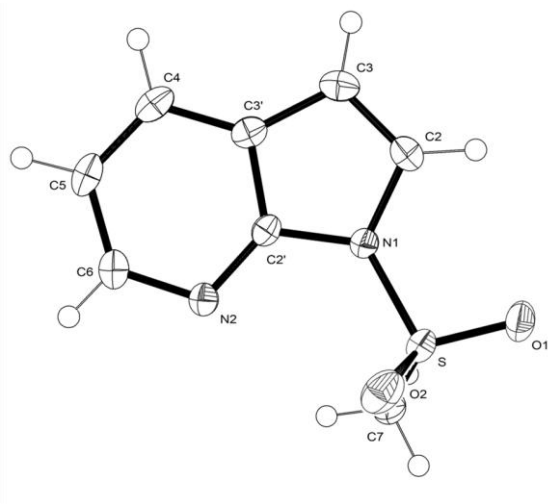

08srv130

08srv269	Coordinates (Å)		
Atom	x	y	z
O1	0.35630 (13)	0.41947 (11)	0.32760 (10)
O2	0.19146 (14)	0.28196 (11)	0.24984 (9)
N1	0.18540 (18)	0.03709 (14)	0.35792 (12)
N7	0.31861 (16)	0.23141 (13)	0.40637 (10)
C1	0.3187 (2)	0.52959 (16)	0.25630 (15)
C2	0.1560 (2)	−0.08148 (18)	0.39507 (16)
H2	0.094 (2)	−0.133 (2)	0.3432 (17)
C3	0.2065 (2)	−0.12976 (18)	0.49406 (15)
H3	0.181 (2)	−0.220 (2)	0.5140 (17)
C4	0.2931 (2)	−0.05552 (18)	0.56218 (14)
H4	0.331 (2)	−0.087 (2)	0.6320 (18)
C5	0.4135 (2)	0.17179 (18)	0.56879 (14)
H5	0.471 (2)	0.174 (2)	0.6365 (17)
C6	0.40718 (19)	0.26783 (18)	0.49620 (14)
H6	0.454 (2)	0.357 (2)	0.4957 (17)
C7	0.27984 (18)	0.31106 (15)	0.31912 (12)
C8	0.26925 (18)	0.10615 (15)	0.42486 (12)
C9	0.32731 (19)	0.06733 (16)	0.52669 (12)
C10	0.1592 (2)	0.56988 (18)	0.27997 (16)
H10-1	0.083 (2)	0.509 (2)	0.2543 (18)
H10-2	0.144 (3)	0.585 (2)	0.361 (2)
H10-3	0.139 (3)	0.656 (2)	0.242 (2)
C11	0.3448 (3)	0.4957 (2)	0.13696 (16)
H11-1	0.447 (3)	0.459 (2)	0.1280 (19)
H11-2	0.266 (2)	0.435 (2)	0.1077 (17)
H11-3	0.344 (3)	0.578 (2)	0.0907 (18)
C12	0.4285 (2)	0.6305 (2)	0.29459 (19)
H12-1	0.408 (2)	0.710 (2)	0.2526 (19)
H12-2	0.412 (3)	0.648 (2)	0.3742 (19)
H12-3	0.527 (3)	0.600 (2)	0.2812 (18)

08srv130	Coordinates (Å)		
Atom	x	y	z
S	0.49597 (4)	0.14297 (3)	0.44156 (3)
O1	0.40702 (15)	0.05745 (8)	0.42014 (8)
O2	0.65713 (14)	0.14581 (8)	0.41919 (9)
N1	0.56725 (15)	0.37029 (9)	0.43389 (9)
N7	0.40783 (14)	0.23395 (9)	0.38539 (8)
C1	0.4689 (2)	0.17716 (14)	0.55438 (11)
H10	0.361 (3)	0.1817 (16)	0.5660 (14)
H11	0.521 (3)	0.2361 (18)	0.5636 (15)
H12	0.519 (2)	0.1274 (17)	0.5890 (16)
C2	0.60044 (19)	0.46435 (12)	0.41432 (11)
H2	0.673 (2)	0.4942 (14)	0.4528 (13)
C3	0.5318 (2)	0.51675 (12)	0.34404 (12)
H3	0.562 (2)	0.5832 (15)	0.3329 (13)
C4	0.42036 (19)	0.47365 (12)	0.28967 (11)
H4	0.372 (2)	0.5081 (14)	0.2418 (14)
C5	0.27982 (19)	0.30370 (13)	0.26915 (11)
H5	0.210 (2)	0.3126 (14)	0.2231 (12)
C6	0.29903 (18)	0.21959 (13)	0.31578 (11)
H6	0.254 (2)	0.1546 (14)	0.3082 (12)
C8	0.46006 (17)	0.33119 (11)	0.38019 (10)
C9	0.38080 (17)	0.37636 (12)	0.30795 (10)

Compound	08srv146	08srv297
Empirical formula	$C_{16}H_{26}N_2Si$	$C_{24}H_{36}B_2N_2O_6$
Formula weight	274.48	470.17
Temperature, K	393(2)	393(2)
Crystal system	triclinic	monoclinic
Space group (no.)	P-1 (# 2)	$P2_1/c$ (# 14)
a, Å	7.6314(7)	10.9374(5)
b, Å	13.4875(12)	22.6949(12)
c, Å	15.6505(14)	10.5540(5)
α, º	90.42(2),	90.00,
β, º	96.49(2)	96.50(1)
γ, º	92.07(2)	90.00
V, $Å^3$	1599.4(2)	2602.9(2)
Z	4	4
ρ (calc.), g/cm^3	1.140	1.200
μ, mm^{-1}	0.137	0.084
Refls collected	16940	35524
Unique reflections	7310	7598
Reflections I>2σ (I)	4939	6272
R_{int} ,%	5.93	4.14
Refined parameters	367	342
R(F) [I>2σ (I)]	0.0593,	0.0414
$wR(F^2)$ [all data],%	0.1588	0.1199

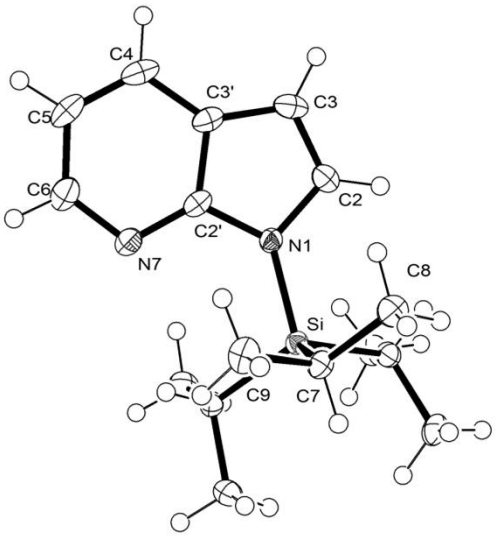

08srv146

08srv146	Coordinates (Å)		
Atom	x	y	z
Si	0.09157 (8)	0.30009 (5)	0.20874 (4)
N1	0.3401 (3)	0.17409 (15)	0.35414 (12)
C2	0.4539 (3)	0.1321 (2)	0.41327 (15)
H2	0.4493	0.0617	0.416
C3	0.5776 (4)	0.1835 (2)	0.47075 (16)
H3	0.6551	0.1483	0.5104
C4	0.5882 (3)	0.2859 (2)	0.46987 (15)
H4	0.6722	0.3224	0.5084
C5	0.4319 (3)	0.43412 (19)	0.38919 (15)
H5	0.4904	0.4921	0.415
C6	0.2969 (3)	0.43115 (17)	0.32514 (15)
H6	0.2462	0.4884	0.2991
N7	0.2401 (3)	0.33362 (14)	0.30194 (11)
C8	0.3504 (3)	0.27302 (18)	0.35509 (14)
C9	0.4708 (3)	0.33373 (19)	0.41059 (14)
C10	−0.0693 (3)	0.40348 (17)	0.19321 (15)
H10	0.0023	0.4671	0.2021
C11	−0.2044 (3)	0.40385 (19)	0.25891 (16)
H111	−0.2633	0.4674	0.2566
H112	−0.1441	0.3947	0.3169
H113	−0.2928	0.3497	0.2454
C12	−0.1657 (3)	0.40619 (19)	0.10137 (16)
H121	−0.2398	0.4641	0.0957
H122	−0.2399	0.3456	0.0902
H123	−0.0789	0.4104	0.0598
C13	−0.0106 (3)	0.17341 (17)	0.22384 (14)
H13	0.0895	0.1273	0.2315
C14	−0.1083 (3)	0.16128 (19)	0.30357 (16)
H141	−0.1374	0.0908	0.3115
H142	−0.2174	0.1981	0.2959
H143	−0.0331	0.1871	0.3544
C15	−0.1281 (3)	0.13735 (18)	0.14260 (15)
H151	−0.1649	0.0677	0.1492
H152	−0.0618	0.1436	0.0926
H153	−0.2328	0.1778	0.1339
C16	0.2262 (3)	0.29775 (17)	0.11525 (14)
H16	0.1426	0.2826	0.0625
C17	0.3180 (3)	0.39912 (18)	0.10156 (16)
H171	0.382	0.3954	0.0508
H172	0.4011	0.4166	0.1523
H173	0.2291	0.4498	0.0928
C18	0.3624 (3)	0.21626 (19)	0.12277 (16)
H181	0.4306	0.2194	0.0734
H182	0.3011	0.1512	0.1236
H183	0.4423	0.2261	0.176

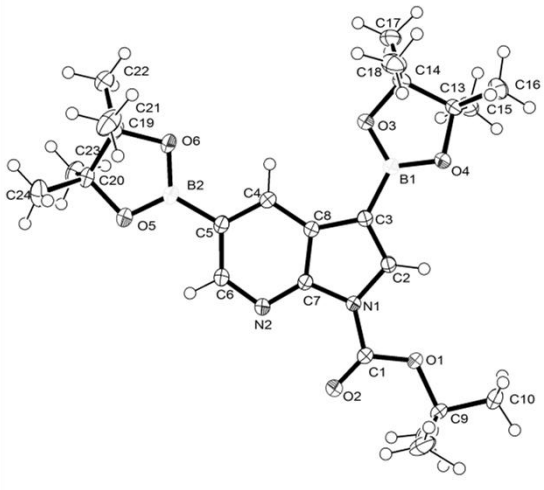

08srv297

08srv297	Coordinates (Å)		
Atoms	x	y	z
O1	0.33919 (6)	0.51945 (3)	0.16906 (6)
O2	0.18288 (7)	0.51562 (4)	0.29310 (8)
O3	0.72813 (6)	0.36388 (3)	0.53448 (7)
O4	0.74137 (6)	0.39314 (3)	0.32835 (6)
O5	0.23510 (7)	0.35770 (3)	0.88546 (7)
O6	0.42950 (7)	0.32143 (4)	0.88006 (7)
N1	0.36881 (7)	0.47047 (3)	0.35279 (7)
N2	0.24818 (7)	0.45365 (4)	0.52914 (8)
C1	0.28468 (9)	0.50419 (4)	0.27065 (9)
C2	0.48650 (8)	0.45333 (4)	0.32764 (8)
H2	0.5228	0.4641	0.2533
C3	0.54252 (8)	0.41916 (4)	0.42374 (8)
C4	0.45514 (8)	0.38639 (4)	0.63407 (8)
H4	0.5243	0.3641	0.6695
C5	0.35054 (9)	0.39158 (4)	0.69838 (9)
C6	0.25209 (9)	0.42602 (4)	0.64197 (9)
H6	0.1825	0.43	0.6875
C7	0.34865 (8)	0.44657 (4)	0.47127 (8)
C8	0.45551 (8)	0.41463 (4)	0.51701 (8)
C9	0.27150 (9)	0.55357 (4)	0.06296 (9)
C10	0.36319 (16)	0.55426 (13)	−0.03412 (17)
H101	0.4389	0.5729	0.0052
H102	0.3295	0.5772	−0.1086
H103	0.3814	0.5142	−0.0609
C11	0.1552 (2)	0.52156 (9)	0.0105 (2)
H111	0.0958	0.5206	0.0733
H112	0.1776	0.4812	−0.0106
H113	0.1183	0.5416	−0.0669
C12	0.2474 (3)	0.61490 (7)	0.10907 (13)
H121	0.3245	0.6346	0.141
H122	0.1946	0.6119	0.1779
H123	0.2051	0.6378	0.0386
C10B	0.3730 (10)	0.5769 (6)	−0.0082 (12)
H104	0.4224	0.5456	−0.0361
H105	0.3375	0.599	−0.0808
H106	0.4235	0.6025	0.0483
C11B	0.1904 (14)	0.5118 (6)	−0.0180 (13)
H114	0.126	0.4968	0.0309
H115	0.2397	0.4788	−0.0439
H116	0.1524	0.5325	−0.0940
C12B	0.1938 (13)	0.6056 (5)	0.1089 (10)
H124	0.1445	0.5907	0.1714
H125	0.2461	0.6366	0.1459
H126	0.1412	0.6209	0.0374
C13	0.86594 (9)	0.37477 (5)	0.37903 (9)
C14	0.84065 (9)	0.33717 (5)	0.49768 (10)
C15	0.93883 (10)	0.43069 (5)	0.41271 (12)
H151	0.9372	0.4557	0.3369
H152	1.0242	0.4204	0.4431
H153	0.9021	0.452	0.4798
C16	0.92170 (11)	0.34043 (6)	0.27593 (11)
H161	0.934	0.3668	0.205
H162	0.866	0.3084	0.2451
H163	1.0011	0.3239	0.3113
C17	0.94058 (10)	0.34154 (6)	0.60938 (11)
H171	0.9192	0.3165	0.6792
H172	0.9479	0.3825	0.6385
H173	1.0191	0.3285	0.5826
C18	0.80917 (11)	0.27309 (5)	0.46539 (13)
H181	0.7788	0.254	0.539
H182	0.883	0.2526	0.4441
H183	0.7455	0.2715	0.3923
C19	0.37618 (10)	0.28685 (5)	0.97738 (9)
C20	0.26360 (9)	0.32516 (4)	1.00476 (9)
C21	0.33837 (14)	0.22778 (5)	0.91606 (11)
H211	0.4109	0.2081	0.8894
H212	0.2779	0.2343	0.8415
H213	0.3019	0.203	0.978
C22	0.47405 (11)	0.27804 (6)	1.08919 (11)
H221	0.5415	0.2544	1.0621
H222	0.4383	0.2576	1.1579
H223	0.5057	0.3165	1.1199
C23	0.29376 (12)	0.37048 (5)	1.10959 (10)
H231	0.222	0.3958	1.1155
H232	0.3634	0.3947	1.0898
H233	0.3153	0.3503	1.1911
C24	0.15002 (12)	0.29061 (6)	1.02939 (12)
H241	0.0832	0.318	1.042
H242	0.1687	0.2664	1.106
H243	0.1247	0.2651	0.9561
B1	0.67236 (10)	0.39221 (5)	0.42880 (10)
B2	0.33839 (10)	0.35720 (5)	0.82377 (10)

Compound	10srv115	10srv117	09srv374	10srv116
Empirical formula	$C_{16}H_{19}BClNO_2$	$C_{16}H_{19}BBrNO_2$	$C_{17}H_{22}BNO_2$	$C_{16}H_{19}BClNO_2$
Formula weight	303.58	348.04	283.17	303.58
Temperature, K	393(2)	393.15	393(2)	135.15
Crystal system	monoclinic	monoclinic	triclinic	monoclinic
Space group (no.)	$P2_1/c$ (# 14)	$P2_1/c$ (# 14)	P-1 (# 2)	$P2_1/c$ (# 14)
a, Å	11.6375(4)	11.6782(3)	7.0095(2)	10.6988(7)
b, Å	14.2064(5)	14.2699(4)	10.8581(3)	10.0350(6)
c, Å	10.3695(5)	10.3543(3)	11.5239(3)	15.0669(10)
α, º	90.00	90.00	115.931(5),	90.00
β, º	113.190(6)	112.982(11)	97.638(6),	105.441(11)
γ, º	90.00	90.00	90.082(5)	90.00
V, $Å^3$	1575.84(11)	1588.55(8)	780.03(4)	1559.23(17)
Z	4	4	2	4
ρ (calc.), g/cm^3	1.280	1.455	1.206	1.293
μ, mm^{-1}	0.245	2.590	0.077	0.248
Refls collected	22051	21607	14334	16841
Unique reflections	4598	4640	4539	3579
Reflections I>2σ (I)	3458	3671	3634	2703
R_{int} ,%	4.89	2.71	4.35	3.90
Refined parameters	266	267	278	266
R(F) [I>2σ (I)]	0.0489	0.0271	0.0435	0.0390
$wR(F^2)$ [all data],%	0.1435	0.0682	0.1342	0.1075

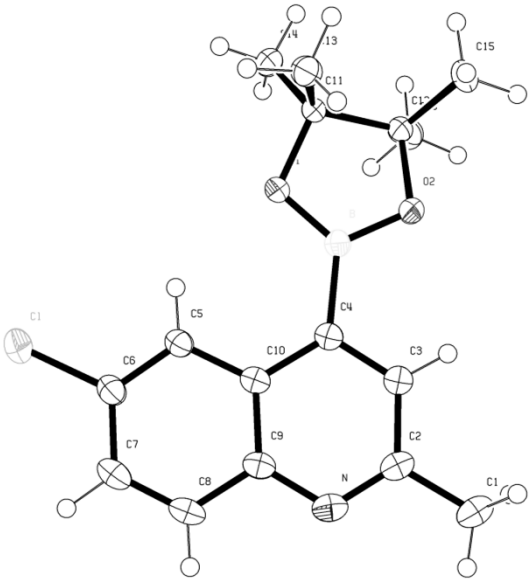

10srv115

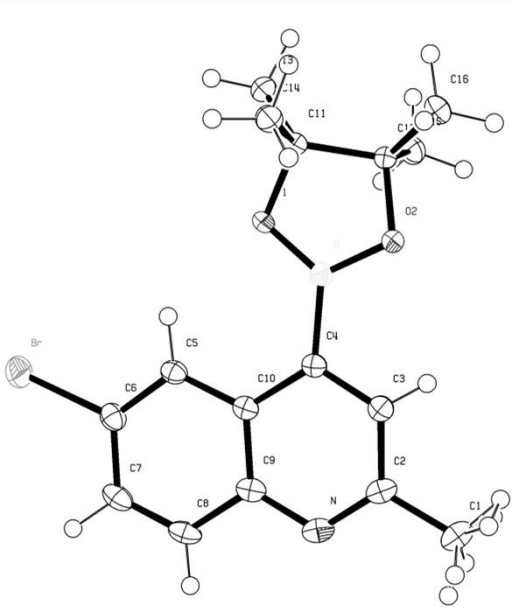

10srv117

10srv115	Coordinates (Å)		
Atom	x	y	z
Cl	0.44250 (4)	0.19855 (3)	0.35926 (4)
O1	0.28643 (8)	0.03025 (7)	−0.11088 (9)
O2	0.10274 (8)	−0.00492 (7)	−0.29483 (9)
N	−0.09531 (11)	0.15804 (8)	0.01260 (13)
C1	−0.27263 (15)	0.11348 (12)	−0.1966 (2)
H1A	−0.304 (2)	0.0500 (17)	−0.232 (3)
H1B	−0.318 (2)	0.1442 (17)	−0.152 (3)
H1C	−0.299 (2)	0.1374 (16)	−0.297 (3)
C2	−0.13463 (13)	0.11630 (9)	−0.11103 (15)
C3	−0.05134 (12)	0.07531 (9)	−0.16500 (14)
H3	−0.0840 (14)	0.0458 (11)	−0.2535 (18)
C4	0.07614 (12)	0.07955 (9)	−0.09267 (13)
C5	0.25029 (13)	0.13835 (9)	0.12581 (14)
H5	0.3111 (16)	0.1157 (12)	0.0948 (17)
C6	0.28445 (14)	0.18291 (10)	0.25329 (15)
C7	0.19632 (15)	0.21751 (10)	0.30232 (16)
H7	0.2192 (16)	0.2484 (13)	0.393 (2)
C8	0.07182 (15)	0.20764 (10)	0.22134 (16)
H8	0.0130 (17)	0.2304 (13)	0.2522 (19)
C9	0.03116 (13)	0.16309 (9)	0.08844 (14)
C10	0.12111 (12)	0.12660 (9)	0.04034 (13)
C11	0.32096 (12)	−0.02856 (9)	−0.20729 (13)
C12	0.20112 (12)	−0.02359 (9)	−0.34627 (13)
C13	0.34796 (15)	−0.12673 (10)	−0.14308 (16)
H13A	0.2760 (17)	−0.1546 (13)	−0.1374 (19)
H13B	0.4164 (17)	−0.1220 (13)	−0.049 (2)
H13C	0.3707 (15)	−0.1672 (12)	−0.2048 (17)
C14	0.43736 (13)	0.01339 (12)	−0.21716 (16)
H14A	0.4301 (15)	0.0816 (13)	−0.2363 (18)
H14B	0.5092 (18)	0.0021 (13)	−0.135 (2)
H14C	0.4556 (16)	−0.0173 (12)	−0.2915 (19)
C15	0.16961 (15)	−0.11433 (11)	−0.43027 (16)
H15A	0.1618 (17)	−0.1685 (13)	−0.3783 (19)
H15B	0.0906 (17)	−0.1052 (13)	−0.5157 (19)
H15C	0.2348 (19)	−0.1314 (14)	−0.459 (2)
C16	0.20006 (14)	0.05946 (11)	−0.44002 (15)
H16A	0.2187 (16)	0.1201 (12)	−0.3891 (18)
H16B	0.1181 (16)	0.0653 (12)	−0.5140 (19)
H16C	0.2611 (17)	0.0507 (13)	−0.4813 (19)
B	0.15872 (14)	0.03379 (10)	−0.16474 (15)

10srv117	Coordinates (Å)		
Atom	x	y	z
Br	0.445508 (15)	0.196062 (12)	0.374691 (16)
O1	0.28326 (8)	0.03083 (7)	−0.11016 (9)
O2	0.10171 (8)	−0.00527 (7)	−0.29451 (9)
N	−0.10083 (11)	0.15805 (8)	0.00735 (13)
C1	−0.27565 (14)	0.11318 (12)	−0.20293 (19)
H1B1	−0.2905	0.0831	−0.2931
H1B2	−0.3177	0.0775	−0.1533
H1B3	−0.3084	0.1773	−0.2193
H1A1	−0.295 (2)	0.1437 (16)	−0.292 (2)
H1A2	−0.308 (2)	0.0504 (17)	−0.237 (2)
H1A3	−0.326 (2)	0.1490 (15)	−0.153 (2)
C2	−0.13832 (13)	0.11579 (9)	−0.11575 (16)
C3	−0.05396 (13)	0.07453 (9)	−0.16711 (15)
H3	−0.0852 (13)	0.0449 (10)	−0.2528 (16)
C4	0.07263 (12)	0.07871 (9)	−0.09362 (13)
C5	0.24362 (13)	0.13677 (9)	0.12740 (14)
H5	0.3086 (14)	0.1113 (10)	0.0999 (16)
C6	0.27566 (14)	0.18080 (10)	0.25431 (15)
C7	0.18562 (15)	0.21673 (10)	0.30086 (16)
H7	0.2093 (16)	0.2432 (12)	0.3950 (19)
C8	0.06334 (15)	0.20782 (10)	0.21751 (16)
H8	0.0013 (16)	0.2297 (11)	0.2450 (17)
C9	0.02441 (14)	0.16302 (9)	0.08500 (15)
C10	0.11555 (13)	0.12594 (9)	0.03953 (14)
C11	0.31898 (12)	−0.02739 (9)	−0.20683 (14)
C12	0.20057 (12)	−0.02263 (9)	−0.34567 (13)
C13	0.43466 (13)	0.01486 (12)	−0.21619 (16)
H13A	0.4242 (16)	0.0824 (13)	−0.2322 (19)
H13B	0.4534 (14)	−0.0180 (11)	−0.2909 (17)
H13C	0.5054 (15)	0.0048 (11)	−0.1331 (17)
C14	0.34588 (15)	−0.12504 (11)	−0.14274 (16)
H14A	0.2721 (16)	−0.1518 (11)	−0.1317 (17)
H14B	0.3708 (16)	−0.1669 (12)	−0.2005 (18)
H14C	0.4113 (15)	−0.1185 (11)	−0.0539 (18)
C15	0.19942 (15)	0.06056 (11)	−0.43822 (15)
H15A	0.1175 (15)	0.0667 (11)	−0.5126 (16)
H15B	0.2165 (15)	0.1212 (12)	−0.3853 (18)
H15C	0.2596 (17)	0.0518 (13)	−0.4830 (19)
C16	0.17037 (15)	−0.11256 (11)	−0.43009 (16)
H16A	0.0943 (16)	−0.1024 (12)	−0.5165 (18)

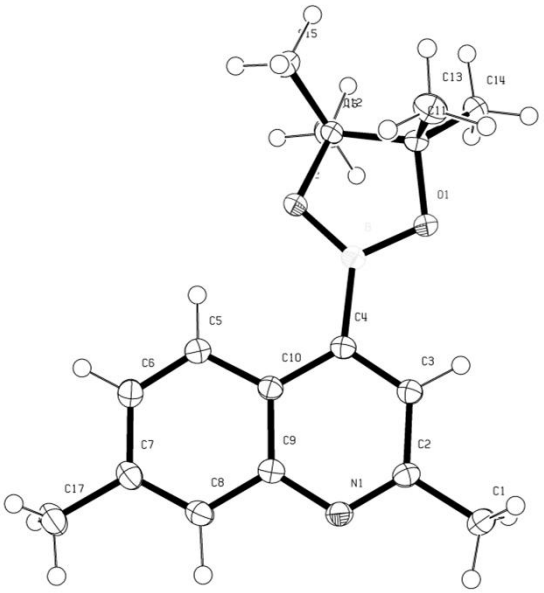

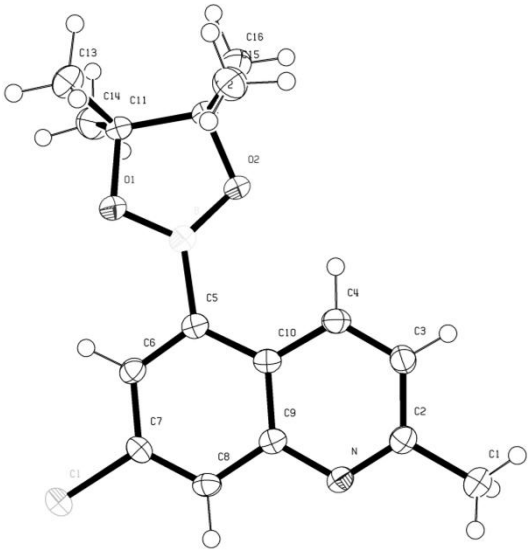

09srv374

09srv374	Coordinates (Å)		
Atom	x	y	z
O1	0.73952 (10)	0.17546 (7)	0.32083 (7)
O2	0.43928 (10)	0.09586 (7)	0.20267 (7)
N1	0.49548 (12)	0.64487 (8)	0.37472 (8)
C1	0.81768 (15)	0.70322 (10)	0.49627 (10)
H1A	0.934 (2)	0.6794 (17)	0.4557 (17)
H1B	0.842 (2)	0.7101 (18)	0.5805 (18)
H1C	0.793 (3)	0.795 (2)	0.4997 (19)
C2	0.65373 (13)	0.59985 (9)	0.41464 (9)
C3	0.67486 (13)	0.45884 (9)	0.38209 (9)
H3	0.7968 (19)	0.4296 (13)	0.4118 (13)
C4	0.52824 (13)	0.36056 (9)	0.30700 (9)
C5	0.18862 (14)	0.31896 (10)	0.18821 (9)
H5	0.1926 (18)	0.2209 (14)	0.1653 (13)
C6	0.02642 (15)	0.37032 (10)	0.14992 (10)
H6	−0.083 (2)	0.3102 (14)	0.0970 (14)
C7	0.01778 (14)	0.51153 (10)	0.18204 (9)
C8	0.17581 (14)	0.59883 (10)	0.25656 (9)
H8	0.179 (2)	0.7045 (15)	0.2823 (14)
C9	0.34536 (13)	0.54985 (9)	0.29983 (9)
C10	0.35391 (13)	0.40712 (9)	0.26393 (9)
C11	0.74225 (13)	0.02626 (9)	0.25971 (9)
C12	0.52328 (13)	−0.02090 (9)	0.21775 (9)
C13	0.85509 (17)	−0.01206 (12)	0.14595 (11)
H13A	0.785 (2)	0.0140 (15)	0.0812 (15)
H13B	0.867 (2)	−0.1132 (15)	0.1033 (14)
H13C	0.988 (2)	0.0376 (14)	0.1804 (14)
C14	0.84401 (15)	−0.01573 (11)	0.36015 (10)
H14B	0.835 (2)	−0.1191 (15)	0.3249 (14)
H14A	0.784 (2)	0.0233 (14)	0.4407 (14)
H14C	0.984 (2)	0.0163 (15)	0.3823 (15)
C15	0.47439 (18)	−0.14872 (11)	0.08916 (12)
H15B	0.515 (2)	−0.1388 (16)	0.0149 (15)
H15A	0.336 (2)	−0.1670 (15)	0.0700 (15)
H15C	0.536 (2)	−0.2284 (16)	0.0966 (15)
C16	0.43049 (16)	−0.03512 (12)	0.32387 (12)
H16A	0.289 (2)	−0.0465 (15)	0.2990 (15)
H16B	0.462 (2)	0.0499 (16)	0.4080 (15)
H16C	0.4746 (19)	−0.1173 (14)	0.3335 (13)
C17	−0.16068 (17)	0.56208 (13)	0.13346 (11)
H17A	−0.194 (3)	0.519 (2)	0.042 (2)
H17B	−0.260 (3)	0.565 (2)	0.174 (2)
H17C	−0.141 (3)	0.658 (2)	0.144 (2)
B	0.56576 (15)	0.20788 (10)	0.27571 (10)

10srv116

10srv116	Coordinates (Å)		
Atom	x	y	z
Cl	0.39657 (4)	0.11294 (4)	0.39182 (3)
O1	0.09430 (11)	0.54240 (11)	0.37590 (8)
O2	0.20139 (11)	0.69741 (11)	0.47907 (8)
N	0.58598 (12)	0.37056 (12)	0.68642 (9)
C1	0.69346 (19)	0.4764 (2)	0.83064 (13)
H1A	0.720 (3)	0.397 (3)	0.8520 (19)
H1B	0.770 (3)	0.517 (3)	0.8215 (18)
H1C	0.672 (3)	0.530 (3)	0.873 (2)
C2	0.58863 (15)	0.47336 (15)	0.74136 (10)
C3	0.49795 (16)	0.57904 (16)	0.71912 (11)
H3	0.5022 (18)	0.6482 (19)	0.7593 (13)
C4	0.40502 (16)	0.57799 (16)	0.63767 (11)
H4	0.3412 (18)	0.6479 (18)	0.6232 (12)
C5	0.30428 (14)	0.46080 (14)	0.48770 (11)
C6	0.30533 (15)	0.34945 (15)	0.43441 (11)
H6	0.2433 (16)	0.3427 (17)	0.3777 (12)
C7	0.39838 (15)	0.24853 (15)	0.46448 (11)
C8	0.49017 (15)	0.25595 (15)	0.54673 (11)
H8	0.5538 (17)	0.1868 (19)	0.5671 (13)
C9	0.49183 (14)	0.36795 (14)	0.60423 (10)
C10	0.39827 (14)	0.47085 (14)	0.57537 (10)
C11	0.02397 (15)	0.66700 (15)	0.34806 (11)
C12	0.07608 (15)	0.75788 (15)	0.43447 (11)
C13	−0.12000 (18)	0.6377 (2)	0.32532 (17)
H13A	−0.148 (2)	0.582 (2)	0.2701 (18)
H13B	−0.136 (2)	0.581 (3)	0.3776 (17)
H13C	−0.172 (2)	0.726 (2)	0.3110 (14)
C14	0.0619 (2)	0.7150 (2)	0.26375 (13)
H14A	0.033 (2)	0.649 (3)	0.2164 (18)
H14B	0.155 (2)	0.735 (2)	0.2752 (15)
H14C	0.0100 (19)	0.796 (2)	0.2401 (14)
C15	−0.0035 (2)	0.7494 (2)	0.50378 (15)
H15A	−0.014 (2)	0.651 (2)	0.5183 (15)
H15B	−0.085 (2)	0.789 (2)	0.4779 (16)
H15C	0.042 (2)	0.801 (2)	0.5573 (16)
C16	0.0983 (2)	0.90150 (18)	0.41348 (15)
H16A	0.1643 (18)	0.8957 (17)	0.3806 (13)
H16B	0.015 (2)	0.947 (2)	0.3795 (16)
H16C	0.130 (2)	0.951 (2)	0.4676 (16)
B	0.19936 (17)	0.56991 (18)	0.44754 (12)